

GERMAN PHARM-TOX SUMMIT 2016

Abstracts

of the

82nd Annual Meeting of the German Society for Experimental
and Clinical Pharmacology and Toxicology (DGPT)

and the

18th Annual Meeting of the Network Clinical Pharmacology
Germany (VKliPha)

in cooperation with the Arbeitsgemeinschaft für Angewandte
Humanpharmakologie e.V. (AGAH)

29th February – 03rd March 2016

Henry-Ford-Bau · Berlin

This supplement was not sponsored by outside commercial
interests. It was funded entirely by the publisher.

Structure

	IDs
Oral presentations	001 – 081
In vitro systems and mechanistic investigations I	001 – 006
Heart	007 – 012
Immunology – inflammation – cancer	013 – 018
Individualized therapy and clinical implications	019 – 023
In vitro systems and mechanistic investigations II	024 – 027
DNA-damage and cancer	028 – 033
GPCR signaling	034 – 038
Cardiovascular pharmacology	039 – 043
Potential drug targets and pharmacotherapy	044 – 048
DNA-damage and –repair	049 – 054
GPCR receptor pharmacology	055 – 060
Ion channels	061 – 066
Organ- and neurotoxicity	067 – 072
Toxic substances, particles and food components	073 – 077
Clinical pharmacology and drug use	078 – 081
Poster presentations	082 – 421
Poster Session I	
Berlin-Brandenburger Forschungsplattform BB3R	082 – 094
Pharmacology – G-protein coupled receptors	095 – 116
Pharmacology – GTP-binding proteins	117 – 124
Pharmacology – Cyclic nucleotides	125 – 135
Pharmacology – Cardiovascular system	136 – 169
Pharmacology – Ion channels	170 – 187
Toxicology – Biotransformation and toxicokinetics	188 – 192
Toxicology – Organtoxicity (immunotoxicity, blood, and kidney)	193 – 195
Toxicology – Neurotoxicity, incl. neurodevelopment	196 – 200
Toxicology – Reproductive/developmental toxicity	201 – 202
Toxicology – Endocrine effects	203 – 207
Toxicology – Immunotoxicology	208 – 209
Toxicology – Nanomaterials	210 – 226
Toxicology – Exposure/effect monitoring	227 – 229
Toxicology – Biomarkers of exposure/Biomonitoring	230 – 236
Toxicology – External exposure	237
Toxicology – Food toxicology	238 – 246
Toxicology – Environmental toxicology/Ecototoxicology	247 – 252
Poster Session II	
Pharmacology – Membrane transporters	253 – 261
Pharmacology – Central nervous system	262 – 269
Pharmacology – Endocrine, immune and pulmonary pharmacology	270 – 280
Pharmacology – Gastrointestinal tract, NO, CO	281 – 290
Pharmacology – Cancer pharmacology	291 – 302
Pharmacology – Drug discovery	303 – 313
Pharmacology – Disease models	314 – 322
Pharmacology – Pharmacokinetics and clinical studies	323 – 335
Pharmacology – Education	336 – 340
Toxicology – Risk assessment	341 – 347
Toxicology – Methods	348 – 349
Toxicology – Substances and compound groups	350
Toxicology – Genotoxicity	351 – 361
Toxicology – Carcinogenesis	362 – 365
Toxicology – Non-animal testing	366 – 371
Toxicology – Non-animal testing in sicilco	372 – 378
Toxicology – Non-animal testing in vitro	379 – 394
Toxicology – Toxic pathway analysis/AOP	395 – 400
Clinical Pharmacology – Drug therapy in pregnancy	401
Clinical Pharmacology – Cardiovascular treatment	402 – 404
Clinical Pharmacology – Antineoplastic treatment	405
Clinical Pharmacology – Safety of drug therapy	406 – 407
Clinical Pharmacology – Personalized therapy	408 – 409
Clinical Pharmacology – Regulatory	410
Clinical Pharmacology – Others	411 – 416
Free topics	417 – 421

Oral presentations

In vitro systems and mechanistic investigations I

001

Crosstalk between macrophages and monocytes: killing in trans

V. Ponath¹, B. Kaina¹

¹University Medical Center Mainz, Department of Toxicology, Mainz, Germany

Monocytes are mononuclear phagocytes that play an important role in the rapid response against invading pathogens. They originate from progenitor cells in the bone marrow before they are released into the bloodstream. Circulating in the blood monocytes migrate into peripheral tissues where they differentiate into tissue-specific macrophages or dendritic cells. Their recruitment to sites of inflammation and infection is crucial in the effective and controlled clearance of pathogens. However, monocytes also contribute to the pathogenesis of inflammatory diseases. Therefore, a mechanism to maintain a healthy balance in the monocyte population is crucial for tissue homeostasis and controlled clearance of inflammatory sites. Previous studies in our lab showed an impaired DNA repair machinery in monocytes, affecting mainly base excision repair and non-homologous end-joining, whereas macrophages (and dendritic cells) were DNA repair competent. Based on these findings we studied the effect of reactive oxygen species (ROS) generated by macrophages on DNA integrity, cell death and differentiation potential of monocytes. Here, we show that monocyte-derived macrophages stimulated with phorbol 12-myristate 13-acetate (PMA) produce intra- and extracellular ROS. Co-cultured with activated macrophages monocytes displayed oxidative DNA damage, *i.e.* 8-hydroxyguanosine and DNA single strand breaks, resulting in apoptosis. In addition, the surviving fraction of monocytes was severely impaired in its differentiation capacity and unable to give rise to new (healthy) macrophages. The data supports the hypothesis that the oxidative burst of macrophages not only kills pathogens, but also DNA repair defective monocytes in the target area, which could be a mechanism regulating the immune response.

002

Neuronal stress response following proteasomal inhibition, and its prevention by astrocytic thiol supply

S. Gutbier¹, M. Leist¹

¹Universität Konstanz, Chair of In vitro toxicology and biomedicine, Konstanz, Germany

Introduction: The underlying mechanisms of neurodegenerative diseases such as Parkinson's disease (PD) are not completely understood. One key event in PD, amongst others, is the disturbance of the ubiquitin proteasome system (UPS). The resulting misfolded and aggregated proteins have been discussed to induce cell death. Various attempts in the past to treat these diseases and to slow down the progressive neuronal loss failed at different clinical stages. Most of these attempts followed the concept of blocking specific stress pathways (e.g. caspase activation). An alternative therapeutic approach would be to identify and harness endogenous cellular defense mechanisms and thereby to prevent the activation of deleterious cascades.

Methods: In this study we used human dopaminergic neurons (LUHMES cells) and treated them with the proteasome inhibitor MG-132 to model neurodegeneration after disturbance of the UPS *in vitro*. Cell death, as well as several biochemical and signaling changes were determined in neuronal cultures and astrocyte-neuron co-cultures.

Results: In a first step, we monitored the stress responses orchestrating the neurodegeneration in LUHMES cells following proteasomal inhibition. Neurons, exposed to MG-132 (nanomolar concentrations), underwent rapid apoptotic cell death. Prior to caspase activation, we observed an increase in AKT and p38 phosphorylation. Moreover, the ATF4 stress response was induced, and this led to an increase in GSH synthesis capacity. In a second step, we identified cysteine supplementation as a protective intervention. This intervention prevented ATF4 activation, AKT and p38 phosphorylation and cell death, while other amino acids showed no effect. Since glia cells are known to support neurons with thiols, we wondered, whether they might have protective properties in a co-culture model. When astrocytes were added to neurons, the latter were protected against MG-132. Under these conditions, the neuronal GSH increase was not observed and ATF4 activation was not detected. The major part of the protective effect of astrocytes was mediated by thiol supply to neurons and this indicates that elevation of cysteine levels in brain might have a protective effect against disturbances of the UPS system in neurons.

Conclusion: The ATF4-mediated induction of DDIT4, NOXA and PUMA, and the mechanism of thiol-transfer from astrocytes to neurons may provide new pharmacological targets to prevent neurodegeneration.

003

Switching from astrocytic neuroprotection to neurodegeneration by cytokine stimulation

P. Chovancova¹, L. Efreanova¹, S. Gutbier¹, S. Schildknecht¹, M. Leist¹

¹University of Konstanz, Konstanz, Germany

Background: Astrocytes are the largest cell population in the human brain, and they react to injury and cytokines with activation. Only few experimental studies have examined the interaction of activated astrocytes with human neurons and the pharmacology thereof.

Experimental approach: Immortalized murine astrocytes (IMA) were combined with human LUHMES neurons, and stimulated with an inflammatory (TNF, IL-1) cytokine mix (CM). Neuronal survival was studied both in co-cultures and in monocultures after transfer of conditioned medium from activated IMA. Interventions with >20 pharmaceutical compounds were used to profile the model system.

Key results: Control IMA supported neurons, and protected them from neurotoxicants. Inflammatory activation reduced this protection, and prolonged exposure of co-cultures to CM triggered neurotoxicity. This neither involved direct effects of cytokines on neurons, nor secretion of nitric oxide from astrocytes, but it was prevented by the corticosteroid dexamethasone. The neurotoxicity-mediating effect of IMA was faithfully reproduced by human astrocytes. Moreover, glia-dependent toxicity was also observed, when IMA cultures were stimulated with CM, and the culture medium was transferred to neurons. Such neurotoxicity was prevented when astrocytes were treated by p38 kinase inhibitors or dexamethasone, whereas such compounds had no effect, when added to neurons. Conversely, treatment of neurons with five different drugs, including resveratrol and CEP1347, prevented toxicity of astrocyte supernatants.

Conclusion: The sequential IMA-LUHMES neuroinflammation model is suitable for separate profiling of both glial-directed and directly neuroprotective strategies. Moreover, direct evaluation in co-cultures of the same cells allows for testing of therapeutic effectiveness in more complex settings, in which astrocytes affect pharmacological properties of neurons.

004

A human hepatic co-culture system for the analysis of cell-cell interactions *in vitro*

F. Wewering¹, J. Florent², D. K. Wissenbach³, S. Gebauer³, R. Pirow¹, M. von Bergen^{2,3,4}, S. Kalkhof², A. Luch¹, S. Zellmer¹

¹Bundesinstitut für Risikobewertung, Chemikalien- und Produktsicherheit, Berlin, Germany

²Helmholtz-Centre for Environmental Research, Department of Proteomics, Leipzig, Germany

³Helmholtz-Centre for Environmental Research, Department of Metabolomics, Leipzig, Germany

⁴Aalborg University, Department of Chemistry and Bioscience, Aalborg, Denmark

The demand of alternative test systems which closely mirror the *in vivo* situation is one of the main challenges in modern toxicity testing. The major goal is the development of *in vitro* systems that partly display the complexity of an organism and thus may mimic *in vivo* conditions. Despite great efforts in the past no adequate *in vitro* systems are available yet. On the other hand, cell cultures from almost every organ are easily accessible and therefore may help to roughly assess the toxic potential of substances at target structures. Nonetheless, the complex interactions which take place *in vivo* cannot be addressed in single cell cultures. In the liver, hepatocytes comprise 80% of the total liver volume while non-parenchymal cells – endothelial cells, stellate cells and Kupffer cells (that is, liver resident macrophages) – contribute only 6.5% of the volume, but 40% of the total cell number (Kmiec 2001). It has been increasingly recognized that in the liver neighboring non-parenchymal cells release molecules which contribute to the inflammatory damage and even aggravate it (Adams et al. 2010).

In our project a human *in vitro* co-culture system was established by combining a hepatic and a monocytic cell line, the latter of which can be differentiated to a macrophage-like phenotype. In this system the hepatotoxicity of substances has been analyzed, and the results were compared to single cultures and to published data from *in vivo* studies. Using ketoconazole, an antifungal, as a known hepatotoxic substance, inflammatory markers were studied and proved to be significantly upregulated only in co-culture. Conversely, cultures of hepatic cells only did not display this increase in inflammatory markers. At the same time, a negative substance, caffeine, failed to show any hepatotoxic potential in the co-culture system.

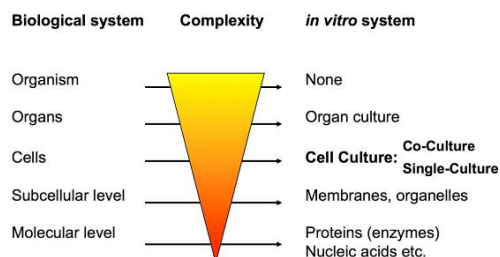
Our results demonstrate that this novel *in vitro* co-culture model represents a promising tool to evaluate the hepatotoxic potential of substances. In drug research, it might help to reduce animal testing as drugs with a high DILI potential can be dropped early in the development phase.

Acknowledgements: Support of the BfR through grant 1322-530 is gratefully acknowledged.

Adams DH, Ju C, Ramaiah SK, et al (2010) Mechanisms of immune-mediated liver injury. *Toxicol Sci* 115:307-321.

Kmiec Z (2001) Cooperation of liver cells in health and disease. *Adv Anat Embryol Cell Biol* 161:III-XIII, 1-151.

Abb. 1



The diagram relates the biological system – the *in vivo* situation – with the degree of complexity to the corresponding *in vitro* system. At the moment, there is no *in vitro* system that displays the high complexity of the whole organism. With decreasing complexity, *in vitro* models are available for the biological counterpart. On cellular level, *in vitro* co-cultures include the cell-cell interactions of the biological system with advantages compared to the single-culture systems.

005

The particle-induced cell migration assay (PICMA) as a model for acute particle-induced inflammation of the lung

I. Schremmer¹, J. Bünger¹, A. Brik¹, N. Rosenkranz¹, D. Weber¹, G. Johnen¹, T. Brünig¹, G. Westphal¹

¹Ruhr-Universität Bochum, Institut für Prävention und Arbeitsmedizin der Deutschen Gesetzlichen Unfallversicherung Institut der Ruhr-Universität Bochum (IPA), Bochum, Germany

Introduction: We aim on a cellular test system that is based on the migration of inflammatory cells in response to particle challenge. Previously we showed chemotaxis of differentiated HL-60 cells (dHL-60 cells) (as a model for neutrophils) and of NR8383 rat alveolar macrophages towards cell supernatants that were yielded from cells which were exposed towards coarse and nanosized quartz, silica, carbon black, and titanium dioxide in concentrations from 32 up to 96 $\mu\text{g}/\text{cm}^2$. BaSO₄ served as inert control. The present study investigates the effects of asbestos fibers.

Methods: NR8383 rat alveolar macrophages were challenged with 1 to 50 $\mu\text{g}/\text{cm}^2$ asbestos (Crysotile A and B, amosite, and crocidolite). The cell supernatants were used to induce migration of differentiated NR8383 rat macrophages and dHL-60 cells.

Results: incubation of NR8383 cells with the asbestos fibers yielded cell supernatants that induced chemotaxis in dHL-60 and un-exposed NR8383- cells in the dose range of 3 up to 50 $\mu\text{g}/\text{cm}^2$. The NR8383 reacted most strongly to amosite, followed by chrysotile A and B, followed by crocidolite. These responses roughly reflect the portion of critical fibers in the samples. The effects were paralleled to the transcription of CCL3, CCL4, CXCL1, CXCL3, IL6, IL10 and TNF- α . These inflammatory mediators were as well elevated following particle challenge.

Conclusions: Asbestos fibers acted significantly stronger as inducers of chemotaxis compared to the previously investigated particles. PICMA is able to differentiate between inert and inflammatory particles as well as strongly inflammatory fibers. The assay may serve as models for particle-induced inflammation of the lung.

006

Label-free and non-invasive monitoring of single cells after drug application using Raman spectroscopy

K. Schütze¹, H. Kremling¹, F. Sekhavati², R. Joachim², K.-F. Becker³, K. Malinowsky³, C. Klopsch⁴

¹CellTool GmbH, Bernried, Germany

²Faculty of Physics, Center for NanoScience and Faculty of Physics, LMU, Munich, Germany

³Institute of Pathology, TUM, Munich, Germany

⁴University of Rostock, Department of Cardiac Surgery, Reference- and Translation Centre for Cardiac Stem Cell Therapy (RTC), Rostock, Germany

Question: Raman spectroscopy (RS) is a highly sensitive analytical method for marker-free and non-invasive identification and characterization of cells. Here, we present RS as a novel tool for gentle yet precise cell analysis in three independent experiments, focusing on monitoring cellular reactions upon treatment. We could provide evidence that RS is a suitable tool to monitor cell differentiation, analyze cell modification and study cell apoptosis after drug application.

Methods: In a first experiment, mesenchymal stem cells (MSCs) were treated with erythropoietin (EPO) for certain time points and subsequently fixed with paraformaldehyde (PFA) for Raman analysis. In addition, SKBR3 breast cancer cells were exposed to the anti-cancer drug Herceptin (20 $\mu\text{g}/\text{ml}$). Cells were then fixed in PFA for RS. In a last experiment, MOLM-13 cells were separately cultivated in microwells and treated with thymidine for different time points prior to Raman analysis.

Results: Raman spectroscopy was able to monitor differentiation of EPO treated MSCs and found that around 35% of treated cells showed fibroblast like Raman profiles. In case of Herceptin treated SKBR3 cells, RS found internal changes of the cell's metabolism as reaction on drug application. Analyzing the most prominent differences in Raman spectra revealed discrimination of cells to be mainly due to changes in amid I, lipid and protein content. In the last experiment, RS was able to follow apoptosis of MOLM-13 cells after thymidine application and discriminate early from late apoptotic states.

Discussion: RS is a photonic marker for gentle yet highly specific cell analysis, which allows monitoring of single cell reaction after drug treatment. Thereby, RS provides information about changes within the entire metabolome on a single cell level. Raman spectra are as characteristic as a "fingerprint". RS works label-free and non-invasive and thus does not impair cell viability. This allows to gain new insights in pharmacological development and toxicological survey.

Acknowledgement: This Project received funding from the EU 7th Health Program grant agreement No 279288.

Figure 1 – MSC differentiation after EPO treatment. A: Representative pictures of untreated (upper image) and EPO treated (lower image) MSCs. B: Raman data of untreated MSCs (dark green: grown in DMEM/ light green: grown in MSCGM) and arterial fibroblasts (blue) form distinct clusters in principal component analysis (PCA). EPO-treated MSCs (red) can be found in both clusters indicating differentiation of a certain population of cells (red circles).

Figure 2 – Monitoring of Herceptin treatment. A: Bright field images of SKBR3 tumor cells. Pins depict sites of Raman measurements. B, C: PCA line plot (B) and scores plot (C) of control cells (blue) and cells incubated for 2h (red) and 8h (green) with Herceptin. D: Mean Raman spectra of cells.

Figure 3 – Apoptosis induction in cells grown in microwells. A: Representative pictures of cells treated in microwells over time. D: PCA scores plot of Raman spectra analysis. Red circled dots indicate early apoptotic cells which already show signs of late apoptosis.

Abb. 1

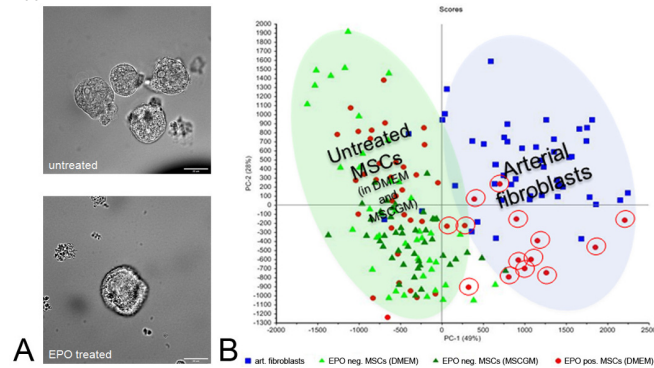


Abb. 2

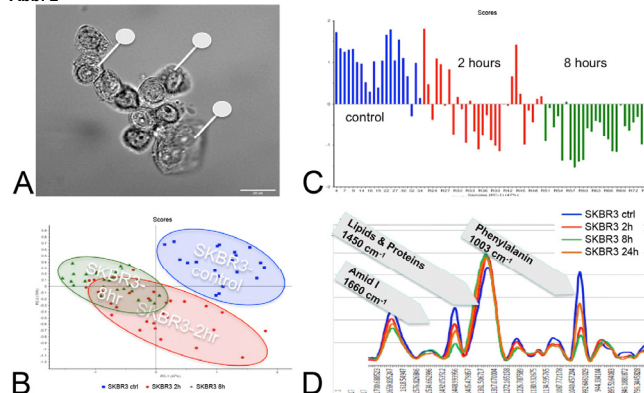
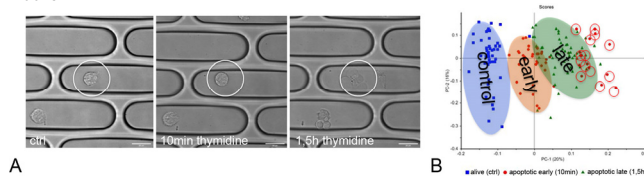


Abb. 3



Heart

007

The dimer interface of ERK1/2 provides an alternative targeting strategy to interfere with ERK1/2 mediated cardiac hypertrophy

A. Tomasovic¹, M. Hümmert¹, S. Kramer¹, T. Gruse¹, H. A. Katus², M. J. Lohse^{1,3}, O. Müller², K. Lorenz^{1,3}

¹Institut für Pharmakologie und Toxikologie, Würzburg, Germany

²Universitätsklinikum Heidelberg, Innere Medizin III, Heidelberg, Germany

³Deutsches Zentrum für Herzinsuffizienz, Würzburg, Germany

Extracellular signal-regulated kinases 1 and 2 (ERK1/2) are essential for the regulation of cell growth and cell survival and their kinase activity is up-regulated for example in different types of cancers and pathological cardiac hypertrophy. While inhibition of ERK1/2 activity by kinase inhibitors prevents tumor growth, it can also lead to exacerbated cardiomyocyte death and impaired heart function. Interestingly, we have previously identified an ERK autophosphorylation at threonine 188 as a prerequisite for nuclear ERK1/2 signaling and ERK-mediated cardiac hypertrophy.

Here, we investigated an alternative strategy to interfere with ERK1/2 signaling: Since activation of ERK1/2 triggers ERK dimerization, a prerequisite for ERK^{T188}-autophosphorylation, we chose the ERK dimer interface as a possible target to selectively interfere with ERK^{T188}-phosphorylation.

First, we investigated the impact of monomeric ERK2 on cardiac function. To address this issue, we generated mice with cardiac overexpression of monomeric ERK2 ^{Δ 174-177} and performed transverse aortic constriction (TAC) to induce cardiac hypertrophy. Compared to wild-type mice, ERK2 ^{Δ 174-177} overexpression attenuated TAC-induced cardiac hypertrophy, interstitial fibrosis and mRNA expression levels of collagen and brain natriuretic peptide (BNP), while cardiomyocyte survival and cardiac function were largely preserved.

Because of the positive effects of monomeric ERK ^{Δ 174-177} in the heart, we designed a peptide to interfere with endogenous ERK dimerization. Cross-linking and co-immunoprecipitation experiments showed that the peptide binds to ERK2 and prevents its dimerization. Moreover, the peptide effectively inhibited ERK^{T188}-phosphorylation and nuclear translocation of YFP-tagged wild-type ERK2 after phenylephrine stimulation. Further, adenoviral or adeno-associated virus serotype 9 (AAV9)-induced overexpression of the peptide in neonatal rat cardiomyocytes (NRCM) or mouse hearts resulted in a significantly reduced hypertrophic response to phenylephrine or TAC,

respectively. Interestingly, the peptide did not impair cardiomyocyte survival or overall ERK1/2 activation. As we found ERK1¹⁸⁸-phosphorylation to be significantly upregulated in colon cancers, we started to evaluate the effectiveness of the peptide on cell proliferation in different colon cancer cells (Colo320, LS174T and HT29). The peptide significantly reduced cancer cell proliferation even to a similar or greater extent than commonly used inhibitors of the ERK1/2 signaling cascade as e.g. PD98059, U0126 and Cetuximab. These data indicate that the more selective ERK1/2 inhibitor approach by the peptide can attenuate ERK1/2 mediated cell growth and proliferation in cancer cells and in cardiomyocytes. Since no adverse effects on cardiomyocytes and cardiac function were observed, the ERK dimer interface might therefore be a valuable and promising target to interfere with ERK1/2 signaling.

008

Dilative cardiomyopathy and increased mortality in β_1 -adrenoceptor overexpressing mice lacking $G\alpha_2$

K. Keller¹, M. Maass², S. Dizayee¹, V. Leiss³, S. Annala⁴, J. Köth¹, W. K. Seemann¹, J. Müller-Ehmsen⁵, K. Mohr⁶, B. Nürnberg³, S. Engelhardt¹, S. Herzig¹, L. Birnbaumer⁸, J. Matthes¹

¹Universität zu Köln, Institut für Pharmakologie, Köln, Germany

²Uniklinik Köln, Herzzentrum, Köln, Germany

³Universitätsklinikum Tübingen, Pharmakologie und Experimentelle Therapie, Tübingen, Germany

⁴Universität Bonn, Institut für Pharmazeutische Biologie, Bonn, Germany

⁵Asklepios Klinik Altona, Kardiologie, Hamburg, Germany

⁶Universität Bonn, Institut für Pharmazie, Bonn, Germany

⁷Technische Universität München, Institut für Pharmakologie und Toxikologie, München, Germany

⁸NIH (Department of Health and Human Services), Laboratory of Neurobiology, Durham, Vereinigte Staaten von Amerika

Background: G₂-proteins have been proposed to be cardioprotective. It's matter of debate whether this depends on the particular G₂ isoform and/or on the particular conditions (e.g. cardiac "stress") only. In our study we investigated effects of a $G\alpha_2$ -knockout on cardiac function and survival in a murine heart-failure model of cardiac β_1 -adrenoceptor overexpression.

Methods and results: β_1 -adrenoceptor overexpressing mice lacking $G\alpha_2$ (β_1 -tg/ $G\alpha_2^{-/-}$) were compared to wild-type (C57BL/6) mice and littermates either overexpressing cardiac β_1 -adrenoceptors (β_1 -tg) or lacking $G\alpha_2$ ($G\alpha_2^{-/-}$). At 300 days of age mortality of mice only lacking $G\alpha_2$ was higher compared to wild-type or β_1 -tg, but similar to β_1 -tg/ $G\alpha_2^{-/-}$ mice. Beyond 300 days mortality of β_1 -tg/ $G\alpha_2^{-/-}$ mice was enhanced compared to all other genotypes (mean survival time: 363±21 days). Echocardiography revealed similar cardiac function of wild-type, β_1 -tg and $G\alpha_2^{-/-}$ mice, but significant impairment for β_1 -tg/ $G\alpha_2^{-/-}$ mice (e.g. ejection fraction 14±2% versus 40±4% in wild-type mice). Significantly increased ventricle- to body-weight ratio (0.71±0.06% versus 0.48±0.02% in wild types), left-ventricular size (length 0.82±0.04 cm versus 0.66±0.03 cm in wild types) and ANP and BNP expression (mRNA: 2819% and 495% of wild type, respectively) clearly indicated hypertrophy. $G\alpha_3$ was significantly upregulated in $G\alpha_2$ -knockouts (protein compared to wild-type mice: 340±90% in $G\alpha_2^{-/-}$ and 394±80% in β_1 -tg/ $G\alpha_2^{-/-}$, respectively). Radioligand binding experiments confirmed cardiac overexpression of β_1 -adrenoceptors in β_1 -tg mice. Of note, overexpression levels differed depending on the particular wild-type background. On an FVB/N background we found the overexpression level to be more than 2-fold higher (B_{max} : 1425 ± 68 fmol/mg) than on the otherwise used C57BL/6 background. Accordingly, FVB/N-based β_1 -tg mice showed a significantly impaired cardiac function at an age of 300d while C57BL/6-based β_1 -tg mice did not.

Conclusions: $G\alpha_2$ -deficiency combined with cardiac β_1 -adrenoceptor overexpression strongly impaired survival and cardiac function. On a C57BL/6 background β_1 -adrenoceptor overexpression alone had not induced cardiac hypertrophy or dysfunction at Day 300 while there was overt cardiomyopathy in mice additionally lacking $G\alpha_2$. We propose an enhanced effect of increased β_1 -adrenergic drive by lack of protection via $G\alpha_2$. The observed $G\alpha_3$ upregulation was not sufficient to compensate for $G\alpha_2$ deficiency suggesting an isoform-specific and/or a concentration-dependent mechanism. The role of $G\alpha_3$ is currently addressed in a subsequent study using β_1 -tg and $G\alpha_3$ -deficient mice.

009

Induction of the inducible cAMP early repressor (ICER) provides protection against cardiac remodeling after beta-adrenergic stimulation in mice

M. D. Seidl¹, A. Sternberg¹, K. Grimm¹, B. Fels¹, F. T. Stümpel¹, N. Kojima², S. Endo³, F. U. Müller¹

¹Westfälische Wilhelms-Universität, Institut für Pharmakologie und Toxikologie, Münster, Germany

²Tokyo Metropolitan Geriatric Hospital, Institute of Gerontology, Tokio, Japan

³Gunma University, Medical School, Maebashi, Japan

Heart failure is accompanied by morphological and functional alterations (e.g. hypertrophy, decreased contractility) which are summarized by the term „cardiac remodeling“. While the β -adrenergic signaling pathway is essential for short-term modulation of cardiac performance, its chronic stimulation by elevated plasma catecholamines and the subsequent activation of cAMP-dependent signal transduction pathways is regarded as a fundamental factor in the pathogenesis of cardiac remodeling. However, the mechanisms mediating the transition of physiological conditions of short-term to detrimental remodeling under long-term β -adrenergic stimulation are not understood in detail so far. In this context, ICER, an isoform of the cAMP dependent transcription factor CREM (cAMP responsive element modulator), acts as an early response gene strongly induced by beta-adrenergic stimulation via cAMP responsive elements (CRE) in its promoter. Contrary to its CRE-mediated induction, ICER is a strong inhibitor of CRE-mediated transcription by itself. Here we study the role of ICER induction in the catecholamine-induced cardiac remodeling in a time dependent manner by the use of ICER deficient mice (IKO) and wild type (WT)

controls, which were treated with isoproterenol (ISO; 10 mg/kg per d) for 6 and 24 hours and 7 days.

Overall 7 days of ISO stimulation resulted in an elevation of cardiomyocyte length in IKO (in μ m; 7d ISO 156±1) vs. WT cardiomyocytes (7d ISO 143±2). At this time point a 29 % decrease of cardiac output and a 16 % decrease of the maximal rate of rise of left ventricular pressure (dp/dt_{max}) in IKO vs. WT animals was detectable. The maximum increase of *Icer* mRNA in WT cardiomyocytes already occurred after 6 h (75-fold), and declined after 24 h (29-fold) to 2.5 fold increase after 7 days, while *Icer* mRNA was not detectable in IKO mice. This raised the hypothesis, that the early induction of ICER modulates transcriptional processes after beta-adrenergic-stimulation, involved in cardiac remodeling of the heart. Profiling of mRNA expression levels between IKO vs. WT cardiomyocytes at the different time points revealed: 55 regulated genes (up-regulated: 45 %) in untreated; 103 altered genes (up 35 %) after 6h; 1437 changed genes (up 97%) after 24 h and 131 altered genes (up 19%) after 7 days of ISO treatment.

In summary, the absence of ICER induction in myocytes resulted in an increase of cardiomyocytes length and a decrease of heart performance after 7 days of beta-adrenergic stimulation. This is preceded by upregulated mRNA levels of several hundred genes at 24 h, which is going along with the induction of transcriptional inhibitor ICER after a few hours of beta-adrenergic stimulation. This suggested a protective role of ICER by inhibiting the progression of cardiac remodeling after beta-adrenergic stimulation in an early responsive manner. (Supported by the DFG)

010

M3 muscarinic receptors limit pacemaker potential during early cardiogenesis

M. Burczyk¹, T. Casar Tena¹, M. Burkhalter¹, S. Matysik¹, S. Wiese², M. Forster¹, M. Rothe^{1,2}, M. Kühn¹, M. Philipp¹

¹Ulm University, Biochemistry and Molecular Biology, Ulm, Germany

²Ulm University, Core Unit Mass Spectrometry and Proteomics, Medical Faculty, Ulm, Germany

The performance of the adult heart is tightly regulated by G protein-coupled receptors. Adrenergic and Angiotensin receptors efficiently control heart rate and contractility. Muscarinic receptors, on the other hand serve as master regulators of the conduction system, which is often lost upon myocardial infarction. This function of muscarinic receptors has been well described in the adult or late embryonic heart. Here we provide evidence that muscarinic receptors are crucial to constrain pacemaker cell identity.

We applied subtype-specific inhibitors of muscarinic receptors to zebrafish embryos of different stages. We observed that both, early cardiac function as well as specification are specifically regulated by muscarinic M3 receptors, while M2 receptors appear to exert a heart-specific function only at later stages. Continuous M3 blockage renders zebrafish with greatly altered cardiac morphology, particularly of the conduction system. Furthermore, embryos with M3 inhibition display impaired ventricular function most likely due to an AV-block and substantial arrhythmia in the atrium. Importantly, to observe these phenotypes it was sufficient to block M3 receptors during stages of cardiac differentiation, which is long before a heart tube has formed. We corroborated our findings regarding these morphological changes using marker gene analysis. Furthermore, we obtained evidence for M3 receptors preventing a transcriptional program towards the induction of pacemaker cells at the expense of AV canal cells. Importantly, this is not only true during heart development. A pacemaker program is also induced in adult hearts upon M3 inhibition. Taken together, we postulate that muscarinic M3 receptors confine a pacemaker lineage during early steps of heart development as well as in the adult heart. Our data suggests M3 receptors as potential new therapeutic targets for the regeneration of hearts with an injured sinoatrial node.

011

Viral vector-based targeting miR-21 in cardiac non-myocyte cells reduces pathologic remodeling of the heart

D. P. Ramanujam¹, Y. Sassi¹, B. Lagerbauer¹, S. Engelhardt^{1,2}

¹Institut für Pharmakologie und Toxikologie, München, Germany

²DZHK (German Center for Cardiovascular Research), partner site Munich Heart Alliance, München, Germany

Systemic inhibition of miR-21 has proved effective against fibrosis of the myocardium and in other organs. MiR-21 has been reported to exert detrimental effects in cardiac fibroblasts and protective roles in cardiac myocytes and other myocardial cell types. A better definition of the cell types that contribute to the beneficial effects of inhibiting miR-21 in vivo may aid the development of strategies with enhanced therapeutic efficacy. Thus far, no approach to selectively manipulate microRNAs in the non-myocyte population of cardiac cells in vivo has been available. In this study, we developed an iCre-encoding MMLV virus for application in miR-21^{fl/fl} mice. Delivery of this vector to neonates achieved targeted genetic ablation of miR-21 in non-myocyte cardiac cells. Immunohistochemistry and flow cytometry confirmed that MMLV was highly selective and effective for cardiac fibroblasts and endothelial cells. In parallel, an AAV9-iCre vector allowed for specific and almost complete deletion of miR-21 in cardiac myocytes. When tested in a model for chronic left ventricular pressure overload, MMLV-iCre-mediated deletion of miR-21 in cardiac fibroblasts and endothelial cells significantly reduced cardiac fibrosis and hypertrophy and improved cardiac function. The benefit of this cell-type-specific inhibition exceeded that observed upon global genetic deletion of the miR-21 gene in mice. AAV9-mediated deletion of miR-21, albeit lowering cardiac hypertrophy, had no effect on fibrosis or cardiac function. Taken together, neonatal delivery of engineered iCre-encoding viruses enabled for the first time a differential gene targeting in non-myocyte and myocyte cells in myocardium. Non-myocyte deletion of miR-21 demonstrated that miR-21 exerts its cardiac profibrotic activity directly in cardiac fibroblasts and in endothelial cells. This novel finding should encourage tailoring of anti-miR-21 therapy towards cellular tropism.

012

Impact of DPP10 on native cardiac I_{to} and action potential in rat epicardial myocytesK. Metzner¹, M. Schaefer¹, S. Kämmerer¹¹University of Leipzig, Rudolf-Boehm-Institute of Pharmacology and Toxikology, Leipzig, Germany

The transient outward potassium current (I_{to}) underlies the early repolarization phase of cardiac action potentials. In patients with heart failure, I_{to} is dramatically reduced due to the down-regulation of the channel subunits Kv4.3 and KChIP2. In contrast, the transmembrane β subunit dipeptidylpeptidase-like protein 10 (DPP10) is up-regulated. The role of this β subunit in cardiomyocytes is still unknown, but the interaction with Kv4.3/KChIP2 channels is well characterized in CHO cells. Co-expression of DPP10 results in higher current amplitudes, acceleration of activation and inactivation and a shift in voltage dependence to more negative values. Here, we have studied whether DPP10 overexpression in rat myocytes exerts similar effects on native cardiac I_{to} . To this end, epicardial myocytes were obtained from adult Wistar rats. Isolated cells were infected with an adenovirus encoding DPP10 and GFP. Control cells were infected with an adenovirus encoding GFP. The cardiomyocytes were cultured for 48 h. Peak and late K^+ currents as well as action potentials were measured at 23°C using the whole-cell patch clamp technique. The peak K^+ current density in cells expressing DPP10 was not increased compared to control cells, but DPP10 significantly increased the late current component. DPP10 overexpression resulted in a faster inactivation and recovery from inactivation. Thus, DPP10 modulates native cardiac I_{to} with respect to the current amplitudes and kinetic properties, in a similar manner as in the heterologous expression system. In addition, DPP10 also affected the rat ventricular action potential (AP) compared to control cells. A significant reduction of the AP amplitude, an acceleration of the upstroke velocity as well as a slowing of the AP duration at 20% and 50% repolarization (APD_{20} , APD_{50}) could be observed in cells expressing DPP10. The influence of DPP10 overexpression on the upstroke component of the AP depolarization in rat cardiomyocytes cannot be explained only by DPP10-dependent modulation of Kv4-bearing channel complexes. This result might indicate a DPP10 interaction with other cardiac ion channels. Ongoing work will focus on the interaction of DPP10 with the voltage-gated sodium channel (Nav1.5) in cardiomyocytes and in expression systems.

Immunology – inflammation – cancer

013

First insights into the action of the carbazole derivative C81 and the role of its primary target BMP2K in the activated vascular endotheliumI. Bischoff¹, B. Dai², B. Ströde³, S. Knapp^{4,5}, F. Bracher³, R. Fürst⁶¹Goethe-University Frankfurt, Germany, Institute of Pharmaceutical Biology, Frankfurt am Main, Germany²University of Munich, Germany, Pharmaceutical Biology, Center for Drug Research, Munich, Germany³University of Munich, Germany, Department of Pharmacy – Center for Drug Research, Munich, Germany⁴Goethe-University Frankfurt, Germany, Institute for Pharmaceutical Chemistry, Frankfurt am Main, Germany⁵University of Oxford, UK, Nuffield Department of Clinical Medicine, Oxford, United Kingdom⁶Goethe-Universität Frankfurt, Institut für Pharmazeutische Biologie, Frankfurt am Main, Germany

Chronic inflammatory diseases, such as psoriasis or rheumatoid arthritis, are characterized by constant leukocyte infiltration and ongoing angiogenesis in the inflamed tissue. As current anti-inflammatory pharmacotherapy is not always satisfying, there is a great demand for the discovery of new drug leads as well as novel drug targets. The synthetic carbazole alkaloid derivative C81 acts as a multikinase inhibitor. Results of a thermal shift assay revealed that C81 shows by far the highest binding affinity to the BMP-2-inducible kinase (BMP2K/BIKE). BMP2K represents an as yet largely uncharacterized protein, which is not regulated by BMP-2 in endothelial cells. Therefore, we aimed to analyze (i) the pharmacological potential of C81 and (ii) the role of BMP2K in angiogenic and inflammatory processes in the vascular endothelium.

Initial experiments show that only high concentrations of C81 affected the viability of human umbilical vein endothelial cells (HUVECs). Both C81 and the knock-down of BMP2K (RNAi) reduced the migratory capacity of a human microvascular endothelial cell line (HMEC-1). Also the proliferation of HMEC-1 was reduced by C81 treatment (IC_{50} : 7 μ M). A tube formation assay on Matrigel demonstrated that C81 significantly impaired the formation of capillary-like structures in a dose-dependent manner. Interestingly, the analysis (Western blot) of signaling molecules in HUVECs that play a crucial role in cell proliferation (e.g. ERK, Akt) revealed that these pathways are not influenced, neither by C81 treatment nor by BMP2K gene silencing. In regard to inflammatory processes, C81 treatment or BMP2K silencing of HUVECs decreased the adhesion of THP-1 cells, a monocytic cell line, onto the activated endothelial cells. As the interaction of leukocytes is mainly mediated by cell adhesion molecules (CAMs), the effect of C81 or BMP2K silencing on their expression was analyzed (flow cytometry, qPCR). While the expression of CAMs was strongly decreased after C81 treatment, the knock-down of BMP2K did not markedly affect their expression. Furthermore, both approaches did not lead to the reduction of TNF-induced I κ B α degradation (Western blot) or p65 translocation into the nucleus (microscopy).

Our study provides first insights into the anti-inflammatory and anti-angiogenic potential of the carbazole alkaloid derivative C81 *in vitro*. The precise role of BMP2K in angiogenic and inflammatory endothelial processes as well as the involved pathways during BMP2K silencing and C81 treatment will be further elucidated. Moreover, since the inhibition of BMP2K seems not to be responsible for all actions of C81, we will investigate the role of other kinases affected by the compound in these processes.

014

The chemokine receptor CXCR4 agonist CTCE-0214D exerts protective effects in endotoxemia *in vivo*S. Seemann¹, A. Lupp¹¹Institute of Pharmacology and Toxicology, Jena University Hospital, Jena, Germany, Jena, Germany

The chemokine receptor CXCR4 is a multifunctional receptor which is activated by its natural ligand C-X-C motif chemokine 12 (CXCL12). CXCR4 seems to be part of the lipopolysaccharide sensing complex, suggesting that an intervention with CXCR4 agonists or antagonists could result in reduced TLR4 signaling. However, the role of CXCR4 and the influence of different CXCR4 ligands in acute as well as chronic inflammatory diseases are still contradictory.

Therefore, we aimed to characterize the systemic effects of CXCR4 activation in severe systemic inflammation and to evaluate its impact on endotoxin induced organ damages by applying a sublethal LPS dose (5 mg/body weight) in mice.

The plasma stable CXCL12 analog CTCE-0214D was synthesized and administered subcutaneously shortly before LPS treatment to ensure a delayed release and thereby a prolonged effect of the drug. 24 hours following LPS administration, mice were sacrificed and blood was obtained for TNF alpha, IFN gamma and blood glucose evaluation. Additionally, histopathological changes and oxidative stress in the liver and spleen were assessed and liver biotransformation capacity was determined. Finally, CXCR4, CXCL12 and TLR4 expression patterns in liver, spleen and thymus tissue as well as the presence of different markers for oxidative stress and apoptosis were evaluated by means of immunohistochemistry.

CTCE-0214D improved the health status and distinctly reduced the LPS mediated effects on TNF alpha, IFN gamma and blood glucose levels by approximately 35%, 50% or 70%, respectively. It attenuated oxidative stress in the liver and spleen tissue and enhanced liver biotransformation capacity unambiguously. CTCE-0214D diminished the LPS induced expression of CXCR4, CXCL12, TLR4, NF- κ B, cleaved caspase-3 and gp91 phox, whereas heme oxygenase 1 expression and activity were induced above average. Furthermore, TUNEL staining revealed anti-apoptotic effects of CTCE-0214D in all organs.

The CXCR4 is undoubtedly involved in inflammation. Its activation was accompanied by anti-inflammatory, anti-oxidative and cytoprotective effects as CTCE-0214D attenuated TLR4 signaling, induced heme oxygenase 1 activity and mitigated apoptosis. Thus, the administration of CXCL12 analogs seems to be a promising treatment option to control acute systemic inflammation, especially when accompanied by a hepatic dysfunction and an excessive production of free radicals.

015

No evidence for a role of the histamine H_4 -receptor in chronic DSS induced colitisB. Schirmer¹, T. Rezniczek¹, R. Seifert¹, D. Neumann¹¹Hannover Medical School, Institut of Pharmacology, Hannover, Germany

In intestinal samples of inflammatory bowel diseases (IBD) from patients as well as from animal models, histamine is found in rather high concentrations. Dextran sulfate sodium (DSS)-induced colitis is a well-established mouse model of IBD. Antagonists of the histamine H_4 -receptor (H_4R) as well as genetic deletion of the H_4R significantly reduce symptoms of acute DSS-induced colitis in mice. In the present study we aimed at analyzing a possible role of the H_4R in the model of chronic DSS-induced colitis in mice. Chronic colitis was induced in BALB/cJ mice, either wild-type or genetically H_4R -deficient ($H_4R^{-/-}$), by 4 cycles of feeding water supplemented with 2 % [w/v] DSS for 7 days. The DSS-cycles were separated by periods of 10 days with pure water alimentation. Control mice always received water without supplementation. Body weights of the mice were recorded every day. One day after termination of the last DSS-cycle mice were sacrificed and sera, caeca, colons, and mesenteric lymph nodes were prepared. Caeca and colons were histologically analyzed. Sera and supernatants of *in vitro* α CD3-stimulated lymph node cells were analyzed for cytokine expression. DSS-feeding induced a dramatic weight loss in wild-type mice, which recovered in the water-only interim periods. In H_4R -deficient mice weight loss and gain was very similar to that in wild-type mice. In chronic colitis, colonic inflammation as detected by histologic analyses was lower as compared to that observed in the acute colitis model. Moreover, no differences between wild type and $H_4R^{-/-}$ mice were observed. Similarly, concentrations of IL-6, IL-10, and MIP-2 in sera and in supernatants of *in vitro* α CD3-stimulated lymph node cells were lower than that observed in the acute model, and without differences between control and DSS-fed wild-type and H_4R -deficient mice. We conclude that the H_4R , which is involved in the regulation of acute DSS-induced colonic inflammation, has no impact on the pathogenesis of the chronic DSS-induced colitis model in Balb/c mice.

016

Epac1 and Epac2 regulate airway smooth muscle tone in miceM. Schmidt¹, A. Oldenburger¹¹University of Groningen, Groningen, Niederlande

Rationale: Dysfunctional regulation of airway smooth muscle (ASM) tone is a feature of obstructive airway diseases such as asthma and chronic obstructive pulmonary disease. cAMP-elevating agents, such as β_2 -adrenoceptor agonists, are potent inhibitors of bronchial constriction. Although used clinically for many years, their precise mechanism of action is still under debate. Activation of protein kinase A (PKA) by β_2 -agonists induces ASM relaxation. Next to PKA, activation of the exchange protein directly activated by cAMP (Epac) induces ASM relaxation. We have recently shown that Epac1 and Epac2 are differentially involved in inflammatory and remodeling processes *in vivo*. Here, we studied the roles of Epac1 and Epac2 in regulating ASM tone.

Methods: To this aim, the effects of the β -agonist isoprenaline, the specific Epac activator's 8-pCPT-2-O-Me-cAMP (8-pCPT) or Sp-8-pCPT-2-O-Me-cAMPS (Sp-8-pCPT) on methacholine (1 μ M)-induced tone were studied in mice open ring preparations, in the absence and presence of specific inhibitors of PKA (Rp-8-CPT-cAMPS (Rp, 100

μ M), Epac1 (CE3F4) or Epac2 (ESI-05). C57Bl/6J wild type animals, Epac1^{-/-} and Epac2^{-/-} were used for all experiments (1).

Results and conclusion: In precontracted rings, isoprenaline dose-dependently reduced methacholine-induced ASM tone by approximately 80 % (pD₂-value 7.58±0.22), both effects were reduced but not diminished by the PKA inhibitor Rp, pointing to PKA-independent mechanisms (E_{max} 63.4±3.5; pD₂-value 7.34±0.13). 8-pCPT and Sp-8-pCPT dose-dependently reduced methacholine-induced ASM tone (pEC₅₀=4.22±0.12 and 4.30±0.10, respectively). The reduction was 25.2±3.0% and 46.0±1.8% for the highest dose used (300 μ M). The effects of the Epac activator^s were unaffected by Rp. Isoprenaline-induced relaxation was not altered in Epac1^{-/-} or Epac2^{-/-} mice. The effects of 8-pCPT were reduced in Epac deficient mice, although to a smaller extent in Epac1^{-/-}. Pharmacological inhibition of Epac1 – to a lesser extent of Epac2 – dose-dependently increased isoprenaline-induced relaxation, effects blunted in Epac deficient mice, confirming the specificity of the Epac inhibitors. Collectively, these data show that Epac1 and Epac2 regulate airway smooth muscle tone in mice by currently unknown mechanisms.

This study was financially supported by the Dutch Lung Foundation (3.2.09.34). (1) Oldenburger et al., FASEB J, 28, 4617-4628.

017

Targeting of the mRNA-binding protein HuR as a putative approach for sensitizing colon carcinoma cells towards anticancer therapies

A. I. M. Badawi^{1,2}, A. Biyane^{1,2}, T. Schmid³, J. Pfeilschifter^{1,4}, W. Eberhardt^{1,4}

¹pharmazentrum frankfurt/ZAFES, pharmakologie, Frankfurt, Germany

²Goethe Universität, Frankfurt, Germany

³Biochemistry II, Frankfurt, Germany

⁴, Germany

Objectives: We have previously shown that HuR knockdown can sensitize colon carcinoma cells to intrinsic apoptotic pathway by increasing translation of the pro-apoptotic caspase-2L. Here, we tested whether HuR knockdown similarly would sensitize colon carcinoma cells towards the established chemotherapeutic drugs Doxorubicin and Paclitaxel. Furthermore, we investigated whether these drugs could modulate different HuR activities.

Results: By using Western blot analysis for cleaved caspase 3 and PARP, we found that siRNA-mediated HuR knockdown sensitizes colon carcinoma cells (DLD-1, RKO) toward doxorubicin or paclitaxel induced apoptosis. By further monitoring apoptosis by measuring sub-G₁ phases and Annexin V-PI staining by FACS, we could demonstrate a clear sensitizing effect after HuR knockdown. The critical role of Caspase-2L in this sensitizing approach was confirmed by double knockdown of HuR plus Caspase-2L which fully rescued the apoptosis sensitizing effect by the HuR knockdown. We furthermore demonstrate that Doxorubicin and Paclitaxel both increased cytoplasmic HuR abundance as shown by Western blot and confocal microscopy, respectively. Using RNA-electrophoretic mobility shift assay (EMSA) we furthermore demonstrate that the increase in cytoplasmic HuR is accompanied by an increased HuR binding to the 3' untranslated region (UTR) of cyclooxygenase-2. A drug-induced increase in HuR binding to the 5' UTR of Caspase-2L was further shown by the use of biotin-pull down assay.

Conclusion: Collectively, our data implicate that transient depletion of HuR sensitizes colon carcinoma cells towards chemotherapeutic drug-induced apoptosis mainly through an upregulation of caspase-2L. Inhibition of HuR illuminates a novel therapeutic option for increasing the efficacy of current chemotherapeutic drugs.

018

The novel MKL target gene MYOF (myoferlin) modulates expansion and senescence of hepatocellular carcinoma

C. Hermans¹, V. Hampf¹, A. Aigner², S. Singer³, A. Thavamani⁴, A. Nordheim⁴, T. Gudermann¹, S. Mühlich¹

¹Ludwig-Maximilians-Universität München, Walther-Straub-Institut für Pharmakologie und Toxikologie, München, Germany

²Universität Leipzig, Rudolf Boehm Institut für Pharmakologie und Toxikologie, Leipzig, Germany

³Universitätsklinikum Heidelberg, Molekulare Hepatopathologie, Heidelberg, Germany

⁴Universität Tübingen, Abteilung Molekularbiologie, Tübingen, Germany

Background & Aims: Megakaryoblastic Leukemia 1 and 2 (MKL1/2) are coactivators of the transcription factor Serum Response Factor (SRF) with an essential role in hepatocellular carcinoma (HCC). We recently showed that depletion of MKL1 and 2 abolished HCC xenograft expansion, associated with oncogene-induced senescence. Our aims were to identify a MKL target gene impacting on HCC growth and senescence.

Methods: We performed gene expression profiling in HCC cells depleted of MKL1 and 2 and verified target genes *in vivo* in HCC xenografts. Out of the newly identified candidate genes, myoferlin (MYOF) was further characterized as a novel MKL- and SRF-dependent target gene by ChIP- and reporter gene assays using MYOF promoter deletion constructs. MYOF expression was determined by immunohistochemical staining of a tissue microarray containing 101 human HCCs and 16 non-tumorous liver samples. Furthermore, MYOF expression was analyzed in murine HCCs triggered by conditional activation of constitutively active SRF-VP16.

Results: This approach revealed MYOF (myoferlin) required for HCC cell proliferation and anchorage-independent cell growth. Consistently, myoferlin was strongly upregulated in human HCCs and in murine HCCs triggered by conditional activation of constitutively active SRF-VP16. Myoferlin plays a critical role in controlling levels of phosphorylated EGFR in HCC cells. Herein, we show that depletion of MKL1 and 2 promotes elevation of phosphorylated EGFR by downregulating myoferlin expression. Reduced myoferlin expression activates downstream MAPK and p16/Rb pathways, thereby contributing to oncogene-induced senescence.

Conclusion: We identify myoferlin as a novel regulator of the balance between proliferation and senescence of HCC cells. Myoferlin represents a mechanistic link between MKL1/2 depletion and oncogene-induced senescence. These findings highlight MKL1/2 and myoferlin as novel therapeutic targets to treat human HCC by a senescence-inducing strategy.

Individualized therapy and clinical implications

019

Characterizing the expression and interindividual variability of human breast cancer resistance protein (BCRP/ABCG2) in renal cell carcinoma

A. Reustle^{1,2}, O. Renner^{1,2}, S. Kruck³, S. Rausch³, A. T. Nies^{1,2}, J. Hennenlotter³, F. Fend¹, J. Bedke³, M. Schwab^{2,5}, E. Schaeffeler^{1,2}

¹Dr. Margarete Fischer-Bosch-Institute of Clinical Pharmacology, Stuttgart, Germany

²University of Tuebingen, Tuebingen, Germany

³University Hospital Tuebingen, Department of Urology, Tuebingen, Germany

⁴University Hospital Tuebingen, Institute of Pathology and Neuropathology, Tuebingen, Germany

⁵University Hospital Tuebingen, Department of Clinical Pharmacology, Tuebingen, Germany

Background: Breast cancer resistance protein (BCRP/ABCG2), an efflux transporter expressed at the apical membrane of proximal tubules in the kidney, is altered in different tumor entities and involved in multidrug resistance to anti-tumor agents. The impact of BCRP expression on clear cell renal cell carcinoma (ccRCC), the most common pathological type of renal carcinomas and the main cause of renal cancer mortality, is still unknown.

Methods: Data of a ccRCC cohort from The Cancer Genome Atlas (TCGA) were analyzed concerning ABCG2 mRNA expression (n=463), DNA methylation (n=288) and somatic variations (n=410). In an independent cohort of 64 ccRCC and corresponding non-tumor tissues, ABCG2 mRNA and protein expression were quantified using Real-Time PCR and immunohistochemical staining of tissue microarrays, respectively. MALDI-TOF mass spectrometry served to genotype a total of 31 variants in the ABCG2 gene region and micro RNA expression was measured using Affymetrics GeneChip technology.

Results: In the TCGA cohort mRNA expression was significantly upregulated in ccRCC compared to normal kidney tissue (P=6.9e⁻⁷). Methylation of the investigated CpG sites was not different in tumor and non-tumor tissue and did not correlate with mRNA expression. Somatic alterations in the ABCG2 gene locus were detected in only a small number of patients. Notably, ABCG2 mRNA expression correlated significantly negative with tumor stage (P=1.2e⁻¹¹), grading (P=1.3e⁻¹⁵), metastasis occurrence (P=4.3e⁻⁶), and cancer-specific survival in Kaplan-Meier analysis (HR=0.22; 95%CI=0.15-0.32; P_{log-rank}=4.5e⁻¹⁴). The data from the second cohort corroborated these findings. Concerning ABCG2 protein, expression was decisively reduced in tumor samples (P<0.0001) and again negatively associated with clinicopathological parameters. However there was no correlation between mRNA and protein expression. Univariate analyses indicate that ABCG2 expression is affected by genetic variants, e.g. rs2725256 was weakly associated with diminished protein expression in ccRCC (P=0.03). Expression of several miRNAs correlated with reduced ABCG2 protein abundance, including mir-145 and mir-212 which have previously been shown to be implicated in ABCG2 regulation.

Conclusions: ABCG2 mRNA expression is induced in ccRCC compared to normal kidney tissue, whereas protein expression is decreased. Lack of correlation between ABCG2 mRNA and protein expression in ccRCC indicates post-transcriptional and post-translational regulation possibly involving genetic variants and miRNAs among other genetic, epigenetic and regulatory factors. Importantly, both ABCG2 mRNA and protein expression are negatively associated with cancer progression and higher expression is found in patients with better survival rates.

020

The novel hepatitis B virus (HBV) entry inhibitor myrcludex B and the nucleotide analogue tenofovir: assessment of a potential drug-drug interaction and elevated plasma bile acids under therapy.

A. Eidan^{1,2}, M. Haag^{3,4,5}, N. Hohmann¹, J. Burhenne¹, L. Witt¹, M. Meyer^{1,6}, M. Schwab^{3,5}, S. Urban^{7,2}, A. Alexandrov⁸, G. Mikus¹, W. E. Haefeli^{1,2}, A. Blank^{1,2}

¹Universitätsklinikum Heidelberg, Klinische Pharmakologie und Pharmakoepidemiologie, Heidelberg, Germany

²Deutsches Zentrum für Infektionsforschung (DZIF), Standort Heidelberg, Heidelberg, Germany

³Dr. Margarete Fischer-Bosch-Institut für Klinische Pharmakologie (IKP), Stuttgart, Germany

⁴Deutsches Zentrum für Infektionsforschung (DZIF), Standort Tübingen, Tübingen, Germany

⁵Universitätsklinikum Tübingen, Klinische Pharmakologie, Tübingen, Germany

⁶Universität des Saarlandes, Experimentelle und Klinische Pharmakologie und Toxikologie, Homburg, Germany

⁷Universitätsklinikum Heidelberg, Molekulare Virologie, Heidelberg, Germany

⁸MYR GmbH, Bad Homburg, Germany

Introduction: A combination therapy of a reverse transcriptase inhibitor (tenofovir) and a HBV entry inhibitor (myrcludex B) may improve therapeutic options for patients with chronic hepatitis B. Myrcludex B binds to hepatic Na-taurocholate cotransporting polypeptide (NTCP), thus preventing the uptake of HBV into hepatocytes. Besides facilitating HBV entry, NTCP also mediates the reuptake of circulating bile acids from the portal blood into the liver. In previous trials, myrcludex B increased plasma bile acid levels, but its impact on individual bile acid kinetics has not been examined. Bile acids inhibit the activity of organic anion transporter 3 in the kidney, of which tenofovir is a substrate. We therefore assessed whether renal tenofovir secretion is reduced by myrcludex B.

Methods: In a prospective, controlled, monocenter, open label, one sequence phase I trial, 12 healthy volunteers received 245 mg of tenofovir disoproxil for 5 days alone followed by 6 days of daily subcutaneous co-administration of 10 mg myrcludex B. Plasma samples were collected to evaluate the influence of myrcludex B on tenofovir pharmacokinetics and plasma bile acid kinetics. Food intake as a physiological confounder of plasma bile acid levels was regulated.

Results: Myrcludex B co-administration did not have a significant effect on tenofovir steady-state pharmacokinetics. Geometric means of the tenofovir area under the concentration-time curve (AUC) over 24 hours without and with myrcludex B were 2198

and 2076 h*ng/ml and 245.7 and 210.0 ng/ml for the tenofovir peak plasma concentration (C_{max}), respectively. Median time to reach C_{max} was 1.75 h during tenofovir monotherapy and 2.0 during combination therapy. The 90% confidence interval of the tenofovir AUC ratio stayed within the standard bioequivalence boundaries of 0.8-1.25 (0.85-1.05, point estimate 0.94), whereas the lower limit of C_{max} ratio extended below this range (0.71-1.03, point estimate 0.85). Total plasma bile acid exposure increased by 1300 % after myrcludex B single dose and by 1800 % after repeated myrcludex B administration, mainly due to conjugated hypercholelomia. With the exception of one asymptomatic grade three increase in lipase levels, only mild and transient treatment-related adverse events occurred.

Conclusions: Co-administration of tenofovir with myrcludex B was well tolerated and did not show any clinically relevant changes in tenofovir pharmacokinetics. Whether plasma bile acid concentrations might serve as a surrogate marker for the pharmacological effect of myrcludex B should now be addressed in clinical trials.

021

Impact of CYP2D6 genotype and co-medication with paroxetine and clarithromycin on clomiphene metabolism *in vivo*

T. Mürdter¹, T. Lehr², S. Igel¹, P. Kröner¹, B. Ganchev¹, E. Schaeffeler¹, G. Böhmer³, M. Sonnenberg¹, H. Brauch¹, R. Kerb¹, M. Schwab^{1,3}

¹Dr. Margarete Fischer-Bosch-Institut für Klinische Pharmakologie und Universität Tübingen, Stuttgart, Germany

²Universität des Saarlandes, Klinische Pharmazie, Saarbrücken, Germany

³Universitätsklinikum Tübingen, Abteilung für Klinische Pharmakologie, Tübingen, Germany

Introduction: Clomiphene (CLOM) citrate as mixture of (*E*-) and (*Z*-) isomer (60:40) is the first line therapy for the treatment of female infertility. Treatment schedule includes dose escalation from 50 mg/d CLOM citrate to up to 150 mg/d in case of non-response. However, therapy outcome is variable and approximately 10 – 30% of patients do not benefit from CLOM treatment. CLOM is bioactivated via 4-hydroxylation of (*E*-)CLOM by the highly polymorphic cytochrome P450 (CYP) 2D6 leading to the active metabolite (*E*-)4-hydroxyclophene ((*E*-)4-OH-CLOM). CYP3A4 mediated de-alkylation and subsequent 4-hydroxylation via CYP2D6 results in the highly potent metabolite (*E*-)4-hydroxy-N-desethylclomiphene ((*E*-)4-OH-DE-CLOM). Therefore, activity of CYP2D6 and CYP3A4 may influence plasma concentrations of both active metabolites. Polymorphism in the CYP2D6 gene results in high variability of enzyme activity. Furthermore, CYP2D6 and CYP3A4 are subject to drug-drug interactions. Here, we investigated the influence of CYP2D6 and co-medication with inhibitors in a pharmacogenetic panel study.

Method: Twenty healthy female volunteers genotyped for CYP2D6 (6 poor metabolizers, PM; 6 intermediate metabolizers, IM; 5 extensive metabolizers, EM; 3 ultra-rapid metabolizers, UM) received either CLOM alone or in combination with the CYP3A4 inhibitor clarithromycin or the CYP2D6 inhibitor paroxetine. Plasma concentrations of CLOM and its metabolites were quantified by LC-MS/MS. Pharmacokinetic (PK) analysis was performed using non-compartmental (Phoenix®) and compartmental (NONMEM®) techniques.

Result: Whereas CYP2D6 genotype did not show any impact on the pharmacokinetics of (*Z*-)CLOM following a single dose of 100 mg CLOM citrate, C_{max} and AUC of (*E*-)CLOM significantly increased with decreasing CYP2D6 activity (ANOVA: p=0.006 and p<0.0001, respectively). A similar correlation was obvious for (*E*-)desethylclomiphene ((*E*-)DE-CLOM). However, such clear correlations were not observed for the 4-hydroxylated metabolites (*E*-)4-OH-CLOM and (*E*-)4-OH-DE-CLOM which showed the highest AUCs in the group of IM. The lack of a stringent gene-dose-effect for CYP2D6 and both active CLOM metabolites could be explained by including a CYP2D6-dependent subsequent metabolic step into the PK-model. Co-administration of clarithromycin led to an approximately two-fold increase in AUC of (*E*-)CLOM independent of CYP2D6 genotype pointing to a decreased clearance to (*E*-)DE-CLOM. In contrast, paroxetine co-medication diminished the differences between CYP2D6 genotypes: (*E*-)CLOM plasma concentrations in IM, EM, and UM were comparable to those observed in PMs independent of paroxetine administration and plasma levels of hydroxylated CLOM metabolites decreased. The inhibition of either of the primary metabolic steps resulted in a metabolic switch.

Conclusion: Genetically determined compromised CYP2D6 activity and co-administration of a CYP2D6 inhibitor led to a significantly lower formation of the active CLOM metabolites (*E*-)4-OH-CLOM and (*E*-)4-OH-DE-CLOM. Further studies including pharmacodynamics are necessary to investigate the clinical implications of our findings. Supported by the Robert Bosch Stiftung, Stuttgart, Germany.

022

Effects of OCT1 polymorphisms on pharmacokinetics and efficacy of tramadol used for postoperative analgesia

M. V. Tzvetkov¹, F. Musshoff¹, F. Stuber¹, J. Brockmüller¹, U. M. Stamer¹

¹Institut für Klinische Pharmakologie, Göttingen, Germany

Background: Tramadol is a synthetic opioid used in step II of pain treatment (according to the WHO's pain ladder classification). Tramadol is a pro-drug that is metabolized by CYP2D6 in the liver to the active metabolite O-desmethyltramadol. Recently we demonstrated that O-desmethyltramadol is a substrate of the hepatic organic cation transporter OCT1 and that common loss-of-function polymorphisms in OCT1 lead to a higher plasma concentration of O-desmethyltramadol and stronger opioidergic effects in healthy volunteers (1). Here we followed up on these findings by analyzing the effects of loss-of-function OCT1 polymorphisms on tramadol pharmacokinetics and efficacy in patients.

Methods: We analyzed a cohort of 181 surgical patients who received tramadol for postoperative pain treatment via patient-controlled analgesia device (PCA). OCT1 genotypes and genotype dependent CYP2D6 activity were determined (i.e. poor, intermediate, extensive and ultra-rapid metabolizers). Patients lacking CYP2D6 activity (poor metabolizer) were excluded from the analyses as they do not produce O-desmethyltramadol. Plasma concentrations of (+)O-desmethyltramadol were measured for three hours and cumulative tramadol consumption for 48 hours after surgery.

Results: We identified 89 patients who carried two, 76 who carried one and 16 who carried zero active OCT1 alleles. The average plasma concentrations of (+)O-desmethyltramadol were significantly higher in carriers of zero (AUC₀₋₃ of 99.3 ng*h/ml) compared to carriers of two active OCT1 alleles (AUC₀₋₃ of 71.7 ng*h/ml, P=0.03). Correspondingly and more importantly, the cumulative tramadol consumption was significantly lower in patients carrying zero compared to patients carrying two active OCT1 alleles (P)

Conclusions: Genetically-determined loss of OCT1 function results in increased plasma concentrations of (+)O-desmethyltramadol and reduced tramadol consumption in patients recovering from surgery. Therefore, loss of OCT1 activity is associated with better efficacy of tramadol in patients. Besides CYP2D6 UM, also extensive CYP2D6 metabolizers with additional loss-of-function OCT1 genotype may be at risk for tramadol related side effects.

(1) Tzvetkov, M.V., Saadatmand, A.R., Lotsch, J., Tegeder, I., Stingl, J.C. & Brockmoller, J. Genetically polymorphic OCT1: another piece in the puzzle of the variable pharmacokinetics and pharmacodynamics of the opioidergic drug tramadol. *Clinical pharmacology and therapeutics* 90, 143-50 (2011).

023

Microfluidic chip for chemosensitivity analysis of primary tumor material

M. Büttner¹, B. Büttner¹, K.-H. Feller¹, J. Wegener², S. Michaelis²

¹Ernst-Abbe-Hochschule Jena, FB Medizintechnik und Biotechnologie, Jena, Germany

²Universität Regensburg, Institut für Analytische Chemie, Chemo- & Biosensorik, Regensburg, Germany

Introduction: Oncology diseases are the main cause of mortality in developed countries. Therefore an important part of the personalized medicine is the immunohistochemical staining for identification of specific biomarker for an accurate prediction of cancer. The second part of cancer characterization is the analysis of individualized chemosensitivity [1]. This presentation will focus on the possibility of lab-on-chip-based chemosensitivity analysis of primary cancer cells (lung cancer) as an improvement of current methods, enabling a continuous measurement without need of labels.

Method: Short-term culture of primary cells from solid tumors has gained significant importance in personalized cancer therapy. The primary tumor cells were isolated in different steps from primary lung cancer tissue. We developed successfully a disaggregation process to cultivate lung tumor cells *in vitro*, see Figure 1. Furthermore this disaggregation process was optimized with a design of experiment (DoE) to obtain high cell yield and cell vitality. Therefore the input and output factors for this process were defined and in cooperation with the responsible hospital to discuss *in vitro* results with clinical correlations.

The chemosensitivity of the primary cancer cells is detected by label-free impedimetric measurement (electric cell-substrate impedance sensing, ECIS) [2]. ECIS is a continuous monitoring system for studying cell behaviors using a noninvasive, real-time, and label-free method.

Results: Moreover, a microfluidic platform was established to allow a convenient, sterile, and incubator-independent time-lapse microscopic observation of the primary cells with integrated ECIS measurement for cytotoxicity detection, see Figure 2. Cell growth was successfully achieved in this microfluidic setup and the cellular response to a cytotoxic substance could be followed in real-time, in a non-invasive and sensitive manner. This study paves the way for the development of micro-total analysis systems that combine microscopic and impedimetric readouts to enable a general quantitative characterization of changes in cell metabolism and morphology as a response to chemotherapeutic agents.

Conclusion: Finally, this cell-based microfluidic chip platform provides a usefully analytical tool for the personalized cancer analysis of lung cancer biopsies.

[1] A. Mitra, L. Mishra, and S. Li, "Technologies for deriving primary tumor cells for use in personalized cancer therapy," *Trends Biotechnol.*, vol. 31, pp. 347-54, Jun 2013.

[2] S. Arndt, J. Seebach, K. Psathaki, H. J. Galla, and J. Wegener, "Bioelectrical impedance assay to monitor changes in cell shape during apoptosis," *Biosens Bioelectron.*, vol. 19, pp. 583-94, Jan 15 2004.

Abb. 1

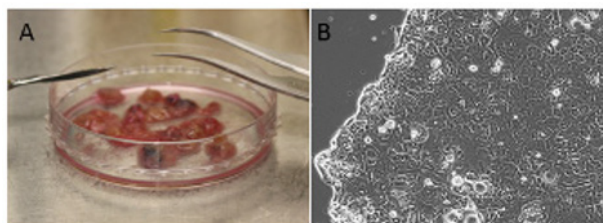
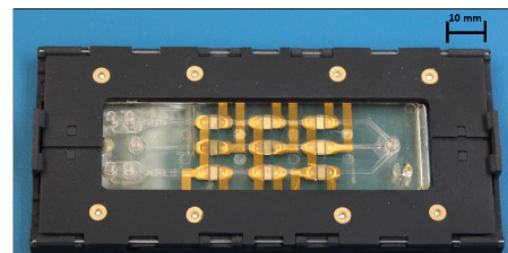


Abb. 2



In vitro systems and mechanistic investigations II

024

Discovery of early and late metabolic events in a new established frataxin knockout model

D. Poburski¹, J. Börner¹, M. Ristow², R. Thierbach¹
¹Institut für Ernährungswissenschaften, Humanernährung, Jena, Germany
²ETH Zürich, Energy Metabolism Laboratory, Zürich, Switzerland

The neurodegenerative disease Friedreich ataxia (FRDA) is caused by a GAA triplet repeat expansion in the first intron of the frataxin gene, which results in a reduction of the corresponding mitochondrial protein. Despite several cellular and animal models the exact function of frataxin is still a matter of debate, but the role of frataxin in iron sulfur cluster biosynthesis is generally accepted. However, we still don't know which primary metabolic events are caused by a frataxin deficit and until now, there is no therapeutic option available.

We developed a new cellular model for FRDA by using the cre/loxP recombination system in mouse embryonic fibroblasts (MEF). C57BL/6J mouse strains with a loxP flanked exon 4 of the frataxin gene and a tamoxifen-inducible cre-recombinase (CreER^{T2}) were crossed and several MEF cell lines isolated. After selection by genotype and growth manner the FX-MEF 2-1 (Fxn^{-/-}) and FX-MEF 2-8 (Fxn^{+/+}) cell lines were finally choosed. The generation of the homozygous or heterozygous frataxin knockout was successfully tested on RNA and protein level. Long maintenance of the frataxin depleted fibroblasts revealed a strong growth inhibition consistent to earlier observations in other cell systems. Therefore, we established a pattern of treatment over 12 days, with medium and substance changes at day 4 and 8, which allows us to get a fully functional knockout and overcome the growth inhibition problem. Endpoint measurements of known metabolic phenomena from mammalian and non-mammalian models were studied at day 12 of our novel cell system. The induced total disruption of frataxin leads to a clearly reduced aconitase activity, cell division and oxygen consumption as well as an increase in ROS production. In the heterozygous knockout with residual frataxin activity no such changes were observed. In addition, our pattern of treatment enables us to monitor the full and partial frataxin knockout in the course of time, to detect early and late metabolic events after frataxin disruption. Therefore we analysed the mentioned parameters (with additional ATP and iron content) in parallel at day 3, 5, 7 and 10 and could identify an initial event followed by secondary consequences and parameters, which seem to play only a minor role in the FRDA pathogenesis. On the contrary, a partial deficit of frataxin didn't result in any differences over time and suggests that there are only cellular alterations below a critical threshold. In conclusion, our new established mammalian cellular FRDA model mimics typical metabolic consequences of the human disease and seems to be qualified for FRDA research. The model shows for the first time six different metabolic events in the course of time in parallel and reveals insights into primary and secondary events of FRDA pathogenesis. These observations can be used to better understand the function of frataxin and can help to develop new therapeutic strategies to address the consequences of frataxin deficiency. Moreover, the transfer of this cell model into 96-well plates offers the possibility for a high-throughput screening of potential therapeutic substances.

025

Role of host cell factors during uptake of diphtheria toxin in human cells

L. Schnell¹, M. Schuster¹, H. Barth¹
¹Institut für Pharmakologie und Toxikologie, Toxikologie, Ulm, Germany

The disease diphtheria is caused by the diphtheria toxin (DT) which belongs to the group of single-chain AB-type bacterial protein toxins. Receptor-binding of the B-domain on the target cell surface is followed by receptor-mediated endocytosis and internalization into early endosomal vesicles. Endosomal acidification triggers membrane insertion and pore formation of the transmembrane (T) domain together with translocation of the (partially) unfolded catalytic (C) domain into the cytosol. Herein, DTA catalyzes ADP-ribosylation of elongation factor 2 which leads to disruption of protein synthesis and finally causes cell death [1]. In HeLa cells, these events are related to cell-rounding functioning as a specific endpoint to monitor the uptake of DTA into the cytosol of the host cell. As for other ADP-ribosylating toxins such as *C. botulinum* C2 toxin, *C. perfringens* iota toxin and *C. difficile* CDT, also in case of native DT we demonstrated the involvement of several host cell factors during the translocation step of the catalytic domain across the endosomal membrane [2,3]. In detail, we confirmed the involvement of the host cell chaperone Hsp90 and the thioredoxin reductase (TrxR), the latter presumably responsible for the reduction of the interchain disulfide bond between the DTA and DTB moieties [4,5,6]. Furthermore, we identified another group of protein folding helpers, the family of peptidyl-prolyl *cis/trans* isomerases (PPIases) including cyclophilin A (CypA), Cyp40 and FK506-binding protein (FKBP)51 as required cytosolic factors for DTA translocation. To characterize the role of the protein folding helpers in more detail, we investigated their interaction with purified DTA *in vitro* by performing dot blot analysis with immobilized recombinant host cell factors, co-precipitation of cellular factors with DTA from HeLa lysate and isothermal titration calorimetry with purified proteins therewith determining the thermodynamic parameters of the individual binding events. Thereby, we detected binding of DTA to Hsp90, CypA, Cyp40, FKBP51 and FKBP52. The data increase the knowledge of the molecular mechanisms underlying DT uptake and especially DTA translocation which can be medically used to develop novel therapeutic strategies against the disease diphtheria.

- [1] Murphy (2011) *Toxins* 3, 294-308.
- [2] Barth (2011) *Naunyn-Schmied Arch Pharmacol* 383, 237-245.
- [3] Kaiser *et al.* (2012) *Cell. Microbiol.* 14, 1193-1205.
- [4] Dmochewicz *et al.* (2011) *Cell. Microbiol.* 13, 359-373.
- [5] Ratts *et al.* (2003) *J. Cell Biol.* 160, 1139-1150.
- [6] Schnell *et al.* (2015) *Toxicon* doi:10.1016/j.toxicon.2015.04.012.

026

Human α -defensin-1 protects cells from intoxication with *Clostridium difficile* toxins A, B and CDT

S. Fischer¹, K. Aktories², H. Barth¹
¹University of Ulm Medical Center, Pharmacology and Toxicology, Ulm, Germany
²University of Freiburg, Experimental and Clinical Pharmacology and Toxicology, Freiburg, Germany

Novel afflictions as for example *Clostridium* (*C.*) *difficile* associated diseases (CDAD) caused by *Clostridium difficile* are on the increase and challenging to treat. CDAD most frequent occur in hospitalized patients after prolonged treatment with antibiotics. CDAD includes among others diarrhea and the severe form of pseudomembranous colitis. Not only the treatment of the infection, but also the treatment of the toxins has a high clinical significance. *C. difficile* secretes the exotoxins A (TcdA) and B (TcdB), which glycosylate and thereby inactivate Rho-GTPases in mammalian cells. TcdA and TcdB are considered as the causative agents of CDAD. In the last few years, more and more hypervirulent strains of *C. difficile* were described. In these hypervirulent strains, the ADP-ribosyltransferase CDT was found as a third toxin in addition to TcdA and TcdB. Given the lack of agents effective against antibiotic-resistant bacterial strains and bacterial exotoxins, the development of novel pharmacological strategies is needed. The antimicrobial activity of naturally occurring substances is already known for a long time. One important mechanism of the innate immune system is the production of natural peptides showing antibiotic features. In recent years, it was shown that human antimicrobial peptides as important part of the native innate immune system plays a crucial role not only in inactivation of bacteria but also in inhibition of bacterial toxins (1). Prompted by these result, we found that only human α -defensin-1 (HNP-1) but not human β -defensin-1 (hBD-1), both important effectors of the innate immune system, protected cultured epithelial cells from intoxication with TcdA and CDT when applied prior to the toxins to the cells. Moreover, α -defensin-1 prevented also the cytotoxic effects of all three *C. difficile* toxins TcdA, TcdB and CDT combined in the medium. The combined investigation of all three toxins might be even more suitable to mimic the situation after an infection with hypervirulent *C. difficile*. The inhibition of the toxins was monitored by cell rounding caused by each of the toxins. Currently, the molecular mechanisms underlying the inhibitory effects are still unknown and will be investigated in different cell lines. In conclusion, our results demonstrate that HNP-1 causes a loss of cytotoxicity of the *C. difficile* toxins and may act as novel drugs to cure *C. difficile* infections that contribute to CDAD.

1. Giesemann T, Guttenberg G, Aktories K. (2008). Human alpha-defensins inhibit *Clostridium difficile* toxin B. *Gastroenterology* 134: 2049-2058.

027

LSR/Angulin-1 – More than a lipoprotein and toxin receptor in intestinal epithelial cells

B. A. Czulkies¹, J. Mastroianni², C. Schwan¹, R. Zeiser², K. Aktories^{1,3}, P. Papatheodorou¹
¹Institut für Experimentelle und Klinische Pharmakologie und Toxikologie, Albert-Ludwigs-Universität Freiburg, 1, Freiburg, Germany
²Universitätsklinikum Freiburg, Klinik für Innere Medizin 1, Hämatologie, Onkologie und Stammzelltransplantation, Freiburg, Germany
³Center for Biological Signaling Studies (BIOSS), Albert-Ludwigs-Universität Freiburg, Freiburg, Germany

The lipolysis-stimulated lipoprotein receptor (LSR; Angulin-1) is a type I single-pass transmembrane protein of the plasma membrane that is mainly expressed in the liver, but also in the intestine and in various other tissues. Previous studies suggested that LSR is involved in the cellular uptake of triglyceride-rich lipoproteins and/or in the organization of tricellular tight junctions. In addition, we found that LSR is the host cell receptor for *Clostridium difficile* binary toxin CDT (Papatheodorou *et al.*, 2011, PNAS). Moreover, increased expression of LSR has recently been associated with the progression of breast cancer. However, less is known about the role(s) of LSR in intestinal epithelial cells. Here, we generated a CaCo-2 LSR knockout cell line via the targeted CRISPR/Cas9 genome editing technique. We show that LSR is required for the maintenance of the epithelial barrier function in CaCo-2 cells. Typical bicellular tight junctions proteins such as occludin and tricellulin, a protein especially found in tricellular tight junctions, were mislocalized in LSR-deficient CaCo-2 cells. Furthermore, we found that LSR-deficient CaCo-2 cells exhibited increased cell proliferation when compared to wild-type CaCo-2 cells. However, tumor growth of the CaCo-2 LSR knockout cells in a xenograft mouse model was strongly impaired. The data indicate, that LSR, the receptor of CDT, plays an essential role in the regulation of cell-cell contacts and controls epithelial barrier functions of intestinal cells. Papatheodorou, P., Carette, J. E., Bell, G. W., Schwan, C., Guttenberg, G., Brummelkamp, T. R. & Aktories, K. 2011, 'Lipolysis-stimulated lipoprotein receptor (LSR) is the host receptor for the binary toxin Clostridium difficile transferase (CDT)', *Proc Natl Acad Sci U S A*, vol. 108 (39), pp. 16422-7.

DNA-damage and cancer

028

Nanoparticles for therapeutic applications – potential and challenges.

A. Aigner¹
¹University of Leipzig, Rudolf-Boehm-Institute for Pharmacology and Toxicology, Leipzig, Germany

Nanoparticles feature special physical and biological properties, thus offering unique possibilities in diagnostic and therapeutic applications. Beyond the alteration of pharmacokinetic drug profiles, nanoparticles can also mediate the delivery of otherwise suboptimal compounds, especially nucleic acid therapeutics. This presentation highlights important groups of nanoparticles and gives examples for their use in pharmacological applications, also with regard to upcoming developments and future concepts.

029

Polyethylenimines (PEI) nanoparticle-mediated delivery of siRNA to silence neuronal gene expression of alpha-synuclein *in vivo*

C. Helmschrodt¹, A. Bauer¹, S. Höbel², A. Aigner², F. Richter¹, A. Richter¹
¹University of Leipzig, Institute of Pharmacology, Pharmacy and Toxicology, VMF, Leipzig, Germany
²University of Leipzig, Rudolf-Boehm-Institute for Pharmacology and Toxicology, Clinical Pharmacology, Faculty of Medicine, Leipzig, Germany

Neurodegenerative diseases like Parkinson's disease (PD) are accompanied by altered gene expression levels in the brain. Recent studies support a role of regulatory non-coding RNAs, such as microRNAs (miRNAs), which silence a specific set of mRNAs at the post-transcriptional level. Upon their aberrant expression, they are likely involved in the pathophysiology of specific neuronal loss. Manipulation of neuronal gene expression is pivotal for understanding the function of proteins and the development of new therapeutic strategies. RNA interference (RNAi) strategies can be employed through the administration of small interfering RNAs (siRNA), which mediate the specific knockdown of a selected target gene. However, the main challenge is the delivery of these RNAs into the neurons of interest.

In this pilot study, we present a method for delivering siRNAs in polymeric nanoparticles based on low molecular weight polyethylenimines (PEIs). Their intracerebroventricular (ICV) injection leads to *in vivo* silencing of neuronal gene expression in the brain of mice overexpressing α -synuclein (Thy1-aSyn mice).

In a first step, PEI-complexed siRNA tagged with a fluorescent dye were injected to track the localization and distribution after ICV administration. Five days later, fluorescent cells were visible throughout the brain, with the highest fluorescence intensity around the ventricles. Fluorescence was also observed in large cells of the lumbar spinal cord. Moreover, preliminary results demonstrate a 42.6% knockdown ($p < 0.05$ student's t-test, $n = 6$) of human α -synuclein (SNCA) in the target structure striatum upon a single ICV injection of PEI-complexed specific siRNA compared to the control injection group ($n = 9$).

Hence, our first results support the usability and efficacy of PEI nanoparticle-mediated delivery of short RNAs, namely siRNAs, for rapidly and efficiently reducing the expression of a neuronal target gene of interest in the brain *in vivo*. This may allow the development of gene therapy strategies for the treatment of neurodegenerative diseases.

030

Metabolism, mutagenicity, and DNA adduct formation of the naturally occurring Alkenylbenzene beta-Asarone

A. T. Cartus¹, S. Stegmüller¹, K. Berg¹, D. Schrenk¹
¹TU Kaiserslautern, Lebensmittelchemie & Toxikologie, Kaiserslautern, Germany

beta-Asarone (bA, (Z)-1,2,4-trimethoxy-5-(1-propen-1-yl) benzene; CAS No 5273-86-9) is a propenyl alkenylbenzene found in several plants, e.g. *Acorus calamus*. bA-containing plant materials are used to flavor foods, and are active ingredients in traditional plant medicines. Thus, human exposure results primarily from the intake of bitters and teas, as well as from *Calamus*-containing medicines and plant food supplements. Although many (positive) pharmacological properties/effects of asarone isomers are described in the literature, bA was found to be carcinogenic in rodents (liver, duodenum) when given daily or in a single dosage. Early experiments indicated that bA is not activated *via* hydroxylation and sulfonation as it is the case for known hepatocarcinogenic allylic alkenylbenzenes such as estragole or methyleugenol. Because the mechanism of metabolic activation of bA is not known, we investigated the metabolism of bA in liver microsomes and human cytochrome P450 (CYP) enzymes, the mutagenicity of bA and its metabolites in the Ames fluctuation assay and the DNA adduct formation in primary rat hepatocytes. We found that side-chain epoxidation (leading to diols and a ketone) was by far the most dominating metabolic route of bA in liver microsomes and human CYP enzymes. bA was mutagenic in the Ames test (+S9 mix), as was the synthesized bA-epoxide (-S9 mix). Furthermore, we were able to synthesize and characterize a bA epoxide-derived DNA adduct with deoxyguanosine. This DNA adduct was formed in a concentration-dependent manner in rat hepatocytes incubated with bA. Our results strongly indicate that bA is genotoxic with the side-chain epoxide being its ultimate carcinogen.

031

Influence of weight loss on oxidative status and genomic damage of Obese Zucker rats

E. E. Bankoouli^{1,2}, F. Seyfried^{1,2}, L. Rotzinger², A. Nordbeck², C. Corteville², C. Jurowich², T. Germer², C. Otto², H. Stopper²
¹University of Wuerzburg, Institute of Pharmacology and Toxicology, Wuerzburg, Germany
²University Hospital of Wuerzburg, Department of General, Visceral, Vascular and Paediatric Surgery, Wuerzburg, Germany

Morbid Obesity is an independent risk factor for cardiovascular disease, Type 2 Diabetes mellitus and certain types of cancer. Bariatric surgery – with the Roux-en-Y gastric bypass (RYGB) being the gold standard – has become the therapeutic option of choice as a sustained weight loss and improvement of associated morbidity is achieved in the majority of patients. There is, however, a lack of evidence focusing on bariatric surgery induced sustained weight loss and its possible impact on cancer risk. We investigated the association between obesity, oxidative stress and genomic damage after Roux-en-Y gastric bypass surgery (RYGB) or caloric restriction induced weight loss in the obese Zucker rat. Obese male Zucker^{fa/fa} rats were divided into three groups: sham surgery (sham), RYGB and caloric restriction (CR) and were compared with lean controls (Lean; Zucker^{+/+} rats).

Shams showed impaired glucose tolerance and elevated plasma insulin levels, which were less severe in RYGB and CR. Oxidative stress was elevated in kidney, liver and colon tissue of sham and reduced again after weight loss induced by either RYGB or

BWM. Urine-derived oxidation products of lipids, DNA and RNA increased in Shams and decreased after weight loss (RYGB and CR). DNA double strand breaks were more frequent in shams than in the weight loss groups or lean. DNA damage in Zucker^{fa/fa} rats correlated with their basal plasma insulin values.

Obese rats showed elevated oxidative stress and genomic damage in comparison to lean rats. After body weight loss, achieved by either RYGB or caloric restriction alone, oxidative stress level and genomic damage were decreased. This may indicate a reduction of the elevated cancer risk in obesity.

032

DNA repair by MGMT causes a threshold in alkylation-induced colorectal carcinogenesis

J. Fahrner¹, J. Frisch¹, G. Nagel¹, A. Kraus¹, B. Dörsam¹, A. D. Thomas¹, S. Reißig², A. Waisman², B. Kaina¹
¹Universitätsmedizin Mainz, Institut für Toxikologie, Mainz, Germany
²Universitätsmedizin Mainz, Institut für Molekulare Medizin, Mainz, Germany

N-nitroso compounds (NOC) are environmental and dietary carcinogens causally linked to colorectal cancer (CRC). In view of recent evidence of non-linear mutagenicity for NOC-like compounds, the question arises as to the existence of threshold doses in CRC formation. NOC induce a variety of DNA adducts, including O⁶-methylguanine (O⁶-MeG) and N-methylated purines, which are removed by O⁶-methylguanine-DNA methyltransferase (MGMT) and N-alkylpurine-DNA glycosylase (AAG)-initiated base excision repair, respectively. Here, we set out to determine the impact of these DNA repair pathways on the dose-response of alkylation-induced CRC. DNA repair-proficient (WT) and -deficient (Mgmt^{-/-}, Aag^{-/-} and Mgmt^{-/-}Aag^{-/-}) mice were treated with the NOC-related compound azoxymethane (AOM) followed by the administration of dextran sodium sulfate to trigger CRC. Tumors were quantified by non-invasive mini-endoscopy, which revealed a non-linear increase in CRC formation in WT and Aag^{-/-} mice. In contrast, a linear dose-dependent increase in tumor frequency was observed in Mgmt^{-/-} and Mgmt^{-/-}Aag^{-/-} mice. The data was corroborated by hockey stick modeling, which yielded similar carcinogenic threshold doses for WT and Aag^{-/-} mice. O⁶-MeG levels and depletion of MGMT activity correlated well with the observed dose-response in CRC formation. AOM dose-dependently induced double strand breaks (DSBs) in colon crypts including in Lgr5-positive colon stem cells, which coincided with ATR-Chk1-p53 signaling. Intriguingly, Mgmt-deficient mice displayed significantly enhanced levels of γ -H2AX, suggesting the usefulness of γ -H2AX as an early genotoxicity marker in the colorectum. This study demonstrates for the first time a non-linear dose-response for alkylation-induced carcinogenesis and reveals DNA repair by MGMT, but not AAG, as a key node in determining a carcinogenic threshold at low alkylation dose levels [2].

[1] Fahrner and Kaina (2013) Carcinogenesis, 34 (11):2435-2442

[2] Fahrner et al. (2015) Carcinogenesis, 36(10):1235-1244

033

Poly(ADP-ribose) polymerase-1 deficiency confers resistance against colitis-associated colorectal cancer

B. Dörsam¹, G. Nagel¹, A. Kraus¹, E. Pfeifer¹, A. Stier², A. Mangerich², S. Reißig³, F. Dantzer⁴, B. Kaina¹, J. Fahrner¹
¹University Medical Center, Toxicology, Mainz, Germany
²University, Biology, Konstanz, Germany
³University Medical Center, Molecular Medicine, Mainz, Germany
⁴University, Strasbourg, Germany

Poly(ADP-ribose) polymerase-1 (PARP-1) plays an important role in plethora of cellular processes such as DNA repair and maintenance of genomic integrity. PARP-1 promotes base excision repair, a DNA repair mechanism that removes base modifications. Including alkylated DNA bases induced by N-nitroso compounds (NOC), which are tightly linked to the etiology of colorectal cancer (CRC) [1]. *In vivo* studies revealed enhanced sensitivity of PARP-1 deficient mice towards alkylating agents in terms of toxicity and genomic instability. The aim of this work is to investigate the impact of PARP-1 on colitis-associated CRC in response to NOC. PARP-1-proficient (WT) and PARP-1 deficient (PARP-1^{-/-}) mice were challenged with the azoxymethane (AOM)/dextran sodium sulfate (DSS) protocol of colorectal carcinogenesis. Tumor number and tumor score were assessed via non-invasive mini-endoscopy. In contrast to the WT, PARP-1 deficient mice displayed a significantly lower rate of tumor formation. To detail the role of PARP-1 in the in the different stages of CRC formation, we first analyzed NOC-induced DNA damage induction and response. We found a time-dependent induction of DNA strand breaks in both mouse strains, which was significantly higher in PARP-1-deficient animals, using the alkaline comet assay and immunoblot analysis of the DNA strand break marker γ H2AX. Determination of the poly ADP-ribose (PAR) levels via mass spectrometry revealed a significant lower induced level in the tissue of PARP-1 k.o. animals after challenge with AOM compared to the WT. PARP-1^{-/-} and WT mice displayed a comparable level of O⁶-methylguanine (O⁶-MeG), the critical lesion driving NOC-induced CRC. Consistent with this, O⁶-MeG repair activity was depleted similarly in both mouse strains. No differences were detectable in basal cell proliferation and cell death induction after AOM treatment as shown by PCNA and TUNEL staining in colorectal tissue of PARP-1 proficient and -deficient mice. As PARP-1 is also a known co-regulator of the pro-inflammatory transcription factor NF- κ B, the acute DSS-induced inflammation was assessed by mini-endoscopy and revealed significantly higher levels of gut inflammation in WT animals compared to PARP-1-deficient mice. In line with these findings, analysis of infiltrated macrophages, monocytes and T-cells via IHC showed a reduced inflammatory response in the colon of PARP-1^{-/-} animals. In addition, we measured lower levels of the pro-inflammatory cytokine TNF α in colon tissue of PARP-1^{-/-} animals. Collectively, we demonstrate that PARP-1 k.o. animals although they display higher levels of initial DNA strand breaks are protected against colitis-associated CRC, which is likely to be attributable to an attenuated inflammatory response. This aspect, which will be dissected in ongoing studies could have significant implications for the etiology and therapy of colitis-associated CRC.

Furthermore we investigate the expression of PARP-1 in human CRC and the impact on PARP inhibitors on colorectal carcinogenesis in PARP-1 proficient animals.

[1] Fahrner and Kaina (2013) *Carcinogenesis*, 34 (11):2435-2442

GPCR signaling

034

Regulation of brown adipose tissue by the adenosine A_{2B} receptor

T. Gnad¹, A. Pfeifer¹

¹University of Bonn, Pharmacology & Toxicology, Bonn, Germany

Obesity has reached pandemic proportions with at least 2.8 million people dying each year as a result of being overweight or obese (WHO). Obesity is a serious risk factor for type 2 diabetes, metabolic syndrome or nonalcoholic fatty liver disease among others.

Brown adipose tissue (BAT) is specialized in dissipating energy in the form of heat by uncoupling ATP synthesis due to its unique *uncoupling protein 1* (UCP1). BAT abundance is correlated with leanness in humans. Thereby, BAT is a potential and self-evident pharmaceutical target for an anti-obesity therapy. We recently showed that adenosine activates human and murine brown adipocytes and that mice are protected from diet-induced obesity when treated with an adenosine receptor A_{2A} agonist. Apart from A_{2A}, the adenosine A_{2B} receptor is abundantly expressed in murine BAT. Here, we analyzed the role of the A_{2B} receptor in BAT differentiation and function.

Histological appearance and UCP1 staining of BAT from A_{2B}^{-/-} mice was alike compared to wild type animals. We found no change in lipid content – visualized with Oil Red-O stain – after differentiation of preadipocytes isolated from BAT of either A_{2B}^{-/-} or wild type newborns. Consistently, expression analysis of the adipogenic markers aP2 and PPAR γ showed no significant difference between the two cell lines. Importantly, thermogenic markers like UCP1 or PGC1a were also not altered on both mRNA and protein level.

First preliminary *in vivo* experiments using non-invasive infrared thermography showed a reduced surface temperature of the interscapular region of A_{2B}^{-/-} pups when compared to wild type littermates indicating a role of A_{2B} in physiological BAT activation. Moreover, cold-exposure of adult knockout mice resulted in decreased whole-body oxygen consumption without changes in locomotor activity when compared to wild type littermates. Consequently, treatment of mice with a specific A_{2B} agonist resulted in increased oxygen consumption compared to vehicle injection.

Our results demonstrate that A_{2B} is expendable for BAT differentiation, but is crucial for full functional activation after physiological stimulation *in vivo*. Besides, pharmacological activation of A_{2B} results in increased whole-body energy expenditure.

035

Role of chemokines and chemokine receptors in adipocellular function

C. Koenig¹, P. Foerster¹, S. Wiese², P. Fischer-Posovszky³, B. Moepps¹

¹Ulm University Medical Center, Pharmacology and Toxicology, Ulm, Germany

²Ulm University, Core Unit Mass Spectrometry and Proteomics Medical Faculty, Ulm, Germany

³Ulm University, Division of Pediatric Endocrinology and Diabetes, Department of Pediatrics and Adolescence Medicine, Ulm, Germany

Obesity is characterized as a status where the excessive accumulation of fat in adipocytes leads to local inflammation and hypoxia; both contributing to severe obesity associated co-morbidities such as cardiovascular disease and type 2 diabetes mellitus. Local inflammation is mediated by macrophages, stromal vascular cells, preadipocytes, and adipocytes as well as by a number of proinflammatory cytokines and chemokines (1). In particular, the chemokines monocyte chemoattractant protein (MCP-1, CCL2), interleukin-8 (IL-8/CXCL8) and stromal cell-derived factor 1 (SDF-1 α /CXCL12) secreted by stromal vascular cells, preadipocytes, and adipocytes exert paracrine effects by recruiting neutrophils, monocytes/macrophages, and T- and B-cells. Interestingly, deficiency in CXCL14 was shown to attenuate obesity in mice (2). The CC chemokine CCL2 is known to stimulate CCR2 receptors, and the CXC chemokines CXCL8 and CXCL12 to activate CXCR1 and CXCR2 or CXCR4 and CXCR7, respectively. The receptor(s) activated by CXCL14 is currently unknown. A role of CXCL14 in modulating CXCR4 signaling has been proposed. We initiated our studies to determine the presence and functional significance of chemotaxis receptors in human adipocytes and their precursor cells. To this end, the mRNA expression pattern of CC chemokine receptors, CXC chemokine receptors formylated peptide receptor FPR1 and the related receptor FPRL1, and CC and CXC chemokines was analyzed during *in vitro* adipose differentiation of human Simpson-Golabi-Behmel-Syndrome (SGBS) preadipocytes, and under conditions mimicking an inflammatory response. In particular, we focused on the expression pattern of human CCR2 receptors, since previous reports indicated a role in adipogenic differentiation. However, our comprehensive analysis using different sources of adipocytes and their precursors indicated that CCR2 receptors were absent (3). Yet, the analysis revealed appreciable levels of mRNA encoding CCL2, CXCL12, and CXCL14, and CCR1, CXCR2, CXCR7, FPR1, and FPRL1, and CXCR4. Of interest, CXCR4- and CXCR7-mRNA were found to be up-regulated under the proinflammatory conditions. To analyze the responses of adipocytes and their precursors to chemokine receptor agonists, we used chemokine-mCherry fusion proteins purified from baculovirus-infected insect cells, e.g. CCL2, CXCL12, CXCL14. While SGBS-preadipocytes and adipocytes did not accumulate CCL2-mCherry upon stimulation, they showed a small accumulation of CXCL12-mCherry, and a strong accumulation of CXCL14-mCherry in the endosomal compartment. Similar results were obtained in murine 3T3L-1 preadipocytes. Using mass spectrometry analysis, we set out to identify the CXCL14-binding putative receptor protein(s) in murine 3T3L-1 preadipocytes.

(1) Makki, K. et al. (2013), *ISRN Inflamm.* 2013:139239. (2) Tanegashima, K. et al. (2010), *PLoS ONE* 5, e10321. (3) Koenig, C. et al. (2013), *Mol. Cell. Endocrinol.* 369: 72-85.

036

New active rac variants in prostate cancer: a sword with two edges

A. Augspach¹, J. Maurer², S. Lassmann³, K. Aktories¹, G. Schmidt¹

¹Institute für Pharmakologie und Toxikologie Freiburg, 1, Freiburg, Germany

²Uniklinikum, Department of Urology, Freiburg, Germany

³Institute für Pathologie, Pathologie, Freiburg, Germany

In personalized medicine tumors are screened for several mutations in oncogenes or tumor suppressors. However, the cellular protein content not exclusively depends on the DNA. We identified new Rac variants generated on the mRNA level in androgen-independent prostate cancer cells. All variants represent active forms of the GTPase. They are capable to suppress RhoA-induced apoptosis and additionally, mediate the synthesis of genes which are under the control of the androgen receptor. Importantly, expression of the Rac variants is sufficient to support tumor growth in mice. We prove the existence of the variants and verify their clinical appearance and relevance in tissue samples of a prostate cancer patient. DNA analysis, however, revealed the wildtype sequence of *rac*. Therefore, routine analysis of patient tumor tissue would miss the detection of active Rac which precludes the success of therapy. The existence of active Rac variants in prostate cancer tissue that promote resistance towards androgen deprivation suggest Rac inhibition as an effective add on therapeutic strategy against prostate cancer.

037

Potential role of cyclic 3',5'-UMP and cyclic 3',5'-CMP as bacterial first messenger molecules

B. Schirmer¹, C. Kloth¹, J. Rothschild¹, S. Hoppe¹, R. Seifert¹

¹Medizinische Hochschule Hannover, Institut für Pharmakologie, Hannover, Germany

The bacterial effector protein Exotoxin Y (ExoY) of *Pseudomonas aeruginosa* is delivered into host cells via the bacterial type III secretion system. Once arrived in the host cell nucleotidyl cyclase activity of ExoY is activated by a yet unknown cofactor and thus has a profound effect on concentrations of cyclic nucleotides: In addition to production of cyclic AMP (cAMP) and cyclic GMP (cGMP) there is a massive synthesis of cyclic 3',5'-uridylylmonophosphate (cUMP) and to some extent of the corresponding cytidylyl analogue cCMP^{1,2}. Currently, the role of cUMP and cCMP during the pathogenesis of *P. aeruginosa* infection remains unknown³. One of our hypotheses is that these cyclic nucleotides fulfill a role as first messengers, e.g. in the communication between individual bacteria or bacterial populations during establishment of acute or chronic infections.

To test this hypothesis, the intra- and extrabacterial concentrations of cyclic nucleotides were measured via HPLC-MS/MS at different time-points in liquid cultures of *P. aeruginosa*, either in a complete (LB medium) or a starving medium (Vogel-Bonner medium). Additionally, we tested if supplementation of the media with extrinsic cUMP or cCMP had an effect on these measured concentrations. The influence of extrabacterial cyclic nucleotides on the bacterial metabolism and homeostasis was evaluated with a microarray of bacterial total cDNA extracted at different time points of *P. aeruginosa* liquid culture with or without extrinsic cUMP/ cCMP. Furthermore we investigated a potential function of the cyclic nucleotides in biofilm formation.

Cyclic UMP and cyclic CMP have differential roles in bacterial metabolism and communication. For example, whereas cCMP is synthesized by *P. aeruginosa* when the bacteria are in a nutrient-rich environment, we could not detect bacterial cUMP under any tested circumstance. In our biofilm formation assays, only cCMP had a biofilm-promoting effect, but only in very high concentrations. The currently ongoing analysis of gene expression data in the presence or absence of cUMP may reveal a role of this cyclic nucleotide as first messenger, too.

In further studies we will elucidate the signal transduction processes underlying the observed cUMP / cCMP effects, for example by identifying cUMP and cCMP binding proteins and their coupling mechanisms to intracellular signalling cascades.

1. Beckert U, Wolter S, Hartwig C, et al. ExoY from *Pseudomonas aeruginosa* is a nucleotidyl cyclase with preference for cGMP and cUMP formation. *Biochem Biophys Res Commun.* 2014;450(1):870-874.

2. Bähre H, Hartwig C, Munder A, et al. cCMP and cUMP occur *in vivo*. *Biochem Biophys Res Commun.* 2015 May 15;460(4):909-14.

3. Seifert R. cCMP and cUMP: Emerging second messengers. *Trends Biochem Sci.* 2014.

038

cAMP microcompartments in *Drosophila* motor neurons

I. Maiellaro¹, M. J. Lohse¹, R. J. Kittel², D. Calebiro¹

¹Institute of Pharmacology, Würzburg, Germany

²Institute of Physiology, Würzburg, Germany

Synapses are complex computational platforms that transmit information encoded in action potentials but also transform their functionality through synaptic plasticity. G protein-coupled receptors (GPCRs) play a major role in modulating the strength of the synapses via the second messenger cAMP¹. However the spatio-temporal dynamics of the mode of action of cAMP underlying synaptic plasticity are still controversial. The role of this study was to investigate the dynamics of cAMP signaling at the *Drosophila* neuromuscular junction, where octopamine binding to its receptors has been shown to cause cAMP-dependent synaptic plasticity². For this purpose, we generated a transgenic *Drosophila* expressing the cAMP sensor Epac1-camps³ in motor neuron. This allowed us to directly follow the octopamine-induced cAMP signals in real time by fluorescence resonance energy transfer (FRET) in different compartments of the motor neuron (i.e. cell body, axon, boutons). We found that octopamine induces a steep cAMP gradient from the synaptic bouton (high cAMP) to the cell body (low cAMP), which was due by higher PDE activity in the cell body. High octopamine concentrations evoked a response also in the soma. Notably, these signals were independent and isolated from each other. Moreover, application of octopamine by iontophoresis to single synaptic boutons induced bouton-confined cAMP signals. These data reveal that a motor neuron

can possess multiple and largely independent cAMP signaling compartments, and provide new basis to explain how cAMP could control neurotransmission at a level of a single synapse.

¹ Kandel, E.R., Dudai, Y. & Mayford, M.R. The molecular and systems biology of memory. *Cell* 157, 163-186 (2014).

² Koon, A.C., et al., Autoregulatory and paracrine control of synaptic and behavioral plasticity by octopamine signaling. *Nat Neurosci.* 14(2): p. 190-9 (2010).

³ Nikolaev VO, Bünemann M, Hein L, Hannawacker A, Lohse MJ Novel single chain cAMP sensors for receptor-induced signal propagation. *J. Biol. Chem.* 279, 37215-37218 (2004)

Cardiovascular pharmacology

039

Hyaluronic acid deposition determines engineered heart muscle characteristics and can be pharmacologically targeted to enhance function

S. Schlick^{1,2}, M. Tiburcy^{1,2}, S. Zeidler^{1,3,2}, S. Lutz^{1,2}, E. Wingender^{3,2}, W.-H. Zimmermann^{1,2}

¹Universitätsmedizin Göttingen, Pharmakologie, Göttingen, Germany

²DZHK (German Center for Cardiovascular Research), Göttingen, Germany

³Universitätsmedizin Göttingen, Bioinformatik, Göttingen, Germany

Background: Engineered human myocardium (EHM) can be generated from PSC derived cardiomyocytes (CMs) and primary fibroblasts suspended in a collagen I hydrogel (70%:30%:0.4 mg/ml). EHM development encompasses an early consolidation phase followed by functional maturation. The presence of fibroblasts is essential for consolidation into a force-generating EHM. Here we assessed the hypothesis that fibroblasts of different origin support EHM formation differentially as a function of hyaluronic acid deposition.

Methods and results: Oscillatory rheology (1% strain, 1 Hz) on cell-free and cell containing collagen I hydrogels directly after casting revealed enhanced consolidation in the presence of human foreskin fibroblasts (FFBs) compared to primary adult cardiac fibroblasts (CFBs) – change in storage modulus over time (Pa/min): collagen 0.03; collagen + CMs 0.03; collagen + CMs + CFBs 0.09, collagen + CMs + FFBs 0.2. We next generated EHM with CMs and FFBs or CFBs. After 4 weeks of culture under serum-free conditions, we assessed EHM function by contraction measurements. FFB-EHMs developed a significantly ($p < 0.01$) higher force of contraction (FOC) per cross sectional area (CSA) than CFB-EHMs (maximal FOC/ CSA are in mN/mm^2 : 1.8 ± 0.1 , $n=29$ vs. 0.3 ± 0.1 , $n=20$). Cross sectional area (CSA) of tissues was greatly increased ($p < 0.01$) in CFB-EHMs (CSA in mm^2 : 1.6 ± 0.1 , $n=20$ vs. 0.6 ± 0.03 , $n=30$) and non-myocyte content was higher in CFB-EHMs (5.6 ± 0.7 , $n=9$ vs. 3.1 ± 0.4 , $n=15$; $\times 10^3$ cells/ml). Histological analysis revealed that cardiomyocytes were only poorly matured in CFB-EHMs compared to FFB-EHMs. Extending EHM functional data, principal component analysis of RNAseq data revealed distinct expression patterns for FFBs and CFBs, in which hyaluronic acid synthase 2 (HAS2) enzyme was significantly ($p < 0.01$) upregulated. Based on these findings, we pharmacologically intervened with HAS2 mediated hyaluronic acid (HA) deposition by treating CFB-EHMs with hyaluronidase during all 4 weeks of culture. Interestingly, ECM manipulation with low concentrations of enzyme significantly ($p < 0.01$) reduced CSA (CSA in mm^2 : control 1.8 ± 0.4 , $n=8$; hyaluronidase of concentrations from 0.15U to 150U 0.9 ± 0.2 , $n=4$) with a concurrent, statistically significant ($p < 0.01$), increase in contractile function and improved cardiomyocyte morphology on a histological level (maximal FOC/CSA in mN/mm^2 : control 0.2 ± 0.05 , $n=8$; hyaluronidase of concentrations from 0.15U to 150U 0.4 ± 0.08 , $n=4$).

Summary and conclusions: Our data suggest that EHM consolidation is influenced differentially by fibroblasts of different tissue origin with HFF-EHM being functionally superior to CFB-EHM. CFB-EHM could be rescued by hyaluronidase leading to reduced HA deposition. The latter demonstrates that extracellular matrix composition is centrally involved in EHM development.

040

cAMP regulates sprouting angiogenesis independent of the VEGF-pathway in endothelial cells

J. Garg¹, Y. Feng¹, M. Schmidt², T. Wieland¹

¹Institute of Experimental Pharmacology, Mannheim, Germany

²University of Groningen, Centre of Pharmacy, Groningen, Niederlande

Angiogenesis is the process of formation of new blood vessels from the pre-existing ones. Vascular endothelial growth factor (VEGF) is the most studied regulator of this process. By binding to its type 2 receptor (VEGFR2), it has been shown to activate a variety of different signaling-pathways leading to enhanced angiogenesis. cAMP, on the other hand, is a versatile second messenger which regulates various endothelial functions including barrier function. It directly activates Protein Kinase A (PKA) or the Exchange protein directly activated by cAMP (Epac) which is a guanine exchange factor (GEF) for the small monomeric GTPase Rap. As Human umbilical vein endothelial cells (HUVEC) express both cAMP effectors (Epac1 and PKA), we investigated the role of cAMP-signaling using a spheroid based sprouting assay as an *in vitro* model for angiogenesis. Interestingly, the activation of β -adrenergic receptors with 5 μM of isoproterenol significantly increased the cumulative sprout length. Similarly, the selective activation of Epac with 30 μM of the cAMP analog 8-pCPT-2'-O-cAMP (007) significantly increased the basal and the VEGF-induced cumulative sprout length. In accordance, siRNA-mediated depletion of Epac1 in HUVEC decreased the basal and VEGF-induced sprouting. Surprisingly, 10 μM of forskolin increased basal and VEGF-induced cumulative sprout length stronger than 007, indicating an additional role of PKA. In accordance, 1 μM of myristoylated PKI, a membrane-permeable specific PKA inhibitor, significantly attenuated the forskolin-induced increase in sprouting. In all conditions tested, 50 ng/ml of VEGF always showed an additive effect to the same extent on cumulative sprout length. Therefore, our data indicate that the VEGF-pathway is acting independently of the cAMP-pathway in the regulation of the sprouting angiogenesis. The

β -adrenergic receptor-mediated activation of cAMP signaling in HUVEC induces angiogenic sprouting by activation of Epac1 and PKA.

041

Endothelial mineralocorticoid receptors play different roles in hypertensive heart vs. kidney disease

A. Lother^{1,2}, D. Fürst¹, S. Bergemann¹, R. Gilsbach¹, F. Grahammer³, T. B. Huber³, I. Hilgendorf², C. Bode², M. Moser², L. Hein¹

¹Institut für experimentelle und klinische Pharmakologie und Toxikologie, Freiburg, Germany

²Universitäts-Herzzentrum Freiburg-Bad Krozingen, Kardiologie und Angiologie I, Freiburg, Germany

³Universitätsklinik Freiburg, Nephrologie, Freiburg, Germany

Introduction: Hypertension is one major risk factor for the development of chronic heart and kidney disease. Mineralocorticoid receptor (MR) antagonists are a cornerstone in the therapy of heart failure and there is first evidence for a beneficial effect on the kidney as well. Inflammation plays an important role in hypertensive organ injury. Thus, this study was designed to evaluate and directly compare the effect of MR deletion in endothelial cells on blood pressure and cardiac vs. renal injury in a mouse model of deoxycorticosterone acetate-induced hypertension.

Methods and results: Mice lacking the mineralocorticoid receptor in endothelial cells ($\text{MR}^{\text{Cdh5Cre}}$) were created using the Cre/loxP system. $\text{MR}^{\text{Cdh5Cre}}$ and Cre-negative littermates ($\text{MR}^{\text{wildtype}}$) underwent unilateral nephrectomy and received 1 % NaCl with drinking water for 6 weeks. The mineralocorticoid deoxycorticosterone acetate (DOCA, 2.5 mg/d) was delivered by subcutaneous pellets. Untreated mice served as controls (CTRL).

Ambulatory blood pressure was determined by implantable telemetry in awake mice. DOCA/salt treatment increased mean blood pressure in $\text{MR}^{\text{wildtype}}$ (141.7 ± 8.0 vs. CTRL 97.8 ± 3.2 mmHg, $P < 0.001$) and $\text{MR}^{\text{Cdh5Cre}}$ (150.0 ± 3.0 vs. CTRL 104.1 ± 4.7 mmHg, $P < 0.001$) without differences between genotypes.

Cardiac hypertrophy after DOCA/salt treatment was ameliorated in $\text{MR}^{\text{Cdh5Cre}}$ mice (ventricle weight 162.4 ± 4.2 mg vs. $\text{MR}^{\text{wildtype}}$ 189.0 ± 10.9 mg, $P < 0.05$). DOCA/salt significantly increased cardiac fibrosis and the expression of fibrotic marker genes in $\text{MR}^{\text{wildtype}}$ but not in $\text{MR}^{\text{Cdh5Cre}}$ mice. This was accompanied by an increased expression of the vascular cellular adhesion molecule (*Vcam1*) in $\text{MR}^{\text{wildtype}}$ cardiac endothelial cells.

Renal function was not altered by MR deletion in endothelial cells at baseline. DOCA/salt treatment led to marked interstitial fibrosis in the kidneys of $\text{MR}^{\text{wildtype}}$ (sirius red fibrosis score: 2.4 ± 0.2 vs. CTRL 0.1 ± 0.1 , $P < 0.001$) and $\text{MR}^{\text{Cdh5Cre}}$ (2.3 ± 0.2 vs. CTRL 0.1 ± 0.1 , $P < 0.001$) mice. mRNA expression of the fibrosis marker gene *Col3a1* ($\text{MR}^{\text{wildtype}}$ 4.3 ± 0.9 -fold; $\text{MR}^{\text{Cdh5Cre}}$ 3.9 ± 1.1 -fold vs. CTRL) was similarly increased.

Periodic acid-Schiff staining revealed glomerular injury in both genotypes. This was associated with a marked rise in urinary albumin / creatinine ratio ($\text{MR}^{\text{wildtype}}$ 20.4 ± 5.7 -fold; $\text{MR}^{\text{Cdh5Cre}}$ 34.3 ± 12.5 -fold vs. CTRL). In the kidney *Vcam1* mRNA expression and the number of macrophages was increased by DOCA/salt treatment independently from endothelial MR deletion.

Conclusion: In conclusion, MR deletion from endothelial cells ameliorated DOCA/salt-induced cardiac but not renal inflammation and remodeling independently from blood pressure. These findings suggest different mechanisms for the beneficial effect of MR antagonists in hypertensive heart vs. kidney disease.

042

Analysis of TRPC cation channels in haemostasis, thrombosis and platelet function

J. E. Camacho Londoño^{1,2,3}, D. Schumacher¹, M. T. Harper⁴, J. Camacho Londoño³, S. E. Philipp⁵, A. Dietrich⁵, V. Flockert³, A. W. Poole⁶, L. Birnbaumer⁷, M. Freichel^{1,2,3}

¹Ruprecht-Karls-Universität Heidelberg, Pharmakologisches Institut, Heidelberg, Germany

²DZHK (German Centre for Cardiovascular Research), Partner site

Heidelberg/Mannheim, Heidelberg, Germany

³Universität des Saarlandes, Experimentelle u. Klinische Pharmakologie und Toxikologie, Homburg, Germany

⁴University of Cambridge, Department of Pharmacology, Cambridge, United Kingdom

⁵Ludwig-Maximilians Universität, Institut für Pharmakologie und Toxikologie, München, Germany

⁶University of Bristol, School of Physiology and Pharmacology, Bristol, United Kingdom

⁷Universidad Nacional de San Martín, IIB-INTECH, Buenos Aires, Argentina

Platelets are relevant cells implicated in morbidity and mortality provoked by cardiovascular thrombosis. Even with the actual antiplatelet therapy there is still a substantial incidence of arterial thrombosis. Therefore, a better understanding of the mechanisms involved in platelet activation and aggregation is required to develop improved antiplatelet therapies. The increase in the intracellular Ca^{2+} concentration due to Ca^{2+} entry from the extracellular space is critical for platelet activation and aggregation. Ca^{2+} entry follows activation of plasma membrane receptors including Gq-coupled receptors for ADP, Thromboxane A_2 (TxA_2) or thrombin, as well as the collagen receptor glycoprotein VI (GPVI). The cellular signalling pathways downstream these receptors involve activation of Phospholipase C and second messengers that are known to mediate activation of TRPC channels. TRPC proteins form receptor-operated cation channels, but their regulation and permeability differ depending on the cell type. It has been proposed that TRPC proteins might contribute to platelet function as constituents of agonist-activated Ca^{2+} entry channels; however, the experimental approaches used so far and the lack of specific agonists or antagonists have not allowed to determine the individual contribution of TRPC proteins for agonist-induced Ca^{2+} entry in platelets, aggregation and thrombosis formation.

We detected the expression of TRPC3 and TRPC6 in human and mouse platelets. We identified that these proteins together are essential components of a system of coincidence detection in cellular Ca^{2+} signalling. This coincidence detection triggered by simultaneous stimulation of both thrombin and collagen receptors is required for the Phosphatidylserine exposure in human and murine platelets, indicating the role of TRPC3/6 proteins for procoagulant activity. In addition, we detected the expression of

TRPC1 transcripts in mouse platelets. Therefore, we tested TRPC1/C3/C6-deficient mice in an *in vivo* model of arterial thrombosis where they showed reduced thrombus formation. Regardless of the protective effect of TRPC1/C3/C6 inactivation observed in the thrombosis model, no differences were detected in tail bleeding. To evaluate the relevance of these TRPC proteins in platelet aggregation we measured *in vitro* platelet aggregation in platelets from TRPC1/C3/C6-deficient mice and we observed that the aggregation was reduced after ADP (3µM) or TxA₂-analogue (1µM) stimulation, but not after collagen stimulation (10µg/ml).

We are currently analyzing the *in vitro* aggregation and the agonist-evoked Ca²⁺ response in platelets from different TRPC-compound and single deficient mouse lines to understand the mechanisms behind this phenotype with regard to its complementarity to actual antiplatelet therapy.

Funding: KFO 196, DZHK (German Centre for Cardiovascular Research) and the BMBF (German Ministry of Education and Research).

043

Biglycan protects from atherosclerosis by inhibiting thrombin generation and platelet activation in ApoE-deficient mice

M. Grandoch^{1,2}, A. Melchior-Becker^{1,2}, C. Kohlmoorgen^{1,2}, K. Feldmann^{1,2}, N. S. Gowert³, J. Müller^{1,2}, S. Homann^{1,2}, L.-S. Kiene^{1,2}, J. Zeng-Brouwers⁴, F. Schmitz^{1,2}, N. Nagy^{1,2}, A. Polzin⁵, P. Skroblin⁶, X. Yin⁶, M. Elvers⁷, M. Mayr⁶, L. Schaefer⁴, L. Tannock⁷, J. W. Fischer^{1,2}

¹Universitätsklinikum der Heinrich-Heine-Universität Düsseldorf, Institut für

Pharmakologie u. Klinische Pharmakologie, Düsseldorf, Germany

²Universitätsklinikum der Heinrich-Heine-Universität Düsseldorf, CARID –

Cardiovascular Research Institute Düsseldorf, Düsseldorf, Germany

³Universitätsklinikum der Heinrich-Heine-Universität Düsseldorf, Institut für

Hämostaseologie, Hämotherapie und Transfusionsmedizin, Düsseldorf, Germany

⁴Pharmazentrum Frankfurt, Klinikum der Goethe-Universität, Institut für Allgemeine

Pharmakologie und Toxikologie/ZAFES, Frankfurt am Main, Germany

⁵Universitätsklinikum der Heinrich-Heine-Universität Düsseldorf, Klinik für Kardiologie,

Pneumologie und Angiologie, Düsseldorf, Germany

⁶Kings' College London, King's British Heart Foundation Centre, London, United

Kingdom

⁷Saha Cardiovascular Research Center, University of Kentucky, Division of

Endocrinology and Molecular Medicine, Lexington, United Kingdom

Background: Thrombin signaling initiates inflammatory events directly and through activation of platelets. Endogenous and pharmacologic inhibitors of thrombin are therefore of relevance during atheroprotection and for therapeutic intervention. The small leucine-rich proteoglycan biglycan (BGN) is such an endogenous thrombin inhibitor that acts through activation of heparin cofactor II (HCII). Here, the effect of genetic deletion of BGN on thrombin activity, inflammation and atherosclerosis was addressed.

Methods and Results: BGN concentrations were elevated in the plasma of patients with acute coronary syndrome. In *ApoE*^{-/-} mice, BGN was detected in the plasma as well as in the glycocalyx of capillaries. Additionally, BGN expression occurred in the subendothelial matrix of arterioles as well as in atherosclerotic plaques. In line with a role of BGN in balancing thrombin activity, *ApoE*^{-/-}/*Bgn*^{0/0} mice exhibited higher activity of circulating thrombin and increased numbers of activated platelets than did *ApoE*^{-/-} mice. Furthermore, higher concentrations of circulating cytokines in *ApoE*^{-/-}/*Bgn*^{0/0} mice suggested a pro-inflammatory phenotype. Likewise, immunohistochemistry and FACS analysis of the aorta demonstrated increased macrophage content in atherosclerotic lesions of these mice. In addition, *ApoE*^{-/-}/*Bgn*^{0/0} mice exhibited higher aortic plaque burden and larger atherosclerotic lesions at the aortic root. Of note, *ApoE*^{-/-}/*Bgn*^{0/0} mice showed progressive dilatation of the aortic arch corresponding to a decrease in collagen fibril density suggestive of an outward remodeling in the absence of BGN. No differences were evident with respect to lipid content of the aortic root plaques or circulating plasma lipids. Treatment with the thrombin inhibitor argatroban reversed platelet activation and aortic macrophage accumulation in *ApoE*^{-/-}/*Bgn*^{0/0} mice.

Conclusions: The present results strongly suggest a protective role of BGN during the progression of atherosclerosis by inhibiting thrombin activity and platelet activation, and ultimately macrophage-mediated plaque inflammation.

Potential drug targets and pharmacotherapy

044

Mechanisms and multi-generational effects of xenosensor activation

K. Dietrich¹, M. Mathás¹, J. Baumgart², L. Eshkind², L. Wojnowski¹

¹Institut für Pharmakologie, Universitätsmedizin der Johannes Gutenberg-Universität

Mainz, Mainz, Germany

²Translational Animal Research Center, Universitätsmedizin der Johannes Gutenberg-Universität Mainz, Mainz, Germany

The exposure to environmental or human-made xenobiotics including drugs induces the hepato-intestinal transcription of metabolizing enzymes and transporters. The time-span of induction is thought not to exceed xenobiotic exposure, in order to minimize disturbances of endobiotic metabolism. In contrast, we find cross-generational transmission of the induction of the Phase I enzyme Cyp2b10 (1200-fold in females, 700-fold in males) in 6-day old offspring of adult female mice exposed one week prior mating to TCPOBOP (3 mg/kg i.p.), the model ligand of the xenosensing nuclear receptor CAR. Such cross-generational effects of xenobiotics are of great clinical interest as they could have profound consequences on the health status of the offspring, including interferences with drug therapies.

The multigenerational transmission of TCPOBOP-driven induction could be mediated by pre-uterine/pre-conceptual epigenetic changes of oocytes. Alternatively, they could be brought about by direct intrauterine/post-conceptual contact with TCPOBOP released from long-term depots. To discriminate between these mechanisms we conducted embryo transfer experiments. Both donor mothers and foster mothers were injected with TCPOBOP (3 mg/kg) prior to mating. The analysis of hepatic Cyp2b10 expression in 6-

day-old offspring is clearly consistent with a post-conceptual onset of TCPOBOP effects. Thus, offspring of solvent-injected donor mothers transferred to TCPOBOP-exposed foster mothers display a 700-fold induction while offspring from the reciprocal experiment show no changes. Cesarean sections on day E18.5 followed by cross-fostering proved transmission to be mediated predominantly via lactation (F1 hepatic Cyp2b10 induction 3000-fold) and only to a minor part via intra-uterine exposure (300-fold). This mechanism is consistent with the absence of induction transmission via the male germline.

To analyze if TCPOBOP leads to functional consequences in drug metabolism of F0 and F1 generation, we conducted *in vivo* zoxazolamine paralysis assays taken as a functional test for Cyp2b10 catalytic activity. In both TCPOBOP-pretreated F0 and in their F1 descendants, the induction reduced the duration of paralysis evoked by zoxazolamine by >50%. The characterization of cross-generational TCPOBOP-mediated effects on other processes controlled by CAR such as energy and bone metabolism is in progress. First tests indicate a transmission of anabolic effects on bone, as evidenced by the induction of serum osteocalcin expression by 45% in 12-weeks-old offspring. In summary, the CAR-mediated Cyp2b10 induction by TCPOBOP is transmitted to the offspring mainly via lactation, resulting in lasting phenotypic consequences in drug and bone metabolism. The effects of similarly lipophilic drugs and anthropogenic environmental pollutants are currently being investigated. Such compounds could affect offspring despite discontinuation of intake or exposure well ahead of pregnancy.

045

Combined treatment of aged rats with donepezil and the Ginkgo extract EGb 761[®] enhances learning and memory superiorly to monotherapy

L. Blümel¹, B. Bert², J. Brosda¹, H. Fink¹, M. Hamann³

¹Institut für Pharmakologie und Toxikologie, Fachbereich Veterinärmedizin, Berlin,

Germany

²Bundesinstitut für Risikobewertung (BfR), Zentralstelle zur Erfassung und Bewertung

von Ersatz- und Ergänzungsmethoden zum Tierversuch, Berlin, Germany

³Institut für Pharmakologie und Toxikologie, Fachbereich Veterinärmedizin, Gießen,

Germany

Age-related cognitive decline can eventually lead to dementia, the most common mental illness in elderly people and an immense challenge for patients, their families and caregivers. Cholinesterase inhibitors constitute the most commonly used antedementia prescription medication. The standardized *Ginkgo biloba* leaf extract EGb 761[®] is approved for treating age-associated cognitive impairment and has been shown to improve the quality of life in patients suffering from mild dementia. A clinical trial with 96 Alzheimer's disease patients indicated that the combined treatment with donepezil and EGb 761[®] had less side effects than donepezil alone (Yancheva et al., 2009). In an animal model of cognitive aging, we compared the effect of combined treatment with EGb 761[®] or donepezil monotherapy and vehicle.

We compared the effect of chronic treatment (15 days of pretreatment) with donepezil (1,5 mg/kg p. o.), EGb 761[®] (100 mg/kg p. o.), or the combination of the two drugs, or vehicle in 18 – 20 month old male OFA rats. Learning and memory performance were assessed by Morris water maze testing, motor behavior in an open field paradigm. In addition to chronic treatment, the substances were administered orally 30 minutes before testing. Compared to the first day and to the control group, only the combination group showed a significant reduction in latency to reach the hidden platform on the second day of testing. Moreover, from the second day of testing onwards, the donepezil, the EGb 761[®] and the combination group required less time to reach the hidden platform compared to the first day. The control group did not reach the same latency reduction until day three. There were no effects on motor behavior. These results suggest a superiority of the combined treatment of donepezil with EGb 761[®] compared to monotherapy.

Literature: Yancheva, S., Ihl, R., Nikolova, G., Panayotov, P., Schlaefke, S., & Hoerr, R. (2009). Ginkgo biloba extract EGb 761(R), donepezil or both combined in the treatment of Alzheimer's disease with neuropsychiatric features: a randomised, double-blind, exploratory trial. *Aging Ment Health*, 13(2), 183-190.

Supported by Dr. Willmar Schwabe GmbH & Co. KG.

046

Handling of FDA-approved drugs by the organic anion transporter 3 (OAT3)

M. Henjakovic^{1,2}, Y. Hagos¹, G. Burckhardt¹, B. Burckhardt¹

¹Institut für Vegetative Physiologie und Pathophysiologie, Göttingen, Germany

²Klinik I für Innere Medizin, Köln, Germany

Question/Aim: Recently the FDA-approved drugs, tyrothostin AG 1478, ceefourin 1, dantrolene, glafenine, nalidixic acid, and prazosine, were identified as multidrug resistance protein 4 (MRP4) inhibitors (Cheung et al. *Biochem Pharmacol* 93:380-388, 2015). Because many of these compounds are zwitterions or organic anions, they could interact with organic anion transporters (OATs) of the SLC22 family. Especially, OAT3 with its broad substrate specificity could be a transporter interacting with these compounds.

Methods: HEK293 cells stably transfected with human OAT3 were used and the uptake of the OAT3 reference substrate, estrone-3-sulfate (ES), was measured in the absence and presence of tyrothostin AG 1478, ceefourin 1, dantrolene, 5-OH dantrolene, glafenine, nalidixic acid, prazosine, and MK571. In all measurements 10 nM of [³H]ES was used.

Results: In OAT3 transfected HEK293 cells, the uptake ES was inhibited by all the above mentioned drugs to more than 50% at a concentration of 100 µM. As compared to tyrothostin AG1478, ceefourin 1, glafenine, nalidixic acid, and prazosine, dantrolene and MK571 were the most potent inhibitors with IC₅₀ values of 0.83 ± 0.51 and 1.6 ± 0.2 µM, respectively. Because dantrolene is the only drug for the specific treatment of malignant hyperthermia, a life-threatening inborn sensitivity of skeletal muscles to volatile anaesthetics, the interactions of dantrolene and its major metabolite, 5-hydroxy dantrolene (5-OH dantrolene), were investigated in more detail. 5-OH dantrolene inhibited ES uptake by OAT3 with an IC₅₀ of 1.1 ± 0.2 µM. Dixon plots revealed competitive inhibition between the ES and dantrolene and 5-OH dantrolene, and the determined K_i values of 0.69 ± 0.06 and 1.37 ± 0.31 µM match the IC₅₀ values. These

values are well below the plasma concentrations (3-28 µM; Just et al. Expert Opin Emerging Drugs 20: 161-164, 2015) observed in patients treated with dantrolene.

Conclusions: Although not yet proven directly, OAT3 may be involved in renal secretion of dantrolene and 5-OH dantrolene by mediating the first step, i.e. the uptake across the basolateral membrane of proximal tubule cells. The second step, the release of these compounds into the urine across the luminal membrane, is possibly mediated by MRP4. Since OAT3 was also detected in the cytoplasmic membrane of skeletal muscle cells (Takeda et al. Europ. J. Pharmacol. 483: 133-138, 2004), dantrolene may reach its target, the intracellular ryanodine receptor, RyR1, by influx through OAT3, where it inhibits calcium efflux by RyR1 thereby preventing severe muscle contraction and malignant hyperthermia. This assumption, however, awaits a direct demonstration of dantrolene transport by OAT3.

In addition, we identified, besides dantrolene and 5-OH dantrolene, several further FDA-approved drugs such as tyrphostin AG 1478, ceefourin 1, glafenine, nalidixic acid, and prazosine, as inhibitors of ES uptake by OAT3.

047

AGTR2 und SIGMAR1 – Association of genetic polymorphisms to neuropathic pain measures

J. Sachau¹, H. Bruckmüller¹, M. Kähler¹, R. Baron², A. Binder², S. Haenisch¹, I. Casorbi

¹Institute of Experimental and Clinical Pharmacology, Kiel, Germany

²University Hospital, Division of Neurological Pain Research and Therapy, Department of Neurology, Kiel, Germany

Background: Drugs used for treatment of neuropathic pain, which arises after dysfunction or lesion of the nervous system, have often limited efficacy and are associated with adverse side effects. Therefore, different ion channels and receptors of the sensor nervous system are intensively investigated as potential new targets in the treatment of neuropathic pain. New candidates are the angiotensin-type 2-receptor (AGTR2) and the sigma-1 receptor (σ_1R , SIGMAR1). Recently, AGTR2 expression on sensory neurons was shown and thus its possible involvement in the development of pain. The chaperon protein SIGMAR1 is expressed in various compartments in human cells causing increased neuronal excitability and pandering pain development by different pathways. Based on these data AGTR2- and SIGMAR1-antagonism are assumed to decrease pain after lesion of nerve fibres.

So far, it is unknown if genetic variants in AGTR2 and SIGMAR1 are associated with different sensory pain qualities in patients suffering from neuropathic pain. Therefore, the aim of this study was to analyse the association of single nucleotide polymorphisms (SNPs) in these two receptors to quantitative measures of this syndrome.

Methods: 241 patients with neuropathic pain and 253 healthy controls were included in this study. All patients were phenotypically characterized using standardized testing of different sensory qualities (QST-parameters) and grouped into clusters (cluster 1 gain; cluster 2 loss of function). Pyrosequencing and TaqMan assays are used for genotyping of five SNPs in SIGMAR1 (rs10814130; rs1799729; rs1800866; rs11559048; rs7865100) and four in AGTR2 (rs5193; rs5194; rs1403543; rs11091046). Statistical analysis was executed using SPSS 22.0. Genotype frequencies were analyzed using Chi-square test. In patients, differences in QST parameters and genotype were calculated by Kruskal-Wallis test. A p-value < 0.05 was considered as statistically significant.

Results: So far, SIGMAR1 rs1799729 and rs10814130 were analyzed showing Hardy-Weinberg equilibrium and in linkage disequilibrium ($p < 0.01$). There was no significant difference in genotype distribution between patients and controls. The minor allelic frequency was 15,618%. Carriers of at least one variant allele of SIGMAR1 rs10814130 and rs1799729 had an increased heat pain threshold (HPT) ($p = 0.026$) as well as less paradoxical heat sensation (PHS) ($p = 0.034$) than carriers of two wildtype alleles. Patients belonging to cluster 1 who carried at least one variant allele showed decreased wind up ratios (WUR) ($p = 0.046$). In patients belonging to cluster 2, a reduced thermal sensory threshold (TSL) ($p = 0.043$) as well as a decreased cold detection threshold (CDT) ($p = 0.037$) were observed for carriers of at least one variant allele. In addition, in cluster 2 vibration detection threshold (VDT) ($p = 0.035$) was elevated compared to carriers of two wildtype alleles.

Conclusion: The results indicated an association of the two analyzed SIGMAR1 SNPs mainly with changes in temperature perception in neuropathic pain patients. Therefore it would be of interest to further investigate the influence of these SNPs on SIGMAR1 function and whether such variants have any impact for the response for treatment of neuropathic pain.

048

Oxidative-stress-mediated teratogenesis and the role of folate

Y. H. Tran¹, J. Bergman², M. Bakker^{2,3}, H. Groen⁴, B. Wilffert^{5,1}

¹University of Groningen, Department of Pharmacy, Groningen, Niederlande

²University of Groningen, University Medical Center Groningen, Eurocat Registration

Northern Netherlands, Department of Genetics, Groningen, Niederlande

³University of Groningen, University Medical Center Groningen, Department of

Obstetrics and Gynecology, Groningen, Niederlande

⁴University Medical Center Groningen, University of Groningen, Department of Epidemiology, Groningen, Niederlande

⁵University of Groningen, University Medical Center Groningen, Department of Clinical Pharmacy & Pharmacology, Groningen, Niederlande

Background: Oxidative stress (OS) is one of the underlying teratogenic mechanisms of medical drugs. Folate is indirectly involved in OS because of its role in the methylation steps in the detoxification of xenobiotics and in the repair of OS-induced DNA damage. Our study was to explore the associations of exposure to OS-inducing drugs in the first trimester of pregnancy and groups of birth defects. Additionally, drugs with folate antagonism (FAA) and folic acid supplementation in the periconceptional period (FOLIC) were investigated.

Methods: A case control study was conducted, using the Eurocat NNL database (birth years 1997-2013). Cases were offspring with a group of birth defects, either isolated or with other defects, not associated with genetic disorders. Two control groups were

controls 1 with other defects and controls 2 with genetic disorders. All drugs used in the first trimester were identified from the database, and were cross-referenced against previously compiled lists of drugs with reactive intermediates and drugs with FAA. Drugs with reactive intermediates, with systemic absorption and with a daily dose ≥ 50 mg were considered OS-inducing drugs. When there was an association between OS-inducing drugs and a group of birth defects, we further investigated two different FAA exposure categories: concurrent exposure to both OS-inducing drugs and FAA drugs (OS+/FAA+) and exposure to OS-inducing drugs only (OS+/FAA-). When the number of subjects allowed (at least five cases/controls were exposed), we examined the role of FOLIC. Odds ratios (ORs) with 95% confidence intervals were adjusted for maternal smoking and alcohol use in the first trimester in controls 1 and additionally adjusted for maternal age in controls 2.

Results: A total of nine groups of birth defects were investigated. Only nervous system defects were associated with OS-inducing drugs. Exposure rates were 65/464 (14.0%) for cases, 512/6033 (8.5%) for controls 1 and 130/1564 (8.3%) for controls 2 and adjusted ORs (95% CIs) were 1.71 (1.29-2.26) and 1.77 (1.27-2.46), respectively. This association was unchanged when we examined OS+/FAA+ and OS+/FAA- separately. The OS+/FAA+ category, however, had slightly higher OR values than the OS+/FAA- (2.41 vs. 1.61 for controls 1, and 2.55 vs. 1.67 for controls 2). Because of the low number of exposed subjects, we could only examine FOLIC in relation to OS+/FAA-. Using OS-/FAA-/FOLIC+ as reference, we found the highest risk with OS+/FAA-/FOLIC- and a lesser magnitude with OS+/FAA-/FOLIC+ (ORs being 2 and 1.6 times respectively for both controls).

Conclusion: Our study suggests an increased risk of having a child with nervous system defects in mothers who were exposed to OS-inducing drugs during pregnancy, and a potential risk reduction with FOLIC.

DNA-damage and –repair

049

Inhibition of the small Rho-GTPase Rac1 for the prevention of topoisomerase II-poison-induced DNA double-strand break formation: Involvement of the actin cytoskeleton and mitochondrial type II topoisomerases

C. Henninger¹, I. Mancinella¹, A. Wagner¹, A. Reck¹, G. Fritz¹

¹Universitätsklinikum Düsseldorf, Institut für Toxikologie, Düsseldorf, Germany

Background: Inhibition of Rho-GTPases with statins as well as specific inhibition of the small GTPase Rac1 protects non-transformed cells from topoisomerase II-(top2)-poison-induced cleavable complex formation and thereof derived DNA double-strand breaks. This effect rests at least partially on Rac1-mediated regulation of topoisomerase II activity. However, the link between Rac1 and top2-poisoning is only poorly understood. Furthermore, it is unclear whether mitochondrial or nuclear type II topoisomerases are the most relevant target for top2-poison-induced cytotoxicity. Here, we investigated the relevance of Rac1-regulated actin cytoskeleton integrity as well as mitochondrial integrity in top2-poison-induced DNA damage responses as well as cytotoxicity under situation of Rac1 inhibition.

Methods: Since endothelial cells are the first barrier for any kind of systemically administered chemicals and cardiomyocytes are particularly sensitive to anthracyclines, endothelial cells (H5V) as well as cardiomyocytes (H9c2) were chosen as *in vitro* model systems for top2-poisoning. The cells were pre-treated with Rac1 inhibitors, statins or actin cytoskeleton disruptors and were subsequently treated with the topoisomerase II poisons doxorubicin or etoposide. To compare the levels of induced DNA damage, γ H2AX foci quantifications as well as the comet assay were employed. Actin disruption was visualized by phalloidin-FITC staining. To be able to detect relevant changes in mitochondrial mass or integrity, high doses of top2-poisons had to be used in both cell lines. Changes in mitochondrial homeostasis as well as integrity were detected by the JC1-assay, mitotracker assay as well as ATP-assay. Additionally, PCR- and gelelectrophoresis-based methods were used for detecting mitochondrial DNA damages. Selected components of the DNA damage response machinery as well as factors of mitochondrial homeostasis were detected by Western Blot.

Results: Disruption of the integrity of the actin cytoskeleton attenuated the DNA damage response to a similar extent as seen by Rac1 inhibition, pointing to a role of actin filaments in the DNA damage response after genotoxic insults. The actin cytoskeleton seems to participate in genotoxin-induced DNA damage, -repair or in the DNA damage response as reflected by reduced numbers of nuclear H2AX-foci as well as the comet assay after treatment with doxorubicin. This was not related to nuclear import or export of doxorubicin. Disturbance of mitochondrial homeostasis or integrity was only detectable at high doses of topoisomerase II poisons. This was largely unaffected by pre-treatment with statins or Rac1-inhibitor. Top2-poison-induced raise in mitochondrial mass was slightly enhanced by the Rac1-inhibitor and statins. Interestingly, inhibition of Rac1 counteracted doxorubicin-induced phosphorylation of the AMP-kinase in endothelial cells but not in cardiomyocytes.

Conclusion: Mitochondrial toxicity seems to play only a minor role in top2-poison-induced cytotoxicity in H9c2 and H5V cells. The data point to a role of Rac1-regulated filamentous (nuclear?) actin in the DNA repair and/or DNA damage response after treatment with top2-poisons.

050

PARP1 is essential for oxidative stress-induced relocalization of WRN from nucleoli to sites of DNA damage

S. Veith¹, A. Schink¹, A. Bürkle¹, A. Mangerich¹

¹Universität Konstanz, Molekulare Toxikologie, Konstanz, Germany

Poly(ADP-ribose) polymerase 1 (PARP1) and the RecQ helicase Werner syndrome protein (WRN) are important caretakers of the genome. They physically interact with each other and are both localized in the nucleus and in particular in the nucleoli. Both participate in various overlapping mechanisms of DNA metabolism, in particular genotoxic stress response and DNA repair [1]. Previously, we and others have shown in biochemical studies that enzymatic functions of WRN are regulated by PARP1 as well as by non-covalent poly(ADP-ribose)-WRN interaction [2-4]. Furthermore, pharmacological PARP inhibition as well as a genetic *PARP1* ablation in HeLa cells

alters the recruitment kinetics of WRN to sites of laser-induced DNA damage [5]. Here we report a novel role for PARP1 and poly(ADP-ribose)ylation in the regulation of WRN's subnuclear spatial distribution upon induction of oxidative stress. We could verify previous reports that WRN is transiently released from nucleoli upon induction of oxidative stress, camptothecin (CPT) treatment, and laser-induced DNA damage in a time-dependent manner. While, CPT-induced translocation appears to be a PARP-independent process, our results reveal that upon H₂O₂-induced oxidative stress, PARP1 is essential for the translocation of WRN from the nucleoli to the nucleoplasm. PARP1 activity only partially contributes to WRN release from nucleoli, underlining the importance of a direct WRN-PARP1 interaction for subnuclear WRN redistribution. Furthermore, we identified a novel PAR-binding motif within the WRN sequence that is located in its RQC domain, which also harbors the binding site for PARP1 and is necessary for WRN's nucleolar localization under non-stress conditions. Currently, we are testing corresponding WRN mutants to analyze if this region is responsible for the PARP1-dependent release of WRN from nucleoli to sites of DNA damage. In conclusion, we provide novel insight into the role of PARP1 in WRN's spatio-temporal regulation in the nucleus during the oxidative stress response.

1. Veith, S. and A. Mangerich, *RecQ helicases and PARP1 team up in maintaining genome integrity*. Ageing Research Reviews, 2015. **23**, Part A(0): p. 12-28.
2. Popp, O., et al., *Site-specific noncovalent interaction of the biopolymer poly(ADP-ribose) with the Werner syndrome protein regulates protein functions*. ACS Chem Biol, 2013. **8**(1): p. 179-88.
3. Mangerich, A., et al., *Quantitative analysis of WRN exonuclease activity by isotope dilution mass spectrometry*. Mech Ageing Dev, 2012. **133**(8): p. 575-9.
4. von Kobbe, C., et al., *Poly(ADP-ribose) polymerase 1 regulates both the exonuclease and helicase activities of the Werner syndrome protein*. Nucleic Acids Res, 2004. **32**(13): p. 4003-14.
5. Khadka, P., et al., *Differential and concordant roles for PARP1 and poly(ADP-ribose) in regulating WRN and RECQL5 activities*. Molecular and Cellular Biology, 2015: p. MCB.00427-15.

051

Enhanced transfection-based assay for DNA repair and epigenetic research

A. Khobta^{1,2}

¹Institut für Pharmazie und Biochemie, Johannes Gutenberg Universität Mainz, Mainz, Germany

²Johannes Gutenberg University of Mainz, Institute of Pharmacy and Biochemistry, Mainz, Germany

Host-cell reactivation (HCR) is an assay used to determine DNA repair capacity of cells. In its canonical layout, the test utilised a virus or a plasmid with a marker gene, inactivated by UV-damage [1,2]. Among the infected or transfected host cells types, only those with functional DNA repair pathway would re-activate the damaged DNA, thus providing a rationale for identification of DNA repair genes in the mutant screens. An obvious advantage of HCR is that repair can be measured in cells that have not been exposed to a damaging agent. However, because of multiple variables of the damage generation, transfection and interpretation of results, the assay has been hard to harmonise and develop into a widely accepted quantitative DNA repair assay.

Over the last years, my team has developed and validated several major improvements of the mammalian HCR assay. Exploiting sequence-specific nicking endonucleases and customised design of the reporter vectors, we proposed an innovative and very efficient technique for incorporation of synthetic oligonucleotides, containing single structurally defined DNA base and backbone modifications, into desired gene elements [3]. This ad hoc approach allows examination of the repair in a stand-specific manner and at single nucleotide resolution. We efficiently applied HCR in its new layout for measurement of the nucleotide excision repair of various DNA adducts. Moreover, we demonstrated that the enhanced HCR assay can differentiate between the transcription-coupled (TC-NER) and global genome (GG-NER) subpathways of NER [4]. We further obtained new significant insights into the lesion-specific mechanisms of base excision repair of several endogenously occurring aberrant DNA bases [5-7] and plan to adapt the assay to the detection of mismatch repair and translesion DNA synthesis. In addition to the applications in the DNA repair field, the enhanced HCR assay provides a tool for investigation of the dynamics and transcriptional impact of the regulatory DNA bases 5-methylcytosine and 5-hydroxymethylcytosine as well as their derivatives (5-formylcytosine and 5-carboxycytosine).

1. Rupert C and Harm W (1966) *Adv Radiat Biol* 2:1-81
2. Protic-Sabljic M and Kraemer KH (1985) *Proc Natl Acad Sci U S A*;82: 6622-6626
3. Lühnsdorf B, et al. (2012) *Analytical Biochemistry* **425**: 47-53
4. Kitsera N, et al. (2014) *PLoS One* **9**: e94405
5. Kitsera N, et al. (2011) *Nucleic Acids Research* **39**: 5926-5934
6. Allgayer J, et al. (2013) *Nucleic Acids Research* **41**: 8559-8571
7. Lühnsdorf B, Epe B, Khobta A (2014) *The Journal of Biological Chemistry* **289**: 22008-22018

052

BPDE activates nucleotide excision repair and adaptive response on the expense of induced mutation frequency

M. Christmann¹, C. Castillo¹, R. Kitzinger¹, C. Berac¹, S. Allmann¹, T. Sommer¹, D. Aasland¹, B. Kaina¹, M. T. Tomicic¹

¹University Medical Center Mainz, Department of Toxicology, Mainz, Germany

A coordinated and faithful DNA damage response is of central importance for maintaining genomic integrity and cell survival. Transcriptional activation of DNA repair genes is an important regulatory mechanism contributing to the adaptation of cells to genotoxic stress and protection against genotoxin-mediated cell death. Here we show that exposure to a low dose of benzo(a)pyrene 9,10-diol-7,8-epoxide (BPDE), the active metabolite of benzo(a)pyrene (B[a]P), which represents the most important carcinogen formed by incomplete combustion during food preparation and smoking, causes upregulation of several DNA repair genes. Combined induction of the nucleotide excision repair (NER) genes *DD22*, *XPC*, *XPF* and *XPB* enhanced repair activity and protected cells against a subsequent BPDE exposure. Furthermore induction of the

translesion polymerase POLH was also involved in protection against BPDE-induced apoptosis, however led to an enhanced mutation frequency in the surviving cells. Activation of these DNA repair pathways was also observed upon exposure to B[a]P and *in vivo* in buccal cells of male individuals upon smoking, indicating that this mechanism may be involved in the formation of smoking-related cancers. Altogether, we could show that low-dose BPDE exposure activates a complex network of transcriptional alterations, leading to protection against cell death, at the cost of increased mutation frequency, highlighting the danger of occasional smoking.

053

Analyzing structure-function relationships of PARP1 during genotoxic stress response by reconstituting HeLa PARP1 knock-out cells with artificial and natural PARP1 variants

L. Rank¹, S. Veith¹, E. Gwosch², J. Demgenski¹, M. Ganz², M. Jongmans³, C. Vogel¹, A. Fischbach¹, S. Bürger⁴, A. Stier¹, S. Beneke¹, J. Fischer¹, C. Renner¹, R. Kuiper², A. Bürkle¹, E. Ferrando-May², A. Mangerich¹

¹Universität Konstanz, Lehrstuhl für molekulare Toxikologie, Konstanz, Germany

²Universität Konstanz, Bioimaging Center, Konstanz, Germany

³University Medical Centre, Department of human genetics, Nijmegen, Niederlande

⁴Universität Konstanz, FlowKon FACS Facility, Konstanz, Germany

Poly(ADP-ribose)ylation (PARYlation) is an essential posttranslational modification with the biopolymer poly(ADP-ribose) (PAR). The reaction is catalyzed by poly(ADP-ribose) polymerases (PARPs) and plays key roles in cellular physiology and stress response by regulating physico-chemical properties of target proteins. Of the 17 members of the human PARP gene family, at least four have been shown to exhibit PAR-forming capacity. Upon DNA damage PARP1 is catalytically activated and is thought to contribute to the bulk of the cellular PAR formation. PARP inhibitors are currently being tested in clinical cancer treatment, in combination therapy, or as monotherapeutic agents by inducing synthetic lethality (Mangerich and Bürkle 2011, Mangerich and Bürkle 2015).

Here we generated a genetic knock out of *PARP1* in one of the most widely used human cell systems, i.e. HeLa *PARP1* KO cells, via TALEN-mediated gene targeting and characterized these cells with regards to PARYlation metabolism and genotoxic stress response. Furthermore, by reconstituting HeLa *PARP1* KO cells with a series of artificial and natural PARP1 variants, we analyzed structure-function relationships of PARP1 in a cellular environment without interfering with endogenously expressed WT-PARP1.

We confirmed that the PARP1E988K mutant exhibits mono-ADP-ribosylation activity and extended previous reports by demonstrating that the PARP1L713F mutant is constitutively active in a cellular environment, leading to high cellular PAR levels even in unchallenged cells. Additionally, both mutants exhibited significantly altered recruitment and dissociation kinetics at sites of laser-induced DNA-damage, which can partially be attributed to non-covalent PARP1-PAR interaction via at least one specific PAR binding motif located in zinc finger 2 of PARP1. Expression of both artificial mutants led to distinct cellular consequences, caused by the altered cellular biochemistry. While the expression of PARP1L713F itself triggered apoptosis, PARP1E988K expression led to a strong G2-arrest during cell cycle and sensitized cells to camptothecin treatment. Interestingly, pharmacological PARP inhibition with ABT888 mitigated effects of the E988K mutant, suggesting distinct functions of mono-ADP-ribosylation.

Finally, by reconstituting *PARP1* KO cells with a natural cancer-associated PARP1 SNP variant (V762A), as well as a newly identified PARP1 mutant present in a patient of pediatric colorectal carcinoma (F304L-V762A), we demonstrate, that these variants exhibit altered biochemical and cellular properties, potentially supporting carcinogenesis. Together, this study establishes a novel model to study PARP1-dependent PARYlation during genotoxic stress response and reveals new insight into the structure-function relationships of artificial as well as natural PARP1 variants in a cellular environment, with implications for PARP research in general.

Mangerich, A. and A. Bürkle (2011). "How to kill tumor cells with inhibitors of poly(ADP-ribose)ylation." *Int J Cancer* **128**(2): 251-265.

Mangerich, A. and A. Bürkle (2015). *Multitasking Roles for Poly (ADP-ribose) ation in Aging and Longevity. PARP Inhibitors for Cancer Therapy*, Springer: 125-179.

054

The Wilms Tumor 1 protein protects leukemic cells from cytotoxic replicative stress

O. H. Krämer¹, N. Mahendrarajah¹, C. M. Reichardt², C. Englert², J. Hartkamp³

¹Institut für Toxikologie Universitätsmedizin der Johannes Gutenberg-Universität Mainz, Mainz, Germany

²Leibniz Institute for Age Research/Fritz-Lipmann-Institute, Molecular Genetics, Jena, Germany

³Institute of Biochemistry and Molecular Biology, Medical School, RWTH Aachen, Aachen, Germany

Leukemic cells frequently overexpress the transcription factor Wilms Tumor 1 (WT1) and the persistence of WT1 expression after chemotherapy indicates remaining leukemic stem cells. Hydroxyurea induces replicative stress by its ability to inhibit ribonucleotide reductase, an enzyme that catalyzes the synthesis of dNTPs from NTPs. We demonstrate that the expression levels of WT1 determines the extent of DNA damage and apoptosis in a panel of leukemic cells treated with hydroxyurea. Accordingly, inhibiting apoptosis through chemical inhibition of caspases or by overexpression of mitochondrial anti-apoptotic BCL proteins prevents the hydroxyurea-induced depletion of WT1 and cell death. In addition, we show that an RNA interference-mediated elimination of WT1 sensitizes leukemic cells to the pro-apoptotic and DNA damaging effects of hydroxyurea. Furthermore, such a loss of WT1 suppresses hydroxyurea-induced erythroid differentiation. Pharmacological approaches that diminish WT1 also sensitize cells to hydroxyurea. These include the tyrosine kinase inhibitor (TKI) imatinib or epigenetic modifiers belonging to the histone deacetylase inhibitor (HDACi) group. Thus, an inhibition of WT1 is therapeutically exploitable for a targeting approach against leukemic cells undergoing replicative stress. Our novel findings reveal that WT1 is a novel biological target of hydroxyurea and they suggest that WT1 has a previously unrecognized ability to prevent DNA damage when replication forks halt and eventually collapse.

GPCR receptor pharmacology

055

Comparison of β_1 - and β_2 -adrenoceptor (AR) signalling using FRET-based assays analyzed with new multichannel fluorescence detectors

H. Lemoine¹, A. Ballweg¹, T. Pfeifer¹, C. Schmidt^{1,2}, F. Boege², V. Nikolaev³
¹UKD Düsseldorf, Inst. für Lasermedizin, Düsseldorf, Germany
²Inst. für Klinische Chemie, Düsseldorf, Germany
³Inst. f. Exp. Cardiovascular Research, Hamburg, Germany

FRET (fluorescence resonance energy transfer)-based cell assays were developed to directly monitor receptor activation and receptor-stimulated cAMP response. Mutant β_1 AR were generated by insertion of cyan and yellow fluorescent proteins (CFP and YFP) into the third intracellular loop and the C-terminus, respectively (Bornholz et al., Cardiovasc Res 97:472, 2013) and stably transfected to HEK 293 cells (Hek β_1 -Fret). To monitor the cAMP response the Epac1-based FRET sensor of cAMP, was stably transfected alone (HekWT-E1) and together with a moderate level of native β_1 AR to HEK293 cells (Hek β_1 -E1; Nikolaev et al. JACC 50: 423, 2007). FRET-activity was measured with recently developed fluorescence detectors (12 channels) equipped with fast semiconductor technology, avoiding any movable optical and mechanical parts, using 438 nm for excitation and 483/540 nm for the emission ratio. Cells were cultivated in 96-format 12-well strips, incubated in physiological HEPES-buffered salt solution and treated with β AR agonists of different selectivity and affinity to determine their β AR-subtype preference. Catecholamines tested in Hek β_1 -Fret cells exhibited EC₅₀-values (-log, M) which matched K_D-values (-log, M) known from native heart receptor membranes (isoprenaline, ISO: 6.9±0.1, adrenaline 5.7±0.1, noradrenaline 6.2±0.1). β AR-expression levels were controlled by radioligand binding with [³H]-(-)-CGP12,177 resulting in different densities of ~4x10⁵ and ~1.4x10⁴ receptors/cell in Hek β_1 -Fret and Hek β_1 -E1, respectively, whereas in HekWT-E1 cells only ~1000 β_1 AR were found. Surprisingly, the low level of β AR in HekWT-E1 cells allowed the measurement of the action of β_2 -sympathomimetics (β_2 SYM), e.g. fenoterol, thereby amplifying receptor binding (pK_D~6.7) to an effective regulation of FRET activity in the presence of 0.06 mM IBMX (pEC₅₀~8.3±0.1), nearly matching the ~100-fold amplification of ISO (pK_D~6.9; pEC₅₀~8.9). In order to determine β_1 AR-mediated side effects of β_2 SYM, Hek β_1 -E1 cells characterized by a 14-fold higher level of β_1 AR over β_2 AR were assayed for FRET activity. Fenoterol maximally inhibited FRET activity with a pEC₅₀~8.4 whereas the high affinity β_2 SYM salmeterol acted a partial agonist (~75% of Iso maximum, pEC₅₀~8.6), both compounds being rather insensitive against the highly effective β_1 AR-blockade with 1 μ M CGP 20,712 A. For that reason Hek β_1 -Fret cells were used characterizing fenoterol as partial agonist (~25%) whereas salmeterol activated less than 10% of maximum receptor activation by ISO. Thus, it has to be concluded that the low level of effectively coupled WT- β_2 AR present in Hek β_1 -E1 cells precludes the exact determination of β_1 AR-mediated side effects of β_2 SYM, and that CFP/YFP labelled receptors have to be used for the determination of the subtype specific intrinsic activity of an agonist.

056

Phosphorylation of the human β_1 -adrenoceptor

L. Hinz¹, A. Ahles¹, B. Ruprecht², B. Küster², S. Engelhardt^{1,3}
¹Technische Universität München, Institute of Pharmacology and Toxicology, Munich, Germany
²Technische Universität München, Chair of Proteomics and Bioanalytics, Freising, Germany
³DZHK (German Center for Cardiovascular Research), partner site Munich Heart Alliance, Munich, Germany

G protein-coupled receptors form the largest group of mammalian surface receptors. They account for about one third of all drug targets. Their regulation from desensitization to internalization and alternative signal transduction is largely dependent on phosphorylation of intracellular serine and threonine residues of the activated receptor. Even though the β_1 -adrenoceptor is of tremendous importance in a number of diseases its phosphorylation remains poorly understood. We addressed this question in a qualitative and quantitative way. By using radioactive phosphorylation assays and mass spectrometry, we were able to elucidate the phosphorylation pattern of the human β_1 -adrenoceptor in vitro. We identified ten previously unknown phosphorylation sites in the third intracellular loop and the receptor's C-terminus. Labeling HEK293 cells with stable heavy isotopes (SILAC) lead to the discovery of a stimulation-dependent regulation of several of these phosphorylation sites. Furthermore, mutagenesis studies in stably transfected HEK293 cells revealed the impact of phosphorylation for arrestin binding and internalization of the receptor. Fluorescence resonance energy transfer experiments with β_1 -adrenoceptor variants carrying point mutations of putative phosphorylation sites identified two C-terminal phosphosites that determine arrestin recruitment. Our current goal is to further investigate the functional implications of these newly identified phosphorylation sites on downstream signal transduction, with an emphasis on the MAP kinase pathway.

057

A moderate increase in arrestin affinity to the β_2 -adrenergic receptor is sufficient to induce arrestin internalization.

D. Zindel¹, A. J. Butcher², S. Al-Sabah³, P. Lanzerstorfer⁴, J. Weghuber⁴, A. B. Tobin², M. Bünemann¹, C. Krasel¹
¹Philipps-Universität Marburg, FB Pharmazie, Institut für Pharmakologie und Klinische Pharmazie, Marburg, Germany
²University of Leicester, MRC Toxicology Unit, Leicester, United Kingdom
³Kuwait University, Dept. of Pharmacology and Toxicology, Kuwait, Kuwait
⁴University of Applied Sciences Upper Austria, Wels, Austria

The homologous desensitization of G-protein-coupled receptors is a two-step process. Initially, G-protein-coupled receptor kinases phosphorylate agonist-occupied receptors which are subsequently bound by arrestins. In many cases, the resulting receptor-arrestin complex is then internalized via clathrin-coated pits. Dependent on the identity of the receptor and the ligand, the complex between receptor and arrestin may exist only in the proximity of the plasma membrane or internalize into the cell interior. We constructed mutants of the β_2 -adrenergic receptor carrying three additional Serine residues in various positions at the C-terminal tail. One of these mutants which carried the Serine residues in close proximity to the endogenous GRK phosphorylation sites (β_2 AR-SSS) showed increased isoprenaline-stimulated phosphorylation and differences in arrestin-3 affinity and trafficking. The affinity of arrestin-3 to the receptor was measured by fluorescence resonance energy transfer (FRET) between the receptor and arrestin-3 and by two-color fluorescence recovery after photobleaching (FRAP). In the FRET assay, arrestin-3 dissociation from the β_2 AR-SSS receptor upon agonist washout was prolonged approximately two-fold compared to the wild-type receptor. FRAP was performed with an N-terminally tagged receptor immobilized with an antibody against the N-terminal tag either in solution or on a micropatterned surface. In these assays, the recovery of arrestin-3 into the bleached region was prolonged between two- and four-fold for the β_2 AR-SSS receptor compared to the wild-type. Even though this two- to four-fold increase in affinity seemed rather modest, it resulted in the trafficking of receptor-arrestin complexes to the early endosome whereas the wild-type receptor interacted only transiently with arrestin at the plasma membrane. Furthermore, the increased affinity of arrestin led to more efficient internalization of the β_2 AR-SSS compared to the wild-type receptor. However, recycling to the plasma membrane after agonist washout was very similar for both receptors. We conclude that even a modest change in affinity between a G-protein-coupled receptor and arrestin can lead to substantial alterations in arrestin trafficking which in turn may have effects on cellular signaling.

058

mAChR – G protein dissociation kinetics reflect coupling efficiencies and allow quantification of G protein subtype selectivity

O. Prokopets^{1,2}, H. Lemoine², M. Bünemann¹
¹Philipps-Universität, Institut für Pharmakologie und klinische Pharmazie, Marburg, Germany
²Heinrich-Heine Universität, Institute für Lasermedizin, Düsseldorf, Germany

Despite recent structural research allow for better understanding of GPCR structure, the crucial aspects of the selectivity mechanism of receptor – G protein subtype coupling remain unresolved. Based on the hypothesis that the affinity of the ternary complex (agonist/GPCR/G-Protein) in the nucleotide-free state determines the selectivity of GPCR-G protein coupling, we set out to measure GPCR-G protein interaction in membranes of single cells. In order to quantify the affinity of G α -subunit towards GPCRs in single cell, we determined the lifetime of the receptor-G protein complex in living cells upon agonist withdrawal under conditions of GTP-depletion. Therefore, we utilized Förster resonance energy transfer (FRET) based assays to study interactions between fluorescent muscarinic receptors and heterotrimeric G proteins in single permeabilized HEK293T cells transfected with the appropriate cDNAs. Here we focused on muscarinic M1-, M2-, and M3-receptors and characterized the kinetics of agonist-induced binding of Go β 1- and Gq/11-proteins to muscarinic receptors and their subsequent dissociation in the absence of nucleotides. As a measure of affinity we calculated the rate constant of G protein dissociation from the receptor after agonist withdrawal. The dissociation kinetics of Go protein from M3- and M1-AChRs was found to be 10-fold faster in comparison to Gq. Similarly, we observed a 15-fold right shift of the concentration-response curves of Go proteins binding to M3-AChR in comparison to Gq. In order to ensure, that the affinity of the ternary complex correlates with the efficiency of G protein activation, we performed experiments on the G protein activity in intact cells expressing non-fluorescent M3-AChR by using a FRET-based assay. Our results showed that Gq activation required 10-fold lower agonist concentration compared to Go activation, suggesting that indeed the stability of the ternary complex in the absence of nucleotides determines the selectivity of GPCR-G protein coupling. We further explored the subtype selectivity of M2-AChR for Gi family members by comparison of dissociation kinetics of Gi1-, Gi2, Gi3-, and Go-proteins from M2-AChR under nucleotide depleted conditions. K_{off} of Gi1 and Gi3 were found to be two-fold higher in comparison to Gi2 and Go proteins, indicating the higher affinity of the latter ones to M2-AChR. Our FRET-based assay to study receptor-G-protein interactions in membranes of single cells has been proven to be a fast and reliable method to quantify the affinity of the ternary complex. The G protein subtype dependent differences in the affinity towards activated receptors correlate with the G protein coupling efficiency of this receptor.

059

Directed evolution of human parathyroid hormone 1 receptor for improved expression and stability

C. Klenk¹, J. Ehrenmann¹, J. Schöppe¹, L. Kummer², M. Schütz², A. Plückthun¹
¹Universität Zürich, Institut für Biochemie, Zürich, Switzerland
²G7 Therapeutics, Schlieren, Switzerland

Despite their tremendous pharmacological relevance and potential for the development of new drugs, our understanding of G protein-coupled receptor (GPCR) architecture and signaling mechanisms are still limited. Major reasons for this are the low abundance and poor biophysical properties of GPCRs, which makes them one of the most challenging class of proteins for structural and biophysical studies. Among the superfamily of GPCRs, the class B receptors comprising 15 receptors are structurally least understood because to date it has not been possible to obtain a crystal structure of this receptor class. To overcome these limitations, we have developed a method for improving functional expression and simultaneous thermo-stabilization of GPCRs by directed evolution which is based on expression of receptors in *Saccharomyces cerevisiae* and subsequent selection of highly expressing variants by flow cytometry with fluorescent ligands. By this strategy, key residues within a receptor sequence can be rapidly identified that are responsible for improved biophysical properties without greatly affecting the pharmacological features of the receptor. We have now applied this method

to the human parathyroid hormone 1 receptor, a member of the class B of GPCRs which is a major regulator of calcium homeostasis in the body and a key target for the treatment of osteoporosis. From two rounds of directed evolution in yeast we obtained several mutants of parathyroid hormone 1 receptor that exhibit strongly improved expression levels and that remain stable after solubilization in detergents. These receptor variants are ideal candidates for subsequent structural and biophysical analysis.

060

MOR-HA knock-in mouse: a new tool to study μ -opioid receptor regulation and expression

A. Kliewer¹, S. Schulz¹

¹Universitätsklinikum Jena, Institut für Pharmakologie und Toxikologie, Jena, Germany

Opioid drugs exert nearly all of their clinically relevant actions through stimulation of MORs (μ -opioid receptors). The molecular biology of endogenous opioid peptides and their cognate receptors has been studied extensively *in vitro*. For MOR, signaling efficiency is tightly regulated and ultimately limited by the coordinated phosphorylation of intracellular serine and threonine residues. Morphine induces a selective phosphorylation of serine 375 that is predominantly catalyzed by G protein-coupled receptor kinase 5. As a consequence, the selective morphine-induced S375 phosphorylation does not lead to a robust β -arrestin mobilization and receptor internalization. By contrast, high-efficacy opioid agonists such as fentanyl or etonitazene not only induce phosphorylation of S375 but also drive higher order phosphorylation on the flanking residues threonine 370, threonine 376, and threonine 379 in a hierarchical phosphorylation cascade that specifically requires GRK2 and GRK3 isoforms. As a consequence, multisite phosphorylation induced by potent agonist promotes both β -arrestin mobilization and a robust receptor internalization. However, little is known about agonist-selective phosphorylation patterns *in vivo* after acute and chronic drug administration. To learn more about MOR regulation *in vivo* we have generated a new μ -opioid receptor knock in mouse with an N-terminal HA-tag. Using these mice, we were able to study *in vivo* phosphorylation of an endogenous G protein-coupled receptor using both mass spectrometry and phosphosite-specific antibodies. We were also able to address the question which of the many putative MOR splice variants detected on the mRNA level are indeed expressed as functional receptors in mouse brain.

Ion channels

061

HCN4 in thalamic relay neurons is necessary for oscillatory activity in the thalamocortical system

A. Blaich¹, M. Zobeir², M. Rottmann², S. Herrmann¹, P. Meuth², H.-C. Pape², T. Budde², **A. Ludwig**

¹Institut für Exp. und Klin. Pharmakologie und Toxikologie, Friedrich-Alexander-Universität, Erlangen, Germany

²Institut für Physiologie I, Westfälische Wilhelms-Universität, Münster, Germany

HCN channels underlie the I_h current and are involved, among other functions, in the genesis of epilepsy. The significance of HCN1 and HCN2 isoforms for brain function and epilepsy has been demonstrated, however the role of HCN4, the third major neuronal HCN subunit, is not known. Here we show an unexpected role of HCN4 in controlling oscillations in the thalamocortical network. HCN4 is predominantly expressed in several thalamic relay nuclei, but not in the thalamic reticular nucleus and the cerebral cortex. HCN4-deficient thalamocortical relay neurons showed a massive reduction of I_h and strongly reduced intrinsic burst firing. Evoked thalamic oscillations in a slice preparation were completely abolished. *In vivo*, brain-specific HCN4 null mutants were protected against induced spike-and-wave discharges (SWD), the hallmark of absence seizures. Our findings indicate that HCN4 is necessary for rhythmic intrathalamic oscillations and that the channels constitutes an important component of SWD generation.

062

Dynamic dissociation of NHERF from TRPC5 proteins determines channel gating by diacylglycerol

U. Storch¹, A.-L. Forst¹, F. Pardatscher¹, S. Erdogmus¹, M. Philipp¹, M. Gregoritz¹, T. Gudermann¹, M. Mederos y Schnitzler¹

¹Ludwig-Maximilians-Universität, Walther-Straub-Institut für Pharmakologie und Toxikologie, München, Germany

TRPC4 and 5 channels are members of the *classical transient receptor potential* (TRPC) family whose activation mechanism downstream of phospholipase C (PLC) largely remained elusive until now. While TRPC3/6/7 channels are directly activated by diacylglycerol (DAG), TRPC4 and 5 channels are commonly regarded as DAG-insensitive. In contrast to TRPC3/6/7 channels, they contain a C-terminal PDZ-binding motif allowing for binding of Na^+/H^+ exchanger regulatory factor (NHERF) 1 and 2. Interestingly, performing electrophysiological measurements, co-immunoprecipitations and intermolecular dynamic FRET experiments, we found that dissociation of NHERF proteins from the C-terminus of TRPC5 confers DAG-sensitivity on TRPC5 channels. TRPC5 channels were DAG-sensitive under the following experimental conditions: inhibition of protein kinase C, amino acid exchange in the C-terminal PDZ-binding motif, PIP₂ depletion with and without involvement of PLC, over-expression of G-protein coupled receptors, down-regulation of endogenous NHERF1 and 2 proteins and over-expression of a NHERF1 mutant incapable of TRPC5 binding. These findings strongly argue for NHERF proteins as molecular determinants for channel activation. Interestingly, PIP₂ depletion itself caused slight TRPC5 current increases while during PIP₂ depletion, the membrane permeable DAG analogue OAG evoked even higher TRPC5 currents suggesting that PIP₂ depletion induces an active and DAG-sensitive channel conformation. Receptor mediated PIP₂ depletion also resulted in dissociation of NHERF1 and 2 from the C-terminus of TRPC5 thereby eliciting a DAG-sensitive TRPC5

channel conformation. Thus, our findings suggest that DAG-sensitivity of TRPC5 is the result of an activation cascade starting with PIP₂ depletion and subsequent dynamic dissociation of NHERF1 and 2 from the C-terminus of TRPC5. Altogether, DAG-sensitivity is a unifying functional hallmark of all TRPC channels.

063

Primidone inhibits TRPM3 and attenuates thermal nociception *in vivo*

U. Krügel¹, I. Straub¹, M. Schaefer¹

¹Universität Leipzig, Institut für Pharmakologie und Toxikologie, Leipzig, Germany

The melastatin-related transient receptor potential channel TRPM3 is a heat-activated nonselective cation channel expressed in sensory neurons of dorsal root ganglia. Since TRPM3-deficient mice show impaired inflammatory thermal hyperalgesia, the pharmacological inhibition of TRPM3 may exert antinociceptive properties.

Fluorometric Ca^{2+} assays and a compound library containing approved drugs were used to identify TRPM3 inhibitors and to characterize their potency and selectivity. Biophysical properties of the block were assessed using electrophysiological patch-clamp methods. Microfluorometry in Fura-2-loaded single cells was applied to monitor $[\text{Ca}^{2+}]_i$ signals in isolated dorsal root ganglion (DRG) neurons. Analgesic effects were assessed applying pregnenolone sulfate (PregS)-induced chemical pain and heat stimuli at mice.

In the screening approach using stably transfected HEK_{TRPM3} cells we identified the nonsteroidal anti-inflammatory drug (NSAID) diclofenac, the tetracyclic antidepressant maprotiline and the anticonvulsant primidone as highly efficient TRPM3 inhibitors. The compounds exhibited half-maximal inhibitory concentrations of 0.6-6 μM .

The selectivity profiles of maprotiline and primidone for TRPM3 were promising with no inhibitory effects on TRPM2, TRPM8, TRPA1, TRPV1, TRPC5, TRPC6 and P2X7 receptor channels. Primidone inhibited PregS-induced $[\text{Ca}^{2+}]_i$ signals in rat DRG neurones, indicating a block of native TRPM3 channels. Consistently, primidone attenuated nociceptive responses of mice to paw-injected PregS. Furthermore, intraplantar primidone reduced nociception in healthy and hyperalgesic CFA-inflamed paws in the hot plate test.

The finding that an approved drug can inhibit TRPM3 at concentrations that may be therapeutically relevant and thereby can act as an analgesic, provides a method to study TRPM3-related effects by acutely challenging the channel's function. Pharmacological interference with TRPM3 applying an approved drug or optimised successor compounds may pave the way to better understanding of physiological functions of TRPM3 in humans and may represent a novel concept for analgesic treatment.

064

SK channel modulation attenuates microglial activation

A. Dolga¹, L. Matschke², F. Wilhelmy¹, B. Honrath³, N. Decher², C. Culmsee³

¹Faculty of Mathematics and Natural Sciences, Molecular Pharmacology — Groningen Research Institute of Pharmacy, Groningen, Germany

²University of Marburg, Inst. of Physiol. and Pathophysiology, Marburg, Germany

³Philipps-Universität Marburg, Inst. für Pharmakologie und Klinische Pharmazie, Marburg, Germany

Excitotoxicity, calcium deregulation, mitochondrial dysfunction and neuroinflammation contribute to progressive cell death in many neurodegenerative diseases. Therefore, proteins that prevent deregulation of these pathways are considered as drug targets. Potential therapeutic approaches may benefit from modulation of small-conductance calcium-activated potassium (SK) channels, since recent data supports the hypothesis that SK channel activity promotes neuronal survival against cellular stress via a dual mechanism of action: i) by controlling neuronal excitability and ii) by preventing mitochondrial dysfunction and inflammation. Our previous studies showed that activation of SK channels in neurons exerted protective effects through inhibition of NMDAR-mediated excitotoxicity. Further, we revealed recently that in a model of glutamate oxytosis, activation of SK channels attenuated mitochondrial fission, prevented the release of pro-apoptotic mitochondrial proteins, and reduced cell death. However, little is known about the function of SK channels in cell metabolism and neuroinflammatory processes in non-neuronal cells, such as microglial cells. In this study, we addressed the question whether SK channel activation affected primary mouse microglia activation upon LPS and α -synuclein challenge. We found that activation of SK channels significantly reduced activation of microglia in a concentration-dependent manner, as detected by real-time xCELLigence cell impedance measurements. Further data on cytokine (TNF- α and IL-6) analysis revealed that activation of SK channels attenuated α -synuclein-induced cytokine release. Inhibition of glycolysis prevented microglial activation and cytokine release. Although SK channel activation slightly reduced ATP levels, it attenuated α -synuclein-induced NO release. Furthermore, glycolytic products and AMPK signaling were evaluated. Overall, our findings show that activation of SK channels attenuates microglial cell activation. Thus, SK channels are promising therapeutic targets for neurodegenerative disorders, where neuroinflammation and cell metabolic deregulation are associated with progression of the disease.

065

An ionic interaction network within the ATP binding site stabilizes the closed-state conformation of the P2X2 receptor

R. Hausmann¹, D. Kuhlmann¹, A. Kless², G. Schmalzing¹

¹RWTH Aachen University, Molecular Pharmacology, Aachen, Germany

²Grünenthal GmbH, Global Drug Discovery, Aachen, Germany

P2X receptors are trimeric ATP-gated cation channels involved in the fast signal transduction in many cells. A closed-state homology model of the rat P2X2 receptor (P2X2R) based on the X-ray structure of the closed-state zebrafish P2X4 receptor revealed that the side chains of the residue pairs E84/R290, E103/K308, E167/R290 and E167/K308 are in close spatial vicinity within the ATP-binding pocket. Indeed, disulfide trapping experiments of cysteine substitution mutants confirmed that the side chains of the residue pairs E84/R290, E167/R290 and E167/K308 are in close proximity when the channel is in the apo closed state. By contrast, the cysteine substitution

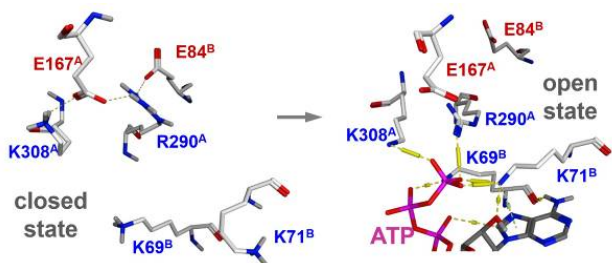
mutant of the residue pair E103/K308 can be crosslinked efficiently in both states, the closed- and open state of the P2X2R. Interestingly, oxidative crosslinking of cysteine substitution mutants of each individual residue pair significantly reduced the ATP-induced current amplitudes. Charge reversal or swapping mutagenesis and cysteine modification by charged MTS-reagents indicated the electrostatic nature of the pairwise interactions in these four residue pairs. Furthermore, preliminary data from triple, tetra and penta mutant cycle analysis indicated energetic coupling between the residue pairs E84/R290, E103/K308, E167/R290 and E167/K308 and thus indicates the cooperative interaction in a larger salt bridge network. Together with the markedly reduced current amplitudes following disulfide crosslinking, our data suggest that the salt bridge network serves to stabilize the closed-state conformation of the P2X2R. The comparison of the closed-state and open-state model of the rat P2X2R showed that ATP promotes a marked rearrangement of the side chains of the residues R290 and K308 to enable the strong ionic coordination of the γ -phosphate oxygen of ATP. In summary, our data are in line with the concept that the electrostatic interaction of R290 and K308 with ATP competitively releases E84, E103 and E167 from their strong electrostatic coupling and thus initiates a destabilization of the closed-state, which favors channel opening.

Fig. 1. Comparison of the apo closed-state (left) and the ATP-bound open-state (right) homology model of the rP2X2R. Selected residues of adjacent subunits A and B are indicated by superscript A and B.

Fig. 1 placeholder

This work was supported by a Deutsche Forschungsgemeinschaft Grant (HA6095/1-1) to RH.

Abb. 1



066

A novel regulator of calcium release from intracellular organelles and constitutive protein secretion in pancreatic acinar cells

U. Kriebs¹, A. Bach¹, U. Wjissenbach², A. Jha³, K. Zimmermann⁴, A. Pfeifer⁴, P. Weissgerber¹, V. Flockerz¹, P. Lipp⁵, S. Muallim⁵, V. Tsvilovsky¹, M. Freichel¹

¹Universität Heidelberg, Pharmakologisches Institut, Heidelberg, Germany

²Universität des Saarlandes, Experimentelle und Klinische Pharmakologie und Toxikologie, Homburg, Germany

³National Institute of Health, Molecular Physiology and Therapeutics Branch, Bethesda, Germany

⁴Universität Bonn, Institut für Pharmakologie und Toxikologie, Bonn, Germany

⁵Universität des Saarlandes, Institut für Molekulare Zellbiologie, Homburg, Germany

In a similarity search using sequence motifs conserved amongst various members of the TRP protein family we identified three non-annotated putative membrane proteins that we initially termed TMEM1, TMEM2 and TMEM4. Expression analysis using the NanoString nCounter system, Northern Blotting and RT-PCR showed that murine TMEM2 is expressed in various tissues including heart, brain, lung, endothelium, colon, cardiac myocytes, cardiac fibroblasts, embryonic fibroblasts, mast cells and pancreatic acinar cells. Hydropathy analysis predicts that TMEM2 proteins exhibit 6 to 10 plasma-membrane spanning domains, but fluorescently labeled TMEM2 fusion constructs expressed in mouse embryonic fibroblasts revealed a vesicular subcellular localization pattern. In contrast to the prediction by the PSORT II algorithm, TMEM2-eYFP could not be identified in the plasma membrane of fibroblasts, cardiac myocytes, mast cells or pancreatic acinar cells but showed a significant colocalization with markers and fusion constructs specific for acidic compartments including lysosomes. In TMEM2^{-/-} mice, a marked elevation of amylase and lipase plasma levels was observed. We found that constitutive but not stimulated amylase secretion from TMEM2-deficient acinar cells is elevated indicating a cell autonomous defect. Calcium (Ca²⁺) is an important signaling molecule regulating stimulated as well as constitutive secretion from pancreatic acinar cells. Microfluorimetric measurements using Fura-2 or Indo-1 indicate higher resting Ca²⁺ concentrations in TMEM2^{-/-} pancreatic acinar cells correlating with elevated basal enzyme secretion. In TMEM2-YFP-knock-add-on mice we identified TMEM2 in organelles of the apical acinar cell pole and a partial colocalisation with Lamp2 proteins. Furthermore, largely increased elevations in cytoplasmic Ca²⁺ concentration were observed upon osmotic lysis of lysosomes triggered by Gly-Phe β -naphthylamide (GPN) or by NH₄Cl application. The role of TMEM2 for Ca²⁺ release was evaluated by stimulation with low concentration of cholecystokinin (CCK-8, 2pM) in the absence of extracellular Ca²⁺ using both microfluorimetric recording of cytosolic Ca²⁺ transients as well as electrophysiological recordings of Ca²⁺-activated chloride currents. These measurements revealed a higher frequency of intracellular Ca²⁺ oscillations and a larger area under the curve of Ca²⁺-activated chloride currents upon CCK-8 stimulation indicating that TMEM2 inactivation leads to an enhancement of the globalization of CCK-8 evoked Ca²⁺ release from intracellular organelles. Taken together, our study identifies TMEM2 as a novel regulator of Ca²⁺ release from intracellular organelles including endo-lysosomes and as a critical determinant of constitutive protein secretion in pancreatic acinar cells.

Organ- and neurotoxicity

067

German Society of Toxicology Working Group on Alternative Approaches to Animal Testing: Quality criteria for *in vitro* methods and *in vitro* research work

U. G. Sauer¹

¹Scientific Consultancy – Animal Welfare, Neubiberg, Germany

While generally highlighting toxicology as a translational science that requires academic anchoring, Gundert-Remy and co-workers [1] have called for efforts to improve the relevance of *in vitro* methodologies in predicting *in vivo* effects. Against this background, the German Society of Toxicology Working Group on Alternative Approaches to Animal Testing proposes specific quality criteria (QC) for *in vitro* methods and for research work using *in vitro* methods. These QC may serve to evaluate *in vitro* methods that are developed or applied in-house or that are described in work plans, peer reviewed articles, etc. For the time being, the QC focus on *in vitro* cell or tissue culture methods that address human health endpoints in the context of substance-related regulatory toxicity testing. Nevertheless, these QC are also generally applicable to *in vitro* research conducted for other toxicological purposes. Relevant work from, e.g., the Organisation for the Economic Co-operation and Development has been taken into account in specifying the QC that cover the following aspects:

- The 3Rs impact of an *in vitro* method in replacing, reducing (and refining) a specific animal test for a specific toxicological endpoint. This aspect also includes scientific hurdles that, in the past, had impeded the successful development of *in vitro* methods for the given toxicological endpoint.
- Scientific relevance and reliability, i.e. which fundamental requirements should an *in vitro* method meet to ensure that its results are relevant and reliable.
- Practicality and applicability, i.e. what is the expected expenditure for the *in vitro* method, and have relevant authorities and industrial sectors been involved in the development of the *in vitro* method.

QC related to the scientific relevance of research work using a specific *in vitro* method provide a tool to justify, e.g., the suitability of the selected test system and *in vitro* endpoint(s) for the given purpose; the selection of test substances, positive and negative controls; the setting and control of test concentrations; and the definition of acceptance criteria to determine the relevance of test results.

The proposed QC may serve as a framework to assess the relevance of *in vitro* methods and *in vitro* research work. Thereby, they aim at improving *in vitro* predictivity of *in vivo* toxicological effects, which in return contributes to reducing and replacing the need for animal testing.

[1] Gundert-Remy, U. *et al.* (2015). Toxicology: a discipline in need of academic anchoring – the point of view of the German Society of Toxicology. Arch Toxicol 89: 1881-93.

068

Implementation of 3R in safety assessment of consumer goods

S. Hoffmann-Dörr¹

¹Henkel AG & Co. KGaA, Düsseldorf, Germany

During the past decades, considerable progress has been made in implementing 3R approaches in routine safety assessment. In spite of these achievements, animal tests still need to be conducted if legal requirements prescribe *in vivo* tests or if no reliable, accepted alternative method exists. Efforts to foster 3R approaches and make them 'ready for use' focus on three levels: Development and validation of scientific methods/strategies, regulatory acceptance of acknowledged approaches and global harmonization of standards. Strong cooperation between toxicological experts from scientific bodies, national and international authorities and industry is needed to advance on all three levels for the benefit of animal welfare.

3R approaches that have already been implemented in routine safety assessment of consumer goods do not focus solely on replacement of animal testing by use of accepted alternative methods. In cases where reliable alternative approaches are not yet available, reduction in animal numbers and refinement of testing procedures can be achieved on a case-by-case basis. A tailor-made, tiered testing strategy is usually pursued that involves knowledge on specific characteristics of the test item and makes use of all available data, including details on exposure and results obtained with structural homologues.

Hurdles to apply alternative approaches can even occur for established methods. As legislations give different priority to alternative approaches, it remains challenging to fulfil conflicting legal requirements in different regions of the world, or even to address horizontal legislations of the same region. Furthermore, successfully validated and legally implemented alternative approaches might not always provide the safety assessor with meaningful test results. With gaining experience, limitations of test systems can become evident that affect for example the applicability domain of the method, as has been the case both for some *in vitro* and *in vivo* methods. In these cases, the new information needs to be shared not only among safety assessors, but also with method developers and regulators to facilitate refinement of scientific approaches and/or amendments of regulations.

069

In vivo imaging of APAP induced liver damage

R. Reif¹, A. Ghallab¹, R. Hassan¹, J. Hengstler¹

¹Leibniz-Institut für Arbeitsforschung (IfADo), VisTox, Dortmund, Germany

Two-photon microscopy facilitates imaging of biological processes *in vivo*. Establishing this recent technique in mouse liver allowed us to record in a real-time the sequence of events during acetaminophen (APAP) induced-liver damage. Although APAP is

intensively studied and described *in vivo* imaging revealed so far unknown scenarios of cell death. The hepatocytes close to the central vein of a liver lobule went within hours into cell death as commonly described due to the toxic metabolite NAPQI. Surprisingly, we observed a distinct way of cell killing at the outer border of the dead cell area which is accompanied by bile acid decompartmentalization. There, within an hour after APAP administration dilatation of bile canaliculi was observed. Subsequently, bile acids containing invaginations arose from the apical side of a hepatocyte into the cytosol. These invaginations ballooned until the bile leaked into the hepatocyte volume and subsequently the plasma membrane of the affected hepatocytes lost its integrity leading to cell death. This mechanism emerged in an environment for hepatocytes where moderate NAPQI levels meet intracellular high bile salt concentrations of the midzonal region. In conclusion, establishing *in vivo* imaging in mouse liver enabled us to identify new cellular mechanisms which cannot be discovered by conventional methods.

070

Protective effects of statins on lung toxicity after fractionated irradiation

V. Ziegler¹, C. Henninger¹, G. Fritz¹

¹Universitätsklinikum Düsseldorf, Institut für Toxikologie, Düsseldorf, Germany

Introduction: Lung inflammation and fibrosis are considered as major toxicities after thoracic cancer radiotherapy. Up to now effective pharmacological interventions for normal tissue protection are largely missing. HMG-CoA reductase inhibitors (statins), which are used in the clinic for lipid-lowering purpose, are reported to have multiple inhibitory effects on genotoxic stress responses. For this reason we aim to investigate the usefulness of statins to protect normal lung cells *in vitro* and lung tissue *in vivo* from damage provoked by ionizing radiation (IR).

Methods: According to clinically relevant anticancer radiation regimens, we used fractionated irradiation schemes (4 x 4 Gy) for both *in vitro* as well as *in vivo* experiments. We analyzed the effect of lovastatin on IR-induced DNA damage formation and repair, DNA damage response (DDR) and cell death in non-proliferating human lung fibroblasts, epithelial as well as endothelial cells. Furthermore, we established an irradiation device that is useful to selectively irradiate the right lung of mice and investigated the influence of lovastatin on lung damage following fractionated and selective irradiation of the lung *in vivo* (BALB/c mice).

Results: Compared to lung fibroblasts and epithelial cells, endothelial cells exhibited the highest radiosensitivity and underwent IR-induced apoptosis which was partly prevented by lovastatin. By contrast fibroblasts and epithelial cells did not undergo apoptosis upon irradiation. Lovastatin did not affect initial DNA damage formation in any of these cells. In all three lung cell types lovastatin enhanced the repair of DNA double-strand breaks as analyzed 24 h after the last irradiation by γH2AX nuclear foci formation. Depending on the cell type lovastatin affected various components of the DDR machinery *in vitro*. *In vivo*, lovastatin prevented IR-mediated increase in breathing frequency as determined two and four weeks after fractionated irradiation. Moreover, statin treatment attenuated the level of residual DNA damage and IR-induced apoptosis as analyzed four weeks after irradiation. These results were mimicked when EHT1864, a small molecule inhibitor of the small Rho-GTPase Rac1, was applied *in vivo*, pointing to an involvement of Rac1 in statin-mediated radioprotective effects.

Conclusion: Bearing in mind that statins are well tolerated in humans, we suggest the application of statins as a promising pharmacological strategy for the prevention of irradiation-induced damage of the lung.

071

A key role for Bid-mediated mitochondrial damage in paradigms of oxytosis and ferroptosis

A. Jelínek¹, S. Neitemeier¹, C. Culumsee¹

¹Philipps-Universität Marburg, Institut für Pharmakologie und Klinische Pharmazie, Marburg, Germany

Targeted genome engineering by CRISPR/Cas9 is an evolving tool for generating specific knockout cell lines. Co-expression of CRISPR/Cas9 allows for efficient DNA cleavage and introduction of so called indel mutations (insertion/deletion point mutations) that lead to either misfolded non-functional proteins or complete knockout. We exploited this tool to generate a Bid (BH3-interacting domain death agonist) knockout cell line in neuronal HT-22 cells. Bid has been shown to be involved in regulated cell death pathways like oxytosis where its activation mediates mitochondrial demise, subsequent release of Apoptosis inducing factor (AIF) and cell death. In the cell death model of oxytosis the cystine/glutamate antiporter (X_c⁻) is inhibited by high extracellular glutamate concentrations. Following events such as increasing lipid peroxidation and ROS production resemble major characteristics of another emerging cell death pathway, called ferroptosis.

In this study we generated a Bid CRISPR/Cas9-knockout cell line to elucidate the role of Bid as a potential link of oxytosis and ferroptosis in the HT-22 cell line. In order to investigate the potential mechanistic overlap at the level of mitochondrial death pathways, we induced oxytosis with glutamate or ferroptosis with erastin in wild-type cells and analyzed the respective effects of the well-established inhibitors ferrostatin-1 and the Bid inhibitor Bi-6c9 on cell death and mitochondrial paradigms. These results were then compared to the effects of glutamate or erastin in CRISPR/Cas9-Bid-knockout cells. Bi-6c9 inhibited glutamate-induced morphological changes of HT-22 cells and also prevented cell death as assessed using the MTT assay and Annexin V/PI staining. Similar results were observed with ferrostatin-1 in the model of erastin-induced ferroptosis. Subsequent FACS analysis of lipid peroxidation by BODIPY staining demonstrated that Bi-6c9 abolishes lipid peroxide formation in the erastin model and ferrostatin-1 in the model of oxytosis. FACS analysis was further employed for the detection of mitochondrial ROS formation. MitoSOX staining revealed a significantly decreased production of mitochondrial ROS by Bi-6c9 and ferrostatin-1 in the respective model systems.

Investigating the CRISPR/Cas9-Bid-knockout HT-22 cell line revealed that Bid knockout prevented cell death, lipid peroxidation and mitochondrial toxicity in both model systems of cell death, oxytosis and ferroptosis. In conclusion, the present study exposes Bid as a pivotal molecular link between the previously separated cell death pathways oxytosis and ferroptosis at the level of mitochondria.

072

Caspase inhibition prevents alpha synuclein-toxicity in human dopaminergic neurons

G. K. Ganjam¹, A. M. Dolga², S. Neitemeier¹, K. Bolte³, M. Hoellerhage⁴, W. E. Oertel⁵, G. Höglinger¹, C. Culumsee¹

¹Philipps-Universität Marburg, Institut für Pharmakologie und Klinische Pharmazie, Karl-von-Frisch-Straße 1, 35032, Marburg, Germany

²University of Groningen, Institute of Pharmacy, Antonius Deusinglaan 1, 9713 AV, Groningen, The Netherlands, Niederlande

³Philipps-Universität Marburg, Department of Biology, Karl-von-Frisch-Straße 8, 35043, Marburg, Germany

⁴German Center for Neurodegenerative Diseases (DZNE), Max Lebsche Platz 30, 81377, Munich, Germany

⁵Philipps-Universität Marburg, Department of Neurology, Rudolf-Bultmann-Strasse 8, 35033, Marburg, Germany

Parkinson's disease is a common neurodegenerative movement disorder characterized by midbrain dopaminergic neuronal loss in the substantia nigra that has been linked to alpha-synuclein toxicity. However, the molecular mechanisms underlying alpha-synuclein-mediated toxicity in human dopaminergic neuronal loss are not well defined. The goal of this study was to investigate the deleterious effects of alpha synuclein in particular mitochondrial toxicity in human dopaminergic cells. Therefore, we have generated neuron specific, adeno associated virus type 2 (AAV2) expressing cytosolic as well as mitochondrial targeted alpha synuclein and EGFP expressing viruses used as respective controls.

Overexpression of both, the cytosolic and the mitochondrial variants of alpha synuclein severely disrupted the dendritic network, induced loss of cellular ATP, enhanced mitochondrial ROS production, and was associated with activation of caspases and dopaminergic cell death in a time-dependent manner. In addition, real-time analysis of mitochondrial bioenergetics using the Seahorse Bioscience system following AAV infection elicited a complete damage to mitochondrial respiration capacity in the dopaminergic neurons. Our results suggested that mitochondrial targeted expression of alpha synuclein appeared to be more toxic than the cytosolic form of alpha synuclein. In addition, ultrastructural mitochondrial morphological analysis by transmission electron microscopy illustrated a number of deformed cristae in cells expressing the cytosolic alpha synuclein and a complete loss of cristae structure and massively swollen mitochondria following the expression of mitochondrial targeted alpha synuclein in the human dopaminergic neurons.

In addition, we found that inhibition of caspases by the broad spectrum caspase inhibitor QVD significantly ameliorated alpha synuclein-induced dopaminergic neuronal death. Interestingly, inhibition of caspases preserved neuronal network integrity, ATP levels and mitochondrial respiration capacity in both paradigms of cytosolic and mitochondrial alpha synuclein overexpression. Overall, our findings show that cytosolic as well as mitochondrial targeted expression of alpha synuclein is detrimental to human dopaminergic neurons, while inhibition of caspases amend alpha synuclein toxicity at the level of mitochondria. Thus, caspase inhibitors provide promising therapeutic potential to prevent dopaminergic neuronal death in Parkinson's syndromes that are associated with alpha synuclein toxicity.

Toxic substances, particles and food components

073

Emerging toxins in medical laser-irradiation of organic pigments in aqueous suspensions and tattooed pig skin

J. Schreiber¹, N. Röder¹, M. Gebhardt¹, C. Hutzler¹, P. Laux¹, H.-P. Berlien², A. Luch¹

¹Bundesinstitut für Risikobewertung, Department of Chemical and Product Safety, Berlin, Germany

²Evangelical Elisabeth Hospital, Department of Laser Medicine, Berlin, Germany

Degradation of and adverse effects caused by tattoo and permanent make-up pigments upon sunlight exposure and laser removal have been occasionally reported in the last decades. Until now, only the ban of certain azo-pigments has been addressed in the national legislation. The regulation was based on a number of studies showing the cleavage of azo-bonds by ultra violet light and laser-irradiation leading to the formation of carcinogenic aromatic amines. As a result, especially German tattoo ink manufacturers switched to the use of more light-fast polycyclic pigments assuming these would be safer for this kind of application when compared to azo-pigments.

To assess the potential risks of polycyclic pigments in terms of decomposition in the skin, we compared the photochemical cleavage of the widely used azo-pigment Orange 13 and the polycyclic pigment copper phthalocyanine blue. Main decomposition products are qualitatively and quantitatively analyzed after Q-switched laser irradiation of 1 mg/ml aqueous suspensions and tattooed pig skin. Irradiated specimen were extracted with ethyl acetate and analyzed with gas chromatography coupled to mass spectrometric detection (GC/MS) using liquid injection and head-space sampling techniques.

We were able to confirm the cleavage of pigment Orange 13 at the azo- and other weak bonds in our experimental set-up (Fig. 1a). Amongst other substances, the carcinogenic aniline (max. conc. 1.01 ± 0.12 µg/mL) and 3,3-dichlorobenzidine (max. conc. 0.88 ± 0.18 µg/mL) are formed. Despite the lack of such weak bonds, the highly stable porphyrin-like structure of copper phthalocyanine blue is as well decomposed upon laser-irradiation (Fig. 1b). Here, 1,2-benzenedicarbonitrile (max. conc. 1.11 ± 0.12 µg/mL) were found as the main decomposition product in all experimental setups. Concentrations of cleavage products were generally higher in aqueous suspensions compared to pig skin extracts with both pigments. Additionally, the highly toxic gas hydrogen cyanide (max. conc. 35.8 ± 4.32 µg/mL) and the human carcinogen benzene (max. conc. 0.19 ± 0.06 µg/mL) were formed from both pigments, dependent on the laser wavelengths used. Cyanide levels of ≥50 µg/mL evolving upon ruby laser irradiation of >1.5 mg/ml aqueous suspensions of phthalocyanine blue were proven to significantly reduce cell viability in human skin cells *in vitro*.¹

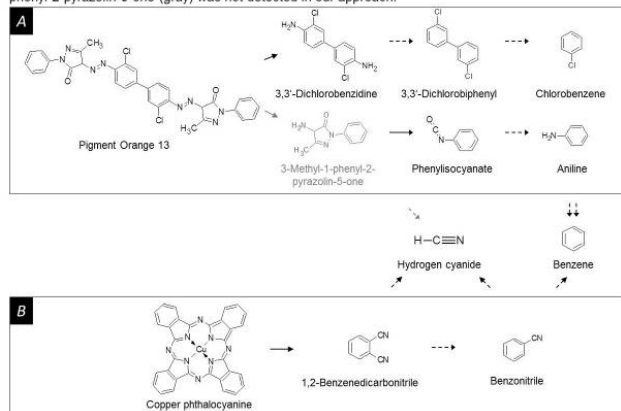
Since temperatures might well exceed 600°C inside the pigment particles, all organic pigments bear the risk of releasing toxic follow-up products upon laser induced combustion. Thus, the evolving substances may harm the skin locally and even systemically.

Reference

1 Schreiber, I., Hutzler, C., Laux, P., Berlien, H. P. & Luch, A. Formation of highly toxic hydrogen cyanide upon ruby laser irradiation of the tattoo pigment phthalocyanine blue. *Sci Rep* 5, 12915 (2015).

Abb. 1

Figure 1: Decomposition pattern of pigment Orange 13 (A) and copper phthalocyanine blue (B). Solid and dashed arrows indicate direct and secondary cleavage products, respectively. 3-Methyl-1-phenyl-2-pyrazolin-5-one (gray) was not detected in our approach.



074

Quantification of cellular uptake of silver nanoparticles in intestinal cell models of various complexities

D. Lichtenstein¹, T. Meyer², L. Böhmert¹, A. F. Thünemann³, I. Estrela-Lopis², A. Braeuning¹, A. Lampen¹

¹Federal Institute for Risk Assessment, Food Safety, Berlin, Germany

²Leipzig University, Institute of Medical Physics & Biophysics, Leipzig, Germany

³Federal Institute for Materials Research and Testing, Polymers in Life Science and Nanotechnology, Berlin, Germany

Understanding the interactions between nanoscaled objects and living cells is of great importance for risk assessment, due to rising application of nanomaterials in food-related products. Several studies show that silver nanoparticles can reach the intestinal epithelia in nanoform in a human *in vitro* digestion model. Nevertheless, only sparse data concerning the direct quantification of cellular uptake of silver nanoparticles are available. Therefore, this study was focused on a systematic quantitative comparison of the cellular uptake of differently coated silver nanoparticles of comparable size.

Intracellular uptake was determined quantitatively via a Transwell™-System with subsequent elemental analysis (AAS) and Ion Beam Microscopy (IBM). Silver nanoparticles were coated with poly (acrylic acid) and polyvinylpyrrolidone and characterized extensively by TEM, DLS, SAXS, Zetasizer and NanoSight. AgPURE™ as a widely used reference nanoparticle coated with Tween 20 and Tagat TO V was also used for comparison. Different intestinal cell models were applied to get closer to the complex *in vivo* situation: Beside the widely used Caco-2 model we also investigated particle uptake in a model which considered the enterocyte-covering mucus layer, as well as in a model specialized on particle uptake, the so-called M-cell model.

Our findings suggest that silver uptake is clearly a particle- and not an ion-related effect. The internalization of silver nanoparticles was enhanced in uptake-specialized M-cells, although no enhanced transport through the cells was observable. Furthermore, the mucus did not providing a substantial additional barrier for nanoparticle internalization. Rutherford Backscattering Spectrometry (RBS) via IBM allowed distinguishing between adsorbed an internalized material and the results were in accordance with the Transwell™-data. Additionally, IBM investigations via Particle-Induced X-Ray Emission (PIXE) showed intracellular association of silver with sulfur.

The quantification of silver nanoparticle internalization revealed a clear particle-specific and a coating-related uptake. Furthermore, a high amount of silver nanoparticles is taken up in cell models of higher complexity. Thus, an underestimation of particle effects *in vitro* might be prevented by considering cell models with greater proximity to the *in vivo* situation.

075

Analyzing iron oxide nanoparticles for drug delivery – innovative investigation tools for nanotoxicology

C. Janke¹, M. Poettler¹, R. Friedrich¹, J. Zaloga¹, H. Unterweger¹, S. Duerr^{1,2}, R. Tietze¹, I. Cicha¹, S. Lyer¹, C. Alexiou¹

¹HNO-Klinik Erlangen, Sektion für Experimentelle Onkologie und Nanomedizin (SEON), Erlangen, Germany

²HNO-Klinik Erlangen, Sektion für Phoniatrie und Pädaudiologie, Erlangen, Germany

Nanoparticles offer promising new possibilities for medical applications including therapy and diagnosis of various diseases. Especially nanoparticle systems with magnetic cores provide a broad application spectrum as contrast agents, magnetic transporters, or heat carriers in hyperthermia treatment. For bench to bedside translation of superparamagnetic iron oxide nanoparticles (SPIONs) for medical applications, safety issues have to be clarified. For that, reliable standards must be established on the basis of comprehensively validated physicochemical and biological characterization methods. SPIONs consisting of maghemite and magnetite are usually of brown or black color. Due to these special properties, SPIONs and other metal oxide nanoparticles are prone to

interfere with classical toxicological assays relying on optical detection of colorimetric, fluorescence or luminescence signals. Particularly, nanoparticle concentration and cellular uptake are further influencing factors. Consequently, for reliable analysis of nanoparticle mediated effects, alternative robust and interference-free readouts have to be established.

Based on long lasting experience working with SPIONs, we suggest a combination of complementary methods to analyse nanoparticle-mediated effects: Multiparameter analyses in flow cytometry deliver statistically relevant data and link uptake of nanoparticles (side scatter increase) with cellular effects in a high-content style. Combination of noninvasive, label-free impedance measurements (xCELLigence system) with real-time (fluorescence) microscopy enables us to monitor cellular proliferation and morphology over several days without interference by nanoparticles. Additional experiments in multicellular tumor spheroids provide information about tissue infiltration and thus, more closely resemble the *in vivo* situation. Using those complementary methods, several drug-loaded SPION systems dedicated for medical applications have been successfully characterized previously.

In sum, nanotoxicology is a complex and interdisciplinary challenge, where physicochemical parameters, as well as *in vitro* and *in vivo* behavior of nanoparticles have to be considered. To address these basic requirements, we are working on a stringent standardized road of characterization for iron oxide nanoparticles synthesized for medical applications.

Reference: Lyer S, Tietze R, Unterweger H, Zaloga J, Singh R, Matuszak J, Poettler M, Friedrich RP, Duerr S, Cicha I, Janko C, Alexiou C. Nanomedical innovation: the SEON concept for an improved cancer therapy with magnetic nanoparticles. *Nanomedicine (Lond)*. 2015; 10(21): 3287-3304.

Acknowledgments: This work was supported by the Bavarian State Ministry of the Environment and Consumer Protection and by the Deutsche Forschungsgemeinschaft (DFG) through the Cluster of Excellence Engineering of Advanced Materials.

076

Studies to establish biomarkers of alimentary acrylamide exposure

E. Richling¹, T. Bakuradze¹, G. Eisenbrand¹, M. Rünz¹

¹TU Kaiserslautern, Lebensmittelchemie & Toxikologie, Kaiserslautern, Germany

Acrylamide (AA) is an α,β -unsaturated compound, which is categorized as probably carcinogenic to humans [1,2]. AA is known to arise in foods by heat treatment in the course of the Maillard reaction between reducing sugars and amino acids at processing temperatures > 120 °C [3]. Dietary AA exposure has mainly been estimated on the basis of dietary recall, assessing consumption of foods with known AA contents. The use of human biomarkers of AA exposure, primarily haemoglobin adducts of AA and its genotoxic metabolite, glycidamide (GA) in red blood cells, as well as mercapturic acids excreted in the urine, is a promising alternative. Such biomarkers are to be validated by exact measurement of AA uptake in duplicates of food as consumed (duplicate diet studies) [4].

We here present results of a nine-day human intervention study with 14 healthy male volunteers. AA contents were determined in duplicates of servings as consumed and kinetics of AA-associated mercapturic acids (AAMA and GAMA) monitored in total urine [5]. The study design included washout periods with an AA-minimized diet (21 – 41 ng/kg bw), a low AA intake day (0.6 – 0.8 µg/kg bw) as well as a high AA intake day (1.3 – 1.8 µg/kg bw). After a three-day washout period an AAMA baseline level of 93 ± 31 nmol/d was determined. Low AA intake led to an AAMA excretion within 24 h of 225 ± 37 nmol/d, high intake to 404 ± 78 nmol/d corresponding to an AAMA excretion rate of about 30% of the ingested AA dose within 24 h, whereas AAMA output within 72 h corresponded to 58% of the respective AA intake. The AAMA baseline after 3 days washout corresponds to a net exposure level of 0.2 – 0.3 µg AA/kg bw/d. Whether this represents a true baseline level is to be clarified in a follow-up study.

In summary, this study provides important quantitative information on kinetics of urinary short-term exposure biomarkers validated by analytically verified dietary AA intake at present day food contamination levels.

[1] Deutsche Forschungsgemeinschaft (DFG). MAK- und BAT-Werte-Liste 2013, 2013 DOI: 10.1002/9783527675135.0th1. [2] IARC. IARC Monographs on the Evaluations of Carcinogenic Risks to Humans 1994, 60. [3] Tareke et al., J. Agric. Food Chem. 2002, 50, 4998-5006. [4] EFSA Panel on Contaminants in the Food Chain (CONTAM), EFSA Journal 2015;13(6):4104 [321 pp.]. [5] Ruenz et al., Arch. Toxicol. 2015 DOI: 10.1007/s00204-015-1494-9.

077

Modulation of redox-active signaling pathways by the flavonoids baicalein and myricetin in the nematode *Caenorhabditis elegans* and Hct116 cells

W. Wätjen^{1,2}, S. Havermann^{1,2}, K. Koch¹, D. Ackermann², C. Büchter^{1,2}

¹Martin-Luther-Universität Halle-Wittenberg, Biofunktionalität sekundärer Pflanzenstoffe, Halle/Saale, Germany

²Heinrich-Heine-Universität, Institut für Toxikologie, Düsseldorf, Germany

Objective: Flavonoids are known to modulate distinct signaling pathways thereby causing different physiological effects. Effects of the flavonoids baicalein and myricetin as well as several methylated derivatives were analyzed in the nematode *Caenorhabditis elegans* and in Hct116 colon carcinoma cells and to get insights in molecular mechanisms modulated by these compounds.

Methods: radical-scavenging activity (TEAC, DCF), stress resistance (SYTOX, sodium arsenite), modulation of signaling pathways (Nrf2/SKN-1, DAF16), life span.

Results: Baicalein enhances the resistance of *C. elegans* against lethal thermal and sodium arsenite stress and dose-dependently prolongs the life span of the nematode (median life span: + 57%). Using RNA interference we were able to show that the induction of longevity and the enhanced stress-resistance were dependent on SKN-1 (homolog to mammalian Nrf2), but not DAF-16 (homolog to mammalian FOXO), another pivotal transcription factor. Negletein was the only methylated derivative which was able to enhance the life span of the nematode. In Hct116 cells, baicalein activates Nrf2; the methylated derivatives oroxylin A and negletein showed a comparable redox-active potential in these cells, but only negletein was able to activate Nrf2.

The dietary flavonoid myricetin as well as the methylated derivatives laricitrin, syringetin and myricitrin strongly enhance life span of *C. elegans*, decreased oxidative stress (DCF) and accumulation of lipofuscin. In contrast to myricetin, the methylated compounds strongly enhanced the resistance against thermal stress. Furthermore, treatment with the derivatives induced a much stronger nuclear localization of the DAF-16 transcription factor.

Conclusion: Baicalein increases stress-resistance and life span in *C. elegans* via SKN-1 but not DAF-16. Experiments with methylated baicalein derivatives suggest that the redox-active potential has a minor impact on the Nrf2/SKN-1 activation since only distinct derivatives activate this pathway. In case of myricetin, the methylation increases the stress resistance of the flavonoid. Methylation seems to enhance the biofunctionality of the flavonoids. Our results may be useful to understand molecular mechanisms of flavonoids and methylated derivatives used as food supplements or pharmacological extracts.

Clinical pharmacology and drug use

078

Effects of intranasal progesterone compared to zolpidem and placebo on sleep EEG and nocturnal hormone secretion in healthy postmenopausal women

A. Steiger¹, P. Schüssler^{1,2}, M. Kluge^{1,3}, M. Adamczyk¹, M. Beiting¹, P. Beiting¹, A. Bleifuß¹, S. Cordeiro¹, C. Mattern⁴, M. Uhr¹, A. Yassouridis¹, E. Friess¹
¹Max Planck Institute of Psychiatry, Munich, Germany
²University of Regensburg, Department of Psychiatry and Psychotherapy, Regensburg, Germany
³University of Leipzig, Department of Psychiatry and Psychotherapy, Leipzig, Germany
⁴M+P Pharma AG, Emmeten, Switzerland

The loss of progesterone during menopause is linked to common sleep complaints of the affected women. Consequently, a previous study of our laboratory demonstrated sleep promoting effects of oral progesterone replacement in postmenopausal women [1]. The oral administration of progesterone, however, is compromised by individual differences in bioavailability and metabolism of the steroid.

We therefore investigated the sleep-EEG effects after intranasal application of progesterone in 12 healthy postmenopausal women (50-70 yrs). In a randomized double-blind protocol each subject received four treatments, 2 doses of intranasal progesterone (4.5mg MPP22; 9.0 mg MPP22), 10mg of zolpidem and placebo. The 4 conditions consisted of 2 experimental nights (adaptation + examination) separated by at least one week. During each examination sleep EEG was recorded from 23:00 to 07:00. Simultaneously blood was collected every 20 min between 22:00 and 07:00 by long catheter for later analysis of the hormones growth hormone (GH), cortisol, melatonin and progesterone.

Conventional sleep-EEG was statistically evaluated by multivariate analyses of variances (MANOVAs) with repeated measures designs after removal of two outliers, which showed a low sleep efficiency index (SEI) after 4.5 and 9.0mg MPP22. Univariate F-tests in the MANOVAs pointed to the following results (significant p-values at $\alpha=0.05$). SEI was higher after zolpidem than after the other three treatments. After 9.0mg MPP22 SEI was elevated significantly in comparison to placebo. Subjects spent more time in NonREM sleep and less time in intermittent wakefulness after 9.0mg MPP22 and after zolpidem than after placebo. Total sleep time was elevated and wake after sleep onset (WASO) was reduced after 9.0mg MPP22 and after zolpidem. After all active treatments with MPP22 and zolpidem the time spent in sleep stage 2 was higher than after placebo. The amount of slow-wave sleep was higher after zolpidem than after placebo. In addition, the higher dose of MPP22 resulted in an increase of spindle and β frequencies combined with a decrease of δ oscillations during NonREM sleep. In comparison, administration of zolpidem resulted in strong increase of δ , spindle and high β frequencies as well as strong decrease in θ and α frequencies. Nocturnal progesterone levels increased after 9.0 mg MPP22. No other changes of hormone secretion were found.

Our study show sleep promoting effects of 9.0 mg MPP. As expected the sleep promoting effect of zolpidem was confirmed. The spectral signature of intranasal progesterone partly resembled the well-known sleep-EEG alterations induced by GABA active compounds. Progesterone levels were elevated after 9.0 mg MPP22. No other endocrine effects were observed.

[1] Schuessler et al, Psychoneuroendocrinology 2008; 33: 1124-31

079

Concomitant use of anticholinergic drugs in a large cohort of geriatric patients

B. Pfistermeister¹, T. Tümena², K.-G. Gaßmann³, R. Maas¹, M. F. Fromm¹
¹Friedrich-Alexander-Universität Erlangen-Nürnberg, Institute of Experimental and Clinical Pharmacology and Toxicology, Erlangen, Germany
²GiB-DAT Database, Nürnberg, Germany
³Waldkrankenhaus St. Marien gGmbH, Internal Medicine III, Geriatrics Center Erlangen, Erlangen, Germany

Introduction: Anticholinergic drugs or drugs with anticholinergic side effects are commonly used for the treatment of various diseases in the elderly population. Elderly patients are particularly vulnerable to anticholinergic-related cognitive effects. Moreover, there is a relationship between anticholinergic exposure and cognitive impairment. However, there is currently a lack of data on the anticholinergic burden in geriatric patients in Germany. It was therefore the aim of this study to evaluate the anticholinergic burden in a large representative cohort of geriatric patients.

Materials and Methods: In this retrospective cohort study, (co)-prescriptions of anticholinergic drugs as well as anti-dementia drugs were evaluated using the discharge medication of geriatric patients between January 2013 and June 2015 from the Geriatrics in Bavaria-Database (GiB-DAT). Anticholinergic drugs were classified according to the Anticholinergic Cognitive Burden (ACB) Scale in three groups (definite anticholinergics with a score of 2 or 3 and possible anticholinergics with a score of 1). The ACB scale was modified by omitting trospium and by adding the three drugs biperiden, metixen and maprotilin, which are used in Germany, with a score of 3. A patient's individual score of 3 or higher is considered to be clinically relevant.

Results: In total, 130,186 geriatric patients (median age 82 years, 66.3% female, median no. of drugs 9) were evaluated. Of these, 41,456 (31.8%) patients took at least one drug with anticholinergic properties. Two or more anticholinergic drugs were co-prescribed in 10,941 (26.4% of the patients taking anticholinergic drugs) patients. 11,241 (27.1% of the patients taking anticholinergic drugs) patients had a score of 3 or higher. The most common anticholinergic drug combinations involving two definite anticholinergic drugs were amantadine/quetiapine (58), amitriptyline/quetiapine (41) and amitriptyline/carbamazepine (35). 2,885 (7.0%) patients received anticholinergic drugs in combination with anti-dementia drugs.

Conclusions: One third of patients in a large geriatric population were prescribed at least one anticholinergic drug. One quarter received a co-prescription of anticholinergic drugs. Caution is advised prescribing anticholinergic drugs to elderly patients especially with dementia.

080

The antiglaucoma agents brimonidine and timolol are novel substrates of the organic cation transporters OCT2 and MATE1 expressed in human eye

C. Neul^{1,2}, D. Süßkind³, T. Lang^{1,2}, U. Hofmann^{1,2}, F. Ziemssen³, U. Schiefer³, M. Schwab^{1,4}, A. T. Nies^{1,2}
¹Dr. Margarete Fischer-Bosch Institute of Clinical Pharmacology, Stuttgart, Germany
²University of Tübingen, Tübingen, Germany
³Center for Ophthalmology, University of Tübingen, Tübingen, Germany
⁴Department of Clinical Pharmacology, Institute of Experimental and Clinical Pharmacology and Toxicology, University of Tübingen, Tübingen, Germany

Purpose: Glaucoma is a leading cause of visual loss in the world population. Lowering intraocular pressure by topical administration of antiglaucoma agents is still the mainstay for glaucoma treatment.^{1,2} Although many effective drugs exist, the major challenge is their efficient intraocular delivery, which is estimated to amount to 3% The involvement of membrane drug transporters in the intraocular delivery of the widely prescribed antiglaucoma prostanoid latanoprost has been described.⁴ However, it is currently unknown whether the cationic drugs brimonidine and timolol, which are also commonly used antiglaucoma agents, are similarly transported by drug transporters and whether these transporters are expressed in human eye. Brimonidine is an α_2 -adrenergic agonist, which inhibits the activity of the adenylate cyclase subsequently leading to a reduced production of aqueous humor. Timolol is a β -adrenergic receptor antagonist, which blocks β -receptors on the ciliary epithelium also resulting in a reduced aqueous humor production.

The aim of the present study was to determine whether brimonidine and timolol are substrates of the organic cation drug transporters OCT1 (encoded by *SLC22A1*), OCT2 (*SLC22A2*), OCT3 (*SLC22A3*) and MATE1 (*SLC47A1*). A further aim was to investigate whether these transporters are localized in different human eye substructures.

Experimental design: Transport of brimonidine and timolol was studied using the mammalian cell line HEK293 stably expressing the organic cation transporters OCT1, OCT2, OCT3 or MATE1.⁵ Intracellular accumulation of brimonidine and timolol was analyzed by mass spectrometry. Immunohistochemistry and immunofluorescence experiments were performed to study the localization of these transporters in different substructures from glaucomatous and non-glaucomatous human eyes.

Results: Uptake experiments revealed that brimonidine is transported by OCT2 and MATE1 in a time- and concentration-dependent manner, but not by OCT1 or OCT3. Timolol is only transported by MATE1, but not by the OCTs. As shown by immunolocalization studies, the OCT2 and MATE1 transporter proteins were expressed in all anterior eye substructures of non-glaucomatous and glaucomatous eyes, i.e. the cornea, the conjunctiva and the ciliary body.

Conclusion: Our data demonstrate that OCT2 and MATE1 may play a role in the ocular disposition of the antiglaucoma drugs brimonidine and timolol and may contribute to interindividual variability of drug concentrations and effects.

References:

- Zhang et al., Nat Rev Drug Discov. 2012 Jun 15;11(7):541-59.
- Lavik et al., Eye (Lond). 2011 May;25(5):578-86.
- Gaudana et al., Pharm Res. 2009 May;26(5):1197-216.
- Kraft et al., Invest Ophthalmol Vis Sci. 2010 May;51(5):2504-11.
- Nies et al., PLoS One. 2011;6(7):e22163.

Supported by the Robert Bosch Foundation, Stuttgart, Germany.

081

Immature platelet count or immature platelet fraction as optimal predictor of antiplatelet response to thienopyridine therapy

C. Stratz¹, T. Nuehrenberg¹, S. Leggewie¹, M. Cederqvist¹, F.-J. Neumann¹, W. Hochholzer¹, D. Trenk¹
¹Universtaets Herzzentrum Freiburg Bad Krozingen, Kardiologie Angiologie II, Bad Krozingen, Germany

Background: Previous data suggest that reticulated platelets impact significantly on antiplatelet response to thienopyridines. It is unknown which of the parameters describing reticulated platelets is the optimal predictor of antiplatelet response to thienopyridine therapy.

Methods: This study is a prespecified subanalysis of the ExcelsiorLOAD trial that randomized elective patients undergoing coronary stenting to loading with clopidogrel 600mg, prasugrel 30mg or prasugrel 60mg (n=300). ADP-induced platelet reactivity was assessed by impedance aggregometry before loading (=intrinsic platelet reactivity) and on day 1 after loading. Multiple parameters of reticulated platelets were assessed by an automated whole blood flow cytometer: immature platelet fraction (IPF, proportion of reticulated platelet of the whole platelet pool), highly immature platelet fraction (hIPF), absolute immature platelet count (IPC).

Results: Each parameter of reticulated platelets correlated significantly with ADP-induced platelet reactivity: IPF ($r_s=0.18$; $p=0.002$), hIPF ($r_s=0.18$; $p=0.002$), IPC $r_s=0.26$; $p<0.001$). In a multivariable model including all three parameters, only IPC remained as significant predictor of platelet reactivity ($p<0.001$). After adjustment to known predictors of on-clopidogrel platelet reactivity including cytochrome P450 2C19 polymorphisms (*2 and *17), age, body mass index, diabetes, smoking and intrinsic platelet reactivity, IPC

was the strongest predictor of on-treatment platelet reactivity (partial $\eta^2=0.045$; $p<0.001$) followed by intrinsic platelet reactivity (partial $\eta^2=0.034$; $p < 0.002$). These findings prevailed when analyzing subgroups of patients on clopidogrel or on prasugrel.

Conclusion: Immature platelet count is the strongest platelet count derived predictor of antiplatelet response to thienopyridine treatment. Given its easy availability together with its even stronger association with on-treatment platelet reactivity when compared to known predictors including the CYP 2C19*2 polymorphism, immature platelet count might become the preferable predictor of antiplatelet response to thienopyridine treatment.

Poster presentations

Poster Session I

Berlin-Brandenburger Forschungsplattform BB3R

082

Development and Characterization of Cutaneous Squamous Cell Carcinoma

C. Wolff¹, M. Ulrich^{2,3}, J. M. Brandner⁴, C. Ulrich³, C. Zoschke¹, M. Schäfer-Korting¹

¹Freie Universität Berlin, Institute for Pharmacy, Berlin, Germany

²Collegium Medicum Berlin, Berlin, Germany

³Charité – Universitätsmedizin Berlin, Department of Dermatology, Venereology and Allergology, Skin Cancer Center Charité, Berlin, Germany

⁴University Hospital Hamburg-Eppendorf, Department of Dermatology and Venereology, Hamburg, Germany

Cutaneous squamous cell carcinoma (cSCC) is the second most common human cancer with continuously rising incidences worldwide. Primarily caused by cumulative UVB exposure, cSCC accounts for considerable costs for health care systems and poses a deadly risk especially to organ transplant recipients [1]. Current chemotherapy needs to be improved, because even the topical treatment for cSCC's carcinoma *in situ* bears limited efficacy and painful adverse effects [2]. However, animal-based approaches in preclinical development contribute to the frequent failure of investigational new drugs in clinical trials [3]. Herein, we characterized a human cell-based cSCC model, normal reconstructed human skin (RHS) served as control.

Whereas RHS exhibited low proliferation, the co-culture with cSCC increased Ki-67 index 23-fold in the cSCC model ($p<0.001$). While the presence of claudin-4 and occludin were distinctly reduced, zonula occludens protein-1 was more wide-spread, and claudin-1 was heterogeneously distributed within the cSCC model compared with RHS. This is in accordance to the *in vivo* situation [4] and likely contributes to the impaired barrier function of the cSCC model, as demonstrated for 2.6-fold increased caffeine permeation. Finally, the ingenol mebutate effects in the cSCC model and RHS closely mimic the anti-tumor effect and the adverse reactions in patients [2], both linked to the drug's inherent cytotoxicity.

In conclusion, the thorough characterization of disease models fosters both advanced preclinical drug development and improved cSCC treatment.

REFERENCES

[1] Alam M et al., N Engl J Med. 2001. 344:975-83.

[2] Gupta et al., The Cochrane database of systematic reviews. 2012. 12:Cd004415.

[3] Hartung et al., ALTEX. 2013. 30: 275-91.

[4] Rachow et al., Plos One. 2013;8:e55116.

ACKNOWLEDGMENTS

This work was financially supported by the German Federal Ministry of Education and Research (Berlin-Brandenburg research platform BB3R).

083

The Berlin-Brandenburg Research Platform BB3R and Integrated Graduate Program

S. Hedtrich¹, L. Japtok², B. Kleuser², V. Kral¹, R. Lauster³, A. Luch⁴, J. Plendl⁵, R. Preissner⁵, **M. Schäfer-Korting**¹, G. Schönfelder⁴, C. Thöne-Reineke⁵, M. Weber⁷, G. Weindl¹

¹Freie Universität Berlin, Institut für Pharmazie, Berlin, Germany

²Universität Potsdam, Potsdam, Germany

³TU Berlin, Institut für Biotechnologie, Berlin, Germany

⁴Bundesinstitut für Risikobewertung, Berlin, Germany

⁵Freie Universität Berlin, Institut für Veterinärmedizin, Berlin, Germany

⁶Charité – Universitätsmedizin Berlin, Institut für Physiologie, Berlin, Germany

⁷Zuse Institut Berlin, Berlin, Germany

Funded by the German government, the Berlin-Brandenburg Research Platform BB3R with integrated graduate education was launched in 2014. The aim of this research platform, along with the associated graduate school, is to close substantial knowledge gaps in the fields of the 3Rs and to find alternatives to animal experimentation within the next years. A panel of 3R experts has been set up to provide advice and assistance and to raise awareness in society for 3R-related issues.

Research in BB3R investigates physiological functions on different levels to establish alternative methods for preclinical drug development and basic research. The principal investigators aim at facilitating research collaborations and sustainable research activities in the region Berlin-Brandenburg and abroad. An integrated BB3R graduate program has been developed to offer structured training to graduate students in a specific, mandatory course program on 3R including modules on ethics and legislation. Currently, 14 PhD students are qualified for management positions in professional areas related to the 3Rs, and three junior research groups are now ready to expand their regional research activities nationwide.

Furthermore, the concept of a novel lecture series for master students and undergraduates has been designed and awarded the Animal Welfare Research Award for Berlin-Brandenburg in teaching and education. The state government of Berlin supports the research platform BB3R and will be funding an additional professorship at the FU Berlin to further promote research on alternative testing. Finally, co-operations with national and international partners are being built to facilitate the project-based exchange of scientists and joint research.

084

Functional characterization of reconstructed human skin with integrated Langerhans-like cells

S. Bock¹, C. Zoschke¹, A. Said¹, M. Schäfer-Korting¹, G. Müller¹, G. Weindl¹
¹Freie Universität Berlin, Institut für Pharmazie, FB Pharmakologie und Toxikologie, Berlin, Germany

Currently, the identification and evaluation of skin sensitizers is mainly restricted to animal testing using the Guinea Pig maximization test, Buehler test or the murine local lymph node assay. Recently, an adverse outcome pathway of skin sensitization has been released by the OECD, identifying the key events leading to allergic contact dermatitis. *In vitro* tests address these key events and two assays are now regulatory adopted (OECD 442C and 442D). The use of the current in chemico and *in vitro* models is, however, limited since they do not reflect dermal penetration, complete biotransformation and cell cross-talk in an organotypic environment. In this study, we aimed to overcome these limitations by establishing reconstructed skin tissues containing Langerhans cells (LCs). *In vitro* generated immature monocyte-derived (MoLCs) or MUTZ-3-derived cells (MUTZ-LCs) cultivated with keratinocytes on a dermal compartment with fibroblasts form a stratified epidermis after 14 days as indicated by the expression of epidermal differentiation markers. MoLCs or MUTZ-LCs were mainly localized in suprabasal layers of the epidermis and distributed homogeneously in accordance with native human skin.

Topical application of the extreme contact sensitizer 2,4-dinitrochlorobenzene (DNCEB) induced IL-6 and IL-8 secretion in skin models with LC-like cells, whereas no change was observed in control RHS lacking immune cells. Increased gene expression of CD83 and PD-L1 in the dermal compartment indicated LC maturation. We confirmed the enhanced mobility from epidermal to dermal compartments for MUTZ-LCs and MoLCs in the presence of DNCEB. In summary, we successfully integrated immature and functional LC-like cells into reconstructed human skin. This fosters the development of animal-free test systems for advanced and potentially individualized hazard assessment of skin sensitization.

085

Computational methods for prediction of *in vitro* activity of new chemical structures.

V. B. Siramshetty^{1,2}, P. Banerjee^{1,3}, M. Dunkel¹, A. Goede¹, R. Preissner^{1,2}, M. N. Drwal¹

¹Charité – Universitätsmedizin Berlin, Structural Bioinformatics Group, Berlin, Germany

²Freie Universität Berlin, BB3R – Berlin Brandenburg 3R Graduate School, Berlin, Germany

³Humboldt-Universität zu Berlin, Graduate School of Computational Systems Biology, Berlin, Germany

Background: With a constant increase in the number of new chemicals synthesized every year, it becomes highly important to employ the most reliable and fast *in silico* screening methods to predict their safety and activity profiles. In recent years, *in silico* prediction methods received great attention as alternatives to animal experiments for evaluation of various toxicological endpoints, complementing the theme of Replace, Reduce and Refine (3Rs). Various computational approaches have been proposed for prediction of toxicity of chemicals ranging from quantitative structure activity relationship modeling to molecular similarity based methods and machine-learning methods. Within the "Toxicology in the 21st Century" screening initiative, a crowdsourced platform was established for development and validation of computational models to predict the interference of chemical compounds in nuclear and stress receptor pathways based on a training set containing more than 10,000 compounds tested in high-throughput screening assays.

Methods: Here we present the results of various molecular similarity-based and machine-learning-based methods over an independent evaluation set containing 647 compounds. Further, we compare the performance of these methods when applied individually and together. In retrospect we also discuss the reasons behind the superior performance of an ensemble approach, that combines a molecular similarity approach and a naive Bayes machine learning algorithm in achieving best prediction rates in comparison with other individual methods, explaining their intrinsic limitations.

Results and Conclusions: Our results suggest that, although prediction methods were optimized individually for each modeled target, an ensemble of similarity and machine-learning approaches provides promising performance indicating its broad applicability in toxicity prediction.

086

In silico prediction of immunotoxicity

J. Nickel-Seeber¹, A. K. Schrey¹, M. N. Drwal¹, R. Preissner¹

¹Charité – Universitätsmedizin Berlin, Structural Bioinformatics Group, Berlin, Germany

A multitude of drug candidates (approx. 20 %) fail in the late drug development due to toxicity and adverse effects [1]. Immunotoxicity can be divided into four types of immune-mediated adverse effects: immunosuppression, immunostimulation, hypersensitivity and autoimmunity. Current safety evaluations of drug candidates with respect to immunotoxicity are comprised of *in vivo* and *in vitro* assays. Here, we present an *in silico* approach for predicting immunotoxic substances based on immune suppressive and not toxic compounds using the Laplacian-modified naive Bayesian model as a supervised machine learning method. Therefore, we examined the relations between about 51,000 compounds and 115 cancer cell lines from the National Cancer Institute's (NCI) NCI-60 growth inhibition data [2] with focus on five immune cell lines (RPMI-8226, CCRF-CEM, MOLT-4, SR and K-562). Different fingerprints encoding the chemical structures have been evaluated for their predictive power (e. g. Extended-connectivity fingerprints, substructure fingerprints) and showed good prediction rates in a retrospective analysis.

[1] Muster et. al. (2008) Computational toxicology in drug development. Drug Discov Today 13: 303-310.

[2] Reinhold et. al. (2012) CellMiner: A web-based suite of genomic and pharmacologic tools to explore transcript and drug patterns in the NCI-60 cell line set. Cancer Res 72: 3499-3511.

087

BB3R Symposium: Computer-based prediction of sulfotransferase 1E1 metabolism using 3D pharmacophores from molecular dynamics simulations

C. Rakers¹, F. Schumacher², W. Meini³, H. Glatt³, B. Kleuser², G. Wolber¹

¹Institut für Pharmazie, Freie Universität Berlin, Berlin, Germany

²Institute of Nutritional Science, University of Potsdam, Nuthetal, Germany

³German Institute of Human Nutrition (DIfE) Potsdam-Rehbrücke, Nuthetal, Germany

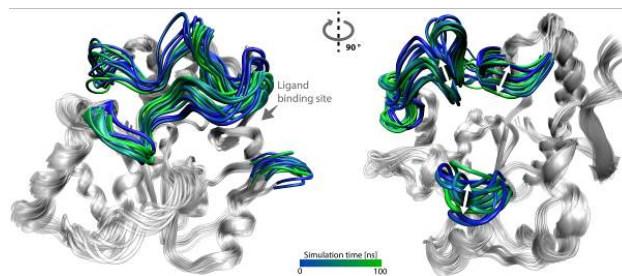
Acting in phase II metabolism, sulfotransferases (SULT) transform endo- and exogenous molecules such as drugs into more hydrophilic entities that are easily excreted from the human body [1]. Although serving detoxification, SULT-mediated transformation of molecules has also been associated with the formation of chemically reactive metabolites that could promote adverse reactions [2]. The development of a computer-based model that allows prediction of molecules susceptible to metabolism would improve drug development and drug safety [3], and encourage the reduction of *in vivo* testing according to the principles of the 3Rs (Replacement, Reduction and Refinement). In our study, we developed an *in silico* model to predict human SULT subtype 1E1 activity acting in phase II metabolism. Structure-based molecular modelling of SULT activity is challenging due to the broad and overlapping substrate spectrum of SULT subtypes. This low substrate specificity can be attributed to the high degree of conformational flexibility of the enzyme, particularly in the active site. Therefore, molecular dynamics simulations were performed to address enzyme flexibility and the broad substrate spectrum of SULT (Figure 1). Based on a collection of selected enzyme conformations from molecular dynamics simulations and a dataset of active SULT1E1 ligands, ensemble docking was utilized to generate ligand-protein complexes that served as a basis for 3D pharmacophore development. Eight specific 3D pharmacophores were created that allow identification of SULT1E1 substrates and inhibitors. For further refinement of the computer-based prediction, machine learning models and post-filtering steps were generated that allow classification of predicted hits. The final prediction model was used to screen the DrugBank (a database comprising over 6,500 experimental and approved drugs). A major part of the predicted hits could be confirmed from literature. From the remaining hits, a representative selection of molecules was experimentally tested for SULT1E1 inhibition or biotransformation. Experimental results were in agreement with our computer-based models and revealed previously-unknown biotransformation by or inhibition of SULT1E1 for compounds listed in the DrugBank.

[1] Drug Metab. Pharmacokin., 30:3-20 (2015)

[2] Curr. Med. Chem., 22:500-527 (2015)

[3] Nat. Rev. Drug Discov., 14:387-404 (2015)

Abb. 1



088

Full-thickness skin constructs: endothelialized versus non-endothelialized. A morphological comparison regarding epidermal differentiation

M. Khiao In¹, L. Wallmeyer², S. Hedtrich², J. Plendi¹, S. Kaessmeyer¹

¹Freie Universität Berlin, Veterinär-Anatomie, Berlin, Germany

²Freie Universität Berlin, Pharmazie, Berlin, Germany

Introduction: Vascularization of the dermal equivalent of full-thickness skin constructs by endothelial cells is highly desirable, because such constructs closely mimic the architecture of real skin. Unfortunately, the realization of a capillary network in skin constructs is still difficult. In our study of full-thickness skin constructs, following the methodologies of Küchler et al. (2011), there were alterations in the epidermal differentiation after endothelialization of the dermal equivalent. The aim of this study was to characterize these changes on a morphological level.

Material and methods: Non-endothelialized constructs (keratinocytes, fibroblasts) were prepared according to Küchler et al. (2011). To obtain endothelialized constructs, the dermal equivalent of the non-endothelialized constructs was enriched with endothelial cells. After two weeks of *in vitro* culture, the skin constructs were processed for quantitative as well as qualitative assessment by light and electron microscopy.

Results: Both types of skin construct developed all strata, i.e., stratum basale, spinosum, granulosum, corneum of a stratified soft-cornified epidermis, although the two constructs displayed differences in every stratum: Significantly more mitoses occurred in the epithelial germ layers of the endothelialized constructs ($p=0.013$). In addition, significantly more keratohyalin granules were counted within their stratum granulosum ($p=0.010$). 50% of the shapes of the spinosum and the granulosum cells were irregular and these cells were separated by wide intercellular spaces. The typical epidermal lamellar bodies appeared in the endothelialized constructs more often than in the non-endothelialized ones. At the stratum granulosum – stratum corneum interface, no cohesion between the strata was present.

Conclusion: The endothelialization of the dermal equivalent caused changes in the epidermal layer of the endothelialized skin constructs that may be interpreted as features of excessive epidermal differentiation.

References: Kuchler S, Henkes D, Eckl KM, Ackermann K, Plendl J, Korting HC, Hennies HC, Schäfer-Korting M. (2011) Hallmarks of atopic skin mimicked *in vitro* by means of a skin disease model based on FLG knock-down. *Altern. Lab. Anim.* 39(5):471-80.

The results of this abstract are published in *Clin Hemorheol Microcirc.* 2015 Sep 5;61(2):157-74. doi: 10.3233/CH-151988.

089

First steps of integrating immunology aspects into a multi-organ-chip platform

J. Hübner¹, I. Maschmeyer², A. Lorenz², S. Gerlach³, J. Kühni³, C. Giese⁴, R. Lauster¹, U. Marx¹

¹Technische Universität Berlin, Berlin, Germany

²TissUse GmbH, Berlin, Germany

³Beiersdorf AG, Hamburg, Germany

⁴ProBioGen AG, Berlin, Germany

Background and novelty: During the last decade organ-on-a-chip technologies received increasing attention in the scientific community. The idea of combining different tissue types on a physiological-like system creates completely new options on how substances can be characterized without the use of animal experiments. Animal models were used for the investigation of skin sensitization as a standard method until animal testing for cosmetic substances was banned in the E.U. in 2013. By combining skin models with an immunological counterpart, new data will be presented to see if the Multi-Organ-Chip add value to the current need of alternative methods regarding skin sensitization and immunotoxicity testing.

Experimental approach: The Multi-Organ-Chip platform is designed to combine different human cell and tissue types like 3D-spheroids, barrier models or biopsies in one microfluidic system. A peristaltic on-chip micropump enables circulation of medium, allowing for a constant perfusion between the compartments. First experiments were performed using a dendritic-cell-only approach in the 2-Organ-Chip. In subsequent cocultivation experiments *ex vivo* human epidermis and dendritic cells were cultivated each in one culture compartment connected by the microfluidic channels. For analysis we measured the typical activation marker CD86 and the vitality of the dendritic cells by flow cytometry. Functionally different sensitizers were selected to investigate their effects in our model.

Finally a more complex 3D matrices including different immunological cell types to emulate *in vivo*-like reactions like in the human lymph node were cultivated in the 2-Organ-Chip.

Results and discussion: Our data show a strong influence of pump pressure and pumping frequency on the activation of dendritic cells. Hence, we established an adequate set up by cultivating the dendritic cells in cell culture inserts, preventing cell activation due to shear stress. Compared to existing sensitization assays, the main advantage of the perfused 2-Organ-Chip sensitization assay is the presence of an epidermis equivalent, partially integrating important parameters such as metabolism and skin barrier function. We compared our data with reference CD86-values from the PBMD (peripheral blood monocyte derived dendritic cells) skin sensitization assay. For identical substances, we observed differences in dendritic cell activation between the PBMD assay and the 2-Organ-Chip perfused assay.

Here we present the first-time cultivation of primary derived immune cells cultivated on our microfluidic system which is a promising enhancement to integrate immunological reactions on further multi-organ combinations.

090

Generation of *in vitro* skin models using ORS cells

A. Löwa¹, N. Charbaji¹, S. Hedtrich¹

¹Freie Universität Berlin/ Institut für Pharmazie, Pharmakologie und Toxikologie, Berlin, Germany

Due to growing social and political pressure, the interest in alternatives to animal testing has constantly increased during the past 10 years stimulating the development and validation of new *in vitro* test systems including reconstructed skin models. Additional to toxicological studies and permeability assays, skin models are of high interest for fundamental research to elucidate basic physiological and pathophysiological processes in human skin [1, 2]. As for today, most of the *in vitro* skin models are grown from primary keratinocytes and fibroblasts that were either isolated from excised human skin or from juvenile foreskin following circumcision.

In this project, we aimed for the generation of *in vitro* skin models using hair follicle-derived cells. Therefore, different methods to optimize cell isolation and expansion of outer root sheath (ORS) cells from human hair follicles were systematically investigated. The best procedure for isolation of ORS cells was the direct cell outgrowth on a cell culture insert which was co-cultured with a feeder layer of postmitotic human dermal fibroblasts. Following outgrowth, the cells were either further cultivated with feeder cells in specific serum-enriched cell culture medium to obtain hair follicle-derived keratinocytes or using the same culture medium without feeder cells to obtain fibroblasts. Afterwards, the generation of hair follicle-derived fibroblasts and keratinocytes was verified via the fibroblast-specific markers vimentin and desmin and the keratinocyte marker cytokeratin (CK) 14 clearly showing that vimentin and desmin are expressed in hair follicle-derived fibroblasts and in dermal fibroblasts. As expected, these cells were negative for CK14, which was abundantly expressed in hair follicle-derived keratinocytes. Moreover, the expression of collagen type I, IV, TGF-beta, alpha SMA and IL-1 alpha in hair follicle-derived fibroblasts and dermal fibroblasts showed no significant differences. Ultimately, hair follicle-derived keratinocytes and fibroblasts were used to grow full-thickness skin models which were subsequently characterized with regard to epidermal differentiation, skin permeability and skin surface pH. Again, no significant differences compared with skin models grown from skin-derived cells were detected showing the potential of using hair follicle-derived cells for generating *in vitro* skin models.

[1] Vávrová, K., Henkes, D., Strüver, K., Sochorová, M., Školová, B. et al. Filaggrin deficiency leads to impaired lipid profile and altered acidification pathways in a 3D skin construct. *The Journal of Investigative Dermatology*. 134, 746-753 (2014).

[2] Kuchler, S., Strüver, K. & Friess, W. Reconstructed skin models as emerging tools for drug absorption studies. *Expert Opinion on Drug Metabolism & Toxicology*. 9, 1255-1263 (2013).

091

Repeated anesthesia in rodents – Assessing severity levels

K. Hohlbaum^{1,2,3}, B. Bert^{4,3}, S. Dietze², H. Fink^{2,3}, C. Thöne-Reineke^{1,3}

¹Freie Universität Berlin, Fachbereich Veterinärmedizin, Institut für Tierschutz, Tierverhalten und Versuchstierkunde, Berlin, Germany

²Freie Universität Berlin, Fachbereich Veterinärmedizin, Institut für Pharmakologie und Toxikologie, Berlin, Germany

³Freie Universität Berlin, BB3R – Berlin Brandenburg 3R Graduate School, Berlin, Germany

⁴Bundesinstitut für Risikobewertung, Experimentelle Toxikologie und ZEBET, Berlin, Germany

Background: The EU Directive 2010/63 has been drawn up with the aim of ultimately replacing animal testing. Wherever animal experimentation is necessary, the 3-R-principle of Russel and Burch (replace, reduce, refine) has to be observed. The primary goal of the 3-R-principle is to replace animal testing with alternative methods. If no alternative method can be applied, the total number of animals is supposed to be reduced. Consequently, some animals are used multiple times in the course of an experiment. For example, in imaging studies, rodents are exposed to anesthesia several times in order to control the progress of a disease. However, the Directive claims that "the benefit of reusing animals should be balanced against any adverse effects on their welfare, taking into account the lifetime experience of the individual animal".

Objective: We are looking into whether multiple exposures to anesthesia cause more stress than a single exposure.

Methods: The most common mouse strain C57/BL6 J and anesthetics isoflurane and the combination of ketamine/xylazine are used. With regard to recent studies, the animals are anesthetized six times for 45 minutes over a period of three weeks. All parameters observed are compared between controls, animals with a single and repeated anesthesia. The interval between the administration of the anesthetics is three to four days. When the animals are under anesthesia, their vital parameters are continuously monitored and afterwards their general condition is examined. The grimace scale is scored 30 and 150 minutes after anesthesia. Besides pain, the grimace scale can also assess anxiety, stress and malaise. The display of so-called luxury behaviors like nest building and burrowing behavior serves as an indicator of wellbeing. Furthermore, activity, food and water intake are monitored for 24 hours. A behavioral test battery including the free exploratory paradigm, open field, balance beam and rota rod test is performed one, seven and ten days after the last anesthesia. Motor coordination and balance are assessed by the balance beam and rota rod. The open field is a test to investigate anxiety-related and exploratory behavior, the free exploratory paradigm estimates trait anxiety. Moreover, corticosterone metabolites are measured in feces and fur in order to prove evidence of cumulative stress.

Results: The first results of our study will be presented at the 82nd meeting of DGPT.

Conclusion: We are confident that the results of our study will contribute to the assessment of the severity level caused by multiple exposures to anesthesia and in this way be a benefit for the welfare of laboratory rodents.

BB3R is funded by BMBF.

References: 1. Langford, D.J., et al., Coding of facial expressions of pain in the laboratory mouse. *Nat Methods*, 2010. 7: 447-9.

2. Albrecht, M., et al., Influence of repeated anaesthesia on physiological parameters in male Wistar rats: a telemetric study about isoflurane, ketamine-xylazine and a combination of medetomidine, midazolam and fentanyl. *BMC Vet Res*, 2014. 10: 963.

3. Jirkof, P., Burrowing and nest building behavior as indicators of well-being in mice. *J Neurosci Methods*, 2014. 234: 139-46.

4. European Union, Directive 2010/63/EU. Official Journal of the European Union 2010. L276/33-L276/29.

092

Individualized pain suppression in mice

J. Rudeck¹, S. Vogl^{1,2}, S. Banneke¹, B. Bert¹, J. Kurreck³, G. Schönfelder^{1,2}

¹Bundesinstitut für Risikobewertung, Experimentelle Toxikologie und ZEBET, Berlin, Germany

²Charité-Universitätsmedizin, Berlin, Germany

³Technische Universität, FG Angewandte Biochemie, Berlin, Germany

In 1959 the 3R-principle was defined by the British scientists William Russel and Rex Burch in their book *The Principles of Human Experimental Techniques*. The 3R refer to Replace, Reduce, and Refine. They set the goals to use alternative non-animal methods (Replace), to reduce the number of laboratory animals (Reduce) and to minimize the distress of laboratory animals and to refine their welfare (Refine). The implementation of the 3R-concept is the overall goal of scientific animal welfare. Article 4 of the *Directive 2010/63/EU on the protection of animals used for scientific purposes* state that the research on Refinement is as important as on Replacement and Reduction [1].

According to the current statistics on laboratory animals, the mouse is the most commonly used animal in experiments with approximately 70 % [2-3]. Effective pain treatment is crucial not only for ethical and legal considerations but also to achieve high-quality results [4]. Pain in mice is only obvious if it is severe or acute pain. However, it is difficult to identify slight or moderate pain. The determination of pain levels and effective dosages of analgesics is therefore challenging. The most commonly used analgesics for postsurgical pain treatment in mice are opioids. However, the recommendations for their use show vast dosage ranges. For example, the recommended dose of buprenorphine ranges from 0.05 to 2.5 mg/kg per bodyweight [5-7] depending on the pain model used. Additionally, putative pharmacogenetic strain differences have to be considered. For example, the analgesic treatment with morphine shows mouse strain specific differences in pain sensitivity [8].

The goal of the project is the refinement of the recommendations for effective dosage of opioid analgesics in laboratory animals for mouse inbred strains by incorporating strain specific differences.

Regarding the phenotype, we want to identify a putative inbred strain dependent pain threshold and measure the drug level in plasma and brain. Additionally the metabolic capacity and mRNA expression level will be investigated. Genotype identification is based on a Data Bank analysis used for correlation with phenotypical parameters.

- [1] RL 2010/63/EU.
 [2] BMEL (2014). *Anzahl der für Versuche und andere wissenschaftliche Zwecke verwendeten Wirbeltiere*.
 [3] EU COMMISSION (2013). Seventh Report on the Statistics on the Number of Animals used for Experimental and other Scientific Purposes in the Member States of the European Union.
 [4] Carbone L (2011) Pain in laboratory animals: the ethical and regulatory imperatives. *Plos One* 6, e21578.
 [5] GV-Solas, A.f.A.d. (2013). *Empfehlung zur Schmerztherapie bei Versuchstieren*.
 [6] Carpenter, J.W., T.Y. Mashima, and D.J. Rupiper (2001). *Exotic Animal Formulary*, 2nd edition, W.B. Saunders Co., Phila.
 [7] Flecknell, P. (1996). *Laboratory Animal Anaesthesia*, 2nd edition, Academic Press, San Diego, CA.
 [8] Mogil JS, Kest B, Sadowski B, & Belknap JK (1996) Differential genetic mediation of sensitivity to morphine in genetic models of opiate antinociception: influence of nociceptive assay. *The Journal of pharmacology and experimental therapeutics* 276(2):532-544.

093

Morphometry of the mandibula in Göttingen Minipigs™: Refining orofacial surgical experiments by 3D-computed tomography

G. M. Corte¹, J. Plendl¹, S. M. Niehues², H. Hünigen¹
¹Freie Universität Berlin, Institut für Veterinär-Anatomie, Berlin, Germany
²Charité Universitätsmedizin Berlin, Institut für Radiologie, Berlin, Germany

Introduction: Göttingen Minipigs™ are frequently used large animal models for orofacial research, for example dental implant surgery. Requests from experimental surgeons for detailed anatomical information can not be answered because there is no existing data, especially not age-related. Because of unavailable data and the false choice of animal age, surgical interventions fail or lead to enormous post-operative suffering. Therefore the aim of this study is the acquisition of detailed anatomical data of the mandibula and other organs and structures without sacrificing pigs for this reason.

Animals, materials and methods: CT scans of a 64-slice scanner were collected from 18 female minipigs, consisting of 6 animals aged 12 months (group 1, n=6) and 12 animals (group 2; n=12) examined at the age of 17 and 21 months. These minipigs were involved in experiments, approved by the Regional Office for Health and Social affairs, Berlin. Image analysis was performed using Vitrea Advanced® (Vital images). More than 50 parameters concerning teeth, the mandibular body, frame and canal, coronoid process and mandibular condyle were defined and measured. For now, we focused on the development of the mandibular canal and the distance between the dorsal borders of the mandibular canal to the alveolar ridge at the most posterior mental foramen, parameters immensely important for planning interventions when testing new dental implants.

Results: The measurements by Computed tomography showed variations of several parameters between left and right ramus mandibulae and within the different age groups. The volume of the Canalis mandibulae increases in time. Animals of the same age show significant differences in volume, with a range of up to 65% where the largest volume was 13,4 ml and the lowest 4,7 ml. The distance between the dorsal borders of the mandibular canal to the alveolar ridge decreases between 12 and 17 months of age. Comparing 17 and 21 months old minipigs, no significant difference in distance could be observed. From the age of 17 months the position of the mandibular canal in relation to the alveolar ridge remains constant.

Conclusion: The decrease of the distance between the mandibular canal and the alveolar ridge between 12 and 17 months of age indicates ongoing anatomical changes of this parameter until the age of 17 months. Therefore animals should be older than 17 months if included in long-term studies after orofacial experiments, like implant surgery of the mandibula. Because of the described individual differences, the authors strongly suggest to support the planning of orofacial interventions by CT imaging or other radiographic techniques.

094

Characterization of stereotypes in FVB/N-Mice and its impact on immune system and metabolism

T. Nitecki¹, B. Kleuser¹, S. Krämer²
¹Universität Potsdam, IEW / BB3R, Nuthetal, Germany
²Deutsches Institut für Ernährungsforschung, Nuthetal, Germany

Background: Laboratory housing conditions are standardized to a high level. Under these conditions, the occurrence of stereotypic behaviour (SB) can be observed. Stereotypies are commonly known as deviations from normal behaviour that are repetitive, invariant and without any obvious function or aim for the animal [1]. Worldwide it is estimated that over 85 million animals perform SB, with the highest prevalence in laboratory animals and the agricultural sector. FVB/N is a typical inbred mouse-strain that shows different types of stereotyped movements. It is known that environmental enrichment decreases the incidence of SB, yet they still occur [2]. Since animal's behaviour highly influences its metabolism and immune system, differences in handling, caring and keeping can lead to varying results, even with an identical experimental setup [3].

Aim: of the study Aim of the study is to observe different life stages of FVB/N-mice and immediately detect the development of SB. Observations are linked to various behavioural tests and the characterisation of the metabolic and immunological phenotype. The results will lead to a better understanding of the mechanisms driving the development of SB and clarify its implication to animal welfare or to what extent the performance of stereotypes even reflect emotional suffering.

Methods: The strain-related behaviour and SB are recorded with computer-assisted programmes. Observational periods already begin with the parental generation. As possible indicators for later developing SB, data on reproductive success and maternal care are collected, such as different behavioural tests. The animals are characterized by a specific protocol for detecting the metabolic and immunological phenotype. Finally, histological and molecular biological analyses follow.

Outlook: It is of paramount importance to take good care for the welfare of laboratory animals (3R-Refinement). Though, the knowledge about the ethological particularities of animals and the motivational base of animals performing SB are not enough to generally avoid stereotypies. Therefore the meaning according to the character of SB has to be analysed more intensively to understand the needs of laboratory animals and evolve recommendations for optimizing the breeding and keeping such as for the assessment of possible distress in animals performing SB.

- Quellen:** 1. Mason GJ. Stereotypies – A critical review. *Animal Behaviour* 41: 1015-1037, 1991.
 2. Coombs EJ. Assessing the Effects of Environmental Enrichment on Behavioural Deficits in C57BL Mice. *Altern Lab Anim.* 42(2):P18-22, 2014.
 3. Garner JP. Stereotypies and other abnormal repetitive behaviors: potential impact on validity, reliability, and replicability of scientific outcomes. *ILAR J.* 46(2):106-117, 2005.

Pharmacology – G-protein coupled receptors

095

Postsynaptic 5-HT_{1A} receptors and regulation of body temperature in mice

M. Feja¹, B. Noto¹, H. Fink¹, S. Dietze¹
¹Institute of Pharmacology and Toxicology, School of Veterinary Medicine, Freie Universität Berlin, Berlin, Germany

Objective: Thermoregulation is a vital function in both humans and animals with the serotonin (5-HT) system, in particular the 5-HT_{1A} receptor, playing a major role. Activating 5-HT_{1A} receptors by the 5-HT_{1A} receptor agonist 8-hydroxy-2-(dipropylamino)tetralin (8-OH-DPAT) leads to reduced body temperature. While there is consensus that hypothermia is induced by the stimulation of postsynaptic 5-HT_{1A} receptors in rats and humans, the regulatory mechanisms in mice are less clear. In our group, within phenotyping a transgenic mouse line permanently overexpressing the 5-HT_{1A} receptor in serotonergic projection areas, Bert et al. (2008, PMID: 18396339) revealed exaggerated 8-OH-DPAT-provoked hypothermic response. Thus, the objective of the present study was to substantiate the contribution of postsynaptic 5-HT_{1A} receptors to thermoregulation, more precisely to the hypothermic effect of 8-OH-DPAT, in mice.

Methods: We used radio telemetry technique to monitor the basal body temperature and the hypothermic effect of different doses of 8-OH-DPAT (0.1 mg/kg – 4 mg/kg i. p.) in male transgenic mice in comparison to NMRI wild-type males. Additionally, we investigated whether reduction of serotonergic activity by pretreatment with the 5-HT synthesis inhibitor parachlorophenylalanine (PCPA; 100 mg/kg, i. p. on four consecutive days) would alter the effects of 8-OH-DPAT on body temperature in transgenic mice postsynaptically overexpressing the 5-HT_{1A} receptor.

Results: 5-HT_{1A} overexpressing mice revealed lower levels of basal body temperature than wild types (transgenic mice: 36.0 °C; NMRI wild-type mice: 37.4 °C). In both genotypes, systemic administration of 8-OH-DPAT dose-dependently decreased body temperature, being significantly more pronounced in mutant mice (-2.8 °C compared to -1.5 °C in NMRI wild types). Dose response curves of 8-OH-DPAT revealed an ED₅₀ = 0.4 mg/kg in transgenic and an ED₅₀ = 0.57 mg/kg in NMRI wild-type mice. PCPA pretreatment did not alter the hypothermic response to 8-OH-DPAT in mice.

Conclusions: The dose-response curves indicate a higher potency of 8-OH-DPAT in transgenic mice. The exaggerated hypothermic response to 8-OH-DPAT in mutant mice implies that postsynaptic 5-HT_{1A} receptors could be involved in thermoregulatory function in mice. This assumption is further confirmed by the fact that 8-OH-DPAT-evoked thermal responses were not influenced by pretreatment with PCPA, most notably in transgenic mice overexpressing 5-HT_{1A} receptors postsynaptically.

096

The p.Arg389Gly variation in the human β₁-adrenoceptor regulates receptor activation and arrestin recruitment

A. Ahles¹, L. Hinz¹, M. Bünemann², S. Engelhardt^{1,3}
¹Technische Universität München, Institut für Pharmakologie und Toxikologie, München, Germany
²Philipps-Universität Marburg, Institut für Pharmakologie und Klinische Pharmazie, Marburg, Germany
³DZHK (Deutsches Zentrum für Herz-Kreislaufforschung), partner site Munich Heart Alliance, München, Germany

Genetic variation within G protein-coupled receptors compromises the therapeutic application of drugs targeting these receptors. One of the most intensely studied variation is p.Arg389Gly in the human beta1-adrenoceptor (ADRB1). The ADRB1 carrying arginine at position 389 in helix 8 in the proximal carboxy terminus is more frequent among Caucasians and is hyperfunctional. Yet, the molecular basis for the differences between the beta1-adrenoceptor variants Arg389-ADRB1 and Gly389-ADRB1 is poorly understood.

Despite its hyperfunctionality, we found the Arg389-variant of the ADRB1 to be hyperphosphorylated upon continuous stimulation with norepinephrine when compared to the Gly389-variant. Using ADRB1 sensors to monitor activation kinetics by fluorescence resonance energy transfer (FRET), the Arg389-ADRB1 exerted faster activation speed and arrestin recruitment than the Gly389-variant. Both depended on phosphorylation of the receptor as shown by knockdown of G protein-coupled receptor kinases and by FRET experiments using phosphorylation-deficient ADRB1 mutants. Point mutation of single serines and threonines in the carboxy terminus of the ADRB1 finally revealed a variant-specific phosphorylation pattern that determines arrestin recruitment.

Taken together, these findings suggest that differences in receptor phosphorylation determine the differences in activation speed, efficacy and arrestin recruitment of ADRB1 variants.

097

μ -opioid receptor phosphorylation is regulated by agonist-selective engagement of G protein-coupled receptor kinase 2 and 3

E. Miess¹, S. Schulz¹

¹Institut für Pharmakologie und Toxikologie, Universitätsklinikum Jena, Jena, Germany

Opioid drugs are the most potent analgesics, which are used in the clinic; however, by activating the μ -opioid receptor (MOR) they also produce several adverse side effects including constipation, antinociceptive tolerance, and physical dependence. There is substantial evidence suggesting that G protein-coupled receptor kinases (GRKs) and β -arrestins play key roles in regulating MOR signaling and responsiveness. Following phosphorylation by GRKs, β -arrestins bind to phosphorylated MORs, which prevents further interactions between the receptor and G proteins even in the continued presence of agonist resulting in diminished G protein-mediated signaling. We have previously shown that agonist-induced phosphorylation of MOR occurs at a conserved 10-residue sequence, ³⁷⁶TREHPSTANT³⁷⁹, in the carboxyl-terminal cytoplasmic tail. Morphine induces a selective phosphorylation of serine³⁷⁵ (S375) in the middle of this sequence that is predominantly catalyzed by G protein-coupled receptor kinase 5 (GRK5). By contrast, high-efficacy opioids not only induce phosphorylation of S375 but also drive higher-order phosphorylation on the flanking residues threonine³⁷⁰ (T370), threonine³⁷⁶ (T376), and threonine³⁷⁹ (T379) in a hierarchical phosphorylation cascade that specifically requires GRK2/3 isoforms. To investigate this mechanism further, we have developed novel β -galactosidase complementation assays to monitor agonist-dependent recruitment of GRK2 and GRK3 to activated MORs. Using this assay, we were able to show that activation of MOR by high-efficacy agonists such as DAMGO results in a robust translocation of GRK2/3. In contrast, activation by low-efficacy agonists such as morphine results in a much less pronounced recruitment of GRK2/3 isoforms. Interestingly, DAMGO-induced β -arrestin recruitment was strongly inhibited by siRNA knock down of GRK2 or GRK3. Conversely, the morphine-induced β -arrestin recruitment was strongly enhanced by overexpression of GRK2 or GRK3. Mutation of S375 to alanine strongly inhibited both GRK and β -arrestin recruitment. However, mutation of all 11 carboxyl-terminal serine and threonine residues of MOR was required to completely abolish its interaction with arrestins and GRKs resulting in a complete loss of MOR internalization and desensitization.

098

Unravel molecular mechanisms of G protein inhibition with radioligand binding experiments

R. Schrage¹, T. Bodefeld¹, G. König², E. Kostenis³, K. Mohr¹

¹University of Bonn, Pharmacology and Toxicology, Bonn, Germany

²University of Bonn, Department of Pharmaceutical Biology, Bonn, Germany

³University of Bonn, Molecular-, Cellular-, and Pharmacobiology Section, Institute of Pharmaceutical Biology, Bonn, Germany

Heterotrimeric G proteins are located at the inner leaflet of plasma membranes and are a major primary transducer of cell signaling initiated by G protein-coupled receptors (GPCRs). Based on sequence similarity, heterotrimeric G proteins can be subdivided into four main classes, i.e. Gi/o, Gs, Gq/11, and G12/13, which interact with distinct cellular effectors to shape the final cellular response¹. Identification of new selective and cell-permeable G protein inhibitors is of great interest as these may be beneficial in complex pathologies that involve signaling of multiple GPCRs². Mechanistically, small molecule G protein inhibitors may, for instance, block nucleotide exchange by inhibiting GDP release (i.e. guanyl nucleotide dissociation inhibitors, GDIs) or allow GDP release but block GTP entry by stabilizing the G protein in an empty pocket conformation³. Here, we set out a new approach to classify G protein inhibitors regarding their mechanism of action in radioligand binding experiments.

In particular, we investigated the influence of the specific G_{q/11/14} inhibitor FR900359⁴ on agonist-radioantagonist binding experiments performed with membranes of CHO cells stably expressing the muscarinic M1 acetylcholine receptor (CHO-M1). Agonist-radioantagonist competition under these conditions is biphasic because agonists bind with higher affinity in the ternary complex consisting of agonist, receptor and nucleotide-free G protein compared with a G protein-free receptor^{1,5}.

We show that FR900359 can be classified as a GDI as it significantly reduced high affinity binding of carbachol in CHO-M1 membranes. In contrast to this, BIM-46187, a pan G protein inhibitor with a cell-type-dependent preference for Gq, did not influence high affinity agonist binding and thus stabilized Gq in an empty pocket conformation³. Interestingly, inhibition of high affinity agonist binding by FR900359 was incomplete in agonist-radioantagonist displacement studies and also when a radioagonist was applied. To fully prevent high affinity agonist binding by FR900359, combined uncoupling of both Gi and Gs proteins from M1 was required by pre-treatment with pertussis toxin and cholera toxin, respectively. These data demonstrate that not only Gq, but also Gi, and Gs, contribute to the high affinity fraction of M1 receptors.

Taken together, our findings show that radioligand binding experiments are an attractive approach to classify new G protein inhibitors according to their mechanism of action.

1. Oldham, W. M. & Hamm, H. E. Heterotrimeric G protein activation by G-protein-coupled receptors. *Nat Rev Mol Cell Biol* **9**, 60-71 (2008).
2. Smrcka, A. V. Molecular targeting of Ga and G β y subunits: a potential approach for cancer therapeutics. *Trends Pharmacol Sci* **34**, 290-298 (2013).
3. Schmitz, A.-L. et al. A cell-permeable inhibitor to trap G α q proteins in the empty pocket conformation. *Chem Biol* **21**, 890-902 (2014).
4. Schrage, R. et al. The experimental power of FR900359 to study Gq-regulated biological processes. *Nat Commun*, accepted article.
5. De Lean, A. Stadel, J. M. & Lefkowitz, R. J. A ternary complex model explains the agonist-specific binding properties of the adenylate cyclase-coupled beta-adrenergic receptor. *J Biol Chem* **255**, 7108-7117 (1980).

099

Dualsteric compounds modulate the signaling pattern of muscarinic M1 acetylcholine receptors

T. Bodefeld¹, C. Matera², C. Dallanocce², R. Messerer³, U. Holzgrabe³, M. De Amici², K. Mohr¹, R. Schrage¹

¹Universität, Pharmakologie und Toxikologie, Bonn, Germany

²Universität, Mailand, Italien

³Universität, Würzburg, Germany

G protein-coupled receptors (GPCRs) are cell surface receptors which, upon a conformational change in the receptor protein induced by an extracellular stimulus, can transduce the signal onto intracellular adaptor proteins such as heterotrimeric G proteins [1]. GPCR-induced cell signaling can be rather complex as several GPCRs may activate multiple different adaptor proteins and can additionally be activated via distinct binding sites, i.e. the orthosteric transmitter binding site and other "allosteric" binding sites [2]. In the present work, we wanted to investigate the influence of an allosteric binding site on receptor activation of muscarinic acetylcholine receptors (mAChRs). To this end, we employed the orthosteric full agonists acetylcholine and iperoxo as well as several dualsteric compounds consisting of iperoxo linked to an allosteric phthalimide (pht) or naphthalimide (naph) moiety through alkyl chains of different length or through a diamide linker (fri). Binding of the allosteric part to the receptor protein may restrict the conformational flexibility of the receptor protein and thus interfere with receptor activation [2]. Therefore, application of different linker length may control the signaling outcome. Here, we applied the human M1 mAChR which preferentially activates G proteins of the G_{q/11} type but can also promiscuously stimulate G_s proteins. G_{q/11}- and G_s-dependent signaling pathways were analyzed by application of CHO cells stably transfected with the human M1 mAChR in IP1 and cAMP accumulation assays, respectively. In comparison to the orthosteric building block iperoxo, all dualsteric compounds under investigation showed a decrease in potency for both G_q-mediated and G_s-mediated signaling. Our findings show that the bulkier allosteric naph residue impaired both signaling pathways to a greater extent than the smaller substituent pht. Particularly, the compound iper-6-naph completely lost intrinsic activity for both G_{q/11} and G_s activation at the M1 mAChR. Moreover, G_s-mediated pathway activation is more sensitive to spatial restriction in the allosteric vestibule than G_q-signaling. Interestingly, longer linker length led to improved signaling for both pathways (G_s and G_q) in both hybrid series. Iper-7-pht seems to be an exception as it had a higher intrinsic efficacy for G_s-dependent signaling than the other pht hybrids with longer linker chains. Strikingly, only iper-fri-pht, which corresponds to iper-8-pht in linker length, but is able to engage increased hydrogen bonding with the receptor protein, acted as a full agonist on M1 mAChR for both signaling pathways under investigation. Taken together, these data strongly suggest that, in comparison to G_{q/11}-mediated signaling, activation of the G_s protein in M1 mAChR is more sensitive to spatial restriction in the allosteric vestibule. Thus, it appears to be possible to control signaling of the M1 mAChR by allosteric constraint of the receptor's conformational flexibility.

[1] Magalhaes, A. et al.: *Br. J. Pharmacol.* 2011, 165(6): 1717-36

[2] Bock, A. et al.: *Nat. Commun.* 2012, 3:1044 doi: 10.1038/ncomms2028

100

In-vitro-pharmacology and structure-activity relationships of derivatives of imidazolylpropylguanidine (SK&F-91,486) at histamine receptors (hH_{1,2,3},R and gpH₁,R)

S. Pockes¹, A. Buschauer¹, S. Elz¹

¹Universität Regensburg, Pharmazeutische/Medizinische Chemie, Regensburg, Germany

For more than three decades 3-(1*H*-imidazol-4-yl)propylguanidine (SK&F-91,486 (1)^[1]) is known as the prototypic pharmacophore of highly potent histamine H₂-receptor (H₂R) agonists of the guanidine class of compounds including, e.g., impromidine and apromidine.^[2] In order to get more insight into the structure-activity relationships of alkylated analogues of SK&F-91,486, we characterized 78 newly synthesized derivatives including several bivalent compounds (e.g., 2) by using different pharmacological *in-vitro* methods.^[3]

The potential H₂R agonists were subjected to a broad screening procedure utilizing radioligand binding assays with membranes of Sf9 cells^[4] (hH_{1,2,3},R). Compounds were also functionally characterized in the [³⁵S]GTPγS assay (hH₂R, Sf9 cell membranes).^[5] Selectivity vs. hH_{1,3},R was determined for selected derivatives also using this technique. Organ bath studies (gpH₁R (ileum), gpH₂R (right atrium)) yielded functional data in a more physiological environment. The major part of the new SK&F-91,486 analogues displayed partial or full agonism via hH₂R and gpH₂R, respectively. The most potent analogue, bivalent thiazole-type bisguanidine 2, was a partial agonist (*E*_{max} = 88%) and 250-times as potent as histamine *vis-à-vis* the gpH₂R. Attempts to antagonize the positive chronotropic effect of (partial) agonists by preincubation with cimetidine, or by adding a cimetidine bolus at the end of the concentration-response curve, respectively, were successful and furnished pA₂ values for the antagonist (5.87 – 6.38) which are in accordance with literature data.

However, in the functional *in-vitro* assay on gpH₂R, the positive chronotropic response evoked by SK&F-91,486 was surprisingly resistant to antagonism by cimetidine and other typical H₂R antagonists (ranitidine, famotidine), although the compound so far has been unanimously classified by others as a weak partial H₂R agonist. This behaviour is unique within the large series of SK&F-91,486 analogues studied so far under similar conditions. Probably the positive chronotropic effect of the lead compound is – at least in part – the result of a second molecular interaction which has been overlooked so far.

[1] Parsons, M.E. et al.; *Agents Actions* **1975**, 5, 464.

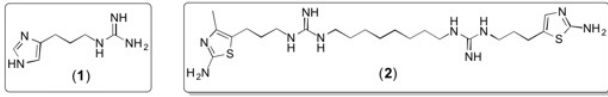
[2] Buschauer, A.; *J. Med. Chem.* **1989**, 32, 1963-1970.

[3] Pockes, S.; Dissertation, *Univ. Regensburg* **2015**.

[4] Seifert, R.; *J. Pharmacol. Exp. Ther.* **2003**, 305(3), 1104-1115.

[5] Schneider, E.H.; Seifert, R.; *Pharmacol. Ther.* **2010**, 128(3), 387-418.

Abb. 1



101

Agonist-induced NOP receptor phosphorylation revealed by phosphosite-specific antibodies

A. Mann¹

¹Institut für Pharmakologie und Toxikologie, Jena, Germany

The nociceptin/orphanin FQ (N/OFQ) peptide (NOP) receptor is the fourth most recently discovered and least characterized member of the opioid receptor family (MOR, KOR and DOR). NOP receptor is widely distributed and modulates several physiological processes by its endogenous ligand nociceptin. The NOP receptor is a potential target for the development of ligands with therapeutic use in several pathophysiological states such as chronic and neuropathic pain. Consequently, there is increasing interest in understanding the molecular regulation of NOP receptor. Recently, we generated two phosphosite-specific antibodies directed against the carboxyl-terminal residues serine³⁵¹ (S351) and threonine³⁶²/serine³⁶³ (T362/S363), which enabled us to selectively detect either the S351- or the T362/S363-phosphorylated forms of the receptor. Our results show that nociceptin, MCOPPB, SCH221510 and Ro64-6198 induce a stably phosphorylation at S351 and T362/S363 followed by a profound internalization of the receptor. The nociceptin-induced S351 and T362/S363 phosphorylation can be blocked by selective NOP receptor antagonists such as J113397 or SB612,111. NNC63-0532, buprenorphine and norbuprenorphine failed to induce a phosphorylation at these sites. In the presence of nociceptin, S351 phosphorylation occurred at a faster rate than phosphorylation at T362/S363 indicating that S351 is the primary site of agonist-dependent phosphorylation. Activation of PKC by phorbol 12-myristate 13-acetate facilitated receptor phosphorylation only at S351 but not at T362/S363, indicating that S351 can also undergo heterologous phosphorylation. Using NOP-GFP *knock in mice*, we detected NOP receptors in brain, spinal cord and dorsal root ganglia (DRG). We were also able to demonstrate a dose-dependent NOP receptor phosphorylation at T362/S363 in mouse brain *in vivo* using Western blot and mass spectrometry. In contrast, MCOPPB and SCH221510 failed to induce phosphorylation *in vivo*. Together, these data provide new insights into the molecular regulation of the NOP receptor *in vitro* and *in vivo*.

102

G-protein-dependent and -independent signaling of human CCR2 chemokine receptors

L. Hipp¹, D. Markx¹, **B. Moepf**¹

¹Universität Ulm, Pharmacology and Toxicology, Ulm, Germany

Several findings indicate that inflammatory diseases are initiated or maintained by an imbalance of receptor biased signaling; the latter referring to the ability of distinct ligands to endue individual receptors with qualitatively different G-protein- and/or b-arrestin-dependent signaling (1). Chemokines and their receptors regulate a wide array of leukocyte functions, including chemotaxis, adhesion, and transendothelial migration, and thus play important roles in regulating inflammation (2). In man, two CC chemokine receptors CCR2a and CCR2b are present that only differ in their carboxyl terminal portions; the latter known to interact with multi-protein complexes made up of heterotrimeric G proteins (pertussis toxin sensitive and -insensitive) and non-G-protein components, including b-arrestin (2). Interested in differential signaling of CCR2a and CCR2b we comparatively analyzed ligand-induced G-protein-regulated signaling pathways (e.g. activation of phospholipase C isoenzymes and RhoGTPase-induced serum response factor [SRF] activity) and b-arrestin-regulated pathways (e.g. internalization of receptors and phosphorylation of ERK1/2) in the presence of CCL2, CCL8, CCL7, and CCL13. All these chemokines have been shown to interact with human CCR2 receptors. In addition, the structural requirements of the carboxyl terminal portions involved in determining specificity in G-protein-dependent signaling was addressed by using CCR2 receptor mutants. The comparative analysis revealed that differences in ligand-induced activation of G-protein-dependent (pertussis-toxin-sensitive versus pertussis-toxin-insensitive) and/or b-arrestin-dependent signaling exist. For example, activation of CCR2b receptors by CCL2 induced both Rho-dependent SRF activation and receptor internalization, while CCL8-stimulation resulted in SRF but little if any receptor internalization. In contrast, CCR2a-expressing cells showed CCL2-dependent SRF-activation but any receptor/ligand internalization. Analysis of the structural requirements of CCR2 receptors for coupling to G proteins revealed that arginine 313 within the putative 'eighth helix' of the carboxyl-terminal portions of CCR2a and CCR2b is not involved in Ga_i-mediated induction of ERK1/2 and plays a minor role in CCR2b receptor internalization, but is specifically required for the CCR2a/ and CCR2b/Ga_i-mediated activation of SRF.

1) Steen, A. et al. (2014): Biased and G protein-independent signaling of chemokine receptors. *Front. Immunol.* 5:277. 2) Bachelier, F. et al. (2014): International Union of Pharmacology. Update on the extended family of chemokine receptors and introducing a new nomenclature for atypical chemokine receptors. *Pharmacol. Rev.* 66, 1-79.

103

Endogenous expression of functional serotonin 5-HT_{2C} receptors in hypothalamic, murine HypoA-2/10 cells

A. Breit¹, L. Lauffer¹, E. Glas¹, T. Gudermann¹

¹LMU, Walther-Straub-Institut, München, Germany

Serotonin 5-HT_{2C} receptors (5-HT_{2CR}) are functionally engaged with G_q proteins and expressed in the central nervous system (CNS). 5-HT_{2CR} significantly regulate emotion, feeding, reward or cognition and thus might serve as promising targets for drugs against

psychiatric disorders or obesity. Due to the technical difficulties in isolating cells from the CNS and the hitherto lack of suitable cell lines that would endogenously express 5-HT_{2CR}, our knowledge about this receptor subtype is rather limited. Recently established hypothalamic mHypoA2-10 cells show some characteristics of appetite-regulating hypothalamic neurons of the *paraventricular nucleus*, where 5-HT_{2CR} *in vivo* expression has been detected. Thus, we tested mHypoA2-10 cells for putative 5-HT_{2CR} expression by performing single cell calcium imaging. We observed that serotonin and the specific 5-HT_{2CR} agonist, WAY161,503 induced robust calcium transients, which were strongly inhibited by two unrelated 5-HT_{2CR}-selective antagonists (SB206,553, RS102,221). Serotonin and WAY161,503 also activated a cAMP response element-dependent reporter gene construct and induced significant phosphorylation of extracellular-regulated kinases-1/2 in a SB206,553 and RS102,221 sensitive manner, providing further evidence for functional 5-HT_{2CR} expression in mHypoA-2/10 cells. Intrinsic activity of WAY161,503 ranged between 0.3 and 0.5 compared to serotonin in all assays, defining WAY161,503 as a partial 5-HT_{2CR} agonist. In conclusion, we provide convincing data that hypothalamic mHypoA-2/10 cells endogenously express 5-HT_{2CR} and thus represent the first cell line to analyse 5-HT_{2CR} pharmacology, signaling and regulation in its natural environment.

104

Optical and electrophysiological methods allow detection and characterization of G_{i/o}-protein coupled receptors

J. Straub¹

¹Walther-Straub-Institut für Pharmakologie und Toxikologie, München, Germany

G-protein mediated signaling pathways are essential components of basic cellular functions. Of note, G-protein coupled receptors (GPCRs) constitute one of the major drug targets in modern medicine. However, despite their clinical importance, fundamental properties of these receptors remain unknown. In particular, regulation of the major second messenger cAMP by G_s- and G_{i/o}-protein coupled receptors is of special interest. The classical biochemical method to detect receptor-mediated cAMP level changes uses pre-labeling with ³H-Adenine and calculation of the conversion rate to ³H-cAMP. Although, this multi-cellular method is highly sensitive and reproducible, it lacks time resolved and spatial assessment of cAMP formation in single living cells. To measure G_s-protein induced increases of intracellular cAMP levels in single living cells in a time resolved manner, the FRET-based cAMP-sensor Epac is commonly used. However, it was unknown whether this sensor might be suitable to detect G_{i/o}-protein mediated decreases of intracellular cAMP levels as well. In this study, we show that FRET-based cAMP sensors can be deployed to reliably monitor G_{i/o}-protein mediated cAMP level decreases. FRET experiments with adrenergic α_{2A} or μ₁ opioid receptors in combination with different FRET-based cAMP sensors showed a notable reduction of intracellular cAMP levels upon receptor activation which could be significantly reduced by selective receptor antagonists. Of note, HEK293 cells had to be pre-incubated with forskolin in submaximal concentration to increase basal cAMP levels. Our findings suggest that FRET based Epac sensors are suitable to detect G_{i/o}-protein activation similar to electrophysiological whole-cell measurements with G_{i/o}-protein coupled receptors and TRPC5 or heteromeric Kir3.1/Kir3.2 or Kir3.1/Kir3.4 channels co-expressing cells. Hereby, agonist stimulations caused current increases with characteristic current-voltage relationships. Altogether, our findings indicate that both optical and electrophysiological approaches allow time resolved detection and characterization of G_{i/o}-protein coupled receptor activation in single living cells.

105

Histamine H₂-receptor overexpression is beneficial for systolic dysfunction in PP2A overexpressing mice

F. Bergmann¹, U. Gergs¹, J. Neumann¹

¹Institute for Pharmacology and Toxicology, Medical Faculty, Martin Luther University Halle-Wittenberg, Halle (Saale), Germany

Histamine can exert positive inotropic and chronotropic effects in humans via histamine H₂-receptors. We have generated and partially characterized transgenic mice (TG) which overexpress the human histamine H₂-receptor specifically in cardiomyocytes via the α-myosin heavy chain promoter. In these mice, but not in wild type mice (WT), histamine increased heart rate and ejection fraction (EF) measured *in vivo* by echocardiography under isoflurane anesthesia. To investigate some aspects of the signaling pathway in these mice, we crossed the TG mice with PP2A mice leading to double transgenic mice (H₂xPP2A = DT). PP2A mice (*J Biol Chem* 2004;279:40827) overexpress the catalytic subunit of protein phosphatase 2A (PP2A) in cardiac myocytes and develop a cardiac hypertrophy. At an age of about 240 days we noted reduced EF in PP2A (33.1 ± 3.5 %, n=16) compared to WT (54.4 ± 4.5 %, n=10) and TG (59.8 ± 2.9 %, n=10). Interestingly, in DT the EF (43.9 ± 4.9 %, n=11) was higher than in PP2A at similar heart rates. E/A was elevated in DT compared to WT. Relative heart weights were unchanged between these groups. In summary, we demonstrated that PP2A is involved in H₂-receptor signaling and we tentatively conclude that the H₂-receptor is able to ameliorate systolic but not diastolic cardiac function of PP2A mice.

106

In 5-HT₄-receptor overexpressing mice, diastolic function is partially preserved in a model of sepsis

T. Geriák¹, U. Gergs¹, J. Neumann¹

¹Institute for Pharmacology and Toxicology, Medical Faculty, Martin Luther University Halle-Wittenberg, Halle (Saale), Germany

Serotonin (5-HT) can exert positive inotropic and chronotropic effects in humans via 5-HT₄-receptors. We have generated transgenic mice (TG) which overexpress the human 5-HT₄-receptor selectively in cardiomyocytes via the α-myosin heavy chain promoter. In these mice, but not in wild type mice (WT), serotonin induced increases in heart rate and ejection fraction. We treated the mice with 30 μg LPS (lipopolysaccharide, i.p.; a

standard model of sepsis) per g body weight or isotonic sodium chloride solution (as solvent control). Echocardiography with isoflurane anesthesia was performed before and 3, 7 and 24 hours after LPS treatment. LPS led to a time-dependent deterioration of cardiac function in both TG and WT. The deterioration included systolic function (left ventricular ejection fraction=EF) as well as diastolic function (height of A and E waves through the mitral valve: E/A). For instance, EF amounted to $58.8 \pm 20.7\%$ seven hours after LPS in WT and to $61.4 \pm 15.9\%$ in TG ($n=10-12$, $p<0.05$ vs pre-LPS value). However, 24 hours after LPS, diastolic function, measured as E/A, amounted to 1.86 ± 0.43 in WT and 1.49 ± 0.17 in TG ($n=6-7$, $p<0.05$ TG vs. WT). Moreover, after 24 hours a less pronounced decline in body temperature (probably due to superficial abdominal hyperemia) occurred in TG versus WT. In contrast, while all flow parameters declined after 3 and 7 hours of LPS, they were not different between WT and TG. For instance, maximum flow (in mm/s) through the ascending aorta declined from 1158.3 ± 212.2 to 782.5 ± 154.3 in WT and from 1208.4 ± 235.1 to 798.8 ± 170.1 in TG (TG vs. WT, $p>0.05$, $n=10-12$; after 7 hours). We tentatively conclude: 5-HT₂-receptors overexpression protects the heart against sepsis, putatively by interference with the intracellular biochemical pathway of LPS in cardiomyocytes.

107

Further characterization of histamine H₂-receptor overexpressing mice

K. Griethe¹, U. Gergs¹, J. Neumann¹

¹Institute for Pharmacology and Toxicology, Medical Faculty, Martin Luther University Halle-Wittenberg, Halle (Saale), Germany

Histamine can exert positive inotropic and chronotropic effects in humans via histamine H₂-receptors. We have generated transgenic mice (TG) which overexpress the human H₂-receptor specifically in cardiomyocytes via the α -myosin heavy chain promoter. In TG, but not in wild type mice (WT), histamine (EC₅₀ = 34 nM) or amthamine (EC₅₀ = 10 nM), a more selective and potent H₂-receptor agonist, induced positive inotropic effects (PIE) and positive chronotropic effects (PCE) in isolated left and right atrial preparations, respectively. In order to investigate the signal transduction for the PIE in atrium, contractile studies using partially depolarized preparations were performed. Therefore, left atrial preparations were equilibrated in the organ bath to 44 mM potassium chloride. Thereafter, histamine (100 μ M) induced a PIE ($31.1 \pm 10.4\%$ of control, $n=7$) in TG but not in WT preparations whereas isoprenaline (10 μ M) increased force in both WT and TG. The PIE of histamine in potassium treated TG atrium could be blocked by cimetidine. Compound 48/80, a releasing agent of endogenous histamine, increased force of contraction in TG left atria to a higher extent than in WT. Furthermore, we tested whether analgetics known to release histamine were inotropically active in TG. However, morphine (10 μ M) was unable to affect contractility in WT or TG, whereas ketamine and fentanyl increased left atrial contractility in both TG and WT. In summary, we demonstrated an involvement of the L-type calcium channel current in the H₂-receptor mediated PIE in TG atria. We failed to release inotropically active histamine using classical analgetics, arguing that a direct effect also in the human heart is unlikely to occur.

108

Interaction of the μ -opioid receptor with G-proteins and GRK2

J. G. Ruland¹, O. Prokopets¹, V. Wolters¹, S. Schulz², C. Krasel¹, M. Bünemann¹

¹Philipps-Universität Marburg, FB Pharmazie, Institut für Pharmakologie und Klinische Pharmazie, Marburg, Germany

²Universitätsklinikum Jena, Institut für Pharmakologie und Toxikologie, Jena, Germany

The initial step in the homologous desensitization of G-protein-coupled receptors is their phosphorylation by one of the G-protein-coupled receptor kinases (GRKs). We demonstrate here measurement of the interaction of GRK2, a ubiquitously expressed GRK, with the μ -opioid receptor (μ OR) by FRET and its dependence on agonist efficacy. HEK293T cells transfected with YFP-tagged μ OR and mTurquoise-tagged GRK2 as well as non-fluorescent G α_{i1} , G β and G γ subunits showed a robust increase in FRET upon superfusion with 10 μ M [D-Ala², N-MePhe⁴, Gly-ol]-enkephalin (DAMGO) which was reversible upon agonist washout. The partial agonist morphine (30 μ M) also caused a FRET increase but the amplitude of the FRET signal was reduced to approximately 15-20% of that of the corresponding DAMGO signal. GRK2 binds G-protein $\beta\gamma$ (G $\beta\gamma$) subunits, and therefore we aimed to find out how cotransfection of GRK2 affected the interaction of G $\beta\gamma$ with the μ OR. However, we could not measure any DAMGO-induced FRET changes between YFP-tagged μ OR and mTurquoise-tagged G β in the presence of non-fluorescent G α_{i1} and G γ . This was unexpected because we had previously successfully determined interactions between G $\beta\gamma$ and the α_{2A} -adrenergic receptor or the M₃ muscarinic acetylcholine receptor. This lack of FRET was not due to an inability of the tagged G β to interact with the μ OR as we could measure DAMGO-induced FRET changes between YFP-tagged G α_{i1} and G $\beta\gamma$ (G β tagged with mTurquoise) in the presence of non-fluorescent μ OR. Moreover, when we attempted to establish an effect of GRK2 on the interaction between the μ OR and G $\beta\gamma$, we could pick up FRET between the μ OR and G $\beta\gamma$. Comparison of the on- and off-kinetics of the μ OR-GRK2 interaction with that of the μ OR-G $\beta\gamma$ interaction in the presence of GRK2 revealed similar time constants both for the on- and off-kinetics (GRK2: k_{on} 0.16 s⁻¹; k_{off} 0.087 s⁻¹; G $\beta\gamma$ in the presence of GRK2: k_{on} 0.23 s⁻¹; k_{off} 0.069 s⁻¹). This suggests that, in the absence of GRK2, the orientation of the two fluorophores on the μ OR and G $\beta\gamma$ may be unfavorable or the interaction may be too short-lived to produce an appreciable FRET signal. In the presence of GRK2, however, G $\beta\gamma$ changes its position relative to the μ OR in a way that allows the interaction of the GRK2-G $\beta\gamma$ complex with the μ OR to be detected by FRET. Similarly, we measured FRET between G $\beta\gamma$ and the α_{2A} -adrenergic receptor or the M₃ muscarinic acetylcholine receptor in the absence and presence of GRK2 and compared the kinetics with the kinetics of GRK2 binding and unbinding to these receptors. In both cases, we found that GRK2 and G $\beta\gamma$ in the presence of GRK2 associate and dissociate from these receptors with comparable kinetics. Our results suggest that ligand efficacy for μ ORs is already apparent on the level of receptor-GRK interaction.

109

RhoA signaling is dependent on caveolae in cardiomyocytes

L. Sommerfeld¹, S. Pasch¹, A. Becker¹, A. Ongherth¹, S. Lutz¹

¹Institute of Pharmacology, University Medical Center Göttingen, AG Lutz, Göttingen, Germany

Introduction: The monomeric GTPase RhoA is dysregulated in heart disease and *in vivo* models provide evidence of RhoA signaling being involved in the progression of cardiac fibrosis and hypertrophy. How RhoA is regulated within this context on a cellular level is not defined.

Objective: The goal of this study was to analyze RhoA activation in adult cardiomyocytes (AMCM) from normal and diseased mouse hearts in response to G protein-coupled receptor activation. This project also aimed at providing new insight into the dependence of RhoA localization and activation on the signaling organizing caveolae in neonatal as well as adult cardiomyocytes and engineered heart muscles.

Methods: Cardiomyocytes from Sham-operated C57BL/6 mice, from mice subjected to transverse aortic constriction (TAC) or from neonatal rats were either directly fixed after isolation or cultured in the presence or absence of methyl- β -cyclodextrin (M β CD). For analyses of RhoA activation cells were treated with endothelin-1 (ET-1) for 90 sec. Cells were prepared for immunofluorescence analysis or lysed for immunoblotting. Imaging was performed using confocal microscopy. Effects of M β CD were further studied in 3D engineered heart muscles (EHM) made from total neonatal rat cardiac cells. The contractile function of EHM was assessed in the organ bath and cells were studied in sections by immunofluorescence analysis.

Results: In AMCM from Sham mice active RhoA mainly localizes at the sarcolemma and is augmented in response to ET-1 treatment. In TAC-AMCM the basal level of active RhoA is increased and surprisingly ET-1 had no further effect. Immunoblot analysis demonstrated that in TAC-AMCM RhoA expression was per se higher and the major caveolae protein caveolin-3 was reduced. To test the influence of caveolae on RhoA activation and expression, we treated NRCM with M β CD and found the expression of RhoA as well as of RhoA target genes CCN1 and CCN2 to be moderately up-regulated after 24h. In addition, an intensified longitudinal alignment of sarcomeric actin fibers was detectable, which could also be seen in M β CD-treated EHM. However, M β CD had no effect on EHM twitch tension but increased the resting tension compared to control. We further treated AMCM with M β CD and found RhoA expression to be increased and its activity less sensitive to ET-1 treatment. Finally, we could show that the perinuclear localization of Cav3 and RhoA was strongly reduced after M β CD treatment.

Conclusion: In cardiomyocytes RhoA expression, activation and effects are dependent on functional caveolae.

110

Evidence for dynamic association of GPCRs, ligands and G-proteins at the Trans Golgi Network of thyroid cells

A. Godbole^{1,2}, M. J. Lohse^{1,2}, D. Calebiro^{1,2}

¹Institute for Pharmacology and Toxicology, University of Wuerzburg, Wuerzburg, Germany

²Rudolf Virchow Center, University of Wuerzburg, Wuerzburg, Germany

Whereas G-protein coupled receptors (GPCRs) have been long believed to signal through cyclic AMP only at cell surface, our group has previously shown that GPCRs not only signal at the cell surface but can also continue doing so once internalized together with their ligands, leading to persistent cAMP production (1). This phenomenon, which we originally described for the thyroid stimulating hormone receptor (TSHR) in thyroid cells, has been observed also for other GPCRs (2-4). However, the intracellular compartment responsible for such persistent signaling was insufficiently characterized. The aim of this study was to follow by live-cell imaging the internalization and trafficking of TSHR, TSH and effector proteins in thyroid cells. Mouse primary thyroid cells were transfected with fluorescent-protein tagged TSHR, G-proteins, nanobody specific for active G-proteins and/or subcellular markers by electroporation, stimulated with fluorescently labeled TSH and visualized using highly inclined thin illumination (HILO) microscopy. Our results suggest that TSH is internalized in complex with its receptor and they traffic retrogradely via the Trans Golgi network (TGN). While we could not find any evidence of internalized TSH/TSHR complexes activating G-proteins in early endosomes, we show that TSH/TSHR complexes meet the intracellular pool of Gas in the TGN and activate it, as visualized in real-time by a nanobody specific for active Gas. Upon acute Brefeldin A-induced Golgi collapse, the retrograde trafficking of TSH/TSHR via TGN is hindered. Bulk TSH stimulations in primary mouse thyroid cells isolated from transgenic mice expressing the cAMP sensor, Epac1-camps, also show a significantly reduced cAMP production in the presence of Brefeldin-A. These data provide evidence that internalized TSH/TSHR complexes meet and activate G-proteins at the TGN, which might serve as the main platform of persistent cAMP signaling after receptor internalization.

1. Calebiro D, Nikolaev VO, Gagliani MC, de Filippis T, Dees C, Tacchetti C, Persani L, Lohse MJ. (2009) Persistent cAMP-signals triggered by internalized G-protein-coupled receptors. *PLoS Biol.* 7:e1000172.

2. Calebiro D, Nikolaev VO, Persani L, Lohse MJ. (2010) Signaling by internalized G-protein-coupled receptors. *Trends Pharmacol. Sci.* 31:221-8.

3. Irannejad R, Tomshine JC, Tomshine JR, Chevalier M, Mahoney JP, Steyaert J, Rasmussen SG, Sunahara RK, El-Samad H, Huang B, von Zastrow M. (2013) Conformational biosensors reveal GPCR signalling from endosomes. *Nature.* 495:534-8.

4. Lohse MJ, Calebiro D. (2013) Cell biology: Receptor signals come in waves. *Nature.* 495:457-8.

111

Dexamethasone downregulates sphingosine 1-phosphate (S1P) receptor 1 expression, which in turn inhibits S1P-induced mesangial cell migration

A. Koch¹, M. Jäger¹, A. Völzke¹, G. Grammatikos^{1,2}, D. Meyer zu Heringdorf¹, A. Huwiler², J. Pfeilschifter¹

¹Klinikum der Goethe-Universität Frankfurt, pharmazentrum frankfurt/ZAFES, Frankfurt am Main, Germany

²Klinikum der Goethe-Universität Frankfurt, Medizinische Klinik 1, Frankfurt am Main, Germany

³Universität Bern, Institut für Pharmakologie, Bern, Switzerland

Objective: Sphingosine 1-phosphate (S1P) is generated by sphingosine kinase (SK)-1 and -2 and acts mainly as an extracellular ligand at five specific G protein-coupled receptors, denoted S1P₁₋₅. After activation, S1P receptors regulate important processes in the progression of renal diseases, such as mesangial cell migration

Methods and Results: Here we demonstrate that dexamethasone treatment lowered S1P₁ mRNA and protein expression levels in rat mesangial cells measured by TaqMan® and Western blot analyses. This effect was abolished in the presence of the glucocorticoid receptor antagonist RU-486. In addition, *in vivo* studies showed that dexamethasone downregulated S1P₁ expression in glomeruli isolated from C57BL/6 mice treated with dexamethasone (10 mg/kg body weight). Functionally, we identified S1P₁ as a key player mediating S1P-induced mesangial cell migration. Using Boyden Chamber assays, we could show that dexamethasone treatment significantly lowered S1P-induced migration of mesangial cells. This effect was again reversed in the presence of RU-486.

Conclusion: We suggest that dexamethasone inhibits S1P-induced mesangial cell migration via downregulation of S1P₁. Overall, these results demonstrate that dexamethasone has functional important effects on sphingolipid metabolism and action in renal mesangial cells (Koch et al., Biol. Chem. 2015; 396: 803-12).

112

The G protein-coupled receptor MrgD is a receptor for angiotensin-(1-7) involving G_α13, cAMP, and phosphokinase A

A. Tetzner^{1,2}, K. Gebols¹, C. Meinert^{1,3}, A. Uhlir¹, I. Villacañas Pérez⁴, T. Walther^{1,2}

¹University College Cork, Pharmacology and Therapeutics, Cork, Ireland

²University of Leipzig, Center for Perinatal Medicine, Department of Obstetrics, Leipzig, Ireland

³Medical Faculty Mannheim – University Heidelberg, Inst. Experimental and Clinical Pharmacology and Toxicology, Mannheim, Ireland

⁴Intelligent Pharma, Computational Chemistry Department, Barcelona, Spanien

Rationale: Angiotensin (Ang)-(1-7) has cardiovascular protective effects and is the opponent of the often detrimental Ang II within the renin-angiotensin system. Although it is well-accepted that the G-protein coupled receptor Mas is a receptor for the heptapeptide, the lack in knowing initial signalling molecules stimulated by Ang-(1-7) prevented final verification of ligand/receptor interaction as well as the identification of further hypothesized receptors for the heptapeptide.

Objective: The study aimed to identify a second messenger stimulated by Ang-(1-7) allowing confirmation as well as discovery of the heptapeptide's receptors.

Methods & Results: We identified cAMP as the second messenger for Ang-(1-7). The heptapeptide elevates cAMP concentration in primary cells such as endothelial or mesangial cells. Using cAMP as readout in receptor-transfected HEK293 cells, we provided final pharmacological proof for Mas to be a receptor for Ang-(1-7). More important, we identified the G-protein coupled receptor MrgD as a second receptor for Ang-(1-7). Consequently, the heptapeptide failed to increase cAMP concentration in primary mesangial cells with genetic deficiency in both Mas and MrgD. Furthermore, we excluded the Ang II type 2 receptor AT2 as a receptor for the heptapeptide, but discovered that the AT2 blocker PD123119 can also block the Mas and MrgD receptors.

Conclusions: Our results lead to an expansion and partial revision of the renin-angiotensin system, by identifying a second receptor for the protective Ang-(1-7) but excluding the AT2 receptor, and by enforcing the revisit of such publications which concluded AT2 function by using PD123119 as a specific AT2 blocker.

113

Activation kinetics of metabotropic glutamate receptor 1

E. Grushevskiy¹, A. Bock¹, M. J. Lohse¹

¹University of Würzburg, Institute of Pharmacology and Toxicology, Würzburg, Germany

Members of the G protein-coupled receptor (GPCR) superfamily are integral membrane proteins that are activated by extracellular ligands and induce cell signaling via G proteins and other adaptor proteins. Rhodopsin, the prototypical GPCR that mediates vision, is activated by photons that isomerize its covalent ligand. Spectroscopic analyses of the cognate agonist retinal allow a detailed description of rhodopsin dynamics at submillisecond resolution. Using rhodopsin as a model, it has been demonstrated that receptor activation, i.e. a switch from the fully inactive to the fully active state, occurs within 1 ms¹. Activation kinetics of other receptors have been studied mainly using fluorescence resonance energy transfer (FRET) which allows kinetic studies with high resolution in living cells². In contrast to rhodopsin, activation constants of several GPCRs using agonist superfusion have been determined to range between 30-80 ms³. However, it is unknown if all GPCRs with diffusible ligands are really activated on a longer timescale or if ligand diffusion to the binding site is rate limiting.

In this study, we intend to overcome ligand diffusion by using photodestruction of caged ligands. We monitor activation-related conformational changes of homodimeric metabotropic glutamate receptor 1 (mGluR1) sensors by FRET after uncaging of an inert glutamate derivative. 4-Methoxy-7-nitroindolyl-L-glutamate (MNI-glutamate) is a caged derivative of glutamate that does not activate mGluR1s. Upon pre-incubation of HEK-TSA cells expressing both CFP- and YFP- tagged mGluR1 protomers with MNI-glutamate, a short UV laser pulse releases active L-glutamate close to the receptor

binding site. We demonstrate very rapid mGluR1 activation kinetics and this allows us to study the process of signal transduction of this homodimeric GPCRs.

References: 1. Vuong et al. Millisecond activation of transducin in the cyclic nucleotide cascade of vision. *Nature* (1984)

2. Lohse et al. Fluorescence/bioluminescence resonance energy transfer techniques to study G-protein-coupled receptor activation and signaling. *Pharmacol Rev* (2012).

3. Lohse and Hofmann. Spatial and Temporal Aspects of Signaling by G-Protein-Coupled Receptors. *Mol Pharmacol* (2015)

4. Hlavackova et al. Sequential Inter- and Intrasubunit Rearrangements during Activation of Dimeric Metabotropic Glutamate Receptor 1. *Science Signal*. (2012)

114

A GIRK-based FLIPR assay for measuring activation of G_i-coupled GPCRs – a versatile technique used for characterization of multi-opioid receptor ligands

T. Günther¹, P. Dasgupta¹, A. Mann¹, E. Miess¹, F. Nagel¹, S. Schulz¹

¹Institut für Pharmakologie und Toxikologie, Jena, Germany

Opioids are still the mainstay of modern pain treatment. Most of the clinically established substances primarily exert their effects via the μ -opioid receptor (MOR). However, many side effects such as tolerance, constipation and respiratory depression limit their therapeutic use. The efficacy of MOR agonists in the treatment of chronic pain is unsatisfactory. In general analgesic effects can be mediated by all four members of the opioid receptor family. The nociception receptor (NOP) is the latest member of the opioid receptor family. There is a rapidly growing interest for the development of novel NOP and combined MOR/NOP agonists. The aim of this development is novel therapeutic agents with improved analgesic characteristics and less classical MOR-mediated side effects. Here we used Buprenorphine as a clinically established opioid which exerts its effect on multiple opioid receptor subtypes. Recently, Nalfurafine, a potent kappa-opioid receptor (KOR) agonist was granted by Japanese authorities for the treatment of uremic pruritus. Even though KOR agonists are known to mediate dysphoria and hallucinations this has not been reported for Nalfurafine.

115

Monitoring the activation of GPCRs, from single cells to high-throughput screening

H. Schihada¹, I. Maiellaro¹, U. Zabel¹, M. J. Lohse^{1,2}

¹Institut für Pharmakologie & Toxikologie, Würzburg, Germany

²Rudolf-Virchow-Zentrum für Experimentelle Biomedizin, Würzburg, Germany

G protein-coupled receptors (GPCRs) belong to a superfamily of cell surface signaling proteins that mediate many physiological responses to hormones and neurotransmitters. They represent the prime targets for therapeutic drugs in healthcare. However, due to the limited knowledge about the pharmacology of the majority of GPCRs, only few of them are employed as therapeutic target. In our lab, the activation kinetics of the α_{2A} -adrenergic receptor, among others receptors, has been extensively studied in single cell assays^(1,2). The activation kinetics of the labeled α_{2A} -adrenergic were monitored by Förster Resonance Energy Transfer (FRET). The goal of our study is to design a sensor to monitor receptor activation kinetics in high throughput screening assays. For the proof of concept, we used the α_{2A} -adrenergic receptor as a prototype. To optimize the FRET efficiency we exchanged the previous acceptor (YFP) with the HaloTag technology⁽³⁾. Additionally, we used HaloTag in combination with the NanoLuc⁽⁴⁾ to explore the possibility of using BRET as a high- throughput approach to monitor receptor activation kinetics. The FRET-based sensor α_{2A} -Halo/CFP showed an increase in FRET upon application of the full endogenous agonist norepinephrine with an EC50 value in accordance with the previously published data. This suggests the functionality of the FRET-based α_{2A} -Halo/CFP sensor. Similar results were obtained with the α_{2A} -adrenergic receptor BRET-based sensor. In contrast to the full agonist norepinephrine, the inverse agonist, Yohimbine, decreased the ratio in both, FRET as well as BRET-based α_{2A} -adrenergic receptor sensors. This suggests the sensitivity of the methods to discriminate among agonist (increased ratio) and antagonist (decreased ratio) induced receptor kinetics. Our results show the feasibility of using HaloTag to monitor receptor activation via FRET in a single cells format and HaloTag, in combination with NanoLuc, can be used to monitor receptor activation in high- throughput format.

1. Vilardaga et al. Measurement of the millisecond activation switch of G protein-coupled receptors in living cells *Nat. Biotechnol.* (2003)

2. Hoffmann et al. A FRET-based FRET approach to determine G protein-coupled receptor activation in living cells *Nat. Methods* (2005)

3. Los et al. HaloTag: A Novel Protein Labeling Technology for Cell Imaging and Protein Analysis *ACS Chemical biology* (2008)

4. Machleidt et al. NanoBRET – a Novel BRET Platform for the Analysis of Protein-Protein Interactions *ACS Chemical biology* (2015)

116

FRET-based β -arrestin biosensors reveal a rapid, receptor-dependent activation/deactivation cycle in living cells

S. Nuber^{1,2}, U. Zabel^{1,2}, K. Lorenz^{1,2}, A. Nuber¹, G. Milligan³, A. B. Tobin⁴, M. J. Lohse^{1,2}, C. Hoffmann^{1,2}

¹University of Würzburg, Institute of Pharmacology and Toxicology, Würzburg, Germany

²University of Würzburg, Rudolf Virchow Center, Würzburg, Germany

³University of Glasgow, Molecular Pharmacology Group, Institute of Molecular, Cell and Systems Biology, College of Medical, Veterinary and Life Sciences, Glasgow, United Kingdom

⁴University of Leicester, MRC Toxicology Unit, Leicester, United Kingdom

β -Arrestins are important regulators of G-protein-coupled receptors (GPCR). They bind to active, phosphorylated GPCRs and thereby shut off "classical" signaling to G-proteins and mediate signaling via "non-classical" pathways. Binding of receptors or their C-terminus as well as certain truncations induce an active conformation of β -arrestins (and

the homologous visual arrestins) that has recently been solved by X-ray crystallography. Here we investigated both the interaction with GPCRs and β -arrestin conformational changes in real time and in living cells with a series of FRET-based β -arrestin2 biosensors. Upon stimulation, β 2-adrenergic receptors bound β -arrestin2 with a time constant $\tau = 1.3 \pm 0.17$ s, indicating that β -arrestin2 binding rapidly terminates their G-protein signaling. We observed a subsequent receptor-mediated conformational change in β -arrestin2 with a $\tau = 2.2 \pm 0.22$ s. Stimulation of β 2-adrenergic vs. M2 muscarinic or FFA4 receptors resulted in different patterns of conformational changes in the various β -arrestin2 sensors and also in downstream kinase signaling, revealing receptor-specificity in β -arrestin2 activation. Upon agonist removal, first the interaction (delay = 1.9 ± 0.51 s) and only then the active state of β -arrestin2 (delay = 4.2 ± 0.85 s) were reversed. Accordingly, β -arrestin localization at the cell membrane lasted much longer than the direct interaction with β 2-adrenergic receptors. Our data indicate a rapid, receptor-specific, two step binding and activation process between GPCRs and β -arrestins; they further suggest that β -arrestins remain active following dissociation from receptors, allowing them to remain at the cell surface and presumably signal independently. Thus, GPCRs trigger a rapid, receptor-specific activation/deactivation cycle of β -arrestins, which permits their active signaling.

Pharmacology – GTP-binding proteins

117

Cytotoxicity of Clostridium difficile Toxin B is determined by glycosylation kinetic of Rho GTPases

L.-A. Beer¹, H. Tatge¹, I. Just¹, R. Gerhard¹
¹Medizinische Hochschule Hannover, Institut für Toxikologie, Hannover, Germany

Pathogenic *Clostridium difficile* produce two large glycosyltransferases, TcdA and TcdB, which are the main pathogenicity factors. The cytotoxin TcdB is about 1,000 fold more potent than TcdA. TcdA and TcdB are A/B structure toxins exhibiting an enzymatically active (A) domain and a binding/translocation domain (B) to deliver the active glycosyltransferase domain into the cytosol of host cells. Beside its glycosyltransferase activity by which the substrate proteins mainly of the family of Rho GTPases are inhibited, TcdB has additional cytotoxic effects that are independent of Rho glycosylation.

To investigate the mechanism by which TcdB induces early cell death, we applied chimeras of TcdB from different toxinotypes where different glycosyltransferase domains were combined with different translocation domains. To this end we cloned TcdB from strain VP110463 (historical strain), strain 1479 (Serotype F, variant TcdBF), strain R20291 (hypervirulent strain, ribotype O27), and strain R9385 (hypervirulent strain with TcdBF characteristics). We were able to investigate the impact of the glycosyltransferase domains with different substrate specificity when translocated into the host cell by identical translocation domains. Furthermore, we tested different translocation domains to deliver the same glycosyltransferase domain into host cells.

We found that the glycosyltransferase domain of TcdBF (strain 1479) is less cytotoxic with respect to early cell death mediated by reactive oxygen species than that from reference strain VP110463. In addition, the translocation domain also showed significant impact on cytotoxicity, probably by faster intracellular delivery of the GTD. By using glycosyltransferase deficient mutants where the highly conserved DXD-motif was changed to NXN, we were able to show that glycosylation of Rho GTPases counteracts the cytotoxic effect, since the mutants were more cytotoxic than wildtype toxins.

In conclusion, the cytotoxicity of TcdB mainly depends on the translocation efficiency into the host cell and on the kinetic of glycosylation of their substrate GTPases. Thus, sensitivity of target cells towards cytotoxic effect also depends on receptor abundance and intracellular status of Rho GTPases, whereas the cytopathic effect, i.e. cell rounding, is predominantly determined by the substrate specificity.

118

p63RhoGEF regulates cardiac tissue properties

A. Ongherth¹, S. Pasch¹, S. Lutz¹
¹Universitätsmedizin Göttingen, Pharmakologie, Göttingen, Germany

Introduction: p63RhoGEF activates the G protein-coupled receptor (GPCR)-mediated induction of RhoA in different cells. However, its role in cardiac fibroblasts (CF) is not defined yet. Thus we studied its localization and function in CF in 2D and 3D culture experiments.

Methods: Neonatal rat cardiac fibroblasts (NRCF) and adult ventricular fibroblasts (AMCF) from wild type mice and p63RhoGEF-knockout mice were adenovirally transduced for 48 to 72 h with recombinant adenoviruses or directly used. For 2D studies the cells were treated with angiotensin II (Ang II). The location of the involved signaling components, RhoA activation and down-stream effects were studied by confocal microscopy and biochemical analyses. In addition, CF were used to prepare CF-containing engineered connective (ECT) or muscle (EHM) tissues.

Results: We could show that p63RhoGEF localizes at the plasma membrane, adjacent to the Golgi apparatus and at the base of primary cilia. In accordance, p63RhoGEF regulates in response to Ang II the expression and secretion of the connective tissue growth factor (CTGF) in NRCF involving the serum response factor. In ECT, p63RhoGEF increases the stiffness of these tissues and in EHM containing CF expressing gain-and-loss-of-function p63RhoGEF variants it influences the contractility. Interestingly, the increase in ECT stiffness was independent of p63RhoGEF's regulatory function of CTGF, as overexpression of CTGF in CF had no impact on ECT properties arguing for a more general role of p63RhoGEF in auto- and paracrine signaling. Moreover, our data on AMCF with a genetic deletion of p63RhoGEF implies that p63RhoGEF is not only a transducer of GPCR-dependent RhoA activation as its loss led to an increase in RhoA expression accompanied by an increase in RhoA-dependent gene expression suggesting a role of p63RhoGEF in the feedback regulation of this signaling cascade.

Conclusion: In summary, our data show that p63RhoGEF regulates auto- and paracrine signaling in cardiac fibroblasts.

119

Pasteurella multocida toxin (PMT) modulates osteocyte function

H. Heni¹, K. Aktories¹, J. H. C. Orth¹
¹Universität Freiburg, Institut für Experimentelle und Klinische Pharmakologie und Toxikologie, 1, Freiburg, Germany

The atrophic rhinitis is characterized by a drastic destruction of nasal turbinate bones in different animals. It leads to shortening and twisting of the snout and a growth retardation of young pigs. This bone degradation is induced by *Pasteurella multocida* toxin (PMT), a toxin produced by *P. multocida* serogroups A and D. This destructive effect indicates an interaction of PMT with bone cells like osteoclasts and osteoblasts. We demonstrated that PMT stimulates the differentiation of osteoclasts and inhibits the differentiation of osteoblasts in a Gq-dependent mechanism. The underlying molecular mechanism of the toxin is the deamidation of an essential glutamine residue in the α -subunits of heterotrimeric G proteins, which results in the constitutive activation of the G protein.

Until now only the function and the PMT-dependent effects on osteoblasts and osteoclasts were studied in detail, but there is also a third important cell type in bone, the osteocytes. Osteocytes are discussed as the regulator of the bone turn-over by interacting with osteoclasts and osteoblasts e.g. via secretion of several osteoclastogenic and osteoblastogenic cytokines. Therefore, we studied the effects of PMT on the function of osteocytes in more detail.

We utilized an osteocyte like cell line and primary osteocytes isolated from tibiae and femurs from mice. The susceptibility of primary osteocytes and the osteocyte like cell line towards PMT was demonstrated by detection of toxin-induced deamidation of G proteins.

We also observed a PMT-induced secretion of different cytokines, like RANKL, IL-6 and TNF- α , which are known to induce osteoclastogenesis or inhibit osteoblastogenesis. Furthermore, we studied the underlying signal transduction pathways and other PMT-induced effects on osteocytes, like morphological changes.

In summary, we show that PMT acts on osteocytes by stimulating heterotrimeric G proteins. This might have impact on overall bone metabolism due to modulation of osteoblast and osteoclast activity.

120

Inhibition of osteoblastogenesis by Pasteurella multocida toxin in the context of fibrodysplasia ossificans progressiva

J. Behr¹, K. Aktories¹, J. H. C. Orth¹
¹Institut für experimentelle und klinische Pharmakologie und Toxikologie, Universität Freiburg, Freiburg, Germany

Pasteurella multocida is an opportunistic pathogen often residing in the nasal pharyngeal space of animals. One virulence factor of *P. multocida* serogroups A and D is the protein toxin PMT (*P. multocida* toxin), which is the causative agent of atrophic rhinitis characterized by degradation of nasal turbinate bones in pigs and other animals. On the molecular level, PMT activates distinct members ($G_{q/11}$, $G_{12/13}$ and G_i) of heterotrimeric G proteins leading to a modulation of bone metabolism: the toxin stimulates osteoclastogenesis but blocks osteoblastogenesis which results in bone loss. This mechanism of action of PMT might be exploited to counteract the human disease fibrodysplasia ossificans progressiva (FOP), a rare and highly disabling disorder of extensive heterotopic bone growth. The underlying cause of FOP is a point mutation in the activation domain of ACVR1 (R206H), a BMP (bone morphogenic protein) type 1 receptor. This mutation leads to an inflated BMP-signaling and heterotopic osteoblastogenesis.

Here, we report that C2C12 cells, a mouse myoblast cell line often used as a FOP model, are susceptible to PMT intoxication. PMT induces deamidation of G proteins in these cells. Furthermore, PMT very efficiently inhibits BMP4-induced osteoblast differentiation in C2C12 cells. This has been shown by measuring alkaline phosphatase expression which is an early marker of osteoblast differentiation. Additionally, the impact of PMT on ACVR1^{R206H} induced osteoblastogenesis will be investigated and the involved cellular signaling pathways will be characterized in detail.

The data indicate that activation of heterotrimeric G-proteins might be a rationale for pharmacological therapy of FOP.

121

p63RhoGEF regulates intracellular membrane compartments in cardiomyocytes

S. Pasch¹, E. Wagner², C. Vettel³, S. Lutz¹
¹University Medical Center Göttingen, Institute of Pharmacology, Göttingen, Germany
²University Medical Center Göttingen, Department of Cardiology and Pneumology, Göttingen, Germany
³Medical Faculty Mannheim, University of Heidelberg, Institute of Experimental and Clinical Pharmacology and Toxicology, Mannheim, Germany

Introduction:

p63RhoGEF is an activator of the monomeric GTPase RhoA and was shown to be expressed in the heart. In cardiac fibroblasts and smooth muscle cells, p63RhoGEF regulates RhoA in response to angiotensin II and controls the actin cytoskeleton as well as protein expression and secretion. Its role in cardiomyocytes, however, has not been elucidated so far.

Methods:

Cardiomyocytes were isolated from neonatal rat hearts (NRCM), wild type mouse hearts (WT-AMCM) and homozygous (KO-AMCM) p63RhoGEF knockout mouse hearts. The cells were either directly fixed or adenovirally transduced for 48 h in culture. For activation of the $G_{q/11}$ -signaling the cells were treated with endothelin-1 (ET-1), angiotensin II (Ang II) or phenylephrine (PE) for 90 s. RhoA activation was assessed by affinity binding or with a specific active-RhoA antibody. Other proteins were detected by immunoblot or immunofluorescence analysis with subsequent confocal imaging.

Results:

In NRCM p63RhoGEF is involved in the regulation of the ET-1-induced RhoA activity and thus increases the expression and secretion of the RhoA target gene CTGF. In

accordance, p63RhoGEF was found to be localized at the sarcolemma as well as in intracellular membrane compartments. The strongest co-localization was detected with the KDELR-receptor 3 (KDELR3) which resides in the endoplasmic reticulum membrane. Next, we analyzed RhoA activation in WT and KO-AMCM and could show that a loss of p63RhoGEF led to an increase in basal RhoA activity and an uncoupling from the GPCRs. Interestingly, in the KO-AMCM caveolin-3 the major component of caveolae, in which several GPCRs are clustered, was reduced in its expression and a shift in localization from transverse to longitudinal membrane tubules was found, arguing for a role of p63RhoGEF in intracellular protein transport. In accordance, Golgi apparatus particles, which were demonstrated to play role in caveolae formation, were reduced in size in KO-AMCM. To further address the role of p63RhoGEF in the transport of membrane proteins, we overexpressed p63RhoGEF in WT-AMCM and could show that this led to an increase in the expression of the KDELR3 and its co-localization with p63RhoGEF in the perinuclear region and at the sarcolemma. No sarcolemmal localization of KDELR3 was found in control-transduced cells. Further, p63RhoGEF was localized adjacent to Golgi apparatus particles which were similar reduced in size as detected in the KO-AMCM. Finally, we expressed the dominant negative construct p63DN and detected similar changes with respect to KDELR3 localization and Golgi structure suggesting that this regulatory function of p63RhoGEF is not dependent on its activity.

Conclusion:

p63RhoGEF mediates the activation of RhoA from GPCRs coupled to G_{q11} proteins. Moreover, it has a function in intracellular transport and distribution of membrane proteins independent of its activity.

122

FR900359: a cyclic depsipeptide to explore the role of Gq proteins in biological systems

S. Annala¹, N. Merten¹, A. Inoue², M. Grundmann¹, A.-L. Schmitz¹, S. Kehraus¹, D. Wenzel³, M. Hesse³, K. Bülesbach¹, R. Schrage⁴, K. Mohr⁴, B. Fleischmann³, J. Gomez¹, G. König¹, E. Kostenis¹

¹Universität Bonn, Pharmazeutische Biologie, Bonn, Germany

²Graduate School of Pharmaceutical Sciences Tohoku University Aoba-ku, Sendai, Japan

³Universität Bonn, Institut für Physiologie I, Life & Brain Center, Bonn, Germany

⁴Universität Bonn, Pharmacology and Toxicology Section, Bonn, Germany

G protein signaling is a means allowing cells to quickly respond and adapt to environmental changes. Four major G protein classes (Gs, Gi/o, Gq/11, G12/13) exist in mammals and these must suffice to convey signals from about 800 G protein-coupled receptors to the cell interior. As such, G proteins receive, interpret, and finally route the GPCR signals to diverse sets of downstream target proteins and thereby permit cells to respond to their ever changing environment.¹ Understanding contribution of individual G protein classes or even isoforms to complex signaling networks in living cells requires capacity to activate or inactivate proteins with great precision and selectivity. One approach towards inactivation of G protein function is via chemical inhibition. However, "true specificity" of chemical inhibitors for their associated targets may often be debated. In this study we posit that FR900359, a cyclic depsipeptide isolated from the leaves of *Ardisia crenata*, may clearly be designated as "truly specific" for inhibition of Gq signaling. Using a broad set of complementary methods based on label-free holistic cell sensing, classical endpoint assays, and bioluminescence resonance energy transfer-based G protein biosensors we assign exceptional selectivity to FR for inhibition of Gq/11/14 over all other mammalian isoforms ("on-target effects"). In holistic label-free recordings using HEK293 cells that lack functional Gq/11 alleles by CRISPR-Cas9 genome editing, bona-fide Gq stimuli were undetectable. However, reintroduction of Gq into the knockout background was required and sufficient to fully restore both, agonist responses and their inhibition by FR. Moreover, FR was completely ineffective in cells lacking Gq/11 using phenotypic assays that examine basic cellular functions such as cell growth, viability, morphology and expression of housekeeping genes ("off-target effects")².

From these results we conclude that FR is of outstanding value as molecular probe to unravel contribution of Gq signaling in complex biological processes *in vitro*, *ex vivo* and *in vivo*. Just as pertussis toxin, applied world-wide by numerous laboratories to diagnose signaling of Gi/o proteins, we anticipate FR to stand out at least equally for investigations into the biological relevance of Gq.

1. Oldham, W. M. & Hamm, H. E. Heterotrimeric G protein activation by G-protein-coupled receptors. *Nat. Rev. Mol. Cell Biol.* 9, 60-71 (2008).

2. Schrage, R et al. The experimental power of FR900359 to study Gq-regulated biological processes. *Nat. Commun. accepted*

123

Possible roles of Rab proteins and septins in the formation of cilia

F. Lehmann¹, C. Schwan¹, K. Østevold¹, K. Aktories¹

¹klinische und experimentelle Pharmakologie und Toxikologie, Abteilung 1, Freiburg, Germany

Binary actin ADP-ribosylating toxins like *C. perfringens* iota toxin and *C. difficile* transferase CDT cause depolymerisation of the cortical actin cytoskeleton, induce the formation of microtubule-based cell membrane protrusions and redirect Rab-dependent intracellular traffic (Schwan et al. 2009). Here, we employed the model of toxin-induced protrusions to study the formation of cilia.

We found that toxin-induced microtubule-based protrusion formation at the cell membrane depends on recruitment of septins, which are highly conserved, small GTP-binding proteins. Similar to toxin-caused protrusions, septins are also recruited to the site of ciliogenesis. Inhibition of septins by shRNA-based knockdown inhibits ciliogenesis as well toxin-induced protrusion formation. Septins are suggested to be involved in exocytotic processes, which are important for ciliogenesis and also for toxin-induced protrusion formation. Accordingly, translocation of septins is accompanied by a recruitment of Rab proteins and proteins of the exocytotic machinery.

The data indicate that septins function as a scaffold at the base of cellular processes like cilia and toxin-induced protrusions, organizing the cross-talk between the actin cytoskeleton and microtubules to regulate the vesicle traffic- and exocytotic machinery.

124

Clostridium difficile toxin CDT induces septin guidance of microtubules

C. Schwan¹, T. Nölke¹, F. Lehmann¹, K. Østevold¹, K. Aktories¹

¹Institut für Experimentelle und Klinische Pharmakologie und Toxikologie, Abteilung 1, Freiburg, Germany

Hypervirulent *Clostridium difficile* strains are associated with increased morbidity and mortality. These strains produce the actin-ADP-ribosylating *Clostridium difficile* toxin CDT. CDT depolymerizes the actin cytoskeleton, causes formation of microtubule-based protrusions and increases pathogen adherence. Septins are essential for CDT-induced protrusion formation. SEPT2, 6, and 7 accumulate at predetermined protrusion sites and form collar-like structures at the base of protrusions. The septins are a prerequisite for protrusion formation. The inhibitor forchlorfenuron or knock-down of septins inhibit protrusion formation. Septins colocalize with active Cdc42 and its effector Borg which act as up-stream regulators of septin polymerization. Microtubules interact with septin structures. Precipitation and surface plasmon resonance studies revealed high-affinity binding of septins to microtubule plus end tracking protein EB1 thereby guiding incoming microtubules.

The data indicate that CDT hijacks conserved regulatory principles involved in microtubule-membrane interaction, depending on septins, Cdc42, Borgs and restructuring of the actin cytoskeleton.

Pharmacology – Cyclic nucleotides

125

Zebrafish as model organism for cNMP research

F. Dittmar¹, S. Abdellah-Seyfried^{2,3}, S. K. Tschirner^{1,4}, V. Kaever^{1,4}, R. Seifert¹

¹Medizinische Hochschule Hannover, Institut für Pharmakologie, Hannover, Germany

²Universität Potsdam, Institut für Biochemie und Biologie, Potsdam, Germany

³Medizinische Hochschule Hannover, Institut für Molekularbiologie, Hannover, Germany

⁴Medizinische Hochschule Hannover, Zentrale Forschungseinrichtung Metabolomics, Hannover, Germany

The zebrafish *Danio rerio* has become an important vertebrate model organism for a wide range of scientific questions [1]. Current studies are mainly focused on development, genetics and disease for which the zebrafish is particularly well suited due to its small size, rapid development, short generation time, optical transparency of embryos and larvae as well as conservation in functional domains [1]. Hitherto, nothing is known about the composition and endogenous level of different cNMPs in various developmental stages and organs of *Danio rerio*. Therefore, we used the zebrafish in our study as a vertebrate model to characterize systematically the temporal- and organ-specific occurrence(s) of all cNMPs including cUMP *in vivo*. Cyclic nucleotides were quantified by high performance liquid chromatography quadrupole tandem mass spectrometry.

We observed specific cNMP patterns in developmental stages and different organs from adult zebrafish, which is in support of the hypothesis of a distinct cNMP signaling code [2]. cAMP, cGMP and cUMP were present in tissue samples of both developmental stages (embryos at 24 hours post fertilization, larvae at 5 days post fertilization) and within all harvested organs. Remarkably, these three cNMPs were the only ones detected in the brain. cAMP concentration of entrails as well as cAMP and cGMP concentrations in the brain were similar to those previously described in mouse tissues [3]. cCMP was detected throughout development and was present in all organs except the brain. The identity of cCMP and cUMP in the zebrafish was confirmed by high performance liquid chromatography quadrupole time-of-flight mass spectrometry (HPLC-MS/TOF). Thus, we unequivocally show for the first time that cUMP occurs in vertebrates. Furthermore, we detected cIMP in several developmental stages of the zebrafish, and observed the highest concentrations in testes and heart, but we were unable to unequivocally identify cIMP via HPLC-MS/TOF. In the zebrafish, sAC is evolutionarily not conserved and absent, since a search in the NCBI gene data base revealed no entry for sAC (also referred to as AC10). Therefore, sAC can be excluded as cUMP- and cCMP generator in this system and sGC remains as the only bona fide cUMP- and cCMP generator in the zebrafish. To test this hypothesis, the effects of NO donors, sGC stimulators and sGC activators on cUMP levels in zebrafish should be examined in future studies. Recently, induction of apoptosis in mouse lymphoma cells by cCMP-AM has been described [4]. Thus, it would be interesting to examine the effect of cCMP-AM on zebrafish embryos in future studies as well.

[1] Seifert, R.: cCMP and cUMP: emerging second messengers, *Trends in Biochemical Sciences* 40, 8-15 (2015).

[2] Dittmar, F. et al.: Temporal and organ-specific detection of cNMPs including cUMP in the zebrafish, *Biochemical and Biophysical Research Communications* (2015).

[3] Bähre, H. et al.: cCMP and cUMP occur *in vivo*, *Biochemical and Biophysical Research Communications* 460, 6-11 (2015).

[4] Wolter, S. et al.: cCMP causes caspase-dependent apoptosis in mouse lymphoma cell lines, *Biochemical Pharmacology* 98, 119-131 (2015).

126

Apoptotic and antiproliferative effects of guanosine-moiety-containing compounds in HuT-78 lymphoma cells

E. Schneider¹, S. Käßle¹, O. Swolski¹, R. Seifert¹

¹Medizinische Hochschule Hannover, Institut für Pharmakologie, Hannover, Germany

An analysis of the effects of extracellularly applied 3',5'-cyclic nucleotides (3',5'-cNMPs) on anti-CD3-antibody (OKT3)-induced IL-2 production of HuT-78 T cell lymphoma cells revealed that 3',5'-cGMP significantly inhibited IL-2 release, while 3',5'-cAMP, 3',5'-

cCMP, 3',5'-cUMP and 3',5'-cIMP were ineffective. To further characterize the action of 3',5'-cGMP on HuT-78 cells, we determined apoptosis (propidium iodide/annexin V staining) and proliferation (carboxyfluorescein succinimidylester staining). 3',5'-cGMP significantly increased apoptosis ($EC_{50} = 75 \mu\text{M}$) and inhibited proliferation ($EC_{50} = 63 \mu\text{M}$) of OKT3-activated HuT-78 cells. Interestingly, also 2',3'-cGMP exhibited comparable effects on apoptosis and proliferation with EC_{50} values of $92 \mu\text{M}$ and $75 \mu\text{M}$, respectively, while 2',3'-cAMP, 2',3'-cCMP and 2',3'-cUMP were ineffective. This indicates that the pro-apoptotic and antiproliferative action of cGMP does not depend on the position of the phosphodiester bond.

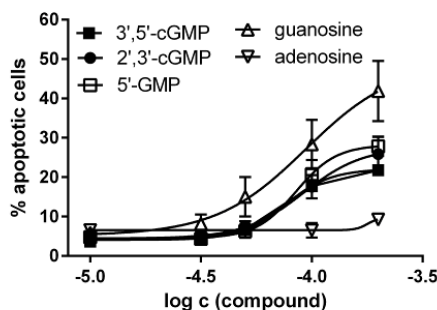
We also tested 3',5'-cGMP degradation products under the same experimental conditions and found that both 5'-GMP and guanosine increased apoptosis and inhibited proliferation with EC_{50} -values between 50 and $100 \mu\text{M}$. By contrast, adenosine did not influence cell growth and viability, suggesting that adenosine receptors are not involved in the observed effects. Our results suggest that the guanosine moiety is responsible for the pro-apoptotic and antiproliferative effects of 3',5'-cGMP, 2',3'-cGMP, 5'-GMP.

It has been reported earlier that guanosine is toxic to Jurkat cells, another T cell lymphoma cell line [1]. 3',5'-cGMP may be hydrolyzed by an ekto-phosphodiesterase on the cell surface of HuT-78 cells (e.g. eNPP1), yielding 5'-GMP, which could be further degraded to guanosine by the 5'-ekto-nukleotidase CD73. A similar pathway may lead from 2',3'-cGMP to guanosine.

[1] Batiuk TD et al. (2001) *Am J Physiol Cell Physiol.* 281:C1776-84.

Abb. 1

Proapoptotic effects of cNMPs and cNMP degradation products on HuT-78 T cell lymphoma cells



127

PDE3B hydrolyzes cUMP

F. Golly¹, J. Ostermeyer¹, V. Kaever², R. Seifert¹, E. H. Schneider¹

¹Medizinische Hochschule Hannover, Institut für Pharmakologie, Hannover, Germany

²Medizinische Hochschule Hannover, Zentrale Forschungseinrichtung Metabolomics, Hannover, Germany

A previous analysis of phosphodiesterases (PDEs) revealed that the dual-specific PDE isoforms 3A and 3B as well as the cGMP-selective PDE9A also degrade the emerging second messenger cUMP [1, 2]. We analyzed the enzyme kinetics of PDE3B-mediated cUMP-hydrolysis using recombinant GST-tagged PDE3B and a highly sensitive and specific HPLC-MS/MS method. Our data show that PDE3B is a low-affinity enzyme for cUMP with a cUMP K_M -value of $>100 \mu\text{M}$. The PDE3-selective competitive inhibitor milrinone inhibited PDE3B-mediated cUMP degradation, suggesting that cUMP binds to the catalytic center.

PDE3B is highly expressed in adipose tissue [3, 4]. Thus, we differentiated murine 3T3-L1-MBX-fibroblasts into adipocytes and analyzed differentiation-dependent alterations of PDE3B expression and basal cNMP-concentrations. In both differentiated and undifferentiated 3T3-L1 cells cUMP and cCMP were detected in addition to the established second messengers cAMP and cGMP. Differentiation to adipocytes reduced cAMP and cGMP by 66 % and 60 %, respectively, while cCMP was reduced by 78 % and cUMP even by 85 %. These findings suggest that cUMP plays a distinct role in adipocyte differentiation. The cUMP-hydrolyzing PDE3B was upregulated ~1000-fold on mRNA level after adipocyte differentiation, which may contribute to the observed reduction of basal cUMP concentrations.

We currently investigate the potential biological role of cUMP in differentiation and lipolysis experiments, analyzing the effects of the membrane-permeant cUMP-acetoxymethyl ester cUMP-AM. In future experiments, we will also analyze the enzyme kinetics of PDE9A-mediated cUMP hydrolysis. PDE9A is the first example of a cGMP-specific cUMP-hydrolyzing PDE.

[1] Reinecke D et al. (2011) *FEBS Lett.* 585:3259-3262

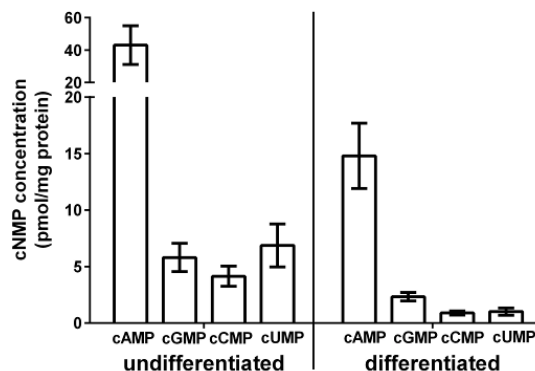
[2] Seifert R (2015) *Trends Biochem Sci.* 40:8-15

[3] Bender and Beavo (2006) *Pharmacol Rev.* 58(3):488-520

[4] Omori and Kotera (2007) *Circ Res.* 100(3):309-27

Abb. 1

cNMP concentrations in differentiated and undifferentiated 3T3-L1-MBX cells (n=3)



128

New cGMP biosensors for cyclic nucleotide research

M. Wolters¹, M. Thunemann¹, H. Subramanian², V. O. Nikolaev², R. Feil¹

¹Universität Tübingen, Interfakultäres Institut für Biochemie, Tübingen, Germany

²Universitätsklinikum Hamburg-Eppendorf, Experimentelle Kardiologie, Hamburg, Germany

Background: cGMP and cAMP are cyclic nucleotide messengers relevant to many physiological and pathophysiological conditions. Live-cell imaging with FRET-based biosensors is a powerful method to study the spatiotemporal dynamics of cGMP and cAMP under close-to-native conditions. However, with the existing biosensors it is difficult to resolve potential membrane-associated cGMP microdomains and to monitor cGMP and cAMP signals in parallel in the same cell. We have generated novel versions of the "green" CFP/YFP-based cytosolic cGMP biosensor, cGi500. They comprise a "green" membrane-targeted version (mcGi500) and a "red" variant (red cGi500) that contains the fluorophores tSapphire and Dimer2.

Methods: The sensors were expressed and characterised in primary vascular smooth muscle cells (VSMCs). Intracellular cGMP was elevated in intact VSMCs by application of a nitric oxide donor or natriuretic peptides, and the sensor's sensitivity to each stimulation and its signal-to-noise ratio were determined. To test each sensor's sensitivity and specificity for cGMP versus cAMP, sensor-expressing cells were permeabilised with β -escin and exposed to defined concentrations of cyclic nucleotides.

Results: The original cGi500 sensor showed a good signal-to-noise ratio, an EC_{50} value of $\approx 1.1 \mu\text{M}$ for cGMP, and a high selectivity for cGMP over cAMP (>100 -fold). FlncG3, a non-FRET-based cGMP sensor, showed similar properties as cGi500. The new membrane-targeted mcGi500 and the new red cGi500 displayed EC_{50} values of $\approx 0.4 \mu\text{M}$ cGMP and a high selectivity for cGMP over cAMP (>300 -fold). In VSMCs, the red cGi500 showed a better signal-to-noise ratio than the previously described "red" cGMP sensor, red cGES-DE5. The "green" FRET-based cAMP sensor, Epac1-camps, showed a signal-to-noise ratio comparable to that of cGi500, an EC_{50} value of $\approx 3 \mu\text{M}$ for cAMP and a selectivity for cAMP over cGMP of ≈ 6 -fold. Finally, imaging of cells expressing both the Epac1-camps and the red cGi500 demonstrated the feasibility of combined visualisation of cAMP and cGMP signals in the same cell.

Conclusion: The new cGMP biosensors should be useful for a broad spectrum of applications requiring real-time monitoring of cGMP signals. For example, mcGi500 would be useful to investigate membrane-associated cGMP compartments and red cGi500 to study the crosstalk between cGMP and cAMP signalling in living cells and tissues.

129

Regulation of renin by cGKI α

A. Schramm¹, F. Hofmann², P. Sandner³, F. Schweda⁴, A. Kurtz⁴, J. Schlossmann¹

¹Universität Regensburg, Pharmakologie und Toxikologie, Regensburg, Germany

²TU München, Carvas-Zentrum, München, Germany

³Bayer Pharma AG, Global Drug Discovery – Cardiology – Heart Lung Diseases, Wuppertal, Germany

⁴Universität Regensburg, Physiologie, Regensburg, Germany

The cGMP-system is a major regulator of blood pressure. cGMP-dependent protein kinases (cGKs), located in the smooth muscle layer of vessels, enable cells to dilate and therefore cause a decrease in blood pressure (BP). To the contrary, the renin-angiotensin-aldosteron-system (RAAS) acts as opponent and causes an increase in BP; furthermore, it influences fluid-electrolyte balance. Renin, which is secreted from renin-producing cells located in the juxtaglomerular apparatus (JGA), is the key regulator enzyme in this system. Pharmacological inhibition of the RAAS, e.g. via ACE-inhibitors or AT1-receptor-antagonists, is a powerful tool to treat hypertension, but chronically challenges this endocrine system, resulting in an enhancement of renin expression. This is caused by an increased number of renin-expressing cells (the so-called renin-recruitment), which derive from a reversible metaplastic retransformation of extraglomerular and smooth muscle cells of afferent arterioles. Next to regulation of renin-function via cAMP/PKA, it has been shown that eNOS-derived NO supports this recruitment via activation of sGC and subsequent generation of cGMP^{P11}. Whether this causes an activation of cGKs is not known. These enzymes exist in 3 different isoforms, cGKI α , cGKI β und cGKII. In contrast to the β -isoform, cGKI α (as well as cGKII) is highly

expressed in the JGA^[2,3]. Therefore, we analyzed, whether cGKI α also plays a role regarding renin synthesis, secretion or recruitment. To characterize the function of cGKI α in JGA-cells, we generated renin-cell specific cGKI α -knockout mice (Ren Cre-cGKI fl/fl) and stimulated renin recruitment via administration of a low salt diet (0.02% Na⁺) and enalapril (10mg/kg/d) for 3 weeks. We analyzed blood pressure, mRNA and renal protein content of renin and cGKI α , plasma renin activity and renin recruitment. Furthermore, we activated the cGMP-system in these mice using BAY41-8543, a sGC-stimulator, and re-analyzed the above-mentioned parameters. Our results indicate that cGKI α could be an additional system supporting renin recruitment but is not a crucial pre-requisite. In contrast, the basal renin concentration and activity appears to be downregulated in Ren Cre-cGKI fl/fl-mice, thus, cGKI could be an important regulator of renin synthesis.

[1] Neubauer et al., "Endothelium-Derived Nitric Oxide Supports Renin Cell Recruitment through the Nitric Oxide Sensitive Guanylate Cyclase Pathway.", *Journal of Clinical Investigation* 98, no. 3 (August 1, 1996): 662-70.

[2] Schinner et al., "The Cyclic GMP-Dependent Protein Kinase Ia Suppresses Kidney Fibrosis.", *Kidney International* 84, no. 6 (December 2013): 1198-1206. doi:10.1038/ki.2013.219.

[3] Gambaryan et al., "Expression of Type II cGMP-Dependent Protein Kinase in Rat Kidney Is Regulated by Dehydration and Correlated with Renin Gene Expression.", *Journal of Clinical Investigation* 98, no. 3 (August 1, 1996): 662-70.

130

Functional analysis of the Jaw1/Lrmp potential cGMP kinase substrate

J. Thoma¹, A. Schramm¹, E. Schinner¹, J. Schlossmann¹
¹Universität Regensburg, Pharmakologie und Toxikologie, Regensburg, Germany

Jaw1/Lrmp (lymphoid-restricted membrane protein) is a type 2 membrane protein, localised to the cytoplasmic face of the endoplasmic reticulum. It encodes a 539 amino acid protein with a highly conserved coiled-coil domain in the middle third of the protein and a COOH-terminal transmembrane domain^[1,2]. Jaw1 and IRAG have a limited homology throughout the length of the protein. The coiled-coil domain and the putative transmembrane anchor at the C-terminus of Jaw1 and IRAG share the highest homology^[3,4]. The coiled coil domains of IRAG and Jaw1 are important for the interaction with IP₃Rs. As already known, IRAG forms a trimeric complex with cGKI β and IP₃R1 and gets phosphorylated by cGKI β ^[5]. Hence we examined if Jaw1 is a new target protein of cGKI β . The recognition site, where a substrate can be phosphorylated by cGKI, is composed of the following amino acids: (K/R)(K/R)X(S/T). In the amino acid sequence of Jaw1 possible phosphorylation sites can be found. Our *in vitro* studies with Jaw1 and cGKI showed that Jaw1 gets phosphorylated in a cGMP-dependent manner by cGKI β . In contrast, Jaw1 was not phosphorylated by cGKI α . Furthermore, no stable interaction between Jaw1 and cGKI β was detected.

To examine the importance of Jaw1 *in vivo*, we generated a conditional knockout mouse. Mating with a CMV Cre mouse, resulted in an ubiquitous deletion of Jaw1. mRNA analysis and western blot analysis approved the deletion. The expression pattern revealed high expression in the thymus and weaker expression in the lung, spleen, colon, pancreas and the tongue. As already published by Shindo et al., Jaw1 was found in sweet, bitter, and umami taste receptor-expressing cells of mouse circumvallate, foliate, and fungiform papillae. We confirmed these results by X-gal staining and mRNA analysis. Therefore, we decided to analyse if Jaw1 influences taste perception. Two bottle preference tests did not result in significant differences between wildtype and knockout mice, indicating that taste perception is not altered by Jaw1. Hence, the function of Jaw1 in taste receptor expressing cells has to be further examined in future studies.

[1]Behrens et al., "Jaw1, A Lymphoid-Restricted Membrane Protein Localized to the Endoplasmic Reticulum."

[2]Behrens et al., "Carboxyl-Terminal Targeting and Novel Post-Translational Processing of JAW1, a Lymphoid Protein of the Endoplasmic Reticulum."

[3]Shindo et al., "Lrmp/Jaw1 Is Expressed in Sweet, Bitter, and Umami Receptor-Expressing Cells."

[4]Mrvil, a Common MRV Integration Site in BXH2 Myeloid Leukemias, Encodes a Protein with Homology to a Lymphoid-Restricted Membrane Protein Jaw1."

[5]Schlossmann et al., "Regulation of Intracellular Calcium by a Signalling Complex of IRAG, IP3 Receptor and cGMP Kinase β ."

131

Characterization of potential cCMP and cUMP binding proteins

T. Koenig¹, T. Hagedorn¹, F. Schwede², R. Seifert¹, S. Wolter¹
¹Medizinische Hochschule Hannover, Institut für Pharmakologie, Hannover, Germany
²BIOLOG life Science Institute, Bremen, Germany

The cyclic purine nucleotides adenosine 3',5'-cyclic monophosphate (cAMP) and guanosine 3',5' cyclic monophosphate (cGMP) are well-characterized second messengers. Both are generated by nucleotidyl cyclases and degraded by phosphodiesterases. Several binding partners of cAMP and cGMP were already identified and functionally analyzed, e.g. cAMP-dependent protein kinase (PKA) and cGMP-dependent protein kinase (PKG) as well as exchange protein activated by cAMP 1 and 2, hyperpolarization-activated cyclic nucleotide gated channels and phosphodiesterases.

Recent data indicate that the cyclic pyrimidine nucleotides cytosine 3',5'-cyclic monophosphate (cCMP) and uridine 3',5'-cyclic monophosphate (cUMP) also fulfill the criteria of second messengers [1, 2]. The interaction of cCMP with the regulatory subunits of PKA (PKAR1 α and PKAR1 α) has already been shown by using cCMP-agarose [3]. Additional cCMP- and cUMP- binding proteins such as calnexin (chaperone), myomegalin (phosphodiesterase-interacting protein) and AKAP9 (A-kinase anchoring protein) were identified by mass spectrometry analysis. To verify the interaction of cCMP and cUMP with these potential target proteins, cCMP and cUMP linked to biotin were used as another approach. The biotin- constructs exhibit lower steric interference than the cCMP- and cUMP-agarose matrices, which were previously used to confirm the binding of PKAR1 α to cCMP and cUMP [4].

FLAG-tagged calnexin, FLAG-tagged myomegalin and myc-tagged Yotiao (smallest splice-variant of AKAP9) were examined as potential cCMP and cUMP target proteins. HEK293 cells were transiently transfected with the cDNA of the respective proteins. The lysates of the protein-overexpressing cells were then incubated with cCMP- and cUMP-biotin matrices and bound proteins were purified using Strep-Tactin® beads (IBA). Afterwards, the interaction of cCMP and cUMP with the potential binding partners was analyzed by western-blotting. A PKAR1 α antibody was used as a positive control. Analogous experiments were also performed using cCMP- and cUMP-agaroses.

Once the interaction between the cyclic pyrimidine nucleotides and the potential binding partners has been confirmed, deletion mutants will be cloned to localize the cCMP- and cUMP-binding area of the target proteins in further studies.

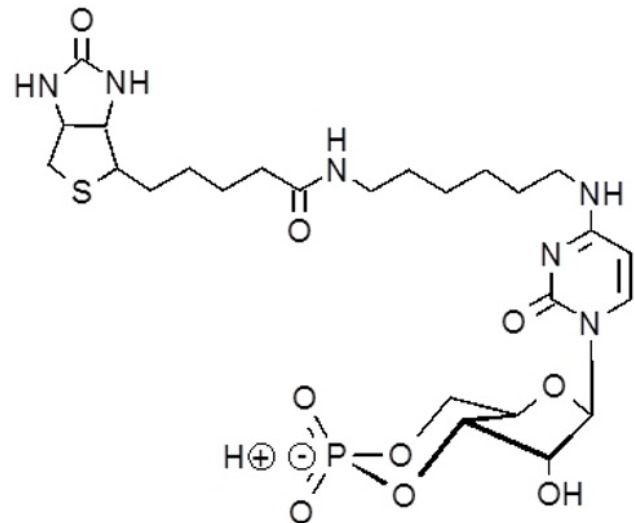
[1] Beste KY and Seifert R (2013) *Biol Chem*. 394:261-270

[2] Seifert R (2015) *Trends Biochem Sci*. 40:8-15

[3] Hammerschmidt A et al. (2012) *PLoS One* 7:e39848

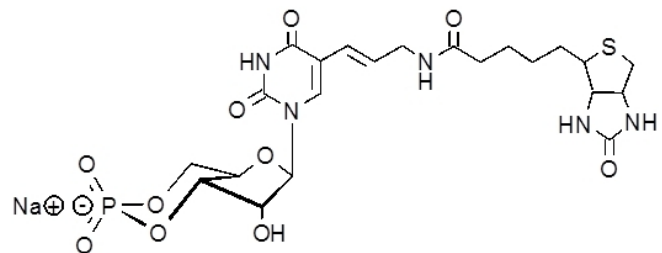
[4] Wolter S et al. (2015) *Naunyn Schmiedebergs Arch Pharmacol*. 388 (Suppl 1):057

Abb. 1



4-[Biotin]-AH-cCMP

Abb. 2



5-[Biotin]-AA-cUMP

132

Role of cGMP degradation and natriuretic peptide clearance receptors for axonal bifurcation of sensory neurons

S. Peters¹, H. Schmidt², K. Frank², L. Wen¹, R. Feil¹, F. G. Rathjen²
¹Universität Tübingen, Interfakultäres Institut für Biochemie, Tübingen, Germany
²Max-Delbrück-Centrum, Berlin, Germany

Axonal branching is essential for the correct formation of neuronal circuits and enables the simultaneous transmission of information throughout the body. In mice, the bifurcation of axons of sensory neurons at the dorsal root entry zone of the developing spinal cord depends on a cGMP signaling cascade that includes C-type natriuretic peptide (CNP), natriuretic peptide receptor 2 (Npr2, also termed GC-B), and cGMP-dependent protein kinase Ia. In this study it was investigated, if a disturbance of cGMP signaling induced by manipulation of cGMP breakdown or CNP scavenging affects axon

bifurcation of murine embryonic dorsal root ganglion (DRG) neurons. RT-PCR screens, *in situ* hybridization, and FRET-based cGMP imaging in living neurons revealed phosphodiesterase 2A (PDE2A) as the major enzyme for degradation of CNP-induced cGMP in embryonic DRG neurons. Interestingly, cGMP measurements and Dil labeling of PDE2A knockout embryos indicated that a strongly elevated concentration of cGMP does not impair sensory axon bifurcation of DRG neurons *in vivo*. The natriuretic peptide receptor 3 (Npr3) was found to be expressed in the roof and floor plate of the spinal cord as well as in the dorsal roots of E12.5 embryos. Because Npr3 binds natriuretic peptides, but does not generate cGMP, it is thought to act as a natriuretic peptide clearance receptor. By scavenging CNP, Npr3 could lower the activity of the CNP-Npr2-cGMP signaling cascade in DRG neurons. In the absence of Npr3, the majority of sensory axons showed normal bifurcation, but »13 % of the axons turned only in rostral or caudal direction. This study shows (1) that PDE2A is important for the degradation of cGMP in embryonic DRG neurons, (2) that the bifurcation of sensory axons in the spinal cord can tolerate high levels of intracellular cGMP in the absence of PDE2A, and (3) that a small population of sensory neurons requires Npr3 to branch correctly.

133

AMPA receptor-induced cGMP signals in cortical and hippocampal neurons

J. Giesen¹, E.-M. Füchtbauer², D. Koesling¹, M. Russwurm¹

¹Ruhr-University Bochum, Institute of Pharmacology and Toxicology, Bochum, Germany

²Aarhus University, Department of Molecular Biology and Genetics-Molecular Cell and Developmental Biology, Denmark, D[Ⓜ]mark

In the central nervous system, NO-dependent cGMP signalling is associated with many different developmental processes and brain functions, and plays an important role in memory consolidation and cognition.

To analyse cGMP signals in primary cells, a *knock-in* mouse was generated which stably and ubiquitously expresses a FRET-based cGMP indicator (cGi500). Cultured cortical and hippocampal neurons were found to respond to exogenously applied NO (GSNO). In these cell types, endogenous NO is mainly generated by the neuronal NO synthase (nNOS) isoform which requires a rise in intracellular calcium for activation of the NO/cGMP-signalling cascade.

Here, we show that AMPA-type ionotropic glutamate receptors were capable to induce cGMP response in cultured cortical and hippocampal neurons. Surprisingly, AMPAR-induced cGMP signals were independent of NMDAR activation, as inhibition of NMDARs with the NMDAR antagonist D-APV (*D*-2-Amino-5-phosphonopentanoic acid) did not block AMPAR-induced cGMP response. However, cGMP accumulation depends on NO synthase activation as the NOS inhibitor L-NNA (*NG*-nitro-*L*-Arginine) completely abolished cGMP accumulation. Whether AMPAR-induced NOS activation depends on calcium influx via calcium permeable AMPARs, VGCCs (*voltage gated calcium channels*) or calcium release from intracellular stores will further be investigated in detail.

134

cAMP nanodomains: role of phosphodiesterases

A. Bock¹, M. J. Lohse¹

¹Universität Würzburg, Pharmakologie und Toxikologie, Würzburg, Germany

Cyclic adenosine monophosphate (cAMP) is an important and ubiquitous cellular second messenger. A dogma in signaling is that cAMP is distributed homogeneously in the cell and that its concentration changes equally upon stimulation. In contrast, a large body of evidence suggests the existence of concentration gradients (so-called microdomains) of cAMP. In this regard, phosphodiesterases (PDEs), the only enzymes which can degrade cAMP, have been suspected to be responsible for maintaining those gradients. However, how PDEs establish cAMP gradients is entirely unknown. Here, we measure local cAMP levels in HEK cells and cytosolic fractions thereof using the cAMP FRET-sensor EPAC1-cAMPs fused to a phosphodiesterase (PDE4A1). We demonstrate the existence of low cAMP concentrations in close proximity to PDEs and show that this gradient is maintained by PDE hydrolytic activity. Further we establish that cAMP gradients cannot be maintained solely on the basis of PDE activity as the cAMP turnover is very slow. We provide evidence that PDEs are structurally organized in yet unspecified 'microstructures' in which cAMP diffusion must be considerably slowed down. Taken together, we suggest that cAMP gradients are established by PDE hydrolytic activity in cellular regions with slow diffusion of cAMP. Our study sheds light on the organization and maintenance of signaling compartments in cells.

135

The influence of PDE hydrolytic activity on cAMP gradients

C. Konrad¹, A. Bock¹, M. J. Lohse¹

¹Universität Würzburg, Pharmakologie und Toxikologie, Würzburg, Germany

Phosphodiesterases (PDEs) are a family of enzymes that degrade cyclic AMP (cAMP) and cyclic GMP (cGMP) to their respective monophosphates. Although several PDEs have been shown to play an important role in a wide variety of physiological and pathological processes, their complexity and function in cell signalling is only beginning to be understood. It is especially astonishing that eukaryotes express more than 100 different PDE isoforms while their single function is to degrade cAMP, cGMP or both. In recent years, a large body of evidence has suggested that PDEs (especially isoforms of the PDE families 3, 4 and 5) are key players in establishing signalling compartments. These so-called microdomains are yet unspecified regions in cells where the concentrations of cAMP and cGMP are higher or lower than in the bulk cytosol. In a companion abstract (Bock & Lohse) we provide evidence that cAMP nanodomains, i.e. regions of low cAMP concentrations, exist in cells in the direct vicinity of PDE4. However, the mechanisms by which PDEs establish and maintain cAMP gradients are largely unknown. Here we study if establishing cAMP gradients is a general role of PDEs and, moreover, if the size of cAMP nanodomains mainly depends on PDE hydrolytic activity. By fusing an ultra-fast PDE2A3 ($V_{max} = 120 \mu\text{mol}/\text{min}/\text{mg}$) to a cAMP FRET sensor (EPAC1-camps) we monitor cAMP concentrations in direct vicinity of PDE2A3. In

comparison to PDE4, we show that PDE2A3, albeit displaying a high cAMP turnover, only establishes a small cAMP gradient in both cytosol preparations of transfected HEK cells and in living cells. Interestingly, this gradient can be increased by deleting the N-terminal regulatory domains while maintaining fast cAMP turnover. Biochemical mapping of the cAMP gradient gives an estimate of the size of nanodomains. Taken together, our data suggest that establishing cAMP gradients does not exclusively depend on PDE hydrolytic activity.

References: Herget *et al.* Real-time monitoring of phosphodiesterase inhibition in intact cells. *Cell. Signal.* **20**, 1423-1431 (2008)

Pharmacology – Cardiovascular system

136

Anti-inflammatory and antiatherogenic effects of the NLRP3 inflammasome inhibitor arglabin

T. Syrovets¹, B. Büchele¹, M. El Gaafary¹, M. Rubio Ayala¹, A. Abderrazak², D. Couchie², D. F. Darweesh Mahmood², R. Elhage², C. Vindis³, M. Laffargue⁴, V. Matéo⁵, M.-N. Slimane⁶, B. Friguet², T. Fulop⁷, K. El Hadri², T. Simmet¹, M. Rouis²

¹Institute of Pharmacology of Natural Products & Clinical Pharmacology, Ulm, Germany

²Biological Adaptation and Ageing (B2A), INSERM -U1164, Paris, France

³Institut des Maladies Métaboliques et Cardiovasculaires, Toulouse, France

⁴Institut des Maladies Métaboliques et Cardiovasculaires, INSERM U1048, Toulouse, France

⁵Centre de Recherche d'Immunologie et Maladies Infectieuses, INSERM U-1135, Paris, France

⁶Biochemistry Laboratory, TN-Monastir, Tunisia

⁷Centre de Recherche sur le Vieillissement, Université de Sherbrooke, Sherbrooke, Canada

Arglabin is a plant-derived sesquiterpene lactone used for cancer therapy in Kazakhstan and Russia. Signaling pathways targeted by arglabin are poorly understood.

We have isolated arglabin by using high performance liquid chromatography from a methanolic extract of *Artemisia glabella*, a plant endemic in Kazakhstan. Mass spectrometric analyses confirmed the chemical structure and the purity of the isolated arglabin.

In J774 macrophages, arglabin strongly induced accumulation of LC3 type II protein in the absence of inflammasome activators, and also in cells activated with LPS and cholesterol crystals. In addition, arglabin induced clustering of LC3-II at autophagosomal membranes, as evidenced from its punctuated pattern in confocal microscopic images of arglabin-treated macrophages, which is a characteristic sign for autophagy. Since autophagy activation leads to increased degradation of NLRP3 and pro-interleukin (IL)-1 β , we further analyzed whether arglabin inhibits the NLRP3 inflammasome. Arglabin reduced expression of NLRP3 and pro-IL-1 β , inhibited activation of caspase-1, and release of mature IL-1 β by LPS- and cholesterol-crystal-stimulated macrophages consistent with inhibition of the NLRP3 inflammasome.

Intraperitoneal injection of arglabin into female ApoE2.KI mice fed a high fat diet resulted in significantly decreased plasma levels of proinflammatory IL-1 β . Moreover, arglabin markedly reduced mean lesion areas in the sinus and whole aorta in mice.

Thus, arglabin may represent a new promising drug to treat diseases associated with inflammasome activation, e.g. atherosclerosis. This work was supported in part by a grant from the Nouvelle Société Francophone d'Athérosclérose (NSFA).

137

Regulation of renin secretion and expression in mice deficient in proteinase-activated receptor 2

L. R. Thurner¹, K. Hoecherl²

¹Institut für Physiologie, Regensburg, Germany

²Institut für Experimentelle und Klinische Pharmakologie und Toxikologie Friedrich-Alexander-Universität Erlangen-Nürnberg, Erlangen, Germany

Recently, we found that activation of the proteinase-activated receptor (PAR) 2 stimulates renin release in the isolated perfused kidney model. Therefore, we determined in the current experiments the response of plasma renin concentration (PRC) to acute intraperitoneal administration of the PAR2 activating peptide SLIGRL (100 $\mu\text{g}/\text{kg}$), hydralazine (2 mg/kg), isoproterenol (10 mg/kg), losartan (3 mg/kg) and furosemide (40 mg/kg) in conscious wild-type (WT) and PAR2-deficient mice.

PRC was measured in plasma obtained by tail vein puncture. Renal renin expression was determined by quantitative RT-PCR. Renal protein expression was measured by immunohistochemistry.

On a control diet (0.6% NaCl), plasma renin concentration (in ng angiotensin I per mL per hour) was significantly lower in PAR2-deficient mice than in wild-type mice (190 \pm 35 versus 380 \pm 91). Renin mRNA expression was 50 \pm 9% of WT. Renin-expressing cells were located at the juxtaglomerular position and renal renin protein expression was lower in PAR2-deficient mice. As measured by tail-cuff method, systolic blood pressure was not different between PAR2 (-/-) and WT mice. Administration of SLIGRL increased renin secretion about 6-fold ($p < 0.01$). Acute stimulation of renin release by furosemide, isoproterenol, losartan and hydralazine caused significant increases of plasma renin concentration in both PAR2 (-/-) and WT mice. The absolute changes (Δ PRC) were similar (3780 \pm 770, 2230 \pm 400, 2780 \pm 70, 1390 \pm 460 in WT, and 2320 \pm 270, 2530 \pm 250, 3010 \pm 210, 1230 \pm 470 in PAR2 (-/-)).

In conclusion, chronic absence of PAR2 reduces basal renin expression and renin release. However, PAR2-deficiency does not alter renin release in response to typical stimuli for renin secretion. Therefore, PAR2 does not appear to be a mandatory and specific requirement for acute regulatory responsiveness.

138

Epigallocatechin-3-gallate shortens relaxation time in cardiac myocytes and decreases Ca²⁺ sensitivity of cardiac myofilaments in an HCM mouse model

F. Friedrich¹, M. Nasib¹, F. Fleener¹, T. Eschenhagen¹, L. Carrier¹
¹Inst. für Exp. Pharmakologie und Toxikologie, Hamburg, Germany

Background: Hypertrophic cardiomyopathy (HCM) is a hereditary cardiac muscle disease with left ventricular hypertrophy, interstitial fibrosis and diastolic dysfunction. Increased myofilament Ca²⁺ sensitivity could be the underlying cause of diastolic dysfunction. We evaluated acute effects of epigallocatechin-3-gallate (EGCG), which has been shown to decrease myofilament Ca²⁺ sensitivity, on cardiac myocyte contractility and force-Ca²⁺ relationship of skinned cardiac muscle strips in an HCM mouse model with left ventricular hypertrophy and both systolic and diastolic dysfunction.

Methods: The HCM mouse model used in this study carries a point mutation in the cardiac myosin-binding protein C gene at the homozygous state (*Mybpc3*-targeted knock-in; KI). We isolated ventricular myocytes from adult KI and WT mice and analyzed sarcomere shortening and Ca²⁺ transients at 37 °C under 1 Hz pacing using the IonOptix system in the absence or presence of EGCG (1.8 µM). Furthermore, force-Ca²⁺ relationships of skinned cardiac muscle strips of KI and WT mice were obtained ±EGCG (30 µM).

Results: In baseline settings and absence of Fura-2, KI cardiomyocytes displayed higher sarcomere shortening (8.2±3.1 µm vs 5.4±1.9%, n=17-20), lower diastolic sarcomere length (1.7±0.06 µm vs 1.8±0.03 µm, n=17-20), longer time to peak shortening (0.06±0.02 s vs 0.04±0.01 s, n=17-20) and time to 50% relengthening (0.04±0.01 s vs 0.02±0.01 s, n=17-20) than WT cardiomyocytes. In WT and KI neither diastolic sarcomere length nor sarcomere shortening were influenced by EGCG treatment, but relaxation time was hastened, to a greater extent in KI cells. EGCG shortened time to peak Ca²⁺ and Ca²⁺ transient decay in Fura-2-loaded WT and KI cardiomyocytes. EGCG did not affect Ca²⁺ transient amplitude, but increased diastolic Ca²⁺ in WT and KI cells. To decipher the mechanism of Ca²⁺ transient abbreviation we investigated phospholamban phosphorylation levels in ±EGCG treated adult ventricular cardiomyocytes. EGCG did not influence phosphorylated phospholamban levels. In skinned cardiac muscle strips EGCG decreased Ca²⁺ sensitivity in both groups.

Conclusion: EGCG accelerated relaxation and Ca²⁺ transient decay in WT and KI cardiomyocytes, which is not due to an influence on phospholamban phosphorylation, but rather Ca²⁺ desensitization of myofilaments and possibly effects on SR calcium content and SERCA/NCX activity.

139

Depressed Ca²⁺ cycling in mice with overexpression of PP1 inhibitor-2 is reversed by chronic β-adrenergic stimulation

U. Kirchhefer¹, T. Herpertz¹, G. Isensee¹, F. U. Müller¹, P. Boknik¹
¹Institut für Pharmakologie und Toxikologie, Münster, Germany

Type-1 serine/threonine protein phosphatase (PP1) comprises a family of enzymes that dephosphorylate cardiac regulatory proteins, thereby modulating Ca²⁺ handling and contractility. All PP1 heterodimers possess a catalytic subunit, which is selectively inhibited by inhibitor 2 (I-2). It has been shown by our group that the heart-directed overexpression of a truncated, constitutively active form of I-2 resulted in an improved basal Ca²⁺ handling and contractility. In contrast, chronic pressure overload by transverse aortic constriction exacerbated the progression of cardiac remodeling and heart failure in transgenic mice. In the present study, we tested whether the overexpression of a₂ full-length form of I-2, regulated by GSK3-dependent phosphorylation at Thr⁷², resulted in comparable functional alterations using a model of induced heart failure. For this purpose transgenic (TG) and wild-type (WT) mice were subjected to chronic application of isoprenaline (ISO, 30 mg/kg/d) via osmotic minipumps. ISO-stimulated mice were compared to mice treated with 0.9% NaCl (n=5). After one week of ISO administration, cardiac hypertrophy was comparable in TG and WT. Ca²⁺ transients were measured in isolated, indo-1-loaded myocytes. The peak amplitude of [Ca]_i was reduced by 39% in TG^{NaCl} compared to WT^{NaCl} (p<0.05), whereas chronic ISO application was associated with comparable effects in TG and WT. [Ca]_i decay kinetics were comparable in NaCl-treated groups but hastened by 25% in TG^{ISO} compared to WT^{ISO} (p<0.05). Consistently, SR Ca²⁺ load was diminished by 28% in TG^{NaCl} compared to WT^{NaCl} (p<0.05). Chronic ISO stimulation led to an unchanged SR Ca²⁺ content in TG and WT myocytes. Biochemical analyses revealed that chronic β-adrenergic stimulation was accompanied by a more than 4-fold higher phospholamban phosphorylation at Ser¹⁶ in TG (p<0.05). Thus, these findings suggest that overexpression of I-2 is able to reduce the progression of heart failure by an improvement of myocyte Ca²⁺ handling.

140

A leogigin derivative as farnesoid X receptor agonist and modulator of macrophage cholesterol efflux

A. Ladurner¹, L. Wang¹, A. Holzer¹, L. Kovářová¹, T. Linder², D. Schuster³, M. D. Mihovlović², A. G. Atanasov¹, V. M. Dirsch¹
¹University of Vienna, Department of Pharmacognosy, Vienna, Austria
²Vienna University of Technology, Institute of Applied Synthetic Chemistry, Vienna, Austria
³University of Innsbruck, Institute of Pharmacy/Pharmaceutical Chemistry and Center for Molecular Biosciences Innsbruck (CMBI), Innsbruck, Austria

The ligand-activated farnesoid X receptor (FXR) is a nuclear receptor highly expressed in gastrointestinal and metabolic tissues, such as the duodenum, jejunum, ileum, colon and the liver, but also in lower amounts for instance in macrophages. The endogenous agonists for this receptor are bile acids with the primary bile acid chenodeoxycholic acid as the most active one. Activation of FXR regulates the transcription of target genes relevant in bile acid homeostasis, glucose and lipid metabolism, liver protection, inflammation, and cancerogenesis. Agonists for FXR have been discussed as possible therapeutic options for the treatment of obesity and the metabolic syndrome.

Atherosclerosis is the main pathology underlying cardiovascular diseases and often occurs side-by-side with the metabolic syndrome. Cholesterol deposition and the formation of cholesterol-loaded foam cells from macrophages lead to the formation of atherosclerotic plaques. This can be prevented by stimulation of cholesterol efflux from macrophages.

Based on leogigin, a lignan-type secondary plant metabolite, naturally occurring in *Leontopodium alpinum* Cass., 168 derivatives were synthesized and subjected to a FXR pharmacophore-based *in silico* screening. Testing of 56 virtual hits in a luciferase-based FXR transactivation assay yielded one compound with promising activity on FXR. Moreover, the heterodimer partner of FXR, RXRα, was not activated by this leogigin derivative in a luciferase-based RXRα assay.

In addition, this compound was able to increase cholesterol efflux in THP-1 macrophages without affecting cell viability. Western blot experiments revealed an increase in ATP-binding cassette transporter A1 (ABCA1) expression in human THP-1 macrophages by this leogigin derivative. The transporters ABCG1 and scavenger receptor class B (SR-BI), which also play a key role in macrophage cholesterol efflux, will be investigated. Moreover, the effect of the leogigin derivative on liver X receptor activation, the nuclear receptor responsible for upregulation of these transporters, has to be studied.

Based on this data, further characterization of the molecular mechanism underlying the described effects will provide valuable insights in a possible crosstalk between macrophage cholesterol efflux and FXR activation.

141

Rho-associated kinases ROCK1 and ROCK2 affect myofibroblast characteristics of cardiac fibroblasts

S. Hartmann^{1,2,3}, A. Jatho^{4,3}, W.-H. Zimmermann^{1,3}, A. J. Ridley², S. Lutz^{1,3}
¹Universitätsmedizin Göttingen, Institut für Pharmakologie, Göttingen, Germany
²King's College London, Randall Division of Cell and Molecular Biophysics, London, Germany
³DZHK (Deutsches Zentrum für Herz-Kreislauf Forschung, Göttingen, Germany
⁴Universitätsmedizin Göttingen, Institut für Herz- und Kreislaufphysiologie, Göttingen, Germany

Background: Rho-associated kinases ROCK1 and ROCK2 are serine/threonine kinases that are downstream targets of the small GTPases RhoA, RhoB, and RhoC. ROCK1 and ROCK2 are known to play a pivotal role in the pathogenesis of myocardial fibrosis. However, their specific function in cardiac fibroblasts (CF) remains unclear. Remodelling of the diseased heart results in the transition of fibroblasts to a myofibroblast phenotype exemplified by an increased proliferation, migration rate and synthesis of extracellular matrix (ECM) proteins. Therefore, we sought to investigate whether ROCK protein signalling intermediates have an impact on cellular characteristics, intracellular protein expression and mechanical properties in CF and engineered tissues.

Methods: Neonatal cardiac fibroblasts were isolated from wild type rats and downregulation of ROCK1 and ROCK2 by 75% was achieved by lentiviral transduction or transfection. Wild type fibroblasts were treated with 10 µM Fasudil or 3 µM H1152p for general ROCK inhibition and 3 µM SLX-2119 for inhibition of ROCK2. Protein expression and modification was determined by immunoblot analysis, gene expression by qPCR analysis, CF morphology and the localisation of cytoskeletal proteins by immunofluorescence analysis, cell proliferation by automated nuclei counting, cell migration on a planar surface by life cell imaging, and rigidity of engineered tissues by rheological measurement.

Results: Our results show that both ROCK1 and ROCK2 influence CF morphology, gene expression, proliferation and migration. The knockdown and inhibition of ROCKs was associated with changes in CF morphology accompanied by a disorganization of higher-order actin structures including stress fibers and geodesic domes. Moreover, the knockdown of ROCK1 and ROCK2 in CF increased adhesion velocity, whereas proliferation was attenuated. Interestingly, downregulation of ROCK2, but not of ROCK1 led to a significantly decreased migration velocity and distance suggesting an isolated principle role for ROCK2 in cardiac fibroblast migratory behavior. Analysis of a three dimensional engineered tissue model composed of cardiac fibroblasts (engineered connective tissue, ECT) suggested that ROCKs are involved in the regulation and turnover of the extracellular matrix (ECM) and thus influence viscoelastic properties of engineered tissues. Destructive tensile strength measurement in ECT treated with ROCK inhibitors showed that rigidity was significantly reduced when compared to control tissues. RNA sequencing of ECT treated with the ROCK inhibitor H1152p and qPCR analysis of CF with a downregulation of ROCK1 and ROCK2 showed that both ROCKs are involved in the regulation of ECM proteins, such as collagens 4a2, 6a, and 8a1, biglycan, decorin, elastin and its respective degrading enzyme MMP12. **Conclusion:** This study demonstrates that ROCK signalling controls myofibroblast characteristics of CF via remodelling of the cytoskeleton and the ECM.

142

Nuclear proteome analysis of newborn and adult mouse cardiomyocytes

M. Zeeb¹, P. Kogan¹, R. Gilsbach¹, V. Dumit², J. Dengjel³, L. Hein¹
¹Institut für experimentelle und klinische Pharmakologie und Toxikologie, Freiburg i. Br., Germany
²ZBSA Center for Biological Systems Analysis, Universität Freiburg, Core Facility Proteomics, Freiburg, Germany
³Medical Center, Universität Freiburg, Dermatologie, Freiburg, Germany

Background: Regulation and fine-tuning of gene transcription in cardiomyocytes (CMs) is a centerpiece of cardiac development, function, and disease. In order to obtain authentic data, cell type-specific analyses are indispensable. Recently, high-purity isolation protocols for CM nuclei were established [Bergmann, Exp Cell Res, 2011] and employed for detailed genetic and epigenetic studies on cardiac gene transcription [Gilsbach, Nat Commun, 2014]. However, corresponding protein analyses, which bridge from transcriptional control to CM function are still lacking.

Therefore, we aimed to map the landscape of nuclear protein expression in newborn and adult mice in order to complement and extend our epigenetic studies.

Methods and Results: Cardiac nuclei were isolated from homogenized adult and P1 mouse frozen hearts by sucrose gradient centrifugation. Magnetic-assisted cell sorting (MACS) with PCM-1 as a nucleus-specific marker was used to enrich CM nuclei to >95%. Proteins were extracted from nuclear lysate with 2% SDS.

Quantitative protein data were obtained from SILAC-based liquid chromatography-tandem mass spectrometry (LC-MS/MS) experiments with an LTQ Orbitrap XL mass spectrometer after in-gel digestion with trypsin. Nuclear protein extracts from 3 murine cell lines served as SILAC (Lys8/Arg10)-labeled internal standard. Finally, protein data are correlated with corresponding mRNA data obtained by RNA-sequencing. We identified 1041 proteins, 688 of which are annotated to the nucleus. 21%/23% (Adult / P1) of nuclear proteins are annotated as DNA-binding. 1.5%/1.4% belong to transcription factor complexes; 7.3%/7.5% are able to bind transcription factors. 7.9%/8.3% have chromatin modification functions; 4.3%/4.4% modify histones. Nuclear-enriched GO terms include mRNA processing and transport, transcription, nucleosome assembly and protein degradation.

71% of proteins are shared between P1 and adult nuclei. 142 proteins are exclusive to P1, 34 are only found in adult. 93 proteins are enriched (1.3-fold increase in abundance) in P1 hearts, 89 proteins in adult. Proteins related to heart development, gene silencing, and DNA replication are more prominent in or exclusive to newborn mice. Adult nuclei strongly express proteins related to regulation of actin fibers and CM function, proteins involved in protein degradation, and chaperones. Although high mRNA expression increases the chance of protein identification, a significant correlation between mRNA and protein level could not be observed on a genome-wide scale.

Conclusions: We present a comprehensive and specific protein landscape of newborn and adult CM nuclei. Young CM nuclei appear as a developing tissue, show the ability for proliferation, and indicate ongoing alterations in gene expression. Adult CM nuclei prominently display a focus on regulation of contractile fibers and CM function, as well as chaperones and proteasomal proteins indicative of its arduous function.

143

Essential role for premature senescence of myofibroblasts in myocardial fibrosis

K. Meyer¹, B. Hodwin¹, S. Engelhardt¹, A. Sarikas¹

¹Technische Universität München, Institut für Pharmakologie und Toxikologie, Muenchen, Germany

Background: Fibrosis is a hallmark of many myocardial pathologies and contributes to distorted organ architecture and function. Recent studies have identified premature senescence as regulatory mechanism of tissue fibrosis. However, its relevance in the heart remains to be established.

Objective: To investigate the role of premature senescence in myocardial fibrosis.

Methods: Murine models of cardiac disease and human heart biopsies were analyzed for characteristics of premature senescence and fibrosis.

Results: Senescence markers p21^{CIP1/WAF1}, senescence-associated β -galactosidase (SA- β -gal) and p16^{INK4a} were increased 2-, 8- and 20-fold (n=5-7; P < 0.01), respectively, in perivascular fibrotic areas after transverse aortic constriction (TAC) compared to sham-treated controls. Similar results were observed with cardiomyocyte-specific β 1-adrenoceptor transgenic mice and human heart biopsies. Senescent cells were positive for vimentin (92 \pm 0.9%), platelet derived growth factor receptor α (94 \pm 0.9%) and α -smooth muscle actin (71 \pm 2.3%), specifying myofibroblasts as the predominant cell population undergoing premature senescence in the heart.

Conclusion: Our data provide first evidence for an essential role of premature senescence of myofibroblasts in myocardial fibrosis. It is tempting to speculate that pharmacologic modulation of premature senescence might provide a novel therapeutic target for anti-fibrotic therapies in the heart.

144

MicroRNAs involved in the antifibrotic effects of cannabinoid receptor 1 inhibition in heart

F. Ariana¹, F. Jan¹, T. Sabrina¹, X. Ke¹, J. Annette¹, Z. Karina¹, S. Katharina¹, G.

Robert¹, N. Chihiro², Z. Andreas³, T. Thomas¹, B. Sandor¹

¹MHH, IMTTS_OE8886, Hannover, Germany

²Helmholtz-Zentrum für Infektionsforschung, Genomanalytik, Braunschweig, Germany

³University of Bonn, Institute of Molecular Psychiatry, Bonn, Germany

Introduction: The endocannabinoid system is increasingly studied in cardiac research due to its role in fibrosis, inflammation and cell fate modulation. The deregulation of this system has been implicated in myocardial infarction (MI) and consequent heart failure development. A recent study suggests cannabinoid receptor 1 (CB1) inhibition to improve cardiac function and to reduce adverse remodeling after cardiac stress, but the exact underlying molecular mechanisms of these beneficial effects are still unknown. MicroRNAs (miRNAs, miRs) provide a complex layer of post-transcriptional regulation modulating key biological processes such as tissue remodeling in heart failure. The aim of the present study was to explore microRNA pathways in the chronic effect of CB1 receptor inhibition after angiotensin-fibrosis induction and left ventricular remodeling.

Methods and Results: Adverse cardiac remodeling was induced in mice by chronic administration of Angiotensin II (AngII, 1,5 mg/kg/day) with osmotic minipumps for 14 days. Treatment with CB1 antagonist, or vehicle was performed every second day during the AngII administration period. Hemodynamic parameters were measured by echocardiography and cardiac pressure volume catheter and tissue samples were taken for molecular and histological analysis. After two weeks of AngII infusion, left ventricular dysfunction was prevented by CB1 antagonist treatment. This was shown by significantly improvements of the myocardial performance index and end-diastolic pressure values. At the tissue level, anti-fibrotic effects of CB1 antagonist treatment was confirmed histologically and by expression analysis of pro-fibrotic genes. These beneficial effects were also observed in CB1 KO mice and in an aging mice model. The particular role of tissue fibroblast in AngII-induced cardiac fibrosis was further explored. Primary cardiac fibroblasts (CF) from each experimental group were isolated and analysed by next generation deep RNA sequencing to identify differentially regulated microRNAs. MicroRNA-181a/b family was downregulated by *in vivo* AngII delivery and vice versa upregulated after CB1 antagonist treatment and Foxb1 (a direct target of miR-

181a family) was differentially regulated, suggesting a possible mechanism of action for the benefits of CB1 receptor inhibition.

Conclusion: We found that in AngII-induced cardiac remodelling, LV function is preserved by chronic CB1 antagonist treatment and that cardiac fibrosis is reduced with concomitant downregulation of fibrogenic genes. Also, CF-enriched miR-181a/b family seems to be sensitive to CB1 antagonist treatment, thereby affecting cardiac fibrosis. The current study employs a novel concept regarding chronic CB1 inhibitor treatment and may provide important details and novel targets for anti-fibrotic approaches in heart failure.

145

Development of atherosclerosis in AGAT/apoE deficient mice

K. Cordts^{1,2}, M. Manderscheid¹, C.-U. Choe^{3,2}, T. Zeller^{2,4}, R. H. Böger^{1,2}, J. Heeren⁵, D. Atzler^{1,2,6}, E. Schwedhelm^{1,2}

¹University Medical Center Hamburg-Eppendorf, Institute of Clinical Pharmacology and Toxicology, Hamburg, Germany

²DZHK (German Centre for Cardiovascular Research), Partner site

Hamburg/Kiel/Lübeck, Hamburg, Germany

³University Medical Center Hamburg-Eppendorf, Department of Neurology, Hamburg, Germany

⁴University Medical Center Hamburg-Eppendorf, Department of Cardiology, Hamburg, Germany

⁵University Medical Center Hamburg-Eppendorf, Department of Biochemistry and Molecular Cell Biology, Hamburg, Germany

⁶University of Oxford, Division of Cardiovascular Medicine, Radcliffe Department of Medicine, Oxford, United Kingdom

Background: Low homoarginine (hArg) was recently identified as an emerging biomarker for stroke, myocardial infarction, and heart failure in clinical and epidemiological studies. hArg competes with arginine as a substrate for nitric oxide (NO) synthase and weakly inhibits arginase. Both mechanisms might lead to increased NO formation *in vivo*. The aim of this study was to investigate whether hArg effects the development of atherosclerosis as a potential underlying mechanism of cardiovascular diseases.

Methods: hArg-deficient AGAT-knockout (AGAT^{-/-}) and wildtype (wt) mice were crossed with apolipoprotein E (ApoE) deficient mice and fed with high fat diet (HFD) for three months to induce atherosclerosis. hArg plasma concentrations were determined using mass spectrometry. En face preparation of aortae followed by red oil staining of atherosclerotic plaques and quantitative evaluation of plaque areas was performed for female mice. Endothelial function of male mice was tested with acetylcholine (ACh) and nitroglycerin (NTG) after contraction with prostaglandin F2 α .

Results: AGAT^{-/-} mice have lower hArg plasma concentrations compared to wt littermates and mean \pm SD hArg plasma concentrations are lower in male mice (0.03 \pm 0.02 (n=13) vs. 0.20 \pm 0.06 μ M (n=13); AGAT^{-/-} vs. wt; P<0.01) compared to female mice (0.06 \pm 0.04 (n=27) vs. 0.41 \pm 0.18 μ M (n=35); P<0.001). After a 3 months HFD, atherosclerotic plaque load in aortic arches is larger in female AGAT^{-/-} mice compared to female AGAT wt mice (22.7 \pm 9.3% vs. 17.9 \pm 8.1% surface area; mean \pm SD; P<0.05). Relaxation analyses of aortae show improved endothelial (ACh; logEC₅₀ -7.33 vs. -7.02; AGAT^{-/-} vs. wt; P<0.05) and non-endothelial (NTG; logEC₅₀ -7.33 versus -7.03; AGAT^{-/-} vs. wt; P<0.001) dependent relaxation in male AGAT^{-/-} mice.

Conclusion: Our study suggests that hArg might affect early plaque development in atherosclerosis, possibly caused by increased NO formation *in vivo*. AGAT^{-/-} mice show higher sensitivity to vasodilators. Low hArg plasma concentrations might have led to an increase in sensitivity to NO, e.g. by altering activities of the NO signaling cascade. Further experimental investigations are needed to reveal the underlying mechanisms.

146

Dabigatran treatment changes macrophage polarization in visceral adipose tissue and atherosclerotic lesions of Low density lipoprotein receptor deficient mice

K. Feldmann^{1,2}, M. Grandoch^{1,2}, C. Kohlmorgen^{1,2}, B. Valentin^{1,2}, N. Nagy^{1,2}, S. Hartwig^{3,4}, S. Lehn^{3,4}, J. W. Fischer^{1,2}

¹Universitätsklinikum der Heinrich-Heine-Universität, Institut für Pharmakologie und Klinische Pharmakologie, Düsseldorf, Germany

²Universitätsklinikum der Heinrich-Heine-Universität, Cardiovascular Research Institute Düsseldorf (CARID), Düsseldorf, Germany

³German Diabetes Center at the Heinrich-Heine-University Düsseldorf, Leibniz Center for Diabetes Research, Institute of Clinical Biochemistry and Pathobiochemistry, Düsseldorf, Germany

⁴German Center for Diabetes Research (DZD), München-Neuherbe, Germany

Background: The direct oral thrombin inhibitor dabigatran etexilate (dabigatran) is used for the prevention and treatment of venous thromboembolism. Obese patients as well as patients with type 2 diabetes mellitus (T2DM) have an increased risk for thrombotic disease and show enhanced thrombin generation. Besides its role in blood coagulation, thrombin is known to be involved in many pro-inflammatory processes. In obesity, adipose tissue (AT) inflammation plays a crucial role in the development of insulin resistance and T2DM and contributes to atherosclerosis development. The aim of the present study was to analyse the effects of dabigatran on AT inflammation in a mouse model of diet-induced obesity in the context of accelerated atherosclerosis.

Methods: 10-week-old female low-density lipoprotein receptor-deficient (*Ldlr*^{-/-}) mice were fed a high-fat diet containing 5 mg/g dabigatran or respective placebo for 20 weeks.

Results: Analysis of visceral AT revealed a significant increase in adipocyte size in dabigatran-treated mice, although body weight, fat mass, glucose tolerance, and insulin resistance were unchanged between groups. This effects seemed to be directly mediated by thrombin, as treatment with another thrombin inhibitor (argatroban) also resulted in the development of adipocyte hypertrophy. Accordingly, *in vitro* studies in 3T3-L1 cells revealed an inhibitory effect of thrombin on lipid accumulation in adipocytes. The amount of pro-inflammatory CD11c-positive macrophages (ATMs) in visceral adipose tissue was significantly reduced, and the secretion of pro-inflammatory IL-6 from visceral AT was significantly lower in dabigatran-treated animals. *In vitro*

studies using 3T3 L1 cells and primary bone marrow-derived macrophages revealed that the changes in macrophage polarization were not directly mediated by thrombin, but indirectly by a change in the secretion profile of adipocytes. A similar reduction in pro-inflammatory macrophages as detected in AT could also be observed in the aortic wall of dabigatran-treated mice. **Conclusions:** The direct thrombin inhibitor dabigatran inhibits AT inflammation and the accumulation of pro-inflammatory macrophages in VAT but also the aortic wall of *Ldlr^{-/-}* mice. These anti-inflammatory effects of dabigatran might contribute to the known atheroprotective effects of dabigatran.

147

Oligomerization enhances basal PLN activity *in vivo* by attenuating PKA-dependent phosphorylation

F. Funk¹, A. Kronenbitter¹, J. P. Schmitt¹

¹Institute of Pharmacology and Clinical Pharmacology, University Hospital, Düsseldorf, Germany

Background: Sarco/endoplasmic reticulum Ca²⁺-ATPase (SERCA2a) and its inhibitor phospholamban (PLN) are critical determinants of cardiomyocyte calcium cycling and hence, cardiac contractility. PLN exists in an equilibrium between mono- and pentamers. While monomeric PLN has been implicated in direct SERCA2a inhibition, a functional role for the pentamers remains ambiguous. Recently it has been shown that PLN pentamers modulate PKA-dependent phosphorylation of PLN monomers *in vitro*.¹ Using transgenic mouse models we now investigated the effects of PLN pentamers on PLN phosphorylation, myocyte Ca²⁺ cycling and contractility in cardiac myocytes.

Methods: Phosphorylation patterns of PLN were analyzed by Western blot using phospho-specific antibodies as well as phosphate affinity SDS-PAGE. To assess the phosphorylation at baseline, PLN knockout (PLN-KO) mice expressing either wild type PLN (TgPLN) or the solely monomeric PLN^{ΔFA} mutant (TgAFA) transgene were deeply anesthetized, whereas PLN phosphorylation by PKA was induced using the beta-adrenergic agonist isoproterenol. The consequences on myocyte Ca²⁺ kinetics were measured in isolated, Fura2-loaded and electrically paced (0.5Hz) cardiomyocytes as the time to 50% decay of the Ca²⁺ signal (T_{50%}). The time to 50% baseline of sarcomere length (T_{50%} baseline) characterized the speed of myocyte relaxation.

Results: Under basal conditions, we found stronger phosphorylation of PLN pentamers than monomers, pointing at pentamers as the preferred PKA target. PLN^{ΔFA} monomers showed 3.3-fold stronger phosphorylation signals if pentamers were absent (P<0.0001). Consistent with a higher basal phosphorylation of PLN^{ΔFA} monomers, measurements of calcium kinetics revealed a faster decay of calcium signals in TgAFA compared with TgPLN cardiomyocytes (T_{50%} [ms]: 92±8 and 122±8, respectively, P<0.05). Notably, T_{50%} of PLN-KO myocytes was 79±5ms (P= not significant versus TgAFA), indicating that the strong basal phosphorylation of monomers leads to near complete inactivation of PLN in TgAFA.

Upon stimulation of PKA, PLN monomer phosphorylation and calcium kinetics of TgPLN and TgAFA mouse myocytes were indistinguishable, because monomer phosphorylation and the speed of cytosolic Ca²⁺ clearance strongly increased only in TgPLN. Acceleration of sarcomere relaxation upon PKA stimulation was also more pronounced in TgPLN than in TgAFA and PLN-KO myocytes (increase of T_{50%}baseline [ms]: 32±8 in TgPLN versus 7±4 in TgAFA-PLN and 5±7 in PLN-KO, P<0.05). Even high-dose isoproterenol induced phosphorylation of only about half of all protomers of PLN pentamers suggesting a high capacity of pentamers to attenuate monomer phosphorylation by acting as a phosphate scavenger.

Conclusions: Our data demonstrate that PLN pentamers reduce basal phosphorylation of PLN monomers in myocytes. Nevertheless, pentamers allow strong phosphorylation of monomers during beta-adrenergic stimulation, thereby extending the range within which PLN can modify diastolic Ca²⁺ kinetics and myocyte relaxation.

1. Wittmann T, Lohse MJ, Schmitt JP. Phospholamban pentamers attenuate PKA-dependent phosphorylation of monomers. *J Mol Cell Cardiol.* 80: 90-97 (2015).

148

Enhancing vector-based therapeutic microRNA inhibition using endogenous 3' untranslated regions

S. Werfel¹, D. Holdhof¹, S. Engelhardt¹

¹Technische Universität München, Institute for Pharmacology and Toxicology, Munich, Germany

Therapeutic inhibition of microRNAs is a promising field in cardiovascular research. Vector-based overexpression of an inhibitor construct (e.g. microRNA sponge) is one approach to achieve sustained inhibition with potential applicability in humans. Yet the strength of expression achieved by the currently available gene therapy vectors (e.g. AAVs) in humans remains a limiting factor, therefore inhibitory constructs with increased potency would provide an improvement of this approach and bring it closer to therapeutic application.

MicroRNAs are believed to discriminate between potential binding sites, based on additional factors provided by the endogenous untranslated regions at the 3' end of mRNAs (3' UTRs) and the proteins that are bound to them. Aim of this project was to investigate whether selected endogenous 3' UTRs can likewise increase the potency of microRNA inhibitory constructs.

To this end several known targets for a cardiac microRNA were selected and their relative potencies of microRNA inhibition was compared. To accurately assess changes in the activity of the respective microRNAs we constructed dual-fluorescent reporter plasmids and established an automated fluorescent microscopy acquisition and analysis pipeline.

Among several tested UTR constructs we found one which strongly increased the inhibitory potency of the microRNA binding site in primary rat cardiac myocytes (NRCMs). Furthermore a similar effect was obtained when the binding site was exchanged for that of a different microRNA and analyzed in the NIH-3T3 fibroblast cell line.

We therefore conclude that endogenous UTR contexts can indeed be successfully applied to increase the potency of vector-based microRNA inhibitors.

149

The immunomodulatory lipid sphingosine-1-phosphate elevates tissue factor expression and enhances thrombin generation in differentiated human monocytes/macrophages

C. Heise¹, C. Joseph¹, A. Böhm¹, A. Welz¹, S. Polster¹, B. H. Rauch¹

¹Universitätsmedizin Greifswald, Pharmakologie, Greifswald, Germany

The G-protein-coupled protease-activated receptor-2 (PAR2) regulates inflammatory responses including monocyte migration and cytokine release. PAR2 is activated by the coagulation factor-Xa or by the tissue-factor (TF)/Factor VIIa complex. The immunomodulatory lipid sphingosine-1-phosphate (S1P) is released from activated platelets and interlinks blood coagulation and inflammation. This study investigates the impact of S1P on the expression of PAR2, TF and of the anticoagulant protein thrombomodulin (TM) in human monocytes and after PMA-induced differentiation into macrophage-like cells.

Monocytic THP1 and U937 cell lines were used as human monocyte models. Primary monocytes were isolated from healthy volunteers using a magnetic bead-based monocyte isolation kit. Expression of PAR2, TF and TM was measured by quantitative real-time PCR and Western blotting. Differentiation of monocytes into macrophage-like cells was induced by incubation with 50 ng/ml PMA (phorbol 12-myristate 13-acetate) over 72 h. Calibrated automated thrombin (CAT) generation was determined in platelet-rich plasma from healthy volunteers.

In THP1 and U937 cells S1P induced a time- (1 to 24 h) and concentration-dependent (0.1 to 10 µM) significant upregulation of PAR2 mRNA and total protein expression. PAR2 total protein was upregulated maximally (about 1.5-fold, n=7) with 1 µM S1P after 16 h incubation. Comparable effects were seen in human primary monocytes. In comparison, TF mRNA and protein were only marginally elevated in non-differentiated THP1 monocytes and TM was not regulated by S1P. After differentiation of cultured monocytic cells with PMA into adhesive macrophage-like cells, incubation with S1P resulted in a time- (1 to 24 h) and concentration-dependent (0.1 to 10 µM) significant upregulation of TF expression within 3 to 6 h of incubation. Conversely, PAR2 total protein expression was reduced by about 50% after 24 h S1P incubation. The expression of TM was again not affected. The generation of thrombin in platelet-rich plasma was determined using PMA-differentiated THP1 cells as TF source. Time-dependent incubation with S1P (1 µM) in differentiated monocytes shortened the time to the onset (lag time) of thrombin generation in plasma from 8.0±1.6 to 6.5±1.4 min and elevated total the thrombin generation capacity from 814±130 to 1286±129 nM. Peak thrombin formation was elevated from 66±31 to 130±30 nM/min (control versus S1P for 6h, mean±SD, n=5, respectively).

These data suggest that S1P induces an enhanced expression of PAR2 in undifferentiated human monocytes while TF and TM are not regulated. In differentiated monocytes/macrophages, S1P does upregulate TF expression but attenuates PAR2 levels. Since PAR2 is involved in regulation cell migration, S1P may stimulate a phenotypic switching from a migratory to a procoagulant phenotype during differentiation of monocytes into macrophages.

150

Activated coagulation factor-X (FXa) induces interleukin-6 expression and secretion in human vascular smooth muscle cells – potential role for vascular inflammation

F. Kostka¹, A. Böhm¹, D. Behrendt², S. Polster¹, W. von Bernstorff², B. H. Rauch¹

¹Universitätsmedizin Greifswald, Pharmakologie, Greifswald, Germany

²Universitätsmedizin Greifswald, Klinik und Poliklinik für Chirurgie, Greifswald, Germany

The pro-inflammatory cytokine interleukin-6 (IL-6) plays an important role in vascular inflammation. Coagulation factors such as the activated factor-X (FXa) may regulate local inflammatory responses of the vessel wall. In this study we investigated whether FXa regulates IL-6 expression and secretion in human vascular smooth muscle cells (SMC) as well as in failed thrombosed vein grafts. Also, we analysed its possible pro-thrombotic impact on monocytes.

IL-6 mRNA expression was determined in primary human saphenous vein SMC by Taqman® real-time PCR. Secretion to the cell culture media was measured by ELISA. Tissue Factor (TF) expression in monocytic THP-1 cells was determined by Western Blot. Immunostainings for IL-6 and the SMC marker smoothelin were performed on paraffin embedded tissue sections from failed thrombosed vein grafts and control veins.

Incubation of cultured human venous SMC with FXa (30 nM) induced a time-dependent (3 – 16 h) increase in IL-6 mRNA expression. Maximum expression was observed within 6 h to a 7.2±3.3 fold increase (mean±SD, n=5, p<0.05). Incubation with an inhibitor of p38 MAP kinase (SB203580, 10 µM) or PI3K (LY294002, 10 µM) significantly attenuated FXa-induced IL-6 mRNA expression (n=5). Inhibition of p42/44 MAPK, Rho kinase or NF-κB had no significant effect. Stimulation with FXa for 24h resulted in a markedly increased IL-6 secretion into the SMC culture media from 0.6±0.2 to 1.1±0.3 ng/ml (p<0.5, n=4). Stimulation of THP-1 cells with IL-6 (1 ng/ml) induced a time dependent (6 – 24 h) increase of up to 2.1±0.6 fold (p<0.05, n=5) in TF protein expression. Immunostainings of tissue sample of failed vein grafts revealed enhanced IL-6 expression in SMC-rich regions in vessel walls compared to non-thrombosed control veins suggesting an elevated IL-6 regulation in thrombosed vein grafts *in vivo*.

In conclusion, FXa induced IL-6 expression and secretion in venous SMC which may be regulated via p38 and PI3K signaling. IL-6 enhanced TF expression in THP-1 monocytes and was found in SMC-rich regions in failed thrombosed vein grafts. FXa-stimulated IL-6 release may be involved in regulating local pro-thrombotic processes during vascular inflammation and possibly vein graft failure.

151

Valproic acid attenuates structural atrial remodeling in CREM-IbΔC-X transgenic mice

B. Scholz¹, J. Stein¹, K. Himmler¹, M. D. Seidl¹, J. S. Schulte¹, S. Hamer¹, E. Wardelmann², E. Hammer³, U. Völker³, F. U. Müller¹

¹Westfälische-Wilhelms-Universität Münster, Institut für Pharmakologie und Toxikologie, Münster, Germany

²Universitätsklinikum Münster, Gerhard-Domagk-Institut für Pathologie, Münster, Germany

³Universitätsmedizin Greifswald, Interfakultäres Institut für Genetik und Funktionelle Genomforschung, Greifswald, Germany

Rationale: The transcription factors cAMP-response element binding protein (CREB) and cAMP-responsive element modulator (CREM) bind to cAMP response elements (CREs) and mediate a cAMP dependent gene regulation. Suppression of CRE mediated transcription is linked to atrial remodeling in genetic mouse models. Inhibition of CREB target genes is associated with atrial fibrillation (AF) susceptibility in patients. CREB and CREM affect histone acetylation recruiting the CREB-binding protein (CBP/p300). The histone acetyltransferase (HAT) activity of CBP facilitates gene transcription by loosening chromatin structure. Histone deacetylases (HDACs) catalyze the inverse reaction: histone deacetylation with consecutive gene silencing. Mice with heart directed expression of the human cardiac isoform CREM-IbΔC-X (TG) show atrial dilatation, morphological and physiological alterations in atria preceding spontaneous-onset AF. The HDAC inhibitor (HDACi) valproic acid (VPA) reduced atrial weight and AF incidence in TG mice. Here we tested the hypothesis, that VPA attenuates the structural remodeling in TG atria by reversing changes in atrial gene regulation due to the transgene.

Methods and Results: TG and WT mice were treated from week 5-16 with VPA (0.71% in drinking water, ad libitum) or vehicle (Veh). Atrial ultrastructure was studied by electron microscopy (EM) (week 7 and 16). Veh-treated TG atria showed a progressive dysorganization of sarcomeres (SM) with less mitochondria and more collagen fibers between cardiomyocytes as compared to Veh-treated WT atria. The fraction of SM structure in Veh-treated TG atria was significantly reduced as compared to Veh-treated WT atria (week 7: TG_{Veh}: 33±2%, WT_{Veh}: 47±1%; week 16: TG_{Veh}: 19±2%, WT_{Veh}: 44±1%, P<0.05). VPA led to a more organized ultrastructure and restored, at least partially, the degradation of the SM in the TG atria (TG VPA at week 7: 40±2%, TG VPA at week 16: 34±1%, P<0.05 vs. TG_{Veh}). The structure of WT atria was not affected by VPA. We further analyzed the protein abundance profiles in the groups of all animals (WT_{Veh}, WT VPA, TG_{Veh}, TG VPA) by using LC-MS/MS. Between Veh-treated genotypes (TG_{Veh} vs. WT_{Veh}, P<0.05) 998 proteins were significantly changed while 854 proteins were differentially abundant between VPA-treated groups (TG VPA vs. WT VPA, P<0.05). 109 proteins were regulated by VPA in WT atria (WT VPA vs. WT_{Veh}, P<0.05), whereas VPA affected 525 proteins in TG atria (TG VPA vs. TG_{Veh}, P<0.05), out of which 43 proteins were common. 295 prominent changed proteins between Veh-treated TG and WT atria were significantly regulated by VPA in TG atria in the opposite direction. A functional pathway analysis showed that pathways activated in TG atria such as cardiac fibrosis, mitochondrial dysfunction were inhibited by VPA treatment.

Conclusion: Similar to human AF, CREM-TG mice present atrial dilatation, ultrastructural changes and impaired conduction and spontaneous AF. While VPA had little to no effect in WT mice, valproate improved the TG phenotype by interfering with pathways involved in structural remodeling. This supports the idea that HDAC inhibition by VPA antagonizes effects of CREM expression in atria. (Supported by EUTRAF, FP7, and the DFG)

152

Functional studies on histamine metabolism in the mammalian heart

J. Grobe¹, U. Gergs¹, J. Neumann¹

¹Institute for Pharmacology and Toxicology, Medical Faculty, Martin Luther University Halle-Wittenberg, Halle (Saale), Germany

In isolated mouse cardiac preparations, histamine is ineffective regarding inotropic or chronotropic effects, presumably because of lack of receptor protein expression. On the other hand, histamine can exert positive inotropic and chronotropic effects in humans via cardiac histamine H₂-receptors. Hence, we have generated transgenic mice (TG) which overexpress the human H₂-receptor specifically in cardiomyocytes. In isolated left and right atrial preparations of these mice, we investigated the histamine metabolism on a functional level. Preparations of wild type mice (WT) served as control. Histamine induced positive inotropic effects (PIE) and positive chronotropic effects (PCE) in left and right atria of TG mice, respectively, but not in WT. Interestingly, the inhibitor of histamine oxidation, aminoguanidine (1 mM), shifted the concentration response curves for the PIE of histamine from EC₅₀ = 110 nM to 37 nM (p<0.05). Furthermore, the unspecific inhibitor of mono amine oxidase, tranylcypromine (10 µM), shifted the PIE of histamine from EC₅₀ = 70 nM to 38 nM and increased the efficacy of histamine for the PIE (p<0.05). These data indicate that exogenously applied histamine is subject to degradation in the mouse heart by two different pathways namely via diaminoxidase and mono amine oxidase. Drugs that inhibit these enzymes could conceivably alter cardiac function also in the human heart.

153

Overexpression of PP2Cβ leads to cardiac hypertrophy in mice and alters cardiac function

P. Bollmann¹, U. Gergs¹, P. Boknik², J. Neumann¹

¹Institute for Pharmacology and Toxicology, Medical Faculty, Martin Luther University Halle-Wittenberg, Halle (Saale), Germany

²Institute for Pharmacology and Toxicology, University Hospital, Münster, Germany

Protein phosphorylation by kinases and dephosphorylation by protein phosphatases has a crucial function in cell signal cascades. It has been shown that cardiomyocytes specific overexpression of serine /threonine protein phosphatases PP1, PP2A, PP2B

(Calcineurin) and PP5 in mice leads to cardiac hypertrophy and alters cardiac function. To examine the function of another important protein phosphatase in the heart we established a mouse model overexpressing protein phosphatase 2Cβ (PP2Cβ) under control of the α-myosin heavy chain promoter. Cardiac overexpression was demonstrated by Western blotting. Like other serine/threonine phosphatases, PP2Cβ can lead to cardiac hypertrophy. In transgenic mice (TG), relative ventricular weight was increased (4.24 ± 0.14 mg/g) compared to wild type (WT) littermates (3.78 ± 0.20 mg/g; p<0.05) whereas weights of right and left atria were unchanged. Therefore, relative heart weight was increased in TG (4.78 ± 0.17 mg/g) vs. WT (4.13 ± 0.22 mg/g; n=8-12; 10-11 months of age; p<0.05). Left ventricular function, measured in vivo by echocardiography under isoflurane anesthesia was diminished in TG compared to WT (ejection fraction: 58.33 ± 3.16 % (TG) versus 76.94 ± 0.92 % (WT); n=12-16; 8-11 months; p<0.05 and fractional shortening: 30.84 ± 2.02 % (TG) versus 44.94 ± 0.87 % (WT); n=12-16; 8-11 months; p<0.05). The left ventricle was dilated (systolic diameter: 2.78 ± 0.21 mm (TG) versus 1.84 ± 0.06 mm (WT); n=12-16; 8-11 months; p<0.05; diastolic diameter: 3.97 ± 0.19 mm (TG) versus 3.33 ± 0.07 mm (WT); n=12-16; 8-11 months; p<0.05). In contrast, atrial function measured as response to β-adrenergic stimulation in isolated left and right atrial preparations was unchanged in TG vs. WT. In summary, our results indicate that PP2Cβ overexpression can lead to ventricular dysfunction and hypertrophy. The underlying signal transduction pathways need to be elucidated.

154

The Insulin-like growth factor binding protein 5 (IGFBP5) – a potential developmental gene is regulated upon cardiac stress

M. Wölfer¹, C. Nöck¹, M. Tiburcy¹, S. Khadjeh², E. Chebbok¹, G. H. Hasenfuß², W.-H. Zimmermann¹, K. T. Toischer², L. C. Zelarayán¹

¹Universitätsmedizin Göttingen, Pharmakologie, Göttingen, Germany

²Universitätsmedizin Göttingen, Kardiologie, Göttingen, Germany

Background: Cardiac remodeling is a complex biological adaptation process of the failing heart accompanied by a re-activation of embryonic gene expression, which so far has unclear pathophysiological relevance. We and others showed that Insulin-like growth factor binding protein 5 (IGFBP5) is expressed in the early pre-cardiac region in mouse embryos and its up-regulation impairs cardiac progenitor differentiation. IGFBP5 functions as an extracellular growth factor binding protein for IGF and also has IGF-independent activities. The role of this factor in the context of cardiac remodeling is still unknown. The aim of this study was to investigate the relevance of IGFBP5 in cardiogenesis and cardiac remodeling and its role as a potential target for ameliorating stress-induced cardiac remodeling.

Methods and Results: We investigated the expression of *Igfbp5* in murine cardiac tissue at different developmental stages by qPCR normalized to *Tpt1* (Tumor Protein, Translationally-Controlled 1). This analysis showed temporal changes of cardiac *Igfbp5* expression from developing to postnatal hearts, where a high expression was detected in early heart stages, which decreased during cardiac development and became low in the postnatal heart. The analysis of *Igfbp5* expression in different heart cells showed a very low *Igfbp5* in adult cardiomyocytes in contrast to a high expression in undifferentiated Sca-1 positive cells. In a mouse model with cardiac specific Wnt/β-catenin activation, which led to cardiac dysfunction, *Igfbp5* was found up-regulated (p<0.05). Further we found an increased *Igfbp5* expression after pressure induced cardiac hypertrophy using mice with transverse aortic constriction (TAC) (p<0.01). In line with this data, an *in vitro* model of human heart muscle hypertrophy using engineered cardiac heart muscle (EHM) showed an up-regulation of *IGFBP5* upon adrenergic activation via norepinephrine stimulation accompanied by a functional deterioration in comparison to untreated controls (p<0.05). All these findings were further supported by RNA-sequencing analysis from human aortic stenosis patient samples, where *IGFBP5* expression was found increased in patients with compensatory hypertrophy and in a higher extent in patients with heart failure in comparison to non-failing heart samples. Interestingly, the expression of *Igfbp5* in angiotensin 2 or norepinephrine stimulated neonatal murine cardiomyocytes, as well as in hearts of mice treated with angiotensin 2, showed the opposite results, namely a reduction in its expression (p<0.01; p<0.05, respectively).

Summary and Conclusion: Our results show active *Igfbp5* transcription in the early developing heart but a low expression in the postnatal heart. A re-activation of expression was found in the process of pathological heart remodeling in mouse and human, *in vivo* as well as *in vitro*, indicate the participation of IGFBP5 in a conserved manner. We hypothesize that IGFBP5 may participate in the developmental gene program becoming activated in the diseased adult heart again. The functional role and regulation of IGFBP5 is under investigation.

155

Crataegus extract WS® 1442 improves vascular function in diet-induced obese mice

N. Xia¹, E. Schramm², E. Koch², M. Burkart², G. Reifenberg¹, U. Förstermann¹, H. Li¹

¹Universitätsmedizin Mainz, Institut für Pharmakologie, Mainz, Germany

²Dr. Willmar Schwabe GmbH & Co. KG, Karlsruhe, Germany

We have recently shown that perivascular adipose tissue (PVAT) plays a crucial role in obesity-induced vascular dysfunction. In PVAT-free aortas isolated from male C57BL/6J mice fed a high-fat diet (HFD) for 22 weeks, the endothelium-dependent nitric oxide (NO)-mediated vasodilator response to acetylcholine remained normal. In contrast, a clear reduction in the vasodilator response to acetylcholine was observed in aortas from obese mice when PVAT was left in place. These results suggest that the reason for vascular dysfunction in diet-induced obese mice is a PVAT dysfunction rather than an endothelial dysfunction. Treatment of HFD mice during the last 4 weeks with Crataegus extract WS® 1442 (150 mg/kg/day) completely normalized vascular function in PVAT-containing aorta. The expression of endothelial NO synthase (eNOS) was not changed by WS® 1442, neither in PVAT nor in aorta. Phosphorylation at Serine 1177 is the most important positive modulation of eNOS activity. HFD-induced obesity was associated with a reduction in eNOS phosphorylation at serine 1177 in PVAT, but not in aorta. WS® 1442 treatment significantly improved eNOS serine 1177 phosphorylation selectively in PVAT but had no effect in aorta. A major upstream kinase for eNOS serine 1177

phosphorylation is Akt. The activity of this kinase is inhibited in the PVAT of HFD mice, which was largely reversed by WS® 1442 treatment. In addition, WS® 1442 treatment enhanced the mRNA expression of the NAD-dependent deacetylase sirtuin-1 (SIRT1), known also as a longevity gene. The activity of SIRT1 depends, among others, on the intracellular content of its cofactor NAD. WS® 1442 treatment led to an upregulation of nicotinamide phosphoribosyltransferase (Namt), a rate-limiting enzyme in the salvage pathway of NAD biosynthesis. One of the non-histone substrates of SIRT1 is eNOS. Deacetylation of eNOS at lysine residues 497 and 507 by SIRT1 enhances the activity of the eNOS enzyme. Currently, we are studying the effect of WS® 1442 on NAD synthesis, SIRT1 activity, and eNOS (de)acetylation. In conclusion, Crataegus extract WS® 1442 reverses obesity-induced vascular dysfunction by improving PVAT function. The molecular mechanisms may involve eNOS phosphorylation at serine 1177 and upregulation of SIRT1.

156

Myocardium-specific expression of the human raf kinase inhibitor protein (RKIP) induces cardiac hypertrophy, ECG abnormalities and signs of heart failure

S. Wolf¹, M. Graemer¹, A. Langer¹, U. Quittner¹
¹ETH Zurich, Molekulare Pharmakologie, Zurich, Switzerland

The raf kinase inhibitor protein (RKIP) inhibits G-protein-coupled receptor kinase (GRK2) and the RAF-ERK1/2 pathway. These two functions of RKIP could counteract each other. While GRK2 inhibition is cardio-protective, inhibition of the pro-survival ERK1/2 axis promotes signs of heart failure in patients and experimental models. In view of this ambivalent nature, the function of RKIP in vivo is not clear. Furthermore, RKIP could have a pathophysiological role because heart specimens from patients with heart failure showed RKIP up-regulation (ref. 1). To investigate the impact of cardiac RKIP up-regulation in vivo, we generated transgenic mice with myocardium-specific expression of the human RKIP gene (*PEBP1*) under control of the alpha-MHC promoter. Two different RKIP-transgenic lines with 2.7-fold and 3.4-fold increased cardiac RKIP protein level were generated (ref. 2, and JAX ID number 911819). We investigated the cardiac phenotype and found that Tg-RKIP mice developed cardiac hypertrophy with a significantly increased heart weight to body weight ratio and a decreased left ventricular ejection fraction relative to non-transgenic FVB controls, as early as 10 weeks of age. Histology analysis revealed progressive atrial and ventricular enlargement of Tg-RKIP hearts. ECG abnormalities, a lower maximum rate of left ventricular pressure rise, and a strongly decreased left ventricular ejection fraction of $32.9 \pm 2.3\%$ ($n=6$; \pm s.d.) were documented at an age of 8 months. Down-regulation of the transgenic RKIP by lentiviral transduction of an RKIP-targeting miRNA retarded the cardiac phenotype of Tg-RKIP mice. Thus, dual-specific inhibition of the GRK2 and RAF-ERK1/2 axis by the human RKIP gene (*PEBP1*) triggers signs of heart failure in vivo, and the documented up-regulation of the cardiac RKIP in heart failure patients could aggravate disease pathogenesis. These findings are in contrast to rodent RKIP (*Pebp1*), which does not seem to inhibit the Raf-ERK1/2 axis in vivo but instead confers GRK2 inhibition-mediated cardioprotection (ref. 1).

References:

- Schmid E. et al. Cardiac RKIP induces a beneficial beta-adrenoceptor-dependent positive inotropy. *Nat. Med.* 21, 1298-1306, 2015.
- Fu X. et al. Inhibition of G-protein-coupled receptor kinase 2 (GRK2) triggers the growth-promoting mitogen-activated protein kinase (MAPK) pathway. *J. Biol. Chem.* 288, 7738-7755, 2013.

157

Analysis of AT1R–B2R heterodimerization in transgenic models with and without deficiency of the B2R gene

A. Langer¹, S. AbdAlia¹, U. Quittner¹
¹ETH Zurich, Molekulare Pharmakologie, Zurich, Switzerland

Heterodimerization between the AT1 receptor (AT1R) for the vasopressor peptide, angiotensin II, and the B2 receptor (B2R) for the vasodepressor peptide, bradykinin, enhances angiotensin II-stimulated signalling in cells. In addition, AT1R–B2R heterodimerization has a major pathophysiological role and contributes to the angiotensin II hypersensitivity in women with preeclampsia hypertension. To analyse the vascular function of the AT1R–B2R heterodimer in vivo, we generated a transgenic model of AT1R–B2R heterodimerization (Tg-B2R+) by transgenic expression of the B2R gene (*BDKRB2*) in the B2R-deficient Tg-B2R-/- strain. Fluorescence resonance energy transfer (FRET) imaging was applied to analyse the interaction between different G-protein-coupled receptors in the aorta of transgenic mice. We report here that FRET imaging detected the close interaction between the aortic AT1R and B2R at a distance of less than 9 nm in Tg-B2R+ mice whereas the AT1R–B2R heterodimer was absent in Tg-B2R-/- mice. In contrast, FRET was not detectable between the endothelin ETA receptor (ETAR) and the B2R in the aorta of Tg-B2R+ mice, although immunofluorescence and immunohistology confirmed the aortic (co-)localization of both, ETAR and B2R. The efficient AT1R–B2R heterodimerization in Tg-B2R+ mice was accompanied by an enhanced angiotensin II AT1R-stimulated vasopressor response relative to that of Tg-B2R-/- mice, which lack the AT1R–B2R heterodimer. As a control, the endothelin-1-stimulated vasopressor response mediated by the ETAR, which did not dimerize with B2R, was not significantly different between Tg-B2R+ and Tg-B2R-/- mice. Together these findings provide strong evidence that AT1R–B2R heterodimerization occurs in vivo and enhances the angiotensin II AT1R-stimulated vasopressor response.

158

Inhibition of GRK2 counteracts the dysfunctional cardiac substrate metabolism of late-stage heart failure

J. Abd Alla¹, M. Graemer¹, S. Wolf¹, U. Quittner¹
¹ETH Zurich, Molekulare Pharmakologie, Zurich, Switzerland

Dysfunction of the cardiac energy substrate metabolism is a characteristic feature of late-stage heart failure. The dysfunctional cardiac substrate metabolism contributes to insufficient energy generation and has limited treatment options. In search for a treatment approach, we investigated whether inhibition of G-protein-coupled receptor kinase 2 (GRK2) could confer cardioprotection by targeting the dysfunctional cardiac substrate use. The impaired substrate metabolism of late-stage heart failure was reproduced in a transgenic model with myocardium-specific expression of fatty acid synthase (*FASN*), which is the major palmitate-synthesizing enzyme. Experiments with a Seahorse XF24 Extracellular Flux Analyzer revealed that in an adult-like lipogenic milieu, *FASN*-transgenic cardiomyocytes reproduced the overall depressed substrate use of late-stage heart failure with a switch from fatty acid to predominant glucose utilization. The impaired substrate use was largely retarded by co-expression of a small peptide inhibitor of GRK2, GRKInh. The GRKInh-mediated protection against cardiometabolic remodelling required an intact RAF-ERK1/2 axis and involved the ERK1/2-dependent inactivation of the heart failure-promoting peroxisome proliferator-activated receptor gamma (*Pparg*) by phosphorylation of serine-273. As a consequence of ERK-dependent phosphorylation of *Pparg* on serine-273, the expression of heart failure-related *Pparg* targets such as fatty acid synthase, resistin and adiponectin was decreased. The importance of *Pparg* serine-273 phosphorylation was further shown in transgenic mice with myocardium-specific expression of the phosphorylation-deficient *PPARG* serine-273A mutant, which was resistant to the cardioprotective activity of GRKInh. Taken together our experiments show that GRK2 inhibition could target cardiometabolic remodelling by inhibition of the heart failure-promoting transcription factor *Pparg*.

159

The effect of sodium valproate on the action potential of atrial myocytes of CREM I Δ C-X transgenic mice

F. Pluteanu¹, B. Scholz¹, J. S. Schulte¹, F. U. Müller¹
¹Westfälische Wilhelms-Universität Münster, Inst. für Pharmakologie und Toxikologie, Münster, Germany

Introduction: In mouse, cardiomyocyte directed over-expression of transcription factor CREM (cAMP response element modulator) causes an atrial phenotype characterized by hypertrophy, reduced contractility and increased duration of the monophasic action potential (MAP). Moreover, this animal model (CREM I Δ C-X) showed spontaneous atrial fibrillation (AF) episodes as early as 5 weeks of age in homozygous mice and 10-12 weeks of age in heterozygous mice (phenotype delayed towards adult stage). Previous studies in heterozygous mice targeted HDAC2 inhibition by sodium valproate (VPA, an anticonvulsant drug, acting also as inhibitor of HDAC class I-II). VPA treatment affected significantly the development of atrial hypertrophy and the incidence of AF episodes, without affecting cellular hypertrophy. Our aim was to investigate the effect of chronic VPA treatment on the electrical activity of atrial myocytes isolated from CREM I Δ C-X and wild type (WT) littermate mice.

Methods and Results: Atrial myocytes were isolated from 12 weeks old wild type mice (WT) and heterozygous CREM I Δ C-X transgenic mice with enlarged atria (TG), treated for 7 weeks with VPA (0.4 mM in the drinking water) vs. water (vehicle control). Action potentials (AP) were measured at room temperature using the patch-clamp technique. Atrial myocytes of water treated TG mice had the AP amplitude significantly reduced by 7 mV compared to water treated WT, and, in line with previous results for the MAP, the TG cells depolarized with a slower slope of 90.2 ± 8 V/s (TG: $n=33$ cells) vs. 109.8 ± 5.1 V/s (WT: $n=30$, $p=0.05$). Moreover, AP of atrial myocytes isolated from water treated TG mice had longer duration (APD) at 50% (TG: 11.6 ± 1.4 ms, $n=35$ vs. WT: 6.9 ± 0.5 ms, $n=30$, $p<0.01$), at 70% (in ms: 21.2 ± 2.5 vs. 13.6 ± 1 , $p<0.05$) and at 90% (in ms: 46.8 ± 4.5 vs. 34 ± 2.5 , $p<0.05$) repolarization. VPA treatment reduced AP amplitude in WT mice by 6 mV ($n=22$, $p<0.05$) vs. water treated WT, without altering the slope of depolarization or the APD. In VPA treated TG mice the APD was reduced (50%: 7.3 ± 0.8 ms, 70%: 13.8 ± 1.5 ms, 90%: 30.9 ± 3.2 ms, $n=21$, $p<0.05$ vs. untreated TG), the amplitude was increased by 5 mV (n.s.) and the slope of depolarization was increased by 21% ($p=0.16$, n.s.). Membrane capacitance evaluation, as an estimation of atrial myocyte size, showed that in untreated TG mice the cells were larger than in WT (TG: 104 ± 7.2 pF, $n=27$ vs. WT: 55 ± 5.4 pF, $n=30$, $p<0.001$), in line with the occurrence of cellular hypertrophy in TG atria. Chronic VPA treatment did not change the cell size in either genotype (WT-VPA: 64.8 ± 7 pF, $n=17$ n.s. vs. WT; TG-VPA: 88 ± 7 pF, $n=14$, $p<0.05$ vs. WT-VPA; $p<0.01$ vs. WT; n.s. vs. TG).

Conclusions: In hypertrophied atrial myocytes of CREM-I Δ C-X, AP were characterized by smaller amplitude, slower onset of depolarization and increased duration compared to WT cells. Despite having no effect on atrial myocytes size, VPA treatment reduced the duration and showed a tendency to increase the amplitude and the slope of depolarization of the action potential in TG mice to values similar to WT. These data suggest that chronic treatment with VPA restored partially the electrical activity of atrial myocytes and may reverse the electrical remodeling via HDAC2 inhibition. (Supported by the DFG)

160

Arrhythmogenic ventricular remodeling by CREM-I Δ C-X in mice – involvement of miRNAs

J. S. Schulte¹, E. Fehrmann¹, M. A. Tekook¹, A. Heinick¹, B. Fels¹, D. Kranick¹, M. D. Seidl¹, F. U. Müller¹
¹Institut für Pharmakologie und Toxikologie, Universität Münster, Münster, Germany

Chronic β -adrenergic stimulation is regarded as a pivotal step in the progression of heart failure which is associated with a high risk for arrhythmia. The small repressor isoforms

of the transcription factor CREM (cAMP response modulator) ICER, smICER and CREM-IbΔC-X are inducible by β-adrenergic stimulation and code for similar or even identical proteins. Thus, these isoforms are able to repress expression of respective target genes in response to cAMP and might play a role in an arrhythmogenic remodeling during the development of chronic heart diseases. Here we test this hypothesis in a mouse model with transgenic expression of CREM-IbΔC-X (TG). These mice develop not only spontaneous onset atrial fibrillation but likewise arrhythmogenic alterations in the ventricle.

Patch clamp experiments revealed an increased $\text{Na}^+/\text{Ca}^{2+}$ exchanger current (I_{NCX}) and decreased transient outward current (I_{to}) in TG ventricular cardiomyocytes (VCMs) vs. wild-type controls (CTL). These alterations were associated with an increased arrhythmogenicity in TG VCMs. Action potentials were prolonged in TG VCMs vs. CTLs leading to an increased proportion of VCMs displaying early afterdepolarizations. Ca^{2+} imaging revealed that the transduction rate of spontaneous sub-threshold Ca^{2+} -waves into supra-threshold transient-like Ca^{2+} -events which is mediated by the NCX was increased in TG VCMs. At the same time the SERCA mediated Ca^{2+} transport rate (r_{SERCA}) was enhanced in TG VCMs potentially limiting Ca^{2+} extrusion by the NCX. Underlining the in-vivo relevance of our findings ventricular extrasystoles (VES) were augmented in ECGs of TG mice (VES/mouse during 10^5 M isoproterenol challenge, TG: 3.65*, CTL: 0.4; n=20/condition). The increase in I_{NCX} and r_{SERCA} and the decrease in I_{to} went along with an increase of NCX1, SERCA2a and decrease of KChIP2 protein levels. However, the respective mRNA levels (Slc8a1, Atp2a2 and Kcnip2) were unaltered between groups pointing to a post-transcriptional regulation of these genes. In a mRNA-sequencing approach we identified the downregulation of precursor miRNAs inter alia for Mir-369 (Fold change in TG: 0.04*) and Mir-1 (Fold change in TG: 0.13*) (n=10/condition). Atp2a2 is a predicted target of Mir-369 and Mir-1 has recently been shown to regulate NCX1 and I_{to} -related potassium channel subunits. (*p<0.05 vs. CTL). Our results demonstrate that transgenic expression of CREM-IbΔC-X in mouse VCMs leads to distinct arrhythmogenic alterations. They further indicate that the repression of micro RNAs by short CREM repressor isoforms may lead to the upregulation of genes in the context of an arrhythmogenic remodeling. Since CREM-repressors are inducible by chronic β-adrenergic stimulation our results suggest that the inhibition of CRE-dependent transcription contributes to the formation of an arrhythmogenic substrate in chronic heart disease. (Supported by the DFG)

161

The role of protein kinase A (PKA) in left ventricular hypertrophy

S. Jaekel¹, A. Ludwig¹, S. Herrmann¹

¹Institut für Experimentelle und Klinische Pharmakologie und Toxikologie, Pharmakologie, Erlangen, Germany

Chronic overstimulation of cardiac β-adrenergic receptors (β-AR) is a major trigger for the development and maintenance of cardiac hypertrophy and heart failure. Although the cAMP activated protein kinase A (PKA) is known as a prominent downstream effector of β-AR signaling, its functional contribution to pathological cardiac remodeling is neither well understood nor directly studied so far. To address this issue we used mice carrying a point mutation in the regulatory PKA subunit R1a (PKAR1aB), which prevents binding of cAMP and consequently diminished kinase activity. This dominant negative mutation was controlled by a tamoxifen (tam) inducible αMHC promoter driven Cre transgene which allows a selective expression in the ventricular myocardium. The inducible and tissue specific gene expression was analyzed and confirmed by PCR, RT-PCR and immunohistochemistry. Furthermore diminished phosphorylation of several PKA targets verifies impaired PKA activity in tam treated double transgenic animals. Hypertrophic response in ventricular PKA mutants was studied in genetic, pharmacological and surgical mouse models of heart disease as well. Genetically induced heart failure was observed following tam treatment in mice expressing an inducible myocardial-specific Cre transgene. This deleterious cardiac phenotype develops independently of the presence of the floxed transgene. 8 days after tam treatment, controls displayed elevated heart weight to bodyweight ratio (HBR) and heart weight to tibia length (HTR). HBR shifted from 6.2(mg/g) in untreated control animals to 10.9(mg/g) in tam injected mice. In contrast PKA inhibited mutants displayed a minor increased HBR of 7.7 (mg/g). For the pharmacological induction of cardiac hypertrophy we implanted osmotic mini pumps, delivering a combination of isoproterenol and phenylephrine. Control animals showed a significantly increased HBR (8.4 mg/g) compared to saline treated animals (6.8mg/g) and PKA mutants (7.1 mg/g). Paradoxically, all PKA inhibited animals displayed a consistent elevation in important hypertrophic markers like ANP. Surgical constriction of the aortic arch (transverse aortic constriction TAC) led to a pressure induced hypertrophic response (HBR: 6.5 vs 7.9 mg/g) followed by a pronounced elevation in several hypertrophic factors such as ANP, Myh6/7 ratio and myocytes size. In contrast PKA mutants displayed an irregular progression of cardiac hypertrophy presented by two groups with either an unchanged (6.9 mg/g) or a strongly elevated HBR (13.5 mg/g). However, additional hypertrophic factors including ANP, Myh6/7 ratio and myocyte size were significantly increased in both groups. To our knowledge this is the first report, which directly studies the role of ventricular PKA activity in cardiac hypertrophy in a genetically altered mouse model. Our results suggest that in an early stage of cardiac remodeling PKA inhibition alleviates cardiac weight gain but provokes a detrimental shift during further progression, which implicates a protective role of ventricular PKA activity in cardiac disease.

162

The acetyl-CoA carboxylase (ACC) inhibitor soraphen A blocks the proliferation and migration of primary endothelial cells

D. Glatzel¹, A. Koeberle², O. Wertz², R. Müller³

¹Institute of Pharmaceutical Biology, Biocenter, Goethe-University, Max-von-Laue-Str. 9, 60438 Frankfurt am Main, Germany, Germany

²Chair of Pharmaceutical/Medicinal Chemistry, Institute of Pharmacy, University Jena, Philosophenweg 14, 07743 Jena, Germany, Germany

³Department of Microbial Natural Products, Helmholtz-Institute for Pharmaceutical

Research Saarland (HIPS), Helmholtz Centre for Infection Research (HZI), Saarland University, Campus Building C2.3, 66123 Saarbrücken, Germany, Germany

Acetyl-CoA carboxylase catalyzes the first step in the biosynthesis of fatty acids in bacterial and eukaryotic cells, i.e. the conversion (carboxylation) of acetyl-CoA into malonyl-CoA. ACC-generated malonyl-CoA functions as a substrate for de novo lipogenesis and acts as an inhibitor of mitochondrial β-oxidation of fatty acids. Because of its role in lipid metabolism this enzyme has become an interesting target in drug discovery in the field of metabolic diseases and cancer. Despite this interest in ACC, no attention has as yet been given to the role of ACC in endothelial cells.

We aimed to investigate the role of ACC in two functional key aspects of angiogenesis: endothelial cell proliferation and migration. We used the ACC inhibitor soraphen A, a polyketidic natural compound isolated from the myxobacterium *Sorangium cellulosum*, as well as an RNAi-based approach to inhibit the function of ACC. Primary human umbilical vein endothelial cells (HUVECs) were used as in vitro model. First, we analyzed the action of soraphen A on cell viability. The compound did neither lower the metabolic activity of HUVECs up to a concentration of 100 μM after 24 and 48 h (CTB assay) nor increase in the apoptosis rate after 24, 48, or 72 h up to 100 μM. Measuring adenosine triphosphate (ATP) levels revealed that 30 μM soraphen A does not alter the ATP levels in HUVECs after 24 h treatment. In contrast, a 48 h treatment significantly lowered the ATP levels by 12 %. Also gene silencing of ACC1 in HUVECs attenuated the ATP levels by 11 %. Mitochondrial membrane potential (MMP) assays showed decreased MMP levels (10 %) in soraphen A-treated cells after 24 h. Interestingly, the compound inhibited the proliferation of endothelial cells with an IC₅₀ value of 34 μM. Cell cycle analysis showed that soraphen A decreases the amount of cells in the G₀/G₁ phase by 26 % and increases the number of cells in the G₂/M phase by 50 %. The compound also inhibited the activation of Akt (Western blot analysis). In a wound healing/scratch assay, 30 μM soraphen A lowered the migration of endothelial cells by 65 %. Gene silencing of ACC1 in HUVECs strongly decreased endothelial migration, whereas a knockdown of ACC2 had no influence. Furthermore, Boyden chamber assays revealed that soraphen A can also lower chemotactic migration by 34 %. Since actin rearrangement is necessary for migratory processes, we analyzed the F-actin cytoskeleton (microscopy) and found that soraphen A decreases the number of filopodia by 60 % but did not influence stress fiber formation. Surprisingly, soraphen A-treated cells did not exhibit significant alterations in their capacity to form tube-like structures on Matrigel. In summary, we could gather first hints that inhibiting ACC has an immense impact on the proliferation and migration of primary endothelial cells. The mechanistic basis of this phenomenon will be investigated in future studies by analyzing the lipid profile and the transcriptome of endothelial cells.

Acknowledgement: This work was supported by the German Research Foundation (DFG, FOR 1406, FU 691/9-2).

163

Statin intolerance – a question of definition

E. Abdel-Hady Algharably^{1,2}, K. Grabowski¹, R. Kreutz¹, I. Filler¹

¹Charité – Universitätsmedizin Berlin, Institut für Klinische Pharmakologie und Toxikologie, Berlin, Germany

²Ain Shams University, Department of Clinical Pharmacy, Cairo, Germany

Introduction: Statins are among the best examined drugs with excellent efficacy and safety profiles. Lowered low-density lipoprotein (LDL) cholesterol goals, new indications for treatment and new knowledge about their pleiotropic effect have promoted a considerable increase in statin use. But as statin use becomes more widespread, awareness of their adverse effects as well as the recognition of statin intolerance problems increase. Statin intolerance is a significant problem in the treatment of dyslipidemia, understood as the inability to tolerate a dose of statin required to reduce individual cardiovascular risk sufficiently and could result from different statin-related side effects. Muscle-related adverse events, elevation of liver enzymes, cognitive problems and new onset diabetes mellitus have all been described, especially at higher doses. Although muscle symptoms are the common side effects observed, excluding other adverse events might underestimate the number of patients with true statin intolerance. These patients represent a target population for the newest lipid lowering drug category i.e. the proprotein convertase subtilisin/kexin type 9 (PCSK9) inhibitors. This work aimed to give an overview of published definitions derived from clinical studies, associations as well as major drug regulatory agencies. We discussed overlaps, differences and limitations in the current definitions.

Methods: Literature based search included PubMed and UpToDate publications in English and German language until October 2015. We performed hand searches of the references retrieved and performed an overview.

Results: A definition of statin intolerance of the European Medicines Agency (EMA) or the US Food and Drug Administration (FDA) is not available. In clinical studies, different definitions are chosen and the results are not comparable. Also different associations, such as the American Heart Association (AHA), the European Atherosclerosis Society (EAS), the Canadian Working Group or the National Lipid Association (NLA) are not able to agree on one common definition. Statin intolerance definitions included different types of muscle symptoms, integration of CK levels and minimal requirements of statin doses. There are currently no validated questionnaires or specific laboratory parameters available. In addition, the term 'myopathy' is often considered as a synonym to statin intolerance. Overall, only a few major studies have been conducted with statin intolerant patients so far using inconsistent definitions.

Discussion and Conclusion: There is an unmet need to find a robust and clear definition of statin intolerance as overemphasizing it might hinder appropriate clinical use of this important drug class. Thus, further work is required to develop a consensus definition on statin intolerance or a more focused definition regarding statin-associated muscle symptoms only. Subsequently, these definitions could be implemented in patient care and their relevance being analyzed and tested in future studies.

164

Characterization of Basic Leucine Zipper and W2 Domain Containing Protein 2 (BZW2), a novel Wnt component

E. Schoger¹, E. Chebbok¹, C. Noack¹, M.-P. Zafiriou¹, A. Renger¹, K. Toischer², G. Hasenfuß², L. C. Zelarayán¹

¹Institut für Pharmakologie, Universitätsmedizin Göttingen, Göttingen, Germany

²Institut für Kardiologie und Pneumologie, Universitätsmedizin Göttingen, Göttingen, Germany

Background: Development of cardiac hypertrophy is characterized by reactivation of genes involved in cardiac development. Wnt/β-catenin signaling is essential for embryonic cardiac development and is known to be dysregulated in pathological heart remodeling. Our previous work suggested a cardiac specific protein complex regulating Wnt/β-catenin/TCF transcription in the adult heart. We aim to identify and to characterize this complex in order to find potentially interesting targets for pharmacological therapy preventing maladaptive cardiac remodeling and the onset of heart failure.

Results: We previously demonstrated that the Krüppel-like-factor 15 (KLF15) is a β-catenin interaction partner and a cardiac specific nuclear inhibitor of the Wnt/β-catenin-dependent transcription. Because KLF15 and β-catenin are ubiquitously expressed, we suggest the existence of cardiac specific co-factors responsible for cardiac specificity in this complex. We identified the Basic leucine zipper and W2 domain containing protein 2 (BZW2), a phylogenetically conserved protein, as a β-catenin and KLF15 interaction partner using yeast-two-hybrid screen. In vitro overexpression experiments and co-immunoprecipitation validated these interactions, which were also confirmed by mass spectrometry. In the developing mouse embryo BZW2 mRNA expression is detectable in the heart, neuronal tissue, somites, limbs and branchial arches as shown by whole mount in situ hybridization. In the adulthood expression of BZW2 is confined to the heart, predominantly in cardiomyocytes and in cardiac progenitor cells compared to cardiac fibroblasts (*p<0.05, CM n=4, cFB n=4, CPC n=2), and skeletal muscle. BZW2 was localized in both the cytosol and in the nucleus. Mutation analysis showed the importance of the N-terminus of BZW2, containing a putative bZip DNA interaction domain, for the nuclear placement of the protein.

BZW2 protein expression was significantly increased under cardiac Wnt/β-catenin signaling activation in vivo in two mouse models (KLF15 knockout (KO) mice **p<0.01 n=3, and in a cardiac specific β-catenin stabilized mouse model, **p<0.01 n=6). A mouse model with constitutively BZW2 loss of function (BZW2 KO) showed cardiac specific upregulation of β-catenin on RNA level (***p<0.001, p<0.05, ctrl n=4, BZW2 KO n=5) and on protein level (**p<0.05, ctrl n=7, BZW2 KO n=9). Echocardiography analysis in eight-weeks-old BZW2 KO mice showed increased left ventricle wall thickness indicating a hypertrophic phenotype at baseline. We also observed increased levels of BZW2 expression in Angiotensin II treated mice as a model for cardiac hypertrophy (*p<0.05 ctrl n=4, AngII n=3) as well as in human samples derived from patients with dilated cardiomyopathy and ischemic cardiomyopathy (*p<0.05 ctrl n=3, DCM n=11, ICM n=10).

Conclusion: These data demonstrated that BZW2 is associated with components of the canonical Wnt cascade and suggest its relevance in the constitutive regulation of the Wnt/β-catenin components specific in the heart. This study further contribute to the elucidation of the tuning of the Wnt-off/on states aiming to establish a proof-of-concept model for Wnt-modulation as a therapeutic strategy in hypertrophic-induced heart failure.

165

Characterization of cholesterol homeostasis in sphingosine-1-phosphate lyase-deficient fibroblasts

H. Vienken¹, A. Rudowski¹, N. Mabrouki¹, A. Koch¹, J. Pfeilschifter¹, D. Meyer zu Heringdorf¹

¹Universitätsklinikum Frankfurt, Institut für Allgemeine Pharmakologie, Frankfurt am Main, Germany

Objective: Sphingosine-1-phosphate (S1P) is involved in the regulation of cell growth, survival, migration and adhesion. It is formed by sphingosine kinases and degraded by phosphatases and S1P lyase [1]. Mice that lack S1P lyase are characterized by the accumulation of S1P and sphingosine in their cells and tissues, and by lymphopenia, generalized inflammation, multiple organ damage, and a strongly reduced life span [2-4]. On the other hand, embryonic fibroblasts from S1P lyase-deficient mice (*Sgpl1*^{-/-}-MEFs) are resistant to chemotherapy-induced apoptosis [5], in part due to an upregulation of multidrug transporters of the ATP-binding cassette (ABC) transporter family [6]. Interestingly, S1P lyase-deficient mice have elevated plasma levels of cholesterol and triglycerides, while suffering from strongly reduced body fat [7]. The aim of the present study was to analyze the link between S1P lyase deficiency and altered cholesterol homeostasis using *Sgpl1*^{-/-}-MEFs.

Results and Conclusions: In *Sgpl1*^{-/-}-MEFs, total cholesterol content measured with Amplex Red was not altered when the cells were kept in serum-free medium, but was elevated when the cells were grown in the presence of 10 % FCS. Furthermore, the uptake of [³H]cholesterol into *Sgpl1*^{-/-}-MEFs was enhanced in the presence of 10 % FCS, but not significantly altered in the presence of 1 % serum albumin. In agreement, the low-density lipoprotein (LDL) receptor was upregulated in *Sgpl1*^{-/-}-MEFs. The release of [³H]cholesterol was not altered, although the transporter involved in reverse cholesterol transport, ABCA1, was upregulated on the mRNA and protein level. The expression of both the LDL receptor and ABCA1 is regulated by the transcription factor, sterol regulatory element-binding protein (SREBP)-2. In agreement, we observed an enhanced proteolytic activation of SREBP-2 in *Sgpl1*^{-/-}-MEFs. On the other hand, the protein expression of HMG-CoA reductase was decreased *Sgpl1*^{-/-}-MEFs. Finally, staining of cellular cholesterol with filipin and confocal laser scanning microscopy revealed a disturbed subcellular distribution of cholesterol in *Sgpl1*^{-/-}-MEFs. It is concluded that both the decreased expression of HMG-CoA reductase and the disturbed intracellular distribution of cholesterol lead to activation of SREBP-2, which in turn by induction of the LDL receptor leads to increased cholesterol uptake in *Sgpl1*^{-/-}-MEFs.

References: [1] Kunkel et al. Nat Rev Drug Discov (2013); [2] Schmahl et al. Nat Genet (2007); [3] Vogel et al. PLoS One (2009); [4] Allende et al. J Biol Chem (2011); [5] Colié et al. Cancer Res (2009); [6] Ihlefeld et al. J Lipid Res (2015); [7] Bektas et al. J Biol Chem (2010).

166

RNA polymerase II dynamics in cardiomyocytes in development and disease

C. Rommel¹, R. Gilsbach¹, T. Schnick^{1,2}, L. Hein¹

¹Universität Freiburg, Institut für Experimentelle und Klinische Pharmakologie und Toxikologie, Freiburg, Germany

²Universität Freiburg, Universitäts-Herzzentrum, Freiburg, Germany

Background: Cardiac gene expression changes during cardiac development and under pathophysiological conditions. These alterations in gene expression are regulated by several processes and the exact regulation of gene expression is essential for the proper development and function of the heart. Crucial steps in transcription regulation are RNA polymerase II (Pol II) recruitment and changes in Pol II activity. Pol II activity is tightly linked with phosphorylation at serine-2 (P-Ser2) of the carboxyterminal domain of Pol II. Thus, the aim of the present study was to identify cardiomyocyte-specific genome-wide Pol II and P-Ser2-Pol II enrichments to get insight into Pol II activity and recruitment in development and disease.

Methods and results: To get insight into RNA polymerase II dynamics, genome-wide maps of RNA polymerase II occupancy were generated by chromatin-immunoprecipitation in cardiomyocyte nuclei purified from normal neonatal and adult mouse hearts. In addition, cardiomyocyte nuclei were obtained from adult hearts after 4 weeks of pressure overload induced by transverse aortic constriction (TAC). Cardiomyocyte nuclei were isolated by magnetic beads with an anti-PCM1 antibody. Nuclei were used for Pol II chromatin-immunoprecipitation followed by deep sequencing (ChIP-seq). To test if Pol II marks correlate with nuclear mRNA expression in cardiomyocyte nuclei all coding genes were ranked according to their expression level. Genes expressed in cardiomyocyte nuclei (> 0.062 FPKM, gene expression rank < 12,653) showed high Pol II enrichment at promoters as well as in genomic regions. Many of the gene promoters showed high levels of Pol II accumulation at the transcription start site, as compared to genic regions, which have been associated with Pol II pausing. In contrast, P-Ser2-Pol II showed enrichment downstream of the transcription start site. The genomic region of troponin I type 1 (*Tnni1*) which is expressed in cardiac muscle only during development but not in adult cardiomyocytes, was enriched for Pol II in neonatal cardiomyocytes. At the *Tnni1* gene, Pol II was absent in adult or pressure-overloaded cardiomyocytes. In contrast, Pol II enrichment at the alpha actin 1 (*Acta1*) locus was only present in pressure-overloaded cardiomyocytes. These data are consistent with cellular RNA-seq data showing an induction of *Acta1* after TAC. Furthermore no Pol II enrichment could be detected in the genomic region of biglycan (*Bgn*), a matrix proteoglycan that is not expressed in cardiomyocytes. This confirms a high purity of cardiomyocyte chromatin.

Conclusions: This study provides, for the first time, cardiomyocyte-specific landscapes of RNA polymerase II occupancy in heart development and disease.

167

Cardiac myocyte maintenance DNA methyltransferase 1 is essential for embryonic heart development but is dispensable for cardiac function and remodeling postnatally

T. Nührenberg^{1,2}, L. Frommherz¹, T. Schnick¹, R. Gilsbach¹, O. Kretz³, F.-J. Neumann⁴, L. Hein¹

¹Institut für experimentelle und klinische Pharmakologie und Toxikologie, Abteilung II, Freiburg, Germany

²Universitäts-Herzzentrum Freiburg • Bad Krozingen, Klinik für Kardiologie und Angiologie II, Bad Krozingen, Germany

³Institut für Anatomie und Zellbiologie, Abteilung für Neuroanatomie, Freiburg, Germany

Background: Recent studies have identified dynamic changes in DNA methylation in cardiac myocytes during development, postnatal maturation and in disease. However, the enzymes involved in shaping the cardiac myocyte DNA methylome are only partially known. Here, we explored the role of *maintenance* DNA methyltransferase Dnmt1 in cardiac development and in remodeling after chronic left ventricular pressure overload.

Methods: In mice, deletion of the *Dnmt1* gene was accomplished by use of two different Cre recombinases. Crosses of homozygous *Dnmt1*^{fl/fl} mice with heterozygous *Dnmt1*^{fl/+} mice expressing a Cre recombinase under control of the atrial myosin light chain gene promoter (*My17-Cre*) resulted in embryonic deletion of *Dnmt1* (KO). Embryos without *My17-Cre* served as controls (CTL). Embryos were dissected and genotyped at E11.5, E12.5, E13.5 and E14.5. RNA-Seq and pyrosequencing of genomic DNA was performed on E11.5 hearts, histology on E12.5 hearts and electron microscopic imaging on E13.5 hearts. For deletion of *Dnmt1* in adult mice, homozygous *Dnmt1*^{fl/fl} mice expressing an inducible Cre recombinase (*Myh6-MCM*) were given tamoxifen i.p. over 4 days. Homozygous *Dnmt1*^{fl/fl} mice not carrying *Myh6-MCM* as well as *Myh6-MCM* carrying mice without *Dnmt1*^{fl} alleles were also injected with tamoxifen and served as controls. Cardiac phenotyping including histology, echocardiography and qPCR was carried out without (sham) or with left ventricular pressure overload induced by transverse aortic constriction (TAC).

Results: *My17-Cre* mediated loss of *Dnmt1* resulted in progressive embryonic lethality with absence of living KO embryos after E14.5. KO embryos displayed loss of cardiomyocyte gene expression patterns, decreased promoter CpG methylation of aberrantly expressed genes and ultrastructural features of wide-spread cardiac myocyte cell death. In contrast, tamoxifen-induced ablation of *Dnmt1* in adult mice did not affect survival of KO mice. Cardiac phenotyping of adult mice revealed no significant differences between KO and CTL mice under sham and TAC conditions.

Conclusion: DNA methyltransferase *Dnmt1* in embryonic cardiac myocytes is essential for proper heart development. In adult cardiomyocytes, *Dnmt1* is dispensable for normal cardiac function and for adaptation to chronic cardiac pressure overload.

168

Cardiomyocyte-specific loss of Tet3 leads to embryonic lethality and impaired demethylation of the *Atp2a2* gene in adult miceD. Kranzhöfer¹, T. Nührenberg¹, R. Gilsbach¹, L. Hein¹¹Institute of Experimental and Clinical Pharmacology and Toxicology, Freiburg, Germany

Background: Recent studies showed that mice with general deletion of the oxidoreductase Tet3 involved in DNA demethylation are embryonic lethal, the underlying cause remaining unknown. This prompted us to investigate whether embryonic lethality is caused by cardiomyocyte-specific loss of Tet3.

Methods: Female mice homozygous for *Tet3^{lox}* and male mice heterozygous for *Tet3^{lox}* and heterozygous for *Myf7-Cre* were mated and offspring were genotyped after weaning. Mice homozygous for *Tet3^{lox}* and heterozygous for *Myf7-Cre* (KO) or homozygous for *Tet3^{lox}* without *Myf7-Cre* (controls) were sacrificed at 12 weeks of age and ventricles were harvested. mRNA of the ventricles was isolated and expression of cardiomyocyte-specific genes was evaluated by quantitative real-time PCR. Cardiomyocyte-specific genomic DNA from KO and control mice was obtained from FACS-sorted cardiomyocyte nuclei and bisulfite-converted for analysis of DNA methylation by pyrosequencing.

Results: KO mice showed embryonic lethality of nearly 50 %. Born KO mice developed without phenotypic abnormalities (normal heart weight/tibia length ratio) and displayed compensatory upregulation of *Tet1* and *Tet2*. Cardiomyocyte genomic DNA of KO mice showed significantly higher methylation levels in the body of the *Atp2a2* gene and at the binding site of the transcription factor GATA4 but not near the promoter and the binding site of the transcription factor TBX5. Higher methylation levels were not accompanied by changes in *Atp2a2* expression. However, both *Myh7* and *Nppb* were upregulated in KO mice compared to control mice.

Conclusions: Our findings suggest that Tet3 is involved in DNA demethylation in cardiomyocytes. Loss of Tet3 expression resulted in embryonic lethality. Compensatory upregulation of *Tet1* and *Tet2* isoenzymes may contribute to the incomplete penetrance of this phenotype. Further studies are ongoing to investigate the functional relevance of Tet3 in cardiomyocytes.

169

Protease inhibitor 16 regulates processing of chemerinM. Regn¹, S. Engelhardt¹¹Institut für Pharmakologie und Toxikologie TU München, München, Germany

To identify novel proteins secreted by the myocardium, we have previously conducted a genetic screen, which led to the identification of protease inhibitor 16 (Pi16). A recent GWAS analysis showed an association of a genetic variant in the Pi16 genomic locus (rs1405069) with chemerin plasma levels.

Here we tested the hypothesis that Pi16 determines chemerin plasma levels through regulation of chemerin processing. We generated mice deficient for Pi16, which did not display an overt phenotype under basal conditions. Plasma levels of chemerin were found significantly lower in Pi16-deficient animals compared to littermate controls. To investigate whether Pi16 and chemerin interact, we performed co-immunoprecipitation experiments. Indeed, we found Pi16 to co-precipitate with chemerin from both murine plasma and cell culture supernatants. As chemerin is proteolytically processed and activated, we next asked whether the presence of Pi16 would affect the processing of pro-chemerin to its processed forms in native tissue. Western blot analysis on cardiac and adipose tissue lysates that detected both the unprocessed precursor and the processed forms of chemerin showed a significant shift towards the processed forms upon genetic deletion of Pi16. When we assayed for the activity of the chemerin-cleaving protease cathepsin K, we found recombinant Pi16 to potently inhibit cathepsin K activity.

Taken together, we propose Pi16 to act as a regulator of chemerin processing.

Pharmacology – Ion channels

170

Structure activity relationship studies of newly synthesized larixol derivatives as potent TRPC6 inhibitorsS. Häfner¹, N. Urban¹, J. Broichhagen², F. Burg², D. Trauner², M. Schaefer¹¹Universität Leipzig, Rudolf-Boehm-Institut für Pharmakologie und Toxikologie, Leipzig, Germany²Ludwig-Maximilians-Universität, Department Chemie, München, Germany

The transient receptor potential canonical 6 (TRPC6) is a second messenger-gated cation channel, which mediates depolarization and Ca²⁺ entry. It is known to be activated by diacylglycerol derivatives (DAG, 1-oleoyl-1-acetyl-sn-glycerol OAG)^[1] in a PKC-independent manner and plays important roles in lung and kidney physiology. Gain-of-function mutations in the *TRPC6* gene can cause focal segmental glomerulosclerosis (FSGS), a kidney dysfunction leading to end stage renal disease.^[2] Thus, the discovery of potent inhibitors of TRPC6 may help to develop new therapeutic strategies. Urban *et al.* discovered that larixol, a natural product with a labdane skeleton found in the oleoresin of the European larch (*Larix decidua*), blocks the OAG-dependent activation of TRPC6.^[3] Larixyl acetate, another component of the resin showed an even higher potency in TRPC6 inhibition (IC₅₀ = 0.26 μM) and a 12-fold selectivity compared to TRPC3. These findings led to the idea that further modifications of the larixol lead structure may reveal even more potent inhibitors. Furthermore, changes in selectivity and efficacy of such compounds may also provide a deeper insight about relevant structural elements for channel binding.

As larixyl carbamate was assumed to exhibit a higher metabolic stability as larixyl acetate, this compound was already investigated in previous studies. It showed a potent and subtype-selective inhibition of TRPC6. Hence, the development of further carbamates was a priority objective. As an alternative to the use of different isocyanates for the introduction of a carbamate function at the C1 position of the molecule we found an elegant way via formation of an active ester with carbonyldiimidazole. This precursor

allowed the design of several isosteric compounds like larixyl methylcarbamate, larixyl hydrazide and larixyl methylcarbonate, which were all able to block TRPC6 with similarly low IC₅₀ values. The introduction of more bulky side chains appeared to diminish the bioactivity of the compounds, the stereochemistry at the C1 position, however, seems to play an important role for the inhibition of TRPC6 currents.

Larixyl methylcarbamate lead to TRPC6 inhibition with an IC₅₀ value of 0.15 ± 0.06 μM. Compared to larixyl carbamate and larixyl methylcarbonate, which are also very potent blockers of TRPC6, this compound bears the benefit of high subtype selectivity towards TRPC3. Even with concentrations up to 50 μM of larixyl methylcarbamate, no complete inhibition of the Ca²⁺ influx via TRPC3 channels could be achieved. This fact distinguishes this larixol derivative as a very promising compound for further studies of TRPC6 in health and disease.

[1] Hofmann *et al.*, Nature (1999) 397:259-263.[2] Winn *et al.*, Science (2005) 308:1801-1804[3] Urban *et al.*, Mol. Pharm. (2015), *in press*.

171

Electrophysiological drug-screening of bispyridinium-non-oxime-compounds on human nicotinic α7 acetylcholine receptors - an alternative approach for the treatment of nerve agent poisoning -C. Scheffel^{1,2}, S. Rappenglück¹, K. Niessen², F. Worek², H. Thiermann², K. Wanner¹, T. Seeger¹¹Ludwig-Maximilians-Universität München, Department für Pharmazie, München, Germany²Institut für Pharmakologie und Toxikologie der Bundeswehr, München, Germany

Poisoning by organophosphorus compounds (OPC) including pesticides and highly toxic nerve agents is based on irreversible inhibition of acetylcholinesterase (AChE) resulting in an excess of acetylcholine causing accumulation. The subsequent overstimulation at nicotinic and muscarinic receptors finally leads to respiratory arrest due to paralysis of the respiratory muscles. Therapy focuses on competitive antagonism at muscarinic acetylcholine receptors and reactivation of inhibited AChE by bisquaternary pyridinium oximes. Thereby, nicotinic malfunction is not directly approached. For that reason, an alternative strategy appears rational using nicotinic acetylcholine receptor (nAChR) active substances to counteract the effects of accumulated acetylcholine and thus to restore the loss of function of nAChRs. Different bispyridinium-non-oxime-compounds (BPs) have been demonstrated to be able to serve as target structures for the identification of new positive allosteric modulators of nicotinic receptors. Unlike nicotinic agonists, positive allosteric modulators can reinforce the endogenous cholinergic neurotransmission despite of acetylcholine accumulation in the synaptic cleft.

To this end, the following electrophysiological *in vitro* study investigated the effect of twelve diversely substituted BPs on human α7 nAChR using whole-cell patch clamping under voltage-clamping conditions (-70 mV) performed with planar electrodes in an automatic system (Nanion Technologies GmbH, Munich). Cholinergic currents of hα7 nAChR that have been expressed in stably transfected CHO cells were activated by the agonist nicotine. Measurements of the effect of various BPs concentrations in the presence of nicotine were performed to establish concentration-response relations. Cholinergic inward currents were generated by human α7 nAChRs in response to low nicotine concentrations. At high concentrations of the drug the currents were decayed reflecting both, desensitization of the receptors and presumably block of the open channel by high agonist concentrations. Four out of twelve BPs co-applied with nicotine showed a concentration-dependent enhancement of peak agonist-evoked currents and, most pronounced, 4-*tert*-butyl-substituted-BP, also demonstrated a marked elongation of the evoked response. This suggests a positive allosteric effect of these compounds on the nicotinic receptor. However, at high BP concentrations in the presence of agonist, responses were decayed significantly, presumably resulting from an open channel block induced by BPs.

Hence, further compounds have to be synthesized to identify promising candidate compounds for improvement of effective therapy against nerve agent poisoning.

172

A benzothiadiazine is a novel activator of homo- and heteromeric TRPC5 channelsH. Beckmann¹, K. Hill¹, N. Urban¹, M. Schaefer¹¹Universität Leipzig, Medizinische Fakultät, Rudolf-Boehm-Institut für Pharmakologie und Toxikologie, Leipzig, Germany

The transient receptor potential channels (TRP) are a family of tetrameric nonselective cation channels, which are involved in a variety of physiological and pathological processes (1). Among the 28 mammalian TRP channels, the canonical channel 5 (TRPC5) is a Ca²⁺-permeable ion channel, which is predominantly expressed in the brain (2). Many aspects of TRPC5 function are still elusive although behavioral experiments with TRPC5-knock-out mice suggest a role in innate fear-response (3) and some studies indicate a TRPC5-mediated down regulation of neurite outgrowth in nerve cells (4,5). To elucidate TRPC5 function on a cellular level, selective and potent compounds are required to acutely control channel activity. Despite extensive research, TRPC5 modulators often lack selectivity or exhibit toxicity, limiting their applicability *in vivo* (6,7). Thus, there is still a need for identifying novel and efficient TRPC5 modulators.

We therefore screened a compound library (ChemBioNet) and identified a benzothiadiazine derivative (BTD) as a novel, potent, and selective TRPC5 activator. HEK293 cells heterologously expressing TRPC5 upon tetracycline induction (HEK_{TRPC5}) show a BTD-induced concentration-dependent activation in both Ca²⁺ assays (EC₅₀ = 0.71 μM) and in electrophysiological whole cell patch clamp recordings (EC₅₀ = 1.1 μM). BTD elicits currents with an N-shaped I/V curve, typical for TRPC5. The resulting activation is long lasting, reversible and sensitive to clemizole, a recently established TRPC5 inhibitor (8). MTT assays revealed that incubating HEK_{TRPC5} cells for 24h with BTD concentrations above 1 μM results in a concentration-dependent decrease in viability and cell proliferation, indicating a Ca²⁺-mediated cytotoxic effect in consequence of sustained channel activity. Non-induced control cells remain unaffected by BTD at concentrations up to 10 μM. Ca²⁺ assays showed no influence of BTD on closely related TRPC4 channels, as well as TRPC3/6/7 at concentrations up to 10 μM. The same

applied to more distantly related TRPV and TRPM channels. Besides a homotetrameric organization, TRPC5 subunits can also assemble to heteromeric channel complexes with their closest relatives TRPC1 and TRPC4 (9). TRPC1/5 and TRPC4/5 heteromers can also be activated by BTd as evident from their typical I/V curves in patch clamp experiments, suggesting a high selectivity of BTd for channel complexes bearing at least one TRPC5 subunit.

- 1 Nilius 2007, *Biochim Biophys Acta*
- 2 Riccio et al. 2002, *Mol Brain Res*
- 3 Riccio et al. 2009, *Cell*
- 4 Greka et al. 2003, *Nature Neurosci*
- 5 Wu et al. 2007, *J Neurosci*
- 6 Richter et al. 2014, *Br J Pharmacol*
- 7 Akbulut et al. 2015, *Angew Chem*
- 8 Richter et al. 2014, *Mol Pharmacol*
- 9 Hofmann et al. 2002, *PNAS*

173

GSK1702934A bypasses the conventional PLC activation pathway to induce a distinct gating mechanism in TRPC3/6 channels

B. Svobodova¹, M. Lichtenegger¹, T. Glasnov², T. Stockner³, M. Poteser¹, K. Groschner

¹Medical University Graz, Institute for Biophysics, Graz, Austria

²University of Graz, Institute of Chemistry, Graz, Austria

³Medical University of Vienna, Institute of Pharmacology, Vienna, Austria

Transient receptor potential canonical channels 3/6 and 7 are controlled by membrane lipids and highly expressed in neuronal and cardiac tissues. The involvement of these channels in development and (patho)physiology of these tissues is well documented, while our understanding of structure-function relations, specifically in terms of the lipid sensing machinery, in these channel proteins is still incomplete.

Using a homology model of TRPC3, based on the recently available structural information on TRPV1, we performed structure-guided mutagenesis and identified a single residue in transmembrane domain 6 (G652), which is conserved within the canonical family of TRP channels. Single point mutations at position 652 in TRPC3 largely eliminated lipid sensitivity. TRPC3^{G652A} expressed in HEK293 cells was found resistant not only to activation via the phospholipase C pathway but also to direct administration of diacylglycerols. On the contrary, a synthetic agonist of TRPC3/6/7 channels (GSK1702934A) activated wild-type TRPC3 and TRPC6 channels as well as the respective lipid insensitive mutants (TRPC3^{G652A}, TRPC6^{G709A}). Interestingly, the synthetic activator was found to generate substantially enhanced TRPC conductances in cells expressing the lipid-insensitive mutants as compared to wild-type proteins. Closer inspection of sensitivity of the WT and mutant proteins to various GSK derivatives argue against a contribution of G652 to GSK recognition by TRPC3.

Our results demonstrate the existence of two different mechanisms of TRPC3/6 activation supposedly involving distinct gating movements in the channel complex.

We suggest that lipid gating of TRPC3/6 involves a hinge-point and/or requires a certain level of flexibility within transmembrane segment S6 provided by G652. Lipids and synthetic activators of TRPC3/6 may be capable of initiating markedly different structural rearrangement in these channels.

174

Affinity and functional effects of non-oxime bispyridinium compounds on muscle-type nicotinic acetylcholine receptors

K. V. Niessen^{1,2}, F. Langguth¹, T. Seeger¹, H. Thiermann¹, F. Worek¹

¹Bundeswehr Institute of Pharmacology and Toxicology, Munich, Germany

²Supervisory Agency for Public Law Tasks of the Bundeswehr Medical Service South, Munich, Germany

Objective: Organophosphorus compounds (OPCs), i.e. nerve agents or pesticides, are highly toxic due to their strong inhibition potency against acetylcholinesterase (AChE). Inhibited AChE results in accumulation of acetylcholine in the synaptic cleft and thus the desensitisation of the nicotinic acetylcholine receptor (nAChR) in the postsynaptic membrane is provoked. As the therapeutic efficacy of oximes is limited, e.g. poisoning by soman or tabun, the direct targeting of nAChR may be an alternative therapeutic approach. Studies with the non-oxime bispyridinium compound (BP) MB327 (1,1'-(propane-1,3-diyl) bis (4-*tert*-butylpyridinium) di(iodide)) demonstrated a therapeutic effect against soman *in vitro* and *in vivo*. Consequently, studying the affinity of BPs at muscle-type nAChRs and functional effects are topics of interest. To identify potential candidates, homologous series of substituted and non-substituted analogues (linker C₁ – C₁₀) of MB327 were investigated by using binding and functional assays.

Experimental procedures: Crude membranes from frozen electric organ of *Torpedo californica* were purified by sucrose-gradient density centrifugation and used in both affinity and functional assays. In competition radio-ligand binding assays, the influence on [³H]epibatidine binding sites of *Torpedo* muscle-type nAChR was determined. Functional assessments were carried out with a bilayer method to investigate the effect on the cholinergic signal induced by 100 μM carbamoylcholine.

Results: Bispyridinium compounds bearing unsubstituted pyridinium rings and long alkyl linkers (> C₇) inhibited the binding of [³H]epibatidine and decreased the cholinergic signal of 100 μM carbamoylcholine in the functional assay. MB327 and several bispyridinium structure analogues (mainly C₂ – C₄ linker) exhibited no regular displacement curves at [³H]epibatidine binding sites and enhanced the carbamoylcholine-induced signal.

Conclusion: The results demonstrate that the described affinity and functional screening methods detected some structure-activity-relationships (SAR). Depending on linker length and substitution pattern, the investigated bispyridinium compounds seemed to interact as positive allosteric modulators. Further research is necessary to verify this hypothesis.

175

Non oxime bispyridinium compounds with an effect on soman-blocked respiratory muscle function have no effect on normal muscle function

T. Seeger¹, J. Rauscher¹, H. Thiermann¹, F. Worek¹

¹Institut für Pharmakologie und Toxikologie der Bundeswehr, Experimentelle Pharmakologie, München, Germany

The life threatening toxicity of organophosphorus compounds (OP), like nerve agents or pesticides, lies in the inhibition of acetylcholinesterase (AChE) which causes cholinergic crisis. The accumulated acetylcholine in neuromuscular synapses results in the desensitization of nicotinic acetylcholine receptors (nAChR) and paralysis of respiratory muscles.

The 4-*tert*-butyl-substituted bispyridinium compound MB327 showed therapeutic efficacy in soman and tabun poisoned guinea pigs *in vivo*. Partial restoration of neuromuscular transmission by bispyridinium compounds (BP), e.g. MB327 or MB420, could also be observed in soman paralysed respiratory muscles *in vitro* and was partly attributed to an interaction of BP with nAChRs. However, it is unknown, whether these BP might affect normal respiratory muscle function in the absence of cholinergic crisis. Therefore this study investigated the effect of BP on physiological rat diaphragm muscle function.

Force generation of rat diaphragm hemispheres was determined after incubation with increasing BP concentrations (1-300 μM) and compare to sham treatment. The diaphragm hemispheres were stimulated every ten minutes by an indirect electrical field (20, 50, 100 Hz). Muscle force was analyzed as time-force integral and is expressed as percentage of the individual control values, measured at the outset of the experiment. The muscle force dropped during the experiment. The application of the bispyridinium compounds MB327 (1,1'-(propan-1,3-diyl) bis (4-*tert*-butylpyridinium) di(iodide)) and MB420 (1,1'-(propan-1,3-diyl) bis (2-ethylpyridinium) di(iodide)) in the tested concentration range (1-300 μM) did not change muscle force production compared to the sham treated muscle. This was equally true for low (20 Hz) and high (50 and 100 Hz) stimulation frequencies.

This study showed that bispyridinium compounds which can partially reverse soman-induced neuromuscular block in rat diaphragms show no effect on respiratory muscle function in absence of the OP-induced neuromuscular block. These results suggest that the BP tested in this study interacted with desensitized nAChRs only, but do not affect physiological neuromuscular transmission. This effect needs to be investigated with further, promising BP compounds.

176

Interaction of recombinant pain-relevant ATP- and proton-gated ion channels in an expression system; potentiation of the P2X3 receptor-induced current by the opening of ASIC3 channels

G. Stephan¹, P. Illes¹

¹Universität Leipzig, Rudolf-Boehm-Institut für Pharmakologie und Toxikologie, Leipzig, Germany

The P2X3 receptor (R) is a ligand-gated cationic channel, which is activated by extracellular ATP. The acid sensing ion channel 3 (ASIC3) belongs to the ENaC/degnerin family and is gated by extracellular protons. Despite their different amino acid sequences both ion channels share the same structure and pore architecture, by i.e. consisting of three identical subunits. Besides, they are both located at partially overlapping subpopulations of dorsal root ganglia neurons and are implicated in acidic pain signaling. Consequently, their physical interaction in the cell membrane or even the formation of heteromeric receptor channels from P2X3 and ASIC3 subunits has to be taken into consideration. We transfected rat (r)P2X3R and rASIC3 constructs individually or together in a ratio of 1:1 into CHO cells. We further used the whole cell patch clamp technique to analyze the current responses either elicited by the application of α,β-methylene-ATP (α,β-meATP) or by a decrease in the extracellular pH value. The functionality of the individually transfected P2X3R- and ASIC3-constructs was verified by recording concentration-response curves for the agonists α,β-meATP and protons, respectively. After co-transfection of both ion channels, a pH-shift from 7.4 to 6.7 caused a rapidly desensitizing current response and a subsequent strong potentiation of the α,β-meATP-induced current. An even larger potentiation was achieved after a decrease of the pH value to 6.5. The opening of ASIC3 channels failed to facilitate the P2X3R current when 2-guanidine-4-methylquinazoline was used to stimulate a non-proton ligand-sensor of ASIC3. Then, we substituted Ca²⁺ in the extracellular medium by Ba²⁺ or decreased the intrapipette concentration of EGTA, to modify the free intracellular Ca²⁺ concentration. In cells individually transfected with the receptor-channels, external Ba²⁺ increased the effect of α,β-meATP but decreased the effect of protons. The lowering of intrapipette EGTA modified P2X3R- and ASIC3-specific currents in a similar manner as external Ba²⁺. In cells co-transfected with P2X3R/ASIC3, the ionic manipulations mentioned above abolished the potentiation of the α,β-meATP currents by ASIC3 activation. Taken together, our results suggest that P2X3R and ASIC3 interact with each other, since the activation of ASIC3 had a marked impact on the P2X3R specific current response. Further experiments are required to clarify the mechanism of this interaction, although it has been shown that extra- and intracellular Ca²⁺ and the proton sensor of ASIC3 appear to critically participate in this process.

177

NAADP and the two-pore channel protein 1 participate in the acrosome reaction in mammalian spermatozoa

L. Arndt¹, E. Artl¹, J. Castonguay², S. Hassan³, S. Zierler¹, G. Wennemuth⁴, A. Breit¹, M. Bief³, C. Wahl-Schott¹, T. Gudermann¹, N. Klugbauer², **I. Boekhoff**¹

¹Ludwig-Maximilians University, München, Walther Straub Institute of Pharmacology and Toxicology, München, Germany

²Albert-Ludwigs-University, Freiburg, Institute for Experimental and Clinical Pharmacology and Toxicology, Freiburg, Germany

³Ludwig-Maximilians University, München, Department of Pharmacy, München, Germany

Germany

¹University of Duisburg-Essen, Institute for Anatomy, Essen, Germany

Background: The sperm acrosome reaction is an all-or-none secretion process, mainly following the conserved principles of calcium-regulated exocytosis in neurons and neurosecretory cells. However, the relationship between the formation of hundreds of fusion pores and the required mobilization of calcium from the lysosome-related acrosomal vesicle has only been partially defined. Hence, the second messenger, nicotinic acid adenine dinucleotide phosphate (NAADP), known to promote efflux of calcium from lysosome-like acidic compartments, was analyzed for its ability to trigger acrosome reaction in mouse sperm. In addition, the expression of two-pore channel (TPC) proteins, which are primarily localized in lysosome-related acidic organelles and which present potential molecular targets of NAADP were examined in mammalian spermatozoa.

Methodology/ Principal Findings: Our results show that treatment of spermatozoa with NAADP resulted in a loss of the acrosomal vesicle, which shows typical properties, described for TPCs: (i) Registered responses were not detectable for its chemical analogue NADP, and (ii) where blocked by the NAADP antagonist trans-Ned-19. In addition, (iii) two narrow bell-shaped dose-response-curves were found, with maxima either in the nanomolar or low micromolar NAADP concentration range. Performing immunogold-electron microscopy with a TPC1 specific antibody, a co-localization with NAADP-binding at the acrosomal region was detectable. Moreover, quantifying loss of the acrosomal vesicle in TPC1 null sperm upon application of different NAADP concentrations, responsiveness to low micromolar NAADP concentrations was completely abolished.

Conclusions/Significance: Our finding that two convergent NAADP-dependent pathways are operative in driving acrosomal exocytosis and that Zona pellucida induced acrosomal exocytosis is prevented by trans-Ned-19 support the concept that both NAADP-gated cascades match local NAADP concentrations with the efflux of acrosomal calcium, thereby ensuring reliable and complete fusion of the large acrosomal vesicle. Since the acrosome reaction shares the same basic sequence of events typical for the conserved process of Calcium regulated exocytosis, such as tethering, docking, priming and final vesicle fusion, the sperm model system may also be useful to comparatively examine whether the same convergence of NAADP-dependent pathways is also operative in cellular systems with many secretory vesicles.

178

Studying the role of transient receptor potential vanilloid 4 (TRPV4) channels in lung edema formation utilizing an isolated perfused lung model

J. Weber¹, M. Kannler¹, T. Gudermann¹, A. Dietrich¹
¹Walther-Straub-Institut, München, Germany

TRPV4 channels are members of the vanilloid family of TRP proteins. The channel is nearly ubiquitously expressed and can be found in brain, kidney, skin, heart, blood vessels as well as in the lung. Pulmonary expression of TRPV4 has been identified in endothelial cells (1), epithelial cells (2) and arterial smooth muscle cells (3). Most interestingly, the channel is known to be involved in the development of several lung diseases such as cough, asthma and pulmonary edema formation, due to its activation by heat, changes in osmolarity and shear stress (reviewed in 4). It is a matter of debate however if TRPV4 activation in pulmonary endothelial as well as epithelial cells induces disruption of the barrier and an increased fluid leak into the alveolus as described for TRPC6 (5) which is also expressed in both cell types. To analyze the potential role of TRPV4 on ischemia-reperfusion-injury(IRI)-induced pulmonary edema formation we utilized the isolated perfused mouse lung model. Much to our surprise, we detected a significantly enlarged edema formation after 90 minutes of ischemia in TRPV4-deficient mice in comparison to wild-type (WT) mice. This effect was observed by constant weight measurements as well as wet-to-dry ratio gain and was not dependent on the initial perfusion rate. Most interestingly, edema formation of TRPV4/TRPC6 double deficient lungs was indistinguishable from WT lungs, indicating antagonizing effects of both channels, because TRPC6 deficiency protected lungs from IRI-induced edema (5). Moreover, we identified reduced expression levels of aquaporin 5 in TRPV4-deficient lung lysates compared to WT lungs. These findings raise the intriguing possibility that TRPV4 might be involved in the regulation of aquaporin expression in lung endothelial cells.

References:

- Earley, et al. (2005) TRPV4 Forms a Novel Ca²⁺ Signaling Complex With Ryanodine Receptors and BK_{Ca} Channels. *Circulation Research* 97: 1270-1279
- Alvarez, et al. (2006) Transient receptor potential vanilloid 4-mediated disruption of the alveolar septal barrier: a novel mechanism of acute lung injury. *Circulation Research* 99: 988 – 995
- Yang, et al. (2006) Functional expression of transient receptor potential melastatin- and vanilloid-related channels in pulmonary arterial and aortic smooth muscle. *American Journal of Physiology – Lung Cellular and Molecular Physiology* 290: 1267-1276.
- Hill-Eubanks, et al. (2014) Vascular TRP channels: performing under pressure and going with the flow. *Physiol.* 29: 343-360
- Weismann, et al. (2012) Activation of TRPC6 channels is essential for lung ischaemia-reperfusion induced oedema in mice. *Nature Commun.* 3: 649

179

Pharmacological tools to selectively patch-clamp early endosomal organelles

C. Grimm¹, C. Wahl Schott¹
¹LMU München, Pharmakologie/Pharmazie, München, Germany

Endosomes and lysosomes are cell organelles involved in transport, breakdown and secretion of proteins, lipids, and other macromolecules. Endolysosomal dysfunction can cause storage disorders such as mucopolisidoses, sphingolipidoses, or neuronal ceroid

lipofuscinoses, but is also implicated in the development of metabolic and neurodegenerative diseases, retinal and pigmentation disorders, trace metal dishomeostasis, infectious diseases, and cancer. Endolysosomal ion channels and transporters are highly critical for the tight regulation of the multiple endolysosomal fusion and fission processes including endo- and exocytotic events as well as the regulation of proton and other ionic concentrations in the lumen of endolysosomal vesicles. Methods to patch-clamp endolysosomal organelles are continuously improving. Yet until now it has not been possible to selectively enlarge endosomal or lysosomal organelles with pharmacological tools for patch-clamp experimentation. We show here by using a combination of two small molecules that we can selectively enlarge early endosomes to a degree sufficient for patch-clamp experimentation. The ability to more selectively patch-clamp intracellular organelles will substantially improve the functional investigation of endolysosomal ion channels under physiological and pathophysiological conditions.

180

Characterisation of renal phenotype of TRPM3^{-/-} mice

D. Huang¹, Z. Kalo¹, F. Theilig², C. Harteneck¹
¹Institut für Pharmakologie und Toxikologie, Abteilung für Pharmakologie und Experimentelle Therapie, Tübingen, Germany
²Department of Medicine, University of Fribourg, Fribourg, Switzerland

The transient receptor potential (TRP) channels are a superfamily of non-selective ion channels involved in a variety of physiological processes and in the pathogenesis of many disorders. In the kidney, TRP channels have been implicated to be involved in diabetic nephropathy, focal, segmental glomerulosclerosis, polycystic kidney disease, hypomagnesemia with secondary hypercalcaemia and idiopathic hypercalcaemia. The melastatin-like TRP channel subfamily 3 (TRPM3) has been shown to be expressed in human kidney^{1,2}. Using newly developed anti-TRPM3 antibodies, we are able to visualize TRPM3 protein in epithelial cells of proximal tubule as well as collecting ducts in the mouse kidneys. Therefore, we compared renal function of male, five month old mice lacking TRPM3 (TRPM3^{-/-}) and their wild type littermates (TRPM3^{+/+}) in metabolic cages and clearance studies. The TRPM3^{-/-} mice presented significantly lower urine osmolarity and imbalances in urine ion composition compared to the TRPM3^{+/+} while creatinine clearance and glomerular filtration rate were comparable in both genotypes. In glomerular filtration experiments, the infusion of physiological Ringer solution showed up with a quite different profile in ion handling in mice lacking TRPM3 compared to wild type littermates. In summary our data provide evidences for renal expression of TRPM3 and possible roles of TRPM3 in renal osmolarity regulation.

1. Grimm et al. JBC 2003
2. Lee et al., JBC 2003

181

Novel mouse models to study the localization and function of the P2X7 receptor in vivo

J. Zhang^{1,2}, K. Kaczmarek-Hájek², A. Saul², T. Jooss¹, R. Stocklauser¹, A. Nicke¹
¹Walther-Straub-Institut für Pharmakologie und Toxikologie, AG Nicke, München, Germany
²Max Planck Institute for Experimental Medicine, Göttingen, Germany

The ATP-gated P2X7 receptor (P2X7R) is a non-selective cation channel widely expressed in epithelia, endothelia, and cells of hematopoietic origin. It plays a central role in cytokine release and *studies* in P2X7^{-/-} animals indicate its involvement in inflammatory and neurodegenerative diseases. In addition, accumulating data suggests a functional role in neurons and its involvement in neurotransmitter release in the brain. However, despite its importance as a drug target, its precise localization and its molecular and physiological functions remain poorly understood. In particular, the location and function of P2X7R in neurons remain a matter of ongoing debate. To clarify the cellular and subcellular distribution of the P2X7R and to investigate its physiological and pathophysiological role in the brain we generated BAC transgenic mouse models in which murine polymorphic variants of EGFP-tagged P2X7R are overexpressed under the control of the endogenous P2X7 promoter.

The EGFP-tagged P2X7Rs are efficiently overexpressed in the plasma membrane and can be directly visualized by green fluorescence or indirectly by anti-EGFP antibodies. The obtained mouse lines show different expression levels but identical expression patterns with predominant expression in the cerebellum, hippocampus, and thalamus. Using cell type-specific markers, P2X7-EGFP was identified in almost all microglia and subpopulations of oligodendrocytes and astrocytes in the brain. In the spinal cord, numerous astrocytes in the white matter showed EGFP immunoreactivity. So far, no EGFP immunostaining was found on MAP2- and NeuN-positive cells indicating that under non-pathological conditions, the P2X7 receptor is not expressed in neurons of the CNS. Interestingly, a higher expression level of CD68 protein was observed in the P2X7R-overexpressing mice. These results suggest that overexpression of P2X7Rs alone is sufficient to induce microglia activation, even under non-pathological conditions. Since CD68 primarily localizes to lysosomes and endosomes, this further supports a role of the P2X7R in the regulation of phagocytosis. To validate these data, conditional knockout mice are generated. The current status of the project will be presented. Supported by the DFG (NI592/7-1)

182

Application of bacterial protein toxins to TPC1 deficient cells reveals the role of two pore channels for intracellular endolysosomal trafficking processes

R. Mallmann¹, J. Orth¹, J. Castonguay¹, T. Müller¹, N. Klugbauer¹
¹Albert-Ludwigs-Universität Freiburg, Experimentelle und Klinische Pharmakologie und Toxikologie, Abteilung I, Freiburg, Germany

The Two-Pore Channels (TPCs) – TPC1 and TPC2 – are located in membranes of intracellular organelles of the endo-lysosomal system. The TPC-protein-monomer

contains two homologous domains with six transmembrane α -helices each. A functional TPC probably consists of a dimer of two TPC-proteins resembling an ion channel architecture with the typical four domain organization like voltage gated Na^+ or Ca^{2+} channels or such as TRP channels. Due to their biophysical properties, TPC1 and TPC2 are assumed to be involved in the efflux of Ca^{2+} from intracellular organelles and thereby contribute to fusion/fission processes of endosomes and lysosomes. Thus, TPCs are supposed to be important regulators for vesicle trafficking, sorting and degradation/recycling processes. Recently, it was shown that virus entry and replication of certain strains of *Filoviridae* – such as Ebola – depends on functional TPCs and that either block or genetic inactivation of TPCs reduces virus infectivity.

A large family of bacterial protein toxins elicit their effects by modification of intracellular target proteins of host cells. These toxins are taken up by receptor mediated endocytosis and follow different endosomal routes to reach their final cytosolic destination. These toxins principally use two different intracellular routes: The first group uses an entry route via early or late endosomes (short-trip toxins), the second group takes a retrograde route via endosomes, Golgi network and the endoplasmic reticulum (long-trip toxins) to get access to the cytosol. Translocation of short-trip toxins – such as Diphtheria toxin (DT), *Pasteurella multocida* toxin (PMT) and *Bacillus anthracis* lethal factor (PA/LF) – from early and late endosomes into the cytosol is driven by ongoing acidification. Long-trip toxins – including Cholera toxin (CT) – are retrogradely transported after endocytosis via the Golgi apparatus to the endoplasmic reticulum (ER). Within the ER a specific peptide-motif allows the translocation into the cytosol.

Due to the role of TPC1 for vesicle fusion & fission processes we investigated a potential impact of TPC1 on the uptake of bacterial toxins. First we determined the precise localization of TPC1 in intracellular compartments. To deduce its role for trafficking processes we performed co-localization and correlation studies with a whole set of established markers such as Rab-GTPases and PIPs. Second we intoxicated wild-type and TPC1 deficient cell lines with different bacterial protein toxins such as Cholera (CT), Diphtheria (DT) or *Pasteurella multocida* (PMT) toxin. Using cell viability and other intoxication assays we investigated the consequences of TPC1-deletion on bacterial toxin uptake, translocation and cytotoxicity.

This work was supported by TRR SFB 152.

References: Sakurai, Y. et al. 2015, Two-pore channels control Ebola virus host cell entry and are drug targets for disease treatment. *Science* 347:995-8.

Grimm, C. et al. 2014, High susceptibility to fatty liver disease in two-pore channel 2-deficient mice. *Nat. Commun.* 5:4699.

Watson, P. & Spooner, R.A. 2006, Toxin entry and trafficking in mammalian cells. *Adv Drug Deliv Rev.* 58(15):1581-96.

183

Alternative initiation of transcription in the pituitary gland creates N-terminal TRPM3 ion channel variants of different abundance and activity

A. Becker¹, E. Gergert¹, C. Lux¹, N. Hasan¹, S. E. Philipp¹

¹Universität des Saarlandes, Institut für Experimentelle und Klinische Pharmakologie und Toxikologie, Homburg/Saar, Germany

TRPM3 ion channels are considered to be involved in hormone release from pancreatic islets and the pituitary gland^{1,2}. The TRPM3 gene encodes a number of different splice variants that differ in their permeation properties and their activity in response to agonists^{3,4}. Variations include the presence or absence of five stretches of 10 to 25 amino acid residues within the aminoterminal, long or short pore loops and long or truncated carboxytermini⁵. Furthermore, three different aminoterminals of human and mouse proteins have been described⁶, but presumably these differences are caused by the activity of different promoters.

Screening of a mouse pituitary gland cDNA library identified 12 variants that differ in exons 8, 13, 15, 17 and 20. However, only variants bearing the short, Ca^{2+} permeable pore loop were detected. 3' rapid amplification of cDNA ends (3'RACE) revealed that TRPM3 proteins of the pituitary gland carry truncated C-termini exclusively. 5'RACE identified five independent regions of transcription initiation within the TRPM3 gene implying the presence of five independent promoters. The different transcripts encode four TRPM3 amino termini α , β , γ and δ of 1-155 amino acid residues including those described in humans (β, γ). However, the activity of these variants after stimulation with pregnenolone sulfate varied largely just as their frequency in the pituitary with shortened γ -variants being most abundant (~76 %).

1 Wagner, T. F. et al. Transient receptor potential M3 channels are ionotropic steroid receptors in pancreatic beta cells. *Nat. Cell Biol.* 10, 1421-1430 (2008).

2 Hasan, N., Beck, A., Mannebach, S., Weißgerber, P. & Philipp, S. E. Expression and function of TRPM3 proteins in mouse pituitary gland. *Naunyn-Schmiedeberg's Arch Pharmacol* 387 (Suppl 1), 510 (2014).

3 Frühwald, J. et al. Alternative splicing of a protein domain indispensable for function of transient receptor potential melastatin 3 (TRPM3) ion channels. *J Biol Chem* 287, 36663-36672 (2012).

4 Oberwinkler, J., Lis, A., Giehl, K. M., Flockerzi, V. & Philipp, S. E. Alternative splicing switches the divalent cation selectivity of TRPM3 channels. *Journal of Biological Chemistry* 280, 22540-22548 (2005).

5 Oberwinkler, J. & Philipp, S. E. Trpm3. *Handb. Exp. Pharmacol.* 222, 427-459 (2014).

184

Functional analysis of the two pore channel TPC1: Conventional black lipid bilayer and multichannel setup

T. Müller¹, E. Zaitseva², G. Baaken², R. Mallmann¹, U. Schulte³, N. Klugbauer¹

¹Albert-Ludwigs-Universität Freiburg, Experimentelle und Klinische Pharmakologie und Toxikologie, Abteilung 1, Freiburg, Germany

²Ionera Technologies GmbH, Freiburg, Germany

³Albert-Ludwigs-Universität Freiburg, Physiologisches Institut, Freiburg, Germany

Two-pore channels (TPCs) are a small family of ion-channels found throughout the endolysosomal system of eukaryotic cells. Phylogenetically TPCs belong to the voltage-gated ion channel superfamily sharing common traits with Ca_v , Na_v , and TRP channels. TPCs show a duplicated architecture with two homologous trans-membrane domains. Each domain is build up by six membrane spanning alpha helices linked by short loops.

It is very likely that TPCs form dimers maintaining the four-fold symmetry found in other members of the voltage-gated ion channel superfamily. Due to their localization in the endolysosomal system TPCs are not accessible to conventional patch clamping.

To investigate TPCs electrophysiological properties we use black lipid bilayer measurements. Purified channels are integrated into an artificial phospholipid bilayer that separates two chambers enabling us to apply different buffers. Upon activation by NAADP ions flow through the channel and can thereby pass the diffusion barrier. The movement of charged molecules through TPCs results in currents which can be amplified and recorded. The controlled environment of the lipid bilayer setup allows testing of different ions as well as putative activating and inhibitory substances.

One of the major drawbacks of conventional lipid bilayer setups are long preparation times between each measurement. Stability of the phospholipid bilayer can pose another issue. Often several membranes have to be established before a measurement can be performed making it very time consuming to achieve adequate experiment numbers. New multichannel systems resolve this issue supporting fast formation of bilayers while allowing measurement of up to 16 different bilayers at a time. Here we utilize the "Orbit" multichannel system with a MECA16 chip by Ionera to measure TPC1 channel activity. We will present data generated by the "Orbit" system and a conventional bilayer setup using different channel constructs and charge carriers.

This work was supported by TRR SFB 152.

References: Sandip Patel, 2015; Function and dysfunction of two-pore channels; *Science Signaling* 8 (384)

185

A new role for the β subunit DPP10 in the heart – influence on Nav1.5 channel

F. Belau¹, K. Metzner¹, M. Schaefer¹, S. Kämmerer¹

¹University of Leipzig, Rudolf-Boehm-Institute of Pharmacology and Toxicology, Leipzig, Germany

Cardiac action potentials are generated and propagated through the coordinated activity of multiple ion channels, including voltage-gated sodium channels (Nav1) and potassium channels (like Kv1, Kv4). The voltage-gated Na^+ channel Nav1.5 initiates the cardiac action potential (AP), is essential for rapid depolarization, and is also known to control the AP duration in cardiomyocytes. The voltage-gated K^+ channel Kv4.3 is responsible for the early repolarization of action potentials in human heart. Similar to many membrane proteins, Nav1.5 and Kv4.3 have been found to be regulated by several interacting proteins. The transmembrane β subunit dipeptidyl aminopeptidase-like protein (DPP) 10 is known to interact with the Kv4.3 channel complex, modulating kinetics and voltage dependence. The overexpression of DPP10 in ventricular cardiomyocytes of rats revealed strong reduction of AP amplitude and significant slowing of AP upstroke velocity and AP duration, which could not be explained by the effects on cardiac Kv4 channels.

To study the potential influence of DPP10 on Nav1.5 channels, we performed whole-cell patch-clamp analysis of transiently transfected CHO-K1 cells, expressing SCN5A alone or with DPP10. Surprisingly, we observed significant effects of DPP10 on Nav1.5 channel voltage dependence and kinetics. Thus, the co-expression of DPP10 significantly shifted the half-maximal voltage of steady-state activation and steady-state-inactivation to more positive potentials compared to Nav1.5 channels alone. In addition we analysed the effects of DPP10 on the kinetics Nav1.5 currents. While time to current peak was not affected in cells co-expressing Nav1.5 and DPP10 compared to Nav1.5 alone, DPP10 slightly accelerated the inactivation. In addition, the time course of recovery from inactivation was clearly accelerated in cells expressing both Nav1.5 and DPP10 compared to Nav1.5 alone.

In summary, we provide first evidence that DPP10 not only interacts with Kv4 channels, but also influences Nav1.5 channels modulating the depolarization as well as the early repolarization phase of the cardiac AP. Therefore, it becomes likely that these ion channels are part of large, multi-protein complexes, and that the pore-forming subunits Kv4.3 and Nav1.5 behave very differently depending on the expression of its associated proteins like DPP10.

186

Analysis of the role of TRPC channels for calcium homeostasis in cardiac fibroblasts

A. Marx^{1,2}, J. E. Camacho-Londono^{1,2}, V. Tsilovskyy^{1,2}, A. Dietrich³, L. Birnbaumer⁴, M. Freichel^{1,2}

¹Universität Heidelberg, Pharmakologisches Institut, Heidelberg, Germany

²DZHK (German Centre for Cardiovascular Research), Heidelberg/Mannheim, Germany

³TU München, Institut für Pharmakologie und Toxikologie, München, Germany

⁴Universidad Nacional de San Martín, IIB-INTECH, Buenos Aires, Argentina

Cardiac fibroblasts (CF) comprise the most abundant cell type of the mammalian heart and it is known that they contribute to maladaptive cardiac remodeling processes. In response to pressure or volume overload, ischemia-reperfusion injury or myocardial infarction, cardiac fibroblasts proliferate and transdifferentiate into myofibroblasts which produce collagen and pro-hypertrophic cytokines influencing cardiomyocyte function and size. It was shown that β -adrenergic stimulation of CFs with isoproterenol leads to Angiotensin II (AT-II) production and autocrine stimulation of these cells (Jaffre et al., 2009). Activation of Phospholipase C triggered by AT-II leads to formation of Inositol trisphosphate (IP_3) and subsequent release of calcium from intracellular stores as well as calcium entry across the cell membrane. The focus of our research is the identification of the plasmalemmal channel proteins such as TRPC channels mediating this calcium entry, and whether these calcium entry pathways in CFs contribute to pathological remodeling. To date the precise role of calcium entry for these pathological processes is largely unknown. TRPC channels are candidates for the analysis of calcium homeostasis in CF. Recently, we showed that TRPC1/C4-deficient mice are protected from maladaptive cardiac remodeling after neurohumoral stimulation or pressure overload, respectively, which can be explained by a significant reduction of a Background Ca^{2+} -Entry (BCGE) pathway in cardiomyocytes; this BCGE is enhanced by stimulation with agonists such as isoproterenol or angiotensin II and it critically depends on TRPC1 and TRPC4 (Camacho Londoño et al., 2015). Nevertheless, the role of

TRPC1/C4 for calcium homeostasis in CFs has not been analyzed so far. We established an *in vitro* model that allows the analysis of calcium release and entry triggered by several (patho)physiological agonists in cultured primary adult CFs from mice. CFs were isolated using Langendorff-perfusion and were cultured for maximal 6 days. Our results show that there is no difference in 100 nM AT-II induced Ca^{2+} -release or Ca^{2+} -entry in TRPC1/C4-deficient CF compared to WT. To evaluate whether the lack of TRPC1/C4 can be compensated by other TRPC channels we currently analyze CFs from TRPC Hepta KO mice lacking all seven TRPC channel proteins concerning AT-II induced Ca^{2+} -release and Ca^{2+} -entry and we will also analyze the influence of other agonists on CFs which are known to evoke a longer lasting rise in the $[Ca^{2+}]_i$, like isoproterenol, 5-HT, thrombin and Endothelin-1.

Supported by: Klinische Forschergruppe 196 and DZHK.
Camacho Londoño JE et al. *Eur Heart J* 36(33): 2257-2266
Jaffre F et al. *Circ Res* 104(1): 113-123

187

Do Kv7.1 channels contribute to control of arterial vascular tone?

J.-Y. Tano¹, D. Tsvetkov², M. Gollasch², M. Kaßmann², J. Schleifenbaum², C. Lan³, J. Voelkl⁴, Y. Huang⁵

¹Universität Würzburg, Pharmacologie, Würzburg, Germany

²Max Delbrück Center for Molecular Medicine, ECRC, Berlin, Germany

³Xiamen Zhongshan Hospital, Xiamen, Germany

⁴University of Tübingen, Physiologie, Tübingen, Germany

⁵Lo Kwee-Seong Integrated Biomedical Sciences, Hong Kong, Germany

Cardiovascular and metabolic diseases are currently the primary cause of morbidity and mortality in the western world and are spreading to the rest of the world following globalization. Adipose tissue, in particular perivascular adipose tissue (PVAT) is recognized as an important player in the development of these diseases. The release of relaxing factor(s) from the PVAT has been a matter of interesting and highly spirited debates about its nature, the channels that govern its activities and its role in vascular dysfunction. Data from our laboratory indicate that Adipose-Derived Relaxing Factor (ADRF) is an important player, however the potential channels necessary for its downstream activities are still under study. Our recent research primarily focuses on Kv7.1 channels, which are known to be expressed in vascular smooth muscle cells.

Kv7.1 voltage-gated potassium channels are expressed in vascular smooth muscle cells (VSMC) of diverse arteries, including mesenteric arteries. Based on pharmacological evidence using R-L3 (Kv7.1 opener), HMR1556, chromanol-293B (Kv7.1 inhibitors), these channels have been suggested to be involved in the regulation of vascular tone. However, the specificity of these drugs *in vivo* is uncertain. We used *Kcnq1-/-* mice to determine whether Kv7.1 plays a role in the regulation of arterial tone. We found that R-L3 produces similar concentration-dependent relaxations ($EC_{50} \sim 1.4 \mu M$) of wild-type (*Kcnq1+/+*) and *Kcnq1-/-* arteries pre-contracted with either phenylephrine or 60 mM KCl. This relaxation was not affected by 10 μM chromanol-293B, 10 μM HMR1556 or 30 μM XE991 (pan-Kv7 blocker). The anti-contractile effects of PVAT were normal in *Kcnq1-/-* arteries. Chromanol-293B and HMR1556 did not affect the anti-contractile effects of perivascular adipose tissue (PVAT). Isolated VSMCs from *Kcnq1-/-* mice exhibited normal peak K_v currents. The Kv7.2-5 opener retigabine caused similar relaxations in *Kcnq1-/-* and wild-type vessels. We conclude that Kv7.1 channels are apparently not involved in the control of arterial tone by α_1 adrenergic vasoconstrictors and PVAT. In addition, R-L3 is an inappropriate pharmacological tool for studying the function of native vascular Kv7.1 channels in mice.

Toxicology – Biotransformation and toxicokinetics

188

DPS1000 – dermatomized porcine skin as ready to use research tool

U. Bock¹, A. Meier², B. Lecher²

¹Bock Project Management, Trier, Germany

²mfd Diagnostics GmbH, Wendelsheim, Germany

Introduction: According to international guidelines [1-7], both human and animal skin *in vitro* models have been used and validated to predict percutaneous penetration in humans. Excellent correlations have been found for domestic pig as surrogate for human skin [8-9].

Material and Methods:

Tissue

The skin samples are descended from female pigs of German Landrace (50 kg weight, approx. 4 month). Process approved under German Welfare Law. After narcotization and euthanization the animals were shaved with an electric shaver, washed and dried. Microbiological investigation swabs from 10 different skin area (Fig. 1) were taken before next preparation step. Skin areas were cut, stretched and subcutaneous fatty tissue was carefully removed. The skin was harvested at thickness of 1.000 μm by dermatome. After dermatomization, samples were taken for histological examination. Skin disks of 30 mm were punched out from the frozen skin stripes and stored at -20°C.

HPLC and Skin Absorption

Waters Corporation HPLC containing 2767 Sample Manager, 2545 binary gradient pump, 2998 PDA detector (optional: 3100 electron spray mass spectrometer); Column: NUCLEODUR® 100-5 C18 ec 50mm x 4.0 mm ID.

Hanson Microette™ Vision® Diffusion Test System (Hanson Vision® AutoPlus™ autosampler/AutoFill™ collector, 6-Cell Drive System with Vertical Diffusion Cell "Standard"). The permeation experiment was performed over a period of 48 h at 32°C. The dosage compartments of each cell were filled with approximately 300 μL of the caffeine solution (10 mg/mL). Samples of 1 mL are taken after 0, 12, 24, 36 and 48 hours from receptor medium of each cell. Aliquots from each VDC are analyzed by HPLC in duplicate.

Results:

Microbiology

Staphylococcus spp. were found explicitly on pig skin surface. Bacteria are facultative anaerobe, gram-positive bacteria that are physiologically colonizing the skin, oropharynx and the gastrointestinal tract.

Histology and Skin thickness

HE staining and mechanical skin thickness determinations confirmed intact dermatomizing process of skin (Fig. 2). Thickness was in the order of magnitude between 897 to 1.230 μm and intra variations were less than 10 %.

Caffeine Skin absorption

Permeability coefficients and lag-phases recorded are in the same order of magnitude of previous work [10], demonstrating intact barrier properties of the membranes after 3 month storage process. Until today, intra-assay variations are superior or equal to inter-regional and inter-animal variations.

Discussion: Well characterized DPS1000 provides ready to use research tool for locally and systemic skin investigations. Ongoing experiments will cover skin structure analysis by Raman Spectroscopy, Biophotonics and storage impact on skin barrier function.

References:

- [1] OECD 428, 2004
- [2] OECD TG 28, 2004
- [3] OECD Series on Testing and Assessment No. 156, 2011
- [4] EMA Guideline on quality of transdermal patches – Annex 1, 2014
- [5] EFSA, Guidance on Dermal Absorption, 2012
- [6] EU, SCCS, Basic criteria for the *in vitro* assessment of dermal absorption of cosmetic ingredients, 2010
- [7] WHO, Dermal Absorption, Environmental Health Criteria 235, 2006
- [8] Takeuchi H. et al., *Biol Pharm Bull.* 2011
- [9] Barbero AM., Frasca HF., *Toxicol In Vitro.* 2009
- [10] Schäfer-Korting M. et al., *ATLA* 2008

Abb. 1

Fig. 1: Schematic representation of pig skin areas L - left side, R - right side, E - ear, Sh - shoulder, H - hip

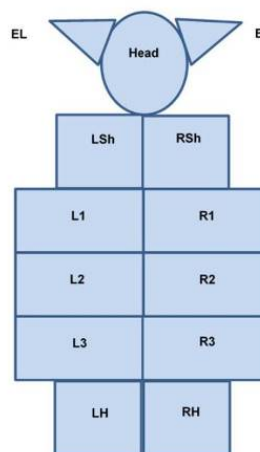


Abb. 2

Fig. 2: HE Stain of histological slices of porcine skin after the dermatomization process (Area RH): A: 5x magnification, B: 10x magnification

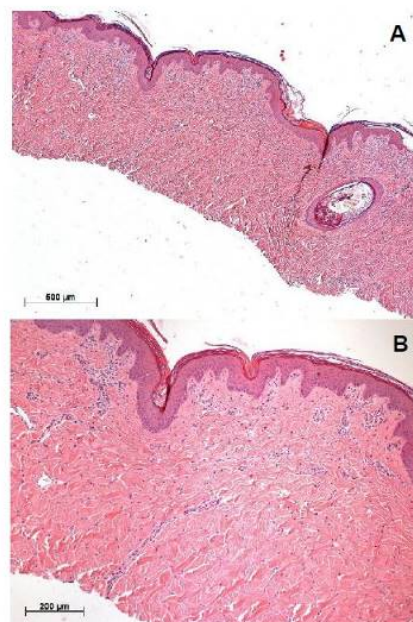


Abb. 3

Tab. 1: Papp values on caffeine permeation on two different animals during 48 h period, n=4, lag phases of approx. 6-8 h.

parameter	cell 1	cell 2	cell 3	cell 4	mean Papp [cm/s]	SD Papp [cm/s]
plg 1/area	R1	R2	R2	R3	-	-
Papp [cm/s] x 10 ⁷	1.38	2.26	1.03	0.94	1.40	0.52
plg 2/area	R2	R2	R2	R2	-	-
Papp [cm/s] x 10 ⁷	5.11	2.20	3.26	3.88	3.61	1.05

189

Method for identification of low soluble, biopersistent susts (GBS) – comparison of intratracheal installation and subacute inhalation

O. Creutzenberg¹, T. Hansen¹, S. Schuchardt¹, T. Tillmann¹, J. Knebel¹
¹Fraunhofer ITEM, Hannover, Germany

Respirable biopersistent granular dusts (GBS) should fulfill the criteria of i.) a negligible solubility in physiological lung fluid that ii.) do not exhibit a specific surface chemistry-related toxicity at volumetric non-overload conditions in lungs. In 2012, the MAK Commission derived a new threshold value of 0.3 mg/m³ for GBS with a density of 1, recognizing that at this concentration a chronic inflammation and increase of the lung cancer risk will not occur. – The objectives of the project were i.) to determine an experimental dissolution value for 'low soluble' GBS using six candidate dusts; ii.) in addition, to measure the inflammatory response in lung lavage fluid and to decide on the criterion 'inert dust'; iii.) to investigate whether nanoscaled dusts could possibly fulfill the criteria to be included in the GBS class. – Six micro- and nanoscaled dusts (one of them a well-characterized inert TiO₂ dust (microscaled; rutile modification) were compared analysing the solubility in the lung fluid (day 3, 28 and 90) and the lung toxicity after intratracheal instillation in rats (day 3 and 28): TiO₂ (rutile, micro), TiO₂ (anatase, nano), Eu₂O₃ (micro-nano mixed), BaSO₄ (micro), ZrO₂ (micro) and amorphous SiO₂ (nano). Two doses of 0.5 and 1.5 µl per rat were administered to Wistar rats; these volume doses resulted in a non-overload and moderate overload of lungs, respectively. – The differential cell count showed only slight inflammatory cell levels after treatment with TiO₂ (rutile) and BaSO₄ (PMN < 5% after 3 days in the low dose group; < 15% in the high dose group; full recovery after 28 days). In contrast, the TiO₂ (anatase) showed a stronger response (PMN > 30% after 3 and 28 days). The rare earth Eu₂O₃ (micro-nano) dust showed the strongest effect (approx. 40% PMN after 3 and 28 days) including a red-coloured lung lavage fluid. µ-ZrO₂ and amorphous SiO₂ showed a strong acute response after 3 days, however, mostly complete recovery after 28 days. The low solubility criterion was met by the following dusts: TiO₂ (both) and ZrO₂. – Similar volumetric lung burdens were deposited in a parallel validation experiment (14-day subacute inhalations). Overall the physiological inhalation route confirmed the results obtained in the instillation study, thus suggesting the applicability of the latter as a tool for identification for GBS dusts. However, for nanoscaled dusts an individual toxicological characterization seems to be adequate.

The project was funded by the Federal Institute for Occupational Safety and Health (BAuA), Dortmund – F 2336 and F2364.

190

Activation of the human nuclear receptors AhR and CAR by different polycyclic aromatic hydrocarbons and their mixtures

S. Hesse¹, T. Füllborn¹, A. Braeuning¹, A. John², A. Seidel², A. Lampen¹
¹Bundesinstitut für Risikobewertung, Lebensmittelsicherheit, Berlin, Germany
²Biochemisches Institut für Umweltcarcinogene Prof. Dr. G. Grimmer-Stiftung, Großhansdorf, Germany

Polycyclic aromatic hydrocarbons (PAH) represent a complex mixture of compounds and occur in considerable amounts as contaminants in the environment and food. Some PAH have been demonstrated to be carcinogenic and mutagenic. Benzo[*a*]pyrene (BP), the most known and studied member of the potent carcinogenic PAH, is classified by IARC as group 1 carcinogen and is present in a wide variety of food items. However, other non-carcinogenic PAH such as pyrene (PYR) and fluoranthene (FA) are also found in substantial amounts in the diet and are strongly suspicious to cause interactive effects.

Reporter gene assays were used for analyzing interactive effects of a ternary mixture including BP, PYR and FA in relative proportions occurring in food on the nuclear receptors aryl hydrocarbon receptor (AHR) and constitutive androstane receptor (CAR). The observed activations were verified at the gene expression level in the human hepatoma cell line HepaRG.

Beside the well characterized ligand BP, 25 µM of PYR and 20 µM FA also activated the AhR, even though to a much lesser extent. No significant higher activation over the level of BP alone was reached when testing different PAH mixtures. However, in HepaRG cells the analysis of CYP1A1 gene expression as a model target gene of AhR showed synergistic effects after PAH co-exposure. In addition, the activation of human CAR was analyzed. PYR and FA are each strong agonists, whereas BP was less potent. For the ternary PAH mixture with BP a strong decrease of the induction was observed. This inhibiting effect was verified at the mRNA level using the model CAR target gene CYP2B6 in HepaRG cells.

In conclusion, really occurring mixtures with non-carcinogenic PAH can modulate the effects of carcinogenic PAH. Such effects warrant to be investigated in more detail to enhance our knowledge of interaction of PAH mixtures at the molecular level.

191

Development of MS- based immunoassays for Cytochrome P450 and transporter quantification

H. S. Hammer¹, O. Pötz¹, P. Artursson², C. Wegler²
¹Naturwissenschaftliches und Medizinisches Institut an der Universität Tübingen, Reutlingen, Germany
²Uppsala Universitet, Department of Pharmacy, Uppsala, Schweden

Cytochrome P450 enzymes and transporters are important for the turnover of pharmaceutical compounds. Their expression levels and activity influence bioavailability and convey drug-drug interactions. Moreover, transporters mediate barrier maintenance of several organs such as blood-brain-barrier and placenta-barrier. Overexpression of export transporters in tumors can lead to multiple drug resistance.

However, membrane associated proteins are difficult to quantify by conventional bioanalytical methods such as sandwich immunoassays because of their hydrophobicity. Antibody – based analysis of cytochrome P450 enzymes and transporters is challenging due to their sequence homology.

Therefore, we developed a test system for protein quantification which combines the sensitivity of immunoprecipitation and the specificity of mass spectrometry. This method is especially convenient for hydrophobic proteins because denatured samples are analyzed on peptide level. One peptide from each protein, which can be assigned unambiguously, is identified via tandem MS and quantified by means of an isotope labeled reference. Prior to MS-read-out, the peptides are enriched by antibodies which recognize a very short c-terminal epitope. These epitopes are selected in such way that they are common in peptides derived from target proteins and therefore allow the analysis of protein groups with few antibodies.

The major advantage of this method is that whole cell or tissue lysates – without preparation of microsomal fractions – can be used for quantification by LC-MS. Also, samples from different model organisms can be analyzed with the same assay which enhances the comparability of experiments.

Currently, we have established assays with 25 antibodies covering 15 Cytochrome P450 enzymes and 17 transporters in eight different species – in total 92 proteins.

References: Gottesman MM, Fojo T, and Bates SE. 2002. Multidrug resistance in cancer: role of ATP-dependent transporters. *Nature reviews*. Cancer Eisen D, Planatscher H, Hardie DB, Kraushaar U, Pynn CJ, Stoll D, Borchers C, Joos TO, and Poetz O. 2013. G protein-coupled receptor quantification using peptide group-specific enrichment combined with internal peptide standard reporter calibration. *Journal of proteomics*:

Hoeppe S, Schreiber TD, Planatscher H, Zell A, Templin MF, Stoll D, Joos TO, and Poetz O. 2011. Targeting peptide termini, a novel immunoaffinity approach to reduce complexity in mass spectrometric protein identification. *Molecular & cellular proteomics* Weiss F, Schnabel A, Planatscher H, van den Berg BH, Serschnitzki B, Nuessler AK, et al. 2015. Indirect protein quantification of drug-transforming enzymes using peptide group-specific immunoaffinity enrichment and mass spectrometry. *Scientific reports* Weiss F, van den Berg BH, Planatscher H, Pynn CJ, Joos TO, Poetz O. 2014. Catch and measure-mass spectrometry-based immunoassays in biomarker research. *Biochimica et biophysica acta*.

192

PBTK modeling of selected potential endocrine modulators: *In vitro-in vivo* extrapolation (IVIVE) and *in silico/in vitro* based risk assessments

C. Haase¹, E. Fabian¹, T. Ramirez¹, B. van Ravenzwaay¹, R. Landsiedel¹
¹BASF SE, Experimental Toxicology and Ecology, 67056 Ludwigshafen am Rhein, Germany

Physiologically Based Toxicokinetic Modeling (PBTK) is an *in silico* tool to predict compound kinetics based on test substance related properties and physiological parameters of the organism. PBTK is a key element for inverse dosimetry to relate effect concentrations *in vitro* to external, e.g. oral doses. In our investigations, we use 8 compartment models for the rat including adrenals and testes or ovaries. Test substance specific properties taken for PBTK modeling are molecular weight and log_{P_{OW}} as well as IVIS based tissue specific partition coefficients, hepatic clearance, intestinal permeability and plasma protein binding. Berkeley Madonna Software was applied to solve consequent differential equations.

Here we present the above described model for the 3 test substances bisphenol A (BPA), fenarimol (FEN) and ketoconazole (KETO). Using the lowest effect concentrations (LOECs) of BPA, FEN and KETO from 1) an *in vitro* yeast based assays with human estrogen and androgen receptor combined with a reporter gene and 2) the interaction of steroidogenesis model calculations were made to relate *in vitro* concentrations to oral doses in the rat. Model calculations, based on *in vitro* LOECs of 10 µM (BPA), 3 µM (FEN) and 0.01 µM (KETO), for concentrations in target organs resulted in estimated oral LOELs of 16, 4 and 0.04 mg/kg. When calculations were made for plasma levels oral LOELs were estimated to be 608, 77 and 16 mg/kg for BPA, FEN and KETO, respectively. When compared to existing *in vivo* data with endocrine related LOELs of 375 mg/kg bw day for BPA (1), 50 mg/kg day for FEN (2) and 6 mg/kg day for KETO (3), it can be concluded that for the exemplary test substances addressed, IVIS related risk assessment approaches based on target tissues seems overpredictive, whereas plasma related LOELs were closer to the *in vivo* situation, 1 Kanno J. et al. (2003) *Environ Health Perspect* 111, 785-794. 2 U.S. EPA (2007) <http://www.epa.gov> (26.09.2015). 3 Shin J-H. et al. (2006) *Arch Toxicol* 80, 797-803.

Toxicology – Organtoxicity (immunotoxicity, blood, and kidney)

193

Structure-dependent activation of PXR and PXR-mediated induction of CYP3A4 expression by hepatotoxic pyrrolizidine alkaloids

C. Luckert^{1,2}, A. Braeuning¹, A. Lampen¹, S. Hessel¹¹Bundesinstitut für Risikobewertung, Lebensmittelsicherheit, Berlin, Germany²Universität Potsdam, Institut für Ernährungswissenschaft, Potsdam, Germany

1,2-unsaturated pyrrolizidine alkaloids (PA) are hepatotoxic plant metabolites and are found predominantly in plants of the plant families *Boraginaceae*, *Asteraceae*, and *Fabaceae*. Acute PA poisoning by food contamination causes severe damage to the liver. Long-term, sub-lethal doses may cause cumulative damage or cancer.

To study the activation of the nuclear receptor PXR a GAL4/UAS-based PXR transactivation assay was used. The PXR-mediated induction of CYP3A4 promoter activity was investigated using a PXR-dependent CYP3A4 reporter gene assay. CYP3A4 induction was analyzed at the mRNA and protein levels in HepG2 cells using qPCR and Western Blot. To cover the most frequently occurring PA structures (retronecine, heliotridine and otonecine type as well as monoester, open-chain diester and cyclic diester) the four PA senecionine, heliotrine, echimidine and senkirkine were selected as representative PA for initial analyses.

Out of the four investigated PA only echimidine activated PXR. Accordingly, PXR-mediated induction of CYP3A4 promoter activity could only be detected for echimidine. CYP3A4 induction by echimidine was verified at the mRNA and protein level in HepG2 wildtype and HepG2 PXR-overexpressing cells. Taking into consideration the structure of the four PA it was hypothesized that only open-chain diesters might act as PXR agonists. The set of analyzed PA was thus extended by five additional PA of the monoester, open-chain diester or cyclic diester type. It was shown that only the open-chain diesters, echimidine and lasiocarpine, activate PXR.

In conclusion: PXR activation and PXR-mediated induction of CYP3A4 expression by PA are structure-dependent. Data suggest that only open-chain diesters act as PXR agonists. This might imply a structure-dependent mode of action of PA resulting in hepatotoxicity that is dependent on PA structure.

194

Investigation of the contribution of different NADPH-oxidases to angiotensin II-induced oxidative stress in kidney and heart

C. Hartmann¹, Z. Anna¹, S. Kretschmar¹, N. Spicker¹, N. Schupp¹¹Heinrich-Heine Universität Düsseldorf, Institut für Toxikologie, Düsseldorf, Germany

Introduction: In higher concentrations, the blood pressure regulating hormone angiotensin II (Ang II), leads to vasoconstriction, hypertension and oxidative stress by activation of the renin angiotensin system (RAS). Here we investigate if NADPH-oxidases are responsible for RAS-mediated oxidative stress in kidney and heart. NADPH-oxidases (7 isoforms are known, Nox 1-5, Duox 1 & 2) are membrane-bound enzymes that produce reactive oxygen species (ROS) for example during the immune response and cell signaling.

Material and Methods: To clarify the role of NADPH-oxidases, wildtype mice and Nox 1-, Nox 2- and Nox 4-deficient mice were equipped with osmotic minipumps, delivering Ang II in a concentration of 600 ng/kg during 28 days to stimulate high blood pressure. Kidney and heart were investigated for steady-state ROS levels and DNA damage (DNA single and double strand breaks).

Results: In wildtype mice, Ang II leads to hypertension, a declined renal function, formation of ROS in kidney and heart and to DNA single and double strand breaks in the kidney. All Nox-knockout mice exhibited Ang II-mediated hypertension and albuminuria. The lack of Nox 2 and Nox 4 could neither protect from the formation of oxidative stress in the kidney nor from DNA double strand breaks in the kidney. Initial findings from the Nox 1-knockout mouse do not show an increase in DNA double strand breaks in the kidney.

Discussion: Contrary to published results of Nox 1-knockout mice, we observed a constant rise in blood pressure over the treatment period compared to the control. This can possibly be due to different Ang II doses. In Nox 4-knockout mice we observed increased oxidative stress and increased renal DNA damage already in untreated control animals, which is in line with reports suggesting a protective effect of Nox4.

Conclusion: Separate eliminations of 3 NADPH-isoforms did not allow the identification of the enzyme which is responsible for Ang II-induced oxidative stress. A possible explanation is that oxidative stress is caused by more than one Nox-isoform or other enzymes like xanthine oxidase or nitrogen synthase take major part in the formation of ROS.

195

Of mice (rats, cats, dogs, monkey) and men – how to measure kidney biomarkers across species

B. van den Berg¹, H. Planatscher¹, X. Zhou², J.-C. Gautier³, T. O. Joos⁴, P. Olté¹¹NMI, Proteinanalytik, Reutlingen, Germany²NCSED National Center for Safety Evaluation of Drugs, Beijing, China³Sanofi, Paris, Frankreich⁴NMI, Reutlingen, Germany

Introduction and Objectives: There is a need for reliable biomarker assays to detect organ toxicity induced by drug candidates. In the last 50 years about 60 drugs were withdrawn from the market due to liver and/or kidney damage. For the detection of drug-induced organ injury, safety-tox studies in rodents, dogs, non-human primates and humans are mandatory in the drug development process. Currently, several protein biomarkers for kidney, liver and cardiovascular organ toxicity are being clinically validated by international consortia like the Safer and Faster Evidence-based

Translation (SAFE-T) or the Predictive Safety Consortium (PSTC). We are developing mass-spectrometry-based immunoassays suitable for the detection of these markers in animal models to support these efforts

Method: Urinary proteins are proteolytically digested to peptides using trypsin. Subsequently synthetic isotope-labelled peptide standards are spiked in at known concentrations. We employ multi-specific antibodies (TXP-antibodies) targeting C-terminal amino acid motifs for the enrichment of peptides derived from the protein biomarkers. Finally, the protein biomarkers are quantified using nanoLC-Parallel Reaction Monitoring-MS. The use of our group-specific TXP-antibodies allows protein analysis of samples from different species using the same antibody.

Results and Discussion: We established an MS-based Immunoassay platform for the analysis of kidney (DIKI) injury protein biomarkers in urine across 5 species; human, cynomolgus, mouse, rat and dog. We analyzed the potential DIKI biomarkers aquaporin 2, podocin, synaptopodin, retinol-binding protein 4, clusterin and osteopontin in urine samples from toxicity studies in cynomolgus monkeys, rodents and humans.

Conclusion: The application of group-specific TXP-antibodies and mass spectrometry allows the quantification of biomarkers in urine of all relevant model organisms. The results strongly support the validation of translational drug-induced organ injury protein biomarkers.

Toxicology – Neurotoxicity, incl. neurodevelopment

196

C. elegans as a model organism to analyze neurotoxicity induced by platinating agents

S. Honnen¹, A. Wellenberg¹, J. Schmutzler¹, S. Hartmann¹, B. Crone², J. Bornhorst³, G. Fritz²¹University Hospital Düsseldorf, Toxicology, Düsseldorf, Germany²University of Münster, Institute of Inorganic and Analytical Chemistry, Münster, Germany³University of Potsdam, Institute of Nutritional Science, Nuthetal, Germany

Although effective anticancer-therapeutic regimen are available, they are accompanied by severe adverse effects on normal tissue, for instance chemotherapy induced peripheral neuropathy (CIPN) caused by platinum compounds. The pathophysiology of this clinically highly relevant side-effect is still unknown and neither prophylaxis nor specific treatment is available. Therefore, further research elucidating the underlying molecular mechanisms of platinating anti-tumor drugs leading to CIPN is required as basis for future development of preventive or therapeutic strategies. In general, platinum compounds lead to cell death mainly via DNA damage induction (mostly intrastrand-crosslinks) and through interference with the redox homeostasis of cells.

Here, we introduce and suggest the well-known nematode model organism *C. elegans* to elucidate mechanisms of neurotoxicity triggered by platinating agents. So far, we determined doses for cis- and oxaliplatin, which have only moderate effects on development, reproduction and body movement (muscular *read-out*). However, these doses are sufficient to trigger apoptosis in *C. elegans* and to induce a considerable amount of 1,2-intrastrand crosslinks in DNA (measured by south-western blotting). Even more important they lead to strong neurotoxicity in a functional *read-out* (pharyngeal pumping). With regard to redox homeostasis, we determined the oxidative stress resistance showing that e.g. cisplatin sensitizes *C. elegans* to reactive oxygen species (ROS), which could be prevented if worms were co- or pretreated with N-acetylcysteine. Furthermore we determined the level of ROS in living *C. elegans* after treatment with platinating agents and also in combination with protective compounds.

Using the advantages of *C. elegans* as a genetic model system, we will further clarify the relevance of different defense mechanisms, including DNA repair (nucleotide excision repair, base excision repair), detoxification systems (antioxidative stress factors, metallothioneins) as well as drug transporters and signaling proteins. This will be achieved by using RNA interference approaches that allow targeting either the whole animal or specific tissues (i.e. neurons) only. First results of this approach will be presented. Finally we aim to use this setup to identify neuroprotective compounds that prevent chemotherapy induced peripheral neuropathy induced by platinating anti-tumor drugs.

197

Role of vimentin in uptake of *Clostridium botulinum* C3 exoenzyme

A. Rohrbeck¹, S. Hagemann¹, A. Pich¹, M. Hötje², G. Ahnert-Hilger², I. Just¹¹MHH, Institut für Toxikologie, Hannover, Germany²Charite-Universitätsmedizin, Centrum für Anatomie, Berlin, Germany

Clostridium botulinum C3 exoenzyme (C3) exclusively ADP-ribosylates RhoA, B and C leading to reorganization of the actin cytoskeleton and morphological changes. In addition to the enzyme-based inhibition of Rho-GTPases, C3 promotes in an enzyme-independent manner axonal and dendritic growth in neurons. As C3 lacks the canonical binding and translocation domains of bacterial protein toxins, cell entry is currently not well understood. Based on overlay assays and mass spec analyses the intermediate filament vimentin was identified as the putative membrane receptor for C3. Knock down of vimentin by siRNA and application of the selective vimentin disruptor acrylamide led to a significantly delayed uptake of C3. Moreover, addition of extracellular vimentin to cells induced an enhanced uptake of C3. Proof of principle experiments in astrocytes and neurons from vimentin knock out mice showed C3-induced morphological changes (astrocyte stellation and axon growth) to a reduced extent and a significantly delayed uptake of C3 compared to wild type cells. As vimentin knock out did not completely inhibit C3 uptake into cells, an additional uptake mechanism or additional receptor for C3 is likely. Nevertheless, our data reveals that C3 employs a specific endocytosis mechanism with involvement of the intermediate filament vimentin to gain access to host cells.

198

New insights in toxicokinetics and toxicity of organic and inorganic mercury species regarding the central nervous systemH. Lohren¹, R. Fitkau¹, J. Bornhorst¹, H.-J. Galla², T. Schwerdtle¹¹Universität Potsdam, Lebensmittelchemie, Nuthetal, Germany²Universität Münster, Biochemie, Münster, Germany

The primary target organ of organic Hg species-mediated toxicity is the central nervous system (CNS). Humans are exposed to organic Hg mainly in the form of methylmercury (MeHg) via the consumption of contaminated fish and other seafood products. In terrestrial food sources Hg is mostly found as inorganic Hg. Thiomeralsal is a further organic Hg compound which is used as a preservative in medical preparations. Exposure to organic Hg promotes primarily neurological effects. The understanding of transfer mechanisms regarding the CNS is an important precondition for an evaluation of Hg species-induced neurotoxicity. Thus, primary porcine *in vitro* models of the blood-brain barrier and the blood-cerebrospinal fluid (CSF) barrier were used to investigate effects of MeHgCl₂, thiomeralsal and HgCl₂ on the barriers as well as transfer properties into and out of the CNS *in vitro*. The results show significant transfer differences of the various incubated species as well as in the different barrier systems. Whereas the blood-brain barrier seems to account for the transfer of organic Hg species from the blood side to the brain side, these species are transferred in the contrary direction by the blood-CSF barrier. Inorganic HgCl₂ was not transferred across both brain barriers towards the brain side but was able to leave the brain side across the blood-brain barrier.

Additionally, cytotoxic effects of the Hg species by themselves as well as the combination of organic and inorganic Hg species have been investigated in human astrocytes and human differentiated neurons. Differentiated neurons were much more sensitive towards all Hg species. Organic species exerted stronger cytotoxic effects in both cell types as compared to HgCl₂. Interestingly, a coincubation of organic and inorganic Hg species led to an increased cytotoxicity in the astrocytes. This cocytotoxic effect is currently investigated in differentiated neurons.

The species-specific differences with respect to both, effects on and transfer across the blood-brain and the blood-CSF barrier *in vitro* as well as toxic effects in brain target cells, clearly emphasizes the necessity for comparative analyses.

199

Inference of several classes of environmental chemicals with human neural crest migrationX. Dolde¹, J. Nyffeler¹, C. Karreman¹, M. Leist¹¹Universität Konstanz, Konstanz, Germany

Introduction: The neural crest is a multipotent stem cell population that arises at the neural plate border during early fetal development. Neural crest cells (NCCs) migrate to target sites in the periphery, where they differentiate into multiple cell types, including melanocytes, cranial bones and peripheral neurons. Failure of NCC migration can lead to severe disorders, such as Hirschsprung's disease.

Aim: To test whether toxicants interfere with human NCC migration, a high-throughput migration assay was established. This test system was used to screen an 80 compound library of potential developmental toxicants.

Methods: NCCs were derived from human embryonic stem cells. The cells were allowed to migrate for 24 h before toxicants were added to the cells. Migration and viability of the cells were then measured after another 24 h by high-content image analysis and a custom-developed software package.

Results: The screening library was assembled by the US national toxicology program (NTP) and consisted of different substance classes, e.g. organophosphates, organochlorines, drug-like compounds, pesticides and polycyclic aromatic hydrocarbons (PAHs). Out of the tested potential developmental toxicants, 26 compounds reduced NCC migration at non-cytotoxic concentrations. Hit-confirmation testing confirmed 23 of the compounds as concentration-dependent inhibitors of NCC migration. Among the potential developmental toxicants identified here, there were several organophosphates (e.g. chlorpyrifos) and drug-like compounds as well as polybrominated diphenyl ethers (PBDEs) and organochlorine pesticides (e.g. DDT and dieldrin), while none of the tested PAHs inhibited NCC migration. The negative controls in the screening library, like acetylsalicylic acid, acetaminophen and saccharin, proved to be non-toxic.

Conclusion/Outlook: The newly established test system allows screening of potential developmental toxicants in a high throughput manner for interference with human NCC migration. Confirmation in other types of migration assays is ongoing, and selected compounds from amongst the screen hits are undergoing mechanistic evaluation.

200

CYLD links oxidative stress to mechanisms of regulated necrosis in a model of erastin-mediated ferroptosis in neuronal cellsI. Eisenbach¹, G. K. Ganjam¹, L. Hoffmann¹, C. Culmsee¹¹Universität Marburg, Institut für Pharmakologie und Klinische Pharmazie, Marburg, Germany

Oxidative stress is regarded as a major trigger for neuronal dysfunction and death in the ageing brain and in multiple neurodegenerative disorders. How oxidative stress mediates neuronal death and whether the associated mechanisms are accessible for therapeutic intervention strategies is not clarified. Increasing evidence suggests, however, that oxidative stress triggers molecular mechanisms of regulated necrosis that involve the activation of receptor interacting protein 1 (RIP1) independently of death receptor activation.

Here, we show that erastin-induced ferroptosis which involves inhibition of the glutamate-cystine transporter (Xc⁻), glutathione depletion and lethal formation of reactive oxygen species (ROS), triggers mechanisms of regulated necrosis independent of TNF α -signaling. In hippocampal HT-22 cells erastin promotes activation of RIP1 and subsequent RIP1-RIP3 necrosome formation which has been investigated as a hallmark of regulated necrosis². In fact, silencing of RIP1 by siRNA or by the RIP1 inhibitor necrostatin-1 prevents ferroptosis-induced cell death whereas the ferroptosis inhibitor ferrostatin-1 fails to protect cells against TNF α -induced classical necroptosis, a form of

programmed cell death that is mediated by receptor interacting protein-1 (RIP1) and RIP3 kinases downstream of death receptor activation (e.g. tumor necrosis factor receptor TNFR)^{2,3}. Recently, a genome-wide siRNA screen linked cylindromatosis (CYLD) to RIP1/RIP3-dependent necroptosis⁴ and also in the present paradigm of ferroptosis, CYLD depletion promotes neuronal survival and decreases RIP1-RIP3 complex formation, suggesting a role of CYLD in intrinsic pathways of regulated necrosis triggered by oxidative stress.

¹ Dixon SJ et al. (2012) Ferroptosis: an iron-dependent form of nonapoptotic cell death. *Cell*. **149**(5), 1060-72

² Vandenabeele P et al. (2010) Molecular mechanisms of necroptosis: an ordered cellular explosion. *Nature Rev. Mol. Cell Biol.* **11**, 700-714

³ Vanden Berghe T et al. (2014) Regulated necrosis: the expanding network of non-apoptotic cell death pathways. *Nat Rev Mol Cell Biol* **15** (2), 135-147

⁴ Hitomi J et al. (2008) Identification of a molecular signaling network that regulates a cellular necrotic cell death pathway. *Cell* **135**, 1311-1323

Toxicology – Reproductive/developmental toxicity

201

Effects of daclatasvir, ledipasvir and sofosbuvir alone and in combination in the embryonic stem cell test (EST)S. Saube¹, F. Partosch¹, R. Stahlmann¹¹Charité Universitätsmedizin Berlin, Institut für Klinische Pharmakologie und Toxikologie, Berlin, Germany

The NS5A inhibitor daclatasvir is used in combination with other antivirals such as the polymerase inhibitor sofosbuvir for treatment of chronic infection with the hepatitis C virus. Daclatasvir is embryotoxic and teratogenic in rats and rabbits at exposures at or above the clinical exposure. In contrast, no teratogenic effects were observed in rat and rabbit developmental toxicity studies with ledipasvir, another NS5A inhibitor.

We studied these compounds in the embryonic stem cell test (EST) alone and in combination with sofosbuvir. The NS5A inhibitors were obtained from Selleckchem, the main metabolite of sofosbuvir, PSI-6202, was from MedChem Express. Murine embryonic stem cells (ES-D3) were obtained from ATCC. They were kept in Iscove's Modified Dulbecco's Medium (IMDM). Substances were dissolved in DMSO at a final DMSO-concentration of 0.1% in the culture medium. A cytotoxicity assay as well as a differentiation assay were performed. After 10 days in culture the cells were evaluated. Cytotoxicity was measured by an MTT test. Differentiation into contracting myocardial cells was determined using direct phase contrast microscopy. The substances were tested at concentrations between 0.1 and 30 mg/l, which is a broad coverage of the therapeutically relevant concentrations reached in patients.

At a concentration of 10 mg daclatasvir / l medium and higher the substance inhibited differentiation of cells. We observed contracting myocytes in 23, 22 and 2 wells out of 24 wells in total at concentrations of 1, 3 and 10 mg/l. At 30 mg/l no differentiation was observed. Effects on cell viability were observed at 30 mg/l. Unexpectedly, we found a higher potency with ledipasvir. At the low, therapeutically relevant concentration of 1 mg/l this NS5A-inhibitor showed a clear impact on differentiation with 6 out of 24 wells affected and no differentiation at higher concentrations. Addition of sofosbuvir or its main metabolite PSI-6206 at concentrations up to 30 mg/l had no influence on the concentration effect curves established for daclatasvir or ledipasvir. This is the first indication of an embryotoxic potential of ledipasvir. The difference to the results from the routinely performed animal experiments is unknown. Possibly, metabolic activity in the maternal organism is responsible for this discrepancy.

202

Comprehensive assessment of reproductive toxicity of dimoxystrobin: no classification warrantedS. Melching-Kollmuss¹, C. Werner¹, I. Fegert¹¹BASF SE, Ludwigshafen, Germany

Dimoxystrobin is a European-registered pesticidal active ingredient. Biologically it is acting as an inhibitor of the fungal respiratory chain. For the purpose of European registration a full set of toxicological studies has been conducted with dimoxystrobin, including reproduction toxicity studies (according to the most recent OECD TG 416) and developmental toxicity studies (OECD TG 414) in rats and rabbits.

Dimoxystrobin interferes with the iron transport in rats and mice. This leads to lower serum iron levels and anemia in rats after repeated exposure. This holds true for treated dams and offspring in reproduction toxicity studies. Furthermore, offspring effects seen at the high dose of the 2-generation toxicity study were a hypochromic microcytic anemia, impaired body weight development, which only developed postnatally, and reversible cardiomegalies in some 21-days old pups. For all effects clear NOAELs were determined.

In the 2-generation toxicity study no dose adjustment during pregnancy and lactation was performed, which resulted in considerably higher food and compound intakes in dams and offspring during these lifestages. As a result, it seemed, that pups were more severely affected by body weight effects compared to the parental generation. By performing a life-stage specific comparison of body weight and substance intakes, as well as benchmark dose calculations (BMD) for these parameters, it could be demonstrated that the point of departures (PODs) and the LOAELs for direct dimoxystrobin-related effects were comparable for offspring and parents. The heart effects (cardiomegaly), which were reversible, occurred only after direct dimoxystrobin-exposure and are considered to be secondary to the detected offspring anemia. Both effects (lower body weights and offspring cardiomegalies) only occur postnatally and are not the consequence of in-utero exposure, as no respective effects at higher doses in rat prenatal toxicity studies were seen.

Two new mechanistic studies (1-generation toxicity study and a 3-week study in young and adult rats, additionally investigating serum iron levels and anemia) confirmed, that pups and young rats were not more sensitive than adult animals to develop anemia or decreased serum iron levels.

In 2006, dimoxystrobin was classified with R63 (possible risk of harm to the unborn child) by the EC, which was the European Authority responsible for classification and

labeling, before ECHA in Helsinki was formed. The R63 (which has been translated into the GHS classification Repr. 2, H361d) was based on offspring body weight and heart effects seen in the 2-generation toxicity study.

Based on a comprehensive re-evaluation of existing and on new data of dimoxystrobin, the conclusion can be drawn, that a classification for reproduction toxicity is scientifically not justified and should be reconsidered.

Toxicology – Endocrine effects

203

Impact of perfluoroalkylated substances (PFAS) on the activity of the hormone receptors ER α and ER β

A.-C. Behr¹, T. Buhrke¹, A. Bräuning¹, A. Lampen¹
¹Federal Institute for Risk Assessment, Berlin, Germany

Perfluorooctanesulfonic acid (PFOS) and perfluorooctanoic acid (PFOA) are perfluorinated substances (PFAS) which are used for the fabrication of surfaces with water- and dirt-repellent properties. Due to their reprotoxic properties and their persistence in the environment, the use of PFOS was restricted in 2009 and a restriction program for PFOA was initiated in 2013. Therefore, industry switches to PFOA and PFOS substitutes, which are predominantly PFAS with a shorter carbon chain length, or structure-related compounds. In contrast to PFOA and PFOS only few toxicological data are available for their substitutes.

Aim of this study was to examine endocrine effects of the substitutes perfluorohexanesulfonic acid (PFHxS), perfluorobutanesulfonic acid (PFBS), perfluorohexanoic acid (PFHxA), perfluorobutanoic acid (PFBA) and 2,3,3,3-tetrafluoro-2-(heptafluoropropoxy)propionic acid (GenX) in comparison to PFOA and PFOS. A HEK-293T cell-based dual-luciferase reporter gene assay was used to investigate the potential of these compounds to affect the activity of the human estrogen receptors hER α and hER β .

The reporter gene assay revealed no activation of hER α or hER β by the PFAS tested in this study. To investigate the potential inhibition of hER α and hER β by PFAS, a co-incubation with the estrogen receptor agonist 17 β -estradiol was performed. None of the tested PFAS inhibited hER α or hER β activity. However, in the case of hER β an enhancement of 17 β -estradiol-stimulated activity was observed. Thus, PFAS do not directly activate or inhibit the human estrogen receptors but have an impact on hER β activity as they amplify the activation mediated by 17 β -estradiol. Further studies will be conducted to examine this synergistic effect in more detail.

204

The XEER-reporter cell line: a novel dual-color luciferase reporter assay for simultaneous detection of estrogen and arylhydrocarbon receptor activation

P. Tarnow¹, S. Bross¹, Y. Nakajima², Y. Ohmiya³, T. Tralau¹, A. Luch¹
¹German Federal Institute for Risk Assessment, Chemical and Product Safety, Berlin, Germany
²Health Research Institute, National Institute of Advanced Industrial Science and Technology (AIST), Takamatsu, Japan
³DAILAB, Biomedical Research Institute, National Institute of Advanced Industrial Science and Technology (AIST), Tsukuba, Japan

Consumers are exposed to a multitude of anthropogenic and natural substances capable of activating or inhibiting ligand activated transcription factors, respectively. This in turn can lead to adverse health effects, particularly for substances acting on signalling pathways that are subject to regulatory crosstalk such as xenoestrogens and polycyclic aromatic hydrocarbons (PAHs). Xenoestrogens are known to activate human estrogen receptors (ERs), whereas PAHs or dioxins act on the arylhydrocarbon receptor (AHR). Importantly, both receptor signalling pathways are interconnected by a complex crosstalk on multiple levels. This ranges from direct protein-protein interactions to competition for common co-factors. However, although this crosstalk has been long known we still lack a deeper understanding of its molecular mechanisms and physiological implications. One reason for this is a lack of tools to visualise and investigate receptor interaction *in vivo*. Based on the breast cancer cell line T47D we thus developed a dual-colour reporter assay which allows time-resolved simultaneous monitoring of the activation of ER and AHR in living cells. The assay uses two beetle luciferases emitting luminescence in the red (SLR) and the green (ELuc) spectrum, respectively. While ELuc is expressed under the control of a 6-fold repeated xenobiotic response element (XRE) SLR is subject to transcription regulation by a 6-fold repeated estrogen response element (ERE). Both constructs were stably transfected into T47D human breast cancer cells, which endogenously express ER α and AHR and are thus ideally suited for monitoring interactions with both receptors. The respective "XEER"-cell line has been successfully subjected to proof of principle studies, using prototypical ER- and AHR-ligands as well as various phytochemicals and xenobiotics. Besides E2 and TCDD ligands included various PAHs, polychlorinated biphenyls, alpha- and beta-naphthoflavone, cosmetic ingredients (butylparaben, benzophenone-2 and 4-MBC), bisphenol A, genistein, resveratrol, diindolymethane as well as pharmacological antagonists of both receptors.

205

Impact of different isoflavone exposure scenarios on estrogen levels and estrogen receptor activation in mammary glands of August Copenhagen Irish rats

R. Hauptstein¹, D. Pemp¹, F. J. Möller², H. L. Esch¹, G. Vollmer², L. Lehmann¹
¹Lehrstuhl für Lebensmittelchemie, Universität Würzburg, Würzburg, Germany
²Lehrstuhl für Molekulare Zellphysiologie und Endokrinologie, TU Dresden, Dresden, Germany

Asian women consuming soy rich food throughout life possess lower levels of 17 β -estradiol (E2) in plasma (PL) than Western women, whose diet is characterized by less soy consumption during early life and possible intake of soy based dietary supplements during adulthood. However, the impact of these soy exposure scenarios on estrogen

(biotrans)formation and the consequence thereof in female mammary glands (MG) has not been investigated yet.

Thus, female August Copenhagen Irish rats were fed either isoflavone (IF) depleted diet (IDD, Western exposure scenario without IF supplement) or IF rich diet (IRD, Asian exposure scenario) until the end of the study at postnatal day (PND) 81. Furthermore, rats fed IDD until PND74 were fed IRD for 7 days (IDD+IRD, Western dietary exposure scenario with IF supplement). Estrous was determined histologically. Levels of transcripts were determined by qPCR and E2 and estrone (E1) in PL and MG were quantified by GC-MS/MS. Statistical analyses of estrogens were performed by Kruskal Wallis and unpaired Wilcoxon tests and of transcript levels by linear regression models considering the explanatory variables tissue levels of E2 and diet (IDD vs IRD and IDD vs IDD+IRD).

E2 levels in PL and MG did not coincide with those predicted by estrous. Furthermore, median levels of E1 and ratios E2/E1 in MG and ratio of E2 levels in PL/MG were not affected by diet. In contrast, diet tended to affect E2 concentrations in PL (p=0.1211) due to an increase in the IRD group (p=0.0056) whereas E2 levels in the IDD+IRD group only tended to be elevated (p=0.0788). In MG, IRD and IDD+IRD increased E2 levels only weakly (p=0.0788 each). Likewise, besides significant changes in transcript levels of *Cyp11a1* and *1a2*, putatively decreasing oxidation of E2 to catechols, in the IDD+IRD group and (not significantly) also in the IRD group, no changes in transcript levels putatively affecting E2 levels were observed. Moreover, no decrease in levels of transcripts indicative for cellular (oxidative) stress (*Gclc*, *Tp53*, *Mt1a*) was observed in the IDD+IRD group.

E2 MG levels were significantly associated with an increase in transcript levels of *Areg* and *Pgr*, indicating activation of estrogen receptor (ER). In contrast, IRD was associated with a significant and IDD+IRD with a not significant decrease in *Pgr* transcript levels. E2 levels but not diet were significantly associated with *Gata3* transcript levels, indicating tissue differentiation. Furthermore, levels of transcripts involved in intercellular communication (*Egfr*, *Wnt4*) were significantly decreased by IDD+IRD and not significantly by IRD and differed from that affected by E2 (increase in *Gdf15*, *Hgf*, *Igf11*, *Wnt5a*). *Bmf*, a marker transcript for apoptosis was increased by IRD, but not affected by E2 and even decreased not significantly by IDD+IRD.

Taken together, despite an increase in E2 levels in PL, less ER activation was observed after dietary exposure to IF. Whereas E2 and transcript levels of enzymes involved in E2 (biotrans)formation as well as ER activation and cellular communication were affected similarly but to a different extend in both Asian and Western IF exposure scenarios, differences in apoptosis were observed between IRD and IDD+IRD groups. Supported by DFG LE 1329/10-1.

206

E2 metabolite profiles and related transcripts during the tumorigenic process in the mammary gland of female August Copenhagen Irish rats: impact of isoflavones

D. Pemp¹, R. Hauptstein¹, F. J. Möller², C. Kleider¹, M. C. Bosland³, H. L. Esch¹, G. Vollmer¹, L. Lehmann¹
¹Lehrstuhl für Lebensmittelchemie, Universität Würzburg, Würzburg, Germany
²Lehrstuhl für Molekulare Zellphysiologie und Endokrinologie, TU Dresden, Dresden, Germany
³Department of Pathology, College of Medicine, University of Illinois at Chicago, Chicago, Vereinigte Staaten von Amerika

August Copenhagen Irish (ACI) rats with 17 β -estradiol (E2)-releasing implants are an accepted model to study the etiology of breast cancer, but neither E2 (biotrans)formation in mammary gland tissues (MG) during tumorigenesis, nor the impact of isoflavones (IF) shown to affect tumorigenesis in ACI rats, has been investigated, yet. Therefore at postnatal day (PND) 75 and 175, placebo (-E2) or silastic implants containing 4 mg E2 were implanted in female ACI rats exposed to either IF depleted diet (IDD) or IF rich diet (IRD) since conception until the end of the study at PND 285. Palpable MG tumors (PT) and 1-2 MG per animal without PT were characterized histologically and categorized into normal (-E2 group, n=12), hyperplasia and non-PT and PT with and without solid tumors (+E2 group, n=32). E2, estrone (E1), their hydroxylation products and methylation (MeO-) products thereof, as well as conjugates of E1 and E2 in plasmas and MG were analyzed by GC- and UHPLC-MS/MS, respectively. Levels of 49 transcripts involved in (biotrans)formation of E2 and estrogen receptor (ER) activation were determined by TaqMan®-PCR. Without exogenous E2, plasma E2 as well as E1 and (borderline) E2 levels in MG were higher in IRD. Plasma E2 as well as E1 and E2 levels in MG were lower in the -E2 group than that in the +E2 group. E2 levels as well as E2/E1 and E2 MG/plasma ratios were elevated in PT, accompanied by a significant increase in transcript levels indicative for estrogen receptor activation (*Areg*, *Pgr*) and proliferation (*Mki67*). IRD increased E2/E1 ratio in PT and, although IRD did not affect ER activation (*Areg*, *Pgr*), IRD increased differentiation (*Gata3*) in normal and hyperplastic tissues and tended to decrease proliferation in hyperplastic (*Ccnd1*) tissues. Levels of E1 and 2-MeO-E1 were highest in hyperplastic tissues, accompanied by an increase in transcript levels of *Hsd17b2* (conversion E2 to E1) and *Cyp11a1*. Transcript levels of *Gstm1* and *Gstm2* were decreased in the whole +E2 group and of *Gstt1* and *Gstt3* in hyperplastic tissues, possibly decreasing inactivation of electrophilic metabolites. Accordingly, maximum transcript levels of *Tp53* and *Mt1a* indicating cellular (oxidative) stress were observed in hyperplastic tissues. IRD did neither affect levels of 2-MeO-E1 nor cellular stress (*Gclc*, *Mt1a*, *Tp53*). Of note, neither 4-MeO-E1, nor E1 catechols, nor E2 catechols nor methylation products of the latter were observed in any sample. Furthermore, no conjugates of E1 or E2 were detected in plasmas and mammary gland tissues. Thus, changes in transcript levels of conjugating enzymes induced by tumorigenesis and by IRD were not related with detectable conjugate levels of E1 or E2. Taken together, whereas hyperplastic tissues were characterized by maximum oxidative metabolism of E1 and cellular (oxidative) stress, PT exhibited highest E2 levels and ER activation. IRD increased differentiation and decreased proliferation in normal and hyperplastic tissues but increased E2/E1 ratio in PT. Supported by DFG Le-1329/10-1.

207

Correlations of tissue levels of soy isoflavones with 17beta-estradiol/estrone ratio in human mammary specimen

C. Kleider¹, D. Pemp¹, R. Hauptstein¹, K. Schmalbach¹, S. T. Soukup², L. Geppert³, C. Köllmann³, P. Eckert⁴, I. Neshkova⁵, K. Ickstadt³, S. Kulling², H. L. Esch¹, L. Lehmann¹
¹Lehrstuhl für Lebensmittelchemie, Universität Würzburg, Würzburg, Germany
²Max-Rubner-Institut, Karlsruhe, Germany
³Chair of Mathematical Statistics with Applications in Biometrics, Dortmund, Germany
⁴Practice for Plastic and Aesthetic Surgery, Würzburg, Germany
⁵University Hospital, Würzburg, Germany

Level of 17beta-estradiol (E2) in human breast tissue is considered to affect breast cancer initiation, promotion and progression. Although putatively beneficial and adverse effects of soy isoflavones (IF) on the human mammary gland, in particular in Western women, have been discussed extensively, the influence of IF levels on estrogen formation in human mammary gland tissue has not been investigated yet.

Thus, glandular tissues were dissected from 37 mammary specimen obtained from women (age 18-66 years old) not taking estrogen active drugs. 14 of these women had been exposed to IF by their usual diet or by intake of a soy-based dietary supplement for 7 days prior to mammary. Information on soy consumption and lifestyle were collected by questionnaire and tissues were characterized histologically. Genistein, daidzein conjugates (n=12) and bacterial metabolites (n=7) as well as the estrogens estrone (E1)-sulfate, E1, E2 and 2-methoxy-E1 were determined by UHPLC- and GC-MS/MS, respectively and transcript levels of 19 enzymes involved in E2 (biotrans)formation were quantified by TaqMan®-PCR in glandular tissues.

Isoflavonoids were categorized into the IF parameters aglycones (Agl) and conjugates (Con) of either genistein, daidzein or sum of both and were further statistically analyzed by Spearman's rank correlation analysis.

A positive correlation of E2/E1 ratio with Agl(+Con) was observed in glandular tissues (R=0.49, p=0.002), accompanied by a significant negative correlation of E1 levels with Agl (R=-0.35/p=0.032), possibly due to reduction of 17beta-hydroxysteroid dehydrogenase 2 (conversion of E2 to E1) expression as indicated by a weak negative correlation of transcript levels of 17beta-hydroxysteroid dehydrogenase 2 with Agl+Con (R=-0.25, p=0.080). Further statistical analysis taking into account multiple variables using linear regression models will provide more insights into variables affecting E1/E2 ratio.

Taken together, estrogen profile in human glandular breast tissue seems to be affected by IF levels. Supported by DFG Le-1329/10-1.

Toxicology – Immunotoxicology

208

Metabonomic and proteomic alterations of THP-1 cells upon exposure to the contact allergen 2,4-dinitrochlorobenzene

F. Mußotter¹, S. Potratz¹, A. Luch¹, A. Haase¹

¹Federal Institute for Risk Assessment, Department Chemicals and Product Safety, Berlin, Germany

Allergic contact dermatitis (ACD) is a widespread disease often caused by substances in consumables. The EU prohibits the testing of cosmetic ingredients *in vivo*. This urges the development of reliable *in vitro* testing strategies.

Activation of dendritic cells (DCs) represents a key step during sensitization as they are essential for selection and priming of allergen specific effector T cells.

In an integrated OMICS approach we aimed to further elucidate the molecular mechanisms of DC activation using quantitative metabolomics and proteomics.

Monocytic THP-1 cells were used as a model system and treated with the sensitizer 2,4-dinitrochlorobenzene (DNCB; 5, 10 and 20 µM) and the irritant sodium dodecyl sulfate (SDS; 100 µM). Samples were taken after 4, 8 and 24 hours. THP-1 activation was analyzed by measuring the established activation markers CD86 and CD54 after 24 hours. A targeted LC-MS/MS approach was used to analyze 188 metabolites including amino acids and lipids. Protein levels were quantified by nano-LC-MALDI-MS/MS after stable isotope labeling by amino acids in cell culture (SILAC).

Data sets were examined by multivariate analyses for identification of biomarker candidates. Regulated metabolites and proteins were subjected to pathway analysis.

The data presented might contribute to the further development of suitable *in vitro* testing methods for chemical-mediated sensitization.

209

Subtoxic concentrations of hepatotoxic drugs lead to macrophage activation in a human *in vitro* liver model

S. Lehmann¹, V. Kegel¹, J. L. Liu², T. Schönfeld¹, D. Seehofer¹, G. Damm¹

¹Charité University Medicine Berlin, Department of General-, Visceral- and Transplantation Surgery, Berlin, Germany

²TU Berlin, Berlin, Germany

Drug induced Liver Injury (DILI) is one of the most frequent causes of acute liver injury and a main cause for drug withdrawals. Currently there are no reliable models to test the DILI potential of new compounds available. Kupffer cells (KC) play an important role in hepatic cell stress mediated through chemokines and release of endogenous proteins. KC activation by damaged or stressed hepatocytes can lead to activation of the NF-κB signaling pathway transmitted by reactive oxygen intermediates (ROI). We have recently established a liver model composed of primary human hepatocytes (PHH) and KC which enables investigation of immune reactions after induction of hepatocyte stress (Kegel et al., 2015).

Aim of the present study was the kinetic investigation of hepatic cell stress induction and macrophage activation after treatment with subtoxic concentrations of hepatotoxic drugs. Primary human hepatocytes (PHH) and KC were isolated from human liver resectates using a two-step collagenase perfusion technique. Initial KC activation was characterized by the DCF assay and immunofluorescence staining. PHH were incubated

with different concentrations of acetaminophen (APAP) and diclofenac (DIC) for different time intervals. Cell stress was evaluated by measurement of oxidative stress (DCF-assay) and viability (XTT-assay). In order to simulate macrophage activation following hepatocyte damage, KC and macrophages derived from the monocytic cell line THP-1 were incubated with supernatants of PHH treated with hepatotoxic compounds. KC and THP-1-macrophage activation were investigated by measuring intracellular formation of ROI using the DCF-assay and cell activity using the XTT-assay.

The characterization of KC activation revealed a donor and disease dependent KC activation resulting in KC differentiation to pro- and anti-inflammatory macrophages. Therefore, KC were substituted by macrophages derived from THP-1 cells. Evaluation of hepatic cell stress showed the strongest effect on THP-1-macrophages when PHH were incubated with APAP or DIC for 4 h. Treatment of KC and THP-1-macrophages with supernatants of PHH challenged for 4 h with hepatotoxic compounds indicates that THP-1-derived macrophages react similar to KC when treated with PHH supernatants in terms of cell activity and ROI-production.

In conclusion, THP-1 derived macrophages might be a suitable alternative to KC concerning macrophage activation. The evaluated kinetic window of 4 h covering hepatic stress induction and immune reaction allows to perform these measurements in a coculture model composed of both cell populations. Further experiments are needed to evaluate the potential of PHH and KC coculture models and their possible use in DILI prediction.

Kegel, V., E. Pfeiffer, B. Burkhardt, J. L. Liu, K. Zeilinger, A. K. Nüssler, D. Seehofer, and G. Damm, 2015. Subtoxic Concentrations of Hepatotoxic Drugs Lead to Kupffer Cell Activation in a Human *In Vitro* Liver Model: An Approach to Study DILI: Mediators Inflamm, v. 2015, p. 640631.

Toxicology – Nanomaterials

210

Toxicity of CeO₂ nanoparticles estimated in a 90-day nose-only inhalation study

D. Schwotzer¹, M. Niehof¹, T. Hansen¹, S. Schuchardt¹, T. Tillmann¹, H. Ernst¹, O. Creutzenberg

¹Fraunhofer Institute for Toxicology and Experimental Medicine, Hannover, Germany

Since the use of cerium dioxide nanoparticles is known to be beneficial e.g. in terms of reducing fuel consumption when added to diesel fuel it has become a frequently used nanomaterial. To compensate the concurrent lack of information on its toxicology a 90-day nose-only inhalation study was initiated. By comparing the results to a combined chronic inhalation toxicity and carcinogenicity study using the same test items and experimental conditions (BASF, Ludwigshafen, Germany) early indicators for genotoxic and carcinogenic effects should be determined. Rats were exposed to 0, 0.1, 0.3, 1 and 3 mg/cm³ CeO₂ as well as 50 mg/m³ BaSO₄ nanoparticles (6 h/day, 5 days/week, 13 weeks). Animal dissections were conducted at five time points (exposure day 1 and 28; recovery day 1, 28 and 90) aiming for endpoints mandatory according to OECD guideline 413. Additionally, gene expression analyses in isolated pneumocytes type II were performed using Pathway Arrays for inflammation, oxidative stress, genotoxicity, apoptosis and lung cancer. The given results intend the identification of marker genes displaying modulated expression in response to nanoparticle exposure. Investigations on CeO₂ and BaSO₄ retention in the lung are also included in this project. In bronchoalveolar lavage fluid (BALF) a time and dose-dependent increase of inflammatory cells has been detected up to the end of exposure. The amount of inflammatory cells decreased during post-exposure; however, in the high dose group a persistent inflammation up to 90 days was detected by BALF and histopathology examination. Based on our current results effects of CeO₂ nanoparticles on the respiratory system are suggested. Its relevance in the context of long term effects such as tumor development needs to be estimated considering all investigations included in this study. The InhaIT-90 project is funded by the German Federal Ministry of Education and Research (BMBF) – 03X0149A.

211

Core or coating material? What dictates the uptake and translocation of nanoparticles *in vitro*?

D. Lichtenstein¹, L. Böhmert¹, T. Meyer², A. F. Thünemann³, I. Estrela-Lopis², A. Braeuning¹, A. Lampen¹

¹Federal Institute for Risk Assessment, Food Safety, Berlin, Germany

²Leipzig University, Institute of Medical Physics & Biophysics, Leipzig, Germany

³Federal Institute for Materials Research and Testing, Polymers in Life Science and Nanotechnology, Berlin, Germany

Nanoparticles are becoming increasingly important role in consumer-related products. Understanding the interactions between nanoscaled objects and living cells is therefore of great importance for risk assessment. In this context, it is generally accepted that nanoparticle size and shape are crucial parameters regarding the potential of nanoparticles to penetrate cell membranes and epithelial barriers. Current research in this field additionally focuses on the particle coating material. In order to distinguish between core- and coating-related effects in nanoparticle uptake and translocation behavior, this study investigated two nanoparticles equal in size, coating and charge but different in core material.

Silver and iron oxide were chosen as core materials to ensure similar nanoparticles characteristics after particle synthesis. Nanoparticles were coated with poly (acrylic acid) (PAS) and extensively characterized by TEM (transmission electron microscopy), SAXS (Small-Angle X-ray Scattering), Zetasizer™ and NanoSight™. For uptake and transport studies the widely used human intestinal Caco-2 model in a Transwell™-system with subsequent elemental analysis (AAS) was used. For evaluation and particle visualization transmission electron microscopy (TEM) and Ion Beam Microscopy (IBM) were conducted.

Although similar in size, charge and coating material, the behavior of particles in Caco-2 cells was quite different. The internalized amount was comparable, but PAS-coated iron oxide nanoparticles were additionally transported through the cells. By contrast, PAS-coated silver nanoparticles remained in the cells. Our findings suggest that the coating

material influenced only the uptake of the nanoparticles whereas the translocation was determined by the core material. In summary, a core-dependent effect on nanoparticle translocation was revealed. Both the uptake and transport of nanoparticles in and through cells should be considered when discussing nanoparticle fate and safety.

212

The DaNa2.0 Knowledge Base Nanomaterials – quality-approved and easy-to-understand information on current nanosafety research

C. Marquardt¹, H. F. Krug², D. Kühnel³, K. Nau¹, F. Paul⁴, C. Steinbach⁴

¹Karlsruher Institut für Technologie (KIT), Institut für Angewandte Informatik (IAI), Eggenstein-Leopoldshafen, Germany

²Empa – Swiss Federal Laboratories for Materials Science and Technology, St. Gallen, Switzerland

³Helmholtz-Centre for Environmental Research (UFZ), Department Bioanalytical Ecotoxicology, Leipzig, Germany

⁴DECHEMA e.V. Society for Chemical Engineering and Biotechnology, Frankfurt a. M., Germany

Nanotechnology is having a great impact not only on basic research but also on many sectors of industry opening the market for numerous new applications ranging from electronics to the health care system. Besides their great innovative potential, the large variety of existing synthetic nanomaterials used in the last decade represents a major challenge for scientists and regulators in terms of measuring and assessing the potential hazard caused by the materials or the products themselves. Equally, consumers often miss reliable and easy-to-understand information on nanomaterials and nanotechnology and do not know where to get such information.

Therefore, the international DaNa^{2.0} expert team brings together its expertise and knowledge from different research areas dealing with all aspects of nanosafety research in order to create and provide easy-to-understand, up-to-date and quality-approved nanomaterials' knowledge base on www.nanopartikel.info. This information platform covers the 25 market-relevant nanomaterials focusing on their effects on the safety of humans and the environment. In order to manage and assess the rapidly increasing number of publications related to nanosafety issues, the DaNa^{2.0} project developed a customised methodology «Literature Criteria Checklist», which includes mandatory and desirable assessment criteria covering physico-chemical characterisation, sample preparation and (biological) testing parameters. This checklist facilitates the discrimination between high- and low quality publications and all positively evaluated literature is then fed into the DaNa knowledge base. Accounting for the need to harmonise experimental practices, the DaNa team also developed a template for Standard Operation Procedures (SOP) to support careful scientific practice. Validated protocols generated within the German BMBF-funded nanosafety research projects are presented together with results from the Swiss CCMX project V.I.G.O. and available for download.

Another unique feature of the DaNa knowledge base is the integrated application-based database that provides a unique link between nanomaterials in real applications (e.g. environmental remediation or medical products) and their potential impacts/ toxicological effect(s) that can be easily accessed by the interested visitor. Additionally, DaNa^{2.0} provides a list of FAQs, a link platform with contact data to other information portals and the opportunity to directly pose questions to our experts via E-mail. DaNa^{2.0} is also present on Twitter, follow us @[nano_info](https://twitter.com/nano_info).

DaNa^{2.0} is a German umbrella project funded by the German Federal Ministry of Education and Research (FKZ 03X0131) and is supported by Swiss Federal Authorities. **References:** Kühnel D., Marquardt C., Nau K., Krug H.F., Mathes B., Steinbach C. (2014). Environmental impacts of nanomaterials: providing comprehensive information on exposure, transport and ecotoxicity – the project DaNa2.0. *Environmental Sciences Europe*, 26(1): 21.

Abb. 1



213

Transcriptome analysis of alveolar epithelial cells after direct exposure to wood combustion emissions

S. Oeder^{1,2,3}, O. Sippula^{4,2}, M. Dilger^{5,2}, H.-R. Paur^{6,2}, T. Streibel^{7,2}, C. Traidl-Hoffmann^{8,1}, C. Weiss⁹, R. Zimmermann^{7,9,2}, C. Schmidt-Weber³, J. Buters^{1,2,3}

¹CK-CARE, Christine Kühne Center for Allergy Research and Education, Davos, Switzerland

²HICE – Helmholtz Virtual Institute of Complex Molecular Systems in Environmental Health – Aerosols and Health, Neuherberg, Germany

³Helmholtz Zentrum München and Technische Universität München, Center of Allergy and Environment (ZAUM), München, Germany

⁴University of Eastern Finland, Department of Environmental Science, Kuopio, Finland

⁵Karlsruhe Institute of Technology, Institute of Toxicology and Genetics (ITG), Karlsruhe, Germany

⁶Karlsruhe Institute of Technology, Institute for Technical Chemistry (ITC), Karlsruhe, Germany

⁷University Rostock, Joint Mass Spectrometry Centre, Chair of Analytical Chemistry, Institute of Chemistry, Rostock, Germany

⁸Technische Universität München, Institute of environmental medicine, UNIKA-T, Augsburg, Germany

⁹Helmholtz Zentrum München, Joint Mass Spectrometry Centre, CMA – Comprehensive Molecular Analytics, Neuherberg, Germany

Background: Particulate matter of combustion processes enhances cardio-vascular diseases and increases associated mortality rates. Around 13% of total PM10 emissions are emitted by wood burners (UBA 2006). How wood combustion aerosols (particles and

gasses) can affect human lung cells and how such cellular responses depend on the usage of different wood types and burners is widely unknown.

Methods: In an exposure chamber imitating the human respiratory tract human alveolar cells (A549) were exposed at an air-liquid-interface (ALI) to gasses and particles of wood combustion aerosols. Log wood of beech, birch and spruce was burnt in a conventional oven and compared to the combustion of wood pellets in a modern pellet burner. The combustion aerosols were diluted 1:40 and directly delivered to the exposure chamber. After 4h exposure the lung cells were lysed and RNA was isolated. In an array based transcription analysis of the whole genome the effects of the aerosol exposures on lung cells was assessed. In parallel, physical and chemical parameters of the combustion aerosols were analyzed.

Results: The combustion aerosol of wood pellets contained less organic substances than the log wood aerosols, but was higher in its zinc content. Genome-wide we found a higher number of regulated genes with combustion of pellets compared to combustion of log wood. The gas phase alone (filtered aerosol) showed comparable gene regulatory activity as the particle-containing total aerosol. Aerosol from log wood burning induced mainly genes of the xenobiotic metabolism and cellular signaling. Pellet aerosols additionally regulated apoptosis and DNA repair processes.

Conclusions: Modern pellet burners reach better combustion efficiencies than conventional log wood ovens, but their emissions seem to stress human lung cells stronger. One reason might be the higher zinc content of wood pellet aerosols.

214

Transcriptome signatures in human peritoneal mesothelial cells after exposure to multiwalled carbon nanotubes support a potential role of cellular senescence in mesothelioma development

S. M. Reamon-Buettner¹, A. Hiemisch¹, I. Voepel¹, **C. Ziemann**¹

¹Fraunhofer ITEM, In Vitro and Mechanistic Toxicology, Hannover, Germany

Multiwalled carbon nanotubes (MWCNTs) may pose as a risk similar to asbestos in causing cancer, notably mesothelioma, which is a malignant tumor originating from mesothelial cells. To identify molecular cues leading to mesothelioma development, we performed genome-wide transcriptome analysis using microarrays in primary human peritoneal mesothelial LP9 cells treated with two different tumor-inducing tailor-made MWCNTs (rat model; Rittinghausen et al. 2014 Part Fibre Toxicol 11:59), or amosite asbestos at 3 µg/cm² for 24 h. Specifically, we determined how the transcriptomic changes of the highly tumorigenic MWCNT A would differ from another tumor-inducing MWCNT with albeit lesser potency (MWCNT D), long amosite asbestos as positive control, and milled MWCNT A as material control. Initial analysis using bioinformatic tools, revealed 3788 significantly differentially regulated genes for MWCNT A, 1680 for MWCNT D, 145 for amosite, and 4 for milled MWCNT. Further analyses with Ingenuity Pathway Analysis comparing the two different MWCNT types and amosite, found common as well as exclusive biomarkers. Interestingly, we identified many differentially regulated genes implicated in cellular senescence, a growth arrest in response to different stressors including DNA damage, disrupted chromatin, and strong mitogenic signals. Paradoxically, cellular senescence can represent both tumor suppression and tumor promotion mechanisms. More important, we found differential expression of genes associated with senescence-associated secretory phenotype (SASP) such as inflammatory cytokines, chemokines, proteases, and growth factors, which were many-folds up- and down-regulated in MWCNT A, compared to MWCNT D and amosite. The mechanisms leading to mesothelioma induction by MWCNTs are from far clear, but the key information emerging from the present transcriptomic data, together with our previously identified senescence markers, indicate that cellular senescence has a likely role.

215

Toxicological effects of synthetic nanoparticles in human colon cancer cells

T. Schneider¹, M. Gle¹

¹Friedrich Schiller University Jena, Department of Nutritional Toxicology, Institute of Nutrition, Jena, Germany

Nanotechnology offers great advantages for the food industry despite its partly unknown risks, whose enlightenment is the main target of nanotoxicology. Due to variability in terms of size, material, shape, surface texture and several endogenous influences, the toxicity of most frequently used and ingested nanomaterials is difficult to estimate. Therefore, the aim of this study was the in vitro investigation of toxicological endpoints such as cell viability, DNA integrity and the induction of apoptotic processes in human colon carcinoma cells (HT29). For this purpose HT29 cells were exposed for 24 hours with metal nanoparticles (gold, silver) and metal oxide nanoparticles (copper oxide, titanium dioxide, zinc oxide) in concentrations of 2-10 µg/ml. At first the cellular uptake of the nanoparticles by means of an ICP-MS was determined. The influence of cell viability was demonstrated by the trypan blue staining and the MTT assay. The alkaline comet assay gave information about possible DNA damages and the use of the repair enzyme formamidopyrimidine DNA glycosylase (FPG) additionally allowed the detection of oxidized bases. The induction of programmed cell death was examined using by Annexin V FITC assay. The ICP-MS data showed a maximum particle content of 1.39 pg per cell for the used concentration range. The metal oxide nanoparticles resulted in a significant reduction of cell viability with a decrease up to 40 % after copper oxide and zinc oxide treatment. For metal particles, only for silver a reduced cell metabolism of about 50 % was detectable by the MTT assay. Low genotoxic effects could be determined for silver nanoparticles (tail intensity about 12%; control about 6%), while for titanium dioxide the amount of oxidized bases was additionally increased (tail intensity about 20%; control about 6%) for concentrations above 8 µg/ml. Induction of apoptosis was determined for silver particles (up to 24% early apoptotic and 20% late apoptotic cells) as well as for titanium dioxide and zinc oxide (10% each early apoptotic cells), whereby the most significant increase in late apoptotic cells was detected for zinc oxide (up to 90%). The results obtained in our studies indicate a clear particle-dependent influence on cell viability and apoptosis-triggering processes, depending on the used material or the concentration deployed, while only minor changes of DNA integrity were detected.

216

Investigating the cytotoxicity of different forms of Multi-walled Carbon Nanotubes and their use as a potential drug delivery carrier

H. Reuquardt¹, T. Hansen¹, S. Hampel², P. Steinberg³, C. Dasenbrock⁴
¹Fraunhofer-Institut für Toxikologie und Experimentelle Medizin, Präklinische Pharmakologie und *in vitro* Toxikologie, Hannover, Germany
²Leibniz-Institut für Festkörper- und Werkstoffforschung, Dresden, Germany
³Stiftung Tierärztliche Hochschule Hannover, Hannover, Germany
⁴Fraunhofer-Institut für Toxikologie und Experimentelle Medizin, Toxikologie und Umwelthygiene, Hannover, Germany

The evolution in the field of Nanotechnology led to a variety of novel materials at the nanoscale. Among them are different carbon materials like buckyballs, graphene nanoplates and carbon nanotubes (CNTs). CNTs are hollow carbon fibres with either one (SW) or multiple sidewalls (MW). MWCNTs usually show a diameter of up to 100nm and can be several micrometres long. Because of their nanoscale diameter CNT-uptake can take place directly through the plasma membrane of cells by the so called *nanoneedle effect* [1]. Additionally CNTs, like most nanomaterials, show a high surface to volume ratio and, because of their micro scale length, a potentially high loading capacity. These properties make CNTs interesting for the potential use as drug delivery carriers (DDCs).

MWCNTs, produced via chemical vapour deposition with a diameter of 45nm and 16µm length, were used in three different forms, unmodified, acid oxidized (Ox_CNT) and ground. Cytotoxicity testing was performed in human umbilical vein endothelial cells (HUVEC). The cells were seeded in 48-well plates and exposed to doses of 1, 5, 10 and 25µg/cm² growth area of the respective CNT type for 24h. The WST-8 assay was applied for testing cell viability and the LDH cytotoxicity assay to identify potential damage to the plasma membrane and to calculate overall cytotoxicity.

The results show that an increased oxidation time for the Ox_CNTs, in a H₂SO₄/HNO₃ mixture, leads to decreased cytotoxicity in HUVEC, compared to unmodified MWCNTs. During the oxidation reactive oxygen groups are formed on the CNT surface [2]. These groups lead to a reduced hydrophobicity of the CNT surface which could be responsible for the decline in cytotoxicity.

Future investigations will include the toxicological analysis of MWCNTs functionalized with polyethylene glycol (CNT-PEG). The hydrophilic polymer PEG will be covalently bound to the CNT surface and is expected to further reduce the cytotoxic effect. For these investigations different analytical methods will be used. Among others, cell cycle analysis, the BrdU assay, pathway arrays and qRT-PCR for the investigation of gene expression and cytokines will be measured. These methods will involve a co-culture model of HUVEC and human umbilical vein smooth muscle cells (HUVSMCs) for a better approximation to the cellular *in vivo* situation. Additionally the PEG modified MWCNTs will be tested for their loading capacity and efficacy with the anticancer drug Doxorubicin for a potential use as an intravenous drug delivery carrier *in vivo*.

References: [1] Bianco A, Kostarelos K, Prato M: Applications of carbon nanotubes in drug delivery. *Current Opinion in Chemical Biology* 2005, 9: 674-679
 [2] Balasubramanian K, Burghard M: Chemically Functionalized Carbon Nanotubes. *Small* 2004, 1(2): 180-192

217

Artificial digestion of Aluminium-containing nanomaterials and their effects on the gastrointestinal tract *in vitro*

H. Sieg¹, B.-C. Krause², D. Lichtenstein¹, L. Böhmert¹, U. Hansen³, C. Kästner³, J. Tentschert², P. Laux², A. Braeuning¹, A. Thuenemann³, A. Luch², A. Lampen²
¹Bundesinstitut für Risikobewertung, Lebensmittelsicherheit, Berlin, Germany
²Bundesinstitut für Risikobewertung, Produktsicherheit, Berlin, Germany
³Bundesanstalt für Materialforschung und -prüfung, Berlin, Germany

Although Aluminium is one of the most common elements in the biosphere, up to now little is known about its impact on human health. Aluminium and its chemical derivatives are highly abundant in food, food contact materials and consumer products what leads to an exposition via the gastrointestinal tract (GI tract), the lung and via skin contact. Recently, Aluminium is hypothesized to cohere with cancer and neurodegenerative disorders. Lately, due to an increasing attentiveness on this topic, limiting values for food additives have been tightened by the EU commission. However, cellular effects of Aluminium and especially Aluminium-containing nanomaterials, are in the focus of our research activities, for example in the international SolNanoTOX project.

We established an *in vitro* simulation system of the GI tract, where nanomaterials undergo the different physiological, chemical and proteinbiochemical conditions of saliva, gastric juice and the intestine. The artificially digested nanomaterials, as well as soluble Aluminiumchloride as ionic control substance, were subjected to several analytical and biochemical methods to characterize their change of appearance and their cytotoxic effects on intestinal cellular models.

We observed the fate of the nanomaterials during typical pH-values of saliva, gastric and intestinal juice with Dynamic light scattering measurements and ICP-MS in the single particle mode. After observable disappearance at pH 2 the particles recovered in the simulated intestinal fluid. The simulation of the GI tract, mainly the change of pH settings, may lead to a certain chemical activation of Aluminium that can increase bioavailability in the intestine after oral uptake of Aluminium-containing food products. *In vitro* assays like CTB, MTT and cellular impedance measurements showed that there were no acute cytotoxic effects measurable after a period up to 48h after incubation, comparable to undigested particles. In contrast, high amounts of Aluminium ions showed additional effects on cell viability compared to non-digested Aluminium ions.

Although toxicological potential of Al ions to healthy tissue appears to be low, increased hazardous potential cannot be ruled out to pre-damaged tissue and can have a relevance for special consumer groups with for example chronic intestinal inflammation or dietary eating behavior combined with high exposure to Al-containing food products.

218

The PHOENIX project: Nano-layered hybrid particles as flame retardant additives – toxicological *in vitro* investigations using lung-relevant cell models

G. Kodandaraman¹, H. Rahmer¹, J. Gómez², D. Schaudien³, H. Brockmeyer¹, I. Voepel⁴, A. Westendorf⁵, O. Creutzenberg⁵, C. Ziemann¹
¹Fraunhofer ITEM, Genetic Toxicology and Epigenetics, Hannover, Germany
²Avanzare Innovacion Tecnologica S.L., Navarre (La Rioja), Spanien
³Fraunhofer ITEM, Pathology, Hannover, Germany
⁴Fraunhofer ITEM, *In vitro* and Mechanistic Toxicology, Hannover, Germany
⁵Fraunhofer ITEM, Inhalation Toxicology, Hannover, Germany

In the EU, there is a strong need for solutions to substitute halogenated flame retardant (HFR) additives, employed in the fabrication of FR thermoplastic and thermoset materials. These materials are used in diverse commercial products, applications and markets, such as electrical/electronic devices, low-voltage wires or household appliances. The PHOENIX project, funded by the European Union 7th Framework Program (grant agreement no. 310187), therefore investigates e.g. several tailor-made, nano-layered hybrid particles as alternatives to HFR additives. Considering "safer-by-design" strategies, potential FR nanomaterials (NM) were physico-chemically characterized (e.g. particle size distribution, zeta potential) and screened early in development for their (geno)toxic and pro-inflammatory potential to timely reject NM with high health hazard. As inhalation is the most important exposure route for NM, lung-relevant cells were used as *in vitro* screening models. To better enable detection and differentiation of the biologic effects of the most promising NM, screening was started with primary rat lung alveolar macrophages (AM; cells of first contact for inhaled NM), at a high concentration of 50µg/cm² (24h of incubation), using membrane damage (lactate dehydrogenase release assay), direct DNA-damage (alkaline comet assay), and IL-8 liberation (ELISA) as primary endpoints, and quartz DQ12 and Al₂O₃ as particulate positive and negative controls, respectively. In this screening system, biologically inert NM could be differentiated from more active ones. Thereby, Mg(OH)₂ nanoplatelets (Mg1; mean lateral size: 1.5-2 µm; mean thickness: 15-20 nm) represented the least, and pristine few layers graphene nanoplatelets (GR1; mean lateral size: 2 µm; mean thickness: 3 nm; graphene layers: 8 ± 0.5) the most biologically active NM. Clear concentration dependencies were detected for GR1 in follow-up experiments. Mg1 and GR1 were further tested in other lung-relevant cell types, i.e. MRC-5 primary human lung fibroblasts and A549 lung adenocarcinoma epithelial cells. Interestingly, MRC-5 cells were less sensitive towards biological effects of GR1, compared to AM, whereas A549 cells showed nearly no effect, keeping in mind that lung epithelial cells are the target cells of lung tumor development. To test the hypothesis that the observed cell-specific differences in sensitivity might in part be based on cellular uptake, cells were exposed for 24 h to 12.5 or 25 µg/cm² of GR1 on chamber slides. Slides were finally stained with DAPI and analyzed by dark field microscopy. Cells indeed demonstrated differences in uptake capacity and also showed unique pattern of cellular localization of GR1, i.e. with tight perinuclear agglomeration in AM, a more scattered cytoplasmic distribution in MRC-5 cells and limited uptake in A549 cells. Additionally, biological activity of the diverse NM seemed also to correlate with cellular uptake, as determined by light and dark field microscopy in AM and MRC-5 cells. In conclusion, an AM-based screening system was able to differentiate biological activity of diverse NM, with morphology, physico-chemical characteristics, and related cellular uptake most likely to be key for NM- and cell type-specific hazard.

219

Histopathological findings after 12 months inhalation to nano Ceria

H. Erns¹, L. Ma-Hock², J. Keller², S. Groeters², B. van Ravenzwaay², T. Gebel³, D. Schaudien¹, S. Rittinghausen¹, R. Landsiedel²
¹Fraunhofer Institute for Toxicology and Experimental Medicine ITEM, Department of Pathology, 30625 Hannover, Germany
²BASF SE, Experimental Toxicology and Ecology, 67056 Ludwigshafen am Rhein, Germany
³Federal Institute for Occupational Safety and Health (BAuA), Friedrich-Henkel-Weg 1-25, 44149 Dortmund, Germany

Lung carcinogenicity and putative systemic effects of low-dose life-time inhalation exposure to biopersistent nanoparticles were examined in a chronic inhalation study performed according to OECD test guideline no. 453 with several protocol extensions. Female rats (100/group) were exposed to cerium dioxide (NM-212, 0.1; 0.3; 1; 3 mg/m³) for two years; a control group was exposed to clean air. After one year exposure, 42 µg/lung was found in animals exposed to 0.1 mg/m³ and 2.6 mg/lung in animals exposed to 3 mg/m³. Histological examination of lungs revealed several adverse and non-adverse effects in the lung. The non-adverse effects comprised accumulation of particle-laden macrophages in alveolar/interstitial areas and in the BALT, particle-laden syncytial giant cells in the BALT and bronchiolo-alveolar hyperplasia (alveolar bronchiolization). The adverse effects included (mixed) alveolar/interstitial inflammatory cell infiltration, alveolar/interstitial granulomatous inflammation, interstitial fibrosis and alveolar lipoproteinosis. The incidence and severity of the effects were concentration-related. Alveolar lipoproteinosis was not observed at low concentrations of 0.1 and 0.3 mg/m³ CeO₂. Neither pre-neoplastic nor neoplastic changes were observed after 12-months exposure. A no observed adverse effect concentration could not be established in this study. The comprehensive histopathological examinations of lungs and other tissues will be finalized in 2017.

This project is part of the EU Project NanoReg. Moreover, German Federal Ministry for the Environment, Nature Conservation, Building and Nuclear Safety, German Federal Institute for Occupational Safety and Health, German Federal Environment Agency funded this project.

220

First results of a chronic inhalation study with ceria and barium sulfate nanomaterialsL. Ma-Hock¹, R. Landsiedel¹, J. Keller¹, P. Laux², T. Gebel³¹BASF SE, Experimental Toxicology and Ecology, 67056 Ludwigshafen am Rhein, Germany²German Federal Institute for Risk Assessment, Department of Product Safety, 14195 Berlin, Germany³Federal Institute for Occupational Safety and Health (BAuA), Friedrich-Henkel-Weg 1-25, 44149 Dortmund, Germany

Lung carcinogenicity and putative systemic effects of low-dose life-time inhalation exposure to biopersistent nanoparticles were examined in a chronic inhalation study performed according to OECD test guideline no. 453 with several protocol extensions. Female rats (100/group) were exposed to cerium dioxide (NM-212, 0.1; 0.3; 1; 3 mg/m³) and barium sulfate (NM-220; 50 mg/m³) for two years; a control group was exposed to clean air. Lung burdens and burdens in extrahepatic tissues were measured at various time-points. The two year exposure period was successfully terminated and 50 animals per dose group were examined for organ burden and histopathology. The remaining animals currently are kept exposure-free for maximally 6 additional months. Up to two years exposure to both nanoparticles did not lead to body weight reduction compared to control animals. The mortality rates were in an acceptable range. Macroscopically evident tumors were not detected after two years. The CeO₂ lung burdens were maximally 3.5 mg/g lung tissue at the highest exposure concentration of 3 mg/m³. In comparison, highest CeO₂ burdens in organs remote to exposure were liver and spleen with maximally roughly 1 x 10⁻³ g/g tissue. In brain, maximum CeO₂ levels were 7x10⁻⁶ mg/g lung tissue. BaSO₄ lung burdens were comparatively low (1 mg/g) within the first 13 weeks of exposure and steeply increased to 6 mg/g lung tissue after one year. The comprehensive histopathological examinations of lungs and other tissues will be finalized in 2017.

221

A decision-making framework for the grouping and testing of nanomaterials (DF4nano Grouping)J. Arts¹, M. Hadi², M.-A. Irfan³, A. Keene⁴, R. Kreiling⁵, D. Lyon⁶, M. Maier⁷, K. Michel⁸, T. Petry⁹, U. Sauer¹⁰, D. Warheit¹¹¹AkzoNobel, Technology and Engineering, 6824 Arnhem, Niederlande²Shell Health, Shell International B.V., 2501 Den Haag, Niederlande³BASF SE, Experimental Toxicology and Ecology, 67056 Ludwigshafen am Rhein, Germany⁴Afton Chemical Corporation, Richmond VA23219, Vereinigte Staaten von Amerika⁵Clariant Produkte GmbH, 65843 Sulzbach am Taunus, Germany⁶Shell Health, Shell Oil Company, Houston, TX 77002, Vereinigte Staaten von Amerika⁷Evonik Degussa GmbH, 63457 Hanau, Germany⁸Henkel AG & Co. KGaA, 40589 Düsseldorf, Germany⁹ToxMinds B.V.B.A., 1200 Brüssel, Belgium¹⁰Scientific Consultancy, 85579 Neubiberg, Germany¹¹DuPont Haskell Global Centers, Newark, DE 19714, Vereinigte Staaten von Amerika

The European Centre for Ecotoxicology and Toxicology of Chemicals (ECETOC) 'Nano Task Force' proposes Decision-making framework for the grouping and testing of nanomaterials (DF4nano) that consists of 3 tiers to assign nanomaterials to 4 main groups, to perform sub-grouping within the main groups and to determine and refine specific information needs. The DF4nanoGrouping covers all relevant aspects of a nanomaterial's life cycle and biological pathways, i.e. intrinsic material and system-dependent properties, biopersistence, uptake and biodistribution, cellular and apical toxic effects. Use (including manufacture), release and route of exposure are applied as 'qualifiers' within the DF4nano to determine if, e.g. nanomaterials cannot be released from a product matrix, which may justify the waiving of testing. The four main groups encompass (1) soluble nanomaterials, (2) biopersistent high aspect ratio nanomaterials, (3) passive nanomaterials, and (4) active nanomaterials. The DF4nano aims to group nanomaterials by their specific mode-of-action that results in an apical toxic effect. This is eventually directed by a nanomaterial's intrinsic properties. However, since the exact correlation of intrinsic material properties and apical toxic effect is not yet established, the DF4nano uses the 'functionality' of nanomaterials for grouping rather than relying on intrinsic material properties alone. Such functionalities include system-dependent material properties (such as dissolution rate in biologically relevant media), bio-physical interactions, in vitro effects and exposure. The DF4nano is a hazard and risk assessment tool that applies modern toxicology and contributes to the sustainable development of nano-technological products. It ensures that no studies are performed that do not provide crucial data and therefore saves animals and resources. The grouping decisions of DF4nano for 24 nanomaterials were validated against grouping by results of existing in vivo data and demonstrated 23 concordant grouping decisions.

222

Serum concentrations in cell culture medium influence the effect of cerium oxide nanoparticles on human lung A549 cells: cytotoxicity, proinflammation, cellular uptake, and particle propertiesK. Burchardt¹, H. Papavlassopoulos¹, C. Röhl^{2,1}¹University Medical School Schleswig-Holstein, Institute of Toxicology and Pharmacology for Natural Scientists, Kiel, Germany²Upper State Agency for Social Services Schleswig-Holstein, Department of Environmental Health, Kiel, Germany

The wide use of cerium oxide (CeO₂) nanoparticles (NP), e.g. as fuel additive and for industrial and biomedical applications, evoked intense studies to understand the effects those particles might have on living organisms. Contradictory results of CeO₂ nanoparticle toxicity have been published as they depend on many variables like shape, size, diluent and others.

In our work we used an in vitro model of CeO₂ nanoparticles and lung carcinoma cells to investigate the role of serum content in the cell culture medium on cellular toxicity, particle uptake, proinflammation and particle characteristics.

Proinflammatory CeO₂ NP with an average diameter of 15-30nm and different concentrations were diluted in cell culture medium with different fetal calf serum (FCS) concentrations (0.01, 0.1, 1 and 10%) and were used to expose human lung adenocarcinoma cells (A549) for up to 24 hours.

At 100µg/ml CeO₂ NP showed little to no toxic effect on growth arrested A549 cells at FCS concentrations of 1% or below, but cell viability was decreased to about 80% in proliferating cells in cultures with 10% FCS.

The proinflammatory effect of CeO₂ NP was investigated through measurement of IL-8 mRNA expression after 3 hours and cellular IL-8 secretion after 24 hours. The qRT-PCR showed that the expression of IL-8 mRNA in cells treated with 100 µg/ml CeO₂ NP in 10% FCS medium was three times higher than in cells treated with lower FCS concentrations. This finding correlated with the cellular IL-8 secretion, which showed a stronger increase by cells treated at 10% FCS.

Differences in cellular uptake of CeO₂ NP was determined by fluorescence-activated cell sorting (FACS) after 2 and 24 hours of exposition. After 2 hours, the cells treated with CeO₂ NP in 10% FCS medium showed a lower mean granularity (ΔGMean) as measure for cellular particle uptake than those with less FCS in medium. After 24 hours all probes showed about the same granularity.

To examine the effect the FCS concentrations on CeO₂ NP characteristics in cell cultures we used dynamic light scattering (DLS) and phase contrast microscopy (PCM). DLS measurements revealed an increasing hydrodynamic diameter of the particles with decreasing FCS concentrations (about 1030nm (10% FCS) to 409nm (0.01% FCS)), which was correlated by an increasing particle agglomeration shown by PCM.

Our results show that the FCS concentration in cell culture medium has a direct or indirect impact on the cytotoxicity, the proinflammatory effect, the FACS parameter for cellular particle uptake as well as on particle properties, which should be taken into account when designing, performing and interpreting in vitro experiments to investigate the toxicity of nanoparticles.

223

Toxic and inflammatory effects of shape-engineered titanium dioxide nanoparticles in NR8383 rat alveolar macrophages.J. Kolling¹, C. Albrecht¹, F. Pellegrino², C. Deiana², A. M. Marucco², R. Schins¹¹IUF-Leibniz Research Institute for Environmental Medicine, Particle, inflammation, genome integrity, Düsseldorf, Germany²University of Torino, Department of Chemistry, Torino, Italien

Knowledge about the contrasting toxicity of nanoparticles (NP) of different chemical composition has steadily increased over the past decade. However, available literature often reveals considerable differences in effects within a specific type of nanomaterial. These contrasts have been contributed to different handling and testing protocols as well as to sample-specific differences in physico-chemical properties of NP that could affect their mode of interaction with cells. Within the nanometrology project SETNanoMetro, the highly controlled generation and characterisation of a large set of shape-engineered TiO₂ NP allows us to investigate the potential role of subtle shape- and surface structure changes on NP toxicity. As inhalation represents the most relevant uptake route of NP, the NR8383 rat alveolar macrophage cell line was selected for *in vitro* toxicological testing. Since oxidative stress and inflammation are considered as key biological pathways in nanotoxicity, we evaluated the expression of the oxidative stress marker genes heme oxygenase-1 (HO-1) and g-glutamylcysteine synthetase (g-GCS) as well as the pro-inflammatory genes interleukin (IL)-1β, IL-6, IL-18 and inducible nitric oxide synthase (iNOS) by qRT-PCR. Protein levels of IL-1β and tumour necrosis factor-α (TNF-α) were measured by ELISA. Cytotoxicity testing of the TiO₂ NP by WST-1 assay overall revealed only minimal toxicity in comparison to SiO₂ NP which were used as reference material. HO-1 and g-GCS mRNA analyses indicated that specific TiO₂ NP triggered a moderate induction of oxidative stress. IL-6 was only induced after SiO₂ treatment, whereas IL-18 was not affected by any of the tested NP. In contrast, various TiO₂ NP caused a significant induction of IL-1β mRNA expression. However, no significant induction of IL-1β and TNF-α protein secretion was observed for any of the TiO₂ NP. The results obtained from these and ongoing investigations will be linked to the physico-chemical database as being developed for all TiO₂ NP within the SETNanoMetro project, with the overall aim to build and model nano-structure activity relationships (NSAR) for this widely applied type of nanomaterial.

Acknowledgements: The SETNanoMetro project is supported by the EU-FP7 Programme. Specific types of TiO₂ particles were obtained by Solarion (Switzerland), Evonik and Cristal.

224

Potential of silver and silver nanoparticles to reduce N-acetyltransferase 1 (NAT1) activityJ. Lichter¹, B. Blömeke¹¹Trier University, Department of Environmental Toxicology, Trier, Germany

Humans are exposed to various kinds of engineered nanoparticles including silver, which is frequently used in consumer and biomedical product due to its bactericidal properties. Despite their widespread usage, knowledge about influences on cellular functions is still incomplete. N-acetyltransferase 1 (NAT1), an enzyme which is ubiquitously expressed in human tissues, catalyzes the transfer of an acetyl group to its substrates and although its endogenous function is not clear yet, it is well known to be involved in the N-acetylation of arylamines. In addition NAT1 enzyme activity is known to be modulated by non-substrates including metals and certain nanoparticles, however, the influence of silver on NAT1 has not been analyzed yet.

To address whether human NAT1 is a target of silver nanoparticles and released ions on protein, purified NAT1 was exposed to silver ions (AgNO₃) and silver nanoparticles (Ag10-COOH, average size 10 nm, carboxyl functionalized), and NAT1 enzyme activity was analyzing the N-acetylation of the NAT1 substrate para-aminobenzoic acid (PABA). Therefore, purified NAT1 (1 ng/µl) was co-exposed for 20 min to PABA (1 mM) and

AgNO₃ or Ag10-COOH (0.01, 0.1, 1, 10 and 100 µg/ml each), resulting in a NAT1:silver relation of 1:0.01-100 (w/w).

Both, AgNO₃ and Ag10-COOH inhibited the N-acetylation of PABA in a concentration dependent manner. Using equal amounts of silver and NAT1 (w/w, 1 µg/ml) enzyme activity was reduced about 98±0.2% (AgNO₃) and 82±0.6% (Ag10-COOH). The lowest concentration analyzed (0.01 µg/ml) reduced NAT1 activity about 24±5% (AgNO₃) and 17±5% (Ag10-COOH). Fifty percent activity reduction was caused by 0.11 ± 0.01 µg/ml of AgNO₃ and 0.21 ± 0.04 µg/ml of Ag10-COOH, which is 10-fold lower compared to the published IC50 values for other metal oxide nanoparticles (3-15 µg/ml).

These data indicate that both chemical silver species are able to modulate PABA acetylation. Further studies will be performed to clarify whether silver ions and/or silver nanoparticles could affect the specific N-acetylation of arylamines in human cells.

225

Proteomic analysis of nanosilver-induced effects in rat kidney after subacute oral exposure

A. Oberemm¹, S. Juling¹, R. Georgi¹, C. Meckert¹, **A. Braeuning¹**, A. Lampen¹
¹BfR, Berlin, Germany

Colloidal silver has been used in medicine for centuries and nanosilver is present in many consumer-related products. However, despite of intense research in the past few years, the potential of nanosilver to induce effects different from ionic silver *in vivo* and *in vitro*, is still under debate. In this study, we compared proteomic effects of nanosilver (AgPURE™) and ionic silver (silver acetate) in the kidney of male rats after repeated oral delivery in a rat 28-days toxicity study. In order to avoid overt signs of toxicity, silver was dosed moderately in amounts of 60 and 6 mg/kg body weight for nanosilver and corresponding amounts of silver acetate (9.3 and 0.93 mg/kg). Accordingly, no pathologic effects, including results from clinical chemistry and hematology, were reported. Kidney tissue protein crude extract was separated by 2-D gel electrophoresis and differentially expressed spots were identified by MALDI-MS. 374 unique proteins, showing a log₂ ratio of ≤ -0.3 for downregulation and ≥ 0.3 for upregulation were identified in all treatment groups. Protein lists were analyzed with Ingenuity Pathway Analysis (IPA). When comparing effects of particulate and ionic treatments, similar alterations were indicated for canonical pathways associated with glycolysis, gluconeogenesis and tricarboxylic acid cycle. Regarding inflammatory responses, stronger effects were derived for ionic treatments. For both types of silver exposures, changes of protein expressions were linked to changes of fatty acid metabolism and NRF2-mediated stress. Mitochondrial dysfunction was highlighted for both nanosilver treatments only, as well as activation of the insulin receptor. In the top-scored network of the higher dose nanosilver treatment, upregulated 14-3-3 protein zeta (YWHAZ) displays a central position. YWHAZ, an important regulator of cell cycle and apoptosis, interacts with the insulin receptor and is well known to be involved in many types of cancer. Overall, both forms of silver treatment revealed similar patterns of affected cellular and molecular functions in rat kidney, supporting common and overlapping mechanisms of particulate compared to ionic silver.

226

Effects of nanoscale Barium sulfate on primary lung cells

S. Thomas¹, B. Schumann¹, J. Wiese¹, F. Glahn¹, H. Foth¹
¹Martin-Luther-University Halle-Wittenberg, Institute of Environmental Toxicology, Halle, Germany

Because of the widespread application of nanomaterials and the fact that for some nanomaterials effects on different organisms where shown, nanomaterials are still in focus of interest. Moreover the fate of NPs is only partially assessed over the lifecycle of products containing nanomaterials. While general toxicological properties of NPs are well described in diverse *in-vitro* and *in-vivo* experiments, the distribution of these particles during the whole and complex process of waste incineration shows big knowledge gaps. In the "NanoEmission"-Project the entire route from the residual material via incineration, filtering of the exhaust gas up to a possible release into the environment are considered together with the toxicological evaluation of effects on humans and the environment. In these experiments the influence of thermal waste treatment on the toxicological profile of nanoparticles, contained in the waste, will be described.

After a complete characterization of the two types of BaSO₄-NPs from two different manufacturers by scanning electron microscopy/ energy dispersive X-ray analysis (SEM/EDX), measurement of the specific surface area (BET) and dynamic light scattering (DLS) we investigated the impact of the pure BaSO₄-NPs on primary cells (normal human bronchial epithelial cells (NHBE) and peripheral lung cells (PLC)). Both materials show statistically significant cytotoxic effects in the Resazurin-Assay (decreased viability below 40 % for 1 mg/ml after 72 h). In general the effects of both NPs were almost similar. Additionally the effects of the BaSO₄-NPs were compared more in detail. Uptake of the BaSO₄ was quantified by ICP-MS after 24 h and 72 h as well as the release of Ba-ions into the cell culture medium after centrifugal separation. The incubation with BaSO₄ of PLC and NHBE to 0.1 mg/ml over 24 h and 72 h leads to ~200 µg BaSO₄/1 mio cells. The uptake is dose dependent but not time dependent. The impact on the secretion of inflammatory cytokines was determined by bead-based multiplex-ELISA flow cytometry. TNF-α, IL-8 and IL-33 could be detected in NHBE and PLC after NP incubation. The possible induction of apoptosis was measured by flow cytometry as well. First investigations showed no induction of apoptosis for both materials. The impact of both NPs on the intracellular glutathione level was measured by HPLC and showed a decrease of GSH after 72 h. Summing up BaSO₄-NPs showed toxic effects in primary human lung cell cultures after 72 h for concentrations under 1 mg/ml.

Toxicology – Exposure/effect monitoring

227

C3 from *C. botulinum* modulates the activity of transcription factors

L. von Elsner¹, S. Hagemann¹, I. Just¹, A. Rohrbeck¹
¹MHH, Institut für Toxikologie, Hannover, Germany

C3 exoenzyme from *C. botulinum* is an ADP-ribosyltransferase that inactivates selectively RhoA, B and C by coupling an ADP-ribose moiety. Rho-GTPases represent a molecular switch integrating different receptor signalling to downstream transcriptional cascades that regulate various cellular processes, such as regulation of actin cytoskeleton, cell proliferation and apoptosis. Previous studies with the murine hippocampal cell line HT22 revealed a C3-mediated inhibition of cell proliferation and a prevention of serum-starved cells from apoptosis (Rohrbeck et al., 2012). Former results of studies on MAP kinase signalling indicated C3-induced modulations of downstream signalling modules. Therefore, HT22 cells treated with 500 nM C3 for 48 h were applied for screening of the activity of 48 various transcription factors followed by Luciferase reporter assays. Five transcription factors namely Sp1, ATF2, E2F-1, CBF, Stat6 were identified as significantly regulated in their activity. For validation of identified transcription factors, studies on the protein level of certain target genes were performed. Western blot analyses exhibited an enhanced abundance of Sp1 target genes p21 and COX-2 as well as a raise in phosphorylation of c-Jun. In contrast, the level of apoptosis-inducing GADD153, a target gene of ATF2, was decreased. Our results suggest that C3 is able to modulate the activity of transcription factors whose target genes are involved in the regulation of cell proliferation and apoptosis.

References: Rohrbeck A, Kolbe T, Hagemann S, Genth H, Just I (2012) Distinct biological activities of C3 and ADP-ribosyltransferase-deficient C3-E174Q. FEBS J 279:2657-71

228

Optimized leucocyte isolation from human buffy coats

M. Hemesberg¹, I. Stadler¹, D. Schrenk¹
¹TU Kaiserslautern, Lebensmittelchemie und Toxikologie, Kaiserslautern, Germany

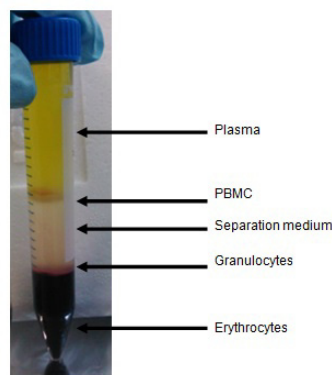
Via covalent binding of chemical compounds to DNA, adducts can be formed. As a consequence, mutations may occur, which represent stages of chemical mutagenesis and carcinogenesis. The isolation of leucocytes represents an essential field of work within DNA-adductomics of blood cells, in which adducts serve as markers of exposure for biological monitoring. Peripheral mononuclear blood cells (PBMC) comprising monocytes and lymphocytes can be separated from other blood cells like granulocytes, erythrocytes (and dead cells) by isopycnic density gradient centrifugation of Buffy Coats (BC's). BC's are blood concentrates rich in leucocytes and thrombocytes, prepared from whole blood samples thorough removal of plasma and erythrocytes. For the experiments only BC's from healthy donors were used. While erythrocytes contain no DNA, lymphocytes, which constitute a subcategory of leucocytes, carry genetic information. A variety of commercially available fluids with a density of 1.077g/cm³, based on different polymers, exists. These materials form the gradient required for the centrifugation. Furthermore, there are several methods available, which differ in the ratio blood vs. fluid, duration of the different work up steps, centrifugation parameters and others. The aim of this work was to compare the effectivity of the different fluids and optimize the workflow.

For isolation of PBMC the fluid was put in a tube and then covered by a thin layer of blood. After centrifugation, five layers were obtained (Figure 1). The interphase was removed carefully, washed and the cells were counted. The yield is expressed as percentage of isolated vs. total leucocytes in the BC, which was based on the leucocyte count of the whole blood sample.

As separation fluids, Ficoll® Paque Plus (GE Healthcare), Histopaque® (Sigma Aldrich) and LSM® (GE Healthcare) were tested. No significant differences between the different fluids were observed. Although dilution is often recommended in literature, it was found that dilution had no effect on the yield. Similarly, using different fluids (RPMI or PBS) for the washing steps did not reveal any differences. Increasing centrifugation speed from 400 to 500 xg resulted in higher yields. In general, large variations in yield (46.8% ± 17.1%) among the various BC's arose. This result is due to the different parameters such as age, storage, leucocyte and erythrocyte counts of the different BC's used. Therefore, the test conditions were optimized using the same batch of BC.

The results show that the low priced separation fluids are comparable in performance to the more expensive ones. By the direct lamination with BC (without dilution) the wastage could be minimized, the yield increased and thus the isolation made more efficient.

Abb. 1



229

Epidermal barrier function challenged by everyday commodities: possible human exposure to polymer additives and their degradation products via skin contacts

N. Bartsch¹, C. Hutzler¹, O. Kappenstein¹, B. Vieth¹, A. Luch¹
¹Bundesinstitut für Risikobewertung, Chemikalien- und Produktsicherheit, Berlin, Germany

The Franz cell is a well-established model in lots of skin research fields. We adapted the diffusion cell system to additives and contaminants of consumer products which are designated for skin contacts. We were aimed to simulate real exposure as realistic as possible.

To meet requirements like longevity, haptic properties and factory costs, different polymers are used as the raw material of choice and modified by a variable number of additives in the majority of commodities. Besides additives with a defined function such as plasticizers, stabilizers, colorants and vulcanization accelerators, contaminants as well as decomposition products or so-called non-intentionally added substances (NIAS) can be part of the material, among them potentially harmful substances.

In a first step, polymers of consumer products like flashlights or tools have been characterized concerning additive composition. Possible breakdown products were identified by means of GC-MS/MS or pyrolysis-GC-MS. We focused on analytes of toxicological relevance including antioxidants such as *N*-phenyl-2-naphthylamine (Neozon D), which is suspected of causing cancer, and on degradation products like cresol and its derivatives (e.g., mesitol or 2-*tert*-butyl-4-methylphenol). Subsequently, analytes of interest were brought into direct skin contact using porcine, human and artificial skin models in the Franz cell chamber assay. The analytes were either followed up layer by layer using tape stripping or examined utilizing cryo sections. For visualization purposes, analytical evaluation has been completed by use of imaging techniques like HE staining or ATR-FTIR (attenuated total reflectance Fourier transform infrared) microscopy. The latter was used with intrinsic markers for tissue specific distribution.

Our project provides evidence for the potential of polymer components to overcome the natural epidermal barrier and, in part, to enter the viable layers of the epidermis. During skin contact with consumer products several substances migrate out of the matrix and penetrate the skin, among them substances which are hazardous to health such as Neozon D.

Toxicology – Biomarkers of exposure/Biomonitoring

230

Post-exposure verification analysis of sulfur mustard poisoning by μ LC-ESI HR MS/MS detection of the alkylated dipeptide HETE-CP after direct proteolysis of human plasma

M. Siegel¹, H. Thiermann², **A. Tsoutsouloupoulos**², H. John²
¹Ludwig-Maximilians-Universität München, Department of Chemistry, Munich, Germany
²Bundeswehr Institute of Pharmacology and Toxicology, Munich, Germany

Depending on its dose, the blister agent sulfur mustard (SM) may lead to painful erythema, blistering with complicated wound healing, pulmonary edema, pulmonary bleeding and temporary blindness. SM is listed as a schedule 1 chemical in the Chemical Weapons Convention and thus its production, stockpiling and use is prohibited. SM still represents a serious threat for civilians and military forces, especially in asymmetric, terrorist and accidental scenarios. After exposure, the highly reactive molecule alkylates nucleophilic sites in endogenous biomacromolecules forming the characteristic and stable hydroxyethylthioethyl (HETE) residue. Hence, bioanalytical methods targeting these adducts in forensic post-exposure verification analysis are of high interest.

Herein, we present an optimized, accurate and comparably simple method to detect adducts of SM and human serum albumin (HSA) alkylated at its cysteine³⁴-residue. Since albumin extraction from human plasma is a time-consuming and expensive step of an established procedure, an alternative method for direct proteolysis of human plasma was developed.

Plasma samples were cleaved directly with pronase resulting in the alkylated dipeptide HETE-cysteine-proline (HETE-CP) which is detected by micro-liquid chromatography-electrospray ionization high-resolution tandem-mass spectrometry (μ LC-ESI HR MS/MS). In order to optimize reproducibility and yield of proteolysis, kinetics were investigated for different kinds of plasma (EDTA-, citrate- and heparin-) as well as serum. Two different mass spectrometers, a triple quadrupole system (4000 QTrap) and a hybrid quadrupole time-of-flight instrument (TT5600⁺), were compared. The latter one proved to be the more selective and sensitive system. The method was successfully applied to *in vitro* and *in vivo* samples of real cases of SM poisoning.

231

Cysteine-proline disulfide adducts from human serum albumin as potential novel biomarkers for verification of exposure to V-type nerve agents

A. Kranawetvogl¹, H. Thiermann¹, **A. Tsoutsouloupoulos**¹, H. John¹
¹Bundeswehr Institute of Pharmacology and Toxicology, Munich, Germany

Organophosphorus compounds (OP), which were originally intended to be used as pesticides to increase agricultural yields at the onset of the 20th century, still represent a considerable threat to human health. By irreversible inhibition of acetylcholinesterase OP lead to cholinergic crisis due to uncontrolled increase of acetylcholine in the synaptic cleft. Finally, sudden death by respiratory failure may result if medical countermeasures are lacking. Therefore exceptionally toxic compounds were designed and synthesized as chemical warfare agents (CWA), among which V-type nerve agents, i.e. VX, Chinese VX and Russian VX, belong to the most toxic artificial substances. Recent events like the First Gulf War, terrorist attacks in Tokyo and the conflict in Syria underline the need for ongoing and strict surveillance of CWA prohibition by the Chemical Weapons Convention. Unambiguous evidence of such substances (verification analysis) plays an important role with great political and legal impact. A variety of such bioanalytical

methods have been established at the Bundeswehr Institute of Pharmacology and Toxicology in Munich, which is accounted for medical chemical defence in Germany.

Exhibiting quite short half-lives *in vivo* nerve agents can hardly be detected days or even weeks after exposure. Accordingly, there is a great need for additional long-term biomarkers like specific protein adducts. Consequently, the current work focuses on examination of adducts between nerve agents and human serum albumin (HSA) as its high abundance and stability *in vivo* provide relative ease of sampling. After incubation of HSA with V-type nerve agents *in vitro* the protein was subjected to proteolysis. Subsequently resulting peptides were separated using microbore high-performance liquid chromatography (μ LC) and detected on-line by modern high-resolution tandem-mass spectrometry (HR MS/MS). This allowed unambiguous identification of already known phosphorylated tyrosines as well as novel adducts between cysteine-proline dipeptides and the thiol-containing leaving group of V-type nerve agents. Simultaneous detection of both biomarkers was realized by a new method, which was applicable even at the very low toxicologically relevant concentrations of V-type agents. Therefore, this method represents a valuable and novel supplement of existing methods for verification.

232

Quantification of hemoglobin adducts for the assessment of the internal exposure to glycidol

J. Hielscher¹, B. Monien¹, K. Abraham¹, A. Seidel², A. Lampen¹
¹Bundesinstitut für Risikobewertung, Lebensmittelsicherheit, Berlin, Germany
²Biochemical Institute for Environmental Carcinogens – Prof Dr. Gernot Grimmer-Foundation, Grosshansdorf, Germany

Fatty acid esters of glycidol (glycidyl esters) are processing contaminants formed as byproducts of industrial deodorizing of plant fats or during other heating processes. Following oral intake, glycidyl esters are mainly cleaved to release the reactive glycidol in the gastrointestinal tract. According to the National Toxicology Program (NTP), glycidol is carcinogenic, genotoxic and teratogenic in rodents. It is classified as probably carcinogenic to humans (IARC group 2A). The exposure assessment of the oral intake of glycidyl esters in humans is difficult, because the current data set for glycidyl ester contents in food is incomplete.

We developed a method for the determination of the internal exposure to glycidol by mass spectrometric quantification of a hemoglobin adduct reflecting the total glycidol burden over approximately three months. A modified Edman degradation was adapted for the cleavage of the valine residues from the *N*-termini of hemoglobin by fluoresceinisothiocyanat (FITC) (von Stedingk et al. (2011) Chem Res Toxicol 24, 1957) resulting in the formation of dihydroxypropyl-valine-fluorescein thiohydantoin (DHP-Val-FTH). The target analyte is purified with mixed-mode anion-exchange solid-phase extraction and analyzed by LC-MS/MS. A major advantage of the technique is the application to whole blood samples, which renders the time-consuming isolation of erythrocytes unnecessary. We synthesized DHP-d₇-Val-FTH as an internal standard for the quantification of the glycidol adduct by LC-MS/MS multiple reaction monitoring. A limit of detection of 5 fmol per injection (5 pmol adduct/g hemoglobin) was achieved. The application of this method will possibly allow future monitoring of the internal exposure of glycidol in human studies.

233

Urinary Biomarker for the internal Exposure to Glycidol and 3-monochloropropane-1,2-diol (3-MCPD)

J. Hielscher¹, B. Monien¹, T. Göen², A. Lampen¹, K. Abraham¹
¹Bundesinstitut für Risikobewertung, Lebensmittelsicherheit, Berlin, Germany
²Friedrich-Alexander Universität, Erlangen, Germany

Glycidol and 3-monochloropropane-1,2-diol (3-MCPD) are carcinogenic food contaminants, which are present in heat-processed oils and fats mainly in form of fatty acid esters. The risk assessment concerning human consumption of these substances is complicated by various reasons. For example, the data on the occurrence in food stuffs is incomplete. Also, the amounts of the proximate carcinogens released from ester hydrolysis in the gastrointestinal tract in humans are not known. Monitoring of the internal exposure would be an alternative strategy to support the assessment of possible health risks related to the intake of glycidol and 3-MCPD and their fatty acid esters.

For short-term monitoring of the internal exposure, urinary metabolites are suitable biomarkers. We study the potential use of two different substances as descriptors of the oral intake of glycidol and 3-MCPD. The metabolite 2,3-dihydroxy mercapturic acid (DHPMA) is generated following glutathione conjugation of both compounds. The second target analyte is 3-MCPD itself, which may also be formed from glycidol in the reaction with hydrochloric acid in the stomach. A method for the quantification of urinary 3-MCPD by GC-MS is currently developed. An LC-MS/MS multiple reaction monitoring technique was devised for the quantification of DHPMA in urine samples with the isotope-labeled reference compound ¹³C₂-DHPMA. The limit of quantification is 10 μ g DHPMA/l. Related to creatinine, the analyte was detected to be in a relatively small concentration range in urine samples from humans. The average concentration in urine samples (n = 45) of one male volunteer collected over ten days was 154 \pm 21 μ g DHPMA/g creatinine. A meal of a highly contaminated, commercially available frying fat (containing 1.1 mg of glycidol equivalents) did not lead to a visible increase of the urinary concentrations. The considerable background levels of DHPMA in urine of humans and also in urine samples of other mammals support the hypothesis that DHPMA may be also be formed from an endogenous C₃-metabolite, as already reported by Eckert et al. (2011).

234

A Hemoglobin Adduct to Determine the Internal Exposure to the Food Carcinogen Furfuryl Alcohol

J. Hielscher¹, K. Abraham¹, A. Lampen¹, **B. Monien¹**
¹Bundesinstitut für Risikobewertung, Lebensmittelsicherheit, Berlin, Germany

Furfuryl alcohol is a common food contaminant formed by acid- and heat-induced dehydration from pentoses. It induced renal tubule neoplasms in male B6C3F1 mice and nasal neoplasms in male F344/N rats in a study of the National Toxicology Program (NTP). The neoplastic effects may originate from sulfotransferase (SULT)-catalyzed conversion of furfuryl alcohol into the DNA reactive and mutagenic 2-sulfoxymethylfuran. The incomplete data set of furfuryl alcohol contents in food does not allow estimating the human exposure. Thus, we sought a method for the determination of the internal exposure. Recently, the DNA adduct of furfuryl alcohol *N*²-[(furan-2-yl)methyl]-2'-deoxyguanosine was detected in specimen of human lung tissue. However, human biomonitoring of DNA adducts has various disadvantages. For example, DNA adducts are removed by various repair systems and human DNA samples are usually not accessible in sufficient quantities. We decided to develop a biomarker for the internal exposure to furfuryl alcohol using blood proteins as dosimetric targets. Following incubation of 2-sulfoxymethylfuran with hemoglobin, we detected adducts of Cys, Lys, His and Trp and the *N*-terminal Val. An Edman degradation-based technique was developed using fluorescein isothiocyanate (FITC) for the removal of the *N*-terminal Val from hemoglobin. The cleavage of 2-sulfoxymethylfuran-modified Val residues leads to the formation of the analyte *N*-[(furan-2-yl)methyl]-Val-FITC thiohydantoin (FM-Val-FTH). This was synthesized by chemical means and characterized by ¹H and ¹³C NMR spectroscopy. In the course of the analytical sample preparation, the Edman analyte was purified with mixed-mode anion-exchange solid-phase extraction and analyzed by LC-MS/MS multiple reaction monitoring. FM-Val-FTH was detected unambiguously in blood samples of FVB/N mice that had received a single oral dose of 400 mg furfuryl alcohol/kg body weight. We synthesized FM-d₅-Val-FTH as an internal standard for the quantification of the furfuryl alcohol adduct by LC-MS/MS. The analyses of blood samples from animal experiments about the influence of sex and ethanol exposure on the bioactivation of furfuryl alcohol in mice are underway.

235

Ultra-slow N-acetyltransferase 2 (NAT2) and prognosis in bladder cancer patients

S. Selinski¹, B. Geis^{1,2}, H. Gerullis^{3,4}, T. Otto⁵, E. Roth⁵, F. Volkert⁵, D. Ovsianikov⁶, J. Salem⁶, O. Moormann⁶, H. Niedner¹, M. Blaszkewicz¹, J. G. Hengstler¹, **K. Golka¹**
¹Leibniz Research Centre for Working Environment and Human Factors at TU Dortmund
²Dortmund, Germany
³TU Dortmund University, Faculty of Statistics, Dortmund, Germany
⁴Lukasklinik, Department of Urology, Neuss, Germany
⁵Carl von Ossietzky University Oldenburg, Department of Urology, Oldenburg, Germany
⁶Evangelic Hospital, Paul Gerhardt Foundation, Department of Urology, Lutherstadt Wittenberg, Germany
⁶St.-Josefs-Hospital, Department of Urology, Dortmund, Germany

Bladder cancer (BC) is a smoking and occupation related disease showing a substantial genetic component. Though the prognosis is generally good, a major problem is the frequent relapses affecting about half of the patients. N-acetyltransferase 2 (NAT2) is well-known to modulate BC risk in persons heavily exposed to carcinogenic aromatic amines. We aim to investigate the impact of NAT2 genotypes, in particular, the ultra-slow genotype, on relapse-free time after first diagnosis in 772 bladder cancer cases. We used follow-ups of three case-control studies from Lutherstadt Wittenberg (n=207), Dortmund (n=167) and Neuss (n=398). NAT2 was genotyped using seven characteristic polymorphisms (rs1801279, rs1041983, rs1801280, rs1799929, rs1799930, rs1208, rs1799931). Haplotypes were reconstructed using PHASE v.2.1.1. We compared slow to rapid acetylators. Additionally, we differentiated between the most frequent slow NAT2*5B/*5B and *5B/other slow haplotypes as well as between the ultra-slow *6A/*6A and *6A/other slow haplotypes compared to rapid acetylators. Chi-square tests used to check the frequency of relapses in ultra-slow, slow and rapid acetylators. Genotype differences in relapse-free time up to 5 yr after first diagnosis of BC were analysed using Cox proportional hazards models adjusted for age, gender, smoking habits, invasiveness and study group. A total of 371 (49%) patients showed a relapse within the first 5 yr after BC diagnosis. Slow acetylators show a higher frequency of relapses than rapid acetylators (51% vs. 46%, P=0.154). This frequency is even higher in ultra-slow acetylators (61%, OR=1.81, P=0.019) but not in slow *5B/*5B genotypes (49%, P=0.609). Ultra-slow acetylators had a significantly shorter relapse free time within 5 yr after BC diagnosis than rapid acetylators (median 0.66 vs. 0.94 yr, HR=1.57, P=0.009). This trend was not that pronounced in all slow acetylators combined (0.78 yr, HR=1.19, P=0.127) nor in the subgroup of NAT2*5B/*5B genotypes (0.79 yr, HR=1.20, P=0.255). The effect of ultra-slow NAT2 is even more pronounced in smokers (HR=1.78, P=0.003) but absent non-smokers (HR=0.89, P=0.781). Ultra-slow NAT2 seems to be associated with a higher recurrence risk and a shorter relapse-free time, especially in smokers. Slow NAT2 in general seems to have less impact on recurrence.

236

A targeted metabolomics approach reveals proline as a biomarker candidate for (xeno)estrogenic effects in MCF-7 cells

S. Potratz¹, P. Tarnow¹, H. Jungnickel¹, S. Baumann^{2,3}, M. von Bergen^{2,4,5}, A. Luch¹
¹German Federal Institute for Risk Assessment (BfR), Department Chemicals and Product Safety, Berlin, Germany
²UFZ – Helmholtz-Centre for Environmental Research, Department Metabolomics, Leipzig, Germany
³University of Leipzig, Institute of Pharmacy, Faculty of Biosciences, Pharmacology and Psychology, Leipzig, Germany
⁴UFZ – Helmholtz-Centre for Environmental Research, Department Proteomics, Leipzig, Germany

Germany

⁵Aalborg University, Department of Biotechnology, Chemistry and Environmental Engineering, Aalborg, Denmark

Xenoestrogens with the potential for endocrine disruption like bisphenol A (BPA) may bind to the estrogen receptors (ERs) and modulate expression of ER target genes mimicking the natural ligand 17β-estradiol (E2). The potential for endocrine adversity is still predominantly assessed *in vivo* as existing *in vitro* tests have only limited value for an exposure-based risk assessment. Thus, the development of reliable bioassays for the detection of endocrine disruptors is one of the paramount challenges faced by modern toxicology.

A targeted metabolomics approach in MCF-7 cells treated with E2 or BPA revealed potential biomarkers for the estrogenic potency of the studied compounds. Among them were several phosphatidylcholines and amino acids. We further addressed proline levels that were found to be strongly increased. Investigations of proline levels over time showed a clear proliferation correlated concentration dependency after both E2 and BPA stimulation. Furthermore, siRNA knockdown experiments suggested an influence of the oncogenic transcription factor MYC and the dependency of ERα activation on the estrogen-mediated proline increase.

Our study demonstrates metabolomics as a powerful tool for biomarker identification and hypothesis generation. The results could be used further to develop bioassays for the detection of endocrine disruptive chemicals.

Toxicology – External exposure

237

Assessing exposure of young children to chemicals: a human biomonitoring project from North Rhine-Westphalia, Germany

Y. Chovolou¹, S. Rudzok¹, S. Sievering¹, M. Kraft¹

¹Landesamt für Natur, Umwelt und Verbraucherschutz NRW, FB33: Umweltmedizin, Toxikologie, Epidemiologie, NIS, Essen, Germany

Children are considered to be more sensitive to most chemicals than the general population due to a variety of factors, including dynamic growth and developmental processes as well as physiological, metabolic and behavioral differences [1]. However, only a few data are available on the magnitude of preschool children's exposure to most chemicals present in many consumer products. Several of these chemicals are linked to endocrine disrupting effects in animal studies and are suspected to have also adverse effects e.g. on development and function of the reproductive organs as well as on neurological and behavioral development in humans. Among of the chemicals that have been a major focus of discussion in the last years are Phthalates, DINCH, Parabens, Bisphenol A, and Triclosan due to their suspected health effects. Therefore we aimed to investigate exposure levels to metabolites of different Phthalates and Parabens as well as to Bisphenol A and Triclosan in urine samples collected from preschool children in German day-care centers from North Rhine-Westphalia (LUPE III; 2011/12). Urine specimens from children aged from 20 to 80 months from 23 different day-care centers were analyzed. In total, 253 preschool children were recruited with mean age of 54 months. Our study results show that nearly all children (>95 %) of the study population had urine concentrations equal to or above the limit of quantification for five most common Phthalates metabolites (MnBP, MiBP, 5OH-MEHP, 5oxo-MEHP, 7oxo-MINP), for Bisphenol A and Methylparaben. Triclosan was detected in 16 % of the study population. In general, the median urinary concentrations of the above mentioned Phthalate metabolites were about 5-50 µg/l in spot urine samples. The highest amount among the Phthalate metabolites was observed for MiBP with maximal values of about 1000 µg/l. Median urinary concentration for Methylparaben and Bisphenol A were about 48 µg/l and 2 µg/l respectively. The maximum Methylparaben, Bisphenol A and Triclosan level found were 1770 µg/l, 72.4 µg/l and 55.6 µg/l respectively. In conclusion, our study shows a widespread exposure of young children to various Phthalates, Parabens and Bisphenol A in North Rhine-Westphalia, Germany. A follow-up human biomonitoring study (2014/2015) has finished recruitment and is in the process of analyzing data.

1. Principles for evaluating health risks in children associated with exposure to chemicals. Environmental Health Criteria (EHC) monograph, Vol 237, WHO 2006

Toxicology – Food toxicology

238

Current levels of polycyclic aromatic hydrocarbons in local smoked fish in Schleswig-Holstein

D. Appel¹, H.-J. Martin¹, E. Maser¹

¹Institut für Toxikologie und Pharmakologie für Naturwissenschaftler Kiel, Kiel, Germany

Polycyclic aromatic hydrocarbons (PAHs) represent a large group of organic compounds that are common environmental contaminants. They are formed by incomplete combustion of organic matter such as coal or crude oil and are often known to be carcinogenic, mutagenic and teratogenic. The acute toxicity of PAHs is rather low, but because of their stability and lipophilic character those compounds can accumulate in the human body and cause severe chronic effects. Additionally PAHs may enter the food chain when preserving meat or fish by exposure to smoke. In the European Union maximum levels of 2 µg/kg benzo[a]pyrene and 12 µg/kg as the sum of benzo[a]pyrene, benzo[a]anthracene, benzo[b]fluoranthene and chrysene in the meat of smoked fish and smoked fishery products are set, respectively.

Smoked fish is often handmade in small fishery stores in Schleswig-Holstein, where self caught fish is prepared in smoke houses. This technique implies the danger of PAHs to accumulate in smoked fishery products above allowed maximum levels.

Here, we report our findings of PAHs in smoked fishery products bought in local convenience and fishery stores in Schleswig-Holstein and give a brief overview about actual contaminant levels. HPLC with fluorescence detection was used to determine the quality and quantity of several toxic PAHs in smoked fishery products made locally. PAHs may constitute risks for human health when exposed to hazardous levels and therefore it is important to have knowledge about given contaminant levels.

239

Heme-iron, but not inorganic iron, induces DNA damage in colon epithelial cells with delayed cytotoxicity

S. Hasselwander¹, N. Seiwert¹, T. Marschall², T. Schwerdtle², B. Kaina¹, **J. Fahrner¹**
¹Universitätsmedizin Mainz, Institut für Toxikologie, Mainz, Germany
²Universität Potsdam, Lehrstuhl für Lebensmittelchemie, Institut für Ernährungswissenschaften, Nuthetal, Germany

Colorectal cancer (CRC) is one of the most frequent cancers worldwide and is tightly linked to dietary habits. Epidemiological studies provided evidence that the intake of red meat is associated with an increased risk to develop CRC [1]. Red meat contains high amounts of heme iron, which is thought to play a causal role in tumor formation. The underlying molecular mechanism, however, remains elusive and may involve increased cell proliferation and DNA damage induction by heme-iron. In this study, we set out to analyze the genotoxic and cytotoxic effects of heme-iron in human colonic epithelial cell lines. We used hemin (Fe^{II}) as commercially available heme source, which was compared to inorganic iron chloride (FeCl₃). First, the time-dependent internalization of hemin and FeCl₃ into HCT116 cells was determined using ICP-MS/MS analysis. Treatment of cells with inorganic iron resulted in a maximum of intracellular iron content after 1 h at all doses tested, while hemin particularly at high doses caused an iron accumulation up to 24 h. Hemin catalyzed the formation of reactive oxygen species (ROS) in a dose-dependent manner in CaCo-2 and HCT116-cells as shown by flow cytometry. Consistent with this finding, hemin dose-dependently induced the oxidative DNA lesion 8-oxoguanine (8-oxoG) as revealed by slot blot analysis and Fpg-modified alkaline Comet assay. Using a pharmacological inhibitor of MutT homologue 1 (MTH1), which protects the nucleotide pool by hydrolysis of 8-oxoGTP, 8-oxoG DNA adduct levels in hemin-treated cells were further enhanced. In contrast, inorganic iron hardly affected the cellular ROS level and only slightly increased oxidative DNA damage. Subsequently, a time- and dose-dependent activation of the DNA damage response (DDR) by hemin was shown in HCT116 and CaCo-2 cells using western blot analysis, which was followed by a reduction in cell viability at high doses after 72 h. Finally, the cytotoxic effects of hemin and inorganic iron were tested using an *ex vivo* model of intestinal crypt organoids. Preliminary results indicate that hemin is highly cytotoxic in organoids, whereas inorganic iron does not impair their viability. Taken together, this study demonstrated that hemin induces oxidative stress and DNA damage, resulting in the activation of the DDR and subsequent cytotoxicity. In contrast, inorganic iron displayed only modest effects. Further *in vivo* studies using DNA-repair deficient and proficient animals will shed light on the contribution of specific DNA lesions to heme-associated colorectal carcinogenesis.

[1] Fahrner and Kaina (2013) Carcinogenesis, 34 (11):2435-2442

240

The role of the enzyme O⁶-alkylguanine DNA alkyltransferase in a non-transformed human colon epithelial cell line

J. Döhning¹, A. Stormetta², M. Christmann³, P. Villalta⁴, S. J. Sturla², P. Steinberg¹
¹University of Veterinary Medicine, Hannover, Institute for Food Toxicology and Analytical Chemistry, Hannover, Germany
²ETH Zurich, Department of Health Sciences and Technology, Zurich, Switzerland
³University Medical Center Mainz, Department of Toxicology, Mainz, Germany
⁴University of Minnesota, Masonic Cancer Center, Minneapolis, Vereinigte Staaten von Amerika

Red and processed meat consumption is known to be a crucial risk factor in the development of colon cancer, which is one of the most common cancers worldwide. A diet rich in red and processed meat increases *N*-nitrosation within the colon leading to an increase in endogenously formed nitroso compounds. These compounds are able to alkylate DNA of gastrointestinal tract cells, resulting in the formation of DNA adducts such as O⁶-carboxymethylguanine (O⁶-CMG) and O⁶-methylguanine (O⁶-MeG). If not repaired, O⁶-CMG and O⁶-MeG adducts can induce GC to AT transition mutations in genes known to be mutated in colorectal cancer such as *ras*. O⁶-CMG and O⁶-MeG DNA adducts may therefore play a role in colon carcinogenesis. The function of the enzyme O⁶-alkylguanine DNA alkyltransferase (MGMT) is to repair DNA adducts that occur at the O⁶-position of guanine. Although it is known that O⁶-MeG is repaired by MGMT, the potential of this enzyme to repair O⁶-CMG in cells is not well characterized. Additionally, adenomas containing a K-ras GC-AT transition mutation have lower MGMT levels than adenomas without this mutation. Therefore, the aim of this study is to determine the role of MGMT in protecting colorectal cells from genotoxicity by repairing O⁶-CMG adducts. For this purpose, an MGMT-deficient non-transformed human colon epithelial cell line was established by stable transfection via RNA interference to inhibit the expression and therefore the activity of MGMT. The transfected cell line was analyzed for complete MGMT gene silencing by activity and expression analyses and cell characterization. Results confirmed that there was neither expression nor activity for MGMT in the transfected cells, and the cell characterization data showed that MGMT deficiency did not lead to differences in growth behavior or cell morphology or malignant cell transformation. Cytotoxicity experiments performed in the transfected and non-transfected cell lines by treatment with DNA alkylating agents suggest that the MGMT-deficient cell line is more sensitive to DNA alkylating agents than the non-transfected cell line. These results were also supported by DNA damage analysis via comet assay. To further understand the role of MGMT in colon epithelial cells, quantitation of O⁶-CMG and O⁶-MeG adducts by LC-MS/MS in the transfected and non-transfected cell lines will reveal if MGMT deficiency leads to more O⁶-CMG and O⁶-MeG adducts and if the MGMT enzyme is responsible for the DNA repair of O⁶-CMG.

241

DNA-adduct formation with α - and β -asarone-epoxide

S. Stegmüller¹, A. Cartus¹, K. Berg¹, D. Schrenk¹
¹Technische Universität Kaiserslautern, Lebensmittelchemie und Toxikologie, Kaiserslautern, Germany

Asarones are secondary plant constituents mainly occurring in *Acorus calamus* L. and *Guatteria gaumeri*. The essential oil of the rhizome of *Acorus calamus* L. is used for flavoring of food and alcoholic beverages. The concentration of β -asarone (bA) in these oils varies between 0.3% and 95%. The bark of *Guatteria gaumeri*, which is rich in α -asarone (aA), is used as cholesterol-lowering drug and to treat gallstones in traditional Mexican medicine. Both, aA and bA are carcinogenic in rodents and mutagenic in the Ames test after metabolic activation and thus classified as genotoxic carcinogens.^[1,2] Previously, the major metabolites in microsomal incubations with aA and bA were identified and synthesized in our laboratory. Side-chain epoxides, the corresponding diols, side-chain alcohols and aldehydes were identified as the major metabolites of aA and bA.^[3] The investigation of the mutagenic potency in the Ames fluctuation test showed positive results in the Salmonella strain TA 100 for aA and bA with metabolic activation and for aA- and bA-epoxide without metabolic activation. While it is known that epoxides are reactive against nucleophiles we set up the hypothesis of DNA-adduct formation by epoxides to explain the mutagenic effect.

First we examined the reactivity between the epoxides and 2'-deoxyadenosine and 2'-deoxyguanosine. This result was confirmed by LC-MS/MS analysis. The adduct N²-2'-deoxyguanosine-1'-hydroxy-asarone with a mass of [M+H]⁺ 492.2 amu showed the characteristic fragments of [M-116]⁺ 376.2 amu and [M-dG]⁺ 225.1 amu. The adduct N²-2'-deoxyadenosin-1'-hydroxy-asarone with a mass of [M+H]⁺ 476.2 amu showed characteristic fragments of [M-116]⁺ 360.2 amu and [M-dA]⁺ 225.1 amu.

This adducts are currently isolated, characterized by NMR-spectroscopy and used to quantify adducts in cells. At the same time primary rat hepatocytes were incubated with non-cytotoxic concentrations of aA and bA for 24 h. After harvest and lysis of the cells, the DNA was isolated by chloroform/phenol extraction and enzymatically hydrolyzed.^[4] The residual hydrolysates will be used to identify the DNA-adducts formed in cells and to determine the adduct formation rate.

Preliminary experiments indicate that both, aA and bA also form DNA-adducts in intact cells in a concentration-dependent manner.

[1] Göggmann, Schimmer (1983). Mutagenicity testing of α -asarone and commercial calamus drugs with *Salmonella typhimurium*. Mutation Research. 121, 191-194

[2] Wiseman *et al.* (1987) Structure-Activity Studies of the Hepatocarcinogenicities of Alkenylbenzene Derivatives Related to Estragole and Safrole on Administration to Preweaning Male C57BL/6J \times C3H/HeJ F1 Mice. Cancer Res, 47; 2275

[3] Cartus *et al.* (2015) Hepatic Metabolism of Carcinogenic β -Asarone. Chem Res Toxicol, 28(9):1760-73

[4] Schumacher *et al.* (2013) Optimized enzymatic hydrolysis of DNA for LC-MS/MS analyses of adducts of 1-methoxy-3-indolylmethyl glucosinolate and methyleugenol. Anal Biochem. 2013; 434(1):4-11.

242

The redox sensor protein DJ-1 is oxidized by the food contaminants 3-chloro-1,2-propanediol (3-MCPD) and 2-chloro-1,3-propanediol (2-MCPD) in different rat tissues

T. Buhre¹, L. Voß¹, A. Briese¹, H. Stephanowitz², E. Krause², A. Braeuning¹, A. Lampen¹

¹Bundesinstitut für Risikobewertung (BfR), Lebensmittelsicherheit, Berlin, Germany
²Leibniz-Institut für Molekulare Pharmakologie, Berlin, Germany

Fatty acid esters of 3-chloro-1,2-propanediol (3-MCPD) and of 2-chloro-1,3-propanediol (2-MCPD) are food process contaminants that are formed, e.g., during refinement of vegetable oils. After ingestion, the esters are hydrolyzed in the gut, thereby releasing free 3-MCPD and 2-MCPD. 3-MCPD has been identified by the International Agency for Research on Cancer (IARC) to be possibly carcinogenic to humans (class 2B) and is therefore in the focus of food safety authorities.

To elucidate the toxicological properties of these compounds at the molecular level (Mode of Action) a proteomic study was conducted in which 10 mg/kg b.w./day of either 3-MCPD or 2-MCPD were orally administered to rats over a period of 28 days. Total protein was extracted from different tissues of the animals and separated via two-dimensional gel electrophoresis (2DE). Among others, the redox sensor protein DJ-1 was identified to be deregulated in liver, kidney, testis, and heart of rats treated either with 3-MCPD or 2-MCPD. Up to six different isoforms of DJ-1 were identified by 2DE-Western blot analysis, all of them having the same molecular weight but different pI values, indicating protein modifications of low molecular weight but with a strong impact on the protein charge. Treatment of the animals with either 3-MCPD or 2-MCPD predominantly led to a shift of the abundance between two DJ-1 isoforms in the rat tissues. This effect was more pronounced with 3-MCPD compared to 2-MCPD. Mass spectrometric analysis of these two isoforms identified an oxidation of a conserved cysteine residue (Cys106) of DJ-1 to a cysteine sulfonic acid to be the protein modification induced by treatment of the rats with either 3-MCPD or 2-MCPD.

DJ-1 is discussed to participate in a number of biological processes such as proteolysis, protein folding, or redox regulation. Oxidation of Cys106 was shown to be crucial for the activity of DJ-1, and the irreversible oxidation of Cys106 to a cysteine sulfonic acid as observed in the present study was shown to result in a loss of protein function and was correlated with diseases related to oxidative stress such as Parkinson's disease. Thus, the potential impact of 3-MCPD and 2-MCPD on cellular oxidative stress and on associated neurodegenerative diseases has to be considered in the ongoing risk assessment of these food contaminants.

243

Molecular modes of action of a long-term exposure to hepatotoxic pyrrolizidine alkaloids in the human hepatoma cell line HepaRG

J. Waizenegger¹, C. Luckert¹, A. Braeuning¹, A. Lampen¹, S. Hessel¹
¹Bundesinstitut für Risikobewertung, Lebensmittelsicherheit, Berlin, Germany

Pyrrolizidine alkaloids (PA) are secondary plant compounds and widely spread in plant kingdom. Humans can therefore be regularly exposed via direct or indirect contamination of food, like herbal teas, honey, wheat or salad. 1,2-unsaturated PA are known for their potentially harmful effects. An acute intoxication may cause veno-occlusive disease leading to hepatomegaly, ascites as well as liver hardening resulting in high mortality. On the other hand, chronic PA intoxications due to regular consumption of small amounts of PA are characterized by hepatic necrosis, fibrosis and cirrhosis.

An initial whole genome transcriptome study in hepatocytes revealed that molecular pathways related to cancer development, cell cycle regulation and cell death are regulated by the four structurally different PA echinidine, heliotrine, senecionine and senkirkine in short-term exposure (24h). Additionally, lipid and bile acid metabolism was affected. However, the uptake of PA by food is more likely to be continuous than singular. Therefore, the aim of this study was to investigate molecular effects of long-term exposure (14d) comparatively to short-term exposure (24h) in the hepatoma cell line HepaRG with the four structurally different PA.

In this context we analyzed selected cellular parameters like cytotoxicity and morphology. In contrast to short-term exposure, structure- and concentration-dependent cytotoxicity was found for the long-term exposure (Sn>He>Em>Ski). Furthermore, obvious morphological changes such as destructure and perforation of the HepaRG cell monolayer were seen after 14d of incubation. Based on these findings, a possible induction of apoptosis or necrosis by PA was examined.

Effects of long-term exposure to PA on gene expression were investigated for a set of genes found to be regulated in the short-term whole genome transcriptome study. The identified regulation of gene expression was confirmed for both terms, with the strongest regulation for CYP7A1 (down-regulation), a gene involved in cholesterol metabolism. Therefore, the effects of PA on various parameters related to cholesterol metabolism were analyzed, showing PA effects on cholesterol levels and bile acid secretion.

Short-term exposure to PA did not affect cell viability. However, repeated doses of PA resulted in severe effects on hepatic cells, concerning viability and morphology. At the mRNA level, short- and long-term incubation with PA seem to affect a wide range of signaling pathways. In conclusion, we show for the first time that HepaRG cells can serve as an *in vitro* model for hepatotoxicity following chronic intake of PA.

244

Characterization of cytotoxic effects caused by the enzyme subunit of subtilase cytotoxin from *Escherichia coli*

A. Schroll¹, H. Schmidt¹, H. Barth¹
¹Universitätsklinikum Ulm, Institut für Pharmakologie und Toxikologie, Ulm, Germany

Shiga toxin-producing *E. coli* (STEC) strains cause a diversity of enteric symptoms in humans, ranging from mild diarrhea to severe diseases such as the hemolytic uremic syndrome (HUS). HUS is a life threatening disease with microvascular endothelial damage in the gastrointestinal tract and the kidneys, which often leads to haemolytic anemia, thrombocytopenia and acute renal failure. Shiga toxin plays a major role for the pathogenesis of HUS but the subtilase cytotoxin, which was identified during an HUS outbreak in 1998 in STEC strains, might contribute as an additional potent enterotoxin. Like Shiga toxin, SubAB is an AB₅ protein toxin. The pentameric binding/transport subunit (SubB) delivers the enzymatic active subunit (SubA), a protease, into the endoplasmic reticulum (ER) of human target cells. In the ER, SubA cleaves the chaperone BiP/GRP78, which results in cell stress and caspase 3/7 dependent cell death.

Recently, we discovered that higher concentrations of SubA (10 mg/mL) causes cytotoxic effects in human epithelial cells (HeLa, Caco-2) in the absence of SubB. The cytotoxic effects were investigated in HeLa cells in more detail. Here, SubA binds in a concentration dependent manner to the cell surface and induces dramatic morphological changes as well as caspase-dependent cell death [1]. In contrast to HeLa and Caco-2 cells, CHO fibroblasts did not respond to SubA. Currently, further cell types including macrophages are tested for SubA effects and the molecular mechanisms underlying the cytotoxic effects caused by SubA and the cell type selectivity are investigated. Although there are strong cytotoxic effects caused by SubA on some human epithelial cells *in vitro*, the situation *in vivo* and the pathogenic relevance of the newly observed SubA effect are not known.

[1] Funk J[§], Biber N[§], Schneider M, Hauser E, Enzenmüller S, Förtsch C, Barth H*, Schmidt H* (2015). Cytotoxic and Apoptotic Effects of Recombinant Subtilase Cytotoxin Variants of Shiga Toxin-Producing *Escherichia coli*. *Infect. Immun.* 83, 2338-2349. (†contributed equally; *corresponding authors).

245

Proteomic effects of 2-monochloropropanediol (2-MCPD) and its dipalmitate in rat heart after subacute oral treatment

K. Schultrich¹, A. Oberemm¹, F. Frenzel¹, A. Braeuning¹, C. Meckert¹, A. Lampen¹
¹BfR, Berlin, Germany

Thermal treatment of fat-containing foodstuff in the presence of salt leads to formation of 3-MCPD and its esters. High amounts of 3-MCPD esters detected in food raised toxicological concern. Recent studies revealed that food may also contain significant amounts of structurally related 2-MCPD and its fatty acid esters. Toxicological studies indicate genotoxicity *in vitro* and a carcinogenic potential of 3-MCPD, pointing to kidney and testes as main target organs. 3-MCPD esters were shown to cause similar, but milder effects. Few unpublished data exist for 2-MCPD, showing similar organ toxicity compared to 3-MCPD and identifying heart as additional target organ. No such data exist for 2-MCPD diesters. In consequence, further toxicological data were required in order to complete risk assessment for 3-MCPD, 2-MCPD and their esters. Hence, an

oral 28-days study was performed in male rats in order to fill data gaps and provide essential information for risk assessment. A proteomic analysis was included in order to compare molecular effects induced by 3-MCPD and 2-MCPD and its dipalmitic ester in rat liver, kidney, testes and heart. In order to avoid overt toxicity, moderate doses of 3-MCPD + 2-MCPD (10 mg/kg body weight), and 2-MCPD-dipalmitate (53 + 13.3 mg/kg body weight) were applied. Accordingly, no pathologic effects were reported. Here, we present proteomic results obtained after analysis of heart tissue. After separation of heart tissue protein crude extract by 2-D gel electrophoresis (2-DE), differentially expressed spots were identified by MALDI-MS. A total of 270 unique proteins deregulated at a log₂ ratio of ≤ -0.5 for downregulation and ≥ 0.5 for upregulation at p ≤ 0.05 were identified. Comparing deregulated spots induced by different treatments revealed that a higher number of spots was deregulated by 2-MCPD versus 3-MCPD. Dipalmitate treatment even caused more deregulation than 2-MCPD. Upregulated cytochrome b-c1 complex subunit Rieske (UCRI) and downregulated Acetyl-CoA acetyltransferase (THIL) were among the top deregulated proteins after 2-MCPD and 2-MCPD dipalmitate treatment. Pronounced upregulation of respiratory chain protein UCRI, not deregulated after 3-MCPD treatment, indicates an effect on energy metabolism. Downregulation of THIL, involved in ketone body metabolism, was only weakly affected after 3-MCPD treatment. Protein DJ-1 (PARK7), a multifunctional redox-sensitive chaperone and protease protecting the cell against oxidative stress, was significantly downregulated after treatment with 3-MCPD and the higher dose of the 2-MCPD diester. Tropomyosin beta chain (TPM2) was commonly upregulated after 3-MCPD and 2-MCPD treatments, possibly indicating a TGF-beta induction of actin stress fibers.

For rat heart, data show that similarities but also some significant differences of 2-MCPD- and 2-MCPD dipalmitate-induced proteomic changes exist compared to 3-MCPD, indicating different mechanisms of toxicity for this structural analogues.

246

Quantitative profiles of autoxidation products of cholesterol in human mammaplasty specimens

M. Mahdiani¹, D. Pemp¹, P. Eckert², I. Neshkova³, H. Esch¹, L. Lehmann¹
¹Lehrstuhl für Lebensmittelchemie, Universität Würzburg, Würzburg, Germany
²Practice for Plastic and Aesthetic Surgery, Wuerzburg, Germany
³University Hospital, Wuerzburg, Germany

Oxidation products (oxy) of cholesterol (ChOL) such as 7α-hydroxy-ChOL (7α-HO-ChOL), 7β-hydroxy-ChOL (7β-HO-ChOL), 7-keto-ChOL (7-O-ChOL), 5,6α-epoxy-ChOL (α-epoxy-ChOL) and 5,6β-epoxy-ChOL (β-epoxy-ChOL) are formed by autoxidation of ChOL and are discussed as biomarkers for inflammation and oxidative stress in human tissues to be used in the identification of risk factors for disease. However, oxy-ChOLs are also present in processed foodstuff where 7β-HO-ChOL (milk) and 7-O-ChOL (fish, meat, and egg) tend to represent the main oxyChOLs, whereas epoxy-ChOLs, are generally minor constituents. Thus, levels of oxyChOLs in tissues may result from both endogenous formation as well as dietary exposure.

Since quantitative profiles of oxy-ChOLs have not been determined in human adipose tissues yet, levels of oxyChOLs and ChOL were quantified using GC-MS/MS (internal standards: deuterated oxyChOLs) and GC-FID (internal standard: 5α-cholestan-3β-ol), respectively in breast adipose tissues of 48 healthy women undergoing mammaplasty. Furthermore, tissue levels of 25 fatty acids in adipose tissues were determined by GC-FID (internal standard: undecanoic acid) to assess relative levels of pentadecanoic acid, docosahexaenoic acid and elaidic acid, indicative for consumption of dairy products, fish, and processed fats, respectively.

All oxyChOLs were detected in all breast adipose tissues. The most abundant oxyChOL was β-epoxy-ChOL (median: 0.36 nmol/g tissue, range: 0.06-1.55 nmol/g), followed by α-epoxy-ChOL > 7-O-ChOL > 7α-HO-ChOL > 7β-HO-ChOL (0.009 nmol/g, range: 0.002-0.11 nmol/g). Tissue levels of ChOL (2.8 micro mol/g, range: 1.88-3.87 micro mol/g) did not correlate (Spearman's rank analysis) with that of epoxy-Chols and correlated even negatively with that of 7α-HO-, 7β-HO-, and 7-O-ChOL (R = -0.29, p=0.024-0.044). Median oxyChOL/ChOL ratios ranged from 0.0119 (5,6β-epoxy-ChOL) to 0.0003 (7β-HO-ChOL).

7-O-Chol and 7-HO-ChOLs correlated strongly with each other (R=0.81-0.91, p Oxy-ChOL levels did not correlate with relative amounts of pentadecanoic acid and docosahexaenoic acid, whereas total oxyChOL, 7β-HO-ChOL, and β-epoxy-ChOL levels correlated with relative amounts of elaidic acid (R=0.30, 0.30, and 0.31, respectively, p=0.037, 0.034, 0.028, respectively).

No correlations of oxyChOL levels, individual or total oxyChOL/ChOL ratios with age or BMI were observed.

Taken together, oxyChOL profiles in breast adipose tissues were different from that usually present in food but could be affected by dietary habits.

Toxicology – Environmental toxicology/Ecotoxicology

247

No hazard pictograms on personal care products due to the exception provision in the European regulation on classification and labelling

U. Klaschka¹, F. Schlichtig¹
¹Hochschule Ulm, Ulm, Germany

Classification and labelling of hazardous substances and hazardous consumer products (1) has proven to be a very efficient tool for risk communication. Consumer products, such as glue, varnish, or washing and cleansing products need to be classified and labelled if they contain dangerous ingredients that render the mixture hazardous. Personal care products, however, need not be classified and labelled if they contain dangerous substances above the thresholds for classification. They are excluded in the CLP regulation. What would happen without this exception?

When I applied the criteria for classification and labelling to a selection of cosmetic product formulas in a conservative approach, most products would have to be labelled and classified, mainly due to hazardous effects to the eye and to the skin (2).

Benefits of personal care products can go along with unwanted properties such as the hazards for the human health, and consumers should be informed about them (3). Risk

communication for every day products like personal care products should be clear, easily and quickly understandable. According to the cosmetic regulation (4) the ingredients must be listed on the containers. It must be questioned whether the listing of the ingredients without hazard pictograms on the products could be considered as a clear, easily and quickly understandable risk communication instrument (3).

The results show that it is urgent to inform consumers better about the potential dangers of personal care products, because cosmetics need to be applied even with more care than any other consumer product. It is strongly recommended to delete the exception provision in the CLP regulation for personal care products.

(1) Regulation No 1272/2008 of the European Parliament and of the Council of 16 December 2008 on classification, labelling and packaging of substances and mixtures (CLP regulation).

(2) Klaschka U. 2012. Dangerous Cosmetics – Criteria for Classification, Labelling and Packaging (EC 1272/2008) applied to Personal Care Products. *Env Sci Europe*, 24:37.

(3) Klaschka U, Rother H-A. 2013. "Read this and be safe!" Comparison of regulatory processes for communicating risks of personal care products to European and South African consumers. *Env Sci Europe* 25:30

(4) Directive 2003/15/EC of the European Parliament and of the Council of 27 February 2003 amending Council Directive 76/768/EEC on the approximation of the laws of the Member States relating to cosmetic products. *Off J Eur Union* 66, 26-35.

248

Infodisruption and the infochemical effect – a new chapter in ecotoxicology

U. Klaschka¹, M. Nendza², F. Schlichtig¹

¹Hochschule Ulm, Ulm, Germany

²Analytisches Laboratorium, Luhnstedt, Germany

Most organisms live in an 'odor environment' and recognize their biotic and abiotic environment via sophisticated, specific and dynamic blends of odorants, called *infochemicals*. The complexity and sophistication of the chemical communication systems for environmental organisms are difficult to imagine from a human perspective. The *infochemical effect* describes that anthropogenic substances can interfere with the chemical communication and influence organisms so that they perceive their chemical environments differently (1,2).

Infochemicals play a role in life history, habitat search, food related aspects and survival which shows that disturbed communication (*infodisruption*) could affect population vulnerability at various decisive points (3).

The classical ecotoxicological standard tests do not allow to observe the infochemical effect. Systematic analyses are needed to find out more about the relevance of this new chapter in ecotoxicology for natural ecosystems. The first crucial step is to select suitable test substances. Repellents (substances used to keep away target organisms, e.g. invertebrates such as midges or fleas via olfaction) enter surface waters mainly indirectly via wastewater discharges from sewage treatment plants or directly by being washed off from the skin and clothes of bathers. There are various indications that repellents which are not toxic for aquatic animals could induce effects like organismic downstream drift of non-target species (downstream dislocation of e.g. crustacean and insect larvae in streams). In a literature study, three repellents were identified to be suitable test compounds for proof of concept of the infochemical effect. DEET (CAS 134-62-3), Icaridine (CAS 119515-38-7) and EBAAP (CAS 52304-36-6) (4). These substances are investigated in new test designs in a subsequent experimental part of the project which are designed to detect and quantify the infochemical effect.

(1) Klaschka U (2008) The infochemical effect: a new chapter in ecotoxicology. *Environ Sci Pollut Res* 15 (6): 448-458

(2) Klaschka U (2009) A new Challenge: Development of Test Systems for the Infochemical Effect. *Env Sci Pollut Res* 16:370-388.

(3) Brönmark C, Hansson LA. 2012. Chemical ecology in aquatic systems OUP Oxford

(4) Nendza M, Klaschka U, Berghahn R (2013) Suitable test substances for proof of concept regarding infochemical effects in surface waters. *Environmental Sciences Europe* 2013, 25:21. (funded by the German Federal Environment Agency)

249

The PBT Assessment of Pharmaceuticals

Astrid Wiemann, Jens Schönfeld, Ines Prutz
Federal Environment Agency, Wörlitzer Platz 1, 06844 Dessau

A. Wiemann¹

¹Umweltbundesamt, IV 2.2, Dessau-Roßlau, Germany

Persistent, bioaccumulative and toxic (PBT) substances or very persistent and very bioaccumulative (vPvB) substances are compounds with hazardous properties. The non-biodegradability (persistence) and high accumulation in organisms (bioaccumulation) may elicit long-term adverse effects in the environment.

Persistent and bioaccumulative substances concentrate in the environmental compartments (water, sediment, soil, air) and can be distributed in the food chains. Ecotoxicological effects are strengthened by bioaccumulation and appear often in remote areas like marine and polar regions. In the framework of PBT assessment, contrary to the risk assessment, the substances are evaluated regardless of the emission into the environment.

An evaluation of medicinal active ingredients under assessment in the German federal environment agency (UBA) identified less than 10% as potential PBT candidates. Due to data lacks in many cases a definite PBT classification is not possible.

250

Pharmaceuticals in the Environment: global occurrence, effects, and potential cooperative action

Silke Hickmann¹, Tim aus der Beek², Axel Bergmann², Ina Ebert¹, Gregor Grüttnert², Arne Hein¹, Juliane Koch-Jugl¹, Anette Küster¹, Johanna Rose¹, Frank-Andreas Weber²

¹Federal Environment Agency (UBA), Germany, ²Adelphi consult GmbH, Germany

S. Hickmann¹

¹Umweltbundesamt, IV 2.2, Dessau-Roßlau, Germany

The poster presents results of an extensive literature research on the global occurrence of pharmaceuticals in the environment. Data on measured environmental occurrences from more than 1,000 international publications have been transferred to a database, with more than 120,000 entries. According to the database, pharmaceuticals have been found in the environment of 71 countries worldwide in all five UN regions. Most published data are for the compartments surface water and sewage effluent; less information is available for groundwater, manure, soil, and other environmental matrices. More than 600 active pharmaceutical substances (or their metabolites and transformation products) have been detected in the environment. Most findings have been published for industrialized countries. Monitoring campaigns are increasingly being conducted in developing and emerging countries. These have revealed the global scale of the occurrence of pharmaceuticals in the environment. For example, diclofenac, a non-steroidal inflammatory drug, has been detected in the aquatic environment in 50 countries worldwide. A number of globally marketed pharmaceuticals have been found in both developing and industrialized countries. The available ecotoxicological information indicates that certain pharmaceuticals pose a risk to the environment at measured concentrations. Options for cooperative action to address the risk of are also presented. The aim of the research presented was to support the discussion of the proposed emerging policy issue pharmaceuticals in the environment under the Strategic Approach to International Chemicals Management (SAICM), which is a global initiative of United Nation Environment Programme (UNEP).

251

Screening for potential endocrine disruptors – evidence from structural alerts, in vitro and in vivo toxicological assays

M. Nendza¹, A. Wenzel², M. Müller²

¹Analytisches Laboratorium für Umweltuntersuchungen und Auftragsforschung,

Luhnstedt, Germany

²Fraunhofer-Institut für Molekularbiologie und Angewandte Ökologie, Schmallenberg, Germany

The European chemicals' legislation REACH aims to protect man and the environment from substances of very high concern (SVHC). Chemicals with (very) persistent, (very) bioaccumulative and toxic properties (PBT and vPvB compounds), substances that are carcinogenic, mutagenic and toxic to reproduction (CMR compounds), as well as chemicals of comparable concern like endocrine disruptors (EDs) may be subject to authorization. The identification of EDs is limited as yet, because specific experimental assessments are not required under REACH. Evidence is currently based on a combination of few experiments, expert judgement and structural analogy with known EDs.

Structural alerts for the identification of potential EDs: Predictions of properties and effects from chemical structures are based on similarities with either active or inactive substances. Structural alerts for the identification of potential estrogen/androgen-ED activities are relevant parts of the structures of compounds that are known to interact with estrogen and androgen receptors as either agonists or antagonists. In addition to the backbones of the chemical structures (pharmacophore) for steric fit to the receptors, modulating factors may be small substructures for local interactions with receptor binding sites and physicochemical properties related to the strength of binding to the receptor.

Comparison of evidence from in silico, in vitro and in vivo assays for potential EDs: Identification of potential EDs based on findings from mammalian long-term reproduction studies, fish life-cycle tests, receptor assays, and chemical alerts were compared and differences analysed. Agreement is limited because in vivo, in vitro and in silico methods address different aspects of potential effects on endocrine systems regarding toxicological targets, modes of action and functional similarity of chemical structures. A combination of toxicological and chemical assays can provide comprehensive and complementary information to support evidence-based identification of potential EDs among the chemicals released into the environment.

Application of structural alerts for the identification of potential EDs to the EINECS inventory: More than 33000 discrete organic EINECS compounds are within the applicability domain of the structural alerts for potential estrogen/androgen-ED activities. Among them, 3585 chemicals (ca. 11%) are indicated as potential candidates for endocrine effects based on structural alerts. Due to the possibility that these chemicals may interact with estrogen/androgen receptors they should be subject to further investigations regarding their potential for endocrine effects, eventually leading to regulatory actions.

252

Evaluation of a metabolomics-based fish embryo assay for predicting drug induced long-term effects in fish

A. Herrmann¹, R. Länge¹, M. Keck¹, T. Steger-Hartmann¹

¹Bayer Pharma AG, Investigational Toxicology, Berlin, Germany

Within the IMI (Innovative Medicine Initiative) project "Intelligence-led assessment of pharmaceuticals of the environment" (iPIE: <http://i-pie.org/>), a more intelligent environmental testing and tools for prioritisation of legacy compounds shall be developed. Regarding the evaluation of fish toxicity, screening approaches in fish embryos are pursued. While the standard fish embryo toxicity (FET) test is restricted to lethal parameters more relevant as substitutes for acute effects, additional sublethal endpoints may provide expanded applicability of the FET assay for chronic effect assessment in fish. In this respect, the analysis of the metabolome could provide additional insights into biochemical processes elicited by pharmaceutical compounds and could potentially support the extrapolation from fish embryo to chronic fish toxicity as displayed in the standard early life stage (ELS) test.

In the context of iPIE a pilot study was performed with the aim to quantify and comparatively assess changes in the metabolic signatures of fish and fish embryos induced by the reference compound amikacin, an aminoglycoside antibiotic, in order to identify metabolic patterns applicable as biomarker profiles that can be linked to apical

endpoints in terms of an integrated approach. Therefore, toxic effects in fathead minnow embryos and ELS fish were investigated following a 4 and 32 days exposure, examining conventional endpoints and additionally using a combined direct injection and LC-MS/MS assay for metabolite identification and quantification.

Metabolic endpoints were found to be at least as sensitive as standard apical endpoints such as growth and mortality as detected in the longer-term fish study. Furthermore, multivariate data analysis (PCA-X, OPLS-DA) revealed substance induced metabolic perturbations specific for fish and fish embryos, respectively. Beyond that, the statistical approach of shared and unique structure (SUS) identified some metabolites from the classes of amino acids, biogenic amines and lipids to be similarly changed in both developmental stages related to amikacin treatment, representing shared biomarker candidates.

In this first pilot study, the integrated metabolomics approach yielded insights into the molecular consequences of amikacin exposure and provided indications for biomarkers for common effects in fish embryos and fish. Due to the different exposure levels in the FET (1 – 100 mg/L) and ELS study (0.0003 – 0.03 mg/L), more definitive conclusions regarding the predictivity of metabolic responses in fish embryos for apical endpoints in chronic fish tests are yet not possible. Further studies are ongoing with a range of pharmaceutical compounds of different chemical classes which will reveal more substantial information on the applicability of this technology in the prediction of long-term effects in fish.

Poster Session II

Pharmacology – Membrane transporters

253

Starvation induces transcription of the human cationic amino acid transporter hCAT-1 in human endothelial cells

S. K. Muther¹, H. Kleinet¹, E. I. Closs¹

¹Unimedizin der Johannes Gutenberg-Universität Mainz, Institut für Pharmakologie, Mainz, Germany

The human cationic amino acid transporter hCAT-1 (SLC7A1) represents the major uptake route for arginine and other cationic amino acids (such as the essential amino acid lysine) in most mammalian cells. It thus provides these amino acids for protein synthesis as well as for essential metabolic pathways. In endothelial cells, special attention has been given to the role of hCAT-1 for supplying arginine to nitric oxide synthase. In spite of its wide distribution, hCAT-1 expression is highly regulated both, on the transcriptional and post-transcriptional level. However, the genetic elements involved in transcriptional regulation a largely unknown.

Here we studied the expressional regulation of hCAT-1 in human EA.hy926 endothelial cells. Starvation of these cells from cationic amino acids led to a pronounced induction of both, hCAT-1 mRNA and protein. The mRNA induction was almost completely abolished by the transcription elongation inhibitor DRB (5,6-Dichloro-1-β-D-ribofuranosylbenzimidazole), suggesting the involvement of transcriptional regulation. We thus aimed at identifying the promoter elements in the hCAT-1 gene responsible for this regulation. To our surprise and in contrast to data published by others¹ the chromosomal region up to 5 kb upstream of the first hCAT-1 exon exhibited no promoter activity in either endothelial or DLD-1 colon carcinoma cells that exhibit a very strong endogenous hCAT-1 expression. We could however identify a promoter element within the first intron of the hCAT-1 gene. Transcriptional activity of this element increased upon amino acid starvation in a similar way as endogenous hCAT-1 expression. Our results indicate starvation-induced transcriptional regulation of hCAT-1 through newly identified promoter regions distinct from those published previously.

¹Reference: Guzman-Gutierrez E, Westermeier F, Salomon C, Gonzalez M, Pardo F, Leiva A, Sobrevia L (2012) Insulin-increased L-arginine transport requires A(2A) adenosine receptors activation in human umbilical vein endothelium. PLoS One 7 (7):e41705. doi:10.1371/journal.pone.0041705

254

Validation of MATE1 and MATE2-K mediated uptake of metformin in comparison to MPP and the interaction of MATE2-K with antineoplastic agents

J. Müller¹, A. Kühne², S. Flör², G. Burckhardt¹, Y. Hagos^{1,2}

¹Universitätsmedizin Göttingen, Vegetative- und Pahtophysiologie, Göttingen, Germany
²PortaCellTec Biosciences GmbH, Göttingen, Germany

The transport of a multitude of drug molecules into the cell is mediated by multispecific organic cation transporters (OCTs), belonging to the solute carrier group (SLC). One of these families within this group of membrane transport proteins is the SLC47-family consisting of the two multidrug and toxin extrusion transporters MATE-1 (SLC47A1) and MATE2-K (SLC47A2). While MATE-1 is highly expressed in several different tissues like kidney, liver, skeletal muscle, adrenal glands, testes and heart, MATE2-K exclusively occurs in the apical membrane of proximal tubular epithelial cells within the kidney. Both transport proteins translocate organic cations in exchange of protons into as well as out of the cell. To define the affinity of both transporters for the anti-diabetic drug metformin and to investigate their interactions with 26 different anti-neoplastic agents comparative transport experiments with the model substrate 1-methyl-4-phenylpyridinium (MPP) have been carried out. Therefore stably transfected HEK293-cells expressing MATE-1 or MATE2-K transport proteins generated by PortaCellTec biosciences GmbH and vector transfected HEK293-cells were used. The interaction analyses were carried out by determining the uptake of [¹⁴C]-metformin and the inhibition of [³H]-MPP-uptake in presence of different anti-neoplastic drugs. Cimetidine was used as positive control. The affinity of MATE-1 and MATE2-K for [¹⁴C]-metformin with a K_m value of $274 \pm 21 \mu\text{M}$ and $934 \pm 200 \mu\text{M}$ respectively, was considerably lower than for the model substrate [³H]-MPP ($89 \pm 9 \mu\text{M}$ and $68 \pm 7 \mu\text{M}$ respectively). Within the group of tested anti-neoplastic drugs in MATE2-K transfected HEK293-cells a distinct inhibition of [³H]-MPP-uptake of more than 50 % could be observed with the substances irinotecan ($K_i = 7.4 \mu\text{M} \pm 1.3 \mu\text{M}$), mitoxantrone ($K_i = 1.3 \mu\text{M} \pm 0.4 \mu\text{M}$), doxorubicine ($K_i = 52.3 \pm 5.1 \mu\text{M}$), vinblastine

($K_i = 91.4 \mu\text{M} \pm 8.1 \mu\text{M}$), etoposide ($K_i = 107.1 \mu\text{M} \pm 4.4 \mu\text{M}$), and paclitaxel ($K_i = 28.6 \mu\text{M} \pm 5.3 \mu\text{M}$). K_i values were determined by Dixon-Blot analyses.

These findings suggest an involvement of MATE2-K in the chemosensitivity of tumour cells expressing this transport protein and show that MATE2-K could be involved in drug-drug-interactions as well as renal drug excretion during chemotherapy.

255

Comparison of human and rat drug transporter OATP2B1/Oatp2b1

J. Hussner¹, S. Nageleisen¹, I. Seibert¹, H. Meyer zu Schwabedissen¹

¹University of Basel, Basel, Switzerland

Drug transporters play a pivotal role in pharmacokinetics by modulating the cellular entry or efflux of compounds. One transporter facilitating the transport of bile acids, steroid hormones, and statins is the organic anion transporting polypeptide (OATP) 2B1 that is highly expressed in placenta, liver, and small intestine. Especially its activity in small intestine and liver is assumed to be basis for specific drug-drug interactions. Understanding mechanisms involved in pharmacokinetics is a prerequisite in drug development. To test whether there are species differences in transport activity we compared the expression and function of the human and rat orthologue.

First, we determined the transport activity of the known OATP2B1 substrate estrone 3-sulfate (E,S), and observed a significantly lower K_m for MDCK-hOATP2B1 compared to MDCK-Oatp2b1 ($14.09 \pm 4.49 \mu\text{M}$ vs. $29.00 \pm 10.23 \mu\text{M}$, * $p < 0.05$ Student's t-test) whereas there was no difference in V_{max} (MDCK-hOATP2B1 $119.4 \pm 11.3 \text{ fmol/min}/\mu\text{g}$ protein; MDCK-Oatp2b1 $102.3 \pm 12.8 \text{ fmol/min}/\mu\text{g}$ protein). The human OATP2B1 exhibits multiple binding sites for its substrates that may explain specific drug-drug interactions [1]. To identify whether rat Oatp2b1 owns the same characteristics, the cellular accumulation of $50 \mu\text{M}$ E,S (low affinity site) or $0.005 \mu\text{M}$ E,S (high affinity site) was determined in presence of specific inhibitors/substrates of OATP2B1. As observed for atorvastatin, a known inhibitor of both affinity sites, the rat transporter failed to exhibit the low affinity site. In detail, while atorvastatin reduced the accumulation of E,S in MDCK-hOATP2B1 cells ($110.0 \pm 14.6 \text{ fmol/min}/\mu\text{g}$ protein vs. $60.7 \pm 7.5 \text{ fmol/min}/\mu\text{g}$ protein, * $p < 0.05$ Student's t-test), there was no inhibition of E,S accumulation in MDCK-Oatp2b1 cells ($53.2 \pm 13.2 \text{ fmol/min}/\mu\text{g}$ protein vs. $49.0 \pm 17.4 \text{ fmol/min}/\mu\text{g}$ protein). Additionally, we observed a different membrane localization of both transporters as assessed by immunofluorescent staining showing an apical localization for rat Oatp2b1 while human OATP2B1 is localized at the basolateral pole of the cellular model. Absolute quantification of mRNA (copy number per 1000 ng of total RNA) in different tissues of rat revealed a high expression of Oatp2b1 in liver (159.6 ± 45.5), a moderate expression in small intestine (14.9 ± 4.0) and colon (57.0 ± 12.3), and a low expression level in kidney (2.3 ± 0.8). The latter is in accordance with previous findings showing that Oatp2b1 is abundant in rat kidney as quantified by absolute proteomics technics [2]. Our data demonstrated species differences in localization and activity of the drug transporter. Further studies are warranted to proof whether this knowledge will help in future drug development and which molecular cause is responsible for the observed data.

[1] Y. Shirasaka, T. Mori, M. Shichiri, T. Nakanishi, I. Tamai, Functional pleiotropy of organic anion transporting polypeptide OATP2B1 due to multiple binding sites, Drug Metab Pharmacokinet 27 (2012) 360-364.

[2] Y. Uchida, T. Toyohara, S. Ohtsuki, Y. Moriyama, T. Abe, T. Terasaki, Quantitative Targeted Absolute Proteomics for 28 Transporters in Brush-Border and Basolateral Membrane Fractions of Rat Kidney, J Pharm Sci (2015).

256

Site-specific miRNA expression affects transporter protein abundance along the human intestine

H. Bruckmüller¹, P. Martin¹, M. Kähler¹, S. Haenisch¹, M. Drozdziak², S. Oswald³, W. Siegmund¹, I. Cascorbi¹

¹University Hospital Schleswig-Holstein, Institute of Experimental and Clinical Pharmacology, Kiel, Germany

²Pomeranian Medical University, Department of Experimental and Clinical Pharmacology, Szczecin, Polen

³Ernst-Moritz-Arndt University, Department of Clinical Pharmacology, Greifswald, Germany

Background: Intestinal drug absorption depends on various factors including aqueous volume, site-specific pH and intestinal motility. Moreover, the expression of efflux- and uptake-transporters vary in dependence of the anatomical localization making the gut a complex barrier for drug transfer into the body. In a recent study, site-specific protein and mRNA expression levels of 10 drug transporters were determined along the entire length of the human gut. Interestingly, discrepancies between mRNA expression and protein levels were observed. Moreover, there were quantitative differences between small intestine and colon. As a consequence the question arose if this observation could be explained by small non-coding RNAs acting as highly tissue-specific post-transcriptional regulators of gene expression. Hence, in our current study, we aimed to investigate the impact of miRNAs on site-specific transporter expression along the human intestine.

Methods: Total RNA was isolated from biopsies obtained from six disease-free organ donors. Tissue samples were acquired from the duodenum, the upper and lower jejunum, the upper and lower ileum, and the transversal or descending colon. The expression of 754 miRNAs was measured using rt-PCR based low density arrays. Expression of all detected miRNAs was correlated with transporter protein data recently determined by LC-MS/MS-based targeted proteomics. miRNAs and transporter genes showing an inverse Pearson's correlation between miRNA and protein expression underwent an *in-silico* search (MicroCosm Targets v.5, TargetScan7.0) for putative miRNA/mRNA interaction. To investigate those interactions in more detail, reporter gene assays and site directed mutagenesis were conducted.

Results: Out of 754 miRNAs, 248 were detected in all tissue types. Out of ten transporters five showed significant inverse correlations with 10 putatively targeting miRNAs (e.g. PEPT1 and hsa-miR-27a, $r = -0.498$, $p = 0.002$). Reporter gene assays indicated interactions of miR-193a/b with PEPT1 3'-UTR ($p = 0.0025$ and $p = 0.0012$) as well as of miR-27a with ABCB1 3'-UTR ($p = 0.0006$).

Conclusion: The site-specific abundance of intestinal drug transporters is significantly affected by microRNA-mediated post-transcriptional regulation under physiological conditions as exemplified for PEPT1 and ABCB1.

257

Analysis of mutations and inhibitors of the human uptake transporter NaCT: a transporter important for energy metabolism and brain development

J. König¹, S. Selch¹, A. Kittel¹, H. Sticht², A. L. Birkenfeld³, M. F. Fromm¹
¹FAU Erlangen, Institut für Experimentelle und Klinische Pharmakologie und Toxikologie, Erlangen, Germany
²FAU Erlangen, Institut für Biochemie, Erlangen, Germany
³Universitätsklinik Carl Gustav Carus, Medizinische Klinik III, Paul Langerhans Institut Dresden (PLID), Dresden, Germany

Background: The human uptake transporter NaCT [gene symbol *SLC13A5*; also known as miNDY, the human orthologue of the *Drosophila* Indy (I'm not dead yet) transporter] is expressed in liver and brain. NaCT is important for energy metabolism and brain development and mediates the uptake of tricarboxylic acid (TCA) intermediate such as citrate and succinate. Reduced expression of this transporter, as studied in knock-out mice, mimics aspects of dietary restriction, promotes longevity and protects against insulin resistance and adiposity. Furthermore, mutations in the human *SLC13A5* gene are associated with epileptic encephalopathy with seizure onset in the first days of life, possibly due to the reduced uptake of TCA intermediates into neurons. To gain more insights into the role of NaCT in drug transport and into structure-function relationships, we studied the inhibition of NaCT-mediated citrate transport by various drugs and analyzed the effect of known mutations in the *SLC13A5* gene on NaCT-mediated transport.

Methods: Drug inhibition studies were performed using HEK cells stably expressing human NaCT with citrate as prototypic substrate. Twenty-four drugs were used as potential inhibitors of NaCT-mediated uptake. The effects of eight mutations, three of them (NaCTp.G219R, -p.T227M and -p.L488P) associated with epileptic encephalopathy, were analyzed using a transient transfection approach. Furthermore, the first computational-based structural model of the NaCT transporter was established and the impact of all mutations on substrate transport was modeled.

Results: Inhibition studies demonstrated that only a few drugs (three out of 24 tested) inhibited NaCT-mediated citrate transport at the tested drug concentration of 100 μ M. From these, benzobromarone shows the strongest inhibition with an IC₅₀ value of 83.2 μ M. Furthermore, citrate transport was also slightly inhibited by pioglitazone and rosiglitazone. Citrate transport of the mutated proteins NaCTp.G219R, -p.G219E, -p.T227M, -p.L420P and -p.L488P was totally abolished and the effect of these mutations could be explained on the basis of the structural model.

Conclusion: Inhibition studies demonstrated that simultaneously administered drugs can inhibit NaCT-mediated uptake of the prototypic substrate citrate. NaCT-mediated uptake is abolished by mutations in the *SLC13A5* gene associated with epileptic encephalopathy. The effect of these mutations can be explained on the basis of the first structural model of this uptake transporter.

258

Regulation of the ABCB1 transporter by MARCKS

T. Wenzel¹, T. Büch¹, M. Schaefer¹, H. Kalwa¹
¹Rudolf-Boehm-Institut für Pharmakologie und Toxikologie, Leipzig, Germany

The ATP-binding cassette subfamily B member 1 (ABCB1) is a drug efflux pump responsible for the classic multi-drug resistance phenotype in cancer cells. Increased activity of ABCB1 in cancer cells contributes to protection against a wide range of chemotherapeutic agents. This dramatically decreases therapeutic options and the chance of patient survival. Knowledge of the underlying mechanisms for ABCB1 deregulation is a critical step for the reversal of this unfavorable condition. Of note, phosphatidylinositol-4,5-bisphosphate (PIP₂) is a known regulator of ABCB1. The protein "Myristoylated Alanine-Rich C-Kinase Substrate" (MARCKS) is known for its ability to bind and sequester the phospholipid PIP₂. In various forms of colorectal cancer the deregulation of MARCKS protein goes hand in hand with an increase in malignancy and therapeutic resistance.

In this study, we characterized the enigmatic MARCKS as a modulator of ABCB1 activity. We focused on a subgroup of colon cancers, where MARCKS resides in a hyperphosphorylated state for which the established cell line HT-29 served as a model. We employed various in-vitro methods for the measurement of ABCB1 activity, in combination with imaging experiments, assays for cellular viability and classical methods of molecular biology. We combined these approaches with pharmacological inhibition of MARCKS phosphorylation state or RNAi-mediated depletion of MARCKS. With these interventions we could modulate endogenous ABCB1 activity and re-sensitize our cell model against chemotherapeutic agents like 5-fluorouracil which are known to be substrates of ABCB1. Taken together, our findings suggest a new way how a cancer cell can gain a state of therapeutic resistance. The exploitation of MARCKS as modulator of ABCB1 might be a new approach to target resistant tumors without interfering with the natural function of ABCB1 in non-malignant tissue.

259

The protective biomarker homoarginine is a substrate of the cationic amino acid transporters (CAT) CAT1, CAT2A and CAT2B

A. Kittel¹, M. F. Fromm¹, J. König¹, R. Maas¹
¹Institute of Experimental and Clinical Pharmacology and Toxicology, Friedrich-Alexander-Universität Erlangen-Nürnberg, Erlange, Erlangen, Germany

Background: In several large clinical studies low blood concentrations of homoarginine were identified as independent risk marker for stroke, cardiovascular events and mortality. Experimental data suggest an active role of homoarginine deficiency in disease development. Interference with L-arginine-dependent pathways and signaling

has been implicated as a possible mechanism. It was the aim of the present study to identify transport mechanisms involved in the cellular uptake and tissue distribution of homoarginine, which is poorly understood, so far. The experiments focused on cationic amino acid transporters (CATs) and possible interactions with known CAT substrates.

Methods: Uptake assays were performed using [³H]-labeled homoarginine as substrate and human embryonic kidney (HEK293) cells stably overexpressing human CAT1 [gene: *SLC7A1* (solute carrier family 7)], CAT2A (*SLC7A2A*) or CAT2B (*SLC7A2B*). Cells transfected with an empty vector were used as control. Unlabeled known CAT-substrates L-arginine and asymmetric dimethylarginine (ADMA) were investigated as inhibitors.

Results: Compared to the uptake into control cells, uptake of homoarginine was significantly higher in HEK cells overexpressing CAT1 (7-fold), CAT2A (1.6-fold) or CAT2B (2.2-fold) after 2.5 min using 100 μ M substrate (each p<0.001). Apparent K_m values for cellular net uptake of homoarginine were 174.6 μ M for CAT1, 3640 μ M for CAT2A and 522.8 μ M for CAT2B. Homoarginine uptake by the three CATs could be inhibited by addition of L-arginine and ADMA.

Conclusion: The protective biomarker homoarginine is a substrate of the human cationic amino acid transporters CAT1, CAT2A and CAT2B. Compared to other CAT substrates, the CAT1- and CAT2B-mediated homoarginine transport is characterized by relatively high affinity. The uptake of homoarginine by all three CATs can be inhibited by L-arginine and ADMA. Taken together these findings make CAT-mediated transport of homoarginine a possible target for interactions and pharmacological interventions aimed at homoarginine homeostasis.

This project is supported by the DOKTOR ROBERT PFLEGER-STIFTUNG.

260

Of mice and men: Characterization of the differences in substrate specificity between human and rodent OCT1 orthologs

T. Seitz¹, M. Meyer¹, H. Massy¹, J. Brockmüller¹, M. V. Tzvetkov¹
¹Institut für Klinische Pharmakologie, Göttingen, Germany

Background and aim: Organic cation transporter 1 (OCT1, alternative name SLCC22A1) is a polyspecific membrane transporter, which has been suggested to play a role in absorption, distribution and elimination of drugs and toxins. Besides endogenous compounds like thiamine (vitamin B1), known OCT1 substrates are toxins like MPP⁺ as well as drugs like metformin, O-desmethyltramadol, ranitidine, and sumatriptan. Tissue distribution of OCT1 has been shown to have strong inter-species differences. In rodents Oct1 is strongly expressed in both the sinusoidal membrane of hepatocytes and the basolateral membrane of kidney epithelial cells. Human OCT1 is strongly expressed on the sinusoidal membrane of hepatocytes, but not in the kidney. Furthermore, substrate specific differences have been observed between the human and rodent OCT1 orthologs. The aim of this study is to characterize the mechanisms causing substrate specificity between rodent and human OCT1 orthologs.

Methods: Overexpression of OCT1 orthologs in mouse, rat and human cells was performed by targeted chromosomal integration of T-REx™ 293. The cells were characterized in detail for their ability to transport the model substrates TEA⁺, MPP⁺, and ASP⁺, the drugs ranitidine, sumatriptan and fenoterol.

Results: Mouse and rat Oct1 orthologs showed similar transport activity for all the model substrates and drugs tested. However, significant differences were observed when rodent orthologs were compared to the human OCT1. Human OCT1 showed a 5-fold higher v_{max} for the uptake of ASP⁺ and 2-fold increase of v_{max} for sumatriptan in comparison to the rodent OCT1 orthologs. Conversely, human OCT1 showed a 4-fold lower v_{max} for the uptake of fenoterol compared to rodent Oct1s. There was no difference between rodent and human OCT1 in the uptake of ranitidine. These differences were further characterized in detail using chimeric mouse-human OCT1 constructs and by comparing the effects of key point mutations in mouse and human OCT1 orthologs.

Conclusions: These data demonstrate strong differences in the substrate specificity between rodent and human OCT1 orthologs. Therefore OCT1 pharmacokinetic data obtained in mouse or rat models could not be directly extrapolated for use in human. Furthermore, comparative functional analyses of orthologs may help reveal the mechanisms underlying polyspecificity of OCT1.

261

Effects of genetic polymorphisms on OCT1-mediated uptake of ranitidine

M. Meyer¹, T. Seitz¹, J. Brockmüller¹, M. V. Tzvetkov¹
¹Institut für Klinische Pharmakologie, Göttingen, Germany

Ranitidine is a histamine H₂-receptor antagonist which is commonly used without prescription for the treatment of pyrosis and gastric ulcers. Approximately 30% of the systemic clearance of ranitidine is via hepatic metabolism. Ranitidine is known to be a substrate of the hepatic organic cation transporter OCT1 [1]. OCT1 is expressed on the sinusoidal membrane of human hepatocytes and is highly genetically variable. Sixteen major OCT1 alleles are known [2]. Thereof 12 alleles confer partial or complete loss of OCT1 activity. The observed loss of activity was highly substrate specific and should be analyzed substrate by substrate. In this study we analyzed the effects of genetic polymorphisms in OCT1 on the uptake of ranitidine.

We used HEK293 cells stably transfected to overexpress wild type or variant OCT1 isoforms. The variant OCT1 alleles OCT1*1A (Met408Val), OCT1*1C (Phe160Leu), OCT1*1D (Pro341Leu/Met408Val), OCT1*2 (Met420del), OCT1*3 (Arg61Cys), OCT1*4 (Gly401Ser), OCT1*5 (Gly465Arg/Met420del), OCT1*6 (Cys88Arg/Met420del), OCT1*7 (Ser14Phe), OCT1*8 (Arg488Met), OCT1*9 (Pro117Leu), OCT1*10 (Ser189Leu), OCT1*11 (Ile449Thr), OCT1*12 (Ser29Leu) and OCT1*13 (Thr245Met) were analyzed. We characterized in ranitidine uptake determined K_m and v_{max} for the different polymorphic OCT1 isoforms.

Wild type OCT1 showed a time and concentration dependent uptake of ranitidine with a K_m of 62.91 ± 4.32 μ M and a v_{max} of 1125.41 ± 86.12 pmol/min/mg protein. Variants OCT1*5, OCT1*6, OCT1*12 and OCT1*13 completely lacked ranitidine transport activity. Variants OCT1*2, OCT1*3, OCT1*4 and OCT1*10 showed v_{max} values decreased by 64, 77, 91 and 50 %, respectively. OCT1*8 variant showed an increase of

v_{max} by 25 %. There was no significant changes in ranitidine uptake by variants OCT1*1A, OCT1*1C, OCT1*1D, OCT1*7, OCT1*9 and OCT1*11 compared to the wild type. There were no significant differences in the K_M values between the wild-type and variants.

In conclusion, we confirmed ranitidine as an OCT1 substrate and demonstrated that genetic polymorphisms in *OCT1* can strongly affect ranitidine uptake. The effects of *OCT1* polymorphisms on ranitidine pharmacokinetics in humans remain to be analyzed.

- Bourdet DL, Pritchard JB, Thakker DR. Differential Substrate and Inhibitory Activities of Ranitidine and Famotidine toward Human Organic Cation Transporter 1 (hOCT1; SLC22A1), hOCT2 (SLC22A2), and hOCT3 (SLC22A3). *J Pharmacol Exp Ther.* 2005; 315: 1288-1297.
- Seitz T, Stalmann R, Dalila N, Chen J, Pojar S, Pereira J, et al. Global genetic analyses reveal strong inter-ethnic variability in the loss of activity of the organic cation transporter OCT1. *Genome Med.* 2015; 7: 56.

Pharmacology – Central nervous system

262

Differential tolerance to lysergic acid diethylamide (LSD) and dimethyltryptamine (DMT) – A matter of serotonin (5-HT) 2A receptor downregulation?

T. Buchborn¹, H. Schröder¹, T. Koch¹, E. Kahl¹, D. C. Dieterich¹, G. Grecksch¹, V. Höllt¹
¹Otto-von-Guericke University, Institute for Pharmacology and Toxicology, Magdeburg, Germany

Serotonergic hallucinogens (μ HGs), such as lysergic acid diethylamide (LSD), induce profound alterations of human consciousness, which are thought to be mediated by activation of 5-HT_{2A} receptors. With repeated application, the mind-altering effects of most μ HGs rapidly are undermined by tolerance. The only exception seems to be dimethyltryptamine (DMT), whose mind-altering effects for reasons unknown even with repeated application do not decrease. Assuming that DMT differs from other μ HGs in its capacity to regulate 5-HT_{2A} receptors, we here compare LSD and DMT with regard to processes of 5-HT_{2A} downregulation. In heat-exposed rats, LSD and DMT induce a marked increase in body core temperature (hyperthermia) accompanied by "defensive hypersalivation". Both effects are mimicked by the 5-HT₂ selective agonist dimethoxybromoamphetamine (DOB) and can be blocked by the selective 5-HT_{2A} antagonists ketanserin and MDL100907. After repeated application, the temperature-regulatory effects of LSD are subject to tolerance, whereas the ones of DMT are not. Tolerance to LSD (as measured by DOB induced [³⁵S]GTPγS binding) is paralleled by a desensitisation of frontocortical 5-HT₂ receptors; for DMT, there is no such decrease. Applying techniques of immunocytochemistry, transphosphatidylation, and quantitative real-time PCR to (HA-5-HT_{2A} transfected) HEK293 and (endogenously 5-HT_{2A} expressing) C6 glioma cells, respectively, we furthermore demonstrate that DMT in contrast to LSD fails to internalise 5-HT_{2A} receptors, fails to activate the phospholipase D (which is needed for 5-HT_{2A} internalisation), and fails to inhibit the synthesis of 5-HT_{2A} receptors. Given that DMT unlike LSD turns out to be inactive as to all processes of 5-HT_{2A} downregulation investigated, our data suggest that the differential tolerance development noted for DMT and LSD indeed might be accounted for by differential regulation of 5-HT_{2A} receptors. LSD and DMT both have recently regained scientific attention as potential therapeutics in the treatment of depression and/or anxiety disorders. Providing mechanistic insights into their action, thus, is of timely clinical relevance.

263

Increased GABA release in human neocortex at high intracellular sodium and low extracellular calcium – an anti-seizure mechanism?

T. Feuerstein¹

¹Universität Freiburg, Sektion Klinische Neuropharmakologie der Neurochirurgischen Klinik, Freiburg, Germany

Fluorescence activated synaptosome sorting (FASS) experiments quantified GABAergic synaptosomes that express GABA transporter (GAT-1) in human neocortical tissue, both from pharmacoresistant epileptic and non-epileptic patients. Pathophysiologically, there is a highly significant difference (21.2% vs 31.0%, respectively).

Before and during the onset of a seizure, the extracellular calcium concentration ($[Ca^{2+}]_e$) decreases. This missing Ca^{2+}_e increased the transporter-mediated release of GABA in human neocortical synaptosomes.

Release was evoked by either veratridine (Na^+ channel activator) or ouabain (Na^+/K^+ -ATPase inhibitor) in the absence or presence of tetanus toxin (TeT, exocytosis inhibitor), KB-R7943 or SEA0400 (Na^+/Ca^{2+} exchanger (NCX) inhibitors) in human tissue.

Evoked GABA release was not affected by TeT. Ca^{2+}_e withdrawal increased and doubling decreased the evoked GABA release in human neocortical synaptosomes. In rats, TeT facilitated an increase in release due to Ca^{2+}_e withdrawal.

Both NCX inhibitors diminished GABA release. The absence of Ca^{2+}_e amplified the NCX activity, leading to elevated $[Na^+]_i$, which, together with the evoked $[Na^+]_i$ increment, enhanced GAT reversal. As heightened $[Ca^{2+}]_e$ diminished GABA release, it may reduce NCX activity. Since incipient seizures are known to reduce $[Ca^{2+}]_e$, this reduction might induce an anti-seizure mechanism by augmenting GAT-mediated GABA release, a mechanism absent in rats.

264

Pharmacological strategies to rejuvenate protein homeostasis in aged neuronal cells

J. Abele¹, A. Müller¹, E. Höhne¹, **D. C. Dieterich**¹

¹Institut für Pharmakologie und Toxikologie Magdeburg, Neurale Plastizität und Kommunikation AG Dieterich, Magdeburg, Germany

Aging is complex on the systems as well as on the molecular level. The process of aging is characterized by a progressive loss of physiological functions and accumulation of cellular damage. One hallmark of aging is an impaired protein homeostasis. The imbalance of the quality control of both *de novo* protein synthesis and protein degradation, therefore, is likely to contribute to the phenotype of aging.

We investigated protein turnover rates with the state-of-the art techniques FUNCAT (Dieterich et al., 2010) and SunSET (Schmidt et al., 2009) in aging neuronal cell cultures. Using these techniques we show a prominent decrease in protein synthesis and degradation that progressed gradually in aging neuronal cells cultured up to DIV 60. In order to rejuvenate the protein turnover in aged neuronal cells we applied the selective eukaryotic elongation factor-2 kinase inhibitor A 484954 and the polyamine Spermidine and observed protein translation utilizing FUNCAT and SunSET.

Whereas both A 484954 and Spermidine had no effect on *de novo* protein synthesis in juvenile neurons (DIV 20), both substances increased the *de novo* protein synthesis to a juvenile level in aged neuronal cultures (DIV60). This effect is seen in neuronal somata and dendritic spines. The molecular function of Spermidine as an "anti-aging agent" is not defined yet. Thus, additional pharmacological interventions are used for further examination of specific molecular Spermidine targets.

In conclusion, the described experimental setup is used to investigate impaired protein homeostasis as one hallmark of aging. Agents with a presumed "anti-aging" effect can be tested for a potential rejuvenating effect on the level of protein homeostasis.

265

A screening approach to test tolerability of multitargeted drug combinations for antiepileptogenesis in mice

R. Klee^{1,2}, K. Töllner^{1,2}, V. Rankovic¹, K. Römermann^{1,2}, A. Schilditzki^{1,2}, W. Löscher^{1,2}

¹Stiftung Tierärztliche Hochschule Hannover, Institut für Pharmakologie, Toxikologie und Pharmazie, Hannover, Germany

²Zentrum für systemische Neurowissenschaften (ZSN), Hannover, Germany

A large variety of brain insults can induce the development of symptomatic epilepsies, particularly temporal lobe epilepsy. In the latent period after the initial insult multiple molecular, structural, and functional changes proceed in the brain and finally lead to spontaneous recurrent seizures. Prevention of these developments, called *antiepileptogenesis*, in patients at risk is a major unmet clinical need.

Several drugs underwent clinical trials for epilepsy prevention, but none of the drugs tested was effective. Similarly, most previous preclinical attempts to develop antiepileptogenic strategies failed. In the majority of studies, drugs were given as monotherapy. However, epilepsy is a complex network phenomenon, so that it is unlikely that a single drug can halt epileptogenesis. Recently, multitargeted approaches were proposed ("network pharmacology") to interfere with epileptogenesis.

Developing novel combinations of clinically used drugs with diverse mechanisms that are potentially relevant for antiepileptogenesis is a strategy, which would allow a relatively rapid translation into the clinic. We developed an algorithm for testing such drug combinations in a screening approach, modelled after the drug development phases in humans. Tolerability of four repeatedly administered drug combinations was evaluated by a behavioral test battery: A, levetiracetam and phenobarbital; B, valproate, losartan, and memantine; C, levetiracetam and topiramate; and D, levetiracetam, parecoxib, and anakinra. As in clinical trials, tolerability was separately evaluated before starting efficacy experiments to identify any adverse effects of the combinations that may critically limit the successful use in preclinical studies on antiepileptogenesis and translation of these preclinical findings to the clinic. Based on previous studies, we expected that tolerability would be lower in epileptic mice than in nonepileptic mice. Therefore nonepileptic mice were used as a first step, followed by epileptic mice and mice during the latent period shortly after status epilepticus.

Except combination B, all drug cocktails were relatively well tolerated. In contrast to our expectations, except combination C, no significant differences were determined between nonepileptic and post-status epilepticus animals. As a next step, the rationally chosen drug combinations will be evaluated for antiepileptogenic activity in mouse and rat models of symptomatic epilepsy.

266

Immunohistochemical analysis of adult neurogenesis in chronic 5-HT_{1A} receptor-stimulated mice

E.-M. Löken¹, B. Noto¹, H. Fink¹, S. E. Sander¹

¹Freie Universität Berlin Fachbereich Veterinärmedizin, Institut für Pharmakologie und Toxikologie, Berlin, Germany

Major depression is one of the most common mental disorders worldwide, with serious social and economic consequences. There are many different hypotheses concerning the pathophysiology of this disease. The complex brain serotonin system and particularly the serotonin_{1A} receptors (5-HT_{1A}R) apparently play a pivotal role in the development of depression. The involvement of an altered, 5-HT_{1A}R-mediated signalling in adult neurogenesis is also discussed. However, in this context the effects of pre- and postsynaptically located 5-HT_{1A}Rs have not been clarified yet. Mice with a permanent overexpression of postsynaptic 5-HT_{1A}Rs (OE mice) represent a unique tool to elucidate the effects of postsynaptic 5-HT_{1A}Rs in adult neurogenesis and depressive-like behaviour. Previous studies demonstrated an increased proliferation and survival of newborn cells in the adult dentate gyrus of female OE mice in comparison to controls. In the present study, we investigate the proliferation and survival of adult born cells after chronic treatment (15 days) with the selective 5-HT_{1A}R agonist 8-OH-DPAT (0,5 mg/kg/day) in young adult OE and WT mice. On the last three days of treatment, newly generated cells of OE and WT mice are labelled by injections with bromodeoxyuridine (BrdU; 50 mg/kg/day). Mice are sacrificed either one day (proliferation) or 21 days (survival) after the last injection. We hypothesise that the data we will present will confirm our previous results, with possibly more pronounced proneurogenic effects and differences in male mice. Further immunohistochemical studies post-exercise and behavioural analyses are in progress to identify the relation between chronic postsynaptic 5-HT_{1A}R stimulation, depressive-like behaviour and hippocampus-dependent learning.

267

Delayed maturation of striatal GABAergic interneurons and altered expression of alpha1 GABA_AR subunits in an animal model of paroxysmal dystoniaB. Christoph¹, C. Spröte¹, F. Richter¹, A. Bauer¹, A. Richter¹¹Institut für Pharmakologie, Pharmazie und Toxikologie, VMF, Uni-Leipzig, Leipzig, Germany

Dystonia is a common movement disorder characterized by intermittent and prolonged muscle contractions resulting in involuntary movements and/or abnormal postures. The lack of knowledge of the pathophysiology of dystonia hampers the development of effective therapeutics. Although benzodiazepines can improve dystonic symptoms, tolerance and side effects limit their use. There is evidence for striatal dysfunctions in human dystonia. GABAergic striatal interneurons (IN) are important for the regulation of striatal signaling. In the *dt^{ex}* mutant hamster, a model of paroxysmal dystonia, immunoreactive IN were reduced at the age of maximum severity of dystonia (33 days), but not after spontaneous remission (age 90 days). As indicated by unaltered homeobox protein *nkx 2.1* (cell density, mRNA), the age-dependent deficit seems not to be related to a disturbed migration, but to a retarded maturation of IN in mutant hamsters.

Here we further determined the maturation of striatal GABAergic neurons in the *dt^{ex}* hamster compared to healthy controls. *KCC2* and *CAVII* mRNA, used as markers for the GABA-switch, were unchanged in 18 and 33 day old mutant hamsters, indicating that there is no general delay in GABAergic maturation. As a retarded maturation seems to be specific for IN, we used another marker for GABAergic maturation: the expression of specific GABA_A receptor (GABA_AR) subunits (mature striatal IN express the alpha1 subunit). By stereological determination, we found a 46% decrease in alpha1 subunit expressing neurons. A lower immunoreactive intensity was restricted to the somata of dorsomedial striatal IN (32%) of *dt^{ex}* hamsters, indicating both a reduced density as well as a delayed maturation. These findings prompted us to examine the effects of the alpha1 GABA_AR preferring compound zolpidem in comparison with the benzodiazepine clonazepam. Zolpidem (2.0 and 10.0 mg/kg i.p.) only exerted moderate antidystonic effects compared to the benzodiazepine clonazepam (0.5 and 1.0 mg/kg i.p.) in the *dt^{ex}* hamster. Examinations of alpha2 GABA_AR preferring compounds are ongoing. In summary our studies indicate that there is no general defect in striatal GABAergic maturation in the *dt^{ex}* mutant but a specific alteration of striatal GABAergic interneurons which express alpha1 GABA_AR subunits. Changes in alpha1 GABA_AR subunit expression and differences in the antidystonic efficacy of zolpidem and clonazepam indicate that further investigations on the role of GABA_AR subunits could lead to new therapeutic approaches for the treatment of dystonia.

268

Interaction between pregnenolone and cannabinoids on GABAergic and glutamatergic synaptic transmissionA. Krohmer¹, M. Brehm¹, B. Szabo¹¹Institut für Pharmakologie und Toxikologie, Abteilung II, Freiburg, Germany

Introduction: The neurosteroid pregnenolone attenuates many *in vivo* behavioural and somatic effects of the phytocannabinoid Δ^9 -tetrahydrocannabinol, and it was suggested that "pregnenolone can protect the brain from cannabis intoxication" (M Vallee et al., Science 343: 94-98, 2014). The primary neuronal cannabinoid action behind most of the behavioural and somatic effects of cannabinoids is presynaptic inhibition of synaptic transmission (Szabo and Schlicker, Cannabinoids [ed. RG Pertwee], Handbook of Experimental Pharmacology vol 168, Springer Press, pp 327-365, 2005). Therefore, the hypothesis of the present study was that pregnenolone attenuates the inhibition of synaptic transmission elicited by cannabinoids.

Methods: 250 μ m-thick slices containing the cerebellum and the nucleus accumbens were prepared from the brains of mice and rats. Spontaneous and electrically evoked GABAergic inhibitory postsynaptic currents (sIPSCs and eIPSCs) and evoked glutamatergic excitatory postsynaptic currents (eEPSCs) were analyzed in superfused brain slices with patch-clamp electrophysiological techniques.

Results: A) The synthetic cannabinoids JWH-018 (5×10^{-9} M) and JWH-210 (5×10^{-6} M) inhibited the spontaneous GABAergic synaptic input (sIPSCs) to Purkinje cells in mouse cerebellar slices. The inhibition by JWH-018 was not affected by pregnenolone (10^{-7} M), the inhibition by JWH-210 was only marginally attenuated. B) The depolarization of the Purkinje cells induced suppression of the GABAergic input to Purkinje cells (DSI); Pregnenolone (10^{-7} M) did not affect this endocannabinoid-mediated form of synaptic suppression. C) In rat nucleus accumbens slices, GABAergic and glutamatergic synaptic input to medium spiny neurons was activated by electrical stimulation of axons. Δ^9 -Tetrahydrocannabinol (2×10^{-5} M) suppressed the GABAergic and glutamatergic synaptic transmission in the nucleus accumbens. These suppressive effects of Δ^9 -tetrahydrocannabinol were not changed by pregnenolone (10^{-7} M). D) Finally, we tested whether we can observe neurosteroid-mediated effects in our brain slice preparations. Tetrahydro-deoxycorticosterone (THDOC, 10^{-6} M) markedly prolonged the decay time constant (τ) of spontaneous GABAergic postsynaptic currents (sIPSCs), similarly as in previous experiments (EJ Cooper et al., J Physiol 521: 437-449, 1999).

Conclusion: The results show that inhibition of GABAergic and glutamatergic synaptic transmission by synthetic-, endogenous-, and phyto-cannabinoids is not changed by pregnenolone. Therefore, it is unlikely that interference with cannabinoid-induced inhibition of synaptic transmission is the mechanism by which pregnenolone attenuates behavioural and somatic effects of Δ^9 -tetrahydrocannabinol *in vivo*.

269

Activation of TRH neurons increases thermogenesis in brown adipose tissueH. Müller-Fielitz¹, M. Richter¹, M. Schwaninger¹¹University of Lübeck, Institute of Experimental and Clinical Pharmacology and Toxicology, Lübeck, Germany

The hypothalamus is one of the key players in the regulation of the energy homeostasis. Cold stress leads to an activation of neurons in the paraventricular hypothalamic nucleus

(PVN) and increases thermogenesis. The Thyrotropin-Releasing-Hormone (TRH) neurons have an important function in this effect. However it is hardly understood which role the TRH neurons exactly play and how they are connected to other regions of the brain.

We have transduced neurons in the PVN of mice with a recombinant adeno associated virus which contains an activating "Designer Receptors Exclusively Activated by Designer Drugs" (DREADD) system under the control of a shortened TRH promoter. Two weeks after transduction the animals were injected with clozapine-N-oxide (CNO). To analyse the physiological function of these neurons we performed indirect calorimetry, measured rectal temperature and thermogenesis in the brown adipose tissue (BAT), analysed drinking feeding behaviour and the home cage activity. After stimulation we measured the expression of genes in BAT as well plasma hormone levels of pituitary hormones. Propranolol and the specific β_3 -antagonist SR59230A were used to analyse the relevance of the sympathetic system. To further characterise the transduced neurons and their projections we used immunohistochemistry methods.

After stimulation with CNO the energy expenditure and body temperature were increased. These effects were mostly driven through an activation of the brown adipose tissue (BAT). In DREADD transduced TRH-receptor 1 (TRH-R1) knockout mice these effects were abolished. In parallel the plasma levels of TSH, the UCP1 mRNA level in the BAT, the home cage activity as well the food and water intake were increased. After the treatment with propranolol and SR59230A the effects on the thermogenesis were reduced, but the home cage activity was not affected. SR59230A treatment normalised the food intake and increased in parallel the plasma leptin concentrations after CNO stimulation. Transduced neurons project into the raphe nucleus, the medial part of the thalamus and the spinal cord.

With our experiments we could provide strong evidence for a sympathetic connection of the transduced neurons in the PVN to the BAT and for the involvement of TRH neurons in these effects. Therefore, this system is a suitable tool to investigate the metabolic relevance of TRH neurons in detail.

Pharmacology – Endocrine, immune and pulmonary pharmacology

270

Anti-adipogenic effects of the PAR-4 thrombin receptor in 3T3L1 adipocytesS. Kaglin¹, V. Fischinger², J. Maier², A. Fender²¹Institut für Pharmakologie & Klinische Pharmakologie, Klinikum der Heinrich-Heine-Universität Düsseldorf, Düsseldorf, Germany²Institut für Pharmakologie & Klinische Pharmakologie, Klinikum der Heinrich-Heine-Universität Düsseldorf, Düsseldorf, Germany

Background & Objective: During obesity development, tissue factor signalling contributes coagulation-independently to inflammatory and metabolic dysfunction of adipose tissue. Adipogenesis involves proliferation and differentiation of preadipocytes, apoptosis and hypertrophic growth of differentiated adipocytes, angiogenesis and extracellular matrix reorganisation. The coagulant protease thrombin promotes similar processes in various cell types, through activation of protease-activated receptors PAR-1, PAR-3 and PAR-4. In human adipose tissue, PAR-1 is found in vascular stromal cells and PAR-4 in preadipocytes and differentiated adipocytes. Thrombin stimulates mitogenic kinase signalling and induces inflammatory cytokine and angiogenic growth factor secretion in adipocytes. We have examined the contribution of thrombin receptor activation to adipogenesis processes in 3T3L1 cells.

Results: Differentiation of 3T3L1 preadipocytes with insulin, dexamethasone and isobutylmethylxanthine increases leptin and PPAR γ gene expression and accumulation of triglycerides and oil red O-stained lipids. PAR-4 is time-dependently upregulated in maturing cells while PAR-1 expression is detectable but not altered. In preadipocytes, thrombin (3 U/ml) activates the mitogenic kinase ERK1/2, promotes cell proliferation and induces gene expression of the maturation markers leptin and PPAR γ and the inflammatory marker tumor necrosis factor alpha (TNF α). Repeated stimulation of differentiating adipocytes with thrombin suppresses induction of leptin and PPAR γ and attenuates lipid accumulation, while expression levels of the proliferation marker Ki67 and the inflammatory cytokine interleukin (IL)-6 are increased compared to differentiated control cells. Similar proliferative and anti-adipogenic effects are seen with the selective PAR4-activating peptide (GYGKGF, 100 μ M) and cathepsin G, a proteolytic PAR-4 activator released from neutrophils and mast cells. Repeated exposure of maturing 3T3L1 cells to conditioned medium from degranulating mouse peritoneal mast cells (MCCM) augments lipid accumulation and IL-6 expression. Pretreatment of MCCM with a PAR-4 inhibitor further drives lipid accumulation, the induction of IL-6 by contrast is suppressed.

Conclusion: PAR-4 activation by thrombin or inflammatory cell-derived cathepsin G appears to suppress adipogenesis, possibly by maintaining proliferative capacity and preventing the growth arrest essential for initiating maturation. Increased PAR-4 expression in maturing adipocytes may instead support inflammatory changes, thereby promoting the onset of insulin resistance.

271

The chemokine receptor CXCR4 antagonist AMD3100 exerts deleterious effects in endotoxemia in vivoS. Seemann¹, A. Lupp¹¹Institute of Pharmacology and Toxicology, Jena University Hospital, Jena, Germany, Jena, Germany

The chemokine receptor CXCR4 is a multifunctional receptor which is activated by its natural ligand C-X-C motif chemokine 12 (CXCL12). Although a blockade of the CXCR4/CXCL12 axis revealed beneficial outcomes in chronic inflammatory diseases, its importance in acute inflammatory diseases remains contradictory and not well characterized. As CXCR4 seems to be part of the lipopolysaccharide sensing complex, CXCR4 agonists or antagonists may have a positive impact on TLR4 signaling. Additionally, CXCR4 is involved in the production of pro-inflammatory cytokines,

suggesting the receptor to be a promising target in terms of mitigating the cytokine storm.

Therefore, we aimed to investigate the impact of a CXCR4 blockade on endotoxemia by applying a sublethal LPS dose (5 mg/body weight) in mice.

The selective CXCR4 inhibitor AMD3100 was administered intraperitoneally shortly after LPS treatment to ensure an immediate effect after endotoxemia onset. 24 hours after LPS administration, the clinical severity score, the body temperature and the body weight of the animals were determined. Afterwards, the mice were sacrificed and serum TNF alpha as well as IFN gamma levels were measured. Furthermore, the oxidative stress in the brain, liver, lung and kidney tissue was assessed. In addition, the biotransformation capacity of the liver was evaluated and finally, the expression of gp91 phox as well as of heme oxygenase 1 in the spleen and liver were determined by means of immunohistochemistry.

The mice of the AMD3100 plus LPS treatment group displayed a significantly impaired general condition, a reduced body temperature and a decreased body weight in comparison to the control and to the LPS treated animals, respectively. TNF alpha levels were significantly increased by more than 200% or 35% when compared to the control or to the LPS group, respectively, whereas IFN gamma levels were elevated by about 11% in comparison to mice which had received LPS only. In all investigated organs, but especially in the liver and in the kidney, co-administration of AMD3100 and LPS caused massive oxidative stress. Furthermore, the protein contents and the activities of several CYP enzymes in the liver were significantly reduced. Immunohistochemistry revealed gp91 phox to occur above average, whereas heme oxygenase 1 expression was distinctly decreased.

Our results indicate that a blockade of the CXCR4 in endotoxemia is disadvantageous and even worsens the disease. Co-administration of AMD3100 and LPS impaired the health status of the animals, caused massive oxidative stress and diminished the biotransformation capacity. Thus, handling acute systemic inflammation with a CXCR4 antagonist cannot be recommended, hence indicating the activation of CXCR4 to be an attractive treatment option.

272

Dexamethasone synergistically enhances TNF α -induced Toll-like receptor 2 expression via inhibition of p38 MAP Kinase and induces TRAF6 in human primary keratinocytes

Q. Su¹, G. Weindl¹

¹Institut für Pharmazie, Freie Universität Berlin, Berlin, Germany

Toll-like receptors (TLRs) recognize microbial pathogens and trigger inflammatory immune responses to control infections. In acne vulgaris, activation of TLR2 by *Propionibacterium acnes* contributes to inflammation. Although glucocorticoids have immunosuppressive and anti-inflammatory effects, acne can be provoked by systemic or topical treatment. Enhanced TLR2 expression by glucocorticoids has been reported in undifferentiated keratinocytes, however, human skin cells of different epidermal and dermal layers have not been investigated. In this study, the modulation of TLR expression by dexamethasone was assessed in monolayer cultures of primary human keratinocytes and dermal fibroblasts, as well as the immortalized keratinocyte cell line HaCaT. Constitutive TLR2, TLR1 and TLR6 mRNA and protein expression was confirmed in basal keratinocytes, calcium-induced differentiated keratinocytes, HaCaT cells and fibroblasts by qPCR and western blotting. Dexamethasone induced TLR2 expression in a time-dependent and concentration-dependent manner and reduced TLR1/6 expression in keratinocytes but not in HaCaT cells or fibroblasts. Stimulation with dexamethasone in the presence of the pro-inflammatory cytokines TNF α or IL-1 β further increased TLR2 mRNA levels. Gene expression of MAPK phosphatase-1 (MKP-1) was also upregulated by dexamethasone. Glucocorticoid-induced TLR2 expression was negatively regulated by p38 MAPK signalling under inflammatory conditions through MKP-1 induction which functions to deactivate MAPKs. As expected, dexamethasone inhibited the immune responses linked to TLR2 signalling as demonstrated by reduced IL-8, IL-1 β , MMP-1 and MCP-1 levels. However, the expression of TRAF6, a critical cytosolic regulator of TLR- and TNF family-mediated signalling, was further upregulated by the TLR2 agonist HKLM (heat-killed *Lysteria monocytogenes*) in dexamethasone-pretreated basal keratinocytes. Conclusively, our results provide novel insights into the molecular mechanisms of glucocorticoid-mediated TLR expression and function in human skin cells.

273

Propranolol induces Th17-related cytokines and inhibits late-stage autophagy in cutaneous dendritic cells

G. Müller¹, G. Weindl¹

¹Freie Universität Berlin, Institut für Pharmazie, FB Pharmakologie und Toxikologie, Berlin, Germany

Psoriasis is a cutaneous chronic inflammatory disease characterized by increased amounts of IL-1 cytokines and T helper 17 (Th17) related cytokines in lesional psoriatic skin. Treatment with beta-adrenoceptor antagonists is associated with induction or aggravation of psoriasis, however, the underlying mechanism is poorly understood. Previously, we could demonstrate a pivotal role for Langerhans Cells and dermal dendritic cells in antimalarial-provoked psoriasis by maintaining a potent Th17 activity. In the present study, we investigated the effect of propranolol on human monocyte-derived Langerhans-like cells (MoLC) and dendritic cells (MoDC) under inflammatory conditions. In the presence of IL-1 β , propranolol induced the Th17 priming cytokines IL-23 and IL-6 in a concentration-dependent manner. The increased cytokine release was not mediated by cAMP suggesting GPCR-independent pathways. In contrast, IL-36 γ and LPS failed to increase IL-23 release in MoLC and MoDC in the presence of propranolol but further induced secretion of IL-1 β . Autophagy has been linked with the secretion of IL-1 family cytokines that are upregulated in chronic inflammatory disorders such as psoriasis. Propranolol upregulated the expression levels of the autophagy marker p62 and LC3-I to LC3-II conversion, induced accumulation of LC3 positive vesicles, as well as expression of IL-1 signalling downstream adapter molecule TRAF6, indicating a late-stage block in autophagy. In summary, our results suggest a prominent role of cutaneous dendritic cell

subtypes in psoriasis-like skin inflammation mediated by propranolol and possibly other beta blockers.

274

TLR2 signalling promotes Th1 induction by acute myeloid leukaemia-derived Langerhans-like cells

S. Bock¹, M. S. Murgueitio², G. Wolber², G. Weindl¹

¹Freie Universität Berlin, Institute of Pharmacy (Pharmacology and Toxicology), Berlin, Germany

²Freie Universität Berlin, Institute of Pharmacy (Pharmaceutical Chemistry), Berlin, Germany

Langerhans cells (LCs) represent a highly specialized subset of epidermal dendritic cells (DCs), yet not fully understood in their function of balancing skin immunity. In the present study, we investigated in vitro generated Langerhans-like cells obtained from the human acute myeloid leukaemia cell line MUTZ-3 (MUTZ-LCs) to study TLR- and cytokine-dependent activation of epidermal DCs. MUTZ-LCs revealed high TLR2 expression and responded robustly to TLR2 engagement, confirmed by increased CD83 and CD86 expression, upregulated IL-6, IL-12p40 and IL-23p19 mRNA levels and IL-8 release. TLR2 activation reduced CCR6 and elevated CCR7 mRNA expression and induced migration of MUTZ-LCs towards CCL21. Similar results were obtained by stimulation with pro-inflammatory cytokines TNF- α and IL 1 β whereas ligands of TLR3 and TLR4 failed to induce a fully mature phenotype. Despite limited cytokine gene expression and production for TLR2-activated MUTZ-LCs, co culture with naive CD4+ T cells led to significantly increased IFN- γ and IL-22 levels indicating Th1 differentiation independent of IL-12. TLR2-mediated effects were blocked by the putative TLR2/1 antagonist CU-CPT22, however, no selectivity for either TLR2/1 or TLR2/6 was observed. Computer-aided docking studies confirmed non-selective binding of the TLR2 antagonist. Taken together, our results indicate a critical role for TLR2 signalling in MUTZ-LCs considering the leukemic origin of the generated Langerhans-like cells.

275

Novel synthetic antimicrobial and LPS-neutralizing peptides suppress inflammatory responses in skin cells and promote keratinocyte migration

A. Pfalzgraff¹, K. Brandenburg², G. Weindl¹

¹Institut für Pharmazie FU Berlin, Pharmakologie und Toxikologie, Berlin, Germany

²Forschungszentrum Borstel Leibniz-Institut für Medizin und Biowissenschaften, Biophysik, Borstel, Germany

The stagnation in the development of new antibiotics during the last decades and the concomitant high increase of resistant bacteria emphasize the urgent need for new therapeutic options. Antimicrobial peptides are promising agents for the treatment of bacterial infections and recent studies indicate that Pep19-2.5, a synthetic antimicrobial and LPS-neutralizing peptide (SALP), efficiently neutralizes pathogenicity factors of Gram-negative and Gram-positive bacteria and protects against sepsis. In the present study, we investigated the potential of Pep19-2.5 and the structurally related compound Pep19-4LF for their therapeutic application in bacterial skin infections. Primary human keratinocytes responded to TLR2 (FSL-1) but not TLR4 (LPS) activation by increased IL-8 production, as determined by ELISA. Western blot analysis showed that both SALPs inhibited FSL-1-induced phosphorylation of NF- κ B p65 and p38 MAPK. Furthermore, the peptides significantly reduced IL-8 release and gene expression of IL-1 β , CCL2 (MCP-1) and hBD-2 as assessed by qPCR. No cytotoxicity (MTT test) was observed at SALP concentrations below 10 μ g/ml. In LPS-stimulated monocyte-derived dendritic cells, the peptides blocked IL-6 secretion, downregulated expression of the maturation markers CD83 and CD86, as analysed by flow cytometry, and inhibited CCR7-dependent migration capacity. Similarly, monocyte-derived Langerhans-like cells activated with LPS and pro-inflammatory cytokines showed reduced IL-6 levels and CD83/CD86 expression in the presence of SALPs. In addition to acute inflammation, bacterial infections often result in impaired wound healing. Since re-epithelialization is a critical step in wound repair, we tested whether Pep 19-2.5 affects keratinocyte migration using the scratch wound assay. The peptide markedly promoted cell migration and accelerated artificial wound closure at concentrations as low as 1 ng/ml and was equipotent to TGF- β . Conclusively, our data suggest a novel therapeutic target for the treatment of patients with acute and chronic skin infections.

276

Nrf2-deficient mice are protected from mild but not moderate acid-induced lung injury

K. Reiss¹, A. Fragouli², C. Wruck², S. Uhlir¹

¹Uniklinik RWTH Aachen, Institut für Pharmakologie und Toxikologie, Aachen, Germany

²Uniklinik RWTH Aachen, Institut für Anatomie und Zellbiologie, Aachen, Germany

Rationale: The acute respiratory distress syndrome (ARDS) is a life-threatening lung disease, characterized by excessive inflammation and hypoxemia. Most ARDS patients require mechanical ventilation and to date there is no pharmacological cure available. Recently, we and others have shown that the transcription factor nuclear factor erythroid 2-related factor 2 (Nrf2), a major regulator of the cellular antioxidant defence system, is activated by mechanical ventilation. During ventilator-induced lung injury, Nrf2 exerts a protective role by interaction with the stretch-induced growth factor amphiregulin. In the current study, we aimed to investigate the role of Nrf2 in acid-induced lung injury, a model for aspiration-induced ARDS.

Methods: Nrf2-deficient (*Nrf2*^{-/-}) mice and wild type (*WT*) littermates were tracheotomised and ventilated for 30min ($V_T=16$ ml/kg, $f=90$ min⁻¹, $PEEP=2$ cmH₂O, $FI_{O_2}=0.3$), before 50 μ l hydrochloric acid (HCl) with pH=1.5 or pH=1.3 were instilled intratracheally, controls received NaCl. Mice were then ventilated for further 6h under monitoring of lung mechanics and vital parameters. Blood gases as well as pro-inflammatory mediators, neutrophil recruitment and microvascular permeability were examined to assess lung injury.

Results: Instillation of HCl pH=1.5 induced mild lung injury, indicated by hypoxemia ($pO_2/FiO_2 \sim 300$ mmHg) and continuously increasing lung tissue elastance (stiffness), from which *Nrf2*^{-/-} mice were protected. Pulmonary inflammation, characterized by liberation of cytokines, chemokines and oedema formation, was attenuated in *Nrf2*^{-/-} mice. In contrast, HCl pH=1.3 caused more severe lung injury ($pO_2/FiO_2 \sim 200$ mmHg) with a steeper incline in elastance and more severe inflammation in both *WT* and *Nrf2*^{-/-} mice.

Conclusion: We conclude that the presence of *Nrf2* augments mild acid-induced lung injury, but plays no role in more severe injury. These discrepant results will be elucidated in future investigations.

277

Implementation of quality management in a mouse intensive care unit

K. Reiss¹, S. Günther², A. Kowalik¹, M. Große Böckmann², S. Uhlir¹

¹Uniklinik RWTH Aachen, Institut für Pharmakologie und Toxikologie, Aachen, Germany

²Fakultät für Maschinenwesen der RWTH Aachen, Werkzeugmaschinenlabor, Aachen, Germany

Rationale: Reproducibility is key to science. In recent times, the reproducibility of biomedical research has been questioned increasingly. This reproducibility crisis also affects complex animal experiments, which – if not reproducible – might also be regarded as unethical and lose public acceptance. Part of the problem is frequently that the provided documentation is not sufficient for reproduction. Therefore, in this study we analyzed the potential of conventional quality management tools – used as standard in machine production – as an approach to improve the documentation and ascertain the quality of complex animal experiments.

Methods: Quality management tools were transferred to an experimental animal set up – the mouse intensive care unit (MICU) – which we use for lung injury studies. The tools included visualization of the experimental set-up, transfer of the experimental procedures to an event-driven process chain (EPC) and statistical process control (SPC) of all crucial pulmonary and cardiovascular parameters. Data from ventilator- and acid-induced lung injury studies acquired in the MICU were analyzed retrospectively.

Results: Schematic visualization of the MICU resulted in a chart comprising medical components, hardware, software and generated data types. The customized EPC included all important activities and the resulting events for preparation of the mouse and the workplace, the actual animal ventilation experiment and sample-taking. In addition, checklists were provided for these activities and events, to ensure standardization of every work step. Lung impedance and cardiac functions from ventilator- and acid-induced lung injury models were analyzed by SPC and correlated with events in the EPC. The SPC proved to be suitable to identify outliers, predict processes and thereby validate the lung injury models.

Conclusions: Conventional quality management tools were successfully adapted to analyze the quality of lung injury experiments in the MICU. We suggest that this new approach is suitable to standardize animal testing procedures and increase the reproducibility of animal studies.

278

Effects of apelin on the L-arginine-nitric oxide pathway in human pulmonary microvascular endothelial cells – implication for pulmonary arterial hypertension?

A. Glatzel¹, N. Lüneburg¹, E. Oetjen¹, R. H. Böger¹, L. Harbaum²

¹Universitätsklinikum Hamburg-Eppendorf, Klinische Pharmakologie und Toxikologie, Hamburg, Germany

²Universitätsklinikum Hamburg-Eppendorf, Sektion Pneumologie, Hamburg, Germany

Background: A dysfunctional endothelial L-arginine-nitric oxide (NO) pathway is a key pathomechanism of idiopathic pulmonary arterial hypertension (IPAH) that can be provoked by hypoxia in cell culture models [1-4]. The small peptide apelin is involved in the maintenance of pulmonary vascular homeostasis and angiogenesis although its precise mechanism of action is still unclear [5]. Asymmetric dimethylarginine (ADMA) is known to be an endogenous inhibitor of endothelial NO synthase and is associated with several cardiovascular diseases [6]. ADMA is degraded by dimethylarginine dimethylaminohydrolase 1 and 2 (DDAH) enzymes [7].

Objective: To determine the effect of apelin on the L-arginine/NO pathway in human pulmonary microvascular endothelial cells (HPMECs).

Methods: HPMECs were cultured under normoxic and PH-related hypoxic conditions and treated with apelin. The expression of regulators of the L-arginine/NO pathway were analysed using real-time PCR. The effect of apelin on the phosphoinositide-3 kinase (PI3K)/Akt signalling pathway was determined using immunoassays and specific inhibitors [LH1]. Apelin and ADMA concentrations were measured in cell culture supernatants using an enzyme-linked immunosorbent assay and a liquid chromatography-tandem mass spectrometry assay.

Results: Treatment with Apelin resulted in a reduced expression of the apelin receptor (AplnR) on HPMECs suggesting a negative feedback mechanism. Apelin directly influenced the L-arginine/NO pathway by increasing the expression of DDAH1 and DDAH2 enzymes. Thus, the concentration of ADMA was decreased in HPMECs supernatant following treatment with apelin. The effect of apelin could be abrogated by modulation of the PI3K/Akt pathway.

Conclusion: Apelin modulates the L-arginine/NO pathway and mediates enhanced degradation of ADMA via an upregulated expression of DDAH 1 and 2 enzymes. The PI3K/Akt pathway might play a decisive role in regulation of the effect of apelin. An Apelin receptor agonist could be a novel and promising therapeutic option for IPAH treatment.

References:

- Rabinovitch, M. et al.: *J Clin Invest.* **2012**,122(12):4306-13.
- Galiè, N. et al.: *Eur Respir J.* **2009**,34(6):1219-63.
- Cooper, C.J. et al.: *Circulation.* **1996**,93(2):266-71.
- Lüneburg, N. et al.: *Biomed Res Int.* **2014**,2014(2014):501612
- Andersen, C. et al.: *Pulm Circ.* **2011**,1(3):334-46.

- Vallance, P. et al.: *J Cardiovasc Pharmacol.* **1992**,20(12):60S-62S.
- Ogawa, T. et al.: *Arch Biochem Biophys.* **1987**,252(2):526-37.

279

Therapeutic time window for angiotensin-(1-7) in acute lung injury

F. Kohse^{1,2}, S. Supé², F. Gemhardt³, W. M. Kuebler^{2,4}, T. Walther⁵

¹Universität Leipzig – Medizinische Fakultät, Klinik und Poliklinik für Kinderchirurgie, Leipzig, Germany

²Charité – Universitätsmedizin Berlin, Institut für Physiologie, Berlin, Kanada

³Universitätsklinikum Carl Gustav Carus Dresden, Medizinische Klinik III – Bereich Nephrologie, Dresden, Germany

⁴Keenan Research Centre for Biomedical Science of St. Michael's, Toronto, Kanada

⁵Universität Leipzig – Medizinische Fakultät, Abteilung für Geburtsmedizin, Leipzig, Irland

Background and purpose: There is presently no proven pharmacological therapy for the Acute Respiratory Distress Syndrome (ARDS). Recently, we and others discovered that the heptapeptide angiotensin (Ang)-(1-7) shows significant beneficial effects in preclinical models of acute lung injury (ALI). Here, we aimed to identify the best time window for Ang-(1-7) administration to protect rats from oleic acid (OA) induced ALI.

Experimental approach: The effects of intravenously infused Ang-(1-7) were examined over four different time windows before or after induction of ALI in male Sprague-Dawley rats. Hemodynamic effects were continuously monitored, and loss of barrier function, inflammation, and lung peptidase activities were measured as experimental endpoints.

Key results: Ang-(1-7) infusion provided best protection from experimental ALI when administered by continuous infusion starting 30min after OA infusion till the end of the experiment (30-240min). Both pretreatment (-60-0min before OA) and short-term therapy (30-90 min after OA) also had beneficial effects although less pronounced than the effects achieved with the optimal therapy window. Starting infusion of Ang-(1-7) 90min after OA (late-term infusion) achieved no protective effects on barrier function or hemodynamic alterations, but still reduced myeloperoxidase and angiotensin converting enzyme activity, respectively.

Conclusions and implications. Our findings indicate that early initiation of therapy after ALI and continuous drug delivery are most beneficial for optimal therapeutic efficiency of Ang-(1-7) treatment in experimental ALI, and presumably accordingly, in clinical ARDS.

280

The ROCK inhibitor Y-27632 enhances primary equine bronchial epithelial cell proliferation and differentiation

J. Bonicelli¹, C. L. Hofmann-Orsetti¹, J. Kazca¹, T. Vahlenkamp¹, G. Abraham¹

¹Universität Leipzig, Veterinärmedizinische Fakultät, Leipzig, Germany

Airway epithelium functions as a physicochemical barrier against dust, air pollutants and other pathogens and plays a critical role in physiological and pathological processes including modulation of the inflammatory response, innate immunity and airway remodeling such as in human asthma, COPD and equine recurrent airway obstruction (RAO). Models of the airway epithelia are, indeed, missing for the horse; thus, we established long-term equine bronchial epithelial cell cultures using the ROCK inhibitor Y-27632 and cell growth and differentiation was characterized. Bronchial epithelial cells (EBEC) from adult horses were cultured in the presence and absence of 10 μ M Y-27632 under conventional and air-liquid-interface (ALI) culture conditions. Cell proliferation and differentiation were analyzed. Formation of a functional epithelial barrier was investigated by transepithelial electric resistance (TEER) measurement and immunocytochemical staining of the Tight-Junction-protein Zonula Occludens-1 (ZO-1). Under conventional culture, Y-27632 induced higher growth rate of primary EBEC and increased the passage number up to 5 passages with retained epithelial cell behavior. In the presence of Y-27632, EBECs under ALI showed higher TEER values. Expression of ZO-1 correlated with the increase in TEER, but in Y-27632-treated EBEC Tight-junction-formation was more rapid, indicating accelerated differentiation, as well H/E-staining and scanning electron microscopic imaging showed a higher amount of cilia and microvilli and PAS-positive cells. In conclusion, the data suggest that the ROCK inhibitor Y-27632 facilitates long-term culture of equine bronchial epithelial cells which can be used to study airway disease mechanisms and to identify pharmacological targets.

Pharmacology – Gastrointestinal tract, NO, CO

281

Activation of Endoperoxide Drugs in *Leishmania*

G. Pichler¹, M. Tonner¹, K. Staniek¹, L. Monzote², L. Gille¹

¹University of Veterinary Medicine, Inst. of Pharmacology and Toxicology, Vienna, Austria

²Institute of Tropical Medicine "Pedro Kouri", Parasitology Department, Havana, Cuba

Leishmaniasis is a neglected disease of tropical and subtropical regions with millions of people at risk of infection with severe consequences including death. Current antileishmanial drugs exhibit serious side effects and also development of resistances is rising. This disease is caused by protozoal organisms from the genus *Leishmania*. In their insect vector they exist in the promastigote form, while in the mammalian host they survive as amastigotes inside the phagolysosomes of macrophages. This makes a specific pharmacotherapy complicated. Due to the success of artemisinin in malaria therapy, it was of interest whether endoperoxides are also useful to treat leishmaniasis. In a previous study we demonstrated that ascaridole, an endoperoxide from *Chenopodium ambrosioides*, can cure cutaneous leishmaniasis in a mouse model and exhibited IC_{50} values for the viability in the low micromolar range [1]. Even though in chemical model systems some basic ideas about the mechanism of activation of these endoperoxides exist, in biological systems including *Leishmania*

parasites this activation step has never been demonstrated. Therefore, we set up experiments to identify primary drug intermediates formed from ascaridole by activation in *Leishmania tarentolae* promastigotes using electron spin resonance spectroscopy in combination with spin trapping methods. Ascaridole was activated in a cell-free system by Fe^{2+} . The radicals were trapped by 2-methyl-2-nitrosopropane (MNP). The resulting ESR spectra consisted of the triplet of doublets. Spectral simulations revealed coupling parameters of $a_N = 16.8$ G, and $a_H = 1.8$ G. These coupling constants are compatible with iso-propyl radicals as primary intermediates. In the cellular system, consisting of *Leishmania tarentolae* promastigotes, instead of MNP the less cytotoxic 5,5-dimethyl-1-pyrroline-N-oxide (DMPO) was used for spin trapping. Without addition of Fe^{2+} a six line ESR signal was observed. Spectral simulations of the DMPO spin adduct revealed coupling constants of $a_N = 16.1$ and $a_H = 24.6$ G. According to previously published data [2] from other spin trapping experiments, this corresponds to the formation of carbon-centered radicals from ascaridole by *Leishmania* parasites. Additional experiments using iron chelators and antioxidants as well as a comparison with the endoperoxide artemisinin were performed. In summary, this study for the first time demonstrated the activation of the endoperoxide ascaridole by a protozoal organism to its active intermediate as a prerequisite to understand its mechanism of action.

[1] L. Monzote, J. Pastor, R. Scull, and L. Gille. Antileishmanial activity of essential oil from *Chenopodium ambrosioides* and its main components against experimental cutaneous leishmaniasis in BALB/c mice. *Phytomedicine* 21:1048-1052, 2014.
[2] G. R. Buettner. Spin trapping: ESR parameters of spin adducts. *Free Radic.Biol.Med.* 3:259-303, 1987.

282

Role of the upstream open reading frame (μ ORF) in the human inducible nitric oxide synthase (iNOS) mRNA

F. Gather¹, A. Pautz¹, H. Kleinert¹

¹Johannes Gutenberg-University Medical Center, Department of Pharmacology, Mainz, Germany

Nitric oxide (NO), produced by the inducible nitric oxide synthase (iNOS) has many functions in physiological and pathophysiological pathways. After induction of iNOS expression by cytokines and other agents the enzyme produces high amounts of NO in a Ca^{2+} -independent way. This high NO production can have beneficial microbicidal, antiparasitic, antiviral and antitumoral effects. In contrast, aberrant iNOS induction may have detrimental consequences and seems to be part of many diseases such as asthma, arthritis, multiple sclerosis, colitis, psoriasis, neurodegenerative diseases, tumor development, transplant rejection or septic shock.

Analysis of the human iNOS-mRNA structure revealed the existence of an upstream open reading frame (μ ORF) and a putative internal ribosome entry site (IRES) in the 5' untranslated region (5'UTR) in front of the start codon of the iNOS coding sequence (cds). To analyze the function of the μ ORF and the putative IRES we cloned different EGFP and luciferase reporter constructs and transfected them into the human colon carcinoma cell line DLD1. Using a plasmid construct with the μ ORF fused with the EGFP cds, we could show that the μ ORF can be translated. However, compared to the positive control plasmid less EGFP was produced, which can be explained by a weak Kozak sequence of the μ ORF. Blocking the mRNA cap-dependent translation by cloning a stem loop structure in front of the iNOS 5'UTR within a luciferase reporter plasmid led to a remarkable loss of luciferase production. Thus, the expression of iNOS seems to be cap-dependent. Furthermore, transfection experiments with DLD1 cells using constructs coding for a bicistronic renilla-firefly luciferase mRNA showed that there is no IRES in front of the iNOS cds. Taken together, the iNOS expression seems to be cap-dependent and without influence of an IRES, while the μ ORF is translatable. Therefore we speculate that iNOS expression is only possible due to a leaky scanning mechanism depending on the weak Kozak sequence of the μ ORF.

283

Vascular oxidative stress induced by genetically destabilized eNOS selectively impairs blood pressure reduction in mice

T. Suvorava¹, S. Pick², G. Kojda²

¹Heinrich-Heine-University, 1-Institute of Pharmacology and Clinical Pharmacology, 2-Cardiovascular Research Laboratory, Division of Cardiology, Pneumology and Angiology, Düsseldorf, Germany

²Heinrich-Heine-University, Institute of Pharmacology and Clinical Pharmacology, Düsseldorf, Germany

Objectives: Vascular oxidative stress is considered a pathophysiological factor promoting cardiovascular diseases such as coronary artery disease, heart failure, diabetes and hypertension. There are several sources of superoxide in vascular smooth muscle and endothelial cells but whether an impairment of the catalytic function of eNOS and thus generation of oxidative stress is involved in blood pressure (BP) regulation and/or the development of hypertensive disease states is unknown.

Methods: We generated a mutant eNOS in which one of the two essential cysteines required for the coordination with the central Zn-ion, correct dimer formation and normal activity is replaced by alanine (C101A-eNOS). Normal eNOS (eNOS-Tg) or a novel dimer-destabilized C101A-eNOS described previously (Antioxid Redox Signal. 2015 Sep 20;23(9):711-23) were introduced in C57BL/6 in an endothelial-specific manner. Mice were monitored for eNOS expression and localization, aortic relaxation, systolic blood pressure, levels of superoxide and several post-translational modifications indicating activity and/or increased vascular oxidative stress. Some groups of mice underwent voluntary exercise training for 4 weeks or treatment with SOD mimetic Tempol.

Results: C101A-eNOS-Tg showed significantly increased superoxide generation, protein- and eNOS-tyrosine-nitration, eNOS-S-glutathionylation, eNOS^{1176/79} phosphorylation and AMP kinase (AMPK α) phosphorylation at Thr172 in aorta, skeletal muscle, left ventricular myocardium and lung as compared to eNOS-Tg and wild type (WT) controls. The localization of eNOS-C101A-Tg was restricted to endothelium as evidenced by immunohistochemically staining for eNOS and an endothelial-specific marker CD31. Exercise training increased phosphorylation of eNOS at Ser 1176/79 and of AMPK α at Thr 172 in WT but not in C101A-eNOS-Tg. Aortic endothelium-dependent and endothelium-independent relaxations were similar in all strains. In striking contrast,

C101A-eNOS-Tg displayed normal blood pressure despite higher levels of eNOS, while eNOS-Tg showed significant hypotension. Tempol completely reversed the occurring protein modifications and significantly reduced BP in C101A-eNOS-Tg but not in WT controls.

Conclusions: By means of a novel transgenic mouse model we demonstrated that vascular oxidative stress generated by endothelial-specific expression of a dimer-destabilized variant of eNOS selectively prevents BP reducing activity of vascular eNOS, while having no effect on aortic endothelial-dependent relaxation. These data suggest that oxidative stress in microvascular endothelium may play a role in the development of essential hypertension.

* TS, SP – equal contribution

284

In vitro studies on the anti-inflammatory potential of chamomile, myrrh and coffee charcoal – components of a traditional herbal medicinal product (Myrrhinil-Intest®)

C. Vissienon¹, K.-H. Goos², R. Jente¹, J. Arnold¹, K. Nieber¹

¹University of Leipzig, Leipzig, Germany

²REPHA GmbH Biologische Arzneimittel, Langenhagen, Germany

The herbal medicinal product Myrrhinil-Intest® consists of myrrh, chamomile flower dry extract and coffee charcoal. Clinical data prove the effectiveness of this herbal preparation for inflammatory intestinal disorders.

To further investigate the anti-inflammatory potential of the single components as part of a multi-target principle, an ethanolic (MY) and aqueous (MYA) myrrh extract, ethanolic chamomile flower extract (KA) and aqueous coffee charcoal extract (CC), were examined in an *in vitro* TNBS inflammation model using rat small intestinal preparations. The effect of the plant extracts on TNBS induced inflammatory damage was characterised based on TNF α -gene expression analysis, isometric contraction measurement and histological analysis. Furthermore, TNF α -release from LPS-stimulated THP-1 cells was determined. Budesonide was used as positive control. Additionally, microarray gene expression analysis was performed in LPS/IFN γ stimulated native human macrophages to determine potential underlying mechanisms.

The TNBS-induced overexpression of TNF α -mRNA was reduced after KA (0.1 mg/ml) and MYA (1 mg/ml) treatment down to 24% and 16% resp.; TNBS-induced loss of contractility and reduction of mucosal layer thickness was inhibited after KA (3 mg/ml) treatment by 26% and 25% resp.; after MYA (0.1-1mg/ml) treatment by 17% and 44% resp. LPS-induced TNF α release from THP-1 cells was inhibited concentration-dependently by MY (IC₅₀ = 60.65 μ g/ml; 97% inhibition), KA (IC₅₀ = 439 μ g/ml; 71% inhibition) and CC (IC₅₀ = 1886 μ g/ml; 44% inhibition). Furthermore, KA (200 μ g/ml) and CC (500 μ g/ml) inhibited the LPS/IFN γ -induced expression of genes associated with chemokine signalling up to 100-fold (for CXCL13). The presented study demonstrates further evidence for anti-inflammatory properties of the herbal components which contribute to the reported clinical effectiveness.

285

Adenosine receptors in inflammation on rat colon preparations. Are they involved in the anti-inflammatory action of STW 5?

K. Nieber¹, U. Voß¹, C. Müller², H. Abdel-Aziz³, O. Kelber³

¹Universität Leipzig, Institut für Pharmazie, Leipzig, Germany

²Rheinische Friedrich-Wilhelms Universität Bonn., Institut für Pharmazie, Bonn, Germany

³Steigerwald Arzneimittelwerk GmbH, Scientific Department, Darmstadt, Germany

Introduction: The purine nucleoside adenosine, which is involved in a variety of physiological functions, regulates immune and inflammatory responses and acts as a modulator of gut functions. Although it is present at low concentrations in the extracellular space, stressful conditions, such as inflammation, can markedly increase its extracellular level up to micromolar range. By activation of different receptor subtypes adenosine is able to induce anti-inflammatory or pro-inflammatory impacts. Aim: The current study examined the impact of adenosine A2A receptors (A2AR) and adenosine A2B receptors (A2BR) to regulate contractility in untreated and inflamed rat colon preparations using a specific A2AR agonist (CGS 21680) and an A2BR antagonist (PSB-1115) on acute inflammation in rat colon preparations. Further it focused on interactions of the multi-herbal drug STW 5 with A2AR as a possible mechanism of the protective effect of STW 5 in gastrointestinal disorders.

Methods: Inflammation was induced by intraluminal instillation of 2,4,6-trinitrobenzene sulfonic acid (TNBS). Contractions were measured isometrically in an organ bath set up. Gene expression was determined using RT-PCR. Radio ligand binding assays (competition experiments) were carried out with rat brain homogenates. Morphological changes were estimated after van Gieson staining.

Results: All four adenosine receptor subtypes were expressed in untreated colon preparations. Activation of A1, A2B, and A3 receptor with specific agonists reduced the acetylcholine (ACh, 10 μ M)-induced contractions, while activation of A2BR enhanced it. After incubation with TNBS morphological damages in colonic mucosa and muscle walls were detectable followed by reduced ACh-contractions. The TNBS-mediated decrease of ACh-contractions as well as the morphological damages were partially normalized by co-incubation of TNBS with CGS 21680 (10 μ M) or with PSB 1115 (100 μ M). The same effects with smaller intensity were found for STW 5 (512 μ g/ml) in female but not in male colon preparations. These results are in accordance with ligand binding studies indicating that STW 5 interact with the A2AR. Conclusion: Anti-inflammatory mechanisms and cell protective actions of STW 5 are partly due to the interaction with adenosine receptors. The results give a clear-cut correlation with symptom improvements in clinical trials and thereby highlight the relevance of STW 5 as a therapeutic approach in IBS.

286

Handling of complex data in gastroenterology: Multi-Step-Clustering of preclinical data on combination phyto-medicineG. Lorkowski¹, H. Abdel-Aziz², O. Kelber², M. Storr³, **K. Nieber**⁴¹GL Pharma Consulting R & D, Gauting, Germany²Steigerwald Arzneimittelwerk GmbH, Scientific Department, Darmstadt, Germany³Zentrum für Endoskopie, Starnberg, Germany⁴Universität Leipzig, Institut für Pharmazie, Leipzig, Germany

Introduction: In functional gastrointestinal disturbances (FGDs) as irritable bowel syndrome (IBS) and functional dyspepsia (FD), a multitude of concomitant causes and likewise also targets for therapeutic interventions have been identified (Allescher 2006). Therefore, a multi-target approach is a promising therapeutic strategy, as is exemplified by STW 5 (Ottillinger et al. 2013). STW 5 (Iberogast®) is a fixed combination of nine plant extracts with *Iberis amara* (STW 6) as one of its components. It is successfully used for treatment of functional dyspepsia and irritable bowel syndrome (IBS).

Aims & Methods: To allow an overview of targets addressed by STW 5 and the role of its components in relation to the different forms and causes of functional GI diseases, an evaluation of the data, which have been gained from more than 150 pharmacological tests, is needed. All data from studies including STW 5 alone, or STW 5 and its components, were retrieved and sorted according to types of study models (Human and animal systems, animal disease models, GI-preparations, cell cultures, in vitro-systems) and respective etiologic mechanisms related to FGDs and then visualized in the form of 2D histograms (Lorkowski et al. 2015).

Results: More than 150 pharmacological tests indicated anti-oxidative activity, electrophysiological effects, ulcer protection, anti-inflammatory actions, pro-kinetic and spasmolytic effects as well as reflux and acid reduction. Moreover, the analysis indicated that the components of STW 5 contribute differently to the overall effect of STW 5. Altogether, the evaluation of the data shows that STW 5 is active in response to multiple etiologic factors involved in FGDs, especially functional dyspepsia and irritable bowel syndrome, and to which extent the herbal extract components of the combination are relevant for the different mechanisms of action and their translation to clinical efficacy. **Conclusion:** Multi step clustering allows the transformation of complex data sets. It makes the allocation of specific actions to the different components of STW 5 manageable, so also giving support to its clinical use in patients with different symptoms. **References:** Ottillinger et al. 2013, *WMM* 163:65; Allescher et al. 2006, *Phytomedicine* 13 SV:2; Lorkowski et al. 2015, *Der Gastroenterologe* 10: 231.

287

Efficacy of the herbal preparation, STW 5 II, in an experimental model of ulcerative colitis**M. T. Khayyal**¹, W. Wadie¹, O. Kelber², H. Abdel-Aziz²¹Faculty of Pharmacy, Cairo University, Dept. of Pharmacology, Kairo, Egypt²Steigerwald Arzneimittelwerk GmbH, Scientific Dept., Darmstadt, Germany

Introduction: STW 5 II has been recently developed in an effort to reduce the number of active extracts in the mother multi-component herbal preparation, STW 5 (Iberogast®, Steigerwald Arzneimittelwerk GmbH, Darmstadt, Germany) without affecting the overall therapeutic efficiency. STW 5 consists of a mixture of 9 standardized extracts: bitter candytuft (*Iberis amara*), lemon balm (*Melissa officinalis*), chamomile (*Matricaria recutita*), caraway fruit (*Carum carvi*), peppermint leaf (*Mentha piperita*), liquorice root (*Glycyrrhiza glabra*), Angelica root (*Angelica archangelica*), milk thistle (*Silybum marianum*) and celandine herb (*Chelidonium majus*), whereas STW 5 II lacks the last 3 components. STW 5 was shown to be effective clinically to treat functional dyspepsia⁽¹⁾ and irritable bowel syndrome⁽²⁾ and was shown experimentally to be effective to guard against the development of radiation induced intestinal mucositis⁽³⁾ and in the management of ulcerative colitis⁽⁴⁾.

Methods & Results: The present study was initiated to show whether STW 5 II with the reduced component extracts would also be as effective in the latter condition. This was induced in Wistar rats by feeding them with 5% Dextran sodium sulfate in drinking water for 1 week when lesions were observed in the colon evidenced by histological examination as well as colon shortening and reduction of colon mass index. This was associated with a rise in myeloperoxidase and a fall in reduced glutathione, glutathione peroxidase, and superoxide dismutase in colon homogenates as well as a rise in TNF α in serum. Oral administration of STW 5 in doses of 2 and 5 ml/kg or STW 5 II in a dose of 2 ml/kg for 1 week before and continued during DSS feeding tended to normalize all the changes in a fashion comparable to sulfasalazine, used as a reference drug in a dose of 300 mg/kg. **Conclusions:** The modified preparation, STW 5 II thus proved to be as effective as STW 5, thereby reflecting its potential usefulness in ulcerative colitis possibly by virtue of its anti-inflammatory and anti-oxidant properties.

References:

- (1) Schmulson MJ (2008) *Nature Clinical Practice Gastroenterology & Hepatology*, 5, 136-137.
- (2) Madisch A et al. (2004) *Aliment Pharmacol Ther*, 19: 271-279.
- (3) El-Ghazaly MA, El-Hazek RM, Khayyal MT (2015) *Int J Radiat Biol.*, 91:150-6.
- (4) Wadie, W. et al. (2012) *Int J Colorectal Dis.* 2012, 11:1445-53.

288

Comparison of NK1 – and 5HT3-receptor mediated effects in cells endogenously and stably expressing these receptors**T. Plötz**¹, A. Aigner¹, G. Abraham², R. Regenthal¹¹Universitätsmedizin Leipzig, klinische Pharmakologie, Leipzig, Germany²Veterinärmedizinische Fakultät, Institut für Pharmakologie, Pharmazie und Toxikologie, Leipzig, Germany

The emetic pathways include the action of neurotransmitters dopamine, serotonin and substance p in the emetic centers localized in the brainstem, area postrema and vagal nerve afferents. Previous in vivo studies in beagle dogs revealed that the plant alkaloid lycorine potentially induce nausea and emesis. Though antagonists of the tachykinin

receptor 1 (maropitant) and serotonin receptor 3 (ondansetron) prevented lycorine-mediated emesis, the molecular mechanism of nausea and vomiting remain still unknown.

To study the mechanism of action of the emetic agents, we analyzed the effect of lycorine (direct activation of NK1) and channel opening (activation of 5HT3) on the intracellular calcium homeostasis (using Fluorometric Ca²⁺ analysis) and cell proliferation rates in endogenously NK1 and 5HT3 Receptor expressing cell lines as well as in CHO and HEK cells stably expressing the receptors.

Neither endogenously receptor expressing NK1 or 5HT3 cells nor receptor overexpressing cells showed calciumflux or calcium mobilization after stimulation with lycorine. Furthermore, we are measuring the receptor number and subtypes using radioligand binding studies. It is planned, moreover, to obtain fluorescent labeled constructs of the NK1 receptor to gain insights into the involvement of receptor internalization which might mediate emesis.

By characterizing these molecular principles of the NK1 and 5HT3 receptors, we are attempting to obtain more information in predicting drug-induced side effects such as nausea and emesis.

289

A role for plexins in differentiation of intestinal epithelial cells**I. Matkovic**¹, T. Worzfeld^{1,2}¹Universität Marburg, Pharmakologisches Institut, Marburg, Germany²Max-Planck-Institut für Herz- und Lungenforschung, Pharmakologie, Bad Nauheim, Germany

The intestinal epithelium is completely renewed every 4-5 days. This process is driven by stem cells, which reside within specialized niches in the intestinal crypts and give rise to several differentiated cell types, including enterocytes, Paneth, enteroendocrine, goblet and Tuft cells. However, the molecular mechanisms that establish and maintain differentiated cell numbers and proportions remain largely unknown. Here, we systematically analyzed the intestinal expression of semaphorins and plexins, which constitute a ligand-receptor system that plays central roles in cell-cell communication in various biological contexts. We identified Plexin-B2 and its semaphorin ligands to be highly expressed in intestinal epithelial cells. Genetic inactivation of Plexin-B2 in intestinal organoids strongly reduced the number of enteroendocrine cells. Our data suggest that semaphorin-Plexin-B2 signaling promotes differentiation of intestinal epithelial cells towards the enteroendocrine lineage.

290

Rasa1 controls differentiation of gastric epithelial cells**R. Xu**¹, T. Worzfeld^{2,1}¹Max-Planck-Institut für Herz- und Lungenforschung, Pharmakologie, Bad Nauheim, Germany²Universität Marburg, Pharmakologisches Institut, Marburg, Germany

The gastric epithelium contains several types of differentiated cells, including foveolar cells that produce mucus, parietal cells that secrete gastric acid and intrinsic factor, chief cells that synthesize pepsinogen and gastric lipase, and enteroendocrine cells that release different hormones. These differentiated cell types all originate from multipotent stem cells, yet little is known about how this differentiation process is regulated on a molecular level. The GAP protein Rasa1 controls the activity of small GTPases of the Ras family, and its expression levels have been shown to inversely correlate with progression of stomach cancers. However, functional studies on the physiological role of Rasa1 in the gastric epithelium are lacking. Here, we established and characterized a mouse line with inactivation of the Rasa1 gene. We observed that these mice showed increased numbers of enteroendocrine cells in the gastric mucosa. Conditional inactivation of Rasa1 in enteroendocrine cells, using a mouse line in which Cre expression is driven by the Atoh1 promoter, further corroborated that Rasa1 expression in enteroendocrine cells determines enteroendocrine cell numbers. These findings identify Rasa1 as a regulator of gastric epithelial cell differentiation.

Pharmacology – Cancer pharmacology

291

Fatty acid amide hydrolase inhibitors confer anti-invasive and antimetastatic effects on lung cancer cells**K. Winkler**¹, R. Ramer¹, S. Dithmer¹, I. Ivanov¹, J. Merckord¹, B. Hinz¹¹Institut für Toxikologie und Pharmakologie, Universitätsmedizin Rostock, Rostock, Germany

Inhibition of endocannabinoid degradation has been suggested as tool for activation of endogenous tumor defense. One of these strategies lies in blockade of the enzyme fatty acid amide hydrolase (FAAH) which catalyzes the degradation of endocannabinoids (anandamide [AEA], 2-arachidonoylglycerol [2-AG]) and endocannabinoid-like substances (N-oleylethanolamine [OEA], N-palmitoylethanolamine [PEA]). The present study investigates the impact of two FAAH inhibitors (arachidonoyl serotonin [AA-5HT], URB597) on A549 lung cancer cell metastasis and invasion. LC-MS analyses revealed increased levels of FAAH substrates (AEA, 2-AG, OEA, PEA) in cells incubated with either FAAH inhibitor. In athymic nude mice FAAH inhibitors were shown to elicit a dose-dependent antimetastatic action. In vitro, a concentration-dependent anti-invasive action of either FAAH inhibitor was demonstrated, accompanied with upregulation of tissue inhibitor of matrix metalloproteinases-1 (TIMP-1). Using siRNA approaches, a causal link between the TIMP-1-upregulating and anti-invasive action of FAAH inhibitors was confirmed. Moreover, knockdown of FAAH by siRNA was shown to confer decreased cancer cell invasiveness and increased TIMP-1 expression. Inhibitor experiments point toward a decisive role of CB₂ and transient receptor potential vanilloid 1 in conferring the anti-invasive effects of FAAH inhibitors and FAAH siRNA. Finally, antimetastatic and anti-invasive effects were confirmed for all FAAH substrates. Collectively, the present

study provides first-time proof for a pronounced antimetastatic action of the FAAH inhibitors AA-5HT and URB597. As underlying mechanism of its anti-invasive properties an upregulation of TIMP-1 was identified.

292

Inhibition of FAAH confers increased stem cell migration via PPAR α

R. Ramer¹, Y. Wollank¹, I. Ivanov¹, A. Salamon², K. Peters², B. Hinz¹
¹Institut für Toxikologie und Pharmakologie, Universitätsmedizin Rostock, Rostock, Germany
²Arbeitsbereich Zellbiologie, Universitätsmedizin Rostock, Rostock, Germany

Regenerative activity in tissues of mesenchymal origin depends on the migratory potential of mesenchymal stem cells (MSCs). The present study focused on inhibitors of the enzyme fatty acid amide hydrolase (FAAH), which catalyzes the degradation of endocannabinoids (anandamide, 2-arachidonoylglycerol) and endocannabinoid-like substances (N-oleylethanolamine, N-palmitoylethanolamine). In Boyden chamber assays, the FAAH inhibitors, URB597 and arachidonoyl serotonin (AA-5HT), were found to increase the migration of human adipose-derived MSCs. LC-MS analyses revealed increased levels of all four aforementioned FAAH substrates in MSCs incubated with either FAAH inhibitor. Following addition to MSCs, all FAAH substrates mimicked the promigratory action of FAAH inhibitors. Promigratory effects of FAAH inhibitors and substrates were causally linked to activation of p42/44 mitogen-activated protein kinase (MAPK), as well as to cytosol-to-nucleus translocation of the transcription factor, peroxisome proliferator-activated receptor α (PPAR α). Whereas PPAR α activation by FAAH inhibitors and substrates became reversed upon inhibition of p42/44 MAPK activation, a blockade of PPAR α left p42/44 MAPK phosphorylation unaltered. Collectively, these data demonstrate FAAH inhibitors and substrates to cause p42/44 MAPK phosphorylation, which subsequently activates PPAR α to confer increased migration of MSCs. This novel pathway may be involved in regenerative effects of endocannabinoids whose degradation could be a target of pharmacological intervention by FAAH inhibitors.

293

Imatinib & ABCG2 – Impact of microRNA-212-regulation on drug-sensitivity and cell survival

M. Kähler¹, H. Bruckmüller¹, K. Kosicka², E. Turrini¹, O. Bruhn¹, I. Cascorbi¹
¹Institute of Experimental and Clinical Pharmacology, University Hospital Schleswig-Holstein, Kiel, Germany
²Department of Physical Pharmacy and Pharmacokinetics, Poznan University of Medical Sciences, Poznan, Polen

Background: The hematopoietic disorder chronic myeloid leukemia (CML) is one of the most extensively studied neoplasms. It is caused by translocation between chromosomes 9 and 22 leading to the formation of the Philadelphia chromosome and the BCR-ABL fusion gene. First-line targeted therapy is still the tyrosine-kinase inhibitor imatinib (IM), which led to tremendous success in treatment. However, the amount of therapeutic resistances is increasing, caused either by BCR-ABL-dependent mechanisms (e.g. BCR-ABL amplification/overexpression, point mutations) or BCR-ABL-independent mechanisms. These might be linked to alterations in drug transporter expression or particularly, microRNA-expression levels. In our previous study, we analyzed the changes of microRNA expression profiles during the development of IM-resistances in the leukemic cell line K562. An inverse correlation of miR-212 expression and protein levels of the efflux transporter ATP-binding cassette transporter G2 (ABCG2) was observed in cells resistant to different IM-concentrations, pointing to a relation of miR-212 to IM-resistance. Hence, we investigate in current studies, how the influence of miR-212 on IM-sensitivity could be explained.

Methods: We transfected K562 cells, sensitive treatment-naïve cells and cells resistant to various IM-concentrations, either with miR-mimic pre-miR-212 or inhibitory anti-miR-212, challenged them with IM and analyzed effects on cell viability, activation of apoptosis and cell death using WST-1-, Caspase Glo 9-assay and cell counting. In addition, we analyzed changes in ABCG2 expression using flow cytometry and qRT-PCR and investigated alterations in IM-efflux using HPLC and Hoechst efflux assay.

Results: Under IM-treatment, sensitive K562 showed an effect of miR-212-inhibition using anti-miR-212. This led to a significant promotion of cell survival apparent on the level of respiratory chain function ($p < 0.01$) and cell membrane integrity and reduced caspase-9 activity ($p < 0.05$). Furthermore, these miRNA-effects are dose-dependent as confirmed in concentration row-experiments. Regarding transport and ABCG2 expression, we found that 2 μ M IM-resistant K562 do not express higher amounts of ABCG2, but showed higher transport rates of IM or the ABCG2-substrate Hoechst 33342.

Conclusions: Overall, these experiments indicate that miR-212 does not only affect ABCG2-expression, but also influences cell sensitivity to IM in a more direct manner. Further analysis will now be performed to reveal the underlying mechanism, how cell sensitivity to IM is altered and if these effects occur due to a direct regulation of ABCG2. In summary, these findings could be relevant in CML-therapy, overcoming IM-resistances with a better understanding of miRNA- and drug transporter alteration in CML.

Acknowledgments: We would like to thank all the authors for their contribution to this project. This work was funded by the University Hospital Schleswig-Holstein.

294

Oxidized silicon nanoparticles and iron oxide nanoparticles for radiation therapy

S. Klein¹, M. Kizaloglu¹, M. L. Dell'Aciprete², W. Neuhuber³, L. V. R. Distel⁴, M. C. Gonzales², C. Krysch¹
¹Institut für Physikalische Chemie I, Universität Erlangen-Nürnberg, Erlangen, Germany
²Universidad Nacional de La Plata, Facultad de Ciencias Exactas, La Plata, Argentina
³Universität Erlangen-Nürnberg, Lehrstuhl für Anatomie I, Erlangen, Germany
⁴Strahlenklinik, Strahlenbiologie, Erlangen, Germany

Radiation therapy often combined with surgery and/or chemotherapy is applied to more than 50 % of patients at some point of their treatment. The cytotoxic effects of ionizing radiation occur from their ability to produce DNA double-strand breaks through the formation of free radicals within cells. However, the curative potential of radiotherapy is often limited by intrinsic radio resistance of cancer cells and normal tissue toxicity. To overcome this resistance and enhance the effectiveness of ionizing radiation, radio sensitizers are used in combination with radiotherapy. In our studies we used amino functionalized, oxidized silicon nanoparticles (SiNP), superparamagnetic iron oxide nanoparticles (SPION) and iron doped silicon nanoparticles (Fe(1%)-SiNP) to increase the formation of reactive oxygen species (ROS) in cells.

Cancer and tissue cells loaded with the various nanoparticles were irradiated with a single dose of 1-3 Gy using a 120 kV X-Ray tube. After irradiation, the formation of the different ROS species including superoxide, hydroxyl radicals and singlet oxygen was investigated.

SiNPs with sizes around 1 nm can easily cross the cell and nuclear membrane. The positively charged amino functionalized SiNPs stick in all membranes as well in those of the mitochondria. Irradiation of the mitochondria may cause the depolarization of the mitochondrial membrane, which enables the release of cytochrome c and simultaneously, an inhibition of the respiratory chain, which leads to an increased generation of superoxide. Amino functionalized SiNPs, as being embedded in the outer mitochondrial membrane, evidently enhance the depolarizing effect of the X-ray radiation on the mitochondria and therefore increase the concentration of superoxide.^[1] Oxidized SiNPs with larger sizes accumulate in the cytoplasm and generate mainly singlet oxygen after irradiation.

SPIONs enter the cells via endocytosis, whereas the uncoated SPIONs remain in the vesicles and the citrate coated SPIONs accumulate in the cytoplasm. Cells loaded with citrate coated SPIONs show no higher ROS concentration than in media-cultured cells. But after irradiation, the ROS formation increased drastically. This enhancing effect is explained with the impact of X-rays onto the surface of SPIONs which is due to the destruction of surface structures. The freed SPION surface contains easier accessible iron ions. This ions can participate in the Fenton and Haber-Weiss chemistry and thus, catalyze the hydroxyl radical formation.^[2]

1 to 5 % iron doped SiNP increase the formation of hydroxyl radicals as well as the generation of singlet oxygen after irradiation.

References :

- [1] S. Klein, M. L. Dell'Aciprete, M. Wegmann, L. V. R. Distel, W. Neuhuber, M. C. Gonzalez, C. Krysch, *Biochem. Biophys. Res. Commun.*, 434, 2 (2013) page 217- page 222.
- [2] S. Klein, A. Sommer, L. V. R. Distel, W. Neuhuber, C. Krysch, *Biochem. Biophys. Res. Commun.*, 425, 2 (2012) page 393- page 397.

295

The H₂S-producing enzyme CSE is dispensable for chronic pain signaling

K. M. J. Syhr¹, M. Boosen², S. W. Hohmann¹, S. Longen², Y. Köhler², J. Pfeilschifter², K.-F. Beck², G. Geisslinger^{1,3}, A. Schmidt^{4,5}, **W. Kallenborn-Gerhardt**^{4,1}
¹Institut für Klinische Pharmakologie, Goethe Universität, Frankfurt, Germany
²Institut für Pharmakologie und Toxikologie, Goethe Universität, Frankfurt, Germany
³Fraunhofer Institut für Molekularbiologie und angewandte Ökologie, Projektgruppe Translationale Medizin und Pharmakologie Fraunhofer, Frankfurt, Germany
⁴Pharmakologisches Institut für Naturwissenschaftler, Goethe Universität, Frankfurt, Germany
⁵Institut für Pharmakologie und Toxikologie, Universität Witten/Herdecke, Witten, Germany

Chronic pain in response to tissue damage (inflammatory pain) or nerve injury (neuropathic pain) is a major clinical health problem, affecting up to 30% of adults worldwide. Currently available treatments are only partially susceptible and are accompanied with therapy limiting side effects. Thus it is important to elucidate molecular mechanisms of pain signaling in detail to obtain new insights in potential future therapies. Recent data indicate that hydrogen sulfide (H₂S) contributes to the processing of chronic pain, however pro- as well as antinociceptive effects have been described so far. Moreover the sources of H₂S production in the nociceptive system are only poorly understood. Here we investigated the expression of the H₂S releasing enzyme cystathionine γ -lyase (CSE) in the nociceptive system and characterized its role in chronic pain signaling using CSE deficient mice. Paw inflammation and peripheral nerve injury led to upregulation of CSE expression in dorsal root ganglia. However, conditional knockout mice lacking CSE in sensory neurons as well as global CSE knockout mice demonstrated normal pain behaviors in inflammatory and neuropathic pain models as compared to WT littermates. Thus, our results suggest that CSE is not critically involved in chronic pain signaling in mice and that sources different from CSE mediate the pain relevant effects of H₂S.

Acknowledgements: This work was supported by the Deutsche Forschungsgemeinschaft (SFB815-A14) and in part by LOEWE-Schwerpunkt "Anwendungsorientierte Arzneimittelforschung".

296

Investigations on the potential anticarcinogenic effects of resveratrol imine analogues

S. Wang¹, M. Krohn², T. Hecker², S. Meckelman², I. Willenberg¹, C. Li³, Y. Pan³, N. H. Schebb^{1,2}, P. Steinberg¹, **M. T. Empl**¹
¹University of Veterinary Medicine Hannover, Institute for Food Toxicology and Analytical Chemistry, Hannover, Germany, Germany
²University of Wuppertal, Institute of Food Chemistry, Wuppertal, Germany, Germany
³Zhejiang University, Department of Chemistry, Hangzhou, China, China

Abstract content cannot be disclosed at this time.

297

Molecular mechanisms of acquired cisplatin resistance in urothelial carcinoma cellsA. Höhn¹, K. Krüger¹, M. Skowron², G. Fritz¹¹Heinrich-Heine-Universität, Institut für Toxikologie, Düsseldorf, Germany²Heinrich-Heine-Universität, Urologie, Düsseldorf, Germany

Background: Cisplatin (CisPt) is frequently used in the therapy of advanced stage urothelial cell carcinoma (UCC). Yet, inherent and acquired drug resistance limits the clinical use of CisPt. Here, we comparatively investigated the response of epithelial-like (RT-112) and mesenchymal-like (J-82) UC cells following CisPt treatment.

Methods: Upon selection with equitoxic doses of CisPt for months, we obtained CisPt resistant variants (RT-112^R, J-82^R). Cell viability was measured using the Alamar Blue Assay. Cell cycle distribution was analysed by flow cytometry. Immunocytochemistry was used to quantify the number of nuclear γH2AX and 53BP1 foci representing DNA double strand breaks (DSBs), while Western blot was used to unravel the role of DNA Damage Response (DDR) to acquired CisPt resistance. qRT-PCR was performed to analyse the mRNA expression of genes associated with CisPt resistance. J-82 and J-82^R cells were treated with different concentrations of lovastatin and selected DDR inhibitors to elucidate their influence on cell viability.

Results: Untreated RT-112 cells showed an about 2-3-fold higher resistance to CisPt than J-82 cells. Both cell lines differed in the expression pattern of genes that are associated with CisPt resistance. RT-112^R and J-82^R revealed a 2-3-fold increased CisPt resistance as compared to the parental cells. During the selection procedure, we observed that acquired CisPt resistance goes along with morphological alterations that resemble epithelial mesenchymal transition (EMT). Cell cycle analysis of RT-112^R cells disclosed a reduced apoptosis and enhanced G2/M arrest following CisPt exposure as compared to RT-112 wild-type cells. By contrast, induction of cell death was similar in J-82 and J-82^R cells. Notably, J-82^R cells showed a reduced formation of CisPt-induced DSBs. Correspondingly, the related DDR was diminished in J-82^R as compared to their parental cells. This was not found when DDR was comparatively analysed between RT-112^R and RT-112 cells. Data obtained from qRT-PCR analysis indicate that different mechanisms contribute to acquired drug resistance of J-82^R and RT-112^R. Unexpectedly, J-82^R and RT-112^R shared the upregulation of XAF-1. Treatment of J-82^R cells with statins and protein kinase inhibitors revealed an enhanced sensitivity to pharmacological inhibition of Chk-1 and, moreover, re-sensitization to CisPt by Chk-1 inhibitor.

Conclusion: Based on the data we suggest that mechanisms of acquired CisPt resistance of epithelial and mesenchymal UC cell lines are different with apoptosis-related mechanisms appear to be more relevant for epithelial-like RT-112 cells and DDR-related mechanisms dominating CisPt susceptibility in mesenchymal-like J-82 cells. Furthermore, our findings indicate that Chk-1 might be an appropriate target to deal with acquired CisPt resistance in UCC.

298

Heregulin-promoted survival of gastric cancer cells after c-met inhibition depends on PKC- and SATB1-dependent upregulation of HER3R. Jenke^{1,2}, M. Rein^{1,2}, F. Lordick², A. Aigner¹, T. Buech¹¹Rudolf-Boehm-Institut f. Pharmakologie u. Toxikologie, Klinische Pharmakologie, Leipzig, Germany²Universitäres Krebszentrum Leipzig (UCCL), Universitätsklinikum, Leipzig, Germany

In many patients, gastric cancer treatment with conventional cytostatic agents shows only limited clinical response. Novel therapeutics, which inhibit RTK signaling by targeting c-met or HER family receptors, have demonstrated some efficacy; however, primary resistance of gastric cancer cells against these inhibitors is still a major problem. In the present study we investigated the mechanism of heregulin (HRG)-promoted survival of gastric cancer cells after treatment with c-met inhibitors or siRNA-mediated downregulation of c-met. We found that HRG treatment of gastric cancer cells with a c-met amplification partially rescued the cells from the antiproliferative effects of pharmacological c-met inhibition or siRNA-mediated downregulation of c-met. Moreover, c-met inhibition or downregulation led to an induction of HER3 expression on mRNA and protein level, whereas other HER family receptors were unaffected. Downregulation of HER3 impaired the HRG-mediated rescue of cell survival upon c-met inhibition. In other tumor entities the chromatin organizer special AT-rich sequence-binding protein 1 (SATB1) has been described as a regulator of HER family receptor expression involved in adaptive responses of tumor cells. Thus, we investigated the contribution of SATB1 in the upregulation of HER3 after c-met inhibition. Of note, c-met inhibitors as well as c-met-specific siRNAs markedly induced SATB1 expression in gastric cancer cells, and the downregulation of SATB1 by siRNAs completely prevented the induction of HER3 upon c-met inhibition. In contrast, HER1 or HER2 expression levels were not affected by SATB1-specific siRNAs. The function of SATB1 as transcriptional regulator is controlled by its phosphorylation status, which in turn is modulated by PKC activity. Thus, we also tested the effect of PKC inhibitors on HER3 expression after c-met inhibition. Interestingly, the upregulation of HER3 in gastric cancer cells was significantly reduced by PKC inhibitors. To summarize, SATB1 and PKC are critically involved in the regulation of HER3 expression in gastric cancer cells after treatment with c-met inhibitors and the oncogene HER3 plays a crucial role for tumor cell survival in this context. Thus, inhibition of PKC or SATB1 may help to overcome resistance against c-met inhibition in this tumor entity.

300

Breast cancer xenograft models for the evaluation of multifunctional nanomaterialsS. Hafner¹, Y. Wu^{1,2}, T. Weil², V. Rasche³, T. Syrovets^{1,3}, T. Simmet¹¹Institute of Pharmacology of Natural Products & Clinical Pharmacology, Ulm, Germany²Department of Organic Chemistry III/Macromolecular Chemistry, Ulm, Germany³Experimental Cardiovascular Imaging, Ulm, Germany

In the rising field of nanomedicine, development of new approaches in diagnosis and treatment of cancer is a challenging task. Typically, a nanocarrier is synthesized and linked to functional compounds displaying either diagnostic or therapeutic effects in cancer models. Recently, nanomaterials combining both diagnostic and therapeutic properties, so-called 'theranostics', became of primary interest. Here we used a human albumin-polyethylene glycol (PEG) copolymer (HSA) as a theranostic platform for molecular integration of the chemotherapeutic drug doxorubicin (Dox) and the magnet resonance imaging (MRI) contrast agent gadolinium (Gd) yielding Gd-HSA-Dox nanoparticles. Besides *in vitro* testing, which demonstrated cytotoxic efficacy of Gd-HSA-Dox, we used the chorioallantoic membrane (CAM) of fertilized chick eggs as a preclinical xenotransplantation model. The CAM assay, which in legal terms does not represent an animal experiment, allows testing of compounds in an *in vivo* setting. This model is particularly helpful to narrow the gap between *in vitro* and *in vivo* applications in rodents, because it can help to reduce number of elaborate experiments with typically nude mice, and it reduces or even avoids exposure of those animals to adverse effects and distress. Treatment-resistant MDA-MB-231 breast cancer cells stably transfected with luciferase were xenotransplanted onto the chorioallantoic membrane. After formation of solid breast cancer xenografts, Gd-HSA-Dox was injected intravenously and its antiproliferative effect was evaluated by IVIS imaging of luciferase activity and by immunohistochemical analysis of the tumor xenografts for the Ki-67 proliferation antigen. In comparison to conventional Dox, Gd-HSA-Dox showed increased antiproliferative efficacy and reduced general toxicity in the CAM assay. On the basis of these findings, a rodent model was established, where the MDA-MB-231 breast cancer cells were orthotopically xenotransplanted into the mammary fat pads of female NMRI nu/nu mice. In this model, we further investigated biocompatibility, as well as diagnostic and therapeutic properties of the engineered nanomaterial. After repeated administration of Gd-HSA-Dox into the tail vein of the animals, biocompatibility of Gd-HSA-Dox was confirmed by uncompromised liver, kidney and hematopoietic parameters. To warrant diagnostic properties, accumulation of the nanomaterial in tumor tissue is indispensable. By small animal MRI of Gd, kinetics of intravenously applied Gd-HSA-Dox in tumor tissue was monitored. An enhancement of the engineered nanomaterial in tumor tissue was detected for up to 47 h after injection indicating successful enrichment of Gd-HSA-Dox within the tumor tissue, which can be ascribed to the enhanced permeability and retention (EPR) effect observed in the microenvironment of many solid tumor tissues. We are currently investigating the antitumor efficacy of Gd-HSA-Dox in this mouse model and preliminary data seem to indicate a dose-dependent anticancer effect. Supported by the VolkswagenStiftung.

301

The anti-metastatic properties of the tubulin-binding agent pretubulysin could be based on the trapping of tumor cells to the endotheliumR. Schwenk¹, T. Stehning¹, I. Bischoff¹, A. Ullrich², U. Kazmaier², R. Fürst¹¹Goethe-Universität Frankfurt, Institut für Pharmazeutische Biologie, Frankfurt am Main, Germany²Saarland University, Institute of Organic Chemistry, Saarbrücken, Germany

Tubulin-binding agents are the most important anti-tumoral drugs. Due to the side effects and the development of resistances, the discovery of new agents is still of importance. Recently, pretubulysin (PT), a naturally occurring precursor of the myxobacterial compound tubulysin, was identified as a novel tubulin-binding compound. In the DFG research group FOR 1406, PT was characterized as anti-tumoral, anti-angiogenic and vascular-disrupting compound. Moreover, PT was also found to inhibit the formation of metastases *in vivo*. Aim of the present study was to gain first insights into the mechanisms underlying this anti-metastatic effect by investigating the influence of PT on the interaction of endothelial and tumor cells *in vitro*.

PT treatment of primary human endothelial cells (HUVECs) strongly increased the adhesion of breast cancer cells (MDA-MB-231) on HUVECs, but limited their transmigration through the endothelium (Transwell assay). Based on this data, the gene expression of presumably involved adhesion molecules was determined by qRT-PCR: ICAM-1, VCAM-1, E-selectin, N-cadherin, and galectin-3. Moreover, the chemokine system CXCL12/CXCR4 was analyzed. It could be demonstrated that the mRNA level of endothelial N-cadherin is upregulated by PT. While total protein expression of N-cadherin was enhanced in PT treated HUVEC, its surface expression was not largely influenced by PT (Western blot, flow cytometry). In line with this, blocking endothelial N-cadherin by a neutralizing antibody revealed that this protein is not involved in PT-evoked tumor cell adhesion. Interestingly, PT strongly augmented the mRNA and protein expression of CXCL12 in HUVECs (qRT-PCR, Western blot), whereas its endothelial secretion was not affected by PT (ELISA). An autocrine action of CXCL12 could be excluded, since blocking the CXCL12 receptor CXCR4 on endothelial cells with plerixafor did not influence cancer cell adhesion. By microscopic analyses, we observed that PT treatment causes transient gaps in the HUVEC monolayer, where tumor cells prefer to adhere. Since β1-integrins on the tumor cells could mediate interactions between cancer cells and extracellular matrix proteins in the gaps (e.g. collagen), their influence in cell adhesion and transmigration assays was examined. Both the PT-evoked increase in cell adhesion and decrease in transmigration was completely abolished when β1-integrins were blocked on MDAs by a neutralizing antibody.

These results indicate that the anti-metastatic action of pretubulysin might be based on the trapping of tumor cells on the endothelium. Whether this effect is also relevant *in vivo*, will be analyzed in future studies using intravital microscopy. This work was supported by the German Research Foundation (DFG, FOR 1406, FU 691/9-2).

302

High-pulsed doses of erlotinib for the treatment of non-small-cell lung cancer: A modeling analysisA. A. Suleiman¹, J. Schöttle^{2,3,4}, U. Jaehde⁵, R. Ullrich^{2,3}, U. Fuhr¹¹University of Cologne, Department of Pharmacology, Cologne, Germany²University of Cologne, Department I of Internal Medicine, Center of Integrated Oncology Köln-Bonn, and Center of Molecular Medicine Cologne (ZMMK), Cologne, Germany³Klaus-Joachim-Zülich Laboratories of the Max Planck Society and the Medical Faculty of the University of Cologne, Max-Planck-Institute for Metabolic Research, Cologne,

Germany

¹University of Cologne, Department of Translational Genomics, Cologne, Germany²University of Bonn, Institute of Pharmacy, Clinical Pharmacy Department, Bonn, Germany

Introduction: Tyrosine kinase inhibitors (TKIs) for the treatment of non-small cell lung cancer (NSCLC) patients harboring activating mutations in the epidermal growth factor receptor have shown prominent success. Nevertheless, patients treated with TKIs eventually acquire resistance and relapse (1). Based on an evolutionary cancer model (2), weekly high dose-pulsed TKI regimens were proposed to delay resistance. Using data from NSCLC bearing mice treated with erlotinib at different dosing regimens, we developed a semi-mechanistic pharmacokinetic/pharmacodynamic model for erlotinib effects on tumor killing and resistance development.

Methods: Data was available from experiments in xenograft mice bearing NSCLC tumors (PC9 and HCC827 cell lines; both erlotinib sensitive) (3). Plasma concentrations from two single-dose groups, 30mg/kg and 200mg/kg, were used for pharmacokinetic modeling. Relative tumor volume changes in mice randomized to five dosing regimens (15mg/kg daily, 30mg/kg daily, 200mg/kg every 2 days, 200mg/kg every 4 days, or vehicle) was the pharmacodynamic endpoint. A tumor growth inhibition model was developed by testing linear, exponential and logistic models to account for the tumor growth kinetics, as well as fitting an Emax model to explain the effect of exposure on killing the sensitive tumor cells, and resistance development. Analysis was performed using NONMEM 7.3.

Results: Absorption was dose dependent, and a precipitate compartment accounted for dissolution limited absorption for the 200mg/kg dose. A 1-compartment model with first order elimination kinetics described distribution and elimination. To describe tumor volume changes, a tumor was assumed to be a mixture of sensitive and resistant cells (represented by distinct compartments and ordinary differential equations). Exponential kinetics best described natural growth (doubling times: 13 and 52 days, for sensitive and fully resistant cells, respectively). A tumor was found to transit through a less sensitive phase before acquiring full resistance. An E_{max} model (less than linear) best described effect on the sensitive cells (EC₅₀=0.53μM for both cell lines), and on the partially sensitive transit phase (EC₅₀=1.24μM and 3.00μM, for HCC827 and PC9 cell lines, respectively), urging to provide adequate trough erlotinib concentrations for optimal effects.

Conclusions & future perspectives: An exposure-driven tumor growth inhibition model accounting for the kinetics of resistance development was developed. The model emphasizes the need for establishing an adequate trough erlotinib concentrations to delay disease progression.

References:

- Engelman J and Jänne P. *Mechanisms of acquired resistance to epidermal growth factor receptor tyrosine kinase inhibitors in non-small cell lung cancer*. Clin Cancer Res. 2008;14:2895-9.
- Chmielecki J, et al. *Optimization of dosing for EGFR-mutant non-small cell lung cancer with evolutionary cancer modeling*. Sci Transl Med. 2011;3(90):90ra59.
- Schöttle J, et al. *Intermittent high-dose treatment with erlotinib enhances therapeutic efficacy in EGFR-mutant lung cancer*. Oncotarget. 2015 Nov 2. doi: 10.18632/oncotarget.6276. [Epub ahead of print]

Pharmacology – Drug discovery

303

Mechanisms underlying the anti-nociceptive properties of the standardised methanol extract of *Ficus platyphylla* stem bark

A. Becker¹, B. Chindo¹, H. Schröder², O. Werz³, A. Koerberle³
¹Kaduna State University, Department of Pharmacology and Toxicology, Faculty of Pharmaceutical Sciences, Kaduna, Nigeria
²Otto-von-Guericke University, Institute of Pharmacology and Toxicology, Magdeburg, Germany
³Friedrich-Schiller-University Jena, Chair of Pharmaceutical/Medical Chemistry, Institute of Pharmacy, Jena, Germany

Extracts of the stem bark of *Ficus platyphylla* (FP) have been used in traditional Nigerian medicine to treat psychoses, depression, epilepsy, pain and inflammation. Previous studies have revealed the analgesic and anti-inflammatory effects of FP in different assays including acetic acid-induced writhing, formalin-induced nociception, and albumin-induced oedema.

In this study, we assessed the effects of the standardised extract of FP on hot plate nociceptive threshold and vocalisation threshold in response to electrical stimulation of the tail root in order to confirm its acclaimed analgesic properties. We also investigated the molecular mechanisms underlying these effects, with the focus on opiate receptor binding and the key enzymes of eicosanoid biosynthesis, namely cyclooxygenase (COX) and 5-lipoxygenase (5-LO).

FP (i) increased the hot plate nociceptive threshold and vocalisation threshold. The increase in hot plate nociceptive threshold was detectable over a period of 30 min whereas the increase in vocalisation threshold persisted over a period of 90 min. (ii) FP showed an affinity for μ opiate receptors but not for δ or κ opiate receptors, and (iii) FP inhibited the activities of COX-2 and 5-LO but not of COX-1.

We provided evidence supporting the use of FP in Nigerian folk medicine for the treatment of different types of pain, and identified opioid and non-opioid targets. It is interesting to note that the dual inhibition of COX-2 and 5-LO appears favourable in terms of both efficacy and side effect profile.

Figure 1: Analgesic index measured by electrical stimulation of the tail root (STR) and thermal pain threshold (TPT) 30 min (A) and 60 min (B) after application of either saline (sal), *Ficus platyphylla* extract (FP), or morphine (MO)

Figure 2: Inhibition of 5-lipoxygenase by the *Ficus platyphylla* (FP) extract.

Abb. 1

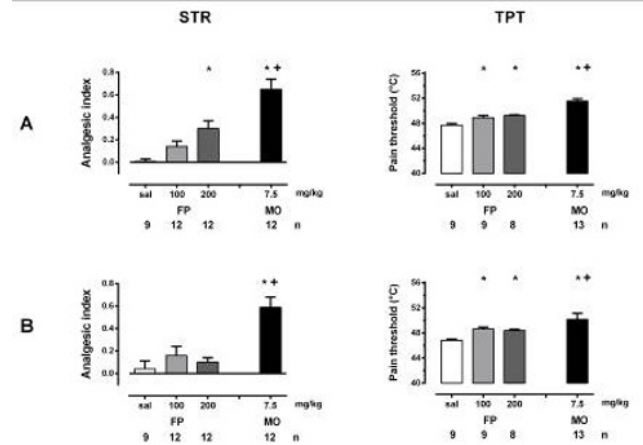
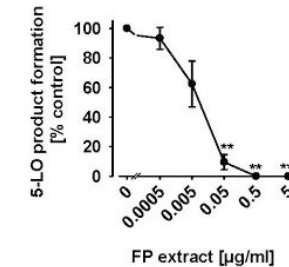


Abb. 2



304

Screening for a small molecule inhibitor targeting the biogenesis of outer membrane virulence factors in gram-negative Enterobacteriaceae

J. M. Schweers¹, M. Buhl¹, U. Bilitewski¹, I. B. Autenrieth¹, M. Schütz¹
¹Institute for med. Microbiology, Tübingen, Germany

Despite the fact, that the enormous economic burden and individual suffering caused by gastrointestinal infections permanently persists in developing and newly industrialized countries, healthcare systems in First world countries underestimated its significance for a long time. The alarming prevalence of multidrug-resistant gram-negative bacteria, combined with a high epidemic potential of gastrointestinal pathogens, however, demonstrates the urgent need for new antibiotics and anti-infectives worldwide. 2.5 million deaths per year were actually caused by acute diarrheal infections. The most common causative agents of acute diarrheal infections, amongst others, are *Yersinia enterocolitica*, *Campylobacter jejuni*, *Salmonella* spp., *Shigella* spp., *Escherichia coli*, *Vibrio cholerae*, and *Clostridium difficile*. The established treatment based on antibiotics is mostly ineffective or may even have adverse side effects and result in prolonged shedding. In either way, antibiotic treatment also eradicates at least parts of the intestinal microbiome, and thereby disrupts colonization resistance, fosters overgrowth of pathogens and prolongs shedding times. Therefore, the development of future drugs should be focused on highly specific anti-infectives, which enable a direct pathogen-specific treatment. One very promising strategy is the inhibition of the biogenesis of outer membrane virulence factors. Due to the fact that many decisive virulence-associated outer membrane proteins (OMPs) of gram-negative enteropathogens are substrates of the periplasmic chaperone SurA exclusively, we developed a new assay format to determine SurA *in vitro* chaperone activity. Previous publications by Behrens *et al.*, 2001 and Buchner *et al.*, 1998 documented an assay to determine SurA *in vitro* chaperone activity with extremely limited sensitivity and minimal detectable concentration, which was not suitable for high throughput screening (HTS). We now developed a luciferase-based screening assay. This highly sensitive and robust test system has been validated extensively and now gives reliable output with an appreciable z-factor of > 0.6. In cooperation with the HZI Braunschweig (Germany) and the HZI Saarbrücken (Germany), we were able to screen over 7000 purified compounds and over 500 extracts of myxobacteria. During the ongoing screening period, the assay generated four validated primary actives, which corresponds to a positive hit rate of 0,05 %. Additionally, we developed an elaborate *follow-up* strategy to validate positive hits, which includes a well-established mouse infection model. We are looking forward to escalate our screening efforts and would like to use this abstract to invite all scientist who are interested in testing compound/natural extract libraries for an activity against the target structure SurA.

305

The potential atypical antipsychotic and dopamine D₂ receptor partial agonist 2-bromoterguride antagonizes phencyclidine- and apomorphine-induced prepulse inhibition and novel object recognition deficits in ratsE. Tarland¹, H. H. Pertz², H. Fink¹, J. Brosda¹¹Freie Universität Berlin, Fachbereich Veterinärmedizin, Institut für Pharmakologie und Toxikologie, Berlin, Germany²Freie Universität Berlin, Institut für Pharmazie, Fachbereich Biologie, Chemie, Pharmazie, Berlin, Germany

Objectives: Schizophrenia is a disabling mental disorder affecting more than 21 million people worldwide. Available medical therapies are effective in the treatment of psychosis and other positive symptoms, however come with considerable side effects and often fail to ameliorate cognitive deficits and negative symptoms of the disorder. The dopamine D₂ receptor partial agonist 2-bromoterguride (2-BT) has recently been shown to exhibit antipsychotic effects in rats without causing adverse side effects common to antipsychotic drugs [1]. To determine its atypical character in vivo, the ability of 2-BT to antagonize the disruptive effects of phencyclidine (PCP) and apomorphine on sensory motor gating was determined in the prepulse inhibition paradigm. The effect of 2-BT on cognitive deficits was assessed in the Novel Object Recognition (NOR) test after object recognition memory deficits were induced by PCP treatment.

Method: 10 week old male Sprague-Dawley rats were injected with 2-BT (0.1 or 0.3mg/kg; i.p.) followed by PCP (1.5mg/kg; s.c.) or apomorphine (0.5mg/kg; s.c.). Prepulse inhibition was measured in two sound-proof startle chambers. The attenuating effect of 2-BT (0.1 or 0.3mg/kg; i.p.) on visual learning and memory deficits following subchronic administration of PCP (5.0mg/kg; i.p. twice daily for 7 days) was assessed in the NOR task consisting of a 3min acquisition trial and a 3min retention trial separated by a 1h inter-trial interval. Clozapine (5.0mg/kg; i.p) or haloperidol (0.1mg/kg; i.p) were used as positive controls.

Results: The dopamine D₂ receptor partial agonist 2-BT (0.3mg/kg) and the typical antipsychotic haloperidol successfully antagonized apomorphine-induced PPI-deficits. Interestingly 2-BT also ameliorated the PCP-induced PPI-deficits to the same extent as the atypical antipsychotic clozapine. Preliminary data from the NOR test indicate that 2-BT reduces subchronic PCP-induced cognitive deficits in novel object recognition analogous to clozapine.

Conclusions: The disrupting effects of PCP on PPI are mediated by non-competitive antagonism at NMDA sites indirectly influencing a series of neurotransmitter systems. Our results indicate that 2-BT mediates actions at multiple neurotransmitter receptors as it successfully ameliorated both the PCP- and apomorphine-induced PPI disruptions in rats, showing an atypical antipsychotic character. Furthermore, our preliminary results support the potential atypical antipsychotic effect of 2-BT as it restored performance in the NOR test, a test with good predictive validity. Due to the previously shown properties and antipsychotic-like effects of 2-bromoterguride [1], this substance may be a promising candidate for treatment of schizophrenic patients. Ongoing experiments investigate the potency of 2-BT to improve social deficits following a sub-chronic PCP regime in rats.

References: [1] F. Jantschak, J. Brosda, R. T. Franke, H. Fink, D. Möller, H. Hübner, P. Gmeiner, H. H. Pertz (2013). Pharmacological profile of 2-bromoterguride at human dopamine D₂, porcine serotonin 5-hydroxytryptamine 2A, and α 2C-adrenergic receptors, and its antipsychotic-like effects in rats. *J Pharmacol Exp Ther.* 347:57-68.

306

Pro-inflammatory obesity in aged cannabinoid-2 receptor deficient miceK. Schmitz¹, N. Mangels², A. Häußler¹, N. Ferreirós¹, I. Fleming², I. Tegeđer¹¹Universitätsklinikum, Klinische Pharmakologie, Frankfurt, Germany²Universitätsklinikum, Vascular Signaling, Frankfurt, Germany

Background and Objectives: Cannabinoid-1 receptor signaling increases the rewarding effects of food intake and promotes the growth of adipocytes, whereas CB2 possibly opposes these pro-obesity effects by silencing the activated immune cells that are key drivers of the metabolic syndrome. Pro- and anti-orexigenic cannabinimetic signaling may become unbalanced with age because of alterations of the immune and endocannabinoid system.

Methods: To specifically address the role of CB2 for age-associated obesity we analyzed metabolic, cardiovascular, immune and neuronal functions in 1.2-1.8 year old CB2^{-/-} and control mice, fed with a standard diet and assessed effects of the CB2 agonist, HU308 during high fat diet in 12-16 week old mice.

Results: The CB2^{-/-} mice were obese with hypertrophy of visceral fat, immune cell polarization towards pro-inflammatory sub-populations in fat and liver and hypertension, as well as increased mortality despite normal blood glucose. They also developed stronger paw inflammation and a premature loss of transient receptor potential responsiveness in primary sensory neurons, a phenomenon typical for small fiber disease. The CB2 agonist HU308 prevented HFD-evoked hypertension, reduced HFD-evoked polarization of adipose tissue macrophages towards the M1-like pro-inflammatory type and reduced HFD-evoked nociceptive hypersensitivity but had no effect on weight gain.

Conclusion: CB2 agonists may fortify CB2-mediated anti-obesity signaling without the risk of anti-CB1 mediated depression that caused the failure of rimonabant.

307

The interference of resveratrol and xanthohumol in the function of leishmanial and mammalian mitochondriaL. Gille¹, A. Lackova¹, K. Staniek¹, S. Steinbauer¹, W. Jäger², L. Monzote³¹University of Veterinary Medicine, Inst. of Pharmacology and Toxicology, Vienna, Austria²University of Vienna, Division of Clinical Pharmacy and Diagnostics, Vienna, Austria³Institute of Tropical Medicine "Pedro Kouri", Parasitology Department, Havana, Cuba

Leishmaniasis is a neglected tropical disease caused by *Leishmania*, eukaryotic protozoal organisms, which infect humans and other mammals. This disease is

transmitted by sandflies of the genus *Phlebotomus*. Due to global warming the endemic region of these vectors expands further to northwards and threatens South European countries as well. The treatment of Leishmaniasis is difficult due to toxicity and resistance development for current drugs. The so far unexplored inhibition of mitochondrial functions in *Leishmania* by natural products or even food ingredients seems to be an interesting alternative. Two food ingredients, resveratrol (Res) and xanthohumol (Xan), were widely studied in mammalian cells but little is known about their actions on protozoal parasites. Therefore, we compared the influence of Res and Xan on the function of leishmanial and mammalian mitochondria. Anti-leishmanial activities of xenobiotics were assessed in cell culture of *Leishmania tarentolae* promastigotes (LTP), *Leishmania amazonensis* amastigotes (LaA) and compared to peritoneal macrophages from mouse (PMM) using viability assays. Furthermore, mechanistic studies regarding mitochondrial functions were conducted in LTP, mitochondrial fractions isolated from LTP and bovine heart submitochondrial particles using oxygen consumption measurements, assays of individual mitochondrial complex activities, membrane potential and superoxide radical formation by photometry, fluorimetry and electron spin resonance spectroscopy. In LTP, Xan inhibited the viability more effective than Res (IC₅₀: Xan 23 μ M, Res 161 μ M). Likewise, Xan and Res demonstrated anti-leishmanial activity in LaA (IC₅₀: Xan 7 μ M, Res 14 μ M) while had less influence on the viability of PMM (IC₅₀: Xan 68 μ M, Res > 438 μ M). In contrast to Res, Xan strongly inhibited oxygen consumption in *Leishmania*. Further studies demonstrated that this is based on the inhibition of the mitochondrial electron transfer complex III/IV by Xan which was less pronounced with Res. However, Xan also demonstrated inhibitory activity on mammalian mitochondrial complex III. In addition, Xan caused no decrease of the membrane potential in leishmanial mitochondria, while Res resulted in mitochondrial uncoupling. Neither Xan nor Res increased mitochondrial superoxide release in LTP. These data show that Res, a major polyphenol from red wine, and Xan, an ingredient of hop-containing beer, may have selective anti-leishmanial activity.

308

Pharmacological targeting of human tryptophan hydroxylase – novel inhibitors for the treatment of serotonin-related diseasesS. Matthes¹, E. Specker², A. Schütz¹, M. Grohmann¹, J. von Kries², M. Nazare², M. Bader^{1,3,4}¹Max-Delbrück-Center, Berlin, Germany²Research Institute for Molecular Pharmacology, Berlin, Germany³Charité-University Medicine, Berlin, Germany⁴University of Lübeck, Institute for Biology, Lübeck, Germany

Tryptophan hydroxylase (TPH) is the rate-limiting enzyme in serotonin (5-HT) biosynthesis.

Its two existing isoforms are exclusively expressed in the periphery (TPH1), or the raphe nuclei of the brainstem (TPH2) and the respective 5-HT populations are distinctly separated by the blood-brain barrier, offering the possibility to pharmacologically modulate central and peripheral functions in an independent manner. Peripheral 5-HT is mainly produced by TPH1-expressing enterochromaffin cells of the gut and taken up into platelets and transported in the blood stream. Upon platelet activation, 5-HT is rapidly released and locally induces multiple effects, such as vasoconstriction, cell proliferation or fibrosis and is furthermore involved in the regulation of e.g. vascular tone, gut motility, primary hemostasis, insulin secretion and T-cell-mediated immune response.

Following the classical early drug development pathway, we developed a fluorescence-based TPH activity assay and performed a high-throughput screening of about 37000 small chemical compounds. We discovered a novel class of TPH inhibitors, which was thoroughly validated in a variety of *in vitro* assay setups. Combining medicinal chemistry and X-ray crystallography, we further aimed to develop these inhibitors into preclinical drug candidates. To date we were able to generate and patent a series of novel TPH inhibitors with optimized affinity and an *in vitro* IC₅₀ in the low nanomolar range.

This novel class of TPH inhibitors could potentially be used to treat a variety of disorders with aberrant peripheral 5-HT signaling, such as gastrointestinal disorders (e.g. irritable bowel syndrome, Crohn's disease, various forms of diarrhea), cardiac valve diseases, pulmonary hypertension, chronic respiratory diseases and some neuroendocrine (carcinoid) tumors.

309

Investigation of the effect of snake venoms on different liver cancer related cell linesM. Kiessig¹, J. Querbach¹, Z. Oezkan², D. Seehofer¹, S. Hinderlich², G. Damm¹¹Charité Berlin, Department of General-, Visceral- and Transplantation Surgery, Berlin, Germany²Beuth Hochschule für Technik Berlin, Faculty of Life Sciences and Technology, Berlin, Germany

Primary hepatocellular carcinoma (HCC) is the most frequent type of liver cancer. Therapeutic options are rare. Beside Sorafenib, a tyrosin kinase inhibitor, which is only used in end stage liver cancer, the surgical intervention is the only successful clinical treatment option. Hence there is an urgent need to develop new therapeutic strategies and to identify new drugs for therapy of HCC. HCC often arises in fibrotic or cirrhotic liver, which is accompanied by a change of the extracellular matrix (ECM) composition. In addition it was shown that hepatoma cells express different integrins, which interact with ECM and intracellular cell signaling, compared to hepatocytes.

Snake venoms have gained increased attention, as it was shown that some of their enzymes and peptides directly act on tumor cells and their multicellular arrangement or indirectly by influencing the stroma environment of the tumor.

Aim of the present study was to investigate the effect of snake venoms on liver cancer related cell lines as well as their specific action on the ECM-integrin axis.

The effects of the snake venoms *Vipera palaestinae* (VP), *Calloselasma rhodostoma* (CR) and *Echis sochureki* (ES) on a cellular level (MTT, LDH release), on cell-cell-connections (Caco2 permeability assay) and on cell-matrix-interactions (adherence test) were investigated. Cell-matrix interactions were tested with an adhesion assay using collagen I (c-I), collagen IV (c-IV), fibronectin (Fn) and laminin (Lm) as ECM compounds.

In our *in vitro* models we used HepG2 as a HCC tumor cell line and the fibroblast cell line F301 as stroma simulation. Additionally Caco2 cells were used, a colon carcinoma cell line representing colorectal liver metastasis.

The toxicity of snake venom on liver cancer related cell lines was determined in the range of 0.01 – 100 µg/ml and plotted into dose response curves. The NOAELs were calculated from these dose response curves: VP: 0.5 µg/ml – CR: 1 µg/ml – ES: 5 µg/ml. Performance of the Caco2-Transwell permeability assay revealed no influence of the tested venom concentrations on the integrity of the cellular arrangement. Investigations for integrin inhibition revealed that the venom from VP reduced adherence on Lm coated plates and the venom of EC reduced adherence on Lm and Fn coated plates compared to untreated cells. There was no effect on the adherence on any matrix from the venom of CR observable.

Co-incubation of the snake venoms of VP and ES (below or near NOAEL concentrations) with 5-Fluorouracil (5FU), which is used as a chemotherapeutic agent, caused a reduction of its IC50 values.

The results indicate that components of VP and EC inhibit the formation of cell-matrix-interactions possibly acting as disintegrins. The co-incubation experiments demonstrated a synergistic effect of 5FU and snake venoms. Further experiments should enable the isolation of therapeutic active venom compounds, identification of disintegrins and their role in synergistic mechanisms in liver cancer therapy.

310

Modulation of the blood-brain barrier with peptidomimetics to improve drug delivery

S. Dithmer¹, C. Staat¹, L. Winkler¹, M.-C. Ku², A. Pohlmann², I. E. Blasig¹

¹Leibniz-Institut für Molekulare Pharmakologie, Berlin, Germany

²Berlin Ultrahigh Field Facility, Max-Delbrueck Center for Molecular Medicine, Berlin, Germany

After decades of research, the blood-brain barrier (BBB) still remains a major problem for successful delivery to the brain for the vast majority of drugs. The main component forming the BBB is the brain microvascular endothelium. The paracellular permeation is limited by tight junctions (TJs), a multiprotein complex composed of the members of the claudin family claudin-1, -3, -5, -12. Claudin-5 is known to be the key TJ protein tightening the BBB. Therefore, claudin-5 has been selected as target to modulate the BBB. For this reason, drug enhancer peptides (peptidomimetics) were designed to modulate transiently claudin-5 and, thereby, permeabilize the BBB. By combining biochemical protein/peptide interaction and tissue culture methods, we identified, validated and optimized peptide sequences modulating claudin-5 containing barriers. The claudin-5 targeting peptides decreased the transcellular electrical resistance and increased the permeability through MDCK-II cell monolayers stably expressing YFP-claudin-5 and immortalized brain endothelial cells (bEND.3). The peptides decreased the amount of claudin-5 and ZO-1 at cell-cell contacts and changed the cell morphology from spindle-shaped to more round-shaped. All tested peptides showed no signs of toxicity on cell cultures and *in vivo* (intravenous injection). Permeability measurements in mice proved enhanced permeation of Na-fluorescein (376 Da) through the BBB, which was confirmed by magnet resonance imaging of contrast agents (Gd-DTPA, 547 Da). In summary, we identified new peptides with the potential to enhance cerebral delivery of small molecules through the BBB.

311

Transient opening of the blood-brain barrier by BO1 – a claudin-5 affecting small molecule

O. Breitreuz-Korff¹, C. Tschek¹, L. Winkler¹, I. E. Blasig¹

¹Leibniz-Institut für Molekulare Pharmakologie, Berlin, Germany

Treatment of cerebral diseases is limited by the capability of pharmacologically active agents to penetrate the blood-brain barrier (BBB). This paracellularly tight diffusion barrier is formed by brain capillary endothelial cells. The paraendothelial cleft is sealed by tight junctions (TJs), a multiprotein complex. Cerebral TJs predominantly consist of claudin-5 (Cldn5) which tightens the BBB for molecules <800 Da. Consequently, Cldn5 is a potential target for transient and size-specific modulation of the BBB to improve CNS penetration for pharmacologically active agents. In high throughput screening using a Cldn5 assay, the barrier opener 1 (BO1) was identified as a Cldn5 modulator. Initially, a significant removal of Cldn5 from the plasma membrane was shown by confocal microscopy using epithelial and endothelial cell lines. Measurement of transcellular electrical resistance and of paracellular permeability using lucifer yellow (mw 521 Da) demonstrated the effect of BO1. Concentration dependent treatment (50-150 µM) of cell monolayers with BO1 reduced tightness of the TJs between some hours and 24 h. Applying 2-hydroxypropyl-β-cyclodextrin as a solubilizer, opening activity of BO1 became detectable in mice. Due to short stability (< 2 h) of BO1 in the blood/plasma repeated administration (1.5 mg/kg i.v.) was required to induce significantly increased permeability of the BBB for Na-fluorescein (mw 376 Da). The small molecule BO1 is a promising new approach for transient opening of the BBB *in vivo*. Further modification of the stability and solubility of BO1 is necessary to optimize its applicability.

312

TricSI – development of a tricellulin peptidomimetic to modify tissue barriers

B. Arslan¹, J. Cording¹, R. Günther¹, C. Staat¹, A. Krüger¹, I. E. Blasig¹

¹Leibniz-Institut für Molekulare Pharmakologie, Berlin, Germany

The complex of tight junction (TJ) proteins is located between opposing epithelial or endothelial cells. TJs restrict the paracellular permeation of ions and other solutes. Tricellulin (Tric) tightens tricellular TJs (tTJs) and regulates bicellular TJ (bTJ) proteins like claudins and occludin (Occl). Current data suggest an important role of tTJs at the blood-brain barrier (BBB). A main pharmacological problem is modulation of the BBB to improve drug delivery to the CNS. Therefore, TricSI has been developed as a peptide taken from Tric to open tissue barriers specifically and transiently. Initially, a recombinant

protein was generated based on a sequence of an extracellular loop of Tric, tagged with maltose binding protein. The fusion protein caused down-regulation of Tric, internalization of both Tric and Occl (confocal laser scanning microscopy), and a significant decrease in transcellular electrical resistance (TER) of a human epithelial colorectal adenocarcinoma cell line. Then, studies with the synthetic peptide TricSI indicated its capacity of cell barrier opening after about 16 h of incubation with concentrations varying from 100 to 150 µM affecting the membrane localization of Tric and Occl. Barrier opening was proven by decreasing TER, increasing permeability coefficient of lucifer yellow (457 Da) and FITC-dextran (10 kDa); the localization of Tric elongated from tTJs towards bTJs and Cldn1 was weakened at bTJs. Physicochemical properties of TricSI examined by circular dichroism spectroscopy suggested β-strand structure and no helical propensity. Taken together, a Tric-derived peptide has been identified increasing the paracellular permeability of tissue barriers and redistributing the cellular localization of TJ proteins. TricSI is a novel, promising tool to overcome cerebral barriers with the potential to improve drug delivery to the CNS. Further experiments are needed to better understand the role of Tric in tissue barriers as well as to clarify the mode of action of TricSI.

313

New properties and applications of the old antimicrobial peptide gramicidin S

M. Berditsch¹, S. Afonin², H. Kern¹, J. Reuster¹, O. Babii¹, A. S. Ulrich^{1,2}

¹Karlsruhe Institute of Technology, Institute of Organic Chemistry, Karlsruhe, Germany

²Karlsruhe Institute of Technology, Institute of Biological Interfaces (IBG-2), Karlsruhe, Germany

Abstract content cannot be disclosed at this time.

Pharmacology – Disease models

314

Progression of airway obliteration induced by orthotopic tracheal transplantation can be monitored by micro CT imaging.

M. Delbeck¹, M. Rosenbruch¹

¹Bayer Pharma AG, Wuppertal, Germany

Introduction: Lung transplantation has become an established treatment option for a variety of end-stage lung diseases, but the long-term survival is often disappointing. The leading cause of death is generally chronic rejection which is characterized by inflammation and fibrous obliteration of the small airways, progressively leading to a reduction of the airflow.

The mouse heterotopic tracheal transplantation model is widely used as an experimental model to study the development of obliterative airway disease. Despite its widespread application, the heterotopic transplantation model does have a number of limitations, as for example the lack of airflow. The present study provides a description of the orthotopic tracheal transplantation mouse model, which shares more similarities with transplant situation in humans, and provides the analysis of airway obliteration via micro CT and histological evaluation.

Methods: A seven-ring donor trachea from BALB/c mice was implanted into the recipient C57BL/6 mice. C57BL/6 mice without transplantation were used as normal controls. Donor C57BL/6 mice to recipient C57BL/6 mice were served as the isograft group. 42 days after transplantation, mice were scanned using an *in vivo* small animal µCT (SkyScan 1176). Tracheal tissue was harvested and fixed in formalin, embedded in paraffin, cut and stained with hematoxylin and eosin (H&E) as well as Sirius-red/Fast-Green.

Results and conclusions: Histologic evaluation showed luminal narrowing with subepithelial inflammatory cell infiltrates and fibrosis, as well as partially damaged and flattened epithelium. The aerated volume of the allogeneic grafts, analyzed by micro CT was significantly reduced compared to the isogenic control grafts and normal controls. Non-invasive imaging via micro CT may offer an option for longitudinal monitoring of the progression of obliterative airway disease as well as response to treatment.

315

Inhibition of the mevalonate synthesis causes a DAF-16 dependent longevity phenotype in *C. elegans*

A. Jahn¹, S. Honnen¹, M. Hertel¹, G. Fritz¹

¹University Hospital Düsseldorf, Toxicology, Düsseldorf, Germany

C. elegans is a well-established model organism to study the aging process as well as effects of various substances *in vivo*. Its lifespan is regulated by multiple signaling pathways (e.g. Insulin or mTOR signaling), which are well conserved up to humans. The insulin/IGF-1 pathway was the first pathway shown to effect ageing in animals. Mutations that decrease the activity of DAF-2 (IGF1R) lead to a significant increase of lifespan accompanied by a decrease of age pigment accumulation in *C. elegans*. The relevant effector of the insulin/IGF-1 pathway is the transcription factor DAF-16 (hFOXO3a). Inhibition of HMG-CoA reductase (enzyme of mevalonate pathway) by statins, which are frequently used as cholesterol-lowering agents in the clinic, has been shown to attenuate protein prenylation and glycosylation. Notably, prenylated-, membrane-bound small GTP-binding proteins are important for the regulation of the afore mentioned age-related signaling pathways like the insulin/IGF-1 pathway. Recently, a cohort study showed that a decreased mortality rate in humans between age 78 – 90 correlates with statin treatment, but is independent of total cholesterol levels. As *C. elegans* harbors the mevalonate pathway, but the branch leading to cholesterol synthesis is missing, it is a well-suited model to study cholesterol-independent effects of statins on aging-associated phenotypes and the underlying molecular mechanisms.

Here, we show that exposure of *C. elegans* to statins substantially decelerated the accumulation of age pigments. While the level of age pigments roughly doubled in control animals, there was only a slight increase in the lovastatin group. The use of atorvastatin gave comparable results indicating a more general effect of the inhibition of

the HMG-CoA reductase. The retarded accumulation of age pigments could be partly phenocopied using an inhibitor of the small GTPase Rac1 or using RNAi against the HMG-CoA reductase. A reduced level of age pigments is prognostic for an elevated mean lifespan (about 20%) in *C. elegans*. A post reproductive treatment with lovastatin, mimicking the use of statins in patients of advanced age increased the mean lifespan in *C. elegans* even further. In addition, we could show a mild reduction of fertility and a developmental delay as well as a marked increase in acute thermal stress resistance mediated by lovastatin. Besides the reduced accumulation of age pigments and the increased lifespan these are phenotypes which are usually observed under accumulation of DAF-16 overactivity. Consequently we found an increased nuclear localization of DAF-16 in the presence of lovastatin and lovastatin completely failed to reduce age pigments in a *daf-16*-KO mutant background. RT-qPCR brought JNK-1, a known activator of DAF-16, into play as a possible effector induced by statins. This is currently under investigation.

In summary, statin exposure induces a longevity phenotype in *C. elegans*, which might be DAF-16 dependent. This findings indicates that a product of the mevalonate pathway might influence the insulin/IGF-1 pathway and particularly the transcription factor DAF-16.

316

High-fat diet and low-dose streptozotocin induced type 2 diabetes: A methodological critique and cross-check

Z. Ozturk¹

¹Izmir Ataturk Research Hospital, Clinical Pharmacology and Toxicology, Izmir, Trkiye

The high-fat diet (HFD)- fed, streptozotocin (STZ)- treated rat model is one of the experimentally-induced animal models of diabetes. This model is often used to evaluate the antidiabetic activity of several agents. According to Srinivasan et al. (2005), prolonged exposure of high-fat diet leads to insulin resistance, and the development of diabetes occurs only in insulin-resistant HFD-fed rats following low dose STZ, because the HFD-fed rats are already mildly hyperglycemic due to insulin resistance (1). In HFD/STZ model, the rats are fed with high-fat diet for 2-4 weeks or for a relatively long time (≥ 3 months) in order to simulate the insulin resistance and/or glucose intolerance. After induction of diabetes with multiple or single low-dose of STZ (30-35 mg/kg), some of the diabetic rats receive treatment (2). In this way, the impact of treatment can be determined by comparing the differences between groups. Despite the lack of methodological information concerning the feeding time in some studies, all rats should be allowed to continue to feed on their respective diets until the end of the study. But what would happen if the HFD was switched to normal pellet diet in these diabetic rats?

In our experience, the feeding of NPD for 4 weeks significantly decreased FBG in diabetic rats compared to HFD-fed diabetic rats (234.40 ± 42.71 mg/dl vs. 464.00 ± 23.88 mg/dl, $p < 0.05$). Although diet regulation could not restore normal blood glucose, such a decrease was unexpected. In addition, the body weights of the NPD-fed diabetic rats were significantly lower than the body weights of the HFD-fed diabetic rats (249 ± 6.00 gvs. 288.00 ± 4.41 g, $p < 0.05$). There was no significant difference in body weight between nondiabetic control rats and diabetic rats fed NPD for 4 weeks. Further details can be found in Table 1.

Diet regulation and weight loss may prevent, control and reverse diabetes. However, at later stages of the disease, it is difficult to improve blood glucose control without medication, because the disease progresses from insulin resistance to insulin deficiency (3). According to some diabetes researchers, the amount of residual functional beta-cells mass is an important issue, and another important question is whether HFD/STZ rat mimics an early or late stage of type 2 diabetes (4). These preliminary findings suggest the possibility that HFD/STZ rat model may simulate the characteristics of early stage more than the final stage of type 2 diabetes, and hyperglycemia in the experimental model can partially reverse with diet regulation.

References: 1. Srinivasan, K., Viswanad, B., Asrat, L., Kaul, C. L., Ramarao, P. (2005). Combination of high-fat diet-fed and low-dose streptozotocin-treated rat: a model for type 2 diabetes and pharmacological screening. *Pharmacol Res* 52(4):313-320.
2. Ozturk Z, Gurbunar T, Vural K, Boyacioglu S, Korkmaz M, Var A. (2015). Effects of selenium on endothelial dysfunction and metabolic profile in low dose streptozotocin induced diabetic rats fed a high fat diet. *Biotech Histochem* 90(7):506-515.
3. Franz, M. J. (2007). The dilemma of weight loss in diabetes. *Diabetes spectr* 20(3):133-136.
4. Skovso, S. (2014). Modeling type 2 diabetes in rats using high fat diet and streptozotocin. *Journal of diabetes investigation* 5(4):349-358.

Abb. 1

Table 1. Effects of diet changes on HFD/STZ induced diabetes in rats

	Initial values	After induction of diabetes (3rd week)	After NPD/HFD (7th week)
Fasting Blood Glucose (mg/dl)			
C	67.00±1.51	72.40±2.60	74.20±3.10
D+NPD	74.00±2.50	344.60±26.19*	234.40±42.71*
D+HFD	78.00±4.72	377.40±18.50*	464.00±23.88*#
Body weight (g)			
C	220.00±4.47	228.00±4.63	231.00±4.84
D+NPD	220.00±5.14	255.00±2.73*	249.00±6.00
D+HFD	230.00±4.30	260.00±4.47*	288.00±4.41*#

C: control rats, D+NPD: diabetic rats fed NPD after induction of diabetes, D+HFD: diabetic rats fed HFD after induction of diabetes. * different from C ($p < 0.05$); # different from D+NPD ($p < 0.05$). Diabetes was induced by a HFD (2 weeks) combined with low dose streptozotocin (35 mg/kg) injection. Values are means \pm S.E.M., n=5 in each group.

317

Phenotyping of a knock-in mouse model of primary torsion dystonia and pharmacological behavioral effects of quinpirole

J. Gerstenberger¹, A. Bauer¹, A. Richter¹, F. Richter¹

¹Universität Leipzig, Veterinärmedizinische Fakultät, Institut für Pharmakologie, Pharmazie und Toxikologie, Leipzig, Germany

Animal models are pivotal for studies of pathogenesis and treatment of movement disorders. Dystonia, characterized by sustained or intermittent muscle contractions causing twisting movements/postures, is regarded as a basal ganglia disorder. The pathophysiology is however poorly understood. In mouse models of DYT1 dystonia, which is caused by a GAG deletion in TOR1A that encodes for the protein torsin A, ex vivo electrophysiological studies have shown an abnormal D2 receptor mediated release of acetylcholine from striatal interneurons. In these models, which do not exhibit a dystonic phenotype, the functional relevance of the increased D2 receptor mediated acetylcholine release has not been examined yet. The aim of present study was to (1) generate more powerful tests to detect behavioural alterations in the DYT1 knock-in mouse and to (2) examine the behavioral effects of the D2 receptor agonist quinpirole.

For this purpose, a sequence of cognitive, motoric and sensorimotor tests were performed in this mouse model. Only the adhesive removal test that explores sensorimotor connectivity revealed significant impairments in the DYT1 knock-in mice compared to controls. To induce a more characteristic and stronger phenotype, the "rotating beam test" was developed. This motoric test measures motor coordination and balance. Interestingly, DYT1 knock-in mice showed significant motor deficits in the rotating beam test.

Based on these results, the acute effects of quinpirole (0.25 -1 mg/kg i.p.) were tested in DYT1 knock-in and wildtype mice. Subsequent to the injections, mice were tested in the open field, the rotating beam test and the adhesive removal test, respectively. In the open field test, DYT1 knock-in mice showed increased thigmotaxis at a dose of 0.5 mg/kg quinpirole. In the rotating beam test, both groups showed a dose-dependently reduced performance. In the adhesive removal test, quinpirole improved the reaction time in DYT1 mice independently of dosage, while no effects were observed in the wildtype littermates. However, in vehicle follow-up (post-drug control), this effect remained consistent in the DYT1 model, suggesting a habituation effect.

In conclusion, we generated a new test, i.e., the rotating beam test which improves the detection of mild motor impairments in DYT1 knock-in mice. Furthermore, the adhesive removal test revealed sensorimotor dysfunctions in this animal model. These results represent an important step for our ongoing optogenetic examinations on the role of abnormal neuronal plasticity in DYT1 dystonia and for pharmacological studies. The first data on the effects of quinpirole do not indicate a critical role of D2 dysregulated acetylcholine release, but this has to be clarified by ongoing local striatal injections of quinpirole and by pharmacological manipulations of the cholinergic system.

318

Effect of stimulation of the cGMP/cGKI signalling pathway by BAY 41-8543 in renal fibrosis

E. Schinner¹, V. Wetzl¹, J. Thoma¹, F. Hofmann², P. Sandner³, J. Schlossmann¹

¹Uni Regensburg, Pharmakologie, Regensburg, Germany

²TU Carvas Zentrum, München, Germany

³Bayer Pharma AG, Wuppertal, Germany

Renal fibrosis is characterized by decreased nitric oxide (NO) bioavailability and pronounced transforming growth factor β (TGF β) signalling subsequently excessive extracellular matrix (ECM) deposition. Here, the effects of the soluble guanylate cyclase (sGC) stimulator BAY 41-8543 after unilateral ureter obstruction (UUO) have been studied.

Kidney fibrosis was induced by unilateral ureter obstruction (UUO) in wild type (WT) and cGKI knock-out (cGKI KO) mice. Starting one day after UUO, the sGC stimulator BAY 41-8543 was (4mg/kg/daily) i. p. injected for seven days. Biomarkers indicating remodelling processes in the kidney were analysed via mRNA expression and protein expression.

BAY 41-8543 administration influenced the activity of the ECM degrading matrix metalloproteases (MMP2 and MMP9) and their inhibitor TIMP-1, the expression pattern of extracellular matrix proteins (e.g. Collagen and fibronectin) of profibrotic mediators (e.g. connective tissue growth factors (CTGF) and plasminogen-activator inhibitor-1 (PAI-1)) and the secretion of cytokines, e.g. IL-6. Thereby, BAY 41-8543 increments the cGMP pool among others via modulation of endothelial NO synthase (eNOS) expression.

Agents, which enhance NO and cyclic guanosine monophosphate (cGMP) ameliorate the progression of fibrotic tissue. However, the molecular mechanism by which cGMP via cGKI affects the development of kidney fibrosis has not fully been elucidated. Accordingly, the present study investigates the functional role of sGC stimulation in regulating the fibrotic process, the signalling pathway and the underlying mechanisms involved. We hypothesize that the antifibrotic potential of BAY 41-8543 might be related to the increased cGMP pool and the inhibition of the MAPK and smad signalling pathway. The elucidation of the signalling allows the development of new therapeutic options.

319

SLY1 regulates T-cell proliferation during *Listeria monocytogenes* infection in a Foxo1 dependent manner

D. Schäll¹, F. Schmitt¹, B. Reis², S. Brandt², S. Beer-Hammer¹

¹Institut für Pharmakologie, Abt. für Pharmakologie und Experimentelle Therapie, Tübingen, Germany

²Institut für Mikrobiologie, Düsseldorf, Germany

Infection of mice with *Listeria monocytogenes* (LM) results in a strong T-cell response that is critical for an efficient defense. Here, we demonstrate that the adapter protein SLY1 (SH3-domain protein expressed in lymphocytes 1) is essential for the generation

of a fully functional T-cell response. The lack of SLY1 leads to reduced survival rates of infected mice. The increased susceptibility of SLY1 KO mice was caused by reduced proliferation of differentiated T cells. Ex vivo analyses of isolated SLY1 KO T cells displayed a dysregulation of Forkhead box protein O1 (Foxo1) shuttling after TCR signaling, which resulted in an increased expression of cell cycle inhibiting genes, and therefore, reduced expansion of the T-cell population. Foxo1 shuttles to the cytoplasm after phosphorylation in a protein complex including 14-3-3 proteins. Interestingly, we observed a similar regulation for the adapter protein SLY1, where TCR stimulation results in SLY1 phosphorylation and SLY1 export to the cytoplasm. Moreover, immunoprecipitation analyses revealed a binding of SLY1 to 14-3-3 proteins. Altogether, this study describes SLY1 as an immunoregulatory protein, which is involved in the generation of adaptive immune responses during LM infection, and provides a model of how SLY1 regulates T-cell proliferation (Schäll et al., Eur J Immunol. 2015).

320

p110y/δ double-deficiency induces eosinophilia and IgE hyperproduction but protects from OVA-induced allergic asthma

K. Bucher¹, B. Mothes¹, S. Ammon-Treiber², B. Nürnberg¹, S. Beer-Hammer¹
¹Institut für Pharmakologie und Toxikologie, Tübingen, Germany
²Institut für Pharmazie, Tübingen, Germany

The catalytic isoforms p110y and p110δ of phosphatidylinositol-4,5-bisphosphate 3-kinase γ (PI3Kγ) and PI3Kδ play an important role in the pathogenesis of asthma. Two key elements in allergic asthma are increased eosinophil and IgE levels. Whereas dual pharmacological inhibition of the catalytic subunits p110y and p110δ reduces asthma-associated eosinophilic lung infiltration and ameliorates disease symptoms, it has been shown that dual genetic deficiency in PI3Kγ and PI3Kδ in p110y^{KO}p110δ^{KO} mice increases serum IgE and basal eosinophil counts in mucosal tissues and blood. This suggests that long-term inhibition of p110y and p110δ might exacerbate asthma. Here we analysed p110y/δ^{-/-} mice and determined IgE and eosinophil counts in a basal state and the immune response to ovalbumin (OVA)-induced allergic asthma. We found that serum concentrations of IgE, IL-5 and eosinophil numbers in blood, spleen and bone marrow were significantly increased in p110y/δ^{-/-} mice in comparison to single knock-out (KO) and wildtype (WT) mice. Nevertheless, p110y/δ^{-/-} mice were protected against OVA-induced infiltration of eosinophils, neutrophils, B cells and T cells into the lung tissue and the bronchoalveolar space. Moreover, p110y/δ^{-/-} mice, but not single KO mice, showed a reduced bronchial hyperresponsiveness as measured with the isolated and perfused lung. We conclude that although the dual deficiency of p110y and p110δ causes eosinophilia and IgE hyperproduction, p110y/δ^{-/-} mice are not prone to develop OVA-induced allergic asthma.

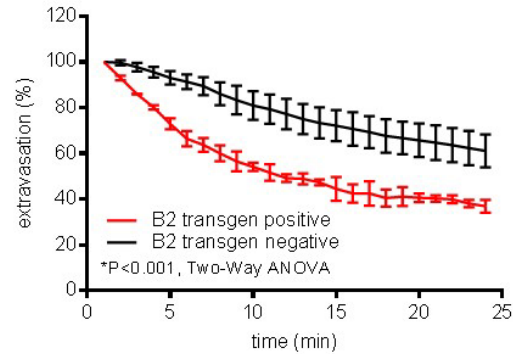
321

Evaluation of non-invasive Two-photon laser microscopy to study endothelial permeability in-vivo

E. Gholamreza-Fahimi¹, F. Khosravani¹, M. Bisha¹, V. T. Dao^{1,2}, T. Suvorava¹, M. van Zandvoort¹, G. Kojda¹
¹Heinrich-Heine-Universität, Institut für Pharmakologie und Klinische Pharmakologie, Düsseldorf, Germany
²Maastricht University, Cardiovascular Research Institute, Maastricht, The Netherlands, Germany

An increase of plasma extravasation induced by activation of constitutively expressed endothelial bradykinin type 2 receptors (B2) has been shown to contribute to the development of angioedema occurring as a sometimes life-threatening side effect of angiotensin-converting enzyme inhibitors such as enalapril (New Engl J Med 2015;372:418-425). These drugs inhibit the degradation of bradykinin and increase its vascular steady-state concentration. Hence, it is reasonable to assume that bradykinin may destabilise the endothelial barrier, i.e. may increase physiologic extravasation. While the commonly used Miles assay provides a useful and relatively easy tool to study the effect of permeabilizing mediators in-vivo, it does not distinguish between intravascular and interstitial Evan's blue dye. Likewise, extravasation can only be quantified at one particular time point per animal, usually 20-30 min. Furthermore, evaluation of physiologic extravasation is not possible. In contrast, non-invasive two-photon laser microscopy may allow separating the intravascular from the interstitial compartment and thereby investigations of changes of the physiologic endothelial barrier induced by drugs or transgenes. Therefore, we have evaluated this methodology for its suitability to study endothelial permeability in mice in vivo. To establish this, we used two different fluorescent dyes of different molecular weight. A 200,000 kDa dextran equipped with a green fluorescent chromophore which cannot leave vascular lumen was injected intravenously to visualize small dermal blood vessels of the mouse ear located approximately 200 μm below the surface. After stabilization of the green fluorescent signal, a 10,000 kDa dextran equipped with a red fluorescent chromophore which easily traverses the endothelial barrier was applied by intravenous injection. The red fluorescence permeates into the interstitium during physiologic extravasation and accumulates in the interstitial space. This process can be followed by measuring the decrease of intravascular red fluorescence over various time periods. Using this methodology we have studied whether endothelial-specific overexpression of B2 changes physiologic endothelial permeability. This newly developed transgenic mouse line (B2^{tg}) was established using a plasmid consisting of pBluescript II SK+ -Vector, the Tie-2-promotor, the human B2 cDNA, the SV40 poly-A-signal and a Tie-2 intron fragment. We observed that B2tg showed a significantly stronger extravasation than their transgene negative littermates as evidenced by the more rapid extravasation of the 10,000 kDa dextran at each time point (Fig. 1). We conclude that two-photon laser microscopy is suitable to study endothelial permeability non-invasively in-vivo and that this methodology allows to study the effects of drugs and transgenes on the endothelial barrier under non-inflammatory conditions. Furthermore, our results suggest that endothelial-specific overexpression of B2 increases physiologic extravasation.

Abb. 1



322

Endothelial-specific overexpression of bradykinin receptor type two in angioedema research

M. Bisha¹, F. Khosravani¹, V. T. Dao², T. Suvorava¹, G. Kojda¹
¹Pharmacology and Clinical Pharmacology, Düsseldorf, Germany
²Maastricht University, Cardiovascular Research Institute Maastricht (CARIM), Maastricht, Niederlande

Non-allergic angioedema such as angioedema induced by angiotensin converting enzyme inhibitors (ACEi) develops as a consequence of increased activation of bradykinin receptor type 2 (B2). Using a plasmid consisting of pBluescript II SK+ -Vector, the Tie-2-promotor, the human B2 cDNA, the SV40 poly-A-signal and a Tie-2 intron fragment a transgenic mouse line harbouring an endothelial-specific overexpression of B2 was generated and backcrossed to C57BL/6 for more than 10 times (B2^{tg}). Lung mRNA using primers specific for the human or the mouse B2 cDNA revealed a 12.5-fold stronger expression of human B2 in B2^{tg} (n=6), while the expression of murine B2 mRNA was unchanged and similar to transgene negative littermates (B2⁻). We have evaluated the specificity of several antibodies directed against B2 and found that a rabbit monoclonal anti B2 antibody appears to be reliable, i.e. there was just a faint staining in lung tissue of B2⁻ mice. However, this antibody primarily stains rodent B2 and has only little cross-reactivity to human B2. Hence, we were not able to detect a significant increase of B2 protein in tissues of B2^{tg}. Previous experiments have shown that bradykinin induced concentration-dependent constrictions of aortic rings with a maximal effect at 1 μM of bradykinin. The contraction due to bradykinin was completely inhibited by icatibant or diclofenac indicating that it is mediated by endothelial B2 activation and dependent on cyclooxygenase activity. In striking contrast to their transgene negative littermates B2⁻, we found a significant icatibant sensitive aortic dilation in B2^{tg} following preincubation with diclofenac which indicates functional overexpression of B2 in conductance vessels of B2^{tg}. To evaluate whether this applies to dermal micro vessels we used the Miles assay to quantify dermal extravasation of the albumin-bound dye Evans blue following intradermal injection of 30 μl of either vehicle, bradykinin, labradimil and histamine (control). Increasing concentrations of bradykinin caused a significant increase of extravasation reaching 4.41±0.11 fold at 18.9 nmol bradykinin in C57BL/6 (n=6 each, P<0.0001 vs. vehicle). A similar increase was found in B2^{tg} (4.45±0.25 fold, n=7, P<0.0001 vs. vehicle), while there was a stronger response in B2⁻ (5.50±0.16 fold, n=7, P<0.0001 vs. vehicle) which was significantly different to B2^{tg} (P<0.01) and C57BL/6 (P<0.01). In another set of experiments the specific and ACE-resistant B2 agonist labradimil (1.89 nmol) was used instead of bradykinin. Labradimil increased extravasation by 3.736±0.121 fold in C57BL/6 (n=6 each, P<0.0001 vs. vehicle), by 4.51±0.11 fold in B2^{tg} (n=7 each, P<0.0001 vs. vehicle) and 4.88±0.21 fold in B2⁻ (n=6, P<0.0001 vs. vehicle) which was significantly different to C57BL/6 (P<0.01) but not to B2^{tg} (P>0.05). The effects of bradykinin and labradimil were largely blocked by 10 nmol icatibant (i.v.) in C57BL/6, B2⁻ and B2^{tg} mice (P<0.0001) and hence mediated by activation of B2. These data suggest that overexpression of B2 in B2^{tg} is functionally active in endothelial cells of large conductance and small dermal vessels. Therefore, B2^{tg} represents a new animal model suitable for cardiovascular and non-allergic angioedema research.

Pharmacology – Pharmacokinetics and clinical studies

323

Pharmacokinetic Pharmacodynamic modeling of irreversible effects: the Rituximab example

F. Keller¹
¹Universitätsklinikum, Innere 1, Nephrologie, Ulm, Germany

Background: For pharmacokinetic-pharmacodynamic modeling usually the sigmoid Emax model is used as described by the Hill equation. However, treatment regimens exist where the effect is only exerted as long as the drug concentration increases whereas decreasing concentrations produce no longer an effect. Examples are the pulse anti-cancer therapy such as originally proposed by the DeVita protocols.

Methods: Here, the new model for irreversible drug action is derived from the time dependent change of the concentration that must be larger than the time-dependent growth of the number of target cells (tumor or bacteria). The irreversible effect can be assumed if the is no further growth of the target cells occurs.

$$dE/dt = + dC/dt - dN/dt$$

$$dN/dt = 0$$

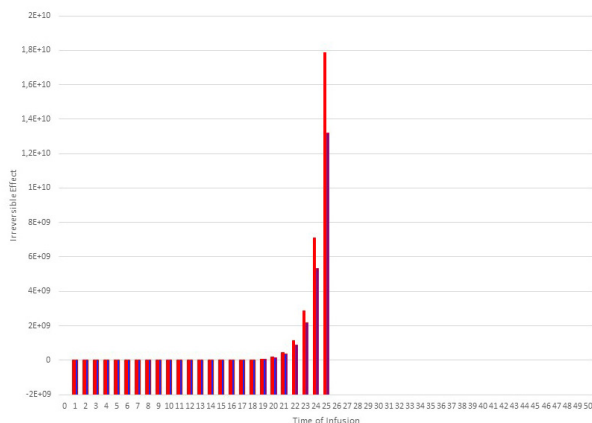
A solution for the above differential equation can be obtained by use of the integral exponential function IEC based on the Euler-Mascheroni constant (gamma = 0.5772 ...).

This model of an irreversible effect was applied to the example of rituximab where the initial effect on CD19+ and CD20+ B-cells completely persists for 6 month. To obtain a numerical solution, the following parameters are needed to be determined: the target concentration $C_{target} = 100$ mcg/ml and the infusion time $T = 2$ hours.

Results: It can be shown that a plausible result for rituximab can be estimated only under the condition that a short distribution half-life is assumed of $T_{1/2} = 2$ hours (not shorter than the time T of infusion). With the terminal half-life of 460 hours no plausible solution is obtained. Under these conditions two observations are made: There is a negative effect both, initially for low concentrations and after cessation of the infusion when concentrations decrease (in reality this means no effect in both cases). The irreversible effect is proportional to the target concentration. The shorter the half-life comes out relative to the infusion time ($T_{1/2} < T$) the stronger is the effect (Figure).

Conclusion: The pharmacodynamics of irreversible effects are different from reversible effects. The present modeling suggests that irreversible effects depend on three parameters: the target concentration, the duration of bolus infusion and on the distribution half-life.

Abb. 1



324

Development of a new *in-vitro* method for investigation of specific ruminant xenobiotic metabolism

B. Birk¹, A. Staehle¹, M. Meier¹, D. Funk¹, N. Sauer², G. Breves³, H. Seulberger¹
¹BASF SE, Global Environmental & Consumer Safety, Limburgerhof, Germany
²LUFA, Speyer, Germany
³TiHo Hannover, Institute of Physiology, Hannover, Germany

For registration of plant protection products (PPP) 14C-metabolism studies are required in rat (OECD 417), livestock (OECD 503) and plants (OECD 501, OECD 502). Occasionally there are specific questions occurring on the ruminant xenobiotic metabolism: 1) are the observed metabolites ruminant specific and formed directly in the rumen? 2) are ruminants able to cleave plant specific metabolites like glycosides to the respective aglycon? In the past new additional *in vivo* goat metabolism studies with at least one animal were performed. The aim of the project was to elucidate an alternative *in-vitro* method to replace the existing *in vivo* method in order to address robustly specific questions on xenobiotic metabolism in ruminants for registration of PPP.

Fresh sheep rumen fluid was incubated *in-vitro* >7 days by using rumen simulation technology (RUSITEC). The conservation of the physiological conditions were proven by measurement of pH (~pH 6.6) and Redox potential (~-300 mV). The microflora composition and their viability (bacteria, protozoa and fungi) of the rumen were monitored by microscopy, incubation on agar plates and performing several viability tests (e.g. Glycosidase-Test, NH3 and Short fatty acids). All the tests showed that the RUSITEC is a successful tool to maintain sheep rumen fluid for at least 7 days *in-vitro*. The metabolic behavior and performance of the rumen fluid was tested by e.g. incubating 14C-triazol derivative metabolites (TDM) like Triazol-Alanin (TA); Triazol-Acetic-acid (TAA) and Triazol-Lactic-acid (TLA), which are usually formed in plants after application of triazol-containing fungicides. It was shown that TA was cleaved within 72 h to 1.2.4.-Triazol, while TAA and TLA were stable under these conditions. These data are in a good accordance with available *in vivo* data in cows. Moreover glycosides (12C-Polydatin, Octyl-14C-β-D-glucopyranosid) were cleaved within 1 hour completely. All these data show, that the rumen fluid maintained its metabolic performance by using RUSITEC.

BASF identified the RUSITEC method, which is usually used in different areas (e.g. investigation of methane production *in-vitro*) as suitable and adapted this method for the purpose of investigation of ruminant xenobiotic metabolism. It was shown that RUSITEC is a robust method to analyze rumen xenobiotic metabolism and therefore can clearly substitute *in vivo* animal studies on ruminant metabolism studies beyond OECD503 and contribute significantly to animal welfare (3R: replacement).

325

Standard dosage of piperacillin leads to subtherapeutic plasma concentrations in burn patients

K. Olberisch¹, P. Mailänder², T. Kisch², J. Thern³, E. Kramme⁴, T. Graf⁵, S. G. Wicha⁶, W. Raasch¹

¹Universität Lübeck, Institut für Experimentelle und Klinische Pharmakologie und Toxikologie, Lübeck, Germany

²Universitätsklinikum Schleswig Holstein, Klinik für Plastische Chirurgie, Lübeck, Germany

³Universitätsklinikum Schleswig Holstein, Apotheke, Lübeck, Germany

⁴Universitätsklinikum Schleswig Holstein, Medizinische Klinik III, Lübeck, Germany

⁵Universitätsklinikum Schleswig Holstein, Medizinische Klinik II, Lübeck, Germany

⁶Uppsala University, Pharmacometrics Research Group, Department of Pharmaceutical Biosciences, Uppsala, Sweden

Background: Infections are a major problem in patients with burn diseases (BD). Due to severe injuries of their total body surface area (TBSA), burn patients have altered pharmacokinetic characteristics. Therefore, insufficient plasma concentrations may be achieved, when standard dosing schedules are applied for antibiotics such as piperacillin. For time-dependent antibiotics, the duration how long drug concentration exceeds the minimal inhibition concentration (MIC) is crucial for their antibacterial effects. Since *Pseudomonas* spp. is the main problematic pathophysiological bacterium for BD patients. The aim of the present study was to monitor the plasma concentrations of piperacillin during piperacillin/tazobactam treatment in BD patients. Patients from Intensive Care Units (ICU) served as controls.

Methods: 10 BD patients (5/5 m/f, 43.4±5.3y, TBSA 40.9±5.9%) and 5 patients (74.4±3.9y) from the ICU were included in this observational study. Blood samples were taken within the 3rd interval of the 8h-lasting dosing period of piperacillin/tazobactam (4/0.5g within 0.5h) at 1, 4 and 7.5h after the end of infusion. Total and free piperacillin concentrations were determined in plasma using HPLC-UV after deprotonisation with acetonitrile and by ultrafiltration, respectively. Pharmacokinetic parameters and dosing simulations were calculated by TDMx (www.tdmx.eu). Free plasma concentrations of piperacillin exceeding at least 1xMIC but preferably 4xMIC over the whole dosing interval were considered to be sufficient for antibiotic efficacy (MIC 16 mg/L for *Pseudomonas* spp., www.eucast.org).

Results: The pharmacokinetic parameters of total piperacillin, calculated for each BD or ICU patient using the concentrations at 1, 4, and 7.5h, were as follows: C_{max} 69.6±7.9 vs. 116.3±10.4 mg/L, $p < 0.05$, half-life 1.8±0.3 vs. 2.3±0.3h, $p > 0.05$, clearance 12.6±1.9 vs. 6.5±0.4 L/h, $p < 0.05$, volume of distribution 27.8±2.0 vs. 20.9±1.3L, $p < 0.05$. Free concentrations (which were included in TDMx calculations) were 87±2 vs. 81±2% ($p < 0.05$) of total concentrations. Duration per day while concentrations exceeded 1xMIC (15.6±1.9 vs. 22.0±1.1h, $p < 0.05$) or 4xMIC (5.4±1.3 vs. 9.4±0.7h, $p < 0.05$) were lower in BD than in ICU patients. Moreover, TDMx simulations predicted that the duration per day for 4xMIC could be enhanced to 16.2±1.5h if the piperacillin amount will be increased to 4x8 g/d and the infusion duration to 3h. Pharmacokinetic parameters have, however, to be determined in a pilot study with BD patients to ensure predicted values.

Conclusions: Standard dosage regimens for piperacillin/tazobactam could result in sub-optimal plasma concentrations of piperacillin in BD patients as well as in ICU patients. Drug monitoring and TDMx simulation of kinetic parameters may easily help to improve piperacillin treatment in BD patients.

326

Development and evaluation of a physiology-based pharmacokinetic model for high-dose methotrexate in children

K. Adam^{1,2}, S. Schmiedl^{1,3}, K. Cobocken⁴, P. Samayoa⁴, J. Szymanski^{1,3}, S. Wirth^{5,6}, K. Sinha^{5,6}, T. Niehues⁷, T. Imschweiler⁸, N. Brauer⁷, A. Abu Hejleh⁸, J. Lippert⁴, S. Willmann⁴, P. Thuermann^{1,3}

¹Witten/Herdecke University, Department of Clinical Pharmacology, School of Medicine, Faculty of Health, Witten, Germany

²Ruhr University Bochum, Children's Hospital, Bochum, Germany

³HELIOS Clinic Wuppertal, Philipp Klee-Institute for Clinical Pharmacology, Wuppertal, Germany

⁴Bayer Technology Services GmbH, Leverkusen, Germany

⁵HELIOS Clinic Wuppertal, Children's Hospital, Wuppertal, Germany

⁶Witten/Herdecke University, Department of Pediatrics, School of Medicine, Faculty of Health, Witten, Germany

⁷HELIOS Clinic Krefeld, Children's Hospital, Krefeld, Germany

⁸HELIOS Clinic Krefeld, Institute for Hygiene and Laboratory Medicine, Krefeld, Germany

Background: High dose methotrexate (HD MTX), defined as >1000mg MTX/m² body-surface-area (BSA) is used in children to treat a variety of malignant diseases since the 1950s. Clinicians observe relevant rates of severe unwanted side effects. Identifying patients having an increased risk for toxicity due to altered MTX pharmacokinetics is urgently needed. We aim to develop and evaluate a Physiology-based Pharmacokinetic (PBPK) Model for HD MTX in children using PK-Sim® (Bayer Technology Services GmbH, Leverkusen, Germany) with a special emphasize on relevant covariates.

Methods: In this non-interventional observational study, children receiving HD MTX intravenously at two major German pediatric oncology departments during the years 2004-2009 were included if at least one MTX serum level (MTX-SL) was determined during clinical routine. 29 Patients aged 2-18 years (male = 19, female = 10) with following diagnoses were included: acute lymphoblastic leukemia, Non-Hodgkin Lymphoma, Burkitt Lymphoma, brain stem glioma and glioblastoma multiforme. In total, 103 MTX treatment cycles corresponding to 300 MTX-SL were used in this study. Patients were randomized into two patient sets (training set and test set). Based on literature data, MTX PBPK-models were developed and slightly adapted taking into account mean relative deviation (MRD) and bias of predicted versus observed MTX-SL of the training set. The PBPK model with the lowest MRD and bias was chosen and finally evaluated using the test set. The impact of the covariates urine pH <6.5, trimethoprim/sulfamethoxazole, proton-pump-inhibitors, non-steroidal anti-inflammatory drugs and β-lactam antibiotics on the prediction quality was assessed using the Mann-Whitney U test.

Results: By using the training set, physicochemical (e.g. lipophilicity) and pharmacokinetic characteristics of MTX (e.g. V_{max} for active tubular secretion) were slightly adjusted. Using the GFR formula of Morris et al. (1982) and including an empiric correction factor, MRD for the training set was 2.49 whereas bias was 2.80 $\mu\text{mol/l}$. By applying the developed PBPK model to the test set the respective values were $\text{MRD}=3.92$ and $\text{Bias}=1.43$ $\mu\text{mol/l}$. For the covariates "at least one potentially interacting co-medication" and "trimethoprim/sulfamethoxazole" a significant impact on the prediction quality was found.

Conclusions: Using the developed PBPK-Model, a good prediction of the pharmacokinetics of HD MTX in severely ill children was found. By including additional factors influencing the prediction of MTX characteristics (e.g. co-medications) an improved prediction of MTX-SL might be reached. In prospective clinical trials, those more complex models should be evaluated and might be helpful to predict HD MTX pharmacokinetics and reduce unwanted side effects.

327

Hypericum extract influences permeation characteristics of hypericin across Caco-2 monolayers

S. Verjee¹, O. Kelber², H. Abdel-Aziz², V. Butterweck¹

¹University of Applied Sciences Northwestern Switzerland, Institute for Pharma Technology, School of Life Sciences, Muttenz, Switzerland

²Steigerwald Arzneimittelwerk GmbH, Scientific Department, Darmstadt, Germany

Hypericin is a natural polycyclic quinone found in *Hypericum perforatum*. Although hypericin reportedly has numerous pharmacological activities, only a limited number of studies have been performed on the absorption and transport characteristics of this compound, presumably, because hypericin is a highly lipophilic compound which is poorly soluble in physiological medium. Recently we have shown that quercitrin and isoquercitrin, but not hyperosid, quercetin or rutin increased the uptake of hypericin in Caco-2 cells.

The major aim of this study was to get a detailed understanding of the exposure and fate of hypericin in the Caco-2 cell system under different experimental conditions. The permeation characteristics of hypericin (5 μM) in absence or presence of hypericum extract STW 3-VI (290, 145, 62.5 $\mu\text{g/ml}$) were studied in the absorptive direction. Following application of hypericin to the apical side of the monolayer only negligible amounts of the compound were found in the basolateral compartment. The amount of hypericin in the basolateral compartment increased concentration-dependently in the presence of the extract (from 0 to 7.5 %). The majority of hypericin was found after cell extraction (44% in absence and 76% in presence of the extract). The recovery was in the range of 90 %, and significant amounts of hypericin found after cell extraction. Fluorescence microscopy and imaging analysis revealed that hypericin is mainly accumulated in the cell membrane. The precise mechanism through which hypericin might overcome the hydrophobic barrier of cell membranes remains to be elucidated. However, our experiments demonstrated that the permeation characteristics of hypericin significantly improved in presence of the extract.

328

Chronic effects of rifampicin on the pulmonary steady-state pharmacokinetics of gamithromycin in healthy foals

S. Berlin¹, S. Wallstabe², S. Oswald¹, D. Wegner¹, M. Venner³, W. Siegmund¹, M. Grube

¹Universitätsmedizin Greifswald, Klinische Pharmakologie, Greifswald, Germany

²Lewitz Stud, Neustadt-Glewe, Germany

³Clinic for Horses, University of Veterinary Medicine, Hannover, Germany

Background: The combination of gamithromycin (GAM), a novel drug with the big advantage of a once weekly administration, and rifampicin (RIF) is used in the treatment of lower airway disease in foals. Both are effective in the therapy of infections with *Rhodococcus equi*, a gram-positive coccobacillus bacterium, which is known to survive and reproduce within alveolar macrophages. Macrolides are combined with RIF to prevent resistance developing with single agent therapy. Both drug classes reach high concentrations in the lung, penetrate into phagocytes and kill intracellular pathogens.

Methods: A controlled, single- and multiple dose study with four-periods was conducted in 10 healthy foals (5 ♂ and 5 ♀, age: 42-63 days, body weight: 100-177 kg) which were treated once with RIF alone (10 mg/kg s.i.d., p.o., A) followed by the administration of GAM (6 mg/kg once weekly, i.v., B) for 3 weeks. Study period 3 ("RIF-GAM acute", C) includes the administration of GAM and RIF for 7 days with an administration interruption after the first RIF dose for blood sampling. For the last study period ("RIF-GAM chronic", D) both GAM and RIF were coadministered for 2 weeks. All periods were completed with blood sampling for pharmacokinetic analysis for 48 (A) or 168 h (B, C, D), respectively. The bronchoalveolar lavage was performed 24 h after the 3rd (treatment B) and 6th (treatment D) i.v. administration of GAM.

RIF, 25-O-Des-RIF, GAM and GAM-M1 were analyzed in serum, epithelial lining fluid (ELF) and bronchoalveolar cells (BALC) using a validated LC-MS/MS method. The 4 β -OH-cholesterol/cholesterol (4 β -OH-cho/cho) ratio was determined as a surrogate for CYP3A4 activity by GC-MS.

Results: Coadministration of GAM and RIF caused an increase of the systemic exposure of GAM for the acute (C) and chronic (D) treatment of about 39 % and 96 %, respectively, compared to the GAM treatment alone (B). Despite the increased GAM concentrations in plasma, relative GAM concentration at the site of action, in ELF and BALC, was lowered significant under RIF treatment (treatment B vs. D: ELF/ $C_{24\text{h}}$: 110 \pm 52.1 vs. 75.7 \pm 43.6; BALC/ELF: 44.0 \pm 32.8 vs. 32.6 \pm 13.1; BALC/ $C_{24\text{h}}$: 4554 \pm 3220 vs. 2283 \pm 1150*). Nevertheless, data also show considerable accumulation of GAM in the ELF and BALC for mono- and combined therapy. Concentration of the measured metabolite of GAM (GAM-M1) is increased about 3-fold under RIF treatment, but is still very low compared to the respective GAM concentration (~2.3-5 %). With regard to RIF the systemic exposure decreases in presence of GAM ($\text{AUC}_{0-24\text{h}}$ in $\mu\text{g}\cdot\text{h/ml}$ for (A): 162 \pm 93.0, (C): 83.0 \pm 30.2 and (D): 108 \pm 36.3). RIF is also accumulated in the lung, but to a much lower degree than GAM (ELF/ $C_{24\text{h}}$: 1.2 \pm 0.5; BALC/ $C_{24\text{h}}$: 2.01 \pm 1.24).

Conclusion: Pharmacokinetic data of the present study provides surprising results. In previous studies coadministration of clarithromycin and RIF show a dramatic decreased

plasma exposure of the macrolide, whereas the BALC/ $C_{24\text{h}}$ -ratio was unaffected (Peters et al. 2011). In contrast, systemic exposure of GAM increase significantly in case of the combined therapy and the BALC/ $C_{24\text{h}}$ -ratio was nearly halved. Both macrolides have in common, that they are intensively accumulated in the lung (ELF << BALC). At the moment there is further research required (e.g. *in vitro* studies) for a better understanding of the very interesting *in vivo* data.

329

Effects of genetic polymorphisms in the organic cation transporter OCT1 on desvenlafaxine pharmacokinetics in healthy volunteers

J. Matthaei¹, T. Prukop¹, F. Faltraco¹, G. Krepinsky¹, M. Abu Abed¹, J. Brockmüller¹, M. V. Tzvetkov¹

¹Institut für Klinische Pharmakologie, Göttingen, Germany

Background and aim: Desvenlafaxine is a selective serotonin and norepinephrine reuptake inhibitor, which is approved in the USA (but not in Europe) for treatment of major depressive disorder. Desvenlafaxine is the major active metabolite of the antidepressant venlafaxine. Desvenlafaxine is produced by O-desmethylation via CYP2D6. Direct administration of desvenlafaxine should bypass the variability in venlafaxine pharmacokinetics caused by the highly polymorphic CYP2D6. However, desvenlafaxine is less lipophilic than venlafaxine and may require carrier-mediated transport to penetrate cell membranes. Based on our *in vitro* data, desvenlafaxine is a substrate of the hepatic organic cation transporter OCT1 and common genetic polymorphisms abolished desvenlafaxine cellular uptake. About 9% of Caucasians are compound heterozygous carriers of loss-of-function OCT1 polymorphisms. Therefore, OCT1 polymorphisms may cause substantial inter-individual variability in the hepatic uptake and plasma concentrations of desvenlafaxine.

In this study we evaluated the influence of genetically-determined loss of OCT1 function on the pharmacokinetics and pharmacodynamics of desvenlafaxine. Primary aim was dependence of desvenlafaxine plasma concentrations (represented by AUC as primary endpoint) on the number of active OCT1 alleles.

Methods: 50 mg desvenlafaxine (Pristiq®) was orally administered to 41 healthy subjects preselected according to their OCT1 genotypes. OCT1*1 allele was regarded full active, OCT1*2 to *6 alleles were regarded loss of function. Plasma concentrations of desvenlafaxine and its main metabolite didesmethylvenlafaxine were quantified in plasma sampled up to 60 hours after administration using LC-MS/MS. Pupillographic measurements were performed as possible surrogate markers for desvenlafaxine pharmacodynamics.

Results: Out of the 41 subjects 14 carried two active, 13 one active, and 14 zero active OCT1 alleles. Age, height and weight were 26.9 \pm 6.4 years (mean \pm standard deviation), 1.75 \pm 0.11 m and 70.9 \pm 12.1 kg with no significant differences among the OCT1 genotypes. There were strong variations in the pharmacokinetics of desvenlafaxine and its metabolite didesmethylvenlafaxine. The $\text{AUC}_{0-\infty}$ of desvenlafaxine varied between 52.8 and 282.2 $\text{min}\cdot\text{mg/L}$ and $\text{AUC}_{0-\infty}$ of didesmethylvenlafaxine between 3.5 and 30.7 $\text{mg}\cdot\text{min/L}$. However, neither desvenlafaxine nor didesmethylvenlafaxine pharmacokinetics significantly differed among the three OCT1 genotypes. Concerning pharmacodynamics of desvenlafaxine, pupil diameters at maximal constriction after a standardized light exposure were on average 14% greater around the time of t_{max} than before administration. In line with the pharmacokinetic results there were no significant differences in maximal constriction or other pupillographic parameters among the OCT1 genotype groups.

Conclusions: Our results suggest that OCT1 genotype does not affect the pharmacokinetics of desvenlafaxine and therefore no dose adjustment in respect to OCT1 genotype should be considered. Other factors like renal transporters or polymorphic glucuronidation may explain the great variability in desvenlafaxine pharmacokinetics.

330

Concomitant cardiovascular medication among elderly patients using psychotropic drugs.

Z. Ozturk¹, A. Turkyilmaz²

¹Izmir Ataturk Research Hospital, Clinical Pharmacology and Toxicology, Izmir, Trkei

²Izmir Ataturk Research Hospital, Neurology, Basın Sitesi Polyclinic, Izmir, Trkei

Background: Cardiovascular disorders and medication are highly prevalent in elderly (1). Due to age related changes in the body, the elderly are particularly vulnerable to side effects and adverse drug reactions. Some psychotropic drugs are linked with reports of cardiac side effects. Additionally, some cardiac drugs may also cause psychiatric symptoms. Of these, angiotensin converting enzyme inhibitors, beta blockers, methylidopa and calcium channel antagonists can induce or exacerbate symptoms of depression (2). The aim of this study was to provide information on the concomitant use of cardiovascular drugs among elderly patients who took psychotropic medication.

Methods: We conducted a single-center, retrospective study between September 2013 and December 2013 using the medical records of elderly patients (≥ 65 years of age) admitted to Basın Sitesi Polyclinic, Izmir Ataturk Research Hospital, Turkey. Demographic characteristics of patients, diagnoses, prescription drugs were evaluated, and SPSS 16.0 statistical software was used for data analysis. Number, percent, mean and standard deviation were used as descriptive statistics.

Results: A total of 541 elderly patients with psychiatric disorders were identified. One in four patients receiving psychotropic medication took at least one cardiovascular agent concomitantly (n=135). Median age was 72 (min:65, max:98), 84 patients were female (62.2%). According to medical records of 135 patients, the most commonly used drugs were escitalopram, sertraline, mirtazapine, quetiapine, mianserin and risperidone. The proportion of the concomitantly use of cardiovascular drugs was higher among the patients who took more than one psychotropic drug (69.6% vs. %30.4) compared to patients taking psychotropic monotherapy. A higher percentage of women used diuretics (65.4% vs. 33.3%) and angiotensin receptor blockers (36.9% vs. 23.5%) concomitantly with psychotropic drugs when compared to men. The proportion of men using angiotensin-converting enzyme inhibitors and lipid-modifying agents was higher than women (58.8% vs. 38%, 68.6% vs. 20.2%, respectively).

Conclusions: The world's population is ageing rapidly. According to World Health Organization, over 20% of elderly suffer from a psychiatric or neurological disorder. Our data showed that use of cardiovascular drugs among elderly patients with psychiatric disorders was extensive. The effects and interactions of these drugs should be discussed and carefully evaluated before starting treatment in the elderly. Further studies focusing on drug use in elderly will increase the success in geriatric pharmacotherapy.

References: 1) Linjakumpu T, Hartikainen S, Klaukka T, Veijola J, Kivelä SL, Isoaho R. Use of medications and polypharmacy are increasing among the elderly. *J Clin Epidemiol.* 2002;55(8):809-17.
2) Shah S, Iqbal Z, White A, White S. Heart and mind: (2) psychotropic and cardiovascular therapeutics. *Postgrad Med J.* 2005;81(951):33-40. doi:10.1136/pgmj.2003.015230.

331

Assessing QTc-prolongation based on data from first-in-man studies

G. Ferber¹

¹Statistik Georg Ferber GmbH, Riehen, Switzerland

Since the adoption of the ICH E14 guideline [1], the Thorough QT (TQT) study has become a standard element of clinical drug development. However, with the IQ/CSRC study [2] the ability to detect QTc-prolongations of about 10 ms in a Phase I setting has been demonstrated. As a consequence, regulatory agencies have begun to grant waivers for a TQT study based on negative QT findings obtained from first-in-man studies. A concentration-response model is the key tool that gives sufficient power to an analysis based on data from single or multiple ascending dose studies. This power has been investigated in subsampling studies that simulate situations comparable to those encountered in first-in-man studies [3, 4]. Other topics to be addressed are the assurance of sufficient quality of the ECGs obtained, in particular in doses that cause adverse reactions, and a replacement for the active control that is part of a TQT study. If a model based statistical analysis is used for confirmatory inference, it must be specified in advance. This pre-specification includes tests to ascertain that the model assumptions are met and alternative methods to be used in case they are violated. In particular linearity and the absence of a hysteresis, i.e. a delay between the drug concentration and the observed QT effect need to be tested. This is an area of active research.

In this contribution, I will share current experience from a statistical perspective, both based on real data and on simulated studies. I will also discuss critical points in the design of first-in-man studies that are intended to be used to obtain a waiver for a TQT study.

1 International Conference on Harmonisation: ICH Topic E 14: The Clinical evaluation of QT/QTc interval prolongation and proarrhythmic potential for non-antiarrhythmic drugs. 2005.

http://www.ich.org/fileadmin/Public_Web_Site/ICH_Products/Guidelines/Efficacy/E14/E14_Guideline.pdf.

2 Darpö B et al.: Results from the IQ-CSRC prospective study support replacement of the thorough QT study by QT assessment in the early clinical phase. *Clin Pharmacol & Therap* 97 (2015) 326 – 335

3 Ferber G, Zhou M, Darpö B: Detection of QTc Effects in Small Studies – Implications for Replacing the Thorough QT Study *Ann Noninvasive Electrocardiol.* 20 (2015) 368-377

4 Ferber G, Lorch U, Täubel J: The Power of Phase I Studies to Detect Clinically Relevant QTc Prolongation: A Resampling Simulation Study. *BioMed Research International*, 2015 (2015) Article ID 293564, 8 pages <http://dx.doi.org/10.1155/2015/293564>

332

Expression and function of the apelin receptor APJ in human platelets is related to cardiac troponin T levels in patients with acute myocardial infarction

A. Böhm¹, A. Strohbach², S. G. Mahajan¹, C. Wirtz¹, H. Wetzel², S. B. Felix², B. H. Rauch¹, R. Busch²

¹Universitätsmedizin Greifswald, Pharmakologie, Greifswald, Germany

²Universitätsmedizin Greifswald, Klinik und Poliklinik für Innere Medizin B (Kardiologie), Greifswald, Germany

Human platelets express the G-protein-coupled angiotensin receptor-like-1 (APJ) receptor. APJ is activated by apelin, which is produced as pre-apelin and cleaved into several bioactive peptides such as apelin-12, -13 and -17. Apelin and APJ are expressed in a variety of tissues such as the heart, the vessel wall, several tumor types, and in platelets. To date, there is no description or a suggested function of the apelin/APJ system in platelets to date. Here, we investigate APJ expression and function in human platelets.

Apelin and APJ expression were determined in platelet-rich plasma from healthy donors by immunofluorescence, Western blotting and flow cytometry. In a pilot study apelin and platelet APJ expression were analyzed in 23 patients with NSTEMI, 4 STEMI patients and 14 controls. Here, platelet aggregation was analyzed by light transmission aggregometry (LTA); platelet CD62 and APJ expression by flow cytometry and circulating plasma apelin by ELISA.

In resting human platelets, APJ receptor expression was observed predominantly in the outer cell membrane, as determined by immunofluorescence staining and flow cytometry. Activation with a selective thrombin receptor-activating peptide (AP1) resulted in decreased APJ protein levels determined by Western blotting in platelet lysates compared to untreated controls. Preincubation of platelets with different apelin isoforms for 30 sec to 5 min reduced platelet aggregation in LTA studies by up to 20 % for apelin-17. This effect was inhibited by preincubation of the platelets with the eNOS inhibitor L-NAME (300 µM), suggesting the involvement of a NO-dependent mechanism. In patients with myocardial infarction the expression of platelet APJ was significantly reduced compared to the control group (56,84% ± 9,28 % in MI versus 100 % ± 19,35 % in controls; p = 0.029). This reduction in APJ expression on platelets was accompanied by decreased plasma levels of apelin-17 in patients with MI (14.95 ± 0.6 pg/mL versus 16.98 ± 0.6 pg/mL; p = 0.035). Interestingly, the decreased APJ expression on platelets

in MI patients significantly correlated inversely with the troponin T plasma levels (r = -0.46; p = 0.03). This may suggest an association of APJ expression with lower plasma levels of troponin T and possibly tissue damage.

In conclusion, our study shows for the first time the expression of APJ and a possible function in human platelets. APJ may act as an endogenous inhibitor of platelet aggregation in response to certain apelin isoforms, predominantly apelin-17. Upon platelet activation, APJ is internalized and surface expression is reduced by about 50 %. In MI patients, plasma levels of apelin-17 and platelet APJ expression were reduced. This correlated inversely with troponin T levels. Reduced circulating apelin-17 levels and platelet APJ expression may be associated or partly account for platelet hyperactivity in MI patients.

333

Anticholinergic drug use, M₁ receptor affinity and dementia risk - a pharmacoepidemiological analysis using claims data

F. Thome¹, K. von Holt¹, W. Gomm¹, W. Maier², K. Broich³, G. Doblhammer^{1,4,5,6}, B. Haenisch¹

¹German Center for Neurodegenerative Diseases (DZNE), Bonn, Germany

²Department of Psychiatry, University of Bonn, Bonn, Germany

³Federal Institute for Drugs and Medical Devices (BfArM), Bonn, Germany

⁴Rostock Center for the Study of Demographic Change, Rostock, Germany

⁵Max-Planck-Institute for Demographic Research, Rostock, Germany

⁶Institute for Sociology and Demography, University of Rostock, Rostock, Germany

Background: Dementia is characterized by cumulative cognitive decline and progressive inability for independent living. The lack of suitable therapies for terminating the progression of this disease underlines the importance of the detection of risk factors. Anticholinergic drugs have been shown to enhance cognitive decline in the elderly. The classification of anticholinergic drugs according to their anticholinergic burden, however, is inconsistent. Since cholinergic transmission is mainly mediated by the M₁ muscarinic acetylcholine receptor in the brain, we classified anticholinergic drugs from anticholinergic risk lists according to their affinity for the M₁ receptor subtype and calculated the risk for the onset of incident dementia.

Methods: Our analyses are based on claims data of the public health insurance fund AOK. Data include information of inpatient and outpatient diagnoses and treatment from 2004 to 2011. Inclusion criteria comprised the initial absence of dementia and age of 75 years or older in 2004. Anticholinergic drugs were taken from three anticholinergic risk lists. The PDSP-database and literature search were used to define K_i-values for the substances. Hazard ratios were calculated using time-dependent Cox regression including covariates like age, gender, and several comorbidities.

Results and Conclusion: Anticholinergic drug exposure increases the risk for dementia. We found that anticholinergics with small K_i-values are at a higher risk than those with greater K_i-values. Furthermore, conventional risk factors for dementia (e.g. age, depression, stroke) could be confirmed.

In conclusion, the intake of anticholinergic drugs increases the risk for incident dementia in the elderly. Taking into account the M₁ receptor affinity may be a contribution in determining the anticholinergic load in view of the risk for incident dementia.

334

Safety signal detection in a large german statutory health insurance database - first results of a feasibility assessment

F. Andersohn^{1,2}, S. Schmiedl^{3,4}, K. Janhsen^{3,5}, P. Thuermann^{3,4}, J. Walker^{6,7}

¹Charité – Universitätsmedizin Berlin, Institute of Social Medicine, Epidemiology and Health Economics, Berlin, Germany

²Frank Andersohn Consulting & Research Services, Berlin, Germany

³Witten/Herdecke University, Department of Clinical Pharmacology, School of Medicine, Faculty of Health, Witten, Germany

⁴HELIOS Clinic Wuppertal, Philipp Klee-Institute for Clinical Pharmacology, Wuppertal, Germany

⁵Hochschule für Gesundheit, Bochum, Germany

⁶Elsevier GmbH, Munich, Germany

⁷Health Risk Institute GmbH, Berlin, Germany

Background: During the last years, approaches to routinely screen health care databases based on electronic medical records or claims to identify drug safety signals were proposed. To evaluate the performance of such methods, reference sets of index drugs have been compiled consisting of (1) drugs with a known association to a certain adverse event (=positive controls) and (2) drugs without any evidence to cause this adverse event (=negative controls). The best possible signal detection method would identify a safety signal for 100% of the positive control drugs, and for none of the negative controls. Ryan et al. 2013 developed drug reference sets for four adverse events of interest (acute myocardial infarction=AMI, acute kidney injury =AKI, acute liver injury=ALI, and upper gastrointestinal bleeding=UGIB) and have shown feasibility of using these reference sets in US health care databases. If the use of these US specific drug lists for evaluation of signal detection methods is also feasible within German health care databases, is unknown.

Aims: To evaluate if the drug reference sets developed by Ryan et al. (Drug Saf. 2013;36 Suppl 1:S33-47) could be used for testing signal detection methods in a large German statutory health insurance database.

Methods: Data source was the Health Risk Institute (HRI) database, an anonymized healthcare database with longitudinal health insurance data from approximately six million Germans. New users (initiators) of index drugs in 2010 to 2013 were identified and followed-up for one year from their first prescription. Exposed person-time to the respective index drug was assessed to estimate for which of these drugs an increase in risk of 50% (relative risk 1.5) compared to the background incidence of the respective adverse event (AMI, AKI, ALI or UGIB) could be identified with 80% statistical power.

Results: From a total of 182 index drugs in the reference sets of Ryan et al., 142 (78.0 %) were also available on the German drug market and were used by at least one insured in the HRI database during the study period. A total of 5,485,722 index drug initiators were included in the analysis. For a total of 16 index drugs, a relative risk of 1.5 could be detected with 80% power. The numbers of index drugs for each of the

outcomes of interest were: AMI (3 positive controls; 6 negative controls); AKI (3 positive controls; 1 negative control); UGIB (2 positive controls; 1 negative control). As the background incidence of ALI was low, no positive or negative control with sufficient power was identified for this outcome.

Conclusions: Using the set of reference drugs proposed by Ryan et al., the number of drug-event pairs with 80% power to detect a relative risk of 1.5 was low, despite the magnitude of the database used. This may be attributable to differences of drug exposure in Germany and the US. Hence, an adaptation of the drug list to the German drug market and consumption data might be relevant for future evaluations of signal detection methods using German databases.

335

Correlation of Sativex™ doses to steady state concentrations of 11-nor-9-carboxy- Δ^9 -tetrahydrocannabinol in urine samples of patients with multiple sclerosis

R. Birke¹, S. Meister², A. Winkelmann², **U. I. Walther¹**

¹Universitätsmedizin Rostock, Institut für Toxikologie und Pharmakologie, Rostock, Germany

²Universitätsmedizin Rostock, Klinik und Poliklinik für Neurologie, Rostock, Germany

Administration of the oromucosal spray Sativex™ represents a therapy option for treatment of spasticity in patients with multiple sclerosis. Sativex™ is an extract containing equal amounts of the Cannabis-derived cannabinoids Δ^9 -tetrahydrocannabinol (THC) and cannabidiol (CBD). In cases of Cannabis abuse a long elimination half life of some THC metabolites is known. Therefore, in patients receiving Sativex™, the long elimination half life of these metabolites should allow a drug monitoring under conditions of steady state. Due to the fact that immunologically based methods for THC determination are very common in medical chemistry, a monitoring might be simply performed even in patients under Sativex™ therapy. In a preliminary observational study 11-nor-9-carboxy- Δ^9 -THC (THC-COOH) concentrations were measured with a commercial immunoassay in urine samples of 16 patients with multiple sclerosis obtaining Sativex™. In addition, THC-COOH, THC, CBD as well as the hydroxy metabolites of THC and CBD were measured by GC/MS in urine and blood samples. Using this analytical technique, only an excessive dosing (as compared to the declaration by the patient) can be detected. As a result of this approach, THC-COOH concentrations determined by the immunoassay were found not to correlate to the daily applied amount of Sativex™ as indicated by the patients (Spearman rang order test: $p > 0.05$). Two patients mentioned not to have taken Sativex™ on the day the samples had been taken, and one patient predicated an additional Cannabis abuse. In three patients the immunological THC-COOH determination was negative or nearly negative. Interpretation of the data is hampered by the fact that an incorrect declaration of Sativex™ applications by the patients cannot be excluded.

Pharmacology – Education

336

Development and validation of a learning analytics platform in undergraduate medical education of pharmacology

F. Kühbeck¹, P. Berbera², S. Engelhardt¹, **A. Sarikas¹**

¹Technische Universität München, Institut für Pharmakologie und Toxikologie, Muenchen, Germany

²Technische Universität München, TUM MeDICAL Center of Medical Education, Muenchen, Germany

Introduction: Learning analytics seeks to enhance the learning process through systematic measurement and analysis of learning related data to provide informative feedback for students and lecturers. However, which parameters have the best predictive power for academic performance remains to be elucidated.

Objective: To analyze the potential of different learning analytics parameters to predict exam performance in undergraduate medical education of pharmacology.

Methods and results: Hypertext Preprocessor (PHP) as server-side scripting language was used to develop a learning analytics platform linked to a My Structured Query Language (MySQL) database for storage and analysis of data (www.tumanalytics.de). The database consisted of 440 lecturer-authored multiple choice questions that were made available to a cohort of undergraduate medical students enrolled in a pharmacology course (winter term 2014/15) at Technische Universität München (TUM). The course consisted of a 28-day teaching period, followed by a 12-day self-study period and a final written exam. Students' assessment data of TUManalytics was collected during the self-study period and correlated to the individual exam results in a pseudonymized manner. A total of 224 out of 393 (57%) students participated in the study. The coefficient of multiple correlation (R) was calculated for different parameters in relation to exam results as a measure of predictive power. Of different parameters investigated, the total score and the score of the first attempt in TUManalytics had the highest positive correlation with exam performance (Abb. 1). No sex-specific differences were observed.

Summary and Conclusion: In this study we systematically investigated the potential of different learning analytics parameters to predict learning outcome and exam performance. Total score and score of the first attempt were identified as parameters with the highest predictive power. In conclusion, our study underscores the potential of learning analytics as valuable feedback source in undergraduate medical education of pharmacology.

Abb. 1

Parameter	Female (N = 150)		Male (N = 74)	
	Correlation (R)	P-value	Correlation (R)	P-value
Login number	- 0.04	0.648	0.09	0.198
Question number	0.03	0.752	- 0.02	0.018
Total score	0.72	< 0.001	0.71	< 0.001
Score 1st attempt	0.71	< 0.001	0.77	< 0.001
Total Time	0.04	0.621	- 0.04	0.722
Time per question	- 0.16	0.057	- 0.25	0.034

337

Test-enhanced learning in the classroom: Evidence from pharmacological teaching

H. Teichert¹, A. Aslan², U. Gergs³, J. Neumann³

¹Center for multimedia teaching and learning, Martin Luther University Halle-Wittenberg, Halle (Saale), Germany

²Institute of Psychology, Martin Luther University Halle-Wittenberg, Halle (Saale), Germany

³Institute for Pharmacology and Toxicology, Medical Faculty, Martin Luther University Halle-Wittenberg, Halle (Saale), Germany

In educational settings, tests (e.g., written or oral exams) are usually considered devices of assessment. However, a recent and intriguing line of evidence from basic cognitive psychological research suggests that tests may not only help to assess what students know, but may also help to improve the learning and long-term retention of information. The goal of the present study was to apply such test-enhanced learning to pharmacological teaching. After the last lecture of a pharmacology class (n=194 3rd-year medical students, n=213 4th-year medical students: basic or clinical pharmacology, respectively), one week prior to the final exam, students were given the opportunity to voluntarily participate in online exam. Because pilot work from previous semesters had revealed relatively low levels of participation in such formative exams, students were offered bonus points for (successful) participation as an incentive. The online exam consisted of 60 items (i.e., selected pieces of information from the lectures and seminars) and was provided on the E-Learning platform ILIAS. Twenty of the 60 items were presented as statements for restudy, 20 items were tested using single-choice questions, and 20 items were tested using short-answer questions. Randomly a third of the students were assigned to different sets of questions. The summative final written exam for each group consisted of 30 single-choice questions, 15 questions of which had not been used before (as a standard of comparison). The remaining 15 questions of the final exam were taken from the previous online exam, but were slightly reworded to avoid ceiling effects. Each of 5 of these reworded 15 questions from the final exam corresponded to restudy items, single-choice items, and short-answer items from the online exam, respectively. The main points of interest were (i) whether the re-processing (rewording and asking for transfer of knowledge) of information in the online exam affected participants' performance on the final exam, and (ii) whether any effect depended on the specific type of re-processing (restudy vs. single-choice test vs. short-answer test). If previous findings from basic cognitive psychological research on test-enhanced learning can be generalized to more applied settings and educationally more relevant materials such as pharmacological information, students' performance in the final exam should be better for questions corresponding to previously tested items than for questions corresponding to previously restudied items. Moreover, if more difficult tests lead to more test-enhanced learning than less difficult tests, as is suggested by recent findings from cognitive psychological research, performance for questions corresponding to (supposedly more difficult) short-answer items should even exceed that for questions corresponding to (supposedly less difficult) single-choice items. The present findings bear direct implications for educational practice.

338

PharmaFrog: Pharmacology learning mobile app

M. Frensch¹, K. Brüll¹, C. Collins², M.- A. Flohr³, J. Greif⁴, S. Hahn¹, I. Krämer², **D. Schütz¹**

¹Universitätsmedizin der JGU, Institut für Pharmakologie, Mainz, Germany

²Apotheke der Universitätsmedizin, Mainz, Germany

³Applikationsentwickler Marc-Anton Flohr, Mannheim, Germany

⁴Opoloo, Mainz, Germany

Safe and rational prescribing is one of future physicians' key skills [1]. In order to address the persisting prescribing deficiencies [2], we set out to develop a learning tool for pharmacotherapies of the most important diseases worldwide. The format, scope, information architecture, and functionalities of the app were identified through assessment of existing apps, literature analysis, app simulation-based student surveys, and expert advice.

A fully functional offline app format for smartphones was selected based on the trends in using digital technologies for educational purposes [3] and on the unreliable internet and power availability in many learning settings. A relational database based on semantic relationships was chosen to minimize information redundancy and to enable the retrieval of drug-related information in the context of mechanisms, contra- and indications, adverse drug reactions, interactions, and common prescribing situations. The usability was optimized using a simulation of the app evaluated by medical students from Germany and Tanzania, and by experts.

A list of 67 indications was assembled beginning with disease burden data for the seven WHO World Bank regions. Each disease accounts for at least 0.3% of life years lost due

to premature death or lived with ill-health or disability (DALY) in at least one region. The list was further complemented according to expert recommendations. Therapeutic recommendations are based on current guidelines, considering cheaper treatment alternatives provided in the WHO List of Essential Medicines.

A novel dual-scale classification system lists drug mechanisms according to the affected physiological process and to the resulting therapeutic effect^[4]. Contraindications, adverse drug reactions, and interactions were compiled using drug monographs of the European Medical Agency, the US Food and Drug Administration, and Health Canada. Unexpectedly, we found significant differences among these sources in respect of adverse drug reactions. This necessitated the ongoing verification through surveying general practitioners and specialists in internal medicine.

During the DGPT meeting we will present the results of testing of the cardiovascular section comprising 8 indications, 28 drugs representing 25 mechanisms, and up to 120 adverse drug reactions.

Supported by Gesellschaft für Internationale Zusammenarbeit and a MAICUM (Mainzer Curriculum Medizin) grant of the University Medical Center Mainz.

[1] H. Nazar et al. Teaching safe prescribing to medical students: perspectives in the UK, *Adv Med Educ Pract*. 2015

[2] Dornan, T., et al. An in-depth investigation into causes of prescribing errors by foundation trainees in relation to their medical education: EQUIP study. London: General Medical Council 1-215, 2009

[3] Harris Interactive National Report: College Students. 2014. Reviewed on 11.13.2015 from Pearson: <http://www.pearsoned.com/wp-content/uploads/Pearson-HE-Student-Mobile-Device-Survey-PUBLIC-Report-051614.pdf>

[4] S. Zhao et al. Systems Pharmacology: Network Analysis to Identify Multiscale Mechanisms of Drug Action, *Annu Rev Pharmacol Toxicol*. 2012

339

Certification within the EPHAR/EACPT European Certified Pharmacologists Programme: the Austrian example

T. Griesbacher^{1,2,3}

¹Medizinische Universität Graz, Institut für Experimentelle und Klinische Pharmakologie, Graz, Austria

²Federation of European Pharmacological Societies, Milano, Austria

³Austrian Pharmacological Society, Vienna, Austria

The European Certified Pharmacologists (EuCP) Programme was launched in July 2014 by the Federation of European Pharmacological Societies with the intention to identify experts in the field of pharmacology whose competency profile, in addition to their personal specialised scientific expertise, covers expert knowledge in all major fields of the discipline. Seventeen EPHAR member societies have declared their active participation in the EuCP programme so far (Austria, Croatia, Czech Republic, Finland, France, Germany, Greece, Hungary, Italy, the Netherlands, Norway, Poland, Portugal, Serbia, Slovenia, Spain, Turkey). EACPT, the European Association of Clinical Pharmacology and Therapeutics, has also recently decided to participate in the EuCP Programme.

National programmes must meet all requirements of the EuCP Guidelines including a clear catalogue of criteria with respect to knowledge, practical awareness and skills, as well as general rules including rules for final assessment of candidates. Such programmes may be based on existing diplomas or training schemes or may consist of a set of rules how applicants may submit credentials for their expertise with respect to the EuCP criteria.

So far, three EPHAR member societies have submitted a national EuCP program: Austria, Italy and the Netherlands. The programmes differ in structure and reflect the flexibility of the EuCP Programme with respect to the respective national conditions. While the Italian programme is based on a catalogue of criteria where applicants have to certify and document their expertise on the basis of this catalogue and the Dutch program is based on a structured PhD training course, the EuCP scheme submitted by the Austrian Pharmacological Society APHAR is based on the legally regulated diploma Medical Specialist (Facharzt) in Pharmacology and Toxicology (APHAR also plans to submit separate regulations for specialists in clinical pharmacology and for non-medically qualified pharmacologists).

The APHAR EuCP scheme has been approved by the EuCP Committee in November 2015 and its regulations are available on the EuCP website (www.euCP-certification.org). The differently structured programs of the Italian and Dutch Pharmacological Societies will also be available at this website, once approved by the EuCP Committee and may thus serve as 'case studies' for other EPHAR and EACPT member societies wishing to take part in the EuCP Programme.

340

Teaching Pharmacovigilance: the WHO-ISO-P Core Elements of a Comprehensive Modular Curriculum

J. Beckmann¹, U. Hagemann²

¹WHO Expert Advisory Panel on Medicine Safety, Berlin, Germany

²International Society of Pharmacovigilance, Berlin, Germany

Introduction: The outstanding importance of pharmacovigilance (PV) for the safe use of medicines has increasingly been recognised during recent years. The multidisciplinary character of PV requires know-how in topics as different as pharmacology, clinical medicine, pharmacoepidemiology, information technology, pharmaceutical manufacturing, legal aspects, public health policies, and medical traditions in different regions of the world. In this complex situation there is a growing need for PV capacity building, in particular by professional training through high quality PV courses with different focuses and different levels of detailing. Against this background, the World Health Organization (WHO) and the International Society of Pharmacovigilance (ISO-P) have co-operated to create a curriculum for teaching PV which can be used for a wide range of audiences and in very different settings and situations. The purpose was to provide an inventory and systematically structured overview of PV including recent developments of topics like pharmacogenomics, consumer reporting of ADRs, risk management and WHO-led international projects, and to propose a range of tasks for practical training.

Methods: We made use of several relevant already existing packages of PV topics and concepts of PV teaching from national and international institutions. We also drew from extensive printed material as well as comprehensive reviews, textbooks and guidelines developed by international organisations which are often available online.

Results: The curriculum includes a main component consisting of a major part for theoretical lecture-based training and a minor component with suggestions for hands-on exercises. The theoretical part has a three-level hierarchical and modular structure with evenly divided tiers. There are 15 chapters. Each of them is divided into four sections and each section into four to six sub-sections. The practical part consists of twelve times three or four proposals for practical tasks which are related to the theoretical lectures.

Since its launch in 2014¹ it has successfully been used in several international courses. Currently a pilot project is under way to explore its use for 'crowd sourcing': it is placed on the ISO-P homepage with a programme allowing for institutions or persons experienced in PV teaching to upload any relevant presentations they may have with a link to related chapters, sections or subsections. These presentations will be offered for downloading by interested users.

Conclusions: The curriculum provides a comprehensive coverage of almost all areas of PV. The structure and content allows almost every kind of focusing on specific issues and going into depth, while maintaining the overall context. It offers opportunities of tailoring courses specifically to the needs of different audiences and can be applied to various forms of training, such as broad, comprehensive and intensive courses, short overviews or focuses on specific narrow topics in perspective.

Reference: 1. Beckmann J, Hagemann U, Bahri P et al. Teaching pharmacovigilance: the WHO-ISO-P core elements of a comprehensive modular curriculum. *Drug Saf*. 2014;37:743-759.

Toxicology – Risk assessment

341

Waiving of information requirements for high tonnage chemicals under reach

A.-K. Müller¹, D. Sittner¹, A. Springer¹, H. Herrmann², U. Herbst¹, A. Schulte¹

¹Federal Institute for Risk Assessment, Department of Chemicals and Product Safety, Berlin, Germany

²Department of Environment and Energy, Hamburg, Germany

According to the REACH Regulation (EC) No. 1907/2006 chemicals produced, marketed or used within the European Union have to undergo a registration process, wherein the registrants have to provide information on hazard and potential risks presented by the substances. However, the standard information requirements defined in Annexes VII to X of the regulation might be waived or adapted by the registrants if adequate documentation and justification according to criteria specified in Annexes VII to XI are provided.

To evaluate the data availability in registration dossiers of high tonnage substances (above 1000 tpa) and their compliance with the REACH Regulation, the Federal Institute for Risk Assessment (BfR) in cooperation with the Federal Environment Agency (UBA) developed a systematic web-based scheme. In total, 1932 dossiers were checked for selected human health and environmental endpoints such as repeated dose toxicity, genetic toxicity and ecotoxicity. A remarkable high rate, 43% to 82 % depending on the endpoint, of the evaluated dossiers included waiving or adaptations from the standard information requirements. Therefore, those dossiers were not concluded, but categorised as 'complex' (Springer et al., 2015).

The use of waiving and adaptations in 'complex' endpoints were part of a follow-up project. Herein, it was evaluated whether the given justifications were in accordance with the criteria set out in the respective REACH Annexes. The results will show the frequency and pattern of waiving/adaptation approaches for the human health as well as the environmental endpoints. Besides this general overview, specific problems regarding the application of the REACH Regulation were identified and their significance with regard to remaining data gaps will be discussed.

References: Andrea Springer, Henning Herrmann, Dana Sittner, Uta Herbst, Agnes Schulte. REACH Compliance: Data Availability of REACH Registrations, Part 1: Screening of chemicals > 1000 tpa. Dessau-Roßlau: Umweltbundesamt, 2015. ISSN 1862-4804.

342

N,N-Dimethylformamide (DMF), a high dose carcinogen

K. Ziegler-Skylakakis¹, **G. Schriever-Schwemmer**², H. Greim¹, A. Hartwig²

¹Karlsruhe Institute of Technology, Institute of Applied Biosciences, Permanent Senate Commission for the Investigation of Health Hazards of Chemical Compounds in the Work Area, Freising-Weihenstephan, Germany

²Karlsruhe Institute of Technology, Institute of Applied Biosciences, Permanent Senate Commission for the Investigation of Health Hazards of Chemical Compounds in the Work Area, Karlsruhe, Germany

The German Commission for the Investigation of Health Hazards of Chemical Compounds in the Work Area has re-evaluated dimethylformamide, and classified it in the Carcinogen Category 4. This category is for chemicals with carcinogenic potential for which a non-genotoxic mode of action is of prime importance and genotoxic effects play no or at most a minor part provided the MAK and BAT values are observed. Under these conditions no contribution to human cancer risk is expected.

DMF was identified as a Substance of Very High Concern by European Commission. The amount of DMF manufactured and/or imported into the EU is, in the range of 10000-100 000 t/y.

N,N-Dimethylformamide is a hepatotoxin in humans and rats. The carcinogenicity studies in both mouse and rat were conducted with test material of an acceptable purity and physical form. The critical study involved administration of DMF via inhalation, which is relevant to human exposure. There is conclusive evidence that DMF induces significant increases of hepatocellular carcinomas in rats after exposure to 800 ml/m³ and in mice in response to 200 ml/m³ and higher. Several in vitro and in vivo studies have indicated that DMF is not genotoxic. The results of the long-term studies reveal that the tumors develop in the liver only after chronic toxic inflammatory and degenerative changes have developed in this organ. The Commission concluded that

the tumors are a result of chronic liver damage, occurring at high exposure concentrations. The available evidence therefore suggests that there is a threshold dose for the carcinogenic effects of DMF. Accordingly, DMF was classified in Carcinogen Category 4 with a MAK-value of 5 ml/m³, an exposure concentration which does not induce liver toxicity and as a consequence is not associated with an increased cancer risk.

343

Does radiofrequency radiation induce effects in human hematopoietic stem cells?

H. Hintzsche¹, K. Taichrib¹, M. Rohland², T. Kleine-Ostmann², T. Schrader², H. Stopper¹
¹Institut für Pharmakologie und Toxikologie, Würzburg, Germany
²Physikalisch-Technische Bundesanstalt, Braunschweig, Germany

Today, a large majority of people is constantly exposed to electromagnetic radiation. Many studies have been performed to investigate whether this type of radiation has a potential to affect biological systems at low intensity levels. Even though no complete consensus has been reached so far in this issue, most of the investigations do not indicate a harmful potential of this radiation. Two questions remain open until today, i. e. long-term effects and specific effects on children. It has been demonstrated that in comparison to adults, children absorb far higher doses of mobile phone radiation in the skull, particularly in the bone marrow, where hematopoiesis takes place. These absorptions occasionally exceed the recommended safety limits. The aim of this study was to elucidate, whether cells of the hematopoietic system can be affected by different forms of mobile phone radiation.

As biological systems, two cell types were investigated, HL-60 cells as an established cell line, and human hematopoietic stem cells. The radiation was modulated according to the two major technologies, GSM (900 MHz) and UMTS (1950 MHz). Additionally, LTE (2.535 MHz) modulation was applied because this technology is used worldwide already but has not been studied sufficiently. Cells were exposed for a short and a long period and with different intensities ranging from 0 to 4 W/kg. Studied endpoints included oxidative stress, differentiation, DNA repair, cell cycle, DNA damage, histone acetylation, and apoptosis. Appropriate negative and positive controls were included and three independent replicate experiments were performed. Exposure to radiofrequency radiation did not induce any alterations of cell functions, measured as oxidative stress and cell cycle. Cell death in the form of apoptosis was not observed. Primary DNA damage was not induced and DNA repair capacity for nucleotide excision repair was not changed. Epigenetic effects (measured as histone acetylation) were not observed. Finally, differentiation was not affected. The effect of treatment with various chemicals as positive controls was different in the two cell types. All in all, mobile phone radiation did not induce effects on human hematopoietic cells.

344

New WHO guidance on uncertainty in hazard characterization – A unified tiered approach integrating deterministic and probabilistic methods

M. Herzler¹, W. A. Chiu², W. Slob³
¹Federal Institute for Risk Assessment (BfR), Chemicals and Product Safety, Berlin, Germany, Germany
²Texas A&M University, Veterinary Medicine & Biomedical Sciences, College Station/TX, USA, Vereinigte Staaten von Amerika
³National Institute for Public Health and the Environment (RIVM), Nutrition, Prevention and Health Services, Bilthoven, The Netherlands, Niederlande

In 2014 WHO published guidance on evaluating and expressing uncertainties in human health hazard characterisation (HC). In this approach, the outcome of HC is expressed as an interval or distribution rather than a „traditional“ deterministic point estimate, such as a Reference Dose (RfD), thereby communicating potential uncertainties more clearly. Risk management protection goals, such as the acceptable magnitude of effect (M) and incidence (I) in the population, are made explicit quantitatively along with the confidence with which they are achieved, e.g. by an RfD.

Specifically, the goal of this approach to HC is to estimate the „HD_{M,I}“, i.e. the „true“ human dose associated with M and I (e.g. body weight decreased by ≥ 10% (M) in 5% (I) of the population). If uncertainties are expressed by providing estimates of the HD_{M,I} as confidence intervals or uncertainty distributions, both the „degree of uncertainty“ (ratio of upper and lower limit of the interval/relevant distribution segment) and the „coverage“ (statistical confidence) associated with a given RfD value can be characterised. Alternatively, one may start from a chosen coverage and calculate the associated „probabilistic RfD“.

Uncertainty in each HC aspect, e.g. inter-/intraspecies or time extrapolation, can be characterised by a „Generic Default Uncertainty Distribution“ which has been derived from historical data, but may be replaced by a substance- or effect-specific distribution (analogous to a chemical-specific adjustment factor in the „traditional“ deterministic approach), where available.

The uncertainty distributions for the individual HC aspects can then be combined into an overall uncertainty interval/distribution in (1) a simple non-probabilistic way, (2) a more refined „Approximate Probabilistic Analysis“ (APROBA, a free spreadsheet tool for easy implementation also by non-statisticians is available from the WHO website), or (3) a fully probabilistic Monte Carlo analysis. The HC aspects contributing most to overall uncertainty are also identified and may be prioritised for refinement in a next assessment tier.

The WHO approach uses a tiered strategy which may start with evaluating the uncertainties in the outcome of a „traditional“ deterministic HC. In this way it represents a unified framework integrating deterministic and probabilistic HC methodologies. Moreover, the concept can be easily combined with exposure uncertainty assessment. Risk managers may use the additional information in better weighing potential health effects against other interests. When they consider the overall uncertainty larger than desirable in view of the problem formulation, they may decide to ask for a more refined (higher tier) assessment. If all possibilities for refinement are exhausted, the new approach can also aid in the selection of new data which might need to be generated.

WHO (2014): Guidance on Evaluating and Expressing Uncertainty in Hazard Assessment. Harmonization Project Document 11. World Health Organization, International Programme on Chemical Safety, Geneva, Switzerland
 Chiu WA & Slob W (2015): A Unified Probabilistic Framework for Dose-Response Assessment of Human Health Effects. EHP, Advance Online Publication 22 May 2015, DOI: 10.1289/ehp.1409385

Abb. 1

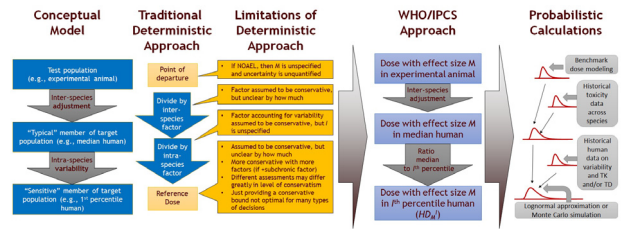
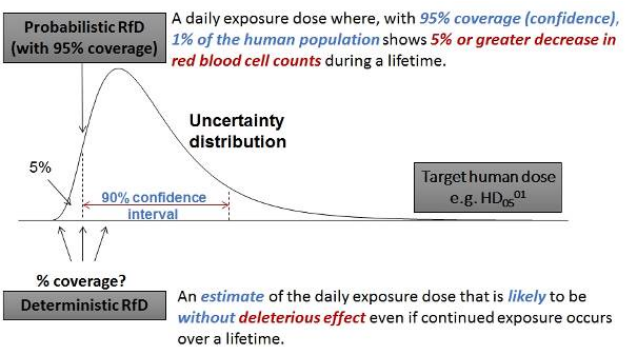


Abb. 2



Target human dose	Probabilistic RfD	Deterministic RfD
HD	“daily exposure dose”	“daily exposure dose”
M (magnitude)=5%	“5% or greater decrease in red blood cell counts”	“deleterious effect”
I (incidence)=1%	“1% of the human population”	“likely...without” (in the sense of variability)
Uncertainty	“95% coverage (confidence)”	“estimate...likely” (in the sense of uncertainty)

345

ToxBox – a new approach for evaluating anthropogenic trace substances in drinking water

A. Eckhardt¹, T. Grummt¹, M. Kramer², T. Braunbeck³, H. Hollert⁴
¹Umweltbundesamt, Toxikologie des Trink- und Badebadeschwassers, Bad Elster, Germany
²RheinEnergie, Wasserlabor, Köln, Germany
³Universität Heidelberg, Centre for Organismal Studies, Heidelberg, Germany
⁴RWTH Aachen, Institut für Umweltforschung, Aachen, Germany

Due to a constant improvement in analytical methods an increasing number of substances are found in drinking water. The joint project ToxBox aimed for the development of a reliable test battery, allowing for a rapid evaluation of single substances in water. Eleven partners either from the research (nine) or the business sector (2) formed the project. The attention was focused on genotoxic, neurotoxic and endocrine effects, which are considered to be of most concern to the consumer. By the end of the project a set of guidelines is published that describes the analytical methods in detail.

The project was based on a theoretical concept, called “Health-related indicator value” (HRIV), which was developed by the German Federal Environment Agency (UBA) for the assessment of substances with incomplete toxicological data. Depending on the type of effect a HRIV between 0.1 and 3.0 µg/laws derived for the substance which had to be evaluated. During the years an increasing amount of substances as well as an increase in finds was observed in drinking water. This called for the creation of an evaluation scheme that offers rapid and at the same time reliable evaluations of chemicals for which there are no data available. The concept is in accordance with Tox21, which envisages the trustworthy evaluation of relevant endpoints by two or three in vitro assays. In the context of ToxBox this was provided for the endpoints genotoxicity, neurotoxicity and endocrine effects. In all cases a hierarchic strategy is applied that enables a first assessment via relatively simple test assays and only when these test give a hint towards an effective more elaborate techniques are applied for a final assessment.

The Ames test and micronucleus assay in combination with the Umu test will form the panel for genotoxicity testing. Neurotoxicity will be assessed by comparing necrotic and apoptotic effects as well as the development of reactive oxygen species in human nervous cell with human liver cells. Additionally neuron specific assay like the Neurite Outgrowth Test are performed. This is complemented by measuring the activity of acetyl choline esterase activity and the development of the side line organ in zebra fish (*Danio rerio*). The test battery for endocrine effects consists of hormone specific reporter gene

assays in addition to the H295R assay. When necessary a reproduction assay in the mud snail *Potamopyrgus antipodarum* is carried out. During the project some 60 substances were evaluated. This allowed for the development of a reliable test strategy. Currently the guidelines for performing the required tests are in the making. Funding: This project was funded by the German Federal Ministry for Education and Research, grant number 02WRS1282A

346

Quality control in metabolomics: Paving the way to regulatory acceptance

S. Sperber¹, E. Fabian¹, M. Frericks¹, M. Herold², G. Kennrich¹, R. Looser², W. Mellert¹, E. Peter¹, T. Ramirez¹, M. Spitzer², V. Strauss¹, A. Strigun², T. Walk², H. Kamp¹, B. van Ravenzwaay¹
¹BASF SE, Ludwigshafen, Germany
²metanomics GmbH, Berlin, Germany

Metabolomics has gained increasing interest over the last years with numerous possible applications ranging from strain optimization for industrial production over drug discovery to improved toxicity testing. However, regulatory acceptance of this promising approach is still not reached, mostly because standardization and evaluation of reproducibility are still mostly lacking.

The MetaMap@Tox database has been developed by BASF over the last ten years containing toxicity and metabolome profiles of more than 750 different compounds. To ensure maximum reliability, data was gained from plasma samples of highly standardized 4 week rat studies. Animal maintenance and treatment, sampling and work-up of plasma, measurement of the metabolome as well as data interpretation and storage were standardized including thorough documentation, the compliance with SOPs and safe data storage.

Data from more than 80 control groups with each 10 males and females were analyzed to assess variability. An in depth analysis of this showed a high stability and robustness of the metabolome over a period of ten years. After artificially splitting the groups of 10 control groups into groups of five animals and comparing the number of statistically significantly regulated (false positive) metabolites, the peak of the distribution curve was located to the left of the exact (gaussian) center, but tailed off to the right more than expected under the normal distribution. From this analysis we were able to calculate density distributions (relative ratio and standard deviation) for the control values of each metabolite, which can serve as a historical control displaying the range of changes which can be expected as normal.

During the course of our project we have used more than ten exact repeats to show reproducibility and reliability of the metabolome analysis (Kamp et al., 2012). Comparing these exact repeats at different levels of statistical significance, we noted that at a level of statistical significance of approximately $p = 0.1$, the best balance between matches (metabolites regulated in the same direction) and mismatches (metabolites regulated in opposite directions) was obtained.

The high quality standards applied as well as the examination of control data increase the robustness of this approach, going also hand in hand with improved data quality. This significantly facilitates decision making based on the gained data. Due to these improvements a new level of transparency is reached, which might allow inclusion of metabolome data in a regulatory environment.

347

Hydroxycitric acid (HCA) in supplements intended for weight loss: Risk assessment regarding toxic effects on reproduction.

N. Bakhiya¹, K. I. Hirsch-Ernst¹, R. Ziegenhagen¹, A. Lampen¹
¹Bundesinstitut für Risikobewertung, Lebensmittelsicherheit, Berlin, Germany

Hydroxycitric acid (HCA) is a fruit acid naturally occurring in fruits of the tropical plant *Garcinia cambogia*. A number of dietary supplements intended for weight loss contain HCA, which is added in form of *G. cambogia* extracts. The composition of these extracts is often not clearly specified. Health concerns about safety of the HCA-containing supplements have been raised, based on results from animal studies, which observed toxic effects on the testes and on spermatogenesis after administration of preparations containing high HCA doses.

In the current risk assessment, the possible health risks associated with consumption of HCA-containing dietary supplements (HCA doses of approximately 1000 to 3000 mg per day) were evaluated based on relevant animal and human studies with the focus on testicular toxicity as a critical endpoint. In several published animal studies, repeated (short-term or subchronic) ingestion of certain HCA-preparations (*G. cambogia*-extract or Ca^{2+} -HCA salt) induced testicular atrophy (i. e. atrophy of seminiferous tubules, degenerative changes of Sertoli cells at histological examination) and impaired spermatogenesis (i. e. decreased sperm counts) in male rats at high doses (NOEL and LOEL of 389 and 778 mg HCA/kg body weight & day, respectively). Animal studies with other HCA-preparations (Ca^{2+} -HCA salt) found no such effects at the highest HCA-doses tested (NOEL: 610.8 mg HCA/kg bwt & day). Human intervention studies which addressed the safety of HCA in healthy test persons reported no substance-specific adverse effects after ingestion of HCA doses up to 3000 mg per day over the period of up to 12 weeks. However, the question of possible adverse effects of HCA on the human testes was not adequately addressed in studies with human volunteers. In a single clinical study with 24 male test subjects, no significant changes in endocrinologically relevant parameters such as serum inhibin B or FSH were observed after consumption of 3000 mg of HCA for 12 weeks. However, no investigations of direct parameters that might inform on potential effects on spermatogenesis, such as sperm quality and sperm count, were conducted in this study.

Considering the serious adverse effects on the testes observed in several animal studies as well as in view of lack of the adequate human data on the safety of the long-term use of HCA-preparations, it is concluded that knowledge gaps and substantial uncertainties exist regarding the safety with respect to human health of high amounts of HCA found in commercially available food supplements, particularly with regard to the human male reproductive system.

Toxicology – Methods

348

A critical look on the Passing-Bablok-regression

B. Mayer¹

¹Universität Ulm, Institut für Epidemiologie und Medizinische Biometrie, Ulm, Germany

Background: The Passing-Bablok (PB)-regression is a commonly used approach to prove the equality of different analytical methods when studying quantitative laboratory data. It is based on the assumption that the measurements of two methods are linearly related. If then one method is regressed onto the other and the respective confidence intervals of the intercept and the slope include 0 and 1, respectively, it is assumed to have a proof of methods equality. However, this conclusion is problematic in respect of an essential principle of statistical hypothesis testing.

Methods: In this talk the general idea behind the PB-regression is discussed critically. Although the method makes use of confidence intervals a decision is made, which is why it is important to discuss how the results of a statistical hypothesis test have to be interpreted. Moreover, alternative statistical approaches to investigate agreement in biometrical practice are pointed out by means of a practical example and their advantages and limitations are addressed.

Results: All approaches applied to a sample data set led to the same conclusions. Demonstrating methods equality though necessitates an a-priori definition of an appropriate equivalence margin.

Conclusion: The PB-regression may give useful advice when comparing two measurement methods towards equality. However, its results are statistically inconclusive, since the PB-method does not follow the principle of equivalence testing. Alternative measures of agreement should be applied instead to ensure results which are not attackable and serve as a statistical proof.

349

Determination of rat insulin in small volumes using an electrochemiluminescence-based 96-well plate assay

A. Freyberger¹, B. Krämer-Bautz¹

¹Bayer Pharma AG, GDD GED Toxikologie P & CP, Wuppertal, Germany

Insulin is an important parameter both in toxicology (toxicity to the endocrine pancreas) and pharmacology (models of diabetes and metabolic syndrome). Currently available ELISA and RIA methodologies for insulin often require up to 100 µl plasma or serum for a single measurement. In order to meet the general trend to include more relevant parameters in animal studies and restrictions through animal welfare requirements to limit the volume of interim blood draws we explored the rat/mouse insulin singleplex assay of Meso Scale Discovery (MSD) as an alternate assay consuming only 10 µl serum or plasma or less for a single measurement. The assay is a sandwich immunoassay, whereby insulin in the sample binds to the capture antibody immobilized on the working electrode surface at the bottom of each well and recruitment of the labeled detection antibody (anti-insulin labeled with electrochemiluminescent compound, MSD SULFO-TAG™ label) by bound analyte completes the sandwich. Voltage applied to the plate electrodes then causes the label bound to the electrode surface to emit light the intensity of which is a quantitative measure of insulin.

The MSD insulin assay was characterized by a robust calibration and only small variations within repeated measurements. The assay presented a broad dynamic range and differences in insulin levels of normal and rats suffering from metabolic syndrome could readily be demonstrated. Furthermore, the high sensitivity may even allow the use of smaller sample volumes. These features render this assay an attractive alternative for the measurement of insulin. The lack of corresponding quality control samples for internal quality control may be considered as a relative drawback. However, the cross reactivity of the assay with human insulin provides the opportunity to use QCs designed for human assays and to possibly participate in ring trials for human insulin for external quality control if needed.

Toxicology – Substances and compound groups

350

Demonstration of surfactant antagonism in Open Source Reconstructed Epidermis (OS-REp) models

R. Wedekind¹, A. Fischer¹, K. R. Mewes¹, O. Holtkötter¹

¹Henkel AG & Co KGaA, Düsseldorf, Germany

Surfactants are main constituents of different consumer products, e.g. detergents or cosmetic cleansing products. Since surfactants show an intrinsic skin irritation potential, dilutions are used in the final products to avoid adverse effects like irritant contact dermatitis from product use. In addition, mixtures of different surfactants are typically formulated, as it is a long-standing experience that those mixtures exhibit much lower acute irritation potential than expected from the mere summation of their individual irritation potential, an effect coined surfactant antagonism.

Only few studies were performed to gain a more fundamental understanding of the effect, and it's mechanistic basis remains unclear. However, a thorough understanding of the surfactant antagonism is not only of value for the formulation of products that are considered 'mild to the skin'. It is also important for the classification of products according to the CLP Regulation in cases when data of the mixtures is missing, because summation of the ingredients' irritating effects usually results in over-classification as skin irritant.

Due to the progress in the development of alternatives to animal testing, different in vitro methods have become available to determine skin irritating properties of substances. Methods like the OECD TG 431 and 439 especially aim at deriving a classification for skin irritation/corrosion effects according to the CLP Regulation. However, even though these methods became the preferred test methods for skin irritation testing, to our

knowledge hitherto isolated investigations on the surfactant antagonism were only performed either by human patch test studies or by non-standard *in vitro* assays. In this study, the irritation potential of binary mixtures of sodium dodecylsulfate (SDS), linear alkylbenzene sulfate (LAS), cocamidopropyl betaine (CABP) and alkylpolyglucosid (APG) compared to the single compounds was investigated using Open Source Reconstructed Epidermis (OS-REp) models. Combinations of SDS or LAS with CABP and APG, respectively, resulted in a clear decrease of the irritation potential compared to the irritation exerted by the single surfactants, even though the total surfactant concentration was higher in the mixtures. In addition, the effect of surfactant antagonism was also observed in a mixture of CABP and APG. The reduced irritation potential of mixed surfactants came along with both reduced skin penetration of fluorescein and reduced release of LDH. Since no surfactant antagonism is observed in monolayer cultures of keratinocytes that were exposed to mixtures of surfactants, it is assumed that keratinocytes in the viable parts of the reconstructed epidermis are promptly damaged by the surfactants once the model's barrier is destroyed. Hence, surfactant antagonism appears to be primarily driven by the mixture's lower ability to damage the skin model's barrier.

Toxicology – Genotoxicity

351

Applicability of the flow cytometry-based micronucleus test in RT4 bladder papilloma cells

F. Schwiering¹, S. Plöttner¹, M. Hagnia¹, T. Brüning¹, H. U. Käfferlein¹
¹Institut für Prävention und Arbeitsmedizin der Deutschen Gesetzlichen Unfallversicherung, Institut der Ruhr-Universität Bochum (IPA), Bochum, Germany

The micronucleus (MN) test is a reliable method for the detection of cytogenetic damage in proliferating cells. In recent years, substantial progress has been made on automated, thus faster and more objective scoring of MN test samples, i.e., methods based on flow cytometry. The aim of the present study was to use the adherently growing human bladder cancer cell line RT4 to carry out a comparison between traditional (fluorescence microscopy) and automated (flow cytometry) MN scoring. For this purpose, different substances which are known to be positive controls were used.

RT4 cells were either continuously incubated for 72 h (approximately 1.5 cell cycles duration) with methyl methanesulfonate (MMS; 50-200 µM), benzo[a]pyrene (B[a]P; 0.1-1 µM), vincristine (3-20 nM), and colcemid (10-20 nM) or cells were irradiated with X-rays (0.5-2 Sv) and then cultured for 72 h. For standard MN scoring, cells were harvested, subjected to hypotonic treatment, fixed with methanol/acetic acid, placed on glass slides, stained with acridine orange and observed by fluorescence microscopy. For the flow cytometric method, harvested cells were stained in two sequential steps. Intact cells were subjected to ethidium monazide bromide followed by photoactivation (75 W, 20 min) to label dead or dying cells. Then, cells were lysed and stained with SYTOX green for a pan-DNA labelling and analyzed on a flow cytometer.

Both, chemically- and radiation-induced treatment led to a dose-dependent induction of MN when evaluated by fluorescence microscopy. When the flow cytometry-based method was applied, clearly positive results including a dose-dependent induction of MN, however, were obtained only for 3 out of the 5 treatments (vincristine, colcemid and X-rays); whereas, treatment with MMS and B[a]P led to only minor increases in relative MN frequencies (≤2-fold), even at the maximum concentrations.

In summary, flow cytometry-based MN scoring has been successfully applied in RT4 cells. However, our initial results suggest that flow cytometry-based MN scoring is less sensitive than microscopic scoring when RT4 cells are used. So far, only few adherently growing cell lines have been applied to flow cytometry-based MN scoring. Further substances (positive and negative controls) and possibly other adherent cell lines need to be tested to expand our knowledge on the effectiveness of automated MN scoring *in vitro* and compared to traditional approaches.

352

Inhibition of cisplatin-induced DNA damage response (DDR) in rat renal proximal tubular epithelial cells (NRK-52E) by the lipid lowering drug lovastatin

K. Krüger¹, G. Fritz¹
¹Heinrich Heine Universität Düsseldorf, Institut für Toxikologie, Düsseldorf, Germany

Background: The platinating agent cisplatin is commonly used in the therapy of various types of solid tumors, especially urogenital cancers. Its anticancer efficacy largely depends on the formation of bivalent DNA intrastrand crosslinks, which impair DNA replication and transcription. These crosslinks stimulate mechanisms of the DNA damage response (DDR), thereby triggering checkpoint activation, gene expression and cell death. The clinically most relevant adverse effect associated with cisplatin treatment is nephrotoxicity, which mainly results from damaged tubular cells. Here, we analyzed the influence of the HMG-CoA-reductase inhibitor lovastatin on the cisplatin-induced geno- and cytotoxicity in the rat renal proximal tubular epithelial cell line NRK-52E.

Methods: Cell viability was determined by using the Alamar Blue assay, as well as by electrical impedance measurements via the iCELLigence system. Alterations in cell cycle progression were assayed by flow cytometric analysis. The formation of Pt-(GpG) intrastrand crosslinks was determined via Southwestern blot. The amount of DNA double-strand breaks (DSBs) was quantified by measuring the level of S139 phosphorylated H2AX (γH2AX) via immunocytochemistry as well as by Western blot. Additionally, neutral and alkaline Comet assays were performed to determine the amount of DNA single- and DNA double-strand breaks. Mechanisms of the DDR were analyzed by Western blot as well as by quantitative real-time PCR.

Results: The data show that pretreatment of NRK-52E cells with a subtoxic dose of lovastatin reduced the cytotoxicity evoked by high doses of cisplatin by protection from cisplatin-stimulated apoptotic cell death. Moreover, Lovastatin had extensive inhibitory effects on cisplatin-induced DDR, as reflected on the level of p-ATM, p-P53, p-CHK1, p-CHK2 and p-KAP1. Furthermore, activation of mitogen-activated kinases (MAPKs) was also reduced. The lovastatin-mediated mitigation of cisplatin-induced DDR was independent of the initial formation of DSBs as well as of Pt-(GpG) intrastrand crosslinks.

Conclusion: Lovastatin protects NRK-52E cells from cisplatin-induced cytotoxicity by interfering with proapoptotic mechanisms of the DDR independently from initial DNA damage formation. With respect to the clinic, the data indicate that lovastatin might be useful to mitigate cisplatin-induced nephrotoxicity.

353

The influence of oxidant tert-butylhydroquinone (tBHQ) on endothelial cell migration in WRN-deficient cells

K. Laarmann¹, G. Fritz¹
¹Institut für Toxikologie, Düsseldorf, Germany

Introduction: WRN is a DNA helicase and possesses a 3'-5' exonuclease and ATPase activity as well as a single strand annealing activity. It is involved in DNA repair, by interacting with proteins of base excision repair (BER) and nucleotide excision repair (NER). Defects of WRN are marked by genome instability which, in turn, is caused by defects in DNA damage repair. Patients with a mutation in the WRN gene show premature aging and early mortality. The latter is mainly caused by arteriosclerosis. Furthermore, WRN participates in the regulation of genotoxic stress responses stimulated by reactive oxygen species (ROS) and alkylating agents. The aim of this study was (i) to investigate whether endothelial cell migration and adhesion were effected by sub-toxic (IC₁₀) and moderate toxic (IC₄₀) concentrations of the oxidant tert-butylhydroquinone (tBHQ) and (ii) whether WRN influences migration and adhesion in the presence or absence of tBHQ.

Methods: Endothelial-like EA.hy926 cells were treated with different concentrations of the redox cycling and thus ROS producing oxidant tBHQ. Viability was measured by the Alamar Blue assay. IC₁₀ and IC₄₀ were determined after 24h permanent treatment. To investigate the influence of WRN on endothelial cell migration and adhesion, a WRN knock-down was performed in EA.hy926 cells using RNA interference. To measure migration, a confluent cell monolayer was scratched using a pipet tip, 24h after permanent tBHQ treatment. Pictures were taken at the time points 0h, 4h and 8h after performing the scratch. The non-closed area was measured. In a second part, adhesion of the calcein-labeled colon adenocarcinoma HT-29 cell line on the EA.hy926 monolayer was investigated. WRN-deficient or non-deficient cells were treated with 100 µM and 160 µM tBHQ or with TNFα.

Results: For EA.hy926 cells, 100 µM and 160 µM tBHQ were determined as IC₁₀ and IC₄₀, respectively. Performing the migration assay, EA.hy926 cells showed 75% gap closure, whereas WRN-deficient cells showed a closure of only 35% after 8h. The gap was closed of 65% and 55% after 100 µM and 160 µM tBHQ treatment. In WRN-deficient cells no remarkable effect on migration was observed after 100 µM tBHQ treatment, whereas the treatment with 160 µM tBHQ showed a slight decrease in migration of about 10% compared to WRN-deficient cells. No effect on adhesion was observed after TNFα treatment. After 160 µM tBHQ treatment a slight increase of adhesion was detected in EA.hy926 cells. The influence of moderate tBHQ concentration on adhesion was reduced in the absence of WRN.

Conclusion: WRN influences endothelial cell migration. In contrast to wild-type EA.hy926 cells, no significant effect of tBHQ was observed on migration of WRN-deficient cells. Furthermore, the moderate toxic concentration of tBHQ showed slightly increased HT-29 adhesion to EA.hy926, which was not found in WRN-deficient cells.

Outlook: In forthcoming studies we analyse the effect of alkylating agents on migration and adhesion. Data will be presented and discussed.

354

Sensitivity of different cell types of the hematopoietic system towards genotoxic agents

G. Kukielka¹, H. Hintzsche¹, H. Stopper¹
¹Institut für Pharmakologie und Toxikologie, Toxikologie, Würzburg, Germany

The aim of the present work was to compare the sensitivity of leukemia cell lines (HL60, Jurkat and TK6) and hematopoietic stem cells with regard to the response to genotoxic agents. Chromosomal damage was analyzed by evaluation of the micronucleus frequency. Furthermore, changes in the proliferation index and the frequencies of apoptotic and mitotic cells were assessed.

Several cytostatic drugs with different mechanisms of action were used as genotoxic agents. Doxorubicin was used as an intercalator, radical producer and topoisomerase II inhibitor. Also, the effects of vinblastine, a mitosis-inhibiting drug and of methyl methanesulfonate, which forms DNA-adducts and stalls replication forks, were analyzed. In general, a difference in sensitivity between the different substances was observed.

With regard to the formation of micronuclei after treatment with doxorubicin, Jurkat and TK6 cells showed similar increasing trends, whereas HL60 cells showed a much higher increase in micronucleus frequency. A clear decrease in proliferation and the frequency of mitotic cells was observed at the highest concentration (100 nM doxorubicin) investigated, and only a slight increase in the number of apoptotic cells could be shown. The biggest differences in formation of micronuclei could be detected after treatment with vinblastine. HL60 cells showed only a slight increase of micronuclei, but the effect on Jurkat cells was stronger. The highest micronucleus frequency after vinblastine treatment was detectable for the TK6 cells. The results for the highest investigated concentrations (31.6 nM and 100 nM vinblastine) showed a significant reduction of the proliferation index. This effect is reflected by the increasing numbers of apoptotic cells in all cell lines. The results for methyl methanesulfonate demonstrated only a small increase in micronucleus formation for the Jurkat cells, but higher values for the TK6 cells. In contrast the HL60 cells did not lead to a concentration-dependent effect with methyl methanesulfonate.

These results are complemented by preliminary findings in hematopoietic stem cells at selected compound concentrations. The different results between the leukemia cell lines and the stem cells might possibly originate from the different p53 status of HL60 (null), Jurkat (multiple mutations), TK6 (wild type) and hematopoietic stem cells (wild type). This difference might also cause differences in cell cycle control or repair mechanisms, and needs further investigations.

355

Metformin protects kidney cells from insulin mediated genotoxicity in vitro and male Zucker diabetic fatty rats

E. M. Othman¹, H. Stopper¹
¹Pharmakologie und Toxikologie, Toxikologie, Würzburg, Germany

Hyperinsulinemia is thought to enhance cancer risk. A possible mechanism is induction of oxidative stress and DNA damage by insulin. Here, the effect of a combination of metformin with insulin was investigated in vitro and in vivo. The rationale for this was reported antioxidative properties of metformin and the aim to gain further insights into mechanisms responsible for protecting the genome from insulin mediated oxidative stress and damage. Comet assay, micronucleus frequency test and a mammalian gene mutation assay were used to evaluate the DNA damage produced by insulin alone or in combination with metformin. For analysis of antioxidant activity, oxidative stress and mitochondrial disturbances, the cell-free FRAP assay, the superoxide-sensitive dye dihydroethidium and the mitochondrial membrane potential-sensitive dye JC-1 were applied. Accumulation of p53 and pAKT were analysed. As an in vivo model, hyperinsulinemic Zucker Diabetic Fatty rats, additionally exposed to insulin during a hyperinsulinemic euglycemic clamp, were treated with metformin. In the rat kidney samples, DHE staining, p53 and pAKT analysis, and quantification of the oxidized DNA base 8-oxodG was performed. Metformin did not show intrinsic antioxidant activity in the cell free assay, but protected cultured cells from insulin mediated oxidative stress, DNA damage and mutation. Treatment of the rats with metformin protected their kidneys from oxidative stress and genomic damage induced by hyperinsulinemia. Metformin may protect patients from genomic damage induced by elevated insulin levels. This may support efforts to reduce the elevated cancer risk that is associated with hyperinsulinemia.

356

Influence of commensal benzo[a]pyrene metabolism on skin UV-damage repair

L. Lemoine¹, A. Luch¹, T. Tralau¹
¹Bundesinstitut für Risikobewertung, Abteilung Chemikalien- und Produktsicherheit, Berlin, Germany

The human skin is the primary barrier against environmental and chemical impacts. As such it shields us against a plethora of xenobiotics such as potentially carcinogenic polycyclic aromatic hydrocarbons (PAHs). At the same time it is the second most densely populated organ, harbouring more than 1000 bacterial species and population densities of up to 10⁷ cfu per cm². Yet little is known about this microbiome's potential to metabolise and detoxify PAHs such as benzo[a]pyrene (B[a]P). Previous work at the BfR showed that degradation of B[a]P and other PAHs is a universal feature of the skin's microbiome (Sowada *et al.*, 2014). The corresponding metabolites only partly overlap with those known from eukaryotic metabolism and possess cytotoxic as well as genotoxic properties. Excretion of these metabolites will lead to exposure times of 20-30 hours or longer for full and partial metabolisers, respectively. While *in vitro* studies show the corresponding substances to exert their effects synergistically, an assessment of their potential impact on human carcinogenesis is pending. One obvious mode of action would be direct genotoxicity. However, another option is interference with UV-damage repair. Ultraviolet radiation (UVR) from sunlight is regarded the main causative factor for the induction of skin cancer. It induces two of the most abundant mutagenic and cytotoxic DNA lesions, that is cyclobutane-pyrimidine dimers (CPDs) and 6-4 photoproducts (6-4PPs). These lesions are repaired primarily by nucleotide excision repair (NER), a system that is also responsible for the removal of PAH-derived DNA adducts. We therefore wanted to know whether and to what extent bacterial B[a]P metabolites have the capacity to interfere with NER, potentially contributing to UV-induced DNA-damage. To investigate this selected genotoxic metabolites were examined for their potential to affect the DNA repair capacity of skin cells (HaCaT). Following treatment with UVA/B and bacterial B[a]P-metabolites the skin's repair capacity was assessed using a modified COMET-Assay.

Sowada J, Schmalenberger A, Ebner I, Luch A und Tralau T (2014) Degradation of benzo[a]pyrene by bacterial isolates from human skin. *FEMS Microbiol. Ecol.* 88: 129-139

357

Autophagy triggered by DNA double-strand breaks is restrained by protein kinase B/Akt

N. Seiwert¹, C. Neitzel¹, T. Frisan², B. Kaina¹, G. Fritz³, J. Fahrner¹
¹University Medical Center, Department of Toxicology, Mainz, Germany
²Karolinska Institute, Department of Cell and Molecular Biology, Stockholm, Sweden
³Heinrich Heine University, Institute of Toxicology, Düsseldorf, Germany

Ionizing Radiation (IR) is a well-established model to induce DNA double-strand breaks (DNA-DSBs), but it also generates a broad range of other DNA lesions including DNA single-strand breaks as well as oxidative DNA base modifications. Furthermore, IR is able to modify membrane components and triggers the activation of epidermal growth factor receptor. A more specific DSB-inducer is cytolethal distending toxin (CDT), which is produced by a variety of gram-negative bacteria and harbours an intrinsic DNase-like endonuclease activity [1]. DSBs are potent cytotoxic lesions and promote genomic instability, e.g. by formation of chromosomal aberrations. A cellular mechanism to prevent genomic instability and maintain cell homeostasis could be autophagy. This process is highly regulated involving the lysosomal degradation of damaged organelles and proteins. Here, we study autophagy induction following DSB generation in human colorectal cancer cells as well as in primary human colonic epithelial cells (HCEC) and analyzed regulatory mechanisms. First, the autophagy-specific marker LC3B was shown to increase in a dose- and time-dependent manner after treatment with both CDT and IR as assessed by confocal immunofluorescence microscopy and Western blot analysis in HCT116. Similar results were obtained in SW48 and HCEC cells via Western blot. These findings are in agreement with the enhanced formation of autophagosomes and

the dose-dependent decrease of the autophagy substrate p62 as observed by flow cytometry and Western blot analysis in HCT116, SW48 and HCEC. CDT- and IR-induced autophagy rates in HCT116 increased over time correlating well with the DSB induction. Importantly, a DNaseI-defective mutant of CDT did neither cause DSBs nor induce autophagy. Additionally, the time-dependent accumulation of the lysosomal associated membrane protein 1 (LAMP-1) was observed by confocal immunofluorescence microscopy. DSB-induced autophagy was blocked by chemical inhibitors. Next, we showed that both IR and, to a lesser degree, CDT induce the phosphorylation of Akt at Ser473. Pharmacological inhibition of Akt in HCT116 cells enhanced the CDT- and IR-induced autophagy shown by accumulation of LC3B and LAMP1 after 48 h and increased autophagosome formation. Upregulation of DSB-induced autophagy by Akt inhibition resulted in a decreased cytotoxicity after 72 h and significantly lower apoptosis/necrosis rates after 48 h, which were determined by MTS cell viability assay and Annexin-V/PI staining. Ongoing studies will evaluate the impact of other DNA damage response pathways and the potential protective role of autophagy against genomic instability.

[1] Fahrner et al. (2014) Cytolethal distending toxin (CDT) is a radiomimetic agent and induces persistent levels of DNA double-strand breaks in human fibroblasts, DNA repair, 18:31-43

358

Development of a mass spectrometric platform for the quantitation of mustard-induced nucleic acid damage

T. Zube¹, W. Burckhardt-Boer¹, A. Schmidt², D. Steinritz², A. Mangerich¹, A. Bürkle¹
¹University of Konstanz, Molecular Toxicology Group, Department of Biology, Konstanz, Germany
²Bundeswehr Institute of Pharmacology and Toxicology, Munich, Germany

Mustard agents are potent DNA alkylating agents. Among them, the bi-functional agent sulfur mustard (SM) was used as a chemical warfare agent due to its vesicant properties. Although the use of SM in warfare has been banned in most countries of the world, its use in terrorist attacks or asymmetrical conflicts, such as the Syrian civil war, still represents a realistic and significant threat. On the other hand, especially nitrogen mustards, such as cyclophosphamide or melphalan, have been used as chemotherapeutic agents due to their cytostatic properties. Thus, mustard-induced DNA damage, in particular DNA crosslinks, can trigger complex pathological states, as it is observed in sulfur mustard exposed victims, but on the other hand also lead to the chemotherapeutic effects of clinically-used nitrogen mustards. Mass spectrometric monitoring and quantitation of mustard-induced DNA adducts can help to unambiguously identify and verify SM-exposed victims and to monitor the efficiency, as well as potential side-effects of mustard-based chemotherapy.

Up to now, the verification of mustard-induced nucleic acid damage is mainly based on immunohistochemical methods, which have several drawbacks such as limited specificity, sensitivity, and low dynamic range of quantitation. With this project, we aim to develop a (HPLC/UPLC)-MS/MS-based platform for the quantitation of the most common mustard-induced DNA adducts including bis(N7-guanine-ethyl) sulfide DNA crosslinks. Up to date, we established methods for the quantitation of the several common DNA adducts induced by the mono-functional sulfur-mustard derivative 2-chloroethyl ethyl sulfide ("half mustard", CEES). For that reason purification protocols, chromatographic conditions and mass spectrometric settings were developed to detect N7-ethylthioethyl-2'-desoxyguanosine (N7-ETE-dG) and N3-ethylthioethyl-2'-desoxyadenosine (N3-ETE-dA) and their thermal hydrolysis products N7-ethylthioethyl-guanine (N7-ETE-Gua) and N3-ethylthioethyl-adenine (N3-ETE-Ade), respectively, and the sensitivity was compared to immunohistochemical methods. Additional non-radioactive isotope-labelled standards are being synthesized, which will be spiked into samples to account for technical variability during sample work-up and to improve MS-based quantitation. This procedure requires minimal cellular material and therefore should be transferred to quantitation of DNA adducts in human blood samples. This will allow to monitor DNA adducts as biomarkers of exposure in potential SM-exposed victims as well as in mustard-based chemotherapy. This method also sets a basis to investigate specific mustard-induced DNA repair mechanisms and their cellular consequences.

359

The γH2AX assay vs. comet assay for genotoxicity testing

T. Nikolova¹, M. Dvorak¹, A. Frumkina¹, B. Kaina¹
¹Universitätsmedizin Mainz, Institut für Toxikologie, Mainz, Germany

DNA damage leads to activation of the cellular DNA damage response (DDR). This signalling network results in activation of various DNA repair proteins and chromatin structure modulators. A frequent manifestation of DDR is the phosphorylation of histone 2AX (γH2AX), which can be visualised as γH2AX foci by immunocytochemistry. In the present study, we tried to assess if γH2AX is a reliable biomarker for detecting the cellular response to DNA damage. We selected 14 well-characterised genotoxic compounds and compared them with 10 non-genotoxic chemicals in the well-characterised CHO cell system. We measured quantitatively γH2AX by manual and automatic scoring of γH2AX foci, and by flow cytometry counting of γH2AX positive cells. The cytotoxicity dose-response was determined by the MTT cell proliferation/viability assay. We show that a) all genotoxic agents were able to induce dose-dependently γH2AX in the cytotoxic range whereas no induction was observed after treatment with non-genotoxicants; b) manual scoring of γH2AX foci and automated scoring gave similar results, with the automated scoring being faster and more reproducible; c) data obtained by foci counting and FACS analysis of γH2AX positive cells showed a significant correlation. Further we compared DNA damage induced by 4 selected genotoxins at the time-points using the alkaline and neutral comet assay. Significant correlation with the alkaline and neutral comet assay was observed for some but not all genotoxins and, predominantly, at earlier time points. We suggest that comet assays detect mainly primary DNA damage, whereas γH2AX assay detects a specific response to DNA damage which can persist longer. The γH2AX foci and flow-cytometry assays allow for a rapid and reliable determination of genetic damage in mammalian cells and can be used as additional genotoxicity assays.

Reference: Nikolova T., Dvorak M., Jung F., Adam I., Krämer E., Gerhold-Ay A., Kaina B. (2014) The γ H2AX Assay for Genotoxic and Nongenotoxic Agents: Comparison of H2AX Phosphorylation with Cell Death Response. *Toxicol Sci.* 140(1):103-17.

360

A multiplexed flow cytometric assay covering mechanistic biomarkers of genotoxicity- experience @Bayer

S. Wilde¹, M. Raschke¹, A. Sutter¹, N. Queisser¹, S. D. Dertinger², S. Bryce²
¹Bayer Pharma AG, Investigative Toxikologie, Berlin, Germany
²Litron Laboratories, New York, United States of America

Available in vitro methods to investigate the genotoxic potential of drugs fall short of throughput, specificity and mode of action information. A set of mechanistic biomarkers for clastogenic, aneugenic or apoptotic effects may help to overcome these limitations. Thus, a staining assay amenable to flow cytometric analysis is being developed by Litron Laboratories, Rochester, NY, supported by international collaborators. The experimental design of this assay consists of 3 stages. The objective of this work is the evaluation of this assay in the laboratories of Bayer Pharma AG.

The biomarkers covered by the assay are associated with DNA damage response pathways that have potential for class discrimination (clastogen/aneugenic/cytotoxicant) of in vitro genotoxicants: DNA double strand breaks (γ H2AX), nuclear division (phospho-H3, DNA content), apoptosis (cleaved PARP).

Based on the pilot work at Litron Laboratories, TK6 cells were introduced to the Genetic Toxicology of Bayer Pharma AG. Cells were exposed for 4 and 24 hrs in triplicates on a 96 microwell plate to one reference clastogen (etoposide, ETO), aneugen (vinblastine, VB) and cytotoxicant (carbonyl cyanide 3-chlorophenylhydrazone, CCCP). After staining, the samples were analyzed with the flow cytometer BD Accuri C6 (BD Biosciences, Heidelberg, Germany).

The reference substances yielded the responses expected from the pilot study at Litron Laboratories: VB showed distinct increases of phospho-H3 events at 4 and 24 hrs and polyploidy at 24 hrs time point. ETO induced a clear increase of γ H2AX with a simultaneous reduction of phospho-H3 at 4 and 24 hrs. Finally, CCCP caused a reduction of phospho-H3 events, increased cleaved PARP events and did not influence γ H2AX.

Moreover, benchmarking experiments under pilot work conditions were performed with high content imaging analysis. We compared γ H2AX and phospho-H3 pilot study results as well as cleaved PARP with Caspase 3/7. In addition, the TUNEL assay (Click-IT[®] TUNEL Alexa Fluor, ThermoFisher) was executed to benchmark cleaved PARP. The benchmarking results support the selected biomarkers of the multiplexed assay.

In stage 2, additional reference compounds (three aneugens/clastogens/cytotoxicants) were investigated. So far, the chosen biomarkers of DNA damage response appear useful for class discrimination and provide additional information to existing genotoxicity tests.

361

Characterization of t-BOOH-induced cell death and DNA damage in murine fibroblasts and human keratinocytes

C. Wenz¹, C. Thurmann¹, D. Faust¹, C. Dietrich¹
¹Universitätsmedizin Mainz, Toxikologie, Mainz, Germany

Cell-cell contacts are involved in keeping a physiological balance between proliferation, differentiation and apoptosis. Far less is known about the role of cell-cell-contacts in regulating necrosis, for instance in response to oxidative stress. Previous findings of our group demonstrated that, in contrast to semi-confluent proliferating cultures, confluent murine fibroblasts (NIH3T3, MEF) and human keratinocytes (HaCaT) are protected against necrosis induced by tert-butyl hydroperoxide (t-BOOH). Comparison of confluent cells (G0/G1 = ~70 %) and semi-confluent cultures, similarly arrested in the G0/G1 phase by serum-starvation or the MEK inhibitor U0126, ascertained that the resistance against t-BOOH is mediated by cell-cell contacts and not by cell cycle arrest. We further revealed that confluent cultures are protected against t-BOOH-induced DNA double strand breaks as assessed by the neutral comet assay and against mitochondrial damage detected by flow cytometric analysis of DiOC6 staining. To better understand the protective role of cell-cell-contacts in ROS-mediated necrosis, we started characterizing the signaling cascade induced by t-BOOH in semi-confluent proliferating cultures. In accordance with the observed formation of DNA double strand breaks in response to t-BOOH, we detected phosphorylation of the checkpoint kinase Chk2. However, inhibition of ATM, the kinase responsible for Chk2 activation, did not influence t-BOOH-induced cell death. Interestingly, first experiments gave a hint for the participation of RIP1, since the chemical RIP1 kinase inhibitor Necrostatin-1 (Nec-1) blocked cell death up to averagely 50 %, what is described as a specific marker for regulated necrosis. In line with this observation, t-BOOH-induced cell death could not be blocked by the pan-caspase inhibitor z-VAD-FMK strongly indicating that caspase activity is not required. Moreover, PARP-1 and p53 are probably not involved. Deeper analyses could give evidence that Nec-1 did not block formation of DNA double strand breaks nor mitochondrial damage indicating that the kinase blocked by Nec-1, possibly RIP1, acts downstream of DNA double strand breaks and / or mitochondrial damage. In the end, we could identify a crucial role of Ca²⁺ signaling for t-BOOH-mediated toxicity. As the calcium chelator BAPTA-AM was able to completely block not only cell death, but also mitochondrial damage and DNA double-strand break formation, there is a strong need for further investigations of the possible interplay between regulated necrosis and calcium, regulated by cell-cell contacts among oxidative stress.

The work was supported by the Hoffmann-Klose-Stiftung, the Promotionsförderung Rheinland-Pfalz, the Johannes Gutenberg-University and the University Medical Center of the Johannes Gutenberg-University.

Toxicology – Carcinogenesis

362

Linking site-specific loss of histone acetylation to repression of gene expression by the mycotoxin ochratoxin A

E. Limbeck¹, J. T. Vanselow², J. Hofmann¹, A. Schlosser², A. Mally¹
¹Universität Würzburg, Institut für Pharmakologie und Toxikologie, Würzburg, Germany
²Universität Würzburg, Rudolf-Virchow-Zentrum, Würzburg, Germany

Ochratoxin A (OTA) is a wide-spread food contaminant and one of the most potent renal carcinogens [1]. Recent data by our group demonstrate that OTA inhibits histone acetyltransferases (HATs), thereby causing a global reduction of lysine acetylation of histones and non-histone proteins [2]. Based on these findings and the importance of specific histone acetylation marks in regulating gene transcription [3], we speculated that repression of gene expression as the predominant transcriptional response to OTA [4, 5] may be linked to loss of histone acetylation. In this study we therefore used a novel mass spectrometry approach, which is based on chemical acetylation of unmodified lysine residues of histones using ¹³C-labeled acetic anhydride and subsequent calculation of the degree of acetylation based on the measured intensities of heavy and light acetylated isotopologues [6], to identify and quantify site-specific alterations in histone acetylation in human kidney epithelial (HK-2) cells treated with OTA. Our results demonstrate OTA-mediated loss of acetylation at almost all important lysine residues at histones H2A, H2B, H3 and H4. We further selected acetylation at histone H3 lysine 9 (H3K9), a well-known euchromatic hallmark that is elevated at promoter regions of transcriptionally active genes [7] and which was reduced from ~3% in controls to <0.1% in response to OTA, to establish a link between loss of H3K9 acetylation and expression of genes consistently shown to be down-regulated in response to OTA [4, 5]. Using chromatin immunoprecipitation followed by quantitative real-time PCR (ChIP-qPCR), we observed OTA-mediated loss of H3K9 acetylation at promoter regions of the selected genes (% of controls: AMIGO2: 45%, CLASP2: 60%, CTNND1: 54%). Overall, these data provide first evidence for a mechanistic link between H3K9 hypoacetylation as a consequence of OTA-mediated inhibition of HATs and repression of gene expression by OTA.

References: 1. National Toxicology, P., Toxicology and Carcinogenesis Studies of Ochratoxin A (CAS No. 303-47-9) in F344/N Rats (Gavage Studies). *Natl Toxicol Program Tech Rep Ser*, 1989. 358: p. 1-142.

2. Czakai, K., et al., Perturbation of mitosis through inhibition of histone acetyltransferases: the key to ochratoxin a toxicity and carcinogenicity? *Toxicol Sci*, 2011. 122(2): p. 317-29.

3. Bannister, A.J. and T. Kouzarides, Regulation of chromatin by histone modifications. *Cell Res*, 2011. 21(3): p. 381-95.

4. Jennings, P., et al., Transcriptomic alterations induced by Ochratoxin A in rat and human renal proximal tubular in vitro models and comparison to a rat in vivo model. *Arch Toxicol*, 2012. 86(4): p. 571-89.

5. Arbillaga, L., et al., In vitro gene expression data supporting a DNA non-reactive genotoxic mechanism for ochratoxin A. *Toxicol Appl Pharmacol*, 2007. 220(2): p. 216-24.

6. ElBashir, R., et al., Fragment Ion Patchwork Quantification for Measuring Site-Specific Acetylation Degrees. *Anal Chem*, 2015.

7. Wang, Z., et al., Combinatorial patterns of histone acetylations and methylations in the human genome. *Nat Genet*, 2008. 40(7): p. 897-903.

363

The mTOR inhibitor rapamycin promotes cell transformation in a BALB/c 3T3 cell model

D. Poburski¹, L. Szymtenings¹, M. Gle², R. Thierbach¹
¹Institut für Ernährungswissenschaften, Humanernährung, Jena, Germany
²Institut für Ernährungswissenschaften, Ernährungstoxikologie, Jena, Germany

The mammalian target of rapamycin (mTOR) forms two multiprotein complexes (mTORC1 and mTORC2) and influences cell growth, proliferation, survival and metabolism. Constitutively activated mTOR was found to be deregulated in several cancer types, which makes it an interesting target for therapeutic cancer strategies. Rapamycin is able to inhibit mTOR and its downstream targets and is currently studied for its anticancer properties in clinical trials. Despite previous evidence, there are studies that show an adverse effect in cancer treatment causing tumour growth, evolving the question of the effectiveness of the drug in cancer treatment. Therefore, we examined the transformational potential of rapamycin in a BALB/c cell transformation assay (CTA) as well as markers of proliferation and protein synthesis.

The BALB/c 3T3 cell transformation assay mimics different stages of in vivo carcinogenicity (initiation, promotion, post-promotion phase) and is a promising alternative to rodent bioassays. BALB/c fibroblasts are treated for 3 days with the tumour initiator MCA (3-Methylcholanthrene) followed by 13 days with the promotor TPA (12-O-Tetradecanoylphorbol-13-acetate). Upon treatment with these chemicals cells are transformed into morphologically aberrant foci and can be visualized after six weeks by giemsa staining. It is possible to apply additional substances during the whole assay or in several phases of transformation and evaluate the colony formation. Furthermore, our improved protocol allows additional westernblot or immunofluorescence analysis.

The influence on cell proliferation of different concentrations of rapamycin was investigated by cell counting (living and dead) to choose a suitable concentration for the CTA. Performances of BALB/c CTAs with 10 nM rapamycin showed, contrary to expectations, an increase in cell transformation. By administration of rapamycin only in the promotion phase we could detect an increase in colony formation, whereas a treatment with rapamycin in the post-promotion phase with already established foci, seemed to reveal its therapeutic properties. To better understand the role of mTOR in our cell transformation system we used another mTOR inhibitor called OSI-027. Surprisingly, an incubation with 3 μ M OSI-027 led to a decrease in colony formation. We are now able to investigate the underlying mechanism with westernblot and immunofluorescence analysis and can compare regulations of downstream targets like the marker of protein synthesis p-S6.

Our investigations revealed different cell transformation outcomes by comparing the two known mTOR inhibitors rapamycin and OSI-027, which need to be further evaluated. In

the ongoing project we want to detect differences between rapamycin and OSI-027 by protein analysis and identify key proteins, which are involved in this opposed colony formation of the BALB/c cells. These results can be helpful to better understand mTOR inhibition in matters of tumour therapy.

364

Investigation of the anti-carcinogenic properties of metformin using the BALB/c 3T3 cell transformation assay

C. Leovsky¹, M. Veit¹, D. Poburski¹, R. Thierbach¹

¹Institut für Ernährungswissenschaften, Humanernährung, Jena, Germany

Introduction: Over the past 50 years, the biguanide compound metformin has been widely prescribed as an insulin sensitizer in type 2 diabetes mellitus. Interestingly, recent meta-analyses of epidemiological studies have shown that metformin might be involved in risk reduction of carcinogenesis. In vitro studies have described AMP-activated protein kinase (AMPK)-dependent, by inhibition of the respiratory chain complex I, as well as AMPK-independent actions of metformin. However, the detailed molecular mechanisms by which metformin affects cell proliferation and carcinogenesis have not been well identified up until now.

Method: To evaluate the protective potential of metformin, BALB/c 3T3 cell transformation assays were performed. This valid toxicological method is an alternative to in vivo carcinogenic testing and mimics the different stages of cell transformation during carcinogenesis. In detail, mouse fibroblasts are treated with metformin and/or the tumour initiator 3-methylcholanthrene (MCA) and the tumour promoter 12-O-tetradecanoylphorbol-13-acetate (TPA). In the first experiment several metformin concentrations (0.1-1 mM metformin) were applied answering the question of an effective metformin concentration. Next, metformin treatment during the different phases of carcinogenesis (initiation, promotion, post-promotion phase) was done determining the most effective phase for an intervention, i.e. chemopreventive or chemotherapeutic properties of metformin. Additionally, the effect of metformin on the energy metabolism of the cells was analysed using various methods like immunoblot and oxygen measurement by Clark electrode.

Results/Discussion: Analysis of different metformin concentrations revealed a concentration-dependent effect of metformin. In detail, decreased colony forming potential of BALB/c cells was most prominent using 1 mM metformin. This effect was not caused by growth inhibition of metformin itself since 1 mM metformin showed no growth inhibitory properties in a cellular growth pretrial. Interestingly, the 2 phase cell transformation assay showed that the metformin effect is more pronounced in the post-promotion phase than in the initiation and promotion phase pointing to a chemotherapeutic potential. Investigating several energy metabolism parameters, the results indicate that metformin may affect cell respiration as well as energy-dependent mechanistic markers like AMPK.

Conclusion: The presented results support rather the idea of the chemotherapeutic potential of metformin than a chemopreventive, using 1 mM metformin. The initial analysis of energy metabolism markers discovered interesting starting points for further investigations.

365

N-Vinyl-2-pyrrolidone (NVP): Investigations on its carcinogenic mechanism

D. Fruth¹, E. Fabian¹, M. Schulz², F.-I. Berger², F. Oesch³, B. van Ravenzwaay¹, R. Landsiedel¹

¹BASF SE, Experimental Toxicology and Ecology, 67056 Ludwigshafen am Rhein, Germany

²BASF SE, Regulatory Toxicology Chemicals, 67056 Ludwigshafen am Rhein, Germany

³Johannes Gutenberg University, Institute of Toxicology, 55131 Mainz, Germany

NVP, widely used e. g. as a monomer for polyvinylpyrrolidones (PVP) with applications in food technology or cosmetics is a known hepatocarcinogen in rats after inhalative exposure to 5, 10, and 20 ppm for 2 years. NVP is tested in a battery of genotoxicity assays (e.g. Ames, HPRT, mouse lymphoma, UDS, chromosome aberration, cell transformation, micronucleus test (MNT) in mice bone marrow) [1] that all yielded negative results. However, NVP induces cell proliferation in liver (LOAEC: 0.5 ppm) after whole body exposure to vapor [2].

To confirm the absence of genotoxicity in the context of a potentially non-genotoxic mode of action, a five day whole body inhalation study to NVP vapor with concentrations of 0, 5, 10, 20 ppm was conducted in Wistar rats (six animals per gender and group, ethyl methanesulfonate 200 mg/kg bw p.o. as positive control). Genotoxicity was investigated by the MNT in bone marrow and the Comet Assay (± FPG) in liver and lung. Further investigated endpoints related to possible non-hepatocarcinogenic MOA were: enzyme induction (EROD, PROD, BROD), oxidative stress (GSH-, GSSG-, non-protein sulfhydryl group level), and peroxisome proliferation (CYP4A, cyanide-insensitive palmitoyl-CoA-oxidase). At carcinogenic inhalative doses, the results of this study proved the absence of genotoxicity in lung, liver and bone marrow as neither the tail intensity in the Comet Assay nor the number of micronuclei in the MNT was increased compared to the controls. However, also the non-genotoxic parameters (CYP-enzyme activity, glutathione levels, cyanide-insensitive-palmitoyl-CoA-oxidase) were not affected by NVP-treatment.

As potential metabolic activation cannot be excluded and may essentially contribute to the understanding of the carcinogenic mechanism, *in vitro* investigations in rat liver systems (subcellular fractions, hepatocytes, precision cut liver slices (PCLS)) were performed additionally. Up to now, 2-pyrrolidone is the only identified *in vitro* metabolite. As these results cannot mimic the *in vivo* situation of two described, ring- and vinyl-majority containing unidentified metabolites [3] detailed investigations on metabolism may be a future perspective to approach the overall understanding of the carcinogenic mechanism of NVP.

¹ Klimisch, H. J.; Deckardt, K.; Gembardt, C.; Hildebrand, B.; Kuettler, K.; Roe, F. J. C. Long-term inhalation toxicity of N-vinylpyrrolidone-2 vapours. Studies in rats. *Food and Chemical Toxicology* 1997, 35, 1041-1060

² MAK Bericht, Nachtigal 2014

³ McClanahan, J.S.; Hawi, A.A.; Digenis, G.A. Disposition and Metabolism of N-vinyl-2-pyrrolidone in the rat. *Proceedings of the 2nd International Symposium on Povidone* 1987, 318-329

Toxicology – Non-animal testing

366

“Emerging angiogenesis” in the chick chorioallantoic membrane.

W. W. Rong¹, B. Reglin¹, W. Xiang¹, B. Nitzsche¹, M. Maibier¹, A. R. Pries¹

¹Charité Universitätsmedizin Berlin, Berlin, Germany

Introduction: In ischemic conditions such as wound healing and myocardial infarction, new vessels are generated by vasculogenesis and angiogenesis. These processes are stimulated by the signalling peptide vascular endothelial growth factor which therefore has been proposed as a promising compound for the treatment of ischemic conditions. However, results of respective clinical studies have not been fully convincing yet. Here, we investigated principles underlying the selforganization of newly formed vessels to functionally adequate microvascular networks indispensable for proper tissue substrate supply. Intravital microscopy of the chick chorioallantoic membrane (CAM), a non animal model as defined by the American National Institutes of Health's Office for Protection from Research Risks, was used to study peripheral expansion of existing arteriolar and venular trees by recruiting segments of the dense polygonal capillary mesh. This process we call “Emerging angiogenesis”.

Methods: White leghorn chicken eggs were put into incubators on embryonic day 0 (E0) at 37.5°C and 82% humidity. On E3, the eggs were cracked open and transferred into petri dishes. On E10, CAM microcirculation was recorded using time-lapse intravital videomicroscopy at discrete time points for up to 48 hours. To improve the visibility of the capillary mesh, videorecordings were processed offline by generating coefficient of variation images of pixel grey values over time. Changes of network topology during the observation time were investigated.

Results: In the CAM, a sequence of specific events leading to extension of existing vessel trees was observed: In a capillary mesh region near terminal branches of existing vessel trees, homogeneous flow distribution is transferred to inhomogeneous flow distribution: Preferred flow pathways through the mesh evolve carrying most of the blood. Over time, these flow pathways exhibit diameter increase, straighten and connect the mesh to arteriolar and venular trees. In contrast, less perfused parallel mesh flow pathways and transversal mesh segments exhibit progressive decrease of flow and diameter resulting in vessel regression. As a result, hierarchical vessel tree structures are extended into the mesh region. While newly generated tree extensions are located above the mesh at the beginning, they sink to a lower level at later stages until they are finally covered by a reconstituted mesh network.

Conclusions: The CAM *ex ovo* model is well suited for studying emerging angiogenesis. Vessel tree extension occurs via parallel processes of vessel maturation and capillary mesh segment regression. At later stages, newly formed vessel tree branches sink and the capillary mesh is reconstituted above. In the next step of our project, we will implement these phenomena in a computer simulation and use theoretical modeling to further investigate and better understand principles underlying microvascular network maturation. This will allow us to derive effective therapeutic strategies which could be tested in the CAM model.

367

Development of a high-throughput method for testing the influence of chemicals on malignant cell transformation

F. Wetzel¹, A.-L. Buchholz¹, N. Loeper¹, D. Poburski¹, M. Gleis², R. Thierbach¹

¹Institut für Ernährungswissenschaften, Humanernährung, Jena, Germany

²Institut für Ernährungswissenschaften, Lehrstuhl für Ernährungstoxikologie, Jena, Germany

Chemicals are able to induce cancer in a wide range of organs. Therefore, it is very important to investigate the toxic properties of chemical substances, especially their carcinogenic potential. In this context the number of animal experiments will drastically increase in the future. In order to avoid the use of expensive and time consuming animal experiments for long-term carcinogenic studies, the development of an *in vitro* system to test the carcinogenic potential of a high number of chemicals in a highly reproducible manner within a short period of time is imperative.

By combination of the well-established BALB/c cell transformation method with the soft agar colony formation assay, we developed a high-throughput *in vitro* system to identify effects of chemicals on cell transformation for the first time.

BALB/c mouse fibroblasts are treated with 3-Methylcholanthrene as a tumour initiator and 12-O-Tetradecanoylphorbol-13-acetate as promoter for several days, whereby foci of transformed cells are developed. After the promotion phase of the common BALB/c cell transformation assay, cells are transferred into soft agar to further monitor the anchorage independent growth of transformed cells only. The established soft agar transformation assay reproduces the foci growth of previous experiments and is performed in 96-well plate format. Hence, we can analyse the carcinogenic potential of several chemical substances in parallel and are also searching for alternative endpoint analysis, e.g. the usage of fluorescing cells stably expressing iRFP, instead of the former time-consuming microscopic assessment.

The here presented new technique is a high-throughput and low priced alternative for the evaluation of the carcinogenic potential of chemical substances in a short period of time without animal testing.

368

Application of serum-free cultured human TK6 cells in the *in vitro* micronucleus test

L. Theis¹, M. Schulz¹, B. van Ravenzwaay¹, R. Landsiedel¹
¹BASF SE, Experimental Toxicology and Ecology, 67056 Ludwigshafen am Rhein, Germany

The effort to develop new or refine established *in vitro* test systems rises due to animal welfare, scientific and/or regulatory reasons (e.g. the animal testing ban concerning the risk assessment of cosmetic product ingredients in March 2013). This progress, among others, leads to an increased performance of cell-based assays. The majority of model cell lines are routinely cultured using medium supplemented with fetal bovine serum (FBS) in amounts between 5-10%. The application of serum-substitutes will provide a reduction of the animal number needed, which corresponds to the guiding principles of the three R's (3R), described by Russel and Burch in 1959. In addition, chemically defined serum-substitutes have the potential to reduce the inter-experimental variability of test conditions caused by the inherent differences in chemical composition across FBS batches¹, resulting in a refinement of *in vitro* testing.

In this study, human TK6 cells were gradually adapted to serum-free conditions, where they show comparable growth gradients at the exponential phase. For cells under serum-free conditions a mean doubling time of 19.3 (± 1.7) h was observed while FBS supplemented cells showed a doubling time of 13.5 (± 0.8) h. The *in vitro* micronucleus test protocol included a 4 h treatment with 0.63, 1.25, 2.50, 5.00, 10.00 and 20.00 µg/mL methyl methanesulfonate, followed by a 20 h recovery period. Both conditions showed a significant increase of the micronucleus frequency. Considering the prolonged doubling time of the serum-free cultures, an extension of the recovery time from 20 h to 26 h would provide a preferable adjustment of the method.

The results indicate that serum-free cultured cells can be used in the *in vitro* micronucleus test. However, further testing of reference substances have to be done to confirm the suitability of this application.

¹Gstraunthaler, Alternatives to the Use of Fetal Bovine Serum: Serum-free Cell Culture, ALTEX 20, 4, 2003

369

The potential of protein reactivity to predict skin sensitizing potency: of peptide depletion, reaction time and tested concentrations

B. Wareing¹, S. Kolle¹, D. Urbisch¹, D. Mulliner², B. van Ravenzwaay¹, R. Landsiedel¹
¹BASF SE, Experimental Toxicology and Ecology, 67056 Ludwigshafen am Rhein, Germany
²BASF SE, Computational Chemistry and Biology, 67056 Ludwigshafen am Rhein, Germany

Several non-animal test methods addressing key events in the sensitization process have passed formal validation and OECD (draft) test guidelines are available. One of these methods is the direct peptide reactivity assay (DPRA) assessing the ability of a chemical to bind to proteins to form a complete antigen (OECD TG 442C). The test is used to obtain a yes/no answer on whether the substance has a protein-binding potential. For a complete risk assessment, however, an estimation of a chemical's potency is also needed.

In this study we examined if an assessment of potency could be achieved by 1) determining reactivity class cut offs based on published data on 199 substances for the DPRA performed according to OECD 442C to predict UN GHS sensitizer classes, 2) a variant of the DPRA assessing reaction kinetics (time and concentration) for 12 substances or 3) an extended protocol testing several test substance concentrations for 50 reference substances and estimating the concentration of a test substance that is needed to cause a peptide depletion of 6.38% (EC6.38%).

Results of the first approach indicated that cut offs to differentiate the UN GHS sensitizer classes 1A and 1B could indeed be defined. Secondly, evaluating the reaction time based assay in which several time points between 5 min and 24 hours were assessed, it was found that not all reactions followed ideal kinetics. Hence further investigations are needed to eventually derive a reaction time based prediction model. The results of the 3rd approach (the standard protocol of the DPRA was amended by testing three concentrations i.e. 1, 10, and 100 mM) indicated that potency classes could be assigned using the EC6.38% value to assess potency. In summary, using quantitative information derived from the DPRA in particular using EC6.38% value may support the assessment of the skin sensitizing potency.

370

Identification of pre- and pro-haptens with non-animal test methods for skin sensitization

D. Urbisch¹, E. Fabian¹, D. Fruth¹, N. Honarvar¹, S. Kolle¹, A. Mehling², T. Ramirez¹, W. Teubner³, B. Wareing¹, R. Landsiedel¹
¹BASF SE, Experimental Toxicology and Ecology, 67056 Ludwigshafen am Rhein, Germany
²BASF Personal Care and Nutrition GmbH, 40589 Düsseldorf, Germany
³BASF Schweiz AG, Product Safety, 4057 Basel, Switzerland

Since pro-haptens may be metabolically activated in the skin, information on xenobiotic metabolizing enzyme (XME) activities in cell lines used for testing of sensitization *in vitro* is of special interest. Metabolic activity of e.g. N-acetyltransferase 1 (NAT1) and esterase in the keratinocyte (KeratinoSensTM and LuSens) and dendritic cell-like cells (U937 and THP-1) was previously demonstrated. Aldehyde dehydrogenase (ALDH) activities were found in KeratinoSensTM and LuSens cells. Activities of the investigated cytochrome P450-dependent alkylresorufin O-dealkylases, flavin-containing monooxygenase, alcohol dehydrogenase as well as UDP glucuronosyl transferase activities were below detection in all investigated cell lines.

A set of 27 putative pre- and pro-haptens (no obvious structural alert for peptide reactivity but positive *in vivo*) was routinely tested using the above mentioned cell lines as well as in the direct peptide reactivity assay (DPRA). 18 of the compounds were unexpectedly positive in the DPRA and further analyzed by LC/MS techniques to clarify the reaction mechanism leading to true positive results in this assay. Oxidation products

like dipeptide formations or the oxidation of the peptide-based sulfhydryl group led to positive results for benzo[a]pyren or 5-amino-2-methylphenol, respectively. In contrast, covalent peptide adducts were identified for 12 putative pre-haptens, indicating the DPRA to be suitable for compounds requiring abiotic oxidation to get activated. For some DPRA negatives, the keratinocyte and dendritic cell based assays provided true positive results.

A combination of DPRA, KeratinoSensTM and h-CLAT within a '2 out of 3' prediction model provided a high sensitivity of 81% for the set of the pre-/pro-haptens. The sensitivity of this combination of non-animal test methods in the '2 out of 3' prediction model in a set of 95 direct haptens was comparable (sensitivity = 87% when compared to LLNA).

Urbisch D¹, Fabian E¹, Fruth D¹, Honarvar N¹, Kolle SN¹, Mehling A², Ramirez T¹, Teubner W³, Wareing B¹, Landsiedel R¹

¹BASF SE, Experimental Toxicology and Ecology, Ludwigshafen, Germany

²BASF Personal Care and Nutrition GmbH, Düsseldorf, Germany

³BASF Schweiz AG, Basel, Switzerland

371

Evaluating non-animal methods for identifying skin sensitisation hazard: A Bayesian value of information analysis

M. Leontaridou^{1,2}, S. Gabbert², E. van Ierland², R. Landsiedel¹, A. Worth³
¹BASF SE, Experimental Toxicology and Ecology, 67056 Ludwigshafen am Rhein, Germany
²Wageningen University, Environmental Economics and Natural Resources Group, 6708 Wageningen, Niederlande
³European Commission Joint Research Centre, Institute for Health and Consumer Protection, 21020 Ispra, Italien

Skin sensitization testing is mandatory for all substances produced or marketed in volumes larger than 1 tonne per year under the European REACH legislation. With REACH supporting *in vivo* testing only "as a last resort" and the marketing ban for finished cosmetic products with ingredients tested in animals, attention has been given to developing integrated testing strategies combining *in vitro*, *in silico* and *in chemico* methods. Key challenges are which tests to select and how to combine non-animal methods into testing strategies. This study suggests a Bayesian value of information (VOI) approach for developing non-animal testing strategies, which consider information gains from testing, but also expected payoffs from adopting regulatory decisions on the use of a substance, and testing costs. The 'value' of testing is defined as the expected social net benefit from decision-making on the use of chemicals with additional, but uncertain information from testing. The VOI is calculated for a set of individual non-animal methods including DPRA, OECD QSAR Toolbox, ARE-Nrf2 luciferase method covered by KeratinoSens and LuSens, and hCLAT, seven battery combinations of these methods, and 86 two-test and 360 three-tests sequential strategies consisting of non-animal methods. Their VOI is compared to the VOI of the local lymph node assay (LLNA) as the animal test. We find that battery and sequential combinations of non-animal methods reveal a higher VOI than the LLNA. In particular, for small prior beliefs (i.e. a chemical is, prior to testing, assumed to be a non-sensitizer), a battery of DPRA + LuSens reveals the highest VOI. If there are strong beliefs that a chemical is a sensitizer, a sequential combination of the battery DPRA + LuSens, followed by KeratinoSens + hCLAT at the second stage and by the OECD QSAR toolbox at the third stage performs best. For given specifications of expected payoffs the VOI of the non-animal strategy significantly outperformed the VOI of the LLNA, for the entire range of prior beliefs. This underlines strong economic potential of non-animal methods for skin sensitization assessment.

Toxicology – Non-animal testing in silico

372

Cardiosafety in silico prediction – Validation results of a multiscale simulation model

L. T. Anger¹, A. Amberg¹, H.-P. Spirkl¹, J.-M. Guillon², V. Ballet², F. Schmidt¹, M. Stolte¹, A. Czich¹, H. Matter¹, J. Gomis-Tena³, L. Rodriguez³, J. Saiz³, M. Pastor³
¹Sanofi-Aventis Germany GmbH, Preclinical Safety, Frankfurt am Main, Germany, Germany
²Sanofi, Preclinical Safety, Paris, France, Frankreich
³Sanofi-Aventis Germany GmbH, LGCR, Frankfurt am Main, Germany
⁴Universitat Politècnica de València, Ci2B, València, Spain, Spanien
⁵IMM, GRIB, Barcelona, Spain, Spanien

A new paradigm to assess the proarrhythmic potential of drugs is proposed by the CiPA (Comprehensive *in vitro* Pro-arrhythmia Assay) initiative combining a suite of *in vitro* assays (7 most important ion channels for cardiac activity) coupled to *in silico* reconstructions of cellular cardiac action potential (AP). The eTOX consortium has developed a multiscale simulation in silico model based on O'Hara/Rudy incorporating the principles of this new paradigm.

The core model simulates the effects of drugs on a virtual cardiac tissue composed by different types of cardiomyocytes. The input of this model, the blockade of a set of 3 ion channels (IKr/hERG, IKs, ICaL), can be obtained experimentally or predicted using advanced 3D-QSAR models. The system predicts the % change of the QT interval at different drug concentrations in order to facilitate risk assessment.

This *in silico* model was validated using Purkinje fiber assay results (input: AP prolongation and arrhythmic risk assessed by early after-depolarisation occurrence) from 500 in-house drug candidates. The validation showed that predictivity is highly dependent on the model's applicability domain (AD): for some chemical series the proarrhythmic potential could not be identified, for others, however, most of the positive drugs were correctly predicted with sensitivities up to 80-90% (average prediction accuracy was 70%). Retraining of this model with additional internal data should help to improve the model AD and predictivity. It is important to note that AP prolongation was correctly predicted for many proarrhythmic drugs with only low (> 30 µM) *in vitro* hERG inhibition. Furthermore, the model showed high additional benefit for read-across within

a chemical series to predict the proarrhythmic potential of drugs with low solubility for which no reliable Purkinje fiber results could be obtained. These validation results showed that this cardiovascular safety *in silico* model can successfully be applied in R&D to predict the proarrhythmic potential of drug candidates within the model AD.

373

In silico assessment of skin permeation of p-Phenylenediamine skeletal structures and tailoring for consecutive *in vitro* studies

U. Bock¹, D. Selzer², D. Neumann²

¹Bock Project Management, Trier, Germany

²Scientific Consilience GmbH, Saarbrücken, Germany

Introduction: The use of p-phenylenediamine (PPD) and derivatives (Tab. 1) in oxidative consumer hair dye products is considered as key in hair dye allergic contact dermatitis [1-4]. In recent supplement, 2-methoxymethyl-PPD (ME+) shows significantly reduced sensitizing properties [5, 6]. Since overcoming the skin barrier is a prerequisite for sensitization, numerous *in vitro* and *in vivo* studies on skin penetration of PPD and derivatives have been performed.

The aim of the present study is the *in silico* prediction of the penetration of PPDs, because such computations may help in understanding the processes involved in sensitization. For the first time, software DSKin [7] is challenged to simulate this class of compounds. *In silico* results are retrospectively compared to previously published experimental data and may assist in future tailoring of *in vitro* experiments.

Material and Methods: The permeabilities, lag-times and the time-dependent accumulated amounts of PPDs were computed using DSKin. Input parameters for the latter were a concentration of 1 mg/mL (1%), finite dosing and 30 min in use incubation periods. Molecular structures were optimized ab initio and the condensed Fukui functions (FF) were estimated from Mulliken population analyses [8] and electrostatic potentials using GAMESS [9].

Results: Initial results agree with experimental results using PPD in white petrolatum, demonstrating the applicability of DSKin to PPDs. The four PPDs exhibit only small differences in permeabilities *in silico* (Tab. 1). Toluene-2,5-diamine shows a higher accumulated mass due to increased lipophilicity (Fig. 1). In general, the FF were very similar for all PPDs and indicated that the N atoms would be the preferred targets for radical and electrophilic attack.

Discussion and Outlook: *In silico* methods may be used to model the permeation of PPDs despite their low molecular weight and low lipophilicity. The low amounts of PPDs under in use conditions result from oxidative conditions. Computed ME+ permeation was not different to other PPDs, therefore other properties account for the reduced sensitization potential.

The very similar FF values hint at similar reaction pathways. Furthermore, PPD and its derivatives are prone to N-acetylation in living skin resulting in metabolites exhibiting higher molecular weight and greater lipophilicity than the parent compounds. The effects of N-acetylation and reactions of PPD and its derivatives with histidine and cysteine residues are subject of upcoming computations.

References: [1] D. Hamann et al. Contact Dermatitis 70:213-218, 2014

[2] SCCP Opinion, COLIPA N° A7, 2006

[3] SCCP Opinion, COLIPA N° A5, 2007

[4] SCCP Opinion, COLIPA N° A80, 2008

[5] SCCP Opinion, COLIPA N° A160, 2013

[6] C. Goebel et al. Toxicol Appl Pharmacol 274:480-487, 2014


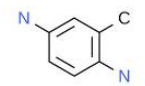
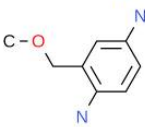
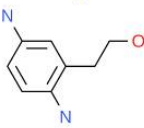
[7] D. Selzer, D. Neumann, U.F. Schaefer. Expert Opin Drug Metab Toxicol 11:1567-1583, 2015

[8] W.J. Mortier et al. J Am Chem Soc 108:4315-4320, 1986

[9] M.W. Schmidt et al. J Comput Chem 14:1347-1363, 1993

Abb. 1

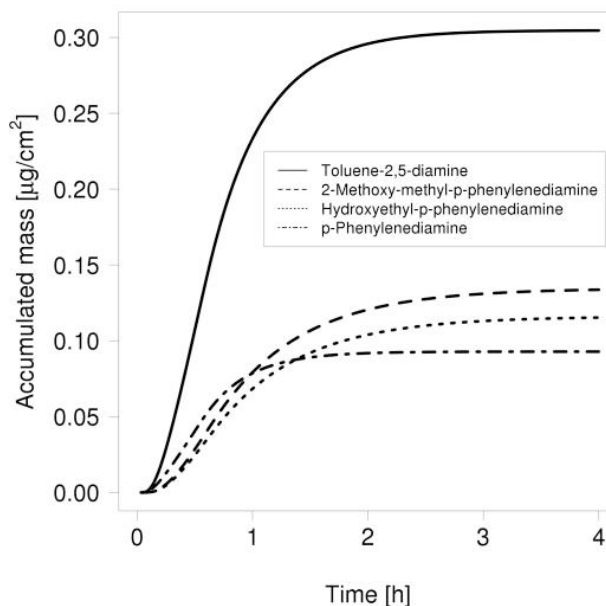
Table 1: PPD and selected derivatives.

Compound Abbreviation (CAS)	Molecular Weight	Xlog3	log k _p [*] [cm/h]	Structure
P-Phenylenediamine, PPD (106-50-3)	108.14	-0.3	-3.93	
Toluene-2,5-diamine (95-70-5)	122.17	0.6	-3.46	
2-Methoxy-methyl-PPD, ME+ (337906-36-2)	152.20	0.2	-3.90	
Hydroxyethyl-PPD (93841-24-8)	152.20	0.1	-3.96	

* Calculated assuming infinite dose conditions

Abb. 2

Figure 1: Accumulated masses permeated through the stratum corneum under simplified in use conditions (conc = 1 mg/mL, application time = 30 min, donor height = 500 µm).



374

The eTOX Project: Data-Sharing and *In Silico* Modelling

M. Pawletta¹, J. Wichard¹, M. Cases¹, T. Steger-Hartmann¹

¹Bayer Pharma AG, Investigational Toxicology, Berlin, Germany

eTOX^[1,2] started in 2010 and is a public-private partnership project within the European Innovative Medicines Initiative (IMI)^[3]. The eTOX project is building a toxicology database relevant to pharmaceutical development and to elaborate innovative strategies and software tools. The overall goal is to better predict the toxicological profiles of new chemical entities in early stages of the drug development pipeline based on existing *in vivo* study results contributed by the participating EFPIA⁴ companies in the consortium. The eTOX database is a relational database with a specifically designed schema to store complex and comprehensive preclinical safety data like the study design, toxicokinetics, ADME data, clinical chemistry, hematology, gross necropsy, histopathological findings and general toxic effects. In addition relevant data from public sources has been included into the database. The primary focus for data collection are systemic toxicity (up to 4 week) repeated dose studies, mostly in rodent. Overall more than 7000 study reports for approximately 1400 investigated compounds.

In order to optimize the usage and mapping of data from different sources the development of common ontologies was a key task within the project. This time-consuming step was necessary to make a high quality read-across analysis possible and valuable. Therefore the OntoBrowser^[4] tool was developed to curate and harmonize the verbatim terms to standardize terms which are used within the eTOX database. Until now more than 13 million verbatim terms were curated.

Additionally to the toxicology database, a web-based user interface called eTOXsys was developed to allow the retrieving of toxicity information, as well as the prediction of toxic endpoints for chemical compounds. Due to the complex search capabilities, the database can be queried for structural similarity, similar target classes and specific toxicological endpoints. Approximately 150 prediction models based on public data are available and first models based on *in vivo* data are in development. The eTOX database therefore represents a valuable tool for early animal-free assessment of drug candidates^[5].

⁴European Federation of Pharmaceutical Industries and Associations

References: [1] <http://www.etoxproject.eu/>

[2] Briggs K, Cases M, Heard DJ, Pastor M, Pognan F, Sanz F, Schwab ChH, Steger-Hartmann T, Sutter A, Watson DK, Wichard JD: Inroads to Predict *In Vivo* Toxicology – An Introduction to the eTOX Project. *Int. J. Mol. Sci.* 2012 (13), 3820.

[3] <http://www.imi.europa.eu/>

[4] <http://opensource.nibr.com/projects/ontobrowser/>

[5] Briggs K, Barber Ch, Cases M, Marc P, Steger-Hartmann T: Value of shared preclinical safety studies – The eTOX database. *Science Direct, Toxicology Reports* 2015 (2), 210.

Abb. 1

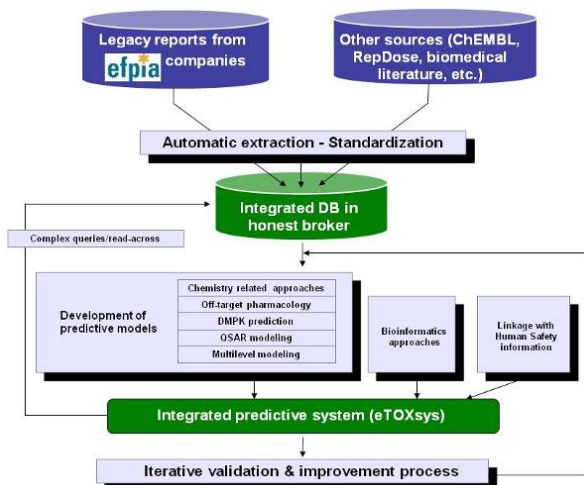


Abb. 2



375

Analysis of selected substances from the SkinAb database

S. Schmeinck¹, A. Bitsch¹, H. Genth²
¹Fraunhofer Institut für experimentelle Medizin und Toxikologie, Hannover, Germany
²Medizinische Hochschule, Institut für Toxikologie, Hannover, Germany

Dermal absorption is an important factor in regulatory science regarding the registration of chemicals, agrochemicals and cosmetics. The issue has gained importance since it has been realized that the skin is not completely impenetrable for chemical substances.[1]

The different ways to assess dermal absorption range from QSAR models to complex in vivo studies including a complete toxicokinetic examination. The choice of method depends on the question that has to be answered as different systems give different results: absorption as % of applied dose in in vivo studies or permeability coefficient and lag time in infinite dose in vitro studies [1]. Ideally both data would be available.

Since the OECD has adopted a guideline for assessing dermal penetration in vitro in 2004 the number of in vitro studies is rising continuously. Depending on the chosen method results may vary in reliability and in acceptance by regulatory authorities.

The SkinAB database[BA1] contains data for about 600 substances on dermal absorption which has been found through the eChemPortal [3] and extended with data from the EDETOX database. For selected substances with a broad spectrum of data available further analysis has now been started.

165 chemicals have been investigated in a comparable test system; from these 79 were shown to have a low dermal absorption of less than 1% and 51 compounds showed a high absorption rate of more than 50%. For the assessment of dermal exposure either the absorbed dose in percent or the flux can be measured. Data analysis showed that

only for 15 substances both is available: flux data from in vitro studies and absorption data from in vivo studies. This data could be used to clarify which parameter would be most useful for exposure assessment regarding dermal exposure.

Seven substances in the dataset were conspicuous for their range of absorption rates in different studies: less than 1% to more than 50%. An in depth analysis revealed the complex influence that different exposure parameters have on the results of dermal absorption studies. For some chemicals the influence of exposure time on increasing absorption values could be clearly demonstrated. Beside other factors such as the chosen vehicle, and the (non-)occlusion of the site of exposure especially the choice species introduced a high variability; this holds even for the most common laboratory animals t. A review published by Jung in 2015 [5] which comes to the conclusion that i.e. hairless species are usually not a good model to predict dermal absorption in humans.

[1]WHO (2006) EHC 235 Dermal absorption
 [2]Scholz et al (2014) Naunyn-Schmiedeberg's Arch Pharmacol 3 (Suppl 1):S86
 [3] www.echemportal.org
 [4]http://edetox.ncl.ac.uk
 [5] Jung et al (2015) J. Appl. Toxicol. 35 1-10
 [BA1]Was hältst du von DADA Dermal Absorption Database
 :-)

376

Risk assessment on sulfamethoxazole and carbamazepine transformation products using molecular dynamics simulations

V. Durmaz¹, M. Weber¹
¹Zuse-Institut Berlin, Berlin, Germany

In-silico methods have evolved to indispensable tools in various areas of life sciences. Several stages in drug development including hit identification and lead optimization, for instance, highly benefit from an accurate estimation of binding free energies associated with biological host-guest systems. As a consequence, the need for laboratory experiments including in-vivo experiments and animal testing is considerably reduced. Another field profiting from free energy calculations is human as well as ecotoxicology. Upon the development and risk assessment of new chemicals, transformation products arising from biotic or abiotic degradation of the parent substance have usually been neglected. However, since few years, the risk assessment of new chemicals often includes transformation products probably causing more harm than the parent substance itself. Such studies as well are mostly carried out on the basis of in-vitro and in-vivo tests. Moreover, many metabolites can be detected but neither enriched nor synthesized in amount sufficient for toxicological evaluations. At this stage, computational methods come into play. Using classical molecular dynamics simulations in combination with an empirical linear prediction model, we have investigated several metabolites of the drugs sulfamethoxazole and carbamazepine and prioritized them according to their estimated binding affinities to potential biological target proteins. Consequently, a couple of metabolites were identified that bind to one or more human cytochrome P450 variants and the bacterial enzyme dihydropteroate synthase, respectively, which are known to be sensitive to the two drugs. The investigations were carried out in the framework of the BB3R project funded by the German government through BMBF.

377

In vitro – in vivo extrapolation – ibuprofen as an example

F. Partosch¹, H. Mielke², E. Di Consiglio³, E. Testai³, U. Gundert-Remy^{1,2}
¹Charité Universitätsmedizin Berlin, Institut für Klinische Pharmakologie und Toxikologie, Berlin, Germany
²Bundesinstitut für Risikobewertung, Berlin, Germany
³Instituto Superiore di Sanità, Environment and Primary Prevention Dept., Rome, Italien

Introduction: *In vitro* methods have been increasingly used to characterize pharmacological and toxicological properties of substances. To address the problem of nominal versus actual concentrations, *in vitro* biokinetic studies were recently undertaken (Truisi et al., Toxicol Lett 233:172-86, 2015). We use those data as input into a physiologically based human kinetic model (PBHKM) to model the *in vivo* doses leading to the *in vitro* measured concentrations.

Methods: A PBHKM was used to simulate the concentration time profile of ibuprofen in the hepatic vein after oral administration. The details of the model and the physiological parameters used have been described elsewhere (Abraham et al., Arch. Toxicology 79: 63-73, 2004). We modelled the concentration time profile exploring the dose which would lead to a concentration at 1 hour and at 24 hour as similar as possible to the concentration measured in the supernatant of human freshly prepared cell cultures after dosing the culture with ibuprofen. We parametrized the PBHKM with the parameters which have been estimated from the *in vitro* kinetic studies (clearance between 3 and 15 $\mu\text{m}^3/\text{sec}$ (Truisi et al., 2015) and an absorption of 100% and an absorption rate of 1/h (Cristofoletti and Dressman, J Pharm Sci 103: 3263-75, 2014).

Results: The data of the *in vitro* study with 100 μM ibuprofen could well be modelled. When assuming a clearance of 15 $\mu\text{m}^3/\text{sec}$ the dose of 1480 mg resulted in an 1 hour concentration of 66.5 μM in the hepatic vein of PBHKM equal to 133.0 nmol/well (volume of the well = 2 ml) in the *in vitro* study in which the measured concentration was 138.75 nmol/well. The concentration at 24 hours of 8.7 μM (equal to 17.4 nmol/well) corresponded with the *in vitro* concentration (16.5 nmol/well).

The modelling approach was less successful with *in vitro* dosing of 1000 μM . The 10 fold higher dose of 14800 mg lead to nearly double the concentration at 1 hour than measured *in vitro*. With a dose of 8500 mg/kg an approximation was feasible resulting in 396.7 μM in the hepatic vein at 1 hour which is equal to 793.4 nmol/well whereas the measured concentration *in vitro* was 782.85 nmol/well. Even with a clearance value as low as the 2.5 percentile (3 $\mu\text{m}^3/\text{sec}$), the concentration at 24 hours was modelled to be lower than the *in vitro* measured value (*in vitro* model: 98.7 μM which corresponds to 197.4 nmol/well; measured *in vitro* concentration: 979.2 nmol/well).

Discussion: This is the first attempt to use kinetic data obtained *in vitro* to feed in a PBHKM for reverse dosimetry finding the dose which corresponds in vivo to the *in vitro* situation. In the case presented here, the *in vitro* dose assumed to be low *in vitro* (100 μM) corresponds to a dose of 1480 mg (note: the highest approved daily dose is 2,400

mg). For the high *in vitro* dose modelling was successful only for the concentration 1 hour after dosing and a dose of 8,500 mg.

Conclusions: *In vitro* kinetic parameters, such as clearance, can successfully be used for parametrizing a PBHKM. It is of utmost importance for the relevance of *in vitro* finding to assure that the concentrations used *in vitro* can be obtained with relevant *in vivo* doses. In this case, the *in vitro* concentrations were within (low dose) and 3.5 fold above (high dose) the *in vivo* relevant therapeutic concentration range.

378

Aciclovir residues in the aquatic environment – an in-silico approach

H. Mückter¹, J. Meyer¹, V. Durmaz², M. Weber², T. Gudermann¹
¹Walther-Straub-Institut, Toxikologie, München, Germany
²Zuse Institut, Berlin, Germany

Introduction: A variety of drug residues have been detected in sewage plant run-offs, rivers and lakes, but also in groundwater and tap water samples. Studies have yet to identify a risk for human health from these contaminants, but adverse health effects have been reported for various species, including fish and birds. It has recently been suggested that for a comprehensive risk assessment toxicologists should also consider transformation products (TPs) of such water contaminants that may arise from abiotic and biotic (metabolic) reactions. With aciclovir (ACV), a well-known antiviral drug, as the parent drug we tried an in-silico approach to identify TPs that might be of interest due to some mutagenic or carcinogenic toxicophores.

Methods: From a literature and database search we picked up 12 ACV-TPs. Predicted acute toxicities and mutagenic / carcinogenic properties for these TPs were derived from an expert system analysis using the LAZAR portal (<http://lazar.in-silico.ch>) as front end.

Results: Two of the identified ACV-TPs could not be handled by LAZAR because of insufficient training data in one out of eight queried categories. The highest score (4 positive out of 8 possible genotoxicity categories) was assigned to 9 of the 12 TPs, including ACV itself. This is a rather low score when compared to other water-borne drug residues, e.g. carbamazepine. COFA, an imidazole derivative of ACV seen in advanced oxidation processes, had shown antiproliferative effects in several ecotoxicologic screening assays, e.g. [1], but was unremarkable in our tests. Additionally, a computer-based simulation of the respective TPs interacting with human CYP isozymes did not support concerns that these TPs may pose a risk for human health.

Conclusions: Our in-silico analyses of 12 ACV-TPs did not provide evidence for any adverse health effects in the micromolar concentration range. Further studies are needed to clarify if the biological activity of some ACV-TPs in ecotoxicological assays may eventually affect yet unidentified biological targets in the human body.

References: [1] Prasse C et al. (2012). Environ Sci Technol 46 (4) 2169-2178.

Toxicology – Non-animal testing in vitro

379

Alkylating agents activate MAPK signaling through TRPA1

B. Stenger¹, A. Breit¹, T. Popp², H. Thiermann², T. Gudermann¹, D. Steinritz^{1,2}
¹Ludwig-Maximilians-Universität, Walther-Straub-Institute of Pharmacology and Toxicology, Munich, Germany
²Sanitätsakademie der Bundeswehr, Institute of Pharmacology and Toxicology, Munich, Germany

Sulfur mustard (SM) is a chemical warfare agent which was first used in World War I, but has found use in several conflicts afterwards. Although SM is prohibited by Geneva Protocol, terrorist attacks cannot be ruled out. Latest news give rise to concern that IS may be in the possession of SM and is willing to deploy it. Even 200 years after the initial synthesis of SM its mode of action is not fully unraveled. Thus, no antidote does exist. However, chemosensing ion channels have been shown to be activated by highly toxic chemicals and might represent a specific therapeutic target.

Previous studies have shown that the SM-surrogate CEES (mono-functional alkylating agent) is able to activate Transient Receptor Potential Ankyrin 1 (TRPA1) channels that are known to affect MAPK cell signaling. MAPK-pathways, especially pERK1/2, are known to increase protein biosynthesis through activation of transcription factors binding to the serum response element (SRE). It is unknown whether alkylating agents have also impact on MAPK signaling mediated through TRPA1 activation.

Our results demonstrate that AITC resulted in phosphorylation of the MAPK pERK1/2 and increased protein biosynthesis of SRE-regulated genes in HEK293 cells overexpressing hTRPA1. CEES increased pERK1/2 levels already after 2.5 min which could be prevented by the TRPA1 blocker AP18. Activation of target genes through pERK1/2 signaling was also evident, but less pronounced compared to AITC.

Our results demonstrate that alkylating agents have impact on cell signaling through TRPA1 channel activation. Thus, TRPA1 might represent a promising target for counteracting SM toxicity.

380

Impaired autophagy in skin injuries induced by sulfur mustard

T. Popp¹, D. Steinritz¹, V. Egea², A. Schmidt¹, C. Ries², H. Thiermann¹
¹Institut für Pharmakologie und Toxikologie der Bundeswehr, München, Germany
²Institute for Cardiovascular Prevention, LMU, München, Germany

Sulfur mustard (SM) is a chemical warfare agent that provokes severe inflammation and blistering upon exposure to the skin accompanied by disturbed wound healing. The potential use of SM in terrorist attacks amplified the interest in understanding the underlying cellular and molecular pathomechanisms in order to improve therapeutical intervention.

Autophagy is a highly conserved catabolic pathway in eukaryotes that ensures the degradation and recycling of cellular components through the lysosomal machinery. Autophagy is important for cell survival in physiological and pathological stress situations. Emerging knowledge indicates that imbalanced regulation of autophagy

disturbs basal cell functions including proliferation, differentiation and migration, thus contributing to the pathophysiology of various diseases.

After penetration into skin cells, SM alkylates and thereby modifies nucleic acids and proteins thus forming aggregates of dysfunctional proteins destined for autophagic disposal.

In our studies, we analyzed the influence of SM on protein expression (Western blotting) of autophagy-related (ATG) genes as well as proliferation (WST-1) of primary normal human keratinocytes (NHEK) and primary normal human dermal fibroblasts (NHDF). Preliminary results demonstrate that SM strongly dysregulates the biosynthesis of ATG proteins that may contribute to the diminished cell migration and proliferation under these conditions.

Our findings suggest that SM affects autophagy in correlation with an impairment of physiological functions in keratinocytes and fibroblasts that are essentially required for normal tissue regeneration. Thus, application of pharmacological modulators of autophagy might be useful in the treatment of the delayed wound healing in skin upon exposure to SM.

This work was supported by contract from the German Federal Ministry of Defense (M/SABX/BA003).

381

The CULTEX® RFS method as an *in vitro* model for the assessment of pulmonary toxicity of inhalable substances

A. Tsoutsouloupoulos¹, H. John¹, T. Gudermann², A. Schmidt¹, H. Thiermann¹, D. Steinritz^{1,2}

¹Bundeswehr Institute of Pharmacology and Toxicology, Munich, Germany
²Ludwig-Maximilians-Universität München, Walther-Straub-Institute of Pharmacology and Toxicology, Munich, Germany

Exposure of the respiratory tract to airborne particles is a major risk to human health. Due to the ubiquitous application of these particles in the field of pharmacy, industry and in daily life, there is a strong necessity to investigate the toxic properties and the underlying pathomechanisms of these inhalable substances. In addition, the EU Chemicals Regulation requires not only that all substances placed on the market have to undergo a toxicological characterization, including the identification of potential toxic inhalation hazards (REACH), but also that animal testing shall be undertaken only as a last resort ("3Rs" principle) and the promotion of the development of alternative methods. Thus, the development, establishment and validation of alternative *in vitro*-based test systems for the assessment of pulmonary toxicity are in the focus of current research. Until now, most of the available *in vitro* cell culture models are limited to some extent as in those studies the exposure is either done under submerged conditions, not resembling the exposure conditions *in vivo*, or a homogeneous particle distribution is not guaranteed. The CULTEX® Radial Flow System (RFS) is a specially designed *in vitro* modular exposure system that overcomes these limitations. It enables the homogenous exposure of human lung epithelial cells at the air-liquid interface (ALI), thereby mimicking the physiological conditions of the alveolae. However, further optimizations are needed for the enhancement of the CULTEX® methodology. Aim of this study was first the optimization of the test methodology in general (i.e. focus on clean air controls of the human lung epithelial cell line A549), and second the improvement of cultivation conditions. Parameters such as handling of the CULTEX® device (proper closing and opening operation of the CULTEX® RFS module; improved washing conditions and media supply), treatment of the incubator controls, adjustment of clean air pressure and flow rates, and integration of two additional filters were sequentially adjusted in order to enhance the methodical setup. Our results show that the test parameters for clean air exposure of the A549 cells were successfully optimized resulting in more accurate and robust data. Cultivation conditions were improved by changing from closed-wall cell culture inserts to open-wall cell culture inserts. The open-wall inserts turned out to be more suitable for exposure experiments as they provided a better medium supply and preserved humidity. Deductively, the change of the cell culture inserts was identified as the deciding factor for the improvement of cell morphology. Hence, we have successfully optimized the CULTEX® RFS methodology for clean air exposure of A549 cells.

382

Comparative analysis of 3D culture methods on human HepG2 cells

C. Luckert^{1,2}, C. Schulz¹, N. Lehmann¹, M. Thomas³, U. Hofmann³, S. Hammad⁴, J. G. Hengstler¹, A. Braeuning¹, A. Lampen¹, S. Hesse¹

¹Bundesinstitut für Risikobewertung, Lebensmittelsicherheit, Berlin, Germany
²Universität Potsdam, Institut für Ernährungswissenschaft, Potsdam, Germany
³Dr. Margarete Fischer-Bosch – Institut für Klinische Pharmakologie, Stuttgart, Germany
⁴Leibniz-Institut für Arbeitsforschung an der TU Dortmund, Dortmund, Germany

Human primary hepatocytes represent the gold standard in *in vitro* liver research. Due to their low availability and high costs, alternative liver cell models with comparable morphological and biochemical characteristics have come into focus.

The human hepatocarcinoma cell line HepG2 is often used as a model for liver toxicity studies. However, under two-dimensional (2D) cultivation conditions the expression of xenobiotic-metabolizing enzymes and typical liver markers is very low. Cultivation for 21 days in a three-dimensional (3D) matrigel culture system has been reported to strongly increase the metabolic competency of HepG2 cells. In our present study we extended previous studies and compared HepG2 cell cultivation in three different 3D culture systems: collagen, matrigel and Alvetex culture system. Cell morphology, albumin secretion, cytochrome P450 monooxygenase (CYP) enzyme activities, as well as expression of xenobiotic-metabolizing and liver-specific enzymes were analyzed after 3, 7, 14, and 21 days of cultivation. Our results show that the previously reported increase of metabolic competency of HepG2 cells is not primarily the result of 3D culture but a consequence of the duration of cultivation. HepG2 cells grown for 21 days in 2D monolayer exhibit comparable biochemical characteristics, CYP activities and gene expression patterns as all 3D culture systems used in our study. However, CYP activities did not reach the level of HepaRG cells.

In conclusion, the increase of metabolic competence of the hepatocarcinoma cell line HepG2 is not due to 3D cultivation but rather a result of prolonged cultivation time.

383

In vitro assessment of the neurotoxic potential of arsenolipids

B. Witt¹, S. Meyer¹, F. Ebert¹, K. A. Francesconi², T. Schwerdtle¹

¹Universität Potsdam, Institut für Ernährungswissenschaft, Lebensmittelchemie, Nuthetal, Germany

²Universität Graz, Institut für Chemie, Analytische Chemie, Graz, Austria

Arsenolipids are organic, lipid-soluble arsenic compounds, which occur mainly in marine organisms. Major human exposure routes are fatty fish including herring or fish oil-based food supplements. About 55 different arsenolipids have been identified so far. Thereby, arsenic-containing hydrocarbons (AsHC) and arsenic-containing fatty acids (AsFA) represent two subgroups of the arsenolipids [1].

Our *in vitro* studies have demonstrated high cellular bioavailability and a high cytotoxic potential of AsHCs in human liver and bladder cells [2], whereas AsFAs were less toxic [3]. A sublethal transfer across an intestinal barrier model (Caco-2) indicated that AsHCs are highly intestinal available. In comparison, AsFAs showed lower intestinal bioavailability and underwent a presystemic metabolism [4]. Moreover, in *Drosophila melanogaster* AsHCs exerted late developmental toxicity and accumulated in the fruit fly's brain. These results suggest that AsHCs might pass the blood-brain-barrier due to their amphiphilic structure [5].

In order to assess the neurotoxic potential we currently investigate the toxicity of several arsenolipids in differentiated, human neurons (LUHMES). After 48 h incubation with AsHCs or AsFAs, cell number (Hoechst) as well as cellular dehydrogenase activity (Resazurin) were measured, with the latter endpoint turning out to be more sensitive. AsHCs showed substantial cytotoxic effects ($IC_{50} \sim 7\text{-}12.5 \mu\text{M}$) in a concentration range comparable to that of arsenite ($IC_{50} \sim 7.5 \mu\text{M}$), whereas AsFAs were less cytotoxic ($IC_{50} > 100 \mu\text{M}$). After incubation with AsHCs the cellular arsenic concentrations increased 10-20fold as compared to incubation with arsenite. Further studies indicated that one possible toxic mode of action of arsenolipids could be a disruption of the cellular energy level. Therefore, the mitochondrial membrane potential was investigated after incubation with the arsenic compounds in differentiated neurons. Whereas arsenite did not exert an impact, AsHCs reduced the mitochondrial membrane potential significantly. This might be due to interactions of the amphiphilic AsHCs with mitochondrial membranes.

Currently we investigate the impact of the arsenolipids on neurite outgrowth as a developmental toxicity endpoint.

[1] Sele *et al.* 2015: *J Trace Elem Med Biol*, 30, 171-179.

[2] Meyer *et al.* 2014: *Metallomics*, 6, 1023-1033.

[3] Meyer *et al.* 2015: *Toxicol Res*, 4, 1289-1296.

[4] Meyer *et al.* 2015: *Mol Nutr Food Res*, 0, 1-13.

[5] Meyer *et al.* 2014: *Metallomics*, 6, 2010-2014.

384

Interactions of antimalarial drugs amodiaquine and chloroquine with human cholinesterases and organophosphorus compounds

A. Bierwisch¹, T. Wille¹, H. Thiermann¹, F. Worek¹

¹Bundeswehr Institute of Pharmacology and Toxicology, Munich, Germany

Standard treatment of poisoning by organophosphorus compounds (OP; e.g. nerve agents and pesticides) consists of co-administration of atropine and an oxime-based reactivator of inhibited cholinesterases. Due to lack of efficacy of clinically used oximes against various OP-inhibited human acetylcholinesterase (AChE) (e.g. soman) research started focusing on new therapeutic approaches. Several research groups conducted *in silico* screenings [1, 2] in order to identify new non-oxime reactivators, presenting amodiaquine as a promising candidate for paraoxon-inhibited hAChE. For decades, antimalarial drugs like amodiaquine and chloroquine have been closely investigated regarding their side effects, thereby discovering interaction with cholinesterases, which could pose a new potential therapeutic benefit for inhibited cholinesterases. Therefore, in this study interactions between antimalarial agents in presence or absence of OPs were examined spectrophotometrically by a modified Ellman assay. Reversible inhibition of cholinesterases was observed with both antimalarial agents. Amodiaquine had higher inhibitory potency for hAChE than human butyrylcholinesterase (BChE), being confirmed by IC_{50} values of $0.67 \pm 0.02 \mu\text{M}$ for hAChE and $81.28 \pm 0.04 \mu\text{M}$ for hBChE. IC_{50} values with chloroquine were $28.37 \pm 0.02 \mu\text{M}$ for hAChE and $55.62 \pm 0.02 \mu\text{M}$ for hBChE, thus representing a weaker inhibition of hAChE than amodiaquine. Furthermore, reactivation of paraoxon- (PXE), sarin- (GB), cyclosarin- (GF), and VX-inhibited hAChE and hBChE by amodiaquine and chloroquine was determined. After 60 minutes, only paraoxon-inhibited hAChE (50%) and cyclosarin-inhibited hBChE (10%) were reactivated by 500 μM chloroquine. On the contrary, 10 μM amodiaquine reactivated all tested OPs after 60 minutes in the following order: PXE > VX > GF > GB. In contrast, with hBChE the highest reactivation was generated with 100 μM amodiaquine in the following order: VX > GB > GF > PXE. Due to the high reversible inhibitory potency of amodiaquine, an increased concentration does not result in a higher reactivation of OP-inhibited hAChE. In summary, our results show that amodiaquine is a reactivator of OP-inhibited cholinesterases. In the future, non-oxime reactivators that are structurally-related to amodiaquine should be further investigated.

[1] Bhattacharjee, A.K., Marek, E., Le, H.T., Gordon, R.K., *Eur. J. Med. Chem.*, 2012, 49, 229-238.

[2] Katz, F.S., Pecic, S., Tran, T.H., Trakht, I., Schneider, L., Zhu, Z., Ton-That, L., Luzac, M., Zlatanic, V., Damera, S., Macdonald, J., Landry, D.W., Tong, L., Stojanovic, M.N., *Chembiochem.*, 2015, 16, 2205-2215.

385

Establishment of a three-dimensional *in vitro* breast cell model for the identification of non-genotoxic carcinogens

A. Engel¹, T. Buhrke¹, B. Niemann¹, A. Braeuning¹, B. Schäfer¹, A. Lampen¹

¹Bundesinstitut für Risikobewertung, Lebensmittelsicherheit, Berlin, Germany

Development of mammary gland tumors is connected to a deregulation of breast epithelial cell differentiation, a complex process which cannot be reproduced *in vitro* under standard cell culture conditions. However, cultivation of cells in a tissue-like environment in an *in vitro* three dimensional (3D) model can mimic general architecture, function and differentiation of mammary bulks.

In this project, a 3D model was used consisting of the permanent breast epithelial cell lines MCF10A (ER⁻, estrogen receptor negative) and MCF12A (ER⁺, estrogen receptor negative) grown in MatrigelTM, which mimics the complex extracellular matrix *in vivo*. The 3D culture of MCF10A and MCF12A cells in MatrigelTM results in the formation of growth-arrested, polarized spheroids with a lumen (acini-like organoids). In order to perform a semi-quantitative estimation on the influence of substances on the differentiation of the breast cells for the identification of non-genotoxic carcinogens a scoring method was developed. This scoring method provides information about substance-induced morphological changes of the spheroids during differentiation based on the following parameters: size of the spheroids, the formation of the lumen, and the degree of polarization. Furthermore, the model allows distinguishing between ER-dependent (MCF12A) and ER-independent (MCF10A and MCF12A) effects.

The 3D *in vitro* model is a useful tool for toxicologists to study substance effects on differentiation processes. The system will be used to examine the potential of e.g. food contaminants such as phthalates or perfluorinated substances (PFAS) to disrupt the differentiation process of breast epithelial cells and will therefore serve as a valuable *in vitro* tool to assess their carcinogenic potential.

386

Prediction of idiosyncratic drug-induced hepatotoxicity: pro-inflammatory stimuli are needed to differentiate between iDILI and non-DILI compounds

A. Granitzny¹, J. W. Knebel¹, P. Steinberg², C. Dasenbrock¹, T. Hansen¹

¹Fraunhofer Institut für Toxikologie und Experimentelle Medizin, In vitro und

mechanistische Toxikologie, Hannover, Germany

²Stiftung Tierärztliche Hochschule Hannover, Hannover, Germany

Inflammatory episodes occur erratically throughout life and are likely to play a critical role in the alteration of the individual susceptibility of a person to idiosyncratic drug-induced liver injury (iDILI), a particular severe form of drug-induced liver injury (DILI). In concordance with the inflammatory stress hypothesis, modest inflammatory stress can lower the threshold for hepatotoxicity and make an individual susceptible to develop liver injury during exposure to therapeutic doses of a drug. In order to evaluate the role of immune cells and its secreted factors during drug therapy, we established an *in vitro* test battery consisting of two cell culture systems in presence or absence of pro-inflammatory factors (LPS, TNF α): (A) the monoculture of human hepatoma (HepG2) cells and (B) co-culture systems of human monocytic or macrophage-like (THP-1) and HepG2 cells. With these different test settings we aimed to identify whether the introduction of inflammatory immune cells and/or pro-inflammatory factors could increase the sensitivity of liver cells towards iDILI compounds. Three reference substance pairs were tested, namely Troglitazone – Rosiglitazone, Trovafloxacin – Levofloxacin, and Diclofenac – Acetylsalicylic Acid, each of them being composed of a compound that is known to induce iDILI and a partner compound of the same substance class that does not induce iDILI. First, all compounds were tested for cytotoxicity towards the single cell systems using the WST-assay. Co-culture experiments with HepG2 and THP-1 monocytes or macrophages as well as co-exposure experiments with LPS or TNF α were then done at about 20% cytotoxicity of the respective substance in the most sensitive cell type. Subsequently the results were compared to the experiments in the monoculture of HepG2. We observed that every iDILI compound showed a significant increase in cytotoxicity in a minimum of one exposure combination while this effect was not observed with the corresponding non-DILI partner compound. In conclusion, a combination of different culture systems and co-exposures with pro-inflammatory factors is needed for a valid differentiation between non-DILI and iDILI compounds. This test battery could provide a useful tool for the prediction of inflammation-associated idiosyncratic drug-induced hepatotoxicity. Furthermore, our results support the inflammatory stress hypothesis and points to an involvement of pro-inflammatory factors in the development of iDILI.

387

Improvement of the BALB/c 3T3 cell transformation assay for mechanistic cancer research

R. Thierbach¹, D. Poburski¹

¹Friedrich-Schiller-Universität Jena, Humanernährung, Jena, Germany

Extensive animal models of carcinogenicity ensure a safe usage of chemicals. To elucidate fundamental molecular mechanisms of carcinogenicity these methods are expensive, time consuming and above all too complex. In contrast, most *in vitro* methods are rather simple and detect only selected endpoints, like DNA damage, mutations or changes in proliferation.

The BALB/c cell transformation assay is a validated toxicological method to identify potential tumour initiators and promoters. First, BALB/c mouse fibroblasts form a monolayer culture and get contact-inhibited after reaching confluence. Upon treatment with a tumour initiator (3-Methylcholanthrene) and promoter (12-O-Tetradecanoylphorbol-13-acetate) transformed cells do not stop proliferation and grow as morphologically aberrant foci over the monolayer of normal cells. After fixation with methanol at day 42, morphological aberrant foci can be visualized with giemsa staining. Because the BALB/c assay mimics different stages of the malignant cell transformation process (initiation, promotion and post-promotion phase) and detects with the colony formation a late endpoint of carcinogenicity we improved this method for mechanistic cancer research.

Using the example of insulin-signalling pathway we can show that
 (1) several substances have a different impact on the transformation process,
 (2) it is possible to identify for each substance the phase with the greatest effectiveness and
 (3) we can detect additional endpoints to elucidate the mechanistic mode of action.
 Therefore we used several compounds (Linsitinib, Metformin, Rapamycin, ...) to manipulate the insulin-signalling pathway on different levels (InsR, AMPK, mTOR, ...) and analysed a number of characteristic endpoints of carcinogenesis. Changes on protein level and signalling (westernblot, immunofluorescence, flow cytometry) or parameters of energy metabolism (oxygen consumption, glucose or ATP measurement) are measurable and enable new insights into the process of cancer origin.
 Summing up, the BALB/c 3T3 assay proves to be a cheap and short-time alternative to rodent bioassays. Although this method does not mimic the whole *in vivo* neoplastic process, it can be used to provide essential information regarding key proteins and their signalling, during the different stages of transformation.

388

Is there hope to correctly classify severe ocular irritant agrochemical formulations using *in vitro* methods: A proof of concept using the Isolated Chicken Eye Test, two modified BCOP protocols and an EpiOcular™ ET50 protocol

K. Susanne¹, R. Landsiedel¹, B. van Ravenzwaay¹
¹BASF SE, Experimental Toxicology and Ecology, 67056 Ludwigshafen am Rhein, Germany

While some *in vitro* methods addressing ocular irritancy have gained regulatory acceptance, to date the Draize rabbit eye test (OECD TG 405) is the only world-wide regulatory accepted test for the determination of the full range of eye irritation potential. Further although several *in vitro* methods for the severe eye irritation have gained regulatory acceptance, agrochemical formulations are not explicitly included nor excluded from the applicability domain to predict severe ocular irritant formulations. Systematic analyses are only available for e.g. the hen's egg test- chorioallantoic membrane (HET-CAM), and bovine corneal opacity and permeability (BCOP, OECD TG 437) assays both showing that the used protocols do not provide sufficient sensitivity to reliably predict severe ocular irritating formulations. The purpose of this study was to evaluate whether the regulatory accepted isolated chicken eye (ICE, OECD TG 438) test including corneal histopathology (as suggested for evaluation of the depth of injury), as well two modified protocols of the BCOP and/or an ET50 (exposure time reducing viability of treated tissue to 50%) protocol using the reconstructed cornea model EpiOcular™ are useful to predict severe ocular irritant agrochemical formulations. A proof of concept comprising the testing of ten to twelve agrochemical formulations with available *in vivo* data in each assay was conducted. In summary, based on the ICE evaluation described in OECD TG 438, one of the five severe ocular irritant formulations (UN GHS Cat 1) was predicted correctly. Using both modified protocol versions of the BCOP the result for one of the four tested UN GHS Cat 1 formulations was just above the UN GHS Cat 1 classification border for using one of the modified protocols. Lastly and most promising, the EpiOcular™ ET50 predicted four of five tested UN GHS formulations correctly with the fifth being close to the classification border. Additional agrochemical formulations will be tested to further evaluate the EpiOcular™ ET50 protocol to identify severe ocular irritant agrochemical formulations.

389

Rat pancreas tissue slices as *in vitro* model for studying drug-induced pancreatic toxicity

M. Hellmund¹, A.-L. Frisk¹, M. Raschke¹
¹Bayer Pharma AG, Berlin, Germany

Drug-induced pancreatic toxicity comprises effects on the exocrine and/or the endocrine pancreas, which both can have serious clinical implications, e.g. acute pancreatitis or diabetes mellitus. Adverse effects on the pancreas are occasionally observed during drug discovery and development and often prohibit further development. Hence, there is a need for reliable *in vitro* models to early on identify the pancreas-toxic potential of drug candidates. Permanent cell lines and primary cells have many shortcomings, e.g. loss of cell-to-cell and cell-to-matrix relationships or changes in cell physiology due to the isolation procedure. Pancreas tissue slices are a potential alternative, circumventing most of these limitations. Their preparation is rather elaborate which may explain its rare use. So far, pancreas tissue slices have predominantly been used to address physiological or pharmacological questions, although they might also serve as valuable *in vitro* model for toxicological applications.

Therefore, this work aimed to establish and characterize rat pancreas tissue slices as *in vitro* model for studying drug-induced pancreatic toxicity. Results will be compared to the responses of the permanent endocrine (INS-1E) and exocrine (AR42J) pancreatic cell lines to evaluate a potential added value.

Rat pancreas tissue slices were prepared by a protocol adapted from Marciniak et al. (Nat Protoc, 2014, 9(12): p. 2809-22). Briefly, pancreas was infused and embedded with agarose. Tissue sections of approx. 200 µm were prepared using a vibratome and maintained in cell culture medium for up to 6 days. Cell viability was determined by daily measurement of lactate dehydrogenase (LDH) in medium supernatants and by microscopic evaluation following fixation in 10 % formalin and H&E staining. Functional integrity of acinar and beta cells were assessed by cell-type specific secretory responses (i.e. insulin, amylase, lipase) to physiological stimuli. Moreover, the effects of the pancreas toxins streptozotocin (STZ), alloxan (ALL), and the cholecystokinin (CCK) analogue cerulein on the viability and functional integrity of tissue slices were compared to the respective responses of the cell lines.

We were able to establish an optimized isolation and cultivation procedure for rat pancreas tissue slices applying minor modifications to the original protocol. Cell viability declined over the cultivation period. Stimulation of the cell lines with glucose or cerulein increased secretion of insulin (INS-1E cells) or amylase/lipase (AR42J cells), respectively. The pancreas slices responded to both stimuli, demonstrating functional integrity of endocrine and exocrine cells. Treatment of INS-1E islet cells with the beta-cell toxicants ALL or STZ only slightly affected islet cell viability, whereas treatment of AR42J acinar cells with cerulein at supraphysiological concentrations had no effect. This

set of experiments is currently completed by investigating the effects of ALL, STZ and cerulein on the viability of acinar and islet cells in pancreas slices. Our preliminary data demonstrate feasibility to prepare and cultivate rat pancreas tissue slices over a period of 6 days thereby maintaining functional integrity to some extent.

390

Coculture of human monocytes with the keratinocyte cell line HaCaT in serum-containing medium leads to higher sensitivity to weak contact allergens: an improvement for the Loose-fit Coculture-based Sensitization Assay (LCSA)

A. Sonnenburg¹, J. Frombach², R. Stahlmann¹, M. Schreiner³
¹Charité Universitätsmedizin Berlin, Institut für Klinische Pharmakologie und Toxikologie, Berlin, Germany
²Charité Universitätsmedizin Berlin, Klinik für Dermatologie, Venerologie und Allergologie, Berlin, Germany
³Bundeswehrkrankenhaus Berlin, Abteilung Innere Medizin, Berlin, Germany

The Loose-fit Coculture-based Sensitization Assay (LCSA) has proved reliable for the *in vitro* detection of contact sensitizers in the past. However, the use of primary human keratinocytes has some disadvantages. To facilitate high throughput screening of chemicals, we replaced primary keratinocytes from the original assay setup (setup A) by the human keratinocyte cell line HaCaT. These cells were cocultured with monocyte-derived dendritic cells in serum-free medium (setup B) or fetal calf serum (FCS)-containing medium (setup C). Upregulation of the dendritic cell maturation marker CD86 assessed by flow cytometry served as endpoint. We have tested four substances known as sensitizers and four non-sensitizers in both new setups as well as in the original setup with primary cells. Three out of four sensitizers (2,4-dinitrochlorobenzene, 2-mercaptobenzothiazole, and coumarin), and three out of four non-sensitizers (glycerol, monochlorobenzene, and salicylic acid) were correctly assessed under all culture conditions. The weak sensitizing potency of resorcinol was only detected by setup B with FCS supplemented medium. A false positive reaction to caprylic (octanoic) acid in all three setups confirms earlier results from our laboratory that some fatty acids are able to induce CD86 on dendritic cells *in vitro*. Culture in FCS supplemented medium led to generation of dendritic cells showing a more pronounced upregulation of CD86 after application of substances with rather high sensitization potency compared to dendritic cells which are formed under serum-free conditions. Therefore, we characterized dendritic cells from setups B and C by flow cytometric measurement of additional dendritic cell surface markers. Dendritic cells from the original setup A had been characterized extensively before (Schreiner et al., Toxicology 2008; 249:146-152). Dendritic cells generated in FCS supplemented medium were CD1a+/CD1c+, whereas dendritic cells from serum free culture conditions were CD1a-/CD1c- regardless whether cocultured with primary human keratinocytes or HaCaT. Populations with CD1a+/CD1c+ dendritic cells in coculture seem to show a higher sensitivity to weak sensitizers, which proved beneficial for the identification of resorcinol. In conclusion, modification of the LCSA protocol led to an increased sensitivity of the assay.

391

**Analysis of miRNA expression profiles in antigen-presenting cells in the presence of epithelial cells
 - A further characterization of the cross talk between THP-1 and HaCaT cells -**

M. Schellenberger¹, J. Hennen¹, B. Blömeke¹
¹University Trier, Department of Environmental Toxicology, Trier, Germany

Due to ethical and social reasons, *in vitro* assays are being developed to replace animal tests for addressing e.g. toxicological questions. For the induction of skin sensitization by chemicals, resulting in tolerance or allergic contact dermatitis after repeated exposure, prerequisites are the induction of inflammatory responses in keratinocytes supporting maturation of dendritic cells (DC), which is needed for the T cell response. Although related *in vitro* assays consisting of one single cell type have good hazard prediction capacities, they have limitations in predicting sensitization potency. One drawback could be the lack of communication between keratinocytes and DC. With respect to the activation of keratinocytes and maturation of DC, intercellular communication between these two cells may include the release of danger molecules such as cytokines, damage-associated molecules such as ATP, and metabolized chemicals. Beside this, microRNA (miRNA), among them those that can regulate DC activation or maturation, can be differentially expressed upon stimulation but can also be transferred between cells.

For skin sensitizers, we reported already that cross talk between HaCaT keratinocytes and THP-1 cells, as model for DC, enhanced CYP1 enzyme activity in HaCaT cells exposed to benzo[a]pyrene (B[a]P) and eugenol, belonging to a subgroup of chemicals (prohaptens) whose sensitizing potential depend on prior metabolic activation e.g. via cytochrome P450 (CYP) enzymes. Furthermore, coculture clearly increased the upregulation of the cell surface molecule CD86 on THP-1 cells after incubation with these prohaptens and also several other skin sensitizers.

In this study we further elucidate the cross talk between THP-1 cells and HaCaT cells by analyzing the impact of HaCaT cells on the expression of miRNAs in THP-1 cells by Microarray technology. We identified 6 differentially expressed miRNAs in cocultured THP-1 cells compared to monocultured THP-1 cells irrespective of the treatment (medium, 0.2% DMSO as solvent control, B[a]P). In the presence of DMSO and B[a]P (after 48h) 8 additional miRNAs are differentially expressed. Up to now it is not clear whether the cross talk between HaCaT and THP-1 cells comprises the exchange of miRNA between the cocultured cells or whether it influences the expression of these miRNA in THP-1 cells, or both. Given that one miRNA has several gene targets these results illustrate that the cross talk between THP-1 and HaCaT cells also impacts on the miRNome.

392

Multi-level omics analysis of combination effects of (tri-)azoles in a set of different cell lines

A. Mentz¹, C. Knebel², P. Marx-Stoelting², J. Kalinowski¹, H. Bednarz¹, K. Niehaus¹, B. Seeger³, R. Pfeil², P. Steinberg³, **T. Heise**²

¹Universität Bielefeld, Centrum für Biotechnologie, Bielefeld, Germany

²Bundesinstitut für Risikobewertung, Sicherheit von Pestiziden, Berlin, Germany

³Stiftung Tierärztliche Hochschule Hannover, Institut für Lebensmitteltoxikologie und Chemische Analytik, Hannover, Germany

Background: Consumers are constantly exposed to chemical mixtures e. g. to multiple residues of different pesticides via the diet. This raises questions concerning potential cumulative effects, especially for substances causing toxicity by a common mode of action. Since substances are tested for regulatory purposes on an individual basis at generally high dose levels, there is only limited data available on potential mixture effects especially in the low dose range. With more than 400 active substances approved for being used in pesticides and over 100000 chemicals registered under REACH there are more possible combinations than one could test with classical animal experiments. The development of *in vitro* tools for assessment of mixture effects consequently is of tremendous importance.

Methods: As a first step in the development of such *in vitro* tools we used a group of fungicides, (tri-)azoles, as model substances in a set of different cell lines from known target tissues, basically liver (human: HepG2, HepaRG, rat: H4IIE) and adrenal gland (human: H295R). Concentrations were taken from measured tissue concentrations *in vivo* to ensure that used concentrations of the (tri-) azoles reflect realistic effect levels. The cell lines were exposed with the triazoles cyproconazole and epoxiconazole as well as with the azole prochloraz as individual substances and in binary or ternary combinations of these substances at three dose levels and three different time periods. The effects of the substances were subsequently analysed by transcriptomics and metabolomics. A support vector machine will be utilized to integrate the data from the different sources to gain a complete picture of affected adverse outcome pathways and mechanistic information about the applied fungicides.

Results & Conclusion: First results indicate combination effects of the substances also at the omics level depending on the specific endpoint and the concentration used. Some of these are comparable to effects found with similar methods in a standard toxicity test, a 28-day feeding study in the rat, thus raising hope for the development of *in vitro* methods suitable to detect combination effects.

393

Toxicity of plant protection and biocide products as compared to active substances *in vitro*

P. Fenske-Uyar¹, J. Wolfrum¹, C. Kneuer¹, L. Niemann¹, P. Marx-Stötting¹, **S. Rieke**¹

¹Bundesinstitut für Risikobewertung, Berlin, Germany

Background: Plant protection and biocide products are chemical mixtures, which contain one or more active substances as well as several co-formulants (e.g. solvents, wetting agents, thickeners or preservatives). Nevertheless, to this day extensive toxicological testing is performed only with the individual active substances, while the plant protection products are only evaluated for acute toxicity, i.e. a single dose group experiment with rats is performed as well as testing for skin- and eye-irritation. Current pesticides regulation foresees testing of potential harmful mixture effects but only when adequate methods are available making the development of such methods a high priority. Several published studies both *in vitro* and *in vivo* have shown fortified toxic effects of plant protection products compared to individual active substances.

Methods: Here we present effects of plant protection products as a whole as compared to the individual active substances or co-formulants in a set of human cell lines of hepatic and renal origin (HepG2, HepaRG, HEK293). Cytotoxicity has been analysed by WST-1 and NRU assay as well as gene expression of several marker genes involved in xenobiotic metabolism. Additionally reporter gene assays have been conducted for nuclear receptors such as AhR and CAR.

Results: While some active substances showed lower toxicity as compared to the respective products, this cannot be confirmed as a general rule for all endpoints for all of the analysed fungicides or herbicides containing active substances such as epoxiconazole, cyproconazole, azoxystrobin or glyphosate.

394

Cross Talk between keratinocytes and dendritic cells modulates capacities for activation and deactivation of chemicals.

J. Hennen¹, B. Blömeke¹

¹University Trier, Department of Environmental Toxicology, Trier, Germany

Chemical compounds may induce skin sensitization in humans, resulting in tolerance or allergic contact dermatitis after repeated exposure. Mechanistically, the activation of dendritic cells is one of the prerequisites for the induction of skin sensitization. A subgroup of sensitizing chemicals, prohaptenes, need metabolic activation, e.g. via cytochrome P450 (CYP) enzymes. Thus, xenobiotic metabolism may crucially impact on a chemical's potential for the induction of skin sensitization by activation, but also deactivation of reactive molecules via conjugation, which determines the concentration and the chemical species available for protein haptation and cell activation.

We established a coculture model consisting of HaCaT keratinocytes and THP-1 as surrogate dendritic cells for the detection of sensitizing chemicals and found enhanced CYP1 enzyme activity in HaCaT cells exposed to benzo[a]pyrene (B[a]P) and eugenol as well as clearly increased expression of cell surface molecule CD86 on THP-1 cells after incubation with these prohaptenes (Hennen et al., 2011). Here, we studied the impact of intercellular cross talk on activation and conjugation capacities in more detail.

Treatment of THP-1 with B[a]P and eugenol in coculture with HaCaT cells augmented CYP1A1 and/or CYP1B1 mRNA levels, while this was not found for THP-1 monoculture. Augmentation of CYP1A1 mRNA needed continuous presence of HaCaT cells. In coculture, levels of 3-OH-B[a]P as exemplary CYP-dependent metabolite were

increased compared to single cultures. In contrast to this, total glutathione contents as well as N-acetyltransferase 1 enzyme activities in both cell types were not modulated in coculture, furthermore the capacity for sulfation/glucuronidation of 3-OH-B[a]P was maintained in coculture. Additionally, the decrease of the total glutathione content in THP-1 cells by 2,4-dinitrochlorobenzene (DNCCB) was much less pronounced when exposed in coculture with HaCaT cells, showing that HaCaT cells provide additional targets for cysteine-reactive chemicals such as DNCCB, diminishing the total amount of chemicals available for THP-1 cells.

Overall, results indicate that the cross talk between keratinocytes and antigen-presenting cells enhances their capacities for metabolic activation of chemicals, while HaCaT cells also provide supplementary capacities for phase II reactions.

References: Hennen J et al. Cross talk between keratinocytes and dendritic cells: Impact on the prediction of sensitzation. Toxicol Sci 2011 123:501-510.

Toxicology – Toxic pathway analysis/AOP

395

Role of superoxide anions and hydroxyl radicals in HEMA-induced apoptosis

M. Godula¹, M. Gallorini^{1,2}, C. Petzel¹, C. Bolay¹, K.-A. Hiller¹, A. Cataldi², S. Krifka¹, W. Buchalla¹, **H. Schweikl**¹

¹Klinikum der Universität Regensburg, Poliklinik für Zahnerhaltung und Parodontologie, Regensburg, Germany

²University "G. d'Annunzio" Chieti-Pescara, Department of Pharmacy, Chieti, Italien

Residual monomers released from dental composite materials interact with tissues of the oral cavity. Monomers like 2-hydroxyethyl methacrylate (HEMA) disrupt vital cell functions e.g. responses of the innate immune system, mineralization and cell differentiation, or induce cell death via apoptosis. These effects are associated with the induction of oxidative stress due to the enhanced formation of reactive oxygen species (ROS). Identifying the kind of ROS which increase in the presence of monomers such as HEMA and lead to apoptosis would be a basis for the development of *new therapeutic strategies* to protect oral tissues from adverse reactions causally related to a monomer-disturbed redox homeostasis. Thus, the present study provides insight into the role of superoxide anions and hydroxyl radicals in monomer-induced apoptosis. General oxidative stress was significantly increased 1.5-fold in cells exposed to HEMA for 1h as indicated after the staining of cells with 2',7'-dichlorodihydrofluorescein diacetate (H₂DCF-DA) as a fluorescent probe and subsequent flow cytometry (FACS). In contrast, DHR123 fluorescence indicating the formation of H₂O₂ was enhanced about 2-fold after 24h exposure. This increase in the formation of hydrogen peroxide was drastically reduced in the presence of the 5 mM tempol, a scavenger of superoxide anions. However, the formation of superoxide anions as detected by dihydroethidium (DHE) was not intensified. Likewise, a significant influence of sodium formate (0-10 mM) used as a scavenger of hydroxyl radicals was not detected in HEMA-exposed cell cultures. Considering the induction of apoptosis, HEMA reduced the number of viable cells in a concentration-dependent manner after a 24h exposure period. About 60% viable cells were detected in cultures exposed to 8 mM HEMA compared to 97% viable cells observed in untreated cultures while the number of cells found in late apoptosis increased in parallel. Low concentrations of tempol (0.05-0.5 mM) caused a shift of the number of cells in HEMA-exposed cultures from late to early apoptosis indicating protection of tempol against the effect of HEMA. Different from tempol, and depending on the concentration, sodium formate reduced the number of cells in the various phases of cell death in cultures exposed to HEMA. These findings demonstrate that the proportion of superoxide anions and hydroxyl radicals in HEMA-induced oxidative stress is unclear. However, the protective effects of tempol or sodium formate indicate that superoxide anions and hydroxyl radicals are involved in HEMA-induced apoptosis. supported by the Deutsche Forschungsgemeinschaft DFG (Schw 431/13-2)

396

A role for TRPA1 as oxygen and toxin sensor in the lung?

M. Kannler¹, T. Gudermann¹, A. Dietrich¹

¹Walther-Straub-Institut der LMU-München, München, Germany

Transient Receptor Potential (TRP) proteins represent a large superfamily of non-selective cation channels sensing toxic stimuli in the human body. TRPA1 expresses a high number of aminoterminal ankyrin repeats and is the only member of the TRPA family. Channel monomers form homotetramers in the plasma membrane with six transmembrane segments (TM) and a pore forming loop between TM5 and 6. TRPA1 has been extensively described in sensory nerve endings as an important cellular detector for toxic stimuli and as an oxygen sensor (reviewed in 1). Although recently two reports identified TRPA1 in pulmonary epithelial and endothelial cells (2, 3), its expression in non-neuronal tissues is still a matter of debate. After isolation and identification of different murine lung cells we were able to identify murine TRPA1 protein in primary endothelial cells, pneumocytes type II (ATII) and fibroblasts by using specific antibodies in a western blot analysis, but not in cells from TRPA1-deficient mice. ATII cells were identified by specific cell markers such as surfactant protein C and were further differentiated to AT1 cells characterized by their specific expression of podoplanin. Quantitative TRP expression patterns will now be evaluated by quantitative reverse transcription (RT)-PCR as well as utilizing NanoString[®] technology in different lung cells. To characterize TRPA1 on a cellular level we cultured a HEK293 cell line stably expressing TRPA1 (4). Allylisothiocyanate (AITC) a specific activator as well as hypoxia and hyperoxia was able to induce Ca²⁺-influx in this cell line, which was blocked by the specific inhibitor A96079. In the future, we will utilize the isolated perfused lung model (5) to quantify toxin-induced edema formation in ex vivo lungs from WT and TRPA1-deficient mice after exposure to potential toxic inhalation hazards (TIH see 6) to challenge the hypothesis of TRPA1 as an important toxin sensor in the lung. By this strategy we hope to understand TRPA1 function in lung cells and to evaluate TRPA1 proteins as potential pharmacological targets for a specific therapeutic intervention during toxin-induced edema formation.

References:

(1) Takahashi et al. Model of O₂ Sensing for TRPA1 channel (2012)., Front. Physiol. 3:324

- (2) Büch et al. Functional expression of the transient receptor potential channel TRPA1 a sensor for toxic lung inhalants, in pulmonary epithelial cells (2013)., *Chem Biol Interact.* 206: 462-71
- (3) Fernandes et al. The functions of TRPA1 and TRPV1: moving away from sensory nerves (2012). *Br. J. Pharmacol.* 166: 510-21
- (4) Schäfer et al. Stimulation of the chemosensory TRPA1 cation channel by volatile toxic substances promotes cell survival of small cell lung cancer cells (2013). *Biochem. Pharmacol.* 85: 426-438
- (5) Weissmann et al. Activation of TRPC6 channels is essential for lung ischaemia-reperfusion induced oedema in mice (2012). *Nature Commun.* 3: 649
- (6) Büch et al. Chemosensory TRP channels in the respiratory tract: role in toxic lung injury and potential as "sweet spots" for targeted therapies. (2013). *Rev Physiol Biochem Pharmacol.* 165: 31-65.

397

Microbiome-related metabolic changes in plasma of antibiotic treated rats

C. Behr¹, B. van Ravenzwaay¹, H. Kamp¹, E. Fabian¹, G. Krennrich¹, W. Mellert¹, E. Peter², V. Strauss¹, T. Walk²
¹BASF SE, Ludwigshafen, Germany
²metanomics GmbH, Berlin, Germany

Metabolism by the intestinal microbiota is likely to contribute essentially to the plasma metabolite profile of the mammalian host organism and it requires adequate identification of effects of the microbiome on the endogenous plasma metabolite patterns. The current investigations present insights in the mammalian-microbiome co-metabolism of endogenous metabolites.

Antibiotics have a profound effect on the micro-organism composition of the microbiome and hence on the mammalian-microbiome co-metabolism. The consequences, however, on the functionality of the microbiome (defined as the production of metabolites absorbed by the host) and which of these changes are related to the microbiome are not well understood.

To identify plasma metabolites related to microbiome changes due to antibiotic treatment, we have employed a metabolomics approach. To this purpose broad-spectrum antibiotics belonging to the class of aminoglycosides (streptomycin, neomycin, gentamicin), fluoroquinolones (moxifloxacin, levofloxacin) and tetracyclines (doxycycline, tetracycline) were administered orally for 28 days to male rats including blood sampling for metabolic profiling after 7, 14 and 28 days. Fluoroquinolones and tetracyclines can be absorbed from the gut whereas aminoglycosides cannot.

To distinguish between metabolite changes caused by systemic toxicity of the antibiotics and microbiome related changes, the metabolites identified in the metabolome pattern were compared to a list of metabolites known to be produced by the gastro-intestinal micro-organisms. Beside changes mainly concerning amino acids and carbohydrates, hippuric acid and indole-3-acetic acid were identified as key metabolites being affected by antibiotic treatment. For each class the following gut metabolites were found to be unique: indole-3-propionic acid for aminoglycosides, taurine for fluoroquinolones, 3-indoxylsulfate, uracil and allantoin for tetracyclines.

For each class of antibiotics specific and selective metabolome patterns could be established. The results suggest that plasma based metabolic profiling (metabolomics) could be a suitable tool to investigate the effect of antibiotics on the functionality of the microbiome and to obtain insight in the mammalian-microbiome co-metabolism of endogenous metabolites.

398

Evaluation of targeted bile acid profiling in a model of Methapyrilene-induced liver injury in rats

M. Slopianka¹, B. Riefke¹, M. Pavkovic², H. Ellinger-Ziegelbauer², M. Segura-Lepe³, M. Keck¹, T. Steger-Hartmann¹
¹Bayer Pharma AG, Investigational Toxicology, Berlin, Germany
²Bayer Pharma AG, Mechanistic Toxicology, Wuppertal, Germany
³Bayer Pharma AG, Bioinformatics, Berlin, Germany

Drug-induced liver injury (DILI) is still a major reason for termination of clinical trials and thus is an important concern in drug development. Identification and prediction of DILI in the clinic and in preclinical safety testing still relies on the classical clinical chemistry panel and histopathology with known limitations in sensitivity and specificity. In the last years bile acids (BAs) have been studied as potential biomarkers to better characterize drug-induced liver injury with promising results (Ellinger-Ziegelbauer et al., 2011; Luo, Schomaker, Houle, Aubrecht, & Colangelo, 2014; Yamazaki et al., 2013). To evaluate whether a targeted bile acid profiling via LC-MS/MS in plasma and liver tissue can improve assessment of liver injury, methapyrilene (MPy) a known hepatotoxin, or corresponding vehicle, was administered daily to male Wistar rats at a low (30 mg/kg) and a high (80 mg/kg) dose. Rats were sacrificed following 3, 7, or 14 consecutive daily doses, or after recovery 10 days following 14 consecutive administrations of MPy or vehicle. In addition to bile acids which were determined both in plasma and tissue, conventional preclinical safety endpoints (Histopathology and Clinical Chemistry) assessment and gene expression profiling was performed in liver to obtain mechanistic information about potential changes in regulation of bile acid levels. Conventional findings included periportal necrosis, inflammation and biliary hyperplasia, and increased liver enzyme activity and bilirubin levels during the treatment phase. The bile acid pattern showed increased levels of conjugated and unconjugated bile acids in low dose and high dose groups compared to the controls after administration of methapyrilene. Furthermore, although liver enzyme activity and bilirubin levels in serum were decreased again in the recovery groups, suggesting recovering liver injury, bile acid concentrations remained elevated with no signs of recovery. Analysis of transcriptomics data revealed decreased levels of mRNA encoding α -Methylacyl-CoA racemase (AMACR) 4 and 15 days after dosing, a gene responsible for bile acid synthesis. Membrane transport systems for bile acids like sodium/taurocholate co-transporting polypeptide (Ntcp) and Organic anion transporting polypeptide 1 (OATP1) expression were down regulated as well, indicating that the increased bile acid concentrations in plasma and tissue could be attributable to reduced uptake by the hepatocyte. In summary the data suggest that

targeted bile acid profiling could be used as potential biomarkers to enhance assessment of drug-induced liver injury.

399

Photorhabdus asymbiotica Toxin PaTox Harbors a C58-like Protease Domain

C. Trillhaase¹, S. Schneider^{1,2}, M. Steinemann¹, K. Aktories¹, T. Jank¹
¹Experimentelle und Klinische Pharmakologie und Toxikologie, Abteilung 1, Freiburg, Germany
²Hermann-Staudinger-Graduiertenschule, Chemie und Pharmazie, Hebelstraße 27, D-79104 Freiburg, Germany

Photorhabdus asymbiotica is an entomopathogen and emerging human pathogen causing soft tissue infections in humans. *Photorhabdus asymbiotica* produces the bacterial protein toxin PaTox, which is cytotoxic for various cell lines and kills insect larvae. Previous studies have established that PaTox harbors two enzymatic active domains, a glycosyltransferase and a deamidase domain. The glycosyltransferase domain inactivates host GTPases of the Rho family by GlcNAcylation of a tyrosine residue in the effector binding loop, which results in the disassembly of the actin cytoskeleton. The deamidase domain deamidates a crucial glutamine residue in heterotrimeric G α and G α_{11} proteins, which renders the G proteins constitutive active. Sequence and structural homology analyses of PaTox revealed a third domain (PaTox^P) resembling peptidases of the C58 protease family. PaTox^P contains the conserved catalytic triade (C/H/D) of papain-like cysteine proteases and shares sequence similarity with effectors from *Yersinia pestis* (*Yersinia* outer protein YopT) and *Pseudomonas syringae* (avirulence protein AvrPphB). Transient expression of PaTox^P in HeLa cells induces cell rounding and indicates a cytotoxic potential of PaTox^P. Incubation of PaTox^P with linearized bovine serum albumin (BSA) results in cleavage products of BSA assuming proteolytic activity of PaTox^P. Mutation of the catalytic cysteine in PaTox^P prevents cleavage of BSA and blocks cytotoxicity. We were not able to observe autocatalytic cleavage of PaTox constructs under various conditions. The intracellular activity of the protease domain is most likely involved in the pathogenicity of PaTox.

400

Vitamin D metabolism – Involved in triazole fungicide toxicity?

A. Lehmann¹, S. Rieke¹, A. Dabrowski¹, T. Heise¹, L. Niemann¹, R. Pfeil¹, P. Marx-Stöling¹, C. Kneuer¹
¹BfR, Berlin, Germany

Background: In a 28-day rat feeding study with the azole fungicides cyproconazole (C), epoxiconazole (E), propiconazole (P), tebuconazole (T), prochloraz (Pz) as well as combinations C+E and C+E+Pz, a reduction of vitamin D (VitD) receptor mRNA levels was reproducibly observed in adrenals for C, E and P. Transcription of various enzymes related to VitD homeostasis (including Cyp2r1, Gc, Cyp3a, Ugt1a) in liver was also affected, while initial indications for modulation of renal Cyp24a1 and renal and hepatic Cyp27b1 could not be confirmed. A possible induction of parathormone (PTH) was noted for the high dose of C, but statistical significance could not be shown. We have now performed supporting analyses for serum VitD levels, measured additional transcript levels and will provide a framework for the interpretation of the findings.

Methods: Male Wistar rats (n=5 for single substances, n=10 for combinations) were treated for 28 days at dose levels tested based on NOAELs from 90-day subchronic feeding studies and ranged from NOAEL/100 to NOAELx10. Quantitative RT-PCR analyses were performed on organ samples obtained at sacrifice. Serum VitD levels were determined using the total (25-OH) Vitamin D ELISA (DRG Instruments GmbH, Marburg, Germany).

Results: The ELISA established for diagnostic analysis of human serum and plasma samples could be applied to rat serum. VitD levels in control animals (n=30) were 64.7±8.3 ng/mL (min/max: 48/78 ng/mL), i.e. in the range of values reported previously for rats. For the high dose of C (1000 ppm in food, n=5), there was a statistically non-significant reduction of VitD levels to 71.3±17.6% of the concurrent control (n=5). However, for 4 of 5 animals of this group, measured VitD level were below the range observed in pooled controls (n=30). An according follow-up is ongoing. qRT-PCR analysis of adrenal tissue showed deregulation of apoptosis related genes (p21 for C, E and Pz; Cdk1 and Gadd45a for E; Cdkn1c for C), which is in agreement with an involvement of VitD in the autocrine/paracrine regulation of cell proliferation.

Conclusion: Reduction of circulating VitD levels would be plausible as a result of induction of hepatic Cyp3a1/2 and Ugt1a. However, this could not be confirmed by ELISA as a general mechanism for all azole fungicides under investigation. Only for rats fed with 1000ppm cyproconazole, there were indications for a moderate reduction of 25-OH Vitamin D, which would correlate with the previously reported moderate increase in serum PTH for this group.

Clinical Pharmacology – Drug therapy in pregnancy

401

Hansen's disease during pregnancy and lactation: two babies born to a mother using antileprosy drugs

Z. Öztürk¹
¹Izmir Atatürk Research Hospital, Clinical Pharmacology and Toxicology, Izmir, Trkei

Hansen's disease, also known as leprosy, during pregnancy has been rarely reported in Europe and United States. Early diagnosis is important, and medication can decrease the risk of those living with leprosy patients from acquiring the disease. This report presents a case of multidrug antileprosy therapy during pregnancy and lactation.

A 26-year-old multiparous woman with a known case of multibacillary leprosy presented with unplanned pregnancy. Her pregnancy was discovered in the 9th week, and she has been taking a multidrug therapy (dapson 100 mg/day, rifampicin 600 mg/month, clofazimine 50 mg /day and clofazimine 300 mg/month) for the past 8 months. Diagnosis of leprosy was established in her previous pregnancy. The patient was informed about

the risks of drugs used in pregnancy. The treatment was continued unchanged during pregnancy. A detailed fetal ultrasonography was offered to scan the development of the fetus at about 20 weeks. In the 8th, 22nd, 28th weeks of pregnancy, prenatal sonographic examinations revealed normal fetal growth and amniotic fluid volume. At 28 weeks pregnant, she was diagnosed with gestational diabetes. Diabetes did not cause any symptoms during pregnancy, and it was controlled with a reduced-calorie diet in a week. The patient delivered a healthy baby girl by vaginal birth in the 39th week of gestation without perinatal complications. The baby was also healthy (APGAR 8-9, 3300 g, 51 cm), and its growth and development were normal during a 6-month follow-up period. The patient decided to breastfeed while taking medication. She had a previous experience with use of anti-leprosy drugs while breastfeeding, her other child was 15 months old and healthy. As well as in the first child, skin discoloration was observed in newborn due to clofazimine during lactation. After 3 months, she stopped breastfeeding, and the infant's skin changes were reversed.

For pregnant women and practitioners, treatment of leprosy in pregnancy can be complicated. Physical and neurological damage may be irreversible even if cured. Multidrug therapy consisting dapson, rifampicin and clofazimine is highly effective for people with leprosy and considered safe, both for the mother and the child. Antileprosy drugs are excreted into human milk but there is no report of adverse effects except for skin discoloration of the infant due to clofazimine. Therefore, multidrug therapy for leprosy patients should be continued unchanged during pregnancy and lactation.

Clinical Pharmacology – Cardiovascular treatment

402

Use of oral anticoagulants and its determinants in elderly

A. Douros¹, E. Schaeffner², O. Jakob³, N. Ebert², R. Kreutz¹

¹Charité-Universitätsmedizin Berlin, Institut für Klinische Pharmakologie und Toxikologie, Berlin, Germany

²Charité-Universitätsmedizin Berlin, Berlin School of Public Health, Berlin, Germany

³Charité-Universitätsmedizin Berlin, Institut für Biometrie und Klinische Epidemiologie, Berlin, Germany

Background: In the past years new oral anticoagulants (NOACs) were approved expanding our pharmacological arsenal. Data regarding their utilisation in elderly compared to vitamin K antagonists are scarce. Moreover, factors affecting physicians' choice in favour of particular anticoagulants have yet to be elucidated. The present study investigated anticoagulant use and factors affecting it in people ≥ 70 years.

Methods: Individuals included in the analysis were participants of the Berlin Initiative Study (BIS). BIS is a population-based prospective cohort study initiated in 2009 in Berlin, Germany, to evaluate kidney function in people ≥ 70 years. Medication was assessed through personal interviews and coded using the Anatomical Therapeutic Chemical Classification System. For estimation of glomerular filtration rate (eGFR) we used the CKD-EPIcr equation. Predictor analysis was conducted via logistic regression.

Results: Figure 1 illustrates the percentage of drug use for the three NOACs and phenprocoumon, the most common vitamin K antagonist in Germany, over the course of four years. Table 1 shows the characteristics of patients for each oral anticoagulant group during the four-year follow-up visit (from January 2014 until April 2015). The probability of dabigatran use rose with increasing age (+12%), and the probability of phenprocoumon use rose in case of eGFR < 60 ml/min/1.73m² (+54%) or male sex (+82%).

Discussion: Our data show that also in the elderly NOAC use increased over the past years. Characteristics such as age, sex or kidney function had an impact on the choice of oral anticoagulation.

Abb. 1

Figure 1 The three NOACs and phenprocoumon over the course of 4 years in the BIS study

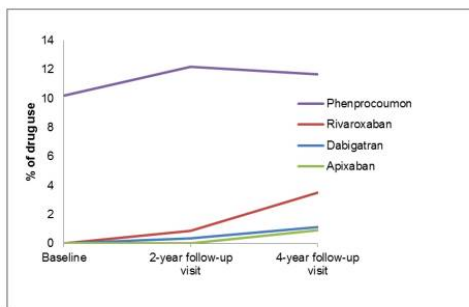


Abb. 2

Table 1 Characteristics of patients for each oral anticoagulant group during the four-year follow-up visit

	Phenprocoumon (n=153)	Dabigatran (n=14)	Rivaroxaban (n=46)	Apixaban (n=12)
Age mean \pm SD (years)	84 \pm 6	87 \pm 4	84 \pm 5	85 \pm 5
Female sex n (%)	62 (41)	4 (29)	24 (52)	9 (75)
eGFR _{CKD-EPIcr} < 60 ml/min/1.73m ² n (%)	64 (42)	3 (21)	16 (35)	5 (42)
Myocardial infarction n (%)	27 (18)	3 (21)	8 (18)	1 (9)
Stroke n (%)	17 (11)	3 (21)	0 (0)	2 (17)

403

Characteristics of patients with orthostatic hypotension in a cohort of very elderly nursing home residents in Germany

K. Grabowski¹, F. Köhner¹, D. Dräger², R. Kreutz¹, J. Bolbrinker¹

¹Charité-Universitätsmedizin Berlin, Institut für Klinische Pharmakologie und Toxikologie, Berlin, Germany

²Charité-Universitätsmedizin Berlin, Institut für Medizinische Soziologie, Berlin, Germany

Objective: Orthostatic hypotension (OH) is an important factor in determining cardiovascular mortality especially in older age. Different factors were discussed to influence OH. Arterial stiffness, medication and frailty were demonstrated as modifying factors of OH. The aim of this study was to assess prevalence of and influencing factors on OH in nursing home residents (NHR) in Germany.

Methods: Systolic (SBP) and diastolic (DBP) blood pressure as well as pulse pressure (PP) and pulse wave velocity (PWV) as markers of arterial stiffness were measured in NHR aged ≥ 65 years in 12 nursing homes in Berlin, Germany. Measurements were first performed in the sitting position and then repeated after standing up. OH was defined as a SBP decrease of > 20 mmHg and/or DBP decrease of > 10 mmHg within 3 min after standing up. Hypertension was defined as the presence of diagnosis arterial hypertension, the prescription of at least one antihypertensive drug, or mean SBP values > 139 mmHg and/or mean DBP > 89 mmHg. Information about antihypertensive medication was received from interviews and medical records. Frailty was determined by geriatric assessments, e.g. "Timed Up and Go Test" (TUG) or Barthel Scale.

Results: OH testing could be performed with 96 NHR (mean age = 84.5 \pm 7.3 years). In total, 15 subjects (15.6%) had OH. The mean change in SBP from sitting to standing was 19.2 \pm 15 mmHg (range +8.5 to -52.5 mmHg) in patients with OH and 1.5 \pm 10.9 mmHg (range +44.5 to -17 mmHg) in patients without OH. Mean SBP was significantly higher (143.6 \pm 17.1 mmHg) in people with OH than in those without (131.5 \pm 20.1 mmHg). All of the NHR with OH were hypertensive compared to 89% of the NHR without OH. Sex, mean age, PWV and PP was not significantly different between individuals with or without OH ($p > 0.05$). Medication data was available for 89 patients. All individuals with OH and 60 NHR without OH (80%) had antihypertensive medication. More than 2 different antihypertensive drugs were present in 11 patients with OH (78.5%) and in 43 patients without OH (57.3%). The intake of beta-blockers had no impact on OH development. Geriatric assessments did not differ significantly between the OH group and the non-OH group. More than 75% of patients in both groups reached 80 points as maximum in Barthel Scale defining a need for assistance and TUG analyses demonstrated that around 50% of patients with OH as well as patients without OH needed more than 19 sec showing a motor slowing.

Conclusion: We found a relatively low prevalence of OH in our very old patient cohort and the overall BP control was good. Similar to earlier publications mean SBP was significantly higher in NHR with OH. All of the other investigated factors were not associated with the occurrence of OH. The small cohort size might have limited the detection of cardiovascular, epidemiological or geriatric associations. In addition, important confounding factors such as the inability to stand of some NHR and the lack of standardized frailty assessments must be addressed.

404

Impact of reticulated platelets on the initial antiplatelet response to thienopyridine loading in patients undergoing elective coronary intervention

C. Stratz¹, T. Nuehnenberg¹, S. Leggewie¹, M. Cederqvist¹, C. Valina¹, F.-J. Neumann¹, W. Hochholzer¹, D. Trenk¹

¹Universtaets Herzzentrum Freiburg Bad Krozingen, Kardiologie Angiologie II, Bad Krozingen, Germany

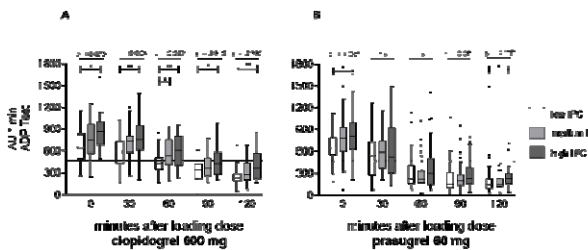
Background: Reticulated platelets are associated with impaired antiplatelet response to thienopyridine treatment. This interaction might be caused by intrinsic properties of reticulated platelets or a decreased drug exposure due to high platelet turnover reflected by reticulated platelets as surrogate. We investigated the impact of reticulated platelets on antiplatelet response to thienopyridines and if this effect is linked to platelet turnover.

Methods: This study randomized elective patients to loading with clopidogrel 600mg or prasugrel 60mg (n=200). ADP-induced platelet reactivity was assessed by impedance aggregometry 30 to 120 minutes and day 1 after loading but before intake of the next dose of thienopyridines. Immature platelet count (IPC) was assessed as marker of reticulated platelets by whole blood flow cytometry.

Results: Platelet reactivity increased with rising tertiles of IPC (Figure). This effect was more pronounced in patients on clopidogrel as compared to patients on prasugrel. Overall, IPC correlated well with on-treatment platelet reactivity at 120min ($r=0.21$; $p < 0.001$). This correlation did not change over time indicating an effect independent of platelet turnover (comparison of correlations 120min/day 1: $p=0.57$ for clopidogrel, $p=0.76$ for prasugrel).

Conclusion: A high immature platelet count is associated with impaired response to thienopyridine loading. This effect is independent of platelet turnover indicating a relation to intrinsic properties of reticulated platelets.

Abb. 1



Clinical Pharmacology – Antineoplastic treatment

405

Combination therapy of a targeted toxin with SO1861: A shooting star in the world of pancreatic carcinoma

C. Bhargava¹, B. von Mallinckrodt¹, H. Dürkop², M. Thakur¹, R. Gilbert-Oriol¹, A. Weng¹, M. F. Meizig³, H. Fuchs¹
¹Charité Universitätsmedizin, Berlin, Germany
²Pathodiagnostik Berlin, Berlin, Germany
³Freie Universität, Berlin, Germany

Introduction: One of the biggest drawbacks of protein-based therapeutics with intracellular targets is their inability to enter the cytosol. Targeted toxins are known to be used in drug delivery. Aim of the study was to target epidermal growth factor (EGF) receptor overexpressed on pancreatic carcinoma using a novel well-defined targeted toxin consisting of EGF fused to the toxic plant ribosome-inactivating protein dianthin and a glycosidic triterpenoid (SO1861) as efficacy enhancer.

Methods: The enzymatic activity of dianthin-EGF was verified by an adenine release assay. The kinetics of cytotoxicity were evaluated in pancreatic adenocarcinoma BxPC-3 and MIAPaCa-2 cells in comparison to the non-target cell line NIH3T3 with an impedance-based real time cell analyzer (xCELLigence) and final cytotoxicity analyses with conventional end-point MTT assays. Acute toxic of dianthin-EGF was studied in male BALB/c mice.

A xenograft solid tumor model was developed in male nude mice by injecting BxPC-3 cells into the dorsal part subcutaneously. Dianthin-EGF was administered at the vicinity of the tumor and SO1861 by subcutaneous injection at the neck. After the tumor reached a diameter of 2 to 3 mm in size 6 treatments were given in total. Tumor volumes and body weight shifts were observed twice weekly to determine the potency of dianthin-EGF when given alone and in combination with SO1861 in comparison to placebo. Immunohistochemical detection of EGF receptor was performed according to the manufacturer's advice (DAKO, Glostrup, Denmark, K1492). Complete blood count analysis was done by Labor 28 GmbH, Berlin.

Results: The adenine release mediated by dianthin-EGF was 47.8 pmol adenine/pmol toxin/h. The in vitro efficacy of the targeted toxin was proven by an IC50 value of approximately 1 nM for EGF receptor expressing MIAPaCa-2 and BxPC-3 cells as compared to 100 nM for non-target NIH3T3 cells. Real time measurement of the cytotoxicity showed a dose-dependent decrease in cell viability from 10 pM to 1 μM. Toxicity studies in BALB/c mice revealed 0.4 μg/mouse to be non-toxic and maximum tolerated dose (MTD) whereas 40 μg caused morbidity accompanied with white ocular discharge. Efficacy studies were performed for a period of 28 days. The combination therapy showed that the average tumor volume measured by a digital vernier caliper was found to be 80% less than for placebo whereas single therapy using dianthin-EGF alone caused a further increase in tumor volume which was although yet 50% less when compared to placebo.

Immunohistochemistry slides showed EGF receptor expression in each of all untreated xenograft tumors, which further confirms the presence of EGF receptor overexpression in the target BxPC-3 cell line. Enlarged spleen was only observed in untreated xenografts. No significant change in various blood parameters (RBC counts, WBC counts, HGB, HCT, MCV, MCH and MCHC) were observed on hematological analysis except for the platelet (PLT) counts in comparison to healthy male nude mice.

Conclusion: Combination therapy with SO1861 proves to be a promising approach for the targeted delivery of toxins instead of single therapy administering targeted toxin alone. The strategy is specific for EGF receptor overexpressing tumors such as pancreatic cancer.

Clinical Pharmacology – Safety of drug therapy

406

In vitro and in silico screening of Moringa oleifera for drug interactions on Cytochrome P450 3A4 and P-glycoprotein

C. Awortwe¹, P. Bouic^{2,3}, B. Rosenkranz¹

¹University of Stellenbosch, Division of Clinical Pharmacology, Faculty of Medicine and Health Sciences, Cape Town, Sd Afrika, Republik
²Synexa Life Sciences, Cape Town, Sd Afrika, Republik
³University of Stellenbosch, Division of Medical Microbiology, Faculty of Medicine and Health Sciences, Cape Town, Sd Afrika, Republik

Introduction: *Moringa oleifera* (MO) is a popular herbal supplement used for treatment and management of diverse diseases in sub-Saharan Africa. Its intake among individuals infected with HIV/AIDS has increased recently due to the purported immune boosting property. Limited information, however, is available regarding its potential to

cause interactions with commonly prescribed medications that are substrates of CYP3A4 and P-glycoprotein.

Methods: The methanol extract and four fractions of MO were tested on recombinant CYP3A4 at different concentrations with and without NADPH to determine the IC₅₀ shift reduction. The crude methanol extract of MO was incubated with testosterone (TST) and cryopreserved hepatocytes to evaluate its influence on clearance of TST. Effect of MO on the efflux transporter, P-glycoprotein was investigated by incubating the methanol extract with MDR1 – MDCKII cells. Virtual screening was conducted to predict physicochemical properties, bioavailability and interaction potential of phytochemical compounds unique to MO using combination of molinspiration version 2014.11 and admetSAR.

Results: Fractions (F1-F3) indicated IC₅₀ shift reduction ≥5 post-incubation with and without NADPH. MO showed moderate interaction (AUC/AUC = 2.46) with TST in cryopreserved hepatocytes. Also, MO mildly inhibited the transport of digoxin (IC₅₀ = 35.45 μg/mL) across MDR1 – MDCKII cells. Niaziminin indicated 85.57% bioavailability via the human intestinal membrane with 61% chance of inhibiting CYP3A4. β-sitosterone showed strong P-gp inhibition (83.27%) with 100% absorption via the intestine.

Conclusions: MO has the potential to inhibit the metabolism or excretion of other medications that are eliminated by CYP3A4 or P-glycoprotein, respectively, if adequate amounts of the active constituents such as niaziminin and β-sitosterone enter the circulation.

Acknowledgements: This study was partly funded by the NIH-Fogarty International Center training grant-Brown AIDS International Training and Research Program (Grant# D43TW00237), The United States Department of Agriculture, Agricultural Research Service, Specific Cooperative Agreement No. 58-6408-1-603 and NRF Indigenous Knowledge Systems (IKS) programme (Grant No: 82641).

407

Hepatotoxicity associated with use of phytotherapeutics

A. Douros^{1,2}, E. Bronder¹, F. Andersohn³, A. Klimpel¹, R. Kreutz¹, E. Garbe², J. Bolbrinker¹

¹Charité-Universitätsmedizin Berlin, Institut für Klinische Pharmakologie und Toxikologie, Berlin, Germany
²Leibniz-Institut für Präventionsforschung und Epidemiologie – BIPS, Abteilung für Klinische Epidemiologie, Bremen, Germany
³Charité-Universitätsmedizin Berlin, Institut für Sozialmedizin, Epidemiologie und Gesundheitsökonomie, Berlin, Germany

Background: Herb-induced liver injury (HILI) has attracted attention in the past years due to an increasing number of publications reporting cases of hepatotoxicity associated with use of phytotherapeutics. Here, we present data on HILI from the Berlin Case-Control Surveillance Study FAKOS.

Methods: FAKOS was initiated in 2000 to study serious toxicity of drugs including hepatotoxicity. Potential cases of liver injury were ascertained in more than 180 Departments of all 51 Berlin hospitals from October 2002 until December 2011. Through a standardised face-to-face interview and review of medical charts information on all previous intakes of drugs or herbals, on co-morbidities, and demographic data was ascertained. Inclusion criteria were an elevation of alanine aminotransferase or aspartate aminotransferase threefold above the upper limit of normal or an elevation of total bilirubin higher than 2 mg/dl. Excluded were patients with underlying liver disease (e.g., alcoholic fatty liver disease). Drug or herbal aetiology was assessed based on the updated Council for International Organizations of Medical Sciences (CIOMS) scale.

Results: Of all 198 cases of hepatotoxicity included into the FAKOS study, herbs were involved in ten cases (5.1%). Demographic, clinical, and laboratory characteristics of these ten cases are illustrated in Table 1. Among the six patients with available liver biopsy results, five patients showed signs of necrosis, either disseminated or predominantly near the central vein. Portal inflammation was more common than lobular inflammation, and the infiltrates contained mostly lymphocytes, neutrophil or eosinophil granulocytes. Herbal aetiology was judged two times as probable (ayurvedic herb in patient 1, pelargonium sidoides in patient 6), and eight times as possible (valeriana in patients 3, 4, 8, 9, 10, mentha piperita in patient 5, hypericum perforatum in patient 2, eucalyptus globulus in patient 7). In nine cases other non-herbal drugs were also suspected as potentially hepatotoxic (exception: patient 6). Seven cases occurred in the ambulatory setting requiring hospitalisation, three cases occurred during hospital stay.

Discussion: This case series provides further information on laboratory and clinical aspects of HILI. It corroborates known risks for valeriana and ayurveda treatment, and suggests that further herbals rarely or never associated with liver injury before such as pelargonium sidoides, hypericum perforatum or mentha piperita could also exhibit a hepatotoxic potential.

Abb. 1

Table 1. Selected demographic, clinical, and laboratory data of the patients with herb-induced liver injury.

	1	2	3	4	5	6	7	8	9	10
Suspected herb	Ayurveda herb	Hypericum perforatum	Valeriana	Valeriana	Mentha piperita	Pelargonium sidoides	Eucalyptus globulus	Valeriana	Valeriana	Valeriana
Sex	Female	Female	Female	Female	Male	Female	Male	Male	Female	Female
Age (y)	63	63	27	70	46	52	50	46	71	47
Grade of liver injury	Hepatohepatic	Mixed	Cholestatic	Hepatohepatic	Hepatohepatic	Hepatohepatic	Hepatohepatic	Hepatohepatic	Cholestatic	Non-classifiable
Laboratory testing										
ALT/ULN	34.9	19.2	7.5	3.5	71.6	14.7	6.1	3.5	4.1	4.6
AST/ULN	49.2	12.8	4.7	4.6	44.6	13.2	3.1	3.3	3.4	2.5
ALP/ULN	1.9	1.2	1.8	0.6	2.0	1.8	0.4	0.8	1.1	Missing
Bilirubin total (mg/dL)	31.3	2.0	7.1	2.8	3.8	1.0	0.5	0.5	0.5	Missing
Cr (mg/dL)	No	No	No	Yes (DNR 1.6)	No	No	No	No	No	No
Serology testing										
Hepatitis A virus	Negative	Negative	Negative	Negative	Negative	Negative	Negative	Negative	Negative	Negative
Hepatitis B virus	Negative	Negative	Negative	Negative	Negative	Negative	Negative	Negative	Negative	Negative
Hepatitis C virus	Negative	Negative	Negative	Negative	Negative	Negative	Negative	Negative	Negative	Negative
Cytomegalovirus	Negative	Missing	Missing	Missing	Missing	Missing	Missing	Missing	Missing	Missing
Epicystic virus	Negative	Missing	Missing	Missing	Missing	Missing	Missing	Missing	Missing	Missing
Hepatitis E virus	Negative	Missing	Missing	Missing	Missing	Missing	Missing	Missing	Missing	Missing
Hepatitis delta virus	Negative	Missing	Missing	Missing	Missing	Missing	Missing	Missing	Missing	Missing
Varicella zoster virus	Negative	Missing	Missing	Missing	Missing	Missing	Missing	Negative	Missing	Missing
Autoimmune antibodies testing	ANA 1:250	Negative	ANA 1:160	Negative	Negative	Negative	Negative	Negative	Negative	Negative
Abdominal sonography	Conducted	Conducted	Conducted	Conducted	Conducted	Conducted	Conducted	Conducted	Conducted	Conducted
Immunology										
Falgor	Yes	Yes	Yes	Yes	Yes	Yes	No	Yes	No	No
Jaundice	Yes	No	Yes	Yes	Yes	Yes	No	No	No	No
Adheleic decompensate	Yes	No	Yes	No	Yes	No	No	No	No	No
Abdominal pain	Yes	Yes	Yes	No	Yes	No	No	No	No	No
Signs of hypernatremia ¹	No	No	No	No	Yes	No	No	No	No	No
Hepatic encephalopathy ²	No	No	No	No	No	No	No	No	No	No
Acute liver failure ³	No	No	No	No	No	No	No	No	No	No

¹ AI, ALP increased normal, the pattern of liver injury was classified as hepatocellular although the ratio ALT/ULN: ALP/ULN was lower than 1 (4/4). DNR: 1:2 = 1:2. *Each, serology, serology, serology, serology and / or serology. ² Serum ceruloplasmin (DNR: 1-5) and hepatic encephalopathy. ³ ALT > 10 times normal, ULN = upper limit of normal, AST = aspartate aminotransferase, ALP = alkaline phosphatase, DNR = International Normalized Ratio, ANA = antinuclear antibodies.

Clinical Pharmacology – Personalized therapy

408

Using the OpenVigil 2 pharmacovigilance tool for guidance for clinical decisions involving newly occurring adverse events

R. Böhm¹, T. Herdegen¹
¹Institut für Experimentelle und Klinische Pharmakologie, UKSH, Campus Kiel, Kiel, Germany

Clinical routine often requires to evaluate the cause of a newly occurring adverse event. If this event is regarded to be iatrogen, further information of the association between the drugs in the current medication list and the adverse event is needed. This information should ideally reflect the true risk and allow ranking of the drugs according to this risk to identify which drug to discontinue first.

We discuss the summary of product characteristics (SPC), the SIDER Side Effect Resource and OpenVigil 2 as possible sources of information.

SPCs are becoming more and more a vindictive charter for pharmaceutical companies that contain misleading information which is not based on evidence (ref. 1). Since it relies on the SPCs, SIDER inherits these shortcomings and flags warnings that result from confounding factors (ref. 1, fig. 1). Furthermore, if any rates are given, they are not easily comparable since they stem from different studies.

Pharmacovigilance data are biased by the very nature of the data and the collection method. However, once confounders are eliminated, pharmacovigilance offers better information on how to rank the drugs than SPCs/SIDER.

We present decision-guiding information obtained by SIDER and by OpenVigil 2 for one of our patients (fig. 2 & 3) and discuss how this information was used to modify the therapy.

Ref. 1: Böhm R., Herdegen Th. Dtsch Apoth Ztg 2009, 149(32), S. 3623. [Risk of infection and liver damage by orlistat] Infektionsrisiko und Leberschädigung unter Orlistat

Abb. 1

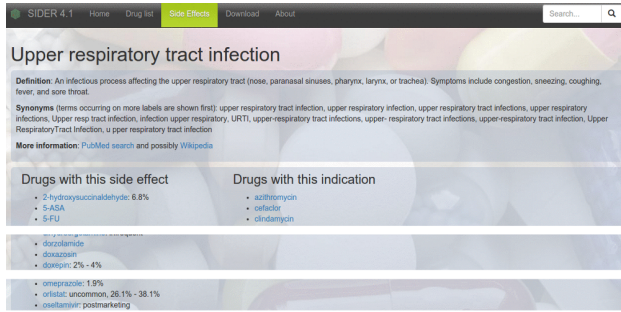


Abb. 2

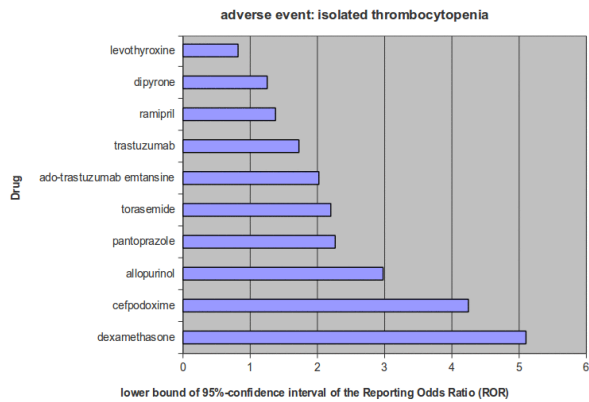
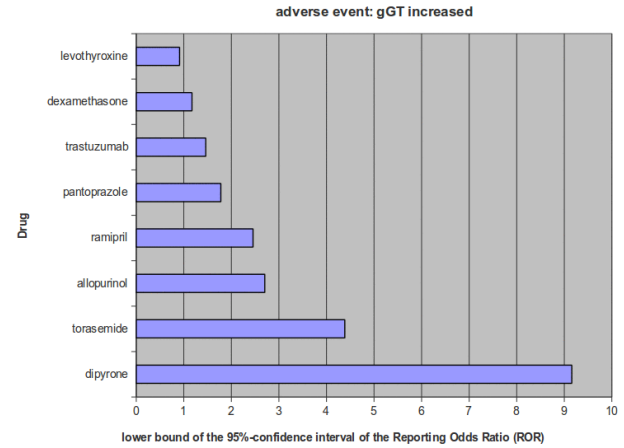


Abb. 3



409

How to individualize drug therapy based on pharmacogenetic information? A systematic review

O. Zolk¹, S. Haubensak¹, T. Paul¹, S. Hafner¹
¹Institut für Naturheilkunde und Klinische Pharmakologie, Universität Ulm, Ulm, Germany

Background: Differences (polymorphisms) in target genes or genes encoding drug transport proteins or drug metabolizing enzymes may be responsible, among other factors, for observed variation in patients' response to medications. Pharmacogenetics aims at identification of patients at higher, genetically determined, risk of adverse drug effects or ineffective medication, to modify dosage or switch to alternative therapy. There is, however, a lack of awareness of pharmacogenetic-based clinical practise guidelines.

Methods: A systematic literature review was conducted which focused on published guidelines on genotype-based (germ-line genetic variants) dosage modification or selection of drugs. We searched the MEDLINE and the Pharmacogenomics Knowledgebase (PharmGKB) databases. Prescribing information was also screened for pharmacogenetic guidance.

Results: The systematic review revealed recommendations for 61 drugs (Table) that enable the translation of genetic test results into actionable prescribing decisions. For 20% of these drugs the respective German drug labels recommend or even require pharmacogenetic testing (Table, 3rd column). Although pharmacogenetic testing is recommended, the prescribing information not always provides guidance on how to adjust the drug dosage based on the pharmacogenetic test result. Compared with the German or European drug labels, the FDA drug labels provide more detailed information on pharmacogenetic dose modifications.

Conclusions: Academic working groups have a front-runner role in the development of prescribing recommendations based on genetic markers. To date, drug labels rarely contain detailed guidelines how available genetic test results should be used to adjust drug dosage. Because pharmacogenetics has a growing role during drug development and pre-prescription genotyping will become more widespread, it is expected that specific pharmacogenetic guidance for the treating physicians will become increasingly important.

Abb. 1

Drug	Gene	Pharmacogenetic tests (German prescribing information)
Abacavir	HLA-B	Genetic testing required (Before initiating treatment with abacavir, screening for carriage of the HLA-B*57:01 allele should be performed in any HIV-infected patient, irrespective of racial origin. Abacavir should not be used in patients known to carry the HLA-B*57:01 allele.)
Acenocoumarol	CYP2C9	
Allopurinol	HLA-B	
Amitriptyline	CYP2C19, CYP2D6	
Aripiprazole	CYP2D6	
Ataluren	DMD	Genetic testing required (Indicated for the treatment of Duchenne muscular dystrophy resulting from a nonsense mutation in the dystrophin gene. The presence of a nonsense mutation in the dystrophin gene should be determined by genetic testing.)
Atomoxetine	CYP2D6	
Azathioprine	TPMT	Genetic testing recommended. However, no guidance on genotype-based dose adjustments is provided.
Capecitabine	DPYD	
Carbamazepine	HLA-A, HLA-B	Genetic testing recommended in patients of Asian descent (Carriers of the HLA-B*15:02 allele; carbamazepine should not be used unless the benefits clearly outweigh the risks.)
Celecoxib	CYP2C9	
Citalopram	CYP2C19	
Clobazam	CYP2C19	
Clomipramine	CYP2D6	
Clopidogrel	CYP2C19	
Clozapine	CYP2D6	
Codeine	CYP2D6	
Dextromethorphan + Quinidine	CYP2D6	
Doxepin	CYP2D6	
Eliglustat	CYP2D6	Genetic testing required (Eliglustat should not be used in patients who are CYP2D6 ultra-rapid metabolizers; poor metabolizers: reduction of the daily dose by 50%.)
Escitalopram	CYP2C19	
Flecainide	CYP2D6	
Fluorouracil	DPYD	
Fluvoxamine	CYP2D6	
Galantamine	CYP2D6	
Haloperidol	CYP2D6	
Iloperidone	CYP2D6	
Imipramine	CYP2C19, CYP2D6	
Irinotecan	UGT1A1	
Ivacaftor	CFTR	Genetic testing required (Ivacaftor is indicated for the treatment of cystic fibrosis in patients who have one of the following gating mutations in the CFTR gene: G551D, G1244E, G1349D, G178R, G551S, S1251N, S1255P, S549N, or S549R.)
Lomitapide	LDLR (and other genes)	Genetic testing recommended (Genetic confirmation of homozygous familial hypercholesterolaemia should be obtained whenever possible.)
Mercaptopurine	TPMT	Genetic testing recommended. However, no guidance on genotype-based dose adjustments is provided.
Metoprolol	CYP2D6	
Nefazodone	CYP2D6	
Nortriptyline	CYP2D6	
Olaparib	BRCA	Genetic testing required (Patients are eligible for olaparib treatment if they have a confirmed deleterious or suspected deleterious BRCA mutation in either the germline or the tumour, detected using an appropriately validated test.)
Omeprazole	CYP2C19	
Oxcarbazepine	HLA-B	
Oxycodone	CYP2D6	
Pantoprazole	CYP2C19	
Paroxetine	CYP2D6	
Pegloticase	G6PD	Genetic testing required for patients with risk for G6PD deficiency e.g., in patients of African and Mediterranean ancestry (Contraindicated in patients with G6PD deficiency.)
Phenprocoumon	CYP2C9	
Phenytoin	CYP2C9, HLA-B	
Pimozide	CYP2D6	Genetic testing recommended in patients treated with high pimozide doses (In poor CYP2D6 metabolizers, pimozide doses should not exceed 0.05mg/kg/day in children or 4 mg/day in adults and doses should not be increased earlier than 14 days.)
Propafenone	CYP2D6	
Rasburicase	G6PD	
Risperidone	CYP2D6	
Sertraline	CYP2C19	
Simvastatin	SLCO1B1	Genetic testing recommended (SLCO1B1 c.521T>C CC genotype: avoid high-dose treatment with simvastatin)
Tacrolimus	CYP3A5	
Tamoxifen	CYP2D6	
Tegafur	DPYD	
Tetrabenazine	CYP2D6	
Thionidazine	CYP2D6	
Thioquinamine	TPMT	
Tamadol	CYP2D6	
Venlafaxine	CYP2D6	
Vortioxetine	CYP2D6	
Warfarin	CYP2C9, VKORC1	
Zuclopenthixol	CYP2D6	

Clinical Pharmacology – Regulatory

410

The *In Vitro* percutaneous absorption and metabolism of radiolabelled bisphenol A (BPA) through fresh human skin

F. Toner¹, G. Allan¹, **D. Bever**², S. S. Dimond³, L. H. Pottenger⁴, J. M. Waechter⁵
¹Charles River Laboratories Ltd, Edinburgh, United Kingdom
²Bayer Pharma AG (on behalf of COVESTRO), Wuppertal, Germany
³SABIC, Pittsfield, MA, USA, Vereinigte Staaten von Amerika
⁴Olin Corporation, Midland, MI, USA, Vereinigte Staaten von Amerika
⁵Cardno Entrix (on behalf of SABIC), Midland, MI, USA, Vereinigte Staaten von Amerika

Bisphenol A (BPA) is a high production volume compound mainly used as a monomer to make polymers for various applications, including food-contact applications. People are exposed to low levels of BPA because very small amounts of BPA may migrate from the food packaging into foods or beverages. However, other potential sources of exposure, such as dermal contact have also been identified (EFSA, 2015).

A substance evaluation process (CoRAP) was initiated for BPA by the European Chemicals Agency (ECHA). As part of the safety evaluation of BPA, a study was required by ECHA to assess absorption and metabolism of BPA following dermal

exposure to human skin. An *in vitro* study with human skin was requested according to OECD TG 428 under consideration of the Scientific Committee on Consumer Safety (SCCS) criteria for the *in vitro* assessment of dermal absorption.

To investigate potential dermal BPA metabolism fresh human skin was used. Abdominal skin was obtained fresh from surgery from 4 different donors. Split-thickness human skin membranes were mounted into flow-through diffusion cells (n=4 per dose and donor) and the receptor fluid was pumped underneath the skin at a constant flow rate. The skin surface temperature was maintained at 32°C throughout the experiment and electrical resistance barrier integrity testing was performed at the start (0 h) and end of the experiment (24 h).

Four test preparations at final BPA concentrations of 2.4, 12, 60, and 300mg/L were investigated. The highest concentration was chosen based on the maximum solubility of BPA in water and the lowest concentration was chosen based upon the specific activity of the radiolabelled [¹⁴C]-BPA that could be used for mass balance. Percutaneous absorption was assessed by collecting receptor fluid (tissue culture medium (DMEM), containing ethanol (ca 1%, v/v), Uridine 5'-diphosphoglucuronic acid (UDPGA, 2 mM) and 3'-phosphoadenosine-5'-phosphosulfate (PAPS, 40 µM)), at multiple time points throughout the experiment. At termination the skin was removed from the cells and the *stratum corneum* was removed with 20 successive tape strips. The exposed epidermis was separated from the dermis using a scalpel. Metabolism was investigated for the highest concentration (300 mg BPA/L) only, using a HPLC with in-line radiodetection and confirmed BPA-glucuronide (BPA-G) and BPA-sulfate (BPA-S) standards for comparison.

No metabolism was observed in any of the epidermis samples, however some metabolism is observed in dermis and receptor fluid samples. Metabolites were identified with retention consistent with BPA-G and BPA-S, and also some more polar components.

The mean Total Absorbed Dose (receptor fluid + receptor chamber wash + receptor rinse) was between 1.7 and 3.6% of the applied dose and the mean Dermal Delivery (epidermis + dermis + total absorbed dose) was between 16 and 20% of the applied dose, with the majority of the radioactivity associated with epidermis samples compared to dermis and receptor fluid samples. A linear dose-response relationship is observed over the whole concentration range.

Study Sponsor: REACHCENTRUM (on behalf of Bisphenol A REACH Consortium), Brussels, Belgium

References: EFSA 2015. EFSA Journal 2015;13(1):3978

Clinical Pharmacology – Others

411

Pharmacokinetics of anastrozole following transdermal application in dogs

F. Baumann¹, J. Teichert¹, G. Abraham², M. Voskanian³, C. Brätter³, A. Aigner¹, **R. Regenthal**¹

¹University of Leipzig, Clinical Pharmacology, Leipzig, Germany
²Universität Leipzig, Institute of Veterinary Pharmacology, Pharmacy and Toxicology, Leipzig, Germany

³Formula GmbH, Pharmaceutical and Chemical Development Company, Berlin, Germany

Anastrozole is a well-known non-steroidal aromatase-inhibiting drug approved for the second-line treatment of breast cancer after surgery and for treating postmenopausal women. Treatment with the only available dosage form, anastrozole film-coated tablets for oral administration, is frequently associated with concentration-dependent unwanted side effects like hot flashes, fatigue, joint pain, joint stiffness, vaginal dryness, hair loss, skin rash, nausea, diarrhea and headache. In order to minimize the local gastrointestinal as well as systemic side effects, a system for transdermal anastrozole delivery has recently been developed.

In this study, we describe the first experimental *in vivo* application of a transdermal therapeutic system (TTS) to Beagle dogs and, as a necessary prerequisite for the analysis of the time course of anastrozole release and uptake, a simple, sensitive and accurate LC-MS method for quantifying anastrozole in plasma. The detection of fragment ions at m/z 225 and 237 instead of the molecule ions (m/z 294 and 306) generated from the elevated collision energy, and the use of a deuterated internal standard resulted in increased relative abundances and improved signal-to-noise ratios. The lower limit of quantification and the limit of detection were 1.4 ng/ml and 0.5 ng/ml, respectively.

The developed method was successfully applied in a pharmacokinetic study of anastrozole plasma levels in beagle dogs, measuring percutaneous drug absorption from an experimental, newly designed glycerol-based patch / TTS. A distinct time course was observed, with an initial linear increase over 24 hours and a plateau thereafter. This offers promising strategies for the transdermal application of anastrozole with improved pharmacokinetics.

412

Comprehensive metabolomic and lipidomic profiling of clear cell renal cell carcinoma for molecular tissue differentiation

P. Leuthold^{1,2}, E. Schaeffeler^{1,2}, T. Mürdter^{1,2}, U. Hofmann^{1,2}, S. Rausch³, J. Bedke³, M. Schwab^{1,2,4}, M. Haag^{1,2}

¹Dr. Margarete Fischer-Bosch – Institute of Clinical Pharmacology (IKP), Stuttgart, Germany

²University of Tübingen, Tübingen, Germany

³University Hospital Tübingen, Department of Urology, Tübingen, Germany

⁴University Hospital Tübingen, Department of Clinical Pharmacology, Tübingen, Germany

Background: Renal cell carcinoma (RCC) is a heterogeneous disease and based on histopathological characteristics it can be classified into different subtypes. Among the different types of kidney cancer, clear cell renal cell carcinoma (ccRCC) represents the most prevalent form (> 70%). The symptoms of ccRCC are usually mild and as a result the disease is often diagnosed in an advanced state which results in poor 5 years survival rates. Many of the mutated genes responsible for the development of ccRCC

are known to be involved in cell metabolism pathways and therefore ccRCC is supposed to be a metabolic disease. In order to facilitate a better understanding of cancer metabolism and to support tumor classification on the metabolite level we have developed a novel analytical approach for comprehensive metabolomic profiling of small molecules and lipids in kidney tissue. The method was established and validated based on porcine tissue and, as proof of concept, applied to a small cohort of human normal and ccRCC tissue samples for molecular tissue differentiation.

Methods: Five fresh frozen ccRCC samples and corresponding normal tissue were used for cancer-specific metabolomic profiling and were derived from patients who underwent partial or radical nephrectomy. Metabolites and lipids were recovered from tissue samples by a two-step extraction protocol. Tissue homogenization and extraction of polar metabolites was performed in methanol/water (aqueous extract) by a bead-beating approach. Lipids were recovered by consecutive extraction of the pellet with methanol/methyl *tert*-butyl ether (organic extract). Metabolites in aqueous extracts were separated by hydrophilic liquid interaction chromatography whereas compounds in organic extracts were separated by reversed phase chromatography prior high resolution mass spectrometry.

Results: Reproducibility of tissue extraction and metabolite analysis was assessed by the analysis of multiple individually prepared porcine kidney samples. More than 1000 metabolic features including amino acids, nucleotides, small organic acids, phospholipids, sphingolipids, glycerolipids and fatty acids could be reproducible (CV \leq 30 %) analyzed with the novel non-targeted metabolomics approach. The validated protocol was applied for metabolomic profiling of kidney tissue derived from ccRCC patients. Based on unsupervised multivariate statistics, a clear differentiation between cancerous and normal tissue for the small metabolites profile as well as for the lipid profile could be observed. A first subset of differentially regulated metabolites responsible for tissue differentiation could be tentatively identified.

Conclusion: Metabolomic profiling of kidney tissue extracts enables differentiation between ccRCC and normal kidney tissue samples based on the lipid and small molecule metabolomic profiles. Further studies on larger and independent sample groups are necessary to confirm and validate our preliminary findings. In summary, the presented approach provides a first basis for comprehensive metabolomics studies in human kidney tissue and thus offers great potential for the metabolic characterization of ccRCC with important prognostic and therapeutic implications in the future.

413

Expression and promoter DNA methylation of the lactate transporter MCT4/SLC16A3 in distant metastases of primary clear cell renal cell carcinoma

P. Fisel^{1,2}, D. Schollenberger³, S. Rausch⁴, S. Winter^{1,2}, S. Kruck³, J. Hennenlotter³, A. T. Nies^{1,2}, M. Scharpf⁴, F. Fend⁴, J. Bedke³, M. Schwab^{1,2,5}, E. Schaeffeler^{1,2}

¹Dr. Margarete Fischer-Bosch-Institute of Clinical Pharmacology, Stuttgart, Germany
²University of Tuebingen, Tuebingen, Germany
³Department of Urology, University Hospital Tuebingen, Tuebingen, Germany
⁴Institute of Pathology and Neuropathology, University Hospital Tuebingen, Tuebingen, Germany
⁵Department of Clinical Pharmacology, University Hospital Tuebingen, Tuebingen, Germany

Background: The monocarboxylate transporter 4 (MCT4), encoded by the *SLC16A3* gene, mediates H⁺-coupled transport of lactate across the plasma membrane. For cells with high glycolytic activity lactate export is of major importance for the maintenance of the glycolytic metabolism and for the prevention of intracellular acidification. In glycolytic tumor cells, the acidic extracellular environment resulting from export of lactate and H⁺, furthermore promotes anti-apoptotic effects and metastasis. Clear cell renal cell carcinoma (ccRCC) is the most common subtype of renal cell carcinoma (RCC) and is characterized by a metabolic shift towards enhanced aerobic glycolysis and hence, increased lactate production. MCT4 and its epigenetic regulation by *SLC16A3* promoter methylation has previously been identified as prognostic marker for ccRCC outcome and as target for ccRCC treatment. Since metastatic ccRCC is associated with poor overall survival and represents a major challenge for treatment, MCT4/SLC16A3 might represent a promising prognostic marker and a target for therapeutic intervention also for metastatic disease.

Methods: MCT4 protein expression was analysed in 130 paraffin embedded tissue samples of distant metastases derived from different organs by immunohistochemical staining of tissue microarrays. Protein expression was evaluated semi-quantitatively using Tissue Studio v.3.6 (Definiens AG). DNA methylation in the *SLC16A3* promoter, specifically at the previously identified CpG site with prognostic potential in primary ccRCC, was analysed in 82 paraffin embedded metastasis samples by MALDI TOF-MS. MCT4 protein expression data and DNA methylation at the specific CpG site in the *SLC16A3* promoter were correlated with clinicopathological parameters and outcome data.

Results: Distant metastases of primary ccRCC showed high MCT4 protein expression irrespective of the affected organ. The most frequently affected organs like lung or bone, with approximately 28% and 14% in our cohort respectively, showed similar expression levels as less frequent metastatic sites such as thyroid gland or spleen. Accordingly, DNA methylation at the identified CpG site in the *SLC16A3* promoter was low in metastatic tissue in all investigated organ sites. An association of low promoter DNA methylation level at the previously identified prognostic CpG site in metastases with poor tumor-specific survival of the patients was observed.

Conclusion: From these results we hypothesize that DNA methylation at specific CpG sites in the 5'-regulatory region of MCT4 may not only serve as a predictor for patient outcome and as potential novel target for therapeutic intervention in primary, but also for metastatic disease.

414

Genome-wide association identifies variants controlling estrogenic tamoxifen metabolites

J. Jöhanning¹, B. Chowbay², C. C. Khor³, D. Eccles⁴, B. Eccles⁴, M. Eichelbaum¹, M. Schwab¹, H. Brauch¹, T. Mürdter¹, W. Schrott¹

¹Dr. Margarete Fischer-Bosch-Institute for Clinical Pharmacology and University of Tübingen, Stuttgart, Germany

²National Cancer Centre Singapore, Clinical Pharmacology Laboratory Division of Medical Sciences, Singapore, Singapore

³Genome Institute of Singapore, Singapore, Singapore

⁴University of Southampton, Faculty of Medicine, Cancer Sciences Academic Unit and University of Southampton Clinical Trials Unit, Southampton, United Kingdom

Tamoxifen is used to treat pre- and postmenopausal women with estrogen-receptor (ER) positive breast cancer. As a prodrug, tamoxifen undergoes extensive hepatic metabolism resulting in a complex mixture of metabolites with estrogenic and anti-estrogenic effects. While endoxifen and (Z) 4-hydroxytamoxifen are the most potent anti-estrogenic metabolites, bisphenol and both isomers (E) and (Z) of metabolite E are the most potent compounds with estrogenic properties at the ER. The mixed antagonist/agonist pharmacodynamic effects of the selective estrogen receptor modulator tamoxifen at the ER have been mainly attributed to tissue specific action of ER coregulators, yet little is known about agonistic metabolites contributing to its estrogenic actions. The aim of the present study was to clarify whether there is a genetic component for interindividual differences in the formation and clinical effect of agonistic tamoxifen metabolites.

A genome-wide association study (GWAS) was conducted on steady-state agonist plasma levels in 390 postmenopausal breast cancer patients of European origin who were treated with 20 mg/day of tamoxifen for at least 6 months. Plasma concentrations of estrogenic metabolites bisphenol, (E), and (Z) metabolite E were quantified using a recently established LC-MS/MS method¹. Promising SNPs for an association between genotype and either plasma metabolite concentration or clinical outcome were confirmed for their relevance in an independent patient cohort of 313 premenopausal breast cancer patients mainly of European descent^{2,3}.

Twelve SNPs close to or above genome-wide significance ($P < 5E-08$) were found to be associated with allele-dependent variable (E) or (Z) metabolite E plasma levels, while no genomic hit was found for the tamoxifen metabolite bisphenol. Here, positive intergenic or genic regions mapped to chromosomes 1, 2 and 16 for (E) metabolite E and to chromosomes 15 and 18 for (Z) metabolite E. Upon genotyping of the validation cohort, two genetic loci with minor allele frequencies $< 5\%$ were confirmed as putative candidates: rs662106 was associated with a 21-39% variant allele-dependent increase of (E) and (Z) metabolite E isomers ($p < 0.05$), and rs3731872, mapping to a gene encoding zinc finger protein ZNF124, was associated with increased risk of recurrence or death ($HR_{carriers} 2.6$, 95% CI: 1.3 – 3.4; $P < 0.005$).

These findings suggest the existence of genetic loci that may contribute to the formation and clinical effect of estrogenic tamoxifen metabolites and therefore could explain therapeutic failure of tamoxifen and/or the occurrence of adverse events during treatment.

¹Jöhanning J, et al. Anal Bioanal Chem 2015;1-6

²Eccles D, et al. BMC Cancer 2007; 7: 160

³Saladores P, et al. TPJ 2015; 15:84-94

415

Regioselective conjugation of active hydroxyclophene metabolites

P. Kröner¹, G. Heinkle¹, S. Igel¹, K. Klein¹, E. Schaeffeler¹, R. Kerb¹, M. Schwab^{2,1}, T. E. Mürdter¹

¹Dr. Margarete Fischer-Bosch-Institute of Clinical Pharmacology and University of Tübingen, Stuttgart, Germany
²University Hospital Tübingen, Department of Clinical Pharmacology, Tübingen, Germany

Introduction: Clomiphene (CLOM) citrate as mixture of *trans*- and *cis*-isomer (60:40) is the first line therapy for the treatment of infertility caused by the polycystic ovary syndrome. Treatment schedule includes dose escalation from 50 mg/d CLOM citrate to up to 150 mg/d in case of non-ovulation. However, therapy outcome is variable and approximately 10 – 30% of patients do not benefit from CLOM treatment. The pro-drug CLOM is bioactivated via 4-hydroxylation of *trans*-CLOM by the highly polymorphic cytochrome P450 (CYP) 2D6 leading to the major active metabolite *trans*-4-hydroxyclophene (*trans*-4-OH-CLOM)^{1,2}. Recently, we identified a less active *trans*-3-OH-CLOM which is also formed by CYP2D6. Besides the formation of the active metabolites, their plasma concentrations are influenced by their clearance e.g. via glucuronidation and sulfation. Here we investigated the glucuronidation and sulfation of both hydroxyl-metabolites.

Methods: Isoforms of UDP-glucuronosyl-transferase (UGT) and sulfotransferase (SULT) responsible for conjugation of OH-CLOM were identified using commercially available supersomes. Glucuronidation and sulfation kinetics were determined in pooled human liver microsomes. Conjugated CLOM metabolites were quantified in plasma and urine samples obtained from healthy female volunteers who received a single dose of 100 mg CLOM citrate.

Results: Incubations with human liver microsomes revealed an almost 60-fold higher glucuronidation rate for *trans*-3-OH-CLOM, which is exclusively catalyzed by UGT2B7, compared to the more potent *trans*-4-OH-CLOM. For the latter a pattern of multiple UGTs was identified. In contrast, the intrinsic clearance of *trans*-4-OH-CLOM to its sulfate is 16-fold higher compared to 3-OH-CLOM. For both metabolites a participation of SULT1A1 and SULT1E1 was identified. These results were in line with previous studies, which identified the same SULTs^{3,4} and UGTs⁵ responsible for the conjugation of the structurally related *trans*-4-hydroxytamoxifen. In addition, *in vivo* data from plasma and urine samples confirmed the reverse regioselective glucuronidation and sulfation of *trans*-3-OH-CLOM and *trans*-4-OH-CLOM. Overall, concentrations of CLOM-glucuronides were significantly higher than those of sulfates. Highest concentrations in plasma and urine samples were measured for *trans*-CLOM-3-O-glucuronide.

Conclusion: Our results suggest a new metabolic route via *trans*-3-OH-CLOM which appears to be a potential inactivation pathway of CLOM.

Acknowledgement: Supported by the Robert Bosch Foundation, Stuttgart, Germany.

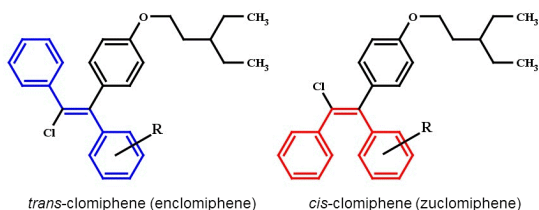
References:

[1] Mürdter T, et al. Hum Mol Genet, 2011, 21:1145-54

[2] Nishiyama T. et al., Biochemical Pharmacology, 2002, 63:1817 – 1830

[3] Sun D. et al., Drug Metabolism and Disposition, 2007, 35:2006 – 2014

Abb. 1



The colored structure emphasize the configuration, which is responsible for the *cis*/*trans*-nomenclature of the parental drug. The R indicates the aromatic ring enzymatically modified in our investigations.

416

LC/MS-based monitoring of drug-induced metabolic alterations of a novel NTCP inhibitor for the treatment of hepatitis B in humans

M. Haag^{1,2}, U. Hofmann^{1,2}, T. E. Mürdter^{1,2}, G. Heinkele¹, P. Leuthold^{1,2}, A. Eidam³, A. Blank^{3,4}, W. E. Haefeli^{3,4}, A. Alexandrov⁵, S. Urban^{6,4}, M. Schwab^{1,7,8}
¹Dr. Margarete Fischer-Bosch-Institute of Clinical Pharmacology, Stuttgart, Germany
²University of Tübingen, Tübingen, Germany
³Heidelberg University Hospital, Department of Clinical Pharmacology and Pharmacoepidemiology, Heidelberg, Germany
⁴German Centre for Infection Research (DZIF), Heidelberg, Germany
⁵Myr GmbH, Bad Homburg, Germany
⁶University Hospital Heidelberg, Department of Infectious Diseases, Molecular Virology, Heidelberg, Germany
⁷University Hospital Tübingen, Department of Clinical Pharmacology, Institute of Experimental and Clinical Pharmacology and Toxicology, Tübingen, Germany
⁸German Centre for Infection Research (DZIF), Tübingen, Germany

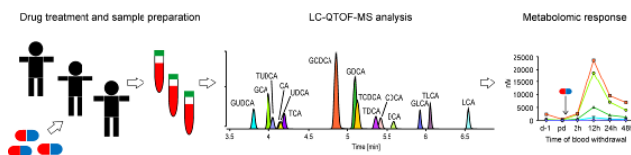
Introduction: Metabolic monitoring of endogenous biomarkers is of increasing importance for the assessment of drug safety and efficacy during clinical drug development. Myrcludex B, a novel lipopeptide-based entry inhibitor for the therapy of hepatitis B and D, exerts its function through inhibition of the hepatic bile acid transporter Na⁺-taurocholate cotransporting polypeptide (NTCP). In order to assess a myrcludex B-induced metabolic response in humans, LC/MS-based monitoring of endogenous metabolites was performed in blood and urine samples from healthy individuals before and during treatment with myrcludex B.

Methods: Plasma and urine samples were collected from healthy volunteers participating in clinical phase I trials to evaluate safety, tolerability, and pharmacokinetics of single doses of the NTCP inhibitor myrcludex B. Using quadrupole time-of-flight mass spectrometry coupled to reversed-phase chromatography (LC-QTOF-MS) a set of 15 known NTCP substrates (bile acids) was quantified by targeted metabolomics. Protein precipitation was performed in the presence of deuterium-labeled internal standards (ISTDs) which allowed absolute bile acid (BA) quantification in low amounts of plasma. BA profiling in urine was performed after dilution with methanol/water (1:1) in the presence of ISTDs. Both methods were validated according to FDA guidance and applied to monitor the effect of myrcludex B treatment on human bile acid homeostasis.

Results: Dynamic quantification in plasma and urine was achieved in the range from 7.8 nM to 10000 nM depending on the BA species analyzed. Intraday- and interday accuracy and precision were in the 15% tolerance range for all analytes in all matrices. Matrix effects were between 39-104% (plasma) and 31-95% (urine), apparent recoveries in plasma were above 97%. Basal plasma BA level (mean ± SD) in fasting healthy subjects were 667 ± 574 nM (unconjugated BAs), 935 ± 629 nM (glycine-conjugated BAs) and 104 ± 62 nM (taurine-conjugated BAs). Urinary BA level (nmol/g creatinine) were 193 ± 225 nM (unconjugated BAs), 89 ± 29 nM (glycine-conjugated BAs) and 6 ± 2 nM (taurine-conjugated BAs). Myrcludex-induced NTCP inhibition resulted in significantly elevated amounts of conjugated BA species demonstrating a spillover of NTCP substrates into the systemic circulation. Furthermore, higher urinary BA level were observed during treatment indicating accelerated elimination of excessive BA from the body.

Conclusion: LC/MS-based monitoring of endogenous biomarkers has been successfully established and applied to study the effect of myrcludex B treatment on human BA metabolism. The results obtained by our assay demonstrate that a myrcludex-induced NTCP inhibition drastically affects human BA homeostasis. This observation provides valuable insights into the drug's mode of action and will be indispensable for the assessment of side effects and dose-finding processes during future clinical trials. Further studies are required to assess a possible role of BA modification (e.g. sulfation) in the process of BA detoxification during myrcludex treatment.

Abb. 1



Free topics

417

What are the characteristics of sulfur mustard (SM) resistant cells?

A. Schmidt¹, S. Rothmiller¹, M. Wolf¹, D. Steinritz¹, F. Worek¹, H. Thiermann¹
¹Institut für Pharmakologie und Toxikologie der Bundeswehr, München, Germany

For decades the biological effect of SM has been investigated. It is well known how SM interacts and destroys cells. Unfortunately, it is still unknown if and how a cell can become resistant against SM. Within the here described experiments we investigated a new approach adapting cells to the presence of SM. Over a time period of nearly three years the cells were cultivated in presence of SM with increasing concentrations. Before starting the initial SM sensitivity was investigated. At the beginning cells were cultivated with a concentration of 0.07 µM SM (IC₁₀). Today the cells are able to tolerate a concentration of 7.2 µM SM (IC₉₀), which reflects to a concentration of which 90% of the original cells would have died.

To determine cellular characteristics, the resistant cells were compared with wildtype cells. The following cell characteristics were investigated: proliferation, apoptosis, clonogenicity, size of nuclei and cytoplasm, cell-cell contacts, DNA adducts formation, secretome, screening of miRNA expression, next generation sequencing, vital observation and scratch assay, NAD(P)⁺/NAD(P)H, H₂O₂, glutathione, Ca²⁺-influx, MDR-channels, resistance to other alkylating agents and the reversibility of the resistance.

The resistant cells demonstrate smaller nuclei and cytoplasm, less DNA adducts, a higher clonogenicity as well as proliferation and less apoptosis. The secretome analysis showed an up-regulation of anti-apoptotic acting cytokines Timp and Ang and the pro-proliferative acting cytokines Timp and PDGF-AA. In contrast, immunologically active cytokines were down-regulated. Concerning cell-cell contacts no differences were seen. In the miRNA screening 49 significant up-regulated and 20 significant down-regulated miRNAs have been observed. Noteworthy was the regulation of various members of 11 different families. During vital observation and in a scratch-assay the resistant cells were shown to have disadvantages. The observed resistance was not unique for SM but also towards other alkylating agents and cytostatic drugs. By analyzing the reversibility cells stayed resistant over more than 35 weeks.

In conclusion, many aspects investigated in this study have an influence on the SM resistance, pointing out that it is a combination of various effects that are involved to switch on resistance. More likely, there are many aspects working together. The present results are an important step in the characterization of the SM-resistant cell line and further studies may be able to directly use these as a start for target identification in antidote or prophylactic agent discovery.

418

On the nucleo-cytoplasmic shuttling of the arylhydrocarbon receptor (AhR)

A. Tkachenko¹, A. Luch¹, F. Henkler¹

¹German Federal Institute for Risk Assessment (BfR), Department Chemicals and Product Safety, Berlin, Germany

The arylhydrocarbon receptor (AhR) is localized in a cytosolic complex that contains several co-chaperones and associated factors. The protein is shifted into the nucleus in response to endogenous and xenobiotic ligands. However, a transient nuclear transport does also occur in the absence of any ligands, while the predominant cytoplasmic compartmentalization is maintained by parallel export. We have analyzed the interplay between this basal nucleo-cytoplasmic shuttling and ligand induced transport in HepG2 cells, using a YFP-tagged fusion protein that is capable to respond to ligands and to trigger the induction of CYP1A1 expression. Basal import was assessed in cells that had been treated with leptomycin B (LMB), an inhibitor of crm1-mediated nuclear export. Interestingly, the apparent AhR import rate in LMB-treated cells was comparable with nuclear import as triggered by xenobiotic (b-naphthoflavone) or endogenous (kynurenine) ligands. This observation was confirmed for endogenous AhR in HepG2 cells, since both ligands and LMB showed comparable effects on nuclear compartmentalization. However, the basal nuclear import rate in LMB-treated cells was strongly increased by AhR ligands. Ligand-induced nuclear transport was therefore confirmed as an import step in receptor activation. Interestingly, LMB did also accelerate nuclear import of AhR after pretreatment of cells with AhR ligands. These data suggest that nuclear export of the AhR is maintained in the presence of ligands. Receptor activation might therefore comprise several rounds of shuttling, thereby involving both accelerated import and continued export of the AhR protein fraction that has not already undergone interactions with ARNT or DNA. We suggest that nuclear export provides an additional kinetic control of AhR activation and function.

419

Mitochondrial Toxicology: Rescuing mitochondria in Wilson disease avoids acute liver failure

H. Zischka¹

¹Institut für molekulare Toxikologie und Pharmakologie, AG Zischka, Neuherberg, Germany

In Wilson disease (WD) functional loss mutations in the hepatocyte *ATP7B* gene cause dramatic copper overload leading to acute liver failure, posing an unmet therapeutic issue. We find that the pathology of severe WD cases is mirrored in LPP^(-/-) rats carrying a functional loss *Atp7b* mutation. This is especially apparent in the hepatocyte mitochondrial compartment. A progressive copper deposition increasingly harms the life-sustaining mitochondrial membrane integrity. Thus, depleting this devastating mitochondrial copper burden is a core requirement for a treatment strategy against acute liver failure in this WD animal model.

420

Master of Science degree program toxicology at Charité Universitätsmedizin Berlin**A. Horvath**¹, A. Sonnenburg¹, F. Partosch¹, R. Stahlmann¹¹Charité Universitätsmedizin Berlin, Institut für Klinische Pharmakologie und Toxikologie, Berlin, Germany

Preparation for the master degree program in toxicology started in 2006 as a cooperation of Charité Universitätsmedizin Berlin with the University of Potsdam and other institutions of the region. First enrollment of students was done in 2008. The program was accredited in 2011 by the Central Evaluation and Accreditation Agency. It offers a modern curriculum encompassing a wide variety of scientific aspects with an interdisciplinary character. This training program in toxicology is organized in modules and ends with the degree "Master of Science" (M.Sc.).

The goal of this program in toxicology is to teach the basis of the interactions between substances at toxic concentrations and living organisms, as well as the molecular mechanism of the adverse effects of chemicals. The understanding of the mechanism of a toxic action is an important prerequisite for the scientifically based evaluation of a hazard associated with a substance. Furthermore, only with the knowledge of the mechanism of action and a deduction of structure activity relationships it is possible to predict toxic effects of new substances. This knowledge should enable students to perform a risk evaluation of chemicals or to predict the adverse effects of chemicals with the aim that human beings and the environment can be protected from harmful consequences of chemical exposure.

The program allocates 30 places per year to an average of 60 applicants. Most applicants have a basic training in the fields biology, chemistry, pharmacy, veterinary medicine and nutritional sciences. About 75% of the students are female. The majority of them have a bachelor's degree before starting the master program, other degrees are diploma and state examination as pharmacists or physicians. Ninety percent of the students pass the final examination consisting of the master's thesis and disputation at the end of the four semesters. Afterwards, most of the graduates aim to obtain a PhD degree.

The program is well established in the education of toxicologists in Germany.

421

Respiratory injury due to chlorine developed from consumer products. still an issue in germany**U. Stedtler**¹, M. Hermanns-Clausen¹¹Uniklinikum Freiburg, Vergiftungs-Informations-Zentrale, Freiburg, Germany

Objective: In the last decades strong efforts have been taken to improve product safety, especially in products intended for domestic use. Hypochlorite-containing cleaners may develop chlorine gas when acidified e.g. by adding an acid sanitary cleaner. Usually these cleaners contain sodium hydroxide or other strong alkalines to avoid this reaction. We analysed reports to our poisons center concerning inhalation exposure to chlorine developed from hypochlorite-containing mixtures.

Method: Retrospective search in the case database of the poisons center. Human inhalative exposures to chlorine released from mixing hypochlorite as well as human inhalative hypochlorite exposure alone were analysed. Frequency and symptoms were compared.

Results: From 2010 to 2015 in total 85 cases of human exposures to chlorine developed from mixtures of hypochlorite and acids (0.8 of 1000 cases) were registered. In 55 Cases the exposure was due to mixtures of products intended for domestic use. 94 % of the exposed patients reported symptoms. Only in two cases the symptoms were not considered to be caused by the inhalation accident. Most frequent symptoms reported were (percent of symptomatic patients): Cough (45 %), dyspnea (33 %), irritated upper airway (26 %), abdominal discomfort (pain, nausea, vomiting) (21 %), thoracic pain (20 %), irritated eyes (11 %), dizziness (8%), and bronchospasm (6 %). Further symptoms were malaise, headache, irritated nose, sweating, muscle pain, and others. In 12 patients (14 %) the symptoms were graded as moderate severe. Main symptoms in this group were dyspnoea (83 %), cough, and irritated airway. One third of the patients experienced bronchial obstruction. All symptomatic patients developed symptoms while exposed or shortly after exposure. There were no severe or fatal cases (especially no lung edema) and all symptoms were expected to resolve completely. Because hypochlorite containing products spontaneously release „chlorine-like“ smelling gases, we additionally analysed inhalation exposures to hypochlorite solutions alone in the same period. There were 42 patients in the same period exposed to hypochlorite evaporation alone. 36 of them (86 %) had symptoms of which in 30 cases these were considered to be caused or possibly be caused by the hypochlorite. Most frequent symptoms were irritated upper airway (33 %), nausea or vomiting (30 %), cough (23 %), irritated eyes (20 %). Dyspnoea was less frequent than in the mixture group (10 %). All symptoms were considered mild. There was no bronchospasm or thoracic discomfort.

Conclusion: Respiratory injuries by chlorine from hypochlorite-containing solutions still occur despite clear warning on the label. The majority of cases was due to products for domestic use. Symptoms develop shortly after exposure.

Author Index

A

Abd Alla, J.	158
Abdel-Hady Algharably, E.	163
Adam, K.	326
Ahles, A.	096
Aigner, A.	028
Andersohn, F.	334
Anger, L. T.	372
Annala, S.	122
Appel, D.	238
Ariana, F.	144
Arslan, B.	312
Arts, J.	221
Augspach, A.	036
Awortwe, C.	406

B

Badawi, A. I. M.	017
Bader, M.	308
Bakhiya, N.	347
Bankoglu, E. E.	031
Bartsch, N.	229
Becker, A.	183
Becker, A.	303
Beckmann, H.	172
Beckmann, J.	340
Beer, L.-A.	117
Beer-Hammer, S.	319
Behr, A.-C.	203
Behr, C.	397
Behr, J.	120
Belau, F.	185
Berditsch, M.	313
Bergmann, F.	105
Berlin, S.	328
Beyer, D.	410
Bhargava, C.	405
Bierwisch, A.	384
Birk, B.	324
Bischoff, I.	013
Bisha, M.	322
Blömeke, B.	224
Blümel, L.	045
Bock, A.	134
Bock, U.	188, 373
Bödefeld, T.	099
Boekhoff, I.	177
Böhm, A.	150, 332
Böhm, R.	408
Bollmann, P.	153
Bonicelli, J.	280
Braeuning, A.	225, 245
Breit, A.	103
Breitkreuz-Korff, O.	311
Bruckmüller, H.	256
Buchborn, T.	262
Bucher, K.	320
Buech, T.	298
Buhrke, T.	242
Burchardt, K.	222
Burckhardt, B.	046
Butterweck, V.	327
Büttner, M.	023

C

Camacho Londoño, J. E.	042
Cartus, A. T.	030
Chovancova, P.	003
Chovolou, Y.	237
Christmann, M.	052
Christoph, B.	267
Cordts, K.	145
Corte, G. M.	093
Creutzenberg, O.	189
Czul Kies, B. A.	027

D

Delbeck, M.	314
Dieterich, D. C.	264
Dietrich, K.	044
Dithmer, S.	310
Dittmar, F.	125
Döhring, J.	240
Dolde, X.	199
Dolga, A.	064
Dörsam, B.	033
Douros, A.	402, 407
Durmaz, V.	376

E

Eckhardt, A.	345
Eidam, A.	020
Eisenbach, I.	200
Empl, M. T.	296
Engel, A.	385
Ernst, H.	219

F

Fahrer, J.	032, 239
Feja, M.	095
Feldmann, K.	146
Ferber, G.	331
Feuerstein, T.	263
Fischer, S.	026
Fisel, P.	413
Freyberger, A.	349
Friedrich, F.	138
Fruth, D.	365
Fuhr, U.	302
Funk, F.	147

G

Ganjam, G. K.	072
Garg, J.	040
Gather, F.	282
Gerigk, T.	106
Gerstenberger, J.	317
Gholamreza-Fahimi, E.	321
Giesen, J.	133
Gille, L.	307
Glatzel, A.	278
Glatzel, D.	162
Gnad, T.	034
Godbole, A.	110
Golka, K.	235
Golly, F.	127
Grabowski, K.	403
Grandoch, M.	043
Granitzny, A.	386
Griesbacher, T.	339
Griethe, K.	107
Grimm, C.	179
Grobe, J.	152
Grushevskiy, E.	113
Günther, T.	114
Gutbier, S.	002

H

Haag, M.	416
Haase, C.	192
Häfner, S.	170
Hafner, S.	300
Hammer, H. S.	191
Hartmann, C.	194
Hartmann, S.	141
Hauptstein, R.	205
Hausmann, R.	065
Heise, T.	392
Hellmund, M.	389
Helmschrodt, C.	029
Hemgesberg, M.	228
Heni, H.	119
Hennen, J.	394
Henninger, C.	049
Herrmann, A.	252
Herzler, M.	344
Hessel, S.	190, 243
Hickmann, S.	250
Hielscher, J.	232, 233
Hintzsche, H.	343
Hinz, L.	056
Hoffmann-Dörr, S.	068
Hohlbaum, K.	091
Höhn, A.	297
Honnen, S.	196
Horvath, A.	420
Huang, D.	180
Hübner, J.	089
Hussner, J.	255

J

Jaekel, S.	161
Jahn, A.	315
Janko, C.	075
Jelinek, A.	071
Joseph, C.	149

K

Kaglin, S.	270
Kähler, M.	293
Kallenborn-Gerhardt, W.	295
Kannler, M.	396
Keller, F.	323
Khayyal, M. T.	287
Khiao In, M.	088
Khobta, A.	051
Kiessig, M.	309
Kirchhefer, U.	139
Kittel, A.	259
Klee, R.	265
Kleider, C.	207
Klein, S.	294
Klenk, C.	059
Kliwer, A.	060
Koch, A.	111
Kodandaraman, G.	218
Koenig, T.	131
Kohse, F.	279
Kolling, J.	223
König, J.	257
Konrad, C.	135
Krämer, O. H.	054
Kranzhöfer, D.	168
Krasel, C.	057
Kriebs, U.	066
Krohmer, A.	268
Kröner, P.	415
Krügel, U.	063
Krüger, K.	352
Kukielka, G.	354

L

Laarmann, K.	353
Ladurner, A.	140
Langer, A.	157
Lehmann, A.	400
Lehmann, F.	123
Lehmann, S.	209
Lemoine, H.	055
Lemoine, L.	356
Leontaridou, M.	371
Leovsky, C.	364
Leuthold, P.	412
Lichtenstein, D.	074, 211
Lichter, J.	224
Limbeck, E.	362
Lohren, H.	198
Löken, E.-M.	266
Lothar, A.	041
Löwa, A.	090
Luckert, C.	193, 382
Ludwig, A.	061

M

Ma-Hock, L.	220
Mahdiani, M.	246
Maiellaro, I.	038
Mallmann, R.	182
Mangerich, A.	050
Mann, A.	101
Marquardt, C.	212
Marx, A.	186
Matkovic, I.	289
Matthaei, J.	329
Matthes, J.	008
Mayer, B.	348
Melching-Kollmuss, S.	202
Metzner, K.	012
Meyer, M.	261
Miess, E.	097
Moepps, B.	035, 102
Monien, B.	234
Mückter, H.	378
Muehlich, S.	018
Müller, A.-K.	341
Müller, G.	084, 273
Müller, J.	254
Müller, T.	184
Müller-Fielitz, H.	269
Mürdter, T.	021
Mußotter, F.	208
Muther, S. K.	253

N

Nendza, M.	251
Neul, C.	080
Neumann, D.	015
Nickel-Seeber, J.	086
Nieber, K.	286
Nieber, K.	284, 285

Niessen, K. V.	174
Nikolova, T.	359
Nitezki, T.	094
Nuber, S.	116
Nührenberg, T.	167

O

Oeder, S.	213
Olberisch, K.	325
Ongherth, A.	118
Othman, E. M.	355
Ozturk, Z.	316, 330, 401

P

Partosch, F.	201, 377
Pasch, S.	121
Pawletta, M.	374
Pemp, D.	206
Peters, S.	132
Pfalzgraff, A.	275
Pfistermeister, B.	079
Philipp, M.	010
Pichler, G.	281
Plöttner, S.	351
Plötz, T.	288
Pluteanu, F.	159
Poburski, D.	024, 363
Pockes, S.	100
Ponath, V.	001
Popp, T.	380
Potratz, S.	236
Pötzt, O.	195
Prokopets, O.	058

R

Rakers, C.	087
Ramanujam, D. P.	011
Ramer, R.	292
Rank, L.	053
Regenthal, R.	411
Regn, M.	169
Reif, R.	069
Reiss, K.	276, 277
Requardt, H.	216
Reustle, A.	019
Richling, E.	076
Rieke, S.	393
Rohrbeck, A.	197
Rommel, C.	166
Rong, W. W.	366
Rudeck, J.	092
Ruland, J. G.	108

S

Sachau, J.	047
Sarikas, A.	143, 336
Sauer, U. G.	067
Schäfer-Kortling, M.	083
Scheffel, C.	171
Schellenberger, M.	391
Schihada, H.	115
Schinner, E.	318
Schirmer, B.	037
Schlichtig, F.	247, 248
Schlick, S.	039
Schmeincck, S.	375
Schmidt, A.	417
Schmidt, M.	016
Schmiedl, S.	334
Schmitz, K.	306
Schneider, E.	126
Schneider, S.	399
Schneider, T.	215
Schnell, L.	025
Schoger, E.	164
Scholz, B.	151
Schrage, R.	098
Schramm, A.	129
Schreiber, I.	073
Schremmer, I.	005
Schriever-Schwemmer, G.	342
Schroll, A.	244
Schroth, W.	414
Schulte, J. S.	160
Schütz, D.	338
Schütze, K.	006
Schwan, C.	124
Schweers, J. M.	304
Schweikl, H.	395
Schwenk, R.	301
Schwotzer, D.	210
Seeger, T.	175
Seemann, S.	014, 271

Seidl, M. D.	009
Seitz, T.	260
Seiwert, N.	357
Sieg, H.	217
Siramshtetty, V. B.	085
Slopianka, M.	398
Sommerfeld, L.	109
Sonnenburg, A.	390
Sperber, S.	346
Stedtler, U.	421
Stegmüller, S.	241
Steiger, A.	078
Stenger, B.	379
Stephan, G.	176
Storch, U.	062
Stratz, C.	081, 404
Straub, J.	104
Su, Q.	272
Susanne, K.	388
Suvorava, T.	283
Svobodova, B.	173
Syrovets, T.	136

T

Tano, J.-Y.	187
Tarland, E.	305
Tarnow, P.	204
Teichert, H.	337
Tetzner, A.	112
Theis, L.	368
Thierbach, R.	367
Thierbach, R.	387
Thoma, J.	130
Thomas, S.	226
Thome, F.	333
Thurner, L. R.	137
Tkachenko, A.	418
Tomasovic, A.	007
Tran, Y. H.	048
Tsoutsouloupoulos, A.	230, 231, 381
Tzvetkov, M. V.	022

U

Urbisch, D.	370
------------------	-----

V

Vienken, H.	165
von Elsner, L.	227

W

Waizenegger, J.	243
Walther, U. I.	335
Wareing, B.	369
Wätjen, W.	077
Weber, J.	178
Weber, M.	376
Wedekind, R.	350
Weindl, G.	274
Wenz, C.	361
Wenzel, T.	258
Werfel, S.	148
Wewering, F.	004
Wiemann, A.	249
Wilde, S.	360
Winkler, K.	291
Witt, B.	383
Wolf, S.	156
Wölfer, M.	154
Wolff, C.	082
Wolters, M.	128

X

Xia, N.	155
Xu, R.	290

Z

Zeeb, M.	142
Zhang, J.	181
Ziegler, V.	070
Ziemann, C.	214
Zischka, H.	419
Zolk, O.	409
Zubel, T.	358